NUREG/CP-0116
CONF-900813
Vol. 2

Proceedings of the 21st DOE/NRC Nuclear Air Cleaning Conference

Sessions 9–16

Held in San Diego, California
August 13–16, 1990

Edited by M. W. First

Sponsored by
U.S. Department of Energy
U.S. Nuclear Regulatory Commission
International Society of Nuclear Air
Treatment Technologies, Inc.
The Harvard Air Cleaning Laboratory

Proceedings prepared by
The Harvard Air Cleaning Laboratory

Available from

Superintendent of Documents
U.S. Government Printing Office
P.O. Box 37082
Washington D.C. 20013-7082

and

National Technical Information Service
Springfield , VA 22161

NUREG/CP-0116
CONF-900813
Vol. 2

Proceedings of the 21st DOE/NRC Nuclear Air Cleaning Conference

Sessions 9–16

Held in San Diego, California
August 13–16, 1990

Date Published: February 1991

Edited by
M. W. First

Sponsored by
Office of Nuclear Safety
U.S. Department of Energy
Washington, DC 20585

Office of Nuclear Regulatory Research
U.S. Nuclear Regulatory Commission
Washington, DC 20555

International Society of Nuclear Air
Treatment Technologies, Inc.
P.O. Box 29246
Columbus, OH 43229

Harvard School of Public Health
The Harvard Air Cleaning Laboratory
665 Huntington Avenue
Boston, MA 02115

Proceedings prepared by
The Harvard Air Cleaning Laboratory

PROGRAM COMMITTEE

W. L. Anderson

R. R. Bellamy

A. G. Evans

H. Gilbert

C. R. Jones

R. T. Jubin

W. H. Miller, Jr.

D. W. Moeller

R. L. Shepard

D. F. Torgerson

A. A. Weadock

R. R. Weidler

CONFERENCE CHAIRMAN

M. W. First
Harvard Air Cleaning Laboratory

TABLE OF CONTENTS

Volume 1

SESSION 2

FILTER TESTING

Monday: [illegible]st 13, 1990
Co-Chairmen: [illegible] Anderson
Consultant
W. Bergman
Lawrence Livermore National Laboratory

SESSION 3

PANEL: CODE ON NUCLEAR AIR AND GAS TREATMENT ASME/ANSI AG-1

Monday: August 13, 1990
Moderator: W. H. Miller, Jr
Sargent & Lundy Engineers

Panel Members:
Thomas J. Vogan
Sargent & Lundy Engineers
Steven G. Banton
Chairman, ASME/CONAGT Subcommittee on Field Test Procedures
Sue A. Hobart
Adams & Hobart Consulting Engineers

SESSION

OPEN SESSION

EUROPEAN COMMUNITY NUCLEAR CODES AND STANDARDS

Monday: August 13, 1990
Co-Chairmen: W. H. Miller, Jr.
Sargent & Lundy
J. L. Kovach
Nuclear Consulting Services

SESSION 4

CHEMICAL PROCESSING OFF-GAS CLEANING

Tuesday: August 14, 1990
Co-Chairmen: R. T Jubin
Oak Ridge National Laboratory
A. C. Vikis
Atomic Energy of Canada, Ltd.

SESSION 5

PANEL: HOW TO USE N510 TESTING METHODS AND ACCEPTANCE CRITERIA FOR AIR TREATMENT SYSTEMS NOT CONSTRUCTED ACCORDING TO N509

Tuesday: August 14, 1990
Moderator: R. R. Weidler
Duke Power Company

Panel Members:
James R. Edwards
Charcoal Service Corporation
John W. Jacox
Jacox Associates
Richard D. Porco
Consultant
Peter Olson
Flakt, Inc.
Philip Roberson
Duke Power Company

SESSION 6

WORKING LUNCHEON

Tuesday: August 14, 1990
Chairman: D. W. Moeller
Harvard School of Public Health

SESSION 7

OPEN END

Tuesday: August 14, 1990
Chairman: M. W. First
Harvard Air Cleaning Laboratory

SESSION 8

A - INCINERATION AND VITRIFICATION
B - SYSTEM DESIGN

Wednesday: August 15, 1990
Co-Chairmen: R. L. Shepard
U.S. Nuclear Regulatory Commission
J. R. Yow
Corporate Consulting & Development Company

SYSTEM DESIGN

Volume 2

SESSION 9

ADSORBENTS

Wednesday: August 15, 1990
Co-Chairmen: A. G. Evans
Westinghouse Savannah River Plant
Li Qi-dong
Fudan University

SESSION 10

NUCLEAR CODES AND STANDARDS

Wednesday: August 15, 1990
Co-Chairmen: A. A. Weadock
U.S. Department of Energy
B. B. Reinert
Los Alamos National Laboratory

SESSION 11

MODELING

Wednesday: August 15, 1990
Co-Chairmen: R. R. Bellamy
U.S. Nuclear Regulatory Commission
J. Pearson
NCS, Inc.

SESSION 12

FILTERS

Wednesday: August 15, 1990
Co-Chairmen: H. Gilbert
Consultant
R. Dorman
Consultant

SESSION 13

SAFETY

Wednesday: August 15, 1990
Co-Chairmen: H. P. Wichmann
Wiederaufarbeitungsanlage Karlsruhe Betriebsgesellschaft mbH
J. P. Mercier
Institut de Protection et Sûreté Nucléaire

SESSION 14

CONTAINMENT VENTING

Thursday: August 16, 1990
Co-Chairmen: J. L. Kovach
NUCON International
P. Mulcey
Commissariat à l'Energie Atomique

SESSION 16

PANEL SESSION: NUCLEAR AIR CLEANING PROGRAMS AROUND THE WORLD

Thursday: August 16, 1990
Co-Chairmen: G.R. Plumb, *IAEA, Austria*
V. Friedrich, *Institute of Isotopes of the Hungarian Academy of Sciences*
Panel Members:
Mr. Lambert Scholten, *The Netherlands*
Dr. M. Lee Hyder, *U.S.A.*
Mr. Christopher Cheh, *Canada*
Mr. David Holman, *United Kingdom*
Mr. Ian Handyside, *United Kingdom*
Mr. Philippe Mulcey, *France*
Mr. Hans Cederqvist, *Sweden*
Dr. Juergen Wilhelm, *Germany*
Dr. Yasuo Hirose, *Japan*
Mr. Vilmos Friedrich, *Hungary*

SESSION 9

ADSORBENTS

Wednesday: August 15, 1990
Co-Chairmen: A. G. Evans
Li Qi-dong

NEW TYPE ADSORBENT MATERIAL OF IMPREGNATED ACTIVATED CARBON FIBERS FOR IODINE FILTER

Li Qi-dong, Ye Changzhuo, Yuam Shunqing
Pang Yafang, Ling Junyue
Fudan University, Shanghai

Gu Xiaochun, Yang Miaoxiang, Zhu Huijian, Liu Zexiang
Shanghai Textile Research Institute

Ma Ruqian, Qian Yingge, Fu Haizhong
Shanghai Nuclear Engineering Research and Design Institute

People's Republic of China

Abstract

Impregnated granular activated carbon bed filters have been used worldwide to treat nuclear power plant exhaust gases of containing iodine and extensive experimental studies have been conducted. It has been discovered that the impregnated granular activated carbon has some inherent defect such as the ignition temperature is lower, the adsorption efficiency and capacity were lower and afected strongly by relative humidity and the adsorption velocity is lower. A new type impregnated activated carbon fibers (IACF) material was developed in our laboratories.

The IACF is a felt material which has a wealth of micropores, low apparent density, high chemical stability, especially higher ignition temperature, low affinity for water, high adsorption velocity and the shape of IACF can be tailored to achive the best adsorption results. Therfore, the IACF is possessed of a high adsorption capacity and efficiency in high relative humidity (>95% R.H.). According to the ASTM D 3803 method A test, the result showed that the adsorption efficiency of >99% in bed depth of 2.5 cm

In this work, the various surface structural parameters, surface chemical characteristics and adsorption dynamics were studied by the X-ray diffraction, infrared absorption, X-ray photoelectron spectrometry method etc.

The results show that the various characteristics of the IACF are better than existing nuclear grade granular activated carbon. For this reason the IACF will be full of promise for the material of iodine filter and it will lead to a significant change for nuclear air cleaning.

I. Introduction

Activated carbon fibers (ACF) is a new type adsorbent material. The research was first recorded more then forty years ago(1), but the time of industrial manufacture was only twenty years. It has a series of advantage such as a high adsorption capacity and efficiency, a high adsorption velocity and a high thermostability etc. besides the whole characteristics of granular activated carbon (GAC). Thus it was extensively used in the military physical protection, air cleaning, water treatment and other pollution controlling. In addition, it also can be used in carrier of catalyst, noble metals recovery and extra-corporeal hemopertusion for adsorbing urea, endotoxin and other toxin from blood.

In the late 1970s, we had found the high capacity of ACF and suggested that a research for iodine removal with ACF was launched when we were studying the iodine filter of Qin-shan nuclear power plant.

The use of impregnated granular activated carbon for iodine removal was getting on for twenty-odd years in the worldwide. From the operational experiences, it have been discovered that the impregnated GAC have some obvious deficiencies such as the adsorption capacity and efficiency were strongly affected by relative humidity, the adsorption velocity is slower and the ignition temperature is lower etc. Therefore, a new type impregnated activated carbon fibers (IACF) adsorbent material was developed in our laboratories.

With regard to the research of IACF for iodine removal, the TOYOBO Co.has published patents(2)(3) in 1983 and 1984. It shows that an adsorbent for removing radioiodine was obtained by looding ACF with TEDA. The yugoslavia VUJISIC(4) it was reported that the adsorption properties of the ACF are equal or better than the same properties of impregnated activated charcoals used on NPP Krsko and it could be promissing for use as a filter materials in iodine filter.

In this work, including these studies of the raw material screeing, carbonization, activation and activator and the method of impregnating etc. From the ACF of some dozens kinds, screening out the IACF in accord with the nuclear grade gas phase adsorbents.

In addition, the structure of surface, the chemical composition of surface, the thermostability, adsorption isotherm and adsorption dynamics were studied.

We expect that the IACF will be used in nuclear air cleaning and other environmental enginerring on these bases of this work.

II. Physical Chemical Properties of Activated Carbon Fibers

The results of studies has shown that the adsorption process is complex. The adsorption capacity was affected by the surface structure, chemical composition of surface and the conditions of adsorption process etc. These basic characteristics of IACF of differential adsorption ability has a very great difference.

In this paper, the surface characteristics of nuclear grade IAC F material which was obtained by the screening GAC narrated as follows

Analyses of Surface Structure

X-ray Diffraction Analysis

The ACF and the GAC were compared; the result shows that the elementary structure is approximately equal. The ACF is a porous high polymers of fibrous carbon. It has a graphite microlite of high disorder. Figure 1. is a x-ray diffraction curve of carbon fiber and activated carbon fibers(the activation temp.of 850°C and 900°C).

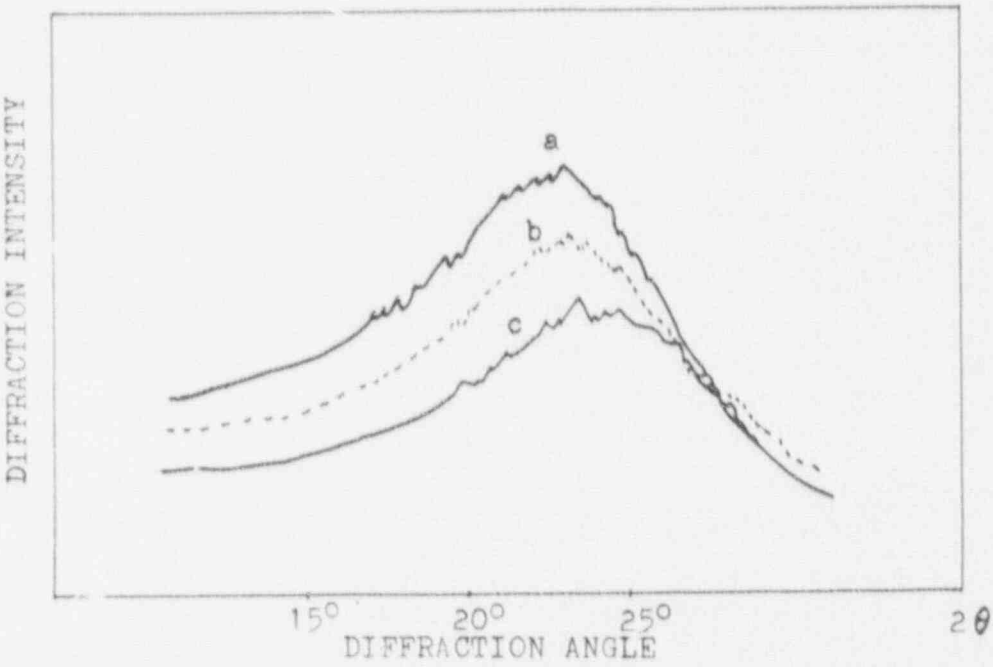

Figure 1 X-ray Diffraction Curve
a. Carbon Fiber
b. Activated carbon fiber of activation Temp.of 850°C
c. Activated carbon fiber of activation Temp. of 900°C

From figure 1. We can see that the disorderty of graphite microlite is progressively increase with increase in the activation temperature and the unit lattice size is decrease with increase in the activation temperature, interplanar distance is roughly the same (see table 1.).

It was generally thinked that the unit lattice size is decrease and the disorderty is increase will cause the active point to be increase on surface and it will advantages the adsorption.

Table 1. Lattice Parameters of ACF

Kind of Carbon	Interplanar Distance d_{002}(Å)	Lattice Size d_c(Å)
Carbon Fiber	3.86	9.76
ACF_1*	3.83	9.65
ACF_2**	3.80	9.01

* ACF_1 The activation temp. of 850°C

**ACF_2 The activation temp. of 900°C

Analyses of Scanning and Transmission electron micrograph

The scanning and transmission electron micrograph was used it were able to observe the micropore structure of adsorbent surface. Figure 2. is scanning electron micrograph and from the figure we can see that there are micropores of large number only in the smooth surface of activated carbon fibers,but opposite, there are macropores and mesopores in the granular activated carbon surface and there are micropores in the interior. (See figure 3.)

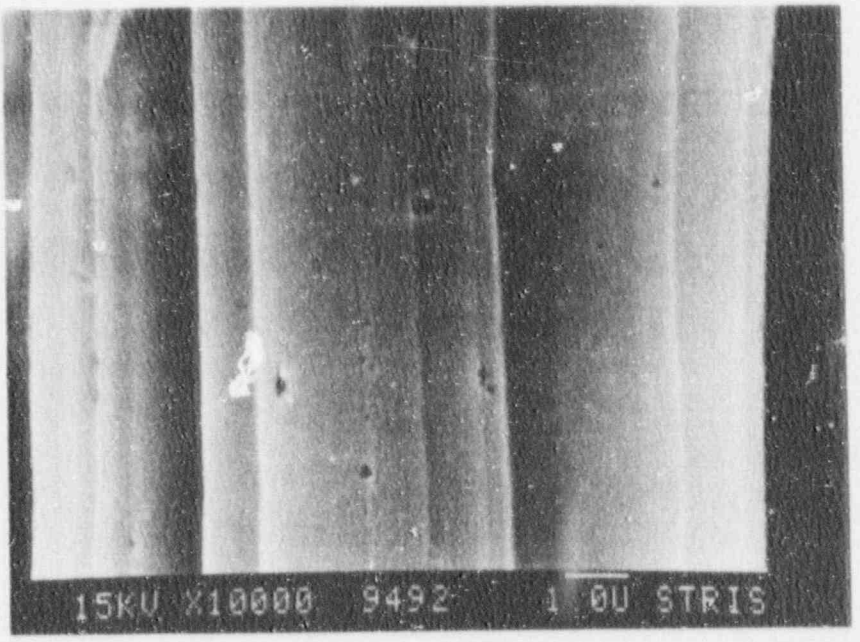

Figure 2 Scanning Electron Micrograph of ACF

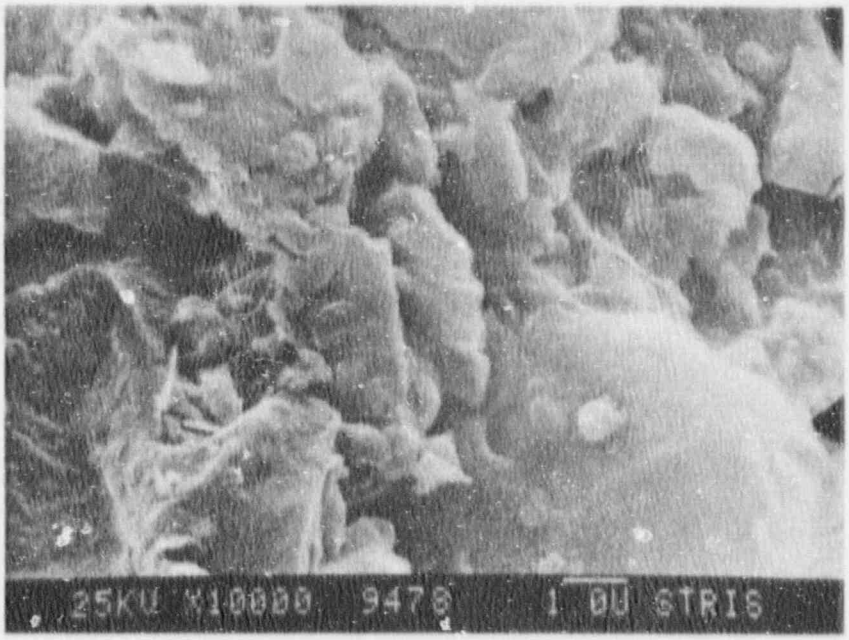

Figure 3 Scanning Electron Micrograph of GAC (x10000)

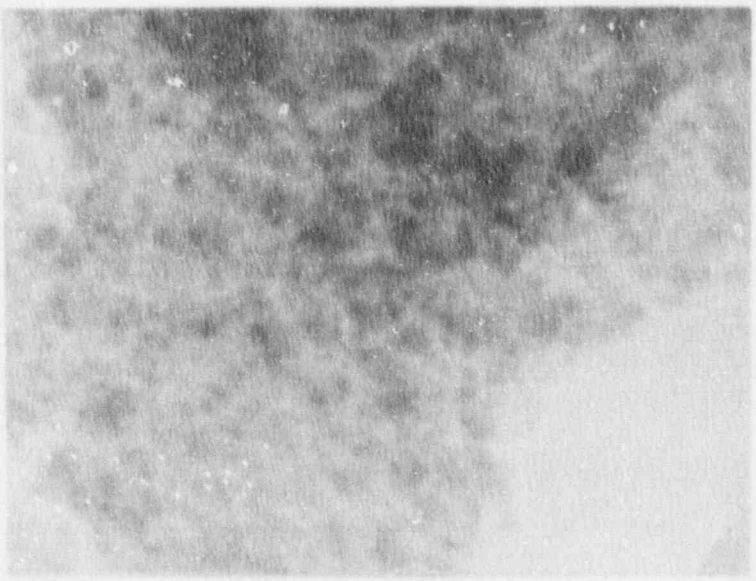

Figure 4 Transmission Electron Micrograph of ACF (x1000000)

Figure 4. is the transmiss[illegible]tron micrograph of ACF which is magnified for a million diame[illegible] the figure, we can see that the micropores was spread all ov[illegible]he activated carbon fiber.

Analyses of specific surface and pore size distribution

In this analyses, the B.E.T. method was used and in the first place the impregnated activated carbon fibers isotherm for adsorption nitrogen were determined then the pore size distribution and specific

surface was obtained by computation. The figure 5. and 6. present the IACF isotherm for nitrogen and the pore size ditribution curve.

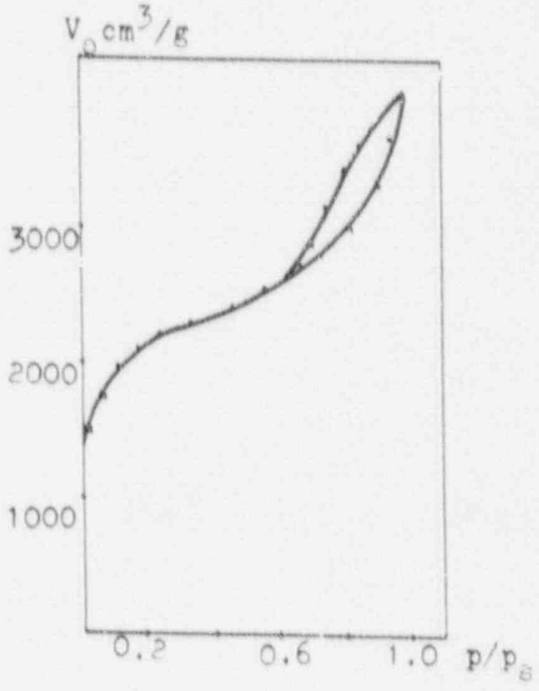

Figure 5 Isotherm for nitrogen at -195.6°C

Figure 5. shows that this is a isotherm with adsorption return line and it belongs to the 2ed type of Brunauer's isotherm which indicated that it will get a good result for specific surface and pore size distribution.

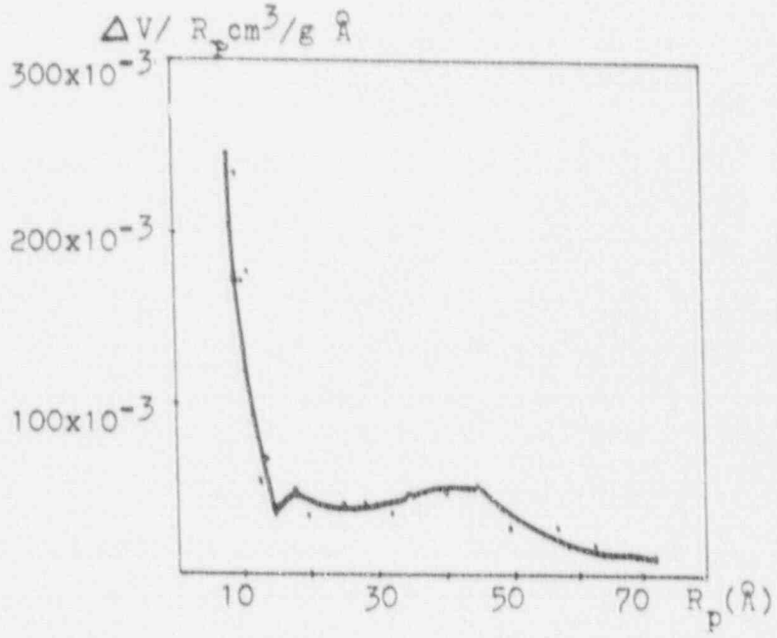

Figure 6 Differential distribution of pore size of ACF

Figure 6. illustrates the micropores are a large number, and the chink between these fibers are as the action of macropores and mesopores in the adsorption process.

The specific surface of 2500 m^2/g about.

In addition, from the results of the scan-ning electron micrograph and pore size distribution demostrate the adsorption velocity was small affected by the pore diffusion. For this reason, it has a rapid velocity and a short retention time in adsorption process.

Analyses of chemical composition of surface

The surface chemical composition are the important characterist -ics of adsorbent.

In this work, the surface chemical composition are some function -al group in the skeleton of carbon, and the results of elementary analysis. And the infra-red absorption spectrophotometry and x-ray photoelectron spectrometry and chemical analysis method were used.

Functional group analysis

The chemical titrimetric analysis was used for the determination of functional group content, the determining result were presented in table 2.

Table 2 Content of Surface Functional Group of ACF

	-COOH	-OH	Internal ester	Acidity group	Basicity group
	meq/g				
ACF	0.0464	0.3343	0.0539	0.4279	0.5605

The functional group of containing oxygen on the surface of ACF was produced in the activation process on the activation point of lattice edge.

The specific surface and functional group content are increase with increase in temperature and time of activation. It will advantage the adsorption. But happen at same time, the recovery and thermostabi -lity of ACF was decreased.

Elementary analysis

The carbon, hydrogen, oxygen, nitrogen, magnesium, calcium and ash etc. of ACF was analysed. The results as follows.

Table 3 Chemical Composition of ACF

	C %	H %	N %	O %	Mg ppm	Ca ppm	Ash %
A C F	87.75	0.8	0.31	11.14	42.57	61.45	1.6

Infra-red Absorption Spectrum

The infra-red absorption spectrum of activated carbon fibers is presented in figure 7. the figure shows that there are absorption peak in 1100 cm^{-1}, 3400 cm^{-1}, it illustrate that there is the hydroxy of phenol in the surface of ACF, and there are continuous little peak in the 2700-2500 cm^{-1} it demonstrates that there are carboxy group in the surface of ACF.

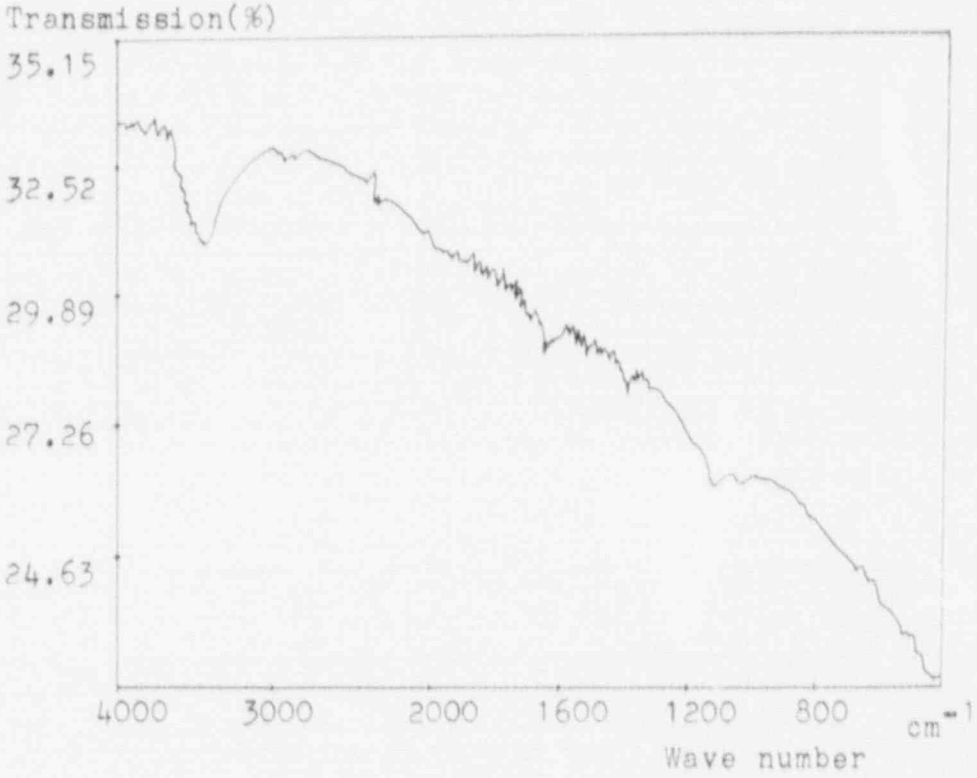

Figure 7 Infra-red Spectrum of ACF

X-ray Photoelectron spectrometry

The x-ray photoelectron spectrometry is able to see the combining status for the carbon atoms. Figure 8 and 9 are the XPS pattern, we can see that the peak shape presented widening and unsymmetry, it shows that there are varied combining status for carbon atoms in the surface, and the ≡C-OH is more in those. In the O_{1s} pattern, there are peak in 532.5 ev, it shows that there are C=O and C-O in the surface of ACF but the C-O is more in those.

Relation between pH value and specific surface

In general, the pH value is a important index of activated carbon and the index has been set, the pH value must be >9 and when the pH<7 the carbon should be changed.

In this work, the relation between pH and the activation degree of ACF was investigated.

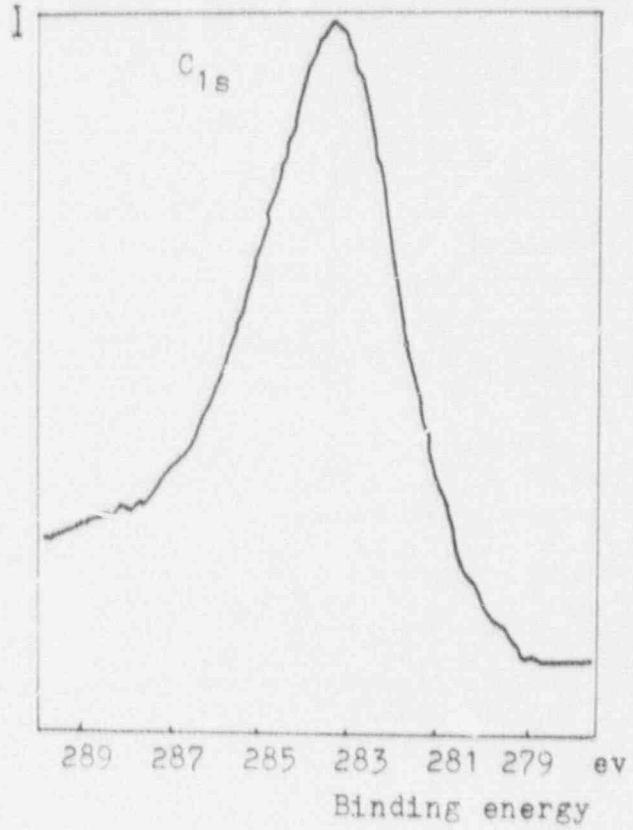

Figure 8 XPS Pattern of ACF

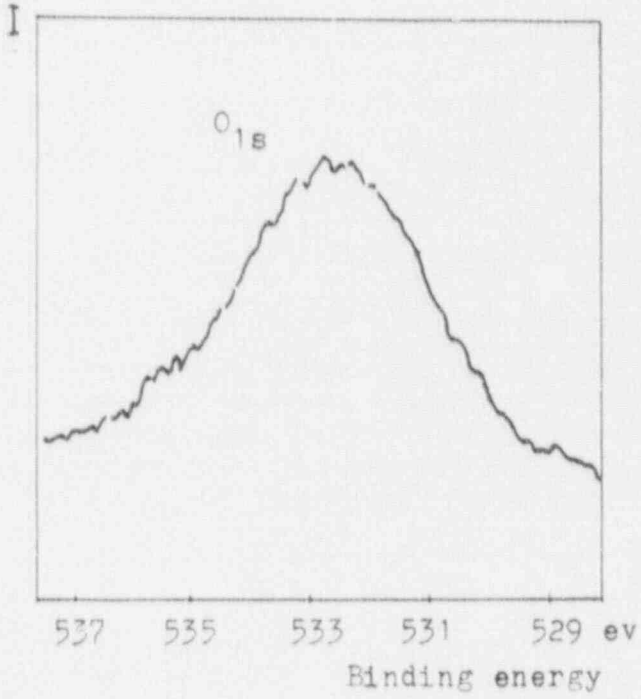

Figure 9 XPS Pattern of ACF

Table 4 Specific Surface and pH Value of ACF

Condition of activation	pH	Specific Surface m^2/g
850°C	6.36	500
	6.27	800
	5.92	1000
900°C	10.06	500
	9.90	800
	9.50	1000

Table 4. shows that the pH of water extract is high in activation temperature of 900°C, but the activation temperature(850°C) is lower and the pH is clear descent.

In addition, when the same condition of activation, the pH value is decreased with increase in the specific surface. This is probably due to the resultant of acidic group which is produced in the activation process.

Test of thermal stability

The spontaneous ignition temperature is a important property of nuclear grade activated carbon. In this paper, the thermal stability of ACF was examined by the thermal gravimetric analysis. Figure 10. shows that the weightlessness curve of two ACF, the ACF_1 has a high activation degree and speficic surface of $1000m^2/g$.and it's weightlessness begins in the after 500°C. The ACF_2 has a lower activation degree and specific surface of $800m^2/g$, it's weightlessness begins in the after 600°C. From figure 10. we can see that the thermal stability is decrease with increase in specific surface.

III. Adsorption characteristics of IACF

Adsorption isotherm of IACF for Methyl iodide

The adsorption isotherm indicates significant adsorption characteristics. Figure 11 is a dynamic adsorption isotherm in low concentration.The condition of test listed below:

Methyl Iodide concentration	0.3 - 27 ppm
Bed Depth	5 cm
Relative Humidity	95 %
Gas velocity	12.2 m/min.
Temperature	30.0±0.5

Figure 11. shows that the experimental adsorption isotherm is very good in accord with the Freundlich adsorption equation, and the following the equation will be used.

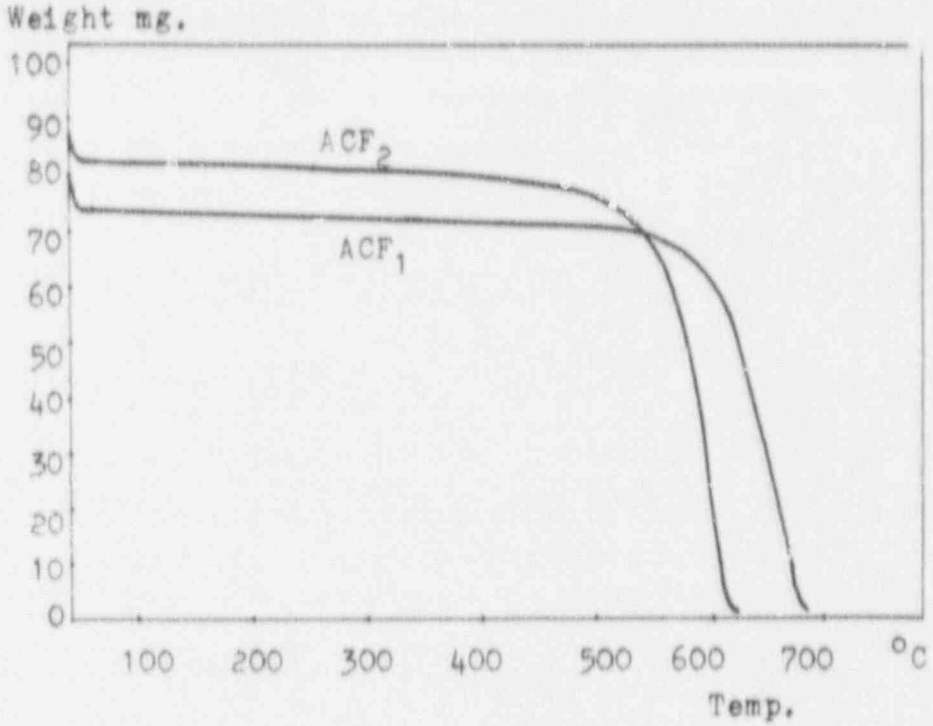

Figure 10. Curve of Weight Loss on Heating of ACF

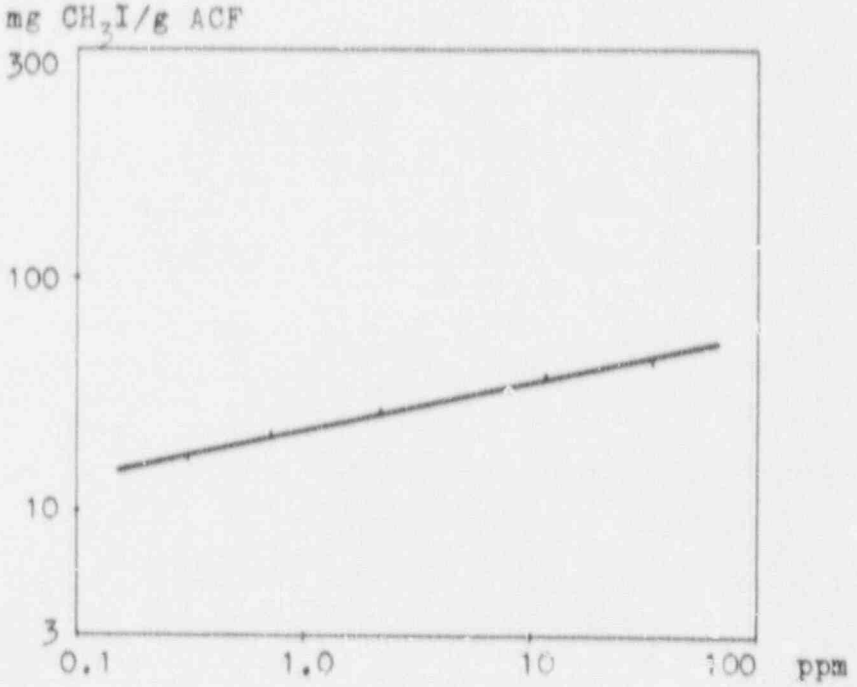

Figure 11. Adsorption Isotherm of ACF for Methyl Iodide

$$\lg q = \lg k + 1/n \lg C$$

Where:

$k = 22.03$ $\quad$ $1/n = 0.218$

c: Saturated Capacity of dynamic adsorption

C: Gas concentration

k, 1/n: Constants

Test of Adsorption Velocity

Because the special micropore structure of IACF the adsorbate is not need passing through the macropores, mesopores then entrance to the micropores of adsorbent. Therefore, the adsorption velocity is very quick.

Adsorption Velocity Test of Saturated Steam of 20°C

The ACF and GAC in the bath of saturated steam of 20°C for 5 hr. For the ACF, the adsorbate amount(steam) up to 80 % of the saturated adsorption amount. For the GAC, the adsorbate amount(steam) up to 22 % of the saturated adsorption amount.

Test of Adsorption Residence Time for Methyl iodide

The residence time of activated carbon is generally 0.25 sec. In order to examine the high speed property of ACF, the residence time of 0.12 sec., 0.072 sec., 0.062 sec., 0.048 sec., and 0.045 sec. respectively was tested. The results of test is in figure 12.

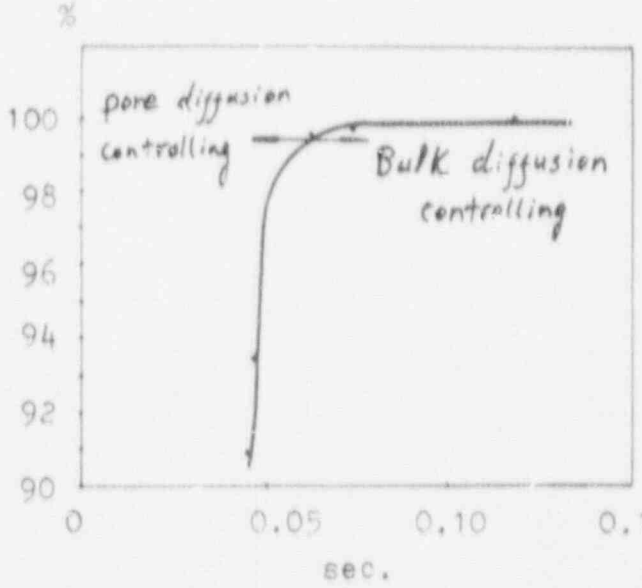

Figure 12. Adsorption efficiency as a function of residence time

Test conditions:

Concentration of methyl iodide	1.75 ± 0.25 mg/m^3
Temperature	30.0 ± 0.5°C
R. H.	>95 %
Duration	120 min.
Bed depth	2.5 cm

Figure 12. shows that the IACF of 5 cm bed depth, when the gas velocity of 70 cm/sec. (residence time is 0.071 sec), the pore diffusion is the rate controlling step. But the correspondence gas velocity is 40.6 cm/sec. (residence time is 0.12sec.) for the GAC.

Affect of Relative humidity on adsorption CH_3I

It is universally acknowledged that the adsorption of activated carbon for methyl iodide was strongly affected by the humidity. recently, Scarpellino reported (5) that in the 96 to 99% R.H. range, a one percent variation in relative humidity can have a 100 percent change in methyl iodide penetration value. For this reason, the high humidity test was conducted.

In the test, the relative humidity of >95 % and >98 % were tested, and other condition in the ASTM D 3803 was followed, the results of test shows that

R.H. >95 % Penetrability=0.25 % and
R.H. >98 % Penetrability=0.85 %,

the penetrability is lower then that of GAC,the penetrability of GAC is 10.5±3.9% in 98 % R.H. the reason is probably the low affinity for water of impregnated activated carbon fibers.

In order to illuminate the phenomenon, the saturated adsorption test was conducted and the results are as follows:

Table 6. Adsorbing water vapor tests

	Amount of Adsorbing Steam 20°C, 120 hr. static	Increment of amount in pre-equilibration period 30°C, 16 hr. dynamic
IACF	28.4 %	25.6 %
GAC	46.8 %	42.4 %

From table 6. we can see that the adsorbing water vapor amount of IACF is small and both static and dynamic are similar. For this reaon, the competitive adsorption of water is small for the methyl iodide, therefore, there are a less effect on adsorption efficiency of methyl iodide in high relative humidity.

Effect of concentration of methyl iodide on penetration

Many studies have been carried out on the relation between the breakthrough time and inlet concentration, and many equations have been established(6), and this paper author have published similar work(7). But between those test conditions and the ASTM D 3803 method A there are some differences. In this study, the test conditions have no difference besides gas concentration and duration time.

The results of tests are presented as a plot of log t_b versus log C_o as figure 13. which shows a good linear relationship in the range of concentrations of the test, and the breakthrough time t_b can be approximated by the following equation

$$DF = 1000, \qquad t_b = 532 C_o^{-0.863}$$

From above equation, we can obtain the breakthrough time-concentration

relation in limited concentration range by extrapolation.

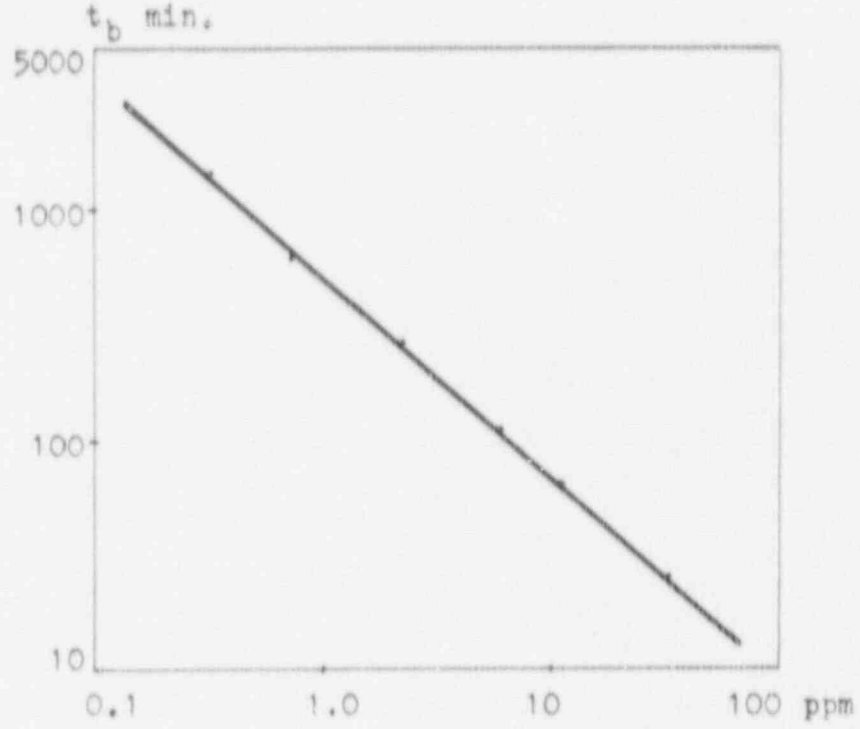

Figure 13.
Breakthrough Curves of IACF for methyl iodide

Test condition:

Relative humidity	>95 %
Gas velocity	12.2 m/sec
Bed depth	5.0 cm
Temp.	30.0 °C
DF	1000

Effect of bed depth on penetration

From the breakthrough time point of view, there are superiority in the deep bed adsorption and the bed depth of 5 cm appears to be inadequate.

In this work, it has been demonstrated that impregnated activated carbon fibers adsorbent material of 2.5 cm bed depth will be able to match the GAC of 5 cm bed depth. Therefore, if it is packed in the bed of 5 cm with the IACF (the amount is 1/10 of granular activated carbon), it will take effect of the deep bed adsorption.

The variation of breakthrough time with the bed depth is presented in figure 14.

Test conditions:

Concentration	0.31 ppm v/v
R.H.	>95 %
Gas velocity	12.2 m/min.
temp.	30.0 °C
DF	1000

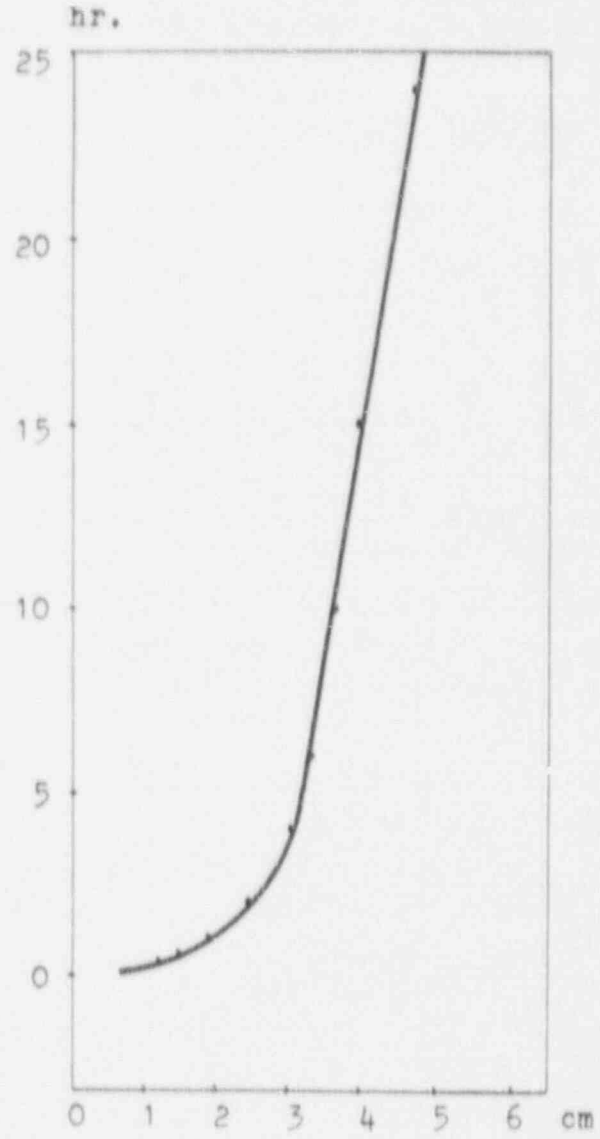

Figure 14.
Breakthrough Time
as a Function of
Bed Depth of IACF

IV. Test of Nuclear Grade Gas Phase Adsorbent

Impregnant

The tests and screening were conducted and the prescription of 5% TEDA + 2% KI were used.

Test of Nuclear Grade Gas Phase Adsorbents

The test procedure outlined in ASTM D 3803 methods A. B. D. E. was followed and the parameters listed below:

		Method A	Method B	Method D	Method E
Test adsorbate		$CH_3{}^{127}I$ +	$CH_3{}^{131}I$	$^{127}I_2$ +	$^{131}I_2$
Concentration	mg/m^3	1.75±0.25	1.75±0.25	17.5±0.5	75±5
Equilibration	Temp.(°C)	30.0±0.5	80.0±0.5	30.0±0.5	
period	R.H.(%)	95		95	
	Duration(h)	16.00		16.00	
Feed period	Temp.(°C)	30.0±0.5	80.0±0.5	30.0±0.5	180±2
	R.H.(%)	95	95	95	Ambient
	Duration(min)	120.0	60.0	120.0	10.0
Elution	Temp. (°C)	30.0±0.5	80.0±0.5	30.0±0.5	180±2
period	R.H.(%)	95	95	95	/
	Duration(min)	240.0	240.0	240.0	240.0
Absolute pressure	(Kpa)	97±3	97±3	97±3	97±3
Gas velocity	(m/min)	12.2±0.3	12.2±0.3	12.2±0.3	12.2±0.3
bed Depth	(mm)	25±1	25±1	25±1	25±1
Adsorption efficiency	(%)	99.7 %	99.8 %	99.95 %	99.78 %
		99.7 %	99.9 %	99.97 %	99.87 %
		99.6 %			
Unimpregnated ACF	(%)	4.2 %		99.91 %	99.50 %
		4.0 %			
		4.2 %			

In the test, monitor temp., pressure, R.H., air flow and pressure drop across the bed at least every 5-10 minutes, and triplicate analyses were preformed for the each sample.

Test of radiation tolerance status of IACF

In order to obtain the radiation tolerance status of IACF which was exposed in a strong radiation field, the radiation dose is 10^5 Gy The samples of radiation treatment was tested by the ASTM D 3803 method A. The results of test shows that the adsorbent material was not injured by the strong radiation and possessed same adsorption efficiency, and triplicate analyses are 99.50 %, 99.40 %, 99.60 % respectively.

Affect of aging treatment in air

The adsorbent aging tests are performed under conditions of 30° C, 95 % R.H..The result shows that the aging treatment was conducted for one year, the adsorption characteristics of IACF was not affected.

The long time aging treatment under the complex environmental conditions will await conduct.

V. Nuclear Grade Impregnated Activated Carbon Fibers Adsorbent Material Specifications

Molecular iodine, 30°C 95% RH		99.96 %
" " 180°C	ASTM D 3803	99.83 %
Methyl iodide, 30°C 95% RH	(Bed depth of 2.5cm)	99.70 %
" " 80°C "		99.80 %
Out ward		Felt
pore size (r)	(B.E.T.)	10-15 Å
pore volume (200 Å)	"	1.2334 ml/g
specific surface	"	2500m^2/g
packing density		0.06-0.1 g/ml
C Cl_4 activity		80mg/g
ash content		1.6 %
Ignition temp.		
IACF		410°C
ACF		500°C
pH of water extract		9.2-10
Benzene activity		55-60 %
monofilament diameter		10-20μ
tensile strength		8-10 Kg/mm^2
thermal stability		
weightlessness 500°C, 50 min		6 %
folding strength		
IACF was curved in diameter		
of 5 mm and 180°,		no break

VI. Concluding remarks

The research has demonstrated that the activated carbon fibers are an adsorbent of excellent function. The ACF was impregnated and car reach to the specifications of nuclear grade gas phase adsorbent. Because the apparent density is less 6-8 times then that of GAC. Therefore, it will be able to be obtained well efficency when the dosage is less. In addition, it have that the moisture content is less and the adsorption velocity is quick.

These characteristics clearly display that the IACF is better then the GAC. This IACF is used as a new type adsorbent which will have important significance in the environmental protection and nuclear air cleaning. About the studies of structre parametors have a certain guide sense on the production and control of the adsorbent.

Reference

(1). TATSUKI MATSUO, NOBUO ISHIZAKI and TAKASHI FUKUDA, " Activated carbon fiber KF " SEN-I GKKAISHI vol. 33 No.6 p.204-208 (1977)

(2). TOYOBO Co. Ltd. " Adsorbent for radioiodine " Jap. Kokai Tokkyo koho JP 58-96299 8,Jun (1983)

(3). TOYOBO Co. Ltd.
Jap. Kokai Tokkyo Koho Jp 59-50399 23 Mach (1984)

(4). Lj. VUJISIC, et al. " New filter material for iodine trapping" Proceedings of Europen conference p. 701-705 (1985)

(5). Scarpellino, C.D., Sill C. W., " Final technical evaluation report for the NRC/INEL activated carbon testing program " USNRC Report EGG-Ga-7653 (1987)

(6). Wood, G.O. et al. " Methyl iodide retention on charcoal sorbents at ppm concentration " 15th DOE nuclear air cleaning conference p. 352 (1978)

(7). Li, Qi-dong et al. " A Study of adsorption properties of impregnated charcoal for airborne iodine and methyl iodide " 18th DOE Nuclear Airborne Waste management and air cleaning conference p.78 (1984)

DISCUSSION

KING: If off-gases contain NO_x is the IACF still good to use for removing iodine?

LI: We have not studied the effect of NO_x, but I think that the IACF will perform acceptably because the thermal and chemical stability of IACF is good.

GLADDEN: What are the physical parameters of the IACF, length, fiber diameter, etc.? Is there a commercial source of the IACF felt? What is the relative cost of this material?

LI: The IACF is like a carpet or cloth, fiber length may be anything you like. It's a monofilament with a diameter of 10-20 μm. A commercial source for IACF felt is being investigated.

A STUDY OF THE EFFECT OF COATINGS OPERATION ON RADIOIODINE REMOVING ADSORBENTS

W. P. Freeman and J. C. Enneking
Nuclear Consulting Services, Inc.

Abstract

Nuclear air treatment systems are designed to remove radioactive contaminants from air. If the contaminants are gaseous in form (iodine and it's compounds), activated carbon is employed to remove them from the air stream by the process of adsorption. The ability of the carbon to perform it's function is checked periodically by sending representative samples to a laboratory for testing. Test methods and conditions are included in the plant technical specification along with failure criteria. When a test sample fails to perform as specified, the carbon in the air cleaning unit must be replaced with new material.

Solvents from coating operations can "poison" carbon by blocking or reducing the surface area available for subsequent reaction of radioiodine compounds. NUCON has developed mathematical models to predict the amount of solvent in the air and residual solvents remaining in the coating at any given time during a coating operation for both normal and accident ventilation modes. Required input parameters for the model include the evaporation rate of the solvents in the coating, the rate of application of the coating, the volume of air treated by the air cleaning system and the air flow rate to the air cleaning system. Output includes the amount of solvent remaining in the coating, the amount of solvent in air and the concentration of solvent vapor in the air.

Presented in this paper are results obtained using the model for nuclear air treatment systems and a number of different types of available coatings. The effect of solvent loading on the carbon beds was performed experimentally by determining the radioiodine removal performance of carbon beds containing a known amount of solvents. These results provide data upon which to base decisions concerning coating operations.

Introduction

Nuclear Air Treatment Systems (NATS) are used at all nuclear power plants for removal of radioactive contaminants from air. These contaminants can be particulates, which are removed by the HEPA filters installed in the NATS. If they are gaseous forms of radioactive iodine, impregnated activated carbon is used.

The ability of the carbon to remove gaseous radioactive iodine compounds from air is affected by many conditions. These include temperature, humidity, bed depth, velocity, adsorbent characteristics, aging effects and the presence of other adsorbed materials. Many papers have dealt with these parameters including the impact of adsorbed solvents on the radioiodine removal efficiency. Kovach and Rankovic [1] identified sources of organic contamination and recommended activated carbon guard beds upstream of the radioiodine adsorbent. Broadbent [2] studied the impact of

various amounts of common paint solvents on the radioiodine removal efficiency of new and aged activated carbons. In order to reduce the possibility of contaminating carbon, some plants have established guidelines for the maximum amount of painting in an area communicating with an air cleaning unit [3].

USNRC Regulatory Guides 1.140 [4] and 1.52 [5] outline general design criteria for NATS components including the adsorber banks. Appropriate sections of ANSI N509 [6] are referenced for design and construction details. The physical property characteristics of new adsorbent and the radioiodine removal requirements are given in Table 5.1 of ANSI N509. The Reg. Guides themselves give guidance for the bed depth of the adsorber banks.

The Reg. Guides also deal with "Laboratory Testing Criteria for Activated Carbon". They include recommendations for testing frequency, test conditions and failure criteria. Of course the technical specifications for each plant contain explicit instructions for testing the activated carbon from each of the air cleaning systems and must be consulted to determine exactly what is required.

Predicting Impact of Adsorbed Solvents

Methods have been developed to predict the amount of organic vapor that will be introduced to an air cleaning system during painting or evaporation of cleaning solvents. In general, higher percentage pick-up of contaminants on the adsorbent will result in lower radioiodine removal efficiencies. Therefore, when the amount of contaminant is compared to the amount of carbon in the adsorber bank, a prediction can be made about the impact on the performance.

The amount of activated carbon in an air cleaning system can vary widely. It is generally proportional to the airflow rate but it depends on the bed depth. Type two trays (2" deep beds) typically contain 55 lbs. of adsorbent and three of them are used for each 1,000 CFM of airflow. Therefore, the carbon weight is approximately 165 lbs. per 1,000 CFM of rated flow. For type III adsorbers, the bed depth can vary. The amount of carbon can be calculated from the following formula.

$$W = \frac{2.67\ Q\ d}{V}$$

W = weight of adsorbent, lbs.
Q = rated airflow, CFM
d = bed depth, inches
V = superficial velocity, ft/min.

For example, a type III adsorber rated for 10,000 CFM at 40 ft/min. superficial velocity with a 4" deep bed would contain 2,670 lbs. of adsorbent.

If the air cleaning unit operates continuously, all of the solvents from the paint being applied, or those vaporized during cleaning operations, will be adsorbed on the carbon. By keeping a

running inventory of the weight of this material, the percentage pick-up on the carbon can be calculated. Then a prediction of the impact on radioiodine removal efficiency can be made.

Most safety-related air cleaning systems, are normally in standby mode. The areas communicating with the units are served by the normal ventilation systems which will exhaust the solvents. However, if painting is being done in the area, there will be some solvent in the air and some remaining in the undried paint. If the air cleaning unit trips on, there will be some exposure to the solvents. However, that can be minimized by using low solvent content paints or by applying smaller quantities of paint during a given time.

It is important to realize that each air cleaning system represents a unique situation. Therefore it is not possible to apply a rule of thumb concerning painting or the permissible quantities of cleaning solvents. Some air cleaning systems contain large amounts of carbon. In some cases, the decontamination factor is low and the failure criteria for lab testing is lenient. If the laboratory test is conducted at high temperature and high humidity, the results will be better than at other conditions (see Freeman, et. al. [7]). A method of studying the impact of adsorbed organic materials on radioiodine adsorbents has been developed which takes all relevant parameters into consideration.

Description of Computer Program

The computer program uses an iterative procedure to calculate the amount of solvent evaporated from a coated surface anytime after a particular coating operation begins. Input variables include: treated air volume, ventilation rate, coating application rate, percent solvent in coating and evaporation rate of the individual solvents. The program sums the evaporation rates for the individual solvents and weights them by a factor that depends on the coating system involved. The program also allows for the calculation of solvent concentrations after switching the ventilation system to an accident mode.

Specific Examples

Shown in Figure 1 is the graphical output of the program for a typical reactor enclosure equipment compartment [8]. With normal ventilation, the solvent concentration in the air does not exceed 1 ppm, while the amount of unevaporated solvent reaches an equilibrium level of about 4.5 lbs. Essentially all of the solvent is evaporated 9 hours after painting is stopped. The ventilation system used here is non-safety related and thus, operates continuously. Since the Keeler and Long Epoxy H contains 0.75 lbs. VOC/gallon, the total burden on the 7,000 lbs of carbon in the system would be < 0.2 Wt%.

In Figures 2 and 3 are solvent concentration versus time curves for a typical reactor building [9]. The corresponding data sheets for the coatings are shown in Tables 1 and 2. Both figures represent normal ventilation modes with no carbon beds involved, Figure 2 is representative of a coating with a relatively small amount of solvent applied at a high rate while Figure 3 represents a

coating with a relatively large amount of solvent applied at a moderate rate.

In Figure 4 is shown the solvent evaporation curve for the coating from Table 3 for normal ventilation. In Figure 5 is the same system now with an accident occurring just as painting ceases and thus, the maximum amount of solvent is available to the carbon beds. The solvent is adsorbed by 16,000 lbs. of carbon in the accident (recirc.) mode.

A similar situation is shown in Figures 6 and 7 for the coating shown in Table 4. This coating system with a large volatile content and high application rate presents a somewhat worse case scenario. Yet, the approximately 70 lbs. of solvent that could be adsorbed during the accident mode amounts to only 0.5 Wt.% burden on the carbon bed.

Effect of Solvent Loading on Methyl Iodide-131 Penetration

A series of methyl iodide removal tests were performed on impregnated carbon samples containing known amounts of adsorbed solvent. The results are shown in Figures 8, 9 and 10 for mineral spirits, xylene and monomethyl glycol ether respectively. These results indicate that more than 10% by weight of these solvents can be adsorbed while still keeping the methyl iodide-131 penetration below 1% for the 30°C, 70% RH test without equilibration.

Conclusions and Recommendations

Using a computer program that calculates the amount of evaporated solvent from coating operations, we have seen that the predicted burden to the carbon in the air cleaning systems involved would have a negligible effect on methyl iodide removal for the cases considered. However, according to current (and proposed) standards, the carbon would still have to be tested but it would be of some comfort to know that, for a given situation, the carbon performance would not be compromised. As we continue to refine the model with input from utilities and coating manufacturers, information can be provided to base procedures for coating operations at nuclear power stations that will minimize risk to nuclear air cleaning systems.

References

1) Kovach, J. L.; Rankovic, L.; Evaluation and Control of Poisoning of Impregnated Carbons Used for Organic Iodide Removal, 15th DOE Nuclear Air Cleaning Conference, Boston (1979) p 368

2) Broadbent, D.; The Ageing and Poisoning of Charcoal Used in Nuclear Plant Air Cleaning System, CEC European Conference on Gaseous Effluent Treatment in Nuclear Installations, Luxembourg (1985)

3) Ginter, W.; Diablo Canyon Power Plant Guidelines for Protection of Carbon Filters, 19th DOE Nuclear Air Cleaning Conference, Seattle (1986)

4) USNRC Regulatory Guide 1.140, Rev. 1, 1979

5) USNRC Regulatory Guide 1.52, Rev. 2

6) ANSI/ASME N509-1976, 1980, 1989

7) Freeman, W. P.; Radioiodine Testing of Used Nuclear Grade Activated Carbon, 20th DOE Nuclear Air Cleaning Conference, Boston (1988) p 997

8) A Study of the Effects of Carbon Contamination by Paint Solvents, 17 January, 1990, NUCON Technical Report 12PE534/02

9) A Study of the Effect of Carbon Contamination by Paint Solvents, 18 June, 1990, NUCON Technical Report 06PH574/02

FIGURE 1

AMOUNTS OF SOLVENT IN THE REACTOR ENCLOSURE EQUIPMENT COMPARTMENT(REEC) FROM PAINTING WITH KEELER AND LONG EPOXY H

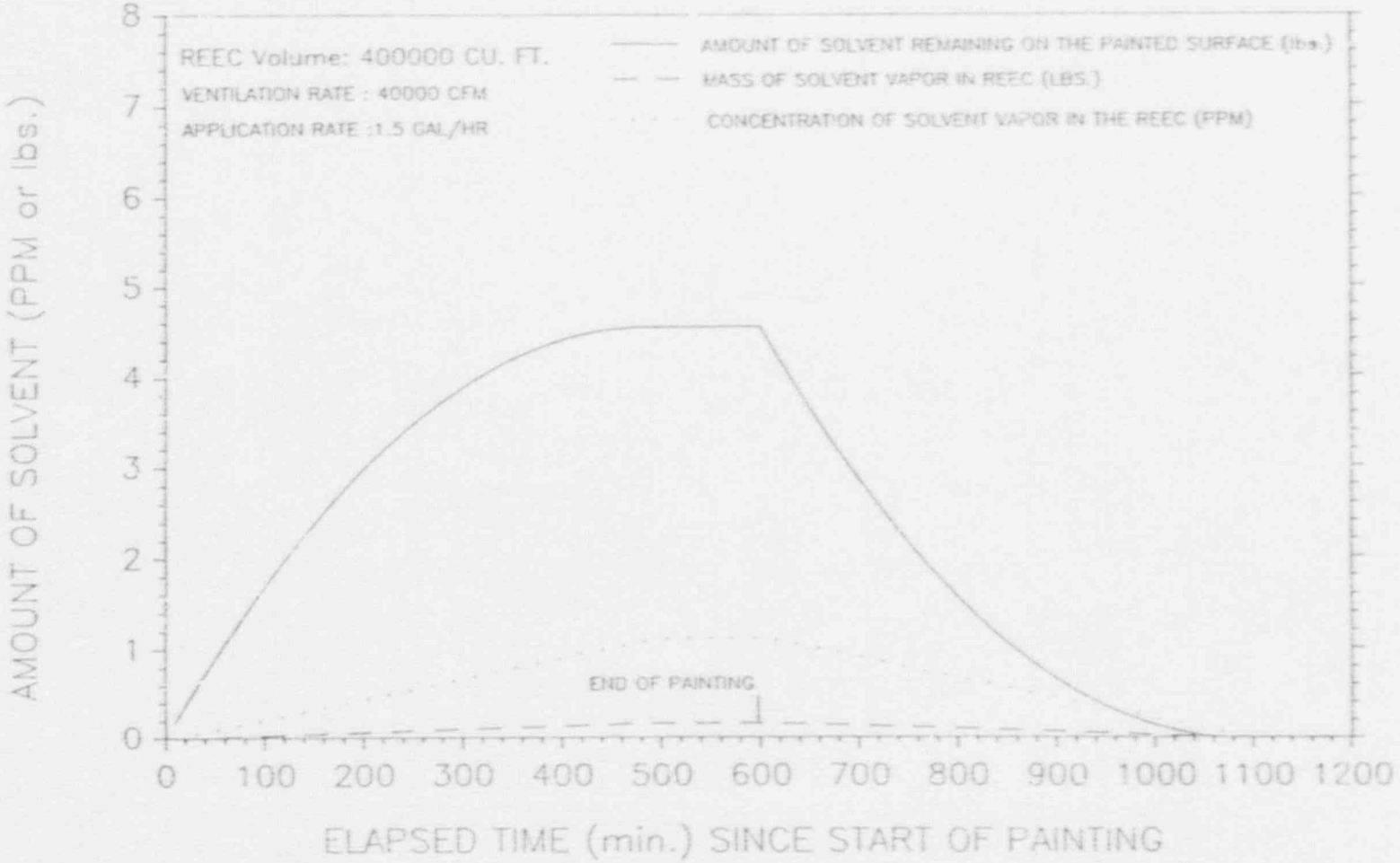

FIGURE 2

AMOUNTS OF SOLVENT IN THE REACTOR BUILDING vs. TIME
FROM PAINTING WITH STARGLAZE 2001

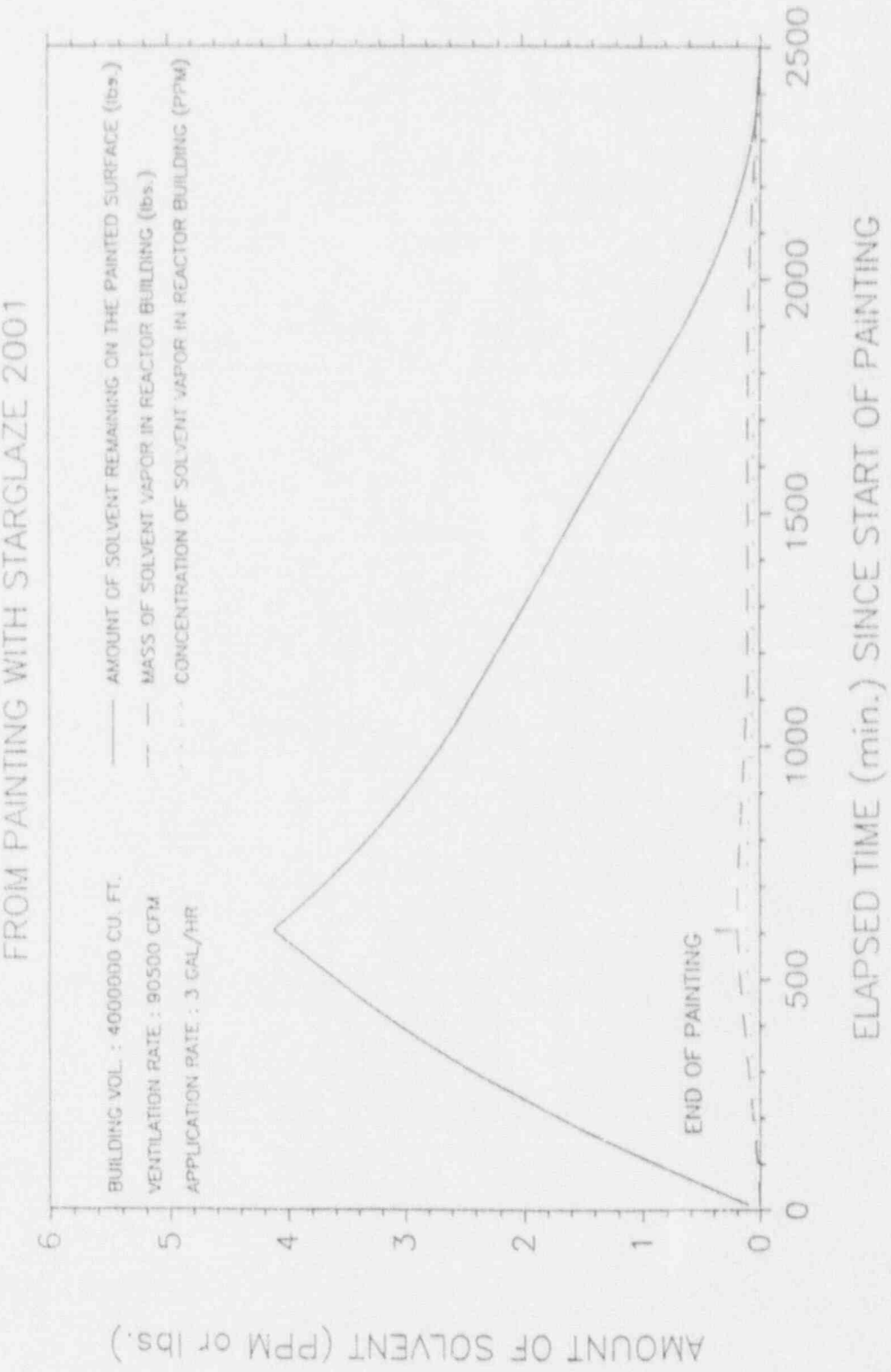

Table 1

Manufacturer: Carboline Company

Paint System: Starglaze 2001

Part A	2.1% Volatile Matter	Density: 10.8 lbs/gal.
	Glycidylether	(less than 15%)
	Mineral Spirits	(less than 5%)
Part B	0.0% Volatile Matter	Density: 8.6 lbs/gal.

Mixed in a 4:1 ration.

Mixture - 1.8% Volatile

Density Mixture - 10.4 lbs/gal.

Application Rate - 20 to 30 gal. per 10 hour day.

FIGURE 3

AMOUNTS OF SOLVENT IN THE REACTOR BUILDING vs. TIME
FROM PAINTING WITH SANITILE SG AND 550 FORTIFIER

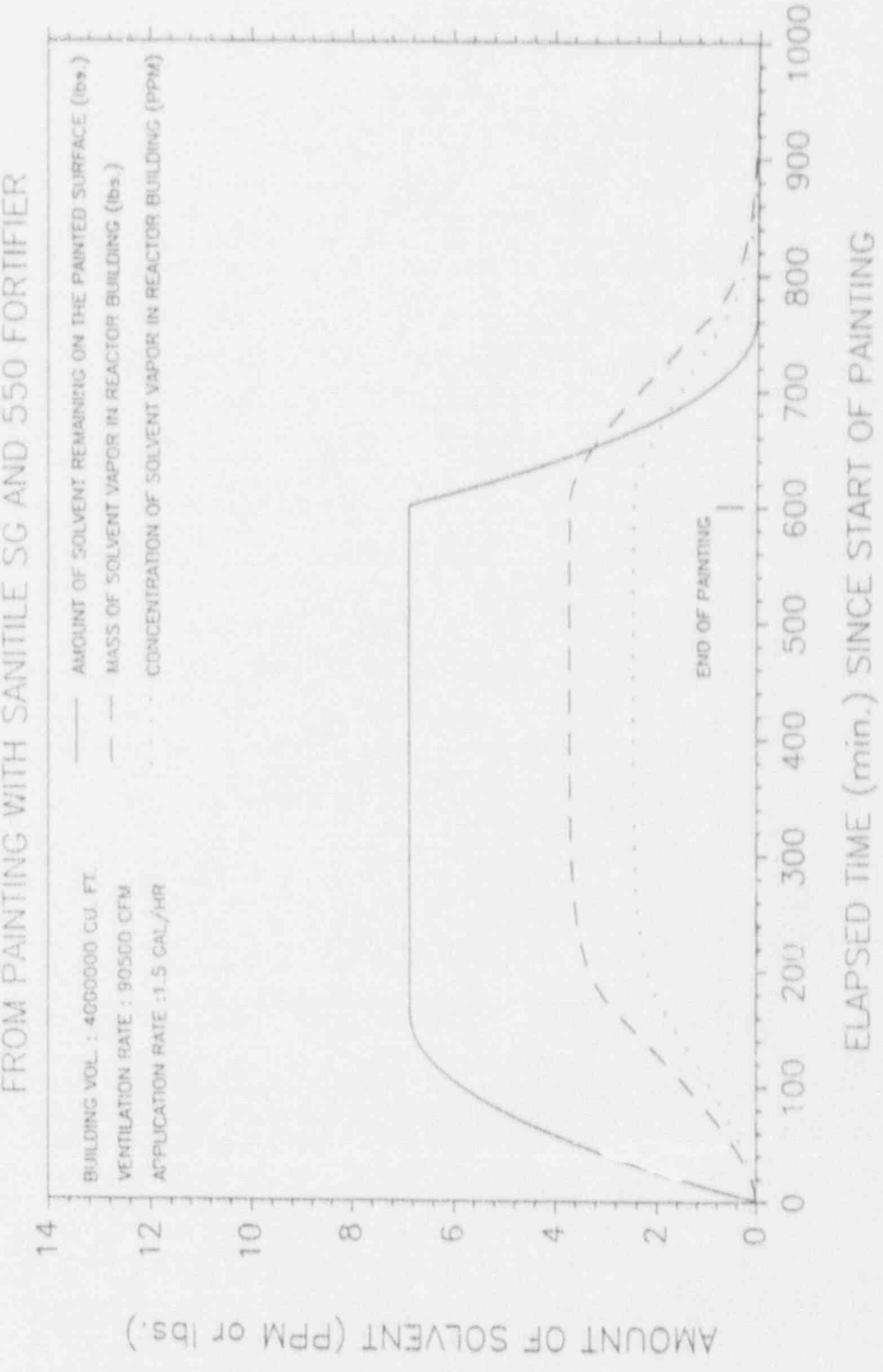

Table 2

Manufacturer: Carboline Company

Paint System: Sanitile SG
Sanitile 550 Fortifier

SG	33.8% Volatile Matter	Density: 10.8 lbs/gal.
	Mineral Spirits	(less than 35%)
550	29.8% Volatile Matter	Density: 8.5 lbs/gal.
	Mineral Spirits	(less than 25%)

Mixed in a 4:1 ratio, SG to 550.

Mixture: 33.1% Volatile - Mineral Spirits

Density of Mixture - 10.3 lbs/gal.

Application Rate - 10 to 15 gal. per 10 hour day.

FIGURE 4

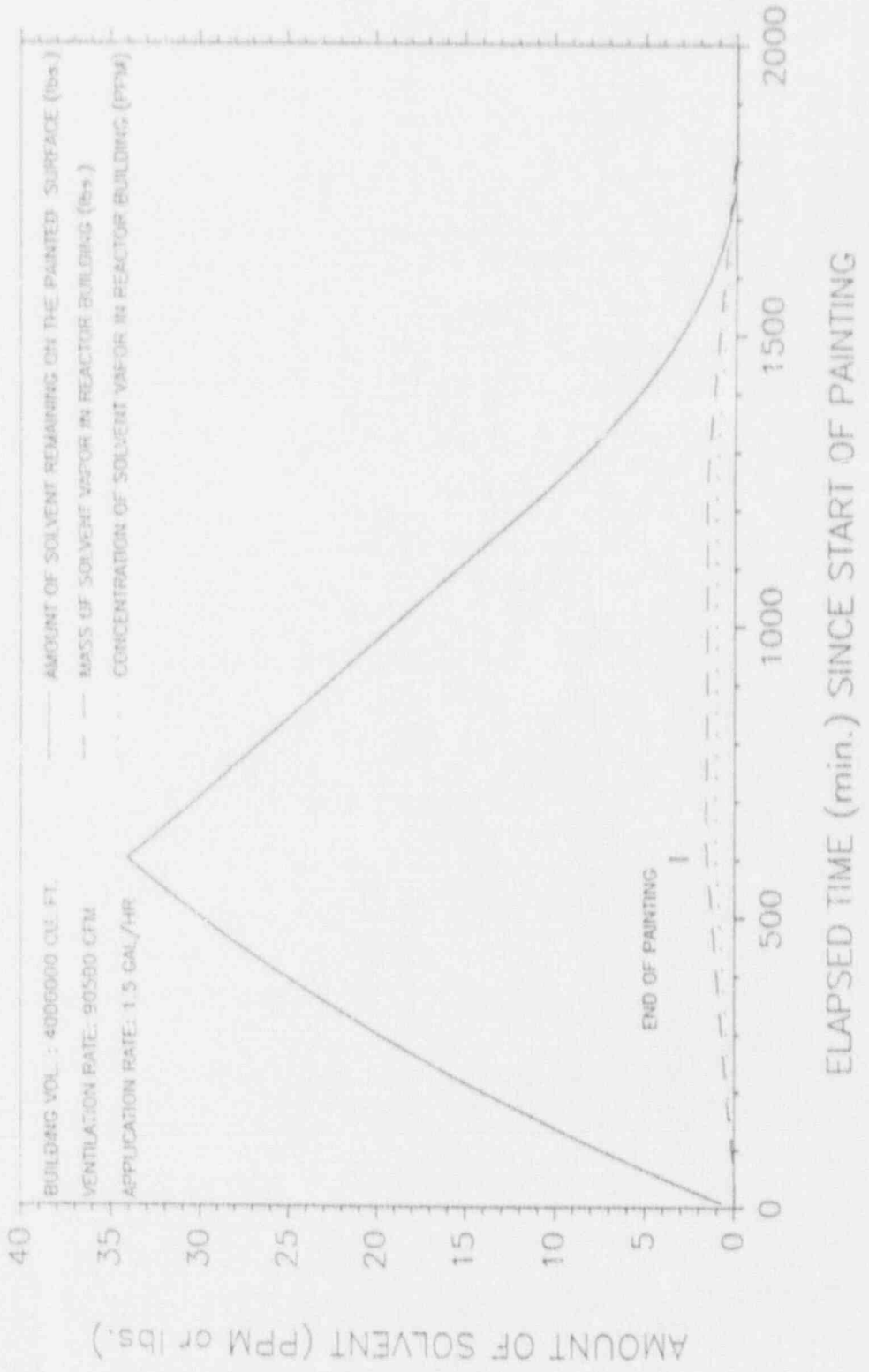
AMOUNTS OF SOLVENT IN THE REACTOR BUILDING vs. TIME
FROM PAINTING WITH PC BASE COAT
BUILDING VOL. : 4000000 CU. FT.
VENTILATION RATE: 90500 CFM
APPLICATION RATE: 1.5 GAL./HR
AMOUNT OF SOLVENT REMAINING ON THE PAINTED SURFACE (lbs.)
MASS OF SOLVENT VAPOR IN REACTOR BUILDING (lbs.)
CONCENTRATION OF SOLVENT VAPOR IN REACTOR BUILDING (PPM)
END OF PAINTING
AMOUNT OF SOLVENT (PPM or lbs.)
ELAPSED TIME (min.) SINCE START OF PAINTING
0
5
10
15
20
25
30
35
40
0
500
1000
1500
2000

FIGURE 5

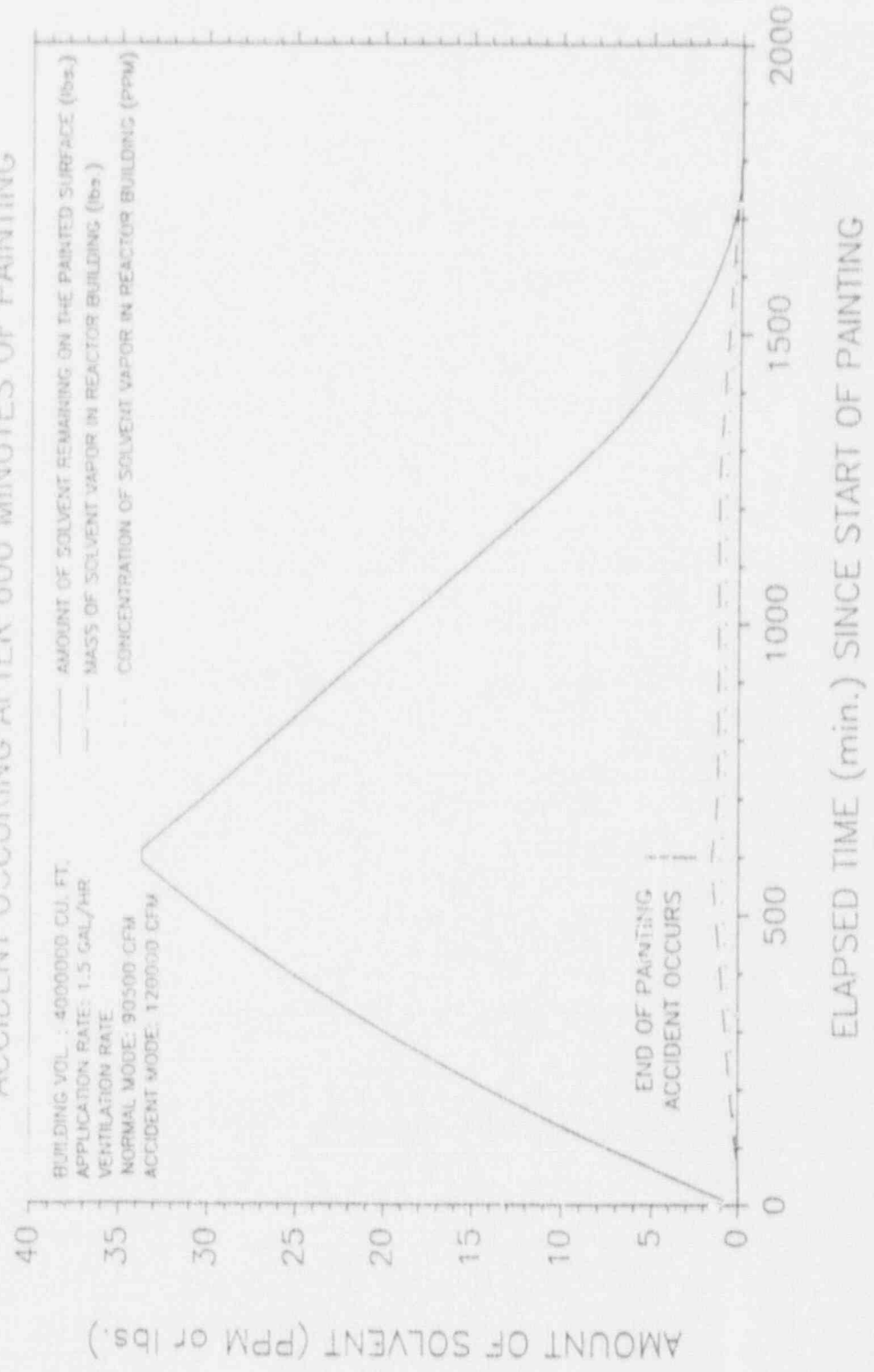
AMOUNTS OF SOLVENT IN THE REACTOR BUILDING vs. TIME
FROM PAINTING WITH PC BASE COAT
ACCIDENT OCCURING AFTER 600 MINUTES OF PAINTING
BUILDING VOL. : 4000000 CU. FT.
APPLICATION RATE: 1.5 GAL/HR
VENTILATION RATE
NORMAL MODE: 90500 CFM
ACCIDENT MODE: 126000 CFM
AMOUNT OF SOLVENT REMAINING ON THE PAINTED SURFACE (lbs.)
MASS OF SOLVENT VAPOR IN REACTOR BUILDING (lbs.)
CONCENTRATION OF SOLVENT VAPOR IN REACTOR BUILDING (PPM)
END OF PAINTING
ACCIDENT OCCURS
AMOUNT OF SOLVENT (PPM or lbs.)
0
5
10
15
20
25
30
35
40
0
500
1000
1500
2000
ELAPSED TIME (min.) SINCE START OF PAINTING

Table 3

Manufacturer: Carboline Company

Paint System: PC Base Coat

28.5% Volatile Matter Density: 12.0 lbs/gal.

Major Component: Mineral Spirits

Minor Components: Xylene (less than 1%)
EBA Solvent (less than 5%)

Application Rate - 10 to 15 gal. per 10 hour day.

FIGURE 6

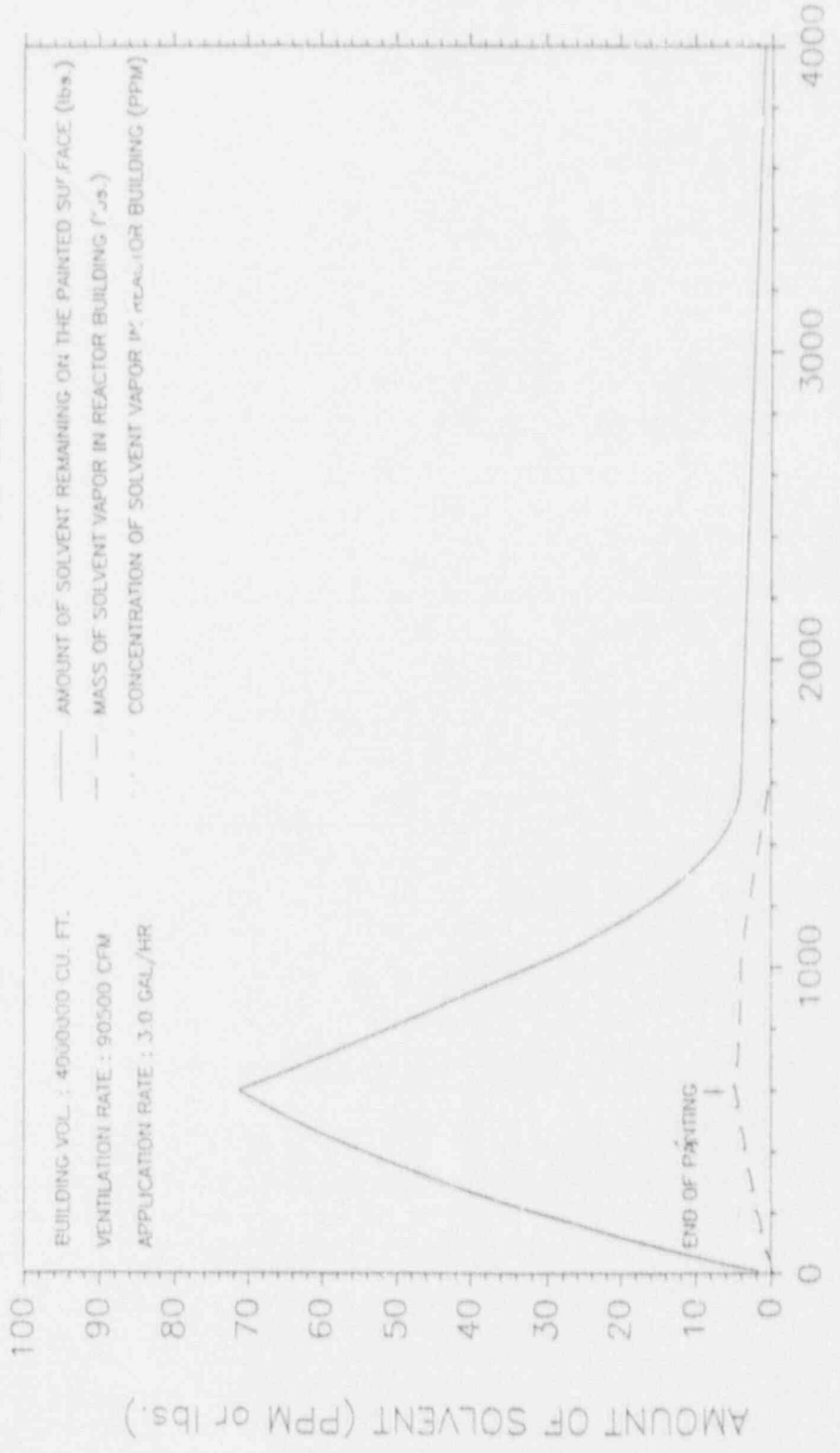
AMOUNTS OF SOLVENT IN THE REACTOR BUILDING vs. TIME
FROM PAINTING WITH STARGLAZE 2011
BUILDING VOL. : 4000000 CU. FT.
VENTILATION RATE : 90500 CFM
APPLICATION RATE : 3.0 GAL/HR
AMOUNT OF SOLVENT REMAINING ON THE PAINTED SURFACE (lbs.)
MASS OF SOLVENT VAPOR IN REACTOR BUILDING (lbs.)
CONCENTRATION OF SOLVENT VAPOR IN REACTOR BUILDING (PPM)
END OF PAINTING
AMOUNT OF SOLVENT (PPM or lbs.)
ELAPSED TIME (min.) SINCE START OF PAINTING
0
10
20
30
40
50
60
70
80
90
100
0
1000
2000
3000
4000

FIGURE 7

AMOUNTS OF SOLVENT IN THE REACTOR BUILDING vs. TIME
FROM PAINTING WITH STARGLAZE 2011–ACCIDENT OCCURING AFTER 10 HOURS OF PAINTING

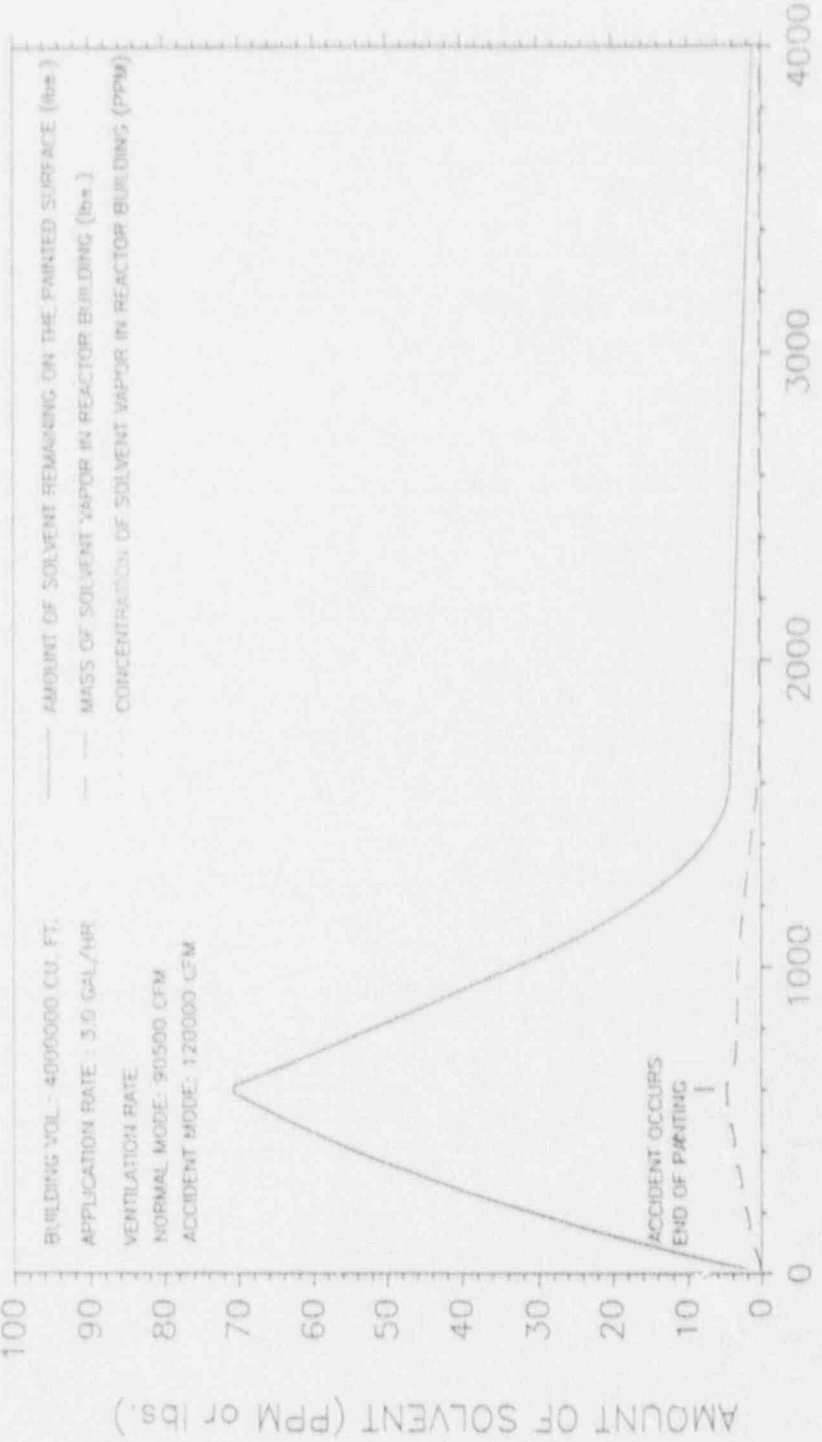

Table 1

Manufacturer: Carboline Company

Paint System: Starglaze 2011s

Part A 32.9% Volatile Matter Density: 9.7 lbs/gal.

2-Ethoxyethanol (less than 10%)

Part B 69.2% Volatile Matter Density: 7.9 lbs/gal.

2-Ethoxyethanol (less than 40%)
2-Butoxyethanol (less than 10%)
1-Nitropropane (less than 10%) Isopropanol
(less than 10%)

Mixed in a 4:1 ration.

Mixture - 40.0% Volatile

2-Ethoxyethanol	33%
2-Butoxyethanol	2%
1-Nitropropane	2%
Isopropanol	3%

Density Mixture - 9.3 lbs/gal.

Application Rate - 20 to 30 gal. per 10 hour day.

Figure 8

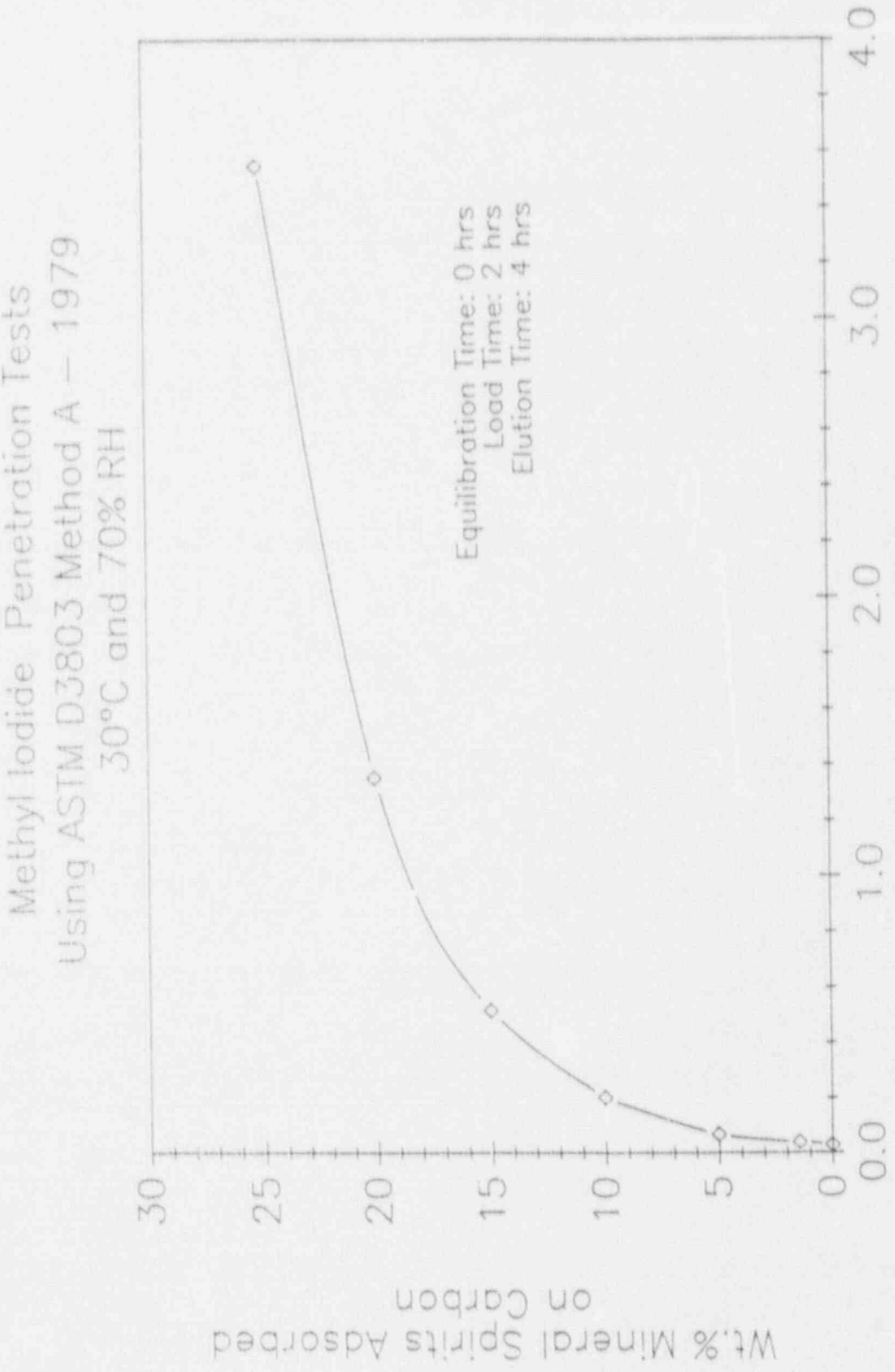
Methyl Iodide Penetration Tests
Using ASTM D3803 Method A – 1979
30°C and 70% RH
Equilibration Time: 0 hrs
Load Time: 2 hrs
Elution Time: 4 hrs
Wt.% Mineral Spirits Adsorbed on Carbon
% Methyl Iodide Penetration at 2 inch Bed Depth.
0
5
10
15
20
25
30
0.0
1.0
2.0
3.0
4.0

Figure 9

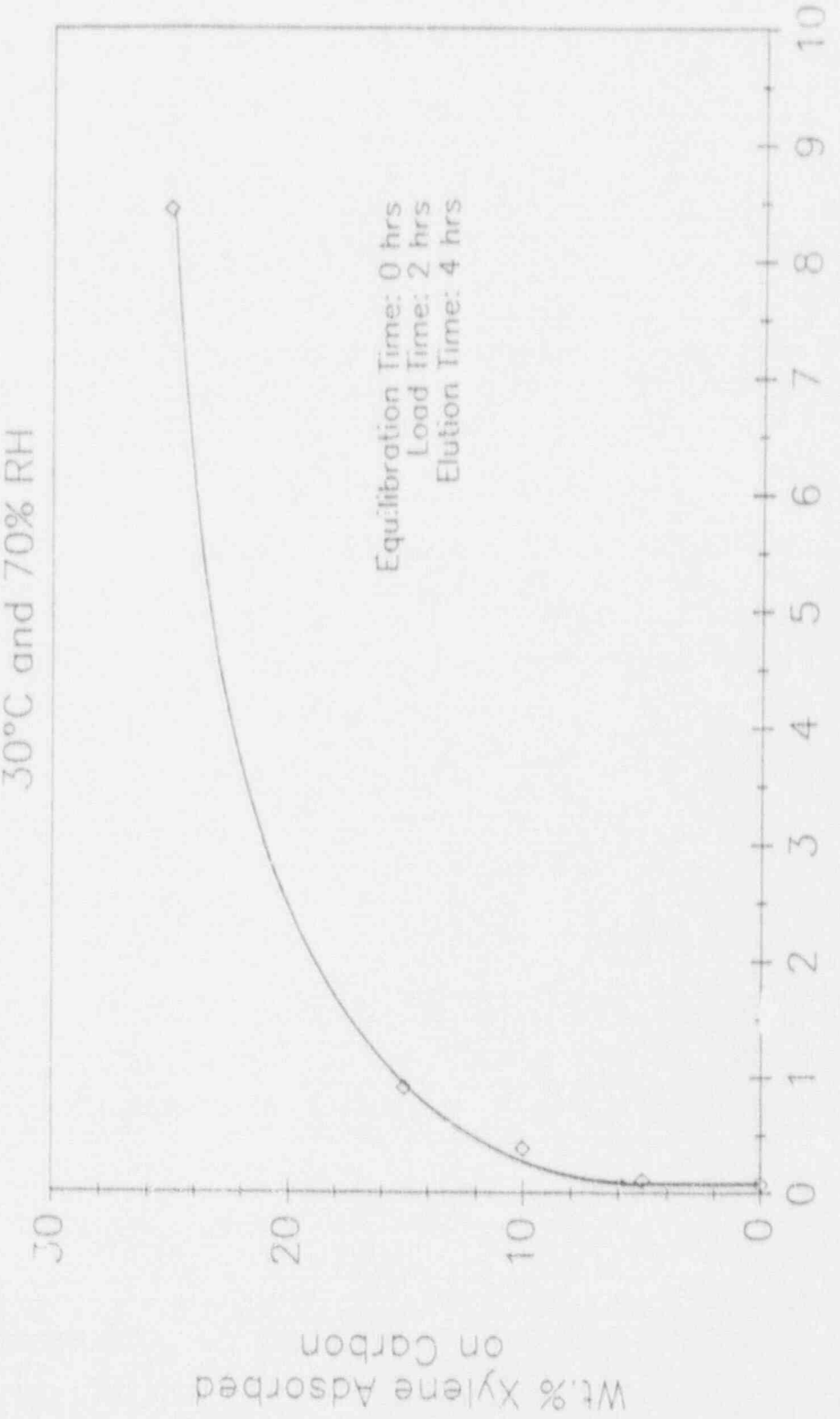
Methyl Iodide Penetration Tests
Using ASTM D3803 Method A – 1986
30°C and 70% RH
Equilibration Time: 0 hrs
Load Time: 2 hrs
Elution Time: 4 hrs
Wt.% Xylene Adsorbed on Carbon
30
20
10
0
0 1 2 3 4 5 6 7 8 9 10
% Methyl Iodide Penetration at 2 inch Bed Depth

Figure 10

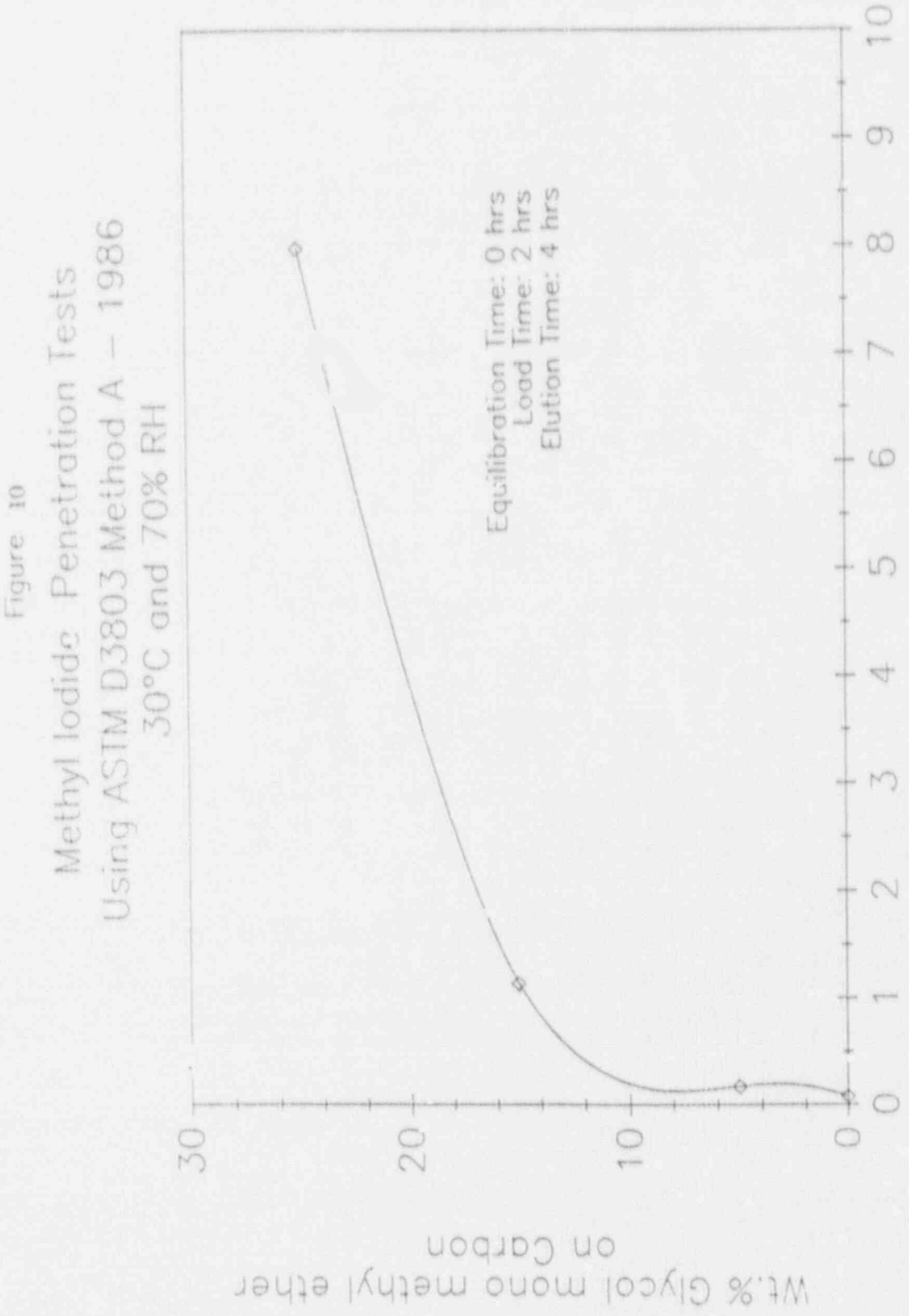
Methyl Iodide Penetration Tests
Using ASTM D3803 Method A – 1986
30°C and 70% RH
Equilibration Time: 0 hrs
Load Time: 2 hrs
Elution Time: 4 hrs
% Methyl Iodide Penetration
at 2 inch Bed Depth
0
1
2
3
4
5
6
7
8
9
10
Wt.% Glycol mono methyl ether
on Carbon
30
20
10
0

DISCUSSION

HAYES: How would your curves of weight percent of loading vs. penetration be effected if you were at 95% relative humidity and if you went to a preequilibration period of 16 hrs?

FREEMAN: I think they would show a little higher penetration based on the fact that they show higher penetration for those conditions without any solvent. The lowest boiling point solvent, glycol ether, was about 124°C. We found that the solvents stay on the charcoal, although we recently obtained some unpublished results that show that solvents like toluene can be removed during preequilibration at 95% RH. So with lower boiling point solvents, the 95% RH equilibration can remove some of the solvent from the carbon and thus the effect of the solvent is diminished.

McVEAN: Does charcoal retain solvent over long periods of time, or does it release it after months?

FREEMAN: This is something we would like to study further but it appears to be dependent upon the affinity of the solvent for carbon and the adsorption process. Some will be removed over a period of time. The lower the boiling point of the solvent, the faster it will be removed. We might try to use a moisture injection system to push solvent off of carbon after we have done a painting operation, but I don't think anybody is ready to put 95% humidity on the charcoal if they don't have to.

ANNON: The only way you can remove some of these solvents from charcoal is to steam clean them. Some are there to stay once they are on the charcoal.

GUEST: Do you have any plans to continue the work using aged or weathered carbons? It is a rare occasion when somebody has brand new carbon in the plant?

FREEMAN: Yes, we do. In fact, this is an example of the work we do in the laboratory on a continuous basis to try to solve our clients' problems regarding radio iodine removal. The next step is to look at a combination of oxidation and solvents which seems to be the worst condition.

KOVACH: The test conditions used here were not the most conservative but those in the Technical Specifications of the Utility Tests at 95% R.H. and 30°C will result in less liberal results, particularly with preequilibration. The effects of each specific paint system have to be known and their solvent effect on CH_3I removal determined under actual use conditions.

HYDER: I agree with these general comments. We have looked at organic contamination of carbon by paint and solvent vapors. Xylene and higher-boiling compounds are retained a long time; more volatile substances apparently are lost from the carbon after sometime in service.

FREEMAN: Yes, I agree. The solvents we looked at (xylene, glycol ether and mineral spirits) all have boiling points greater than 124°C and are strongly retained by the carbon.

DENARD: What are the effects of evaporation at no flow during off situations? We have ESSF systems which do not run and the only exposure will be from evaporation.

FREEMAN: The evaporated solvents should be removed by the normal ventilation system. As long as the isolation dampers for the ESF system are in good repair, little or no solvent should reach the ESF carbon.

FACTORS AFFECTING THE RETENTION OF METHYL IODIDE BY IODIDE-IMPREGNATED CARBON

M. L. Hyder and K. A. Malstrom
Westinghouse Savannah River Company
Savannah River Laboratory
Aiken, South Carolina 29808

Abstract

Iodide-impregnated activated carbon that had been in use for up to 30 months was studied to characterize those factors that affect its interaction with and retention of methyl iodide. Humidity and competing organic sorbents were observed to decrease the residence time of the methyl iodide on the carbon bed. Additionally, changes in the effective surface area and the loss of iodide from the surface are both important in determining the effectiveness of the carbon for retaining radioactive iodine from methyl iodide. A simple model incorporating both factors gave a fairly good fit to the experimental data.

Introduction

This paper comprises two sets of studies of methyl iodide retention by iodide-impregnated carbon. In the first of these, the retention of the methyl iodide on the carbon surface and its subsequent evolution were observed directly by a technique of combustion and phosphorescence. In the second, the methyl iodide retention in a standard test was compared with surface area measurements and the concentration of unreacted iodine. A correlation among these parameters was identified and characterized. Carbon quality was varied through the selection of used material with differing service histories.

Air from the Savannah River Site reactor buildings is vented through carbon beds for control of radioiodine before release to the atmosphere. The carbon used is North American Carbon Co. type GX-176 coconut shell carbon impregnated with one percent triethylenediamine (TEDA) and two percent potassium iodide by weight. Replacement intervals for the carbon have been as long as thirty months. Analysis of samples withdrawn at much shorter times has shown that the TEDA is lost after a few months, and the performance of the carbon for methyl iodide retention is dependent on the iodide impregnant. Efficient methyl iodide retention is not a requirement for carbon in this service; however, methyl iodide retention as measured by the ASTM Test D3803 (method B) has been found to correlate well with other desirable properties of the carbon such as radiation stability. The studies undertaken here were intended to shed light on the changes taking place in this carbon during long-term service and to provide a basis for simpler measurements of carbon quality.

Experiments

Carbon of known and widely varied service history was obtained from routine sampling operations at the Savannah River reactors. Portions were analyzed for methyl iodide penetration by Nuclear Containment Systems of Columbus, Ohio. A modification of ASTM Method D3803 (B) was used, in which two 25-mm (one-inch) thick carbon beds were mounted in series and individually analyzed instead of the specified 51-mm (two-inch) bed. Penetration values cited are for the 25-mm beds.

Iodide on the carbon was measured by a water leach method in which a five-gram sample of carbon was stirred for ten minutes at ambient temperature in 50 mL of a slightly alkaline aqueous solution. The ingrowth of iodide was measured by an iodide-selective electrode. The leach solution consisted of equimolar (0.05 M) sodium carbonate and sodium bicarbonate with 0.001 M sodium iodide added to provide a baseline for the electrode. The electrode response versus concentration was determined in a set of dilution experiments. Control experiments showed that most iodide was dissolved in the ten-minute leach.

The surface area of carbon samples was determined using a Micromeritics Digisorb 2600 surface area analyzer. The samples were approximately 0.2 g and were heated to 110 degrees Celsius for three hours before analysis at a pressure of 0.050 torr or less. Nitrogen was used as the adsorbate.

Methyl iodide sorption on carbon was observed using the apparatus shown in Figure 1. An aspirator was used to pull air at a steady rate through a train consisting of a sample bulb, a pyrolysis cell, a fluorescence cell, and finally a bed of ion exchange resin for iodine retention. For each experiment, a small quantity of methyl iodide (typically 50 microliters) was placed in the five-liter bulb and allowed to evaporate. After a mixing period of ten minutes or more, flow through the test train was initiated with no carbon in the carbon bed. Once a base line was established, the carbon bed was loaded with carbon (normally two grams or about 4 mL) and flow resumed. (The carbon bed height was about 1.5 cm.) The gas flow rate was measured by a water displacement flow meter. A typical flow rate was about eight mL per second.

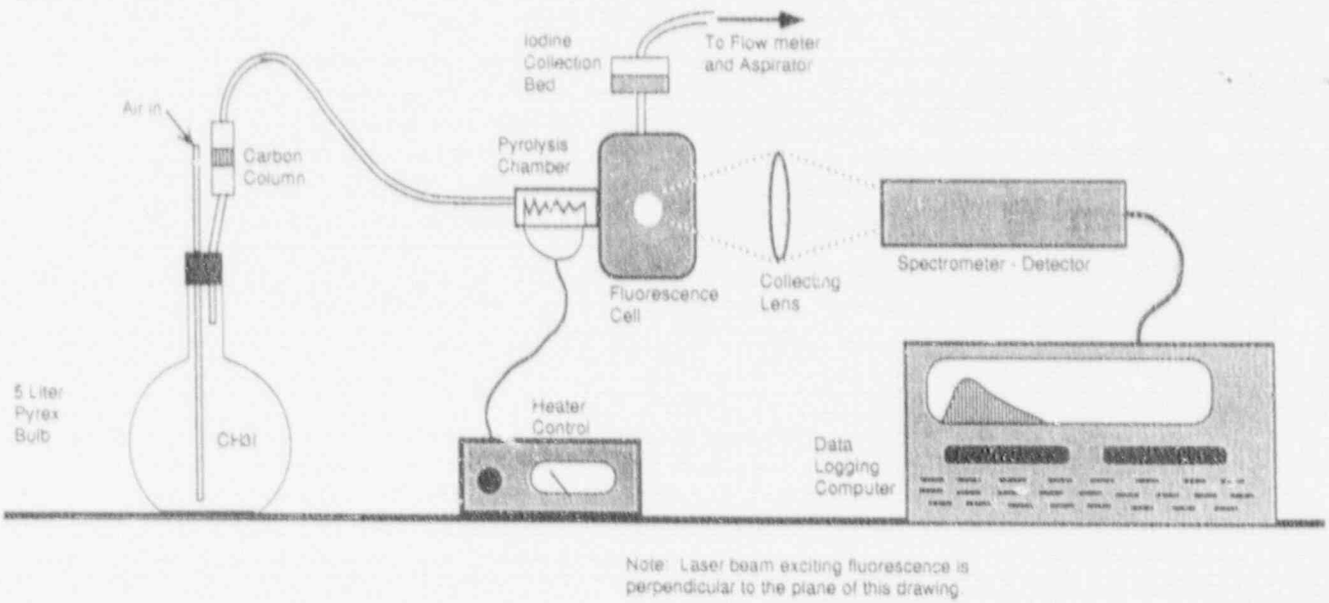

Figure 1. Schematic drawing of laser fluorescence apparatus for methyl iodide detection.

Methyl iodide passing through the carbon was detected and measured by laser-induced phosphorescence of elemental iodine. The effluent from the carbon bed was passed through a small cell containing a heater that decomposed the methyl iodide into methyl and iodide radicals. The methyl radicals were combusted forcing the iodide radicals to recombine into iodine molecules. The gas stream then passed into a long rectangular cell with optically flat windows at either end (Figure 2). This cell was illuminated along its length by a five-watt argon-ion laser (Spectra-Physics Model 2020). To ensure a constant light output, the laser was operated under light control mode at 1 watt and 514.5nm. This caused the iodine in the air stream to be excited to the $B^3{}_{p2m}$ electronic state. Emission from that state back to the ground state was collected by a f/1.7 lens. The emission was filtered by a 550-nm-long wave pass filter and focused into an f/3.5 Instruments SA 1/3 meter monochromator. An EG&G/Princeton Applied Research 1420 diode-array was used to detect the emission. The detection point along the axis of the laser beam was chosen to maximize the signal. Elemental iodine was found to be incompletely formed at the point at which the gas stream entered the detection cell, so a point several inches from the entry point was chosen for detection. Spectral data from the detector were regularly logged to a computer in which background correction and peak summing over the spectral range of interest could be performed automatically and recorded for subsequent study.

During the course of the experiment, it became evident that the humidity in the building air was affecting the results, even though the building is air conditioned. This effect was studied using a commercial wet- and dry-bulb humidity instrument.

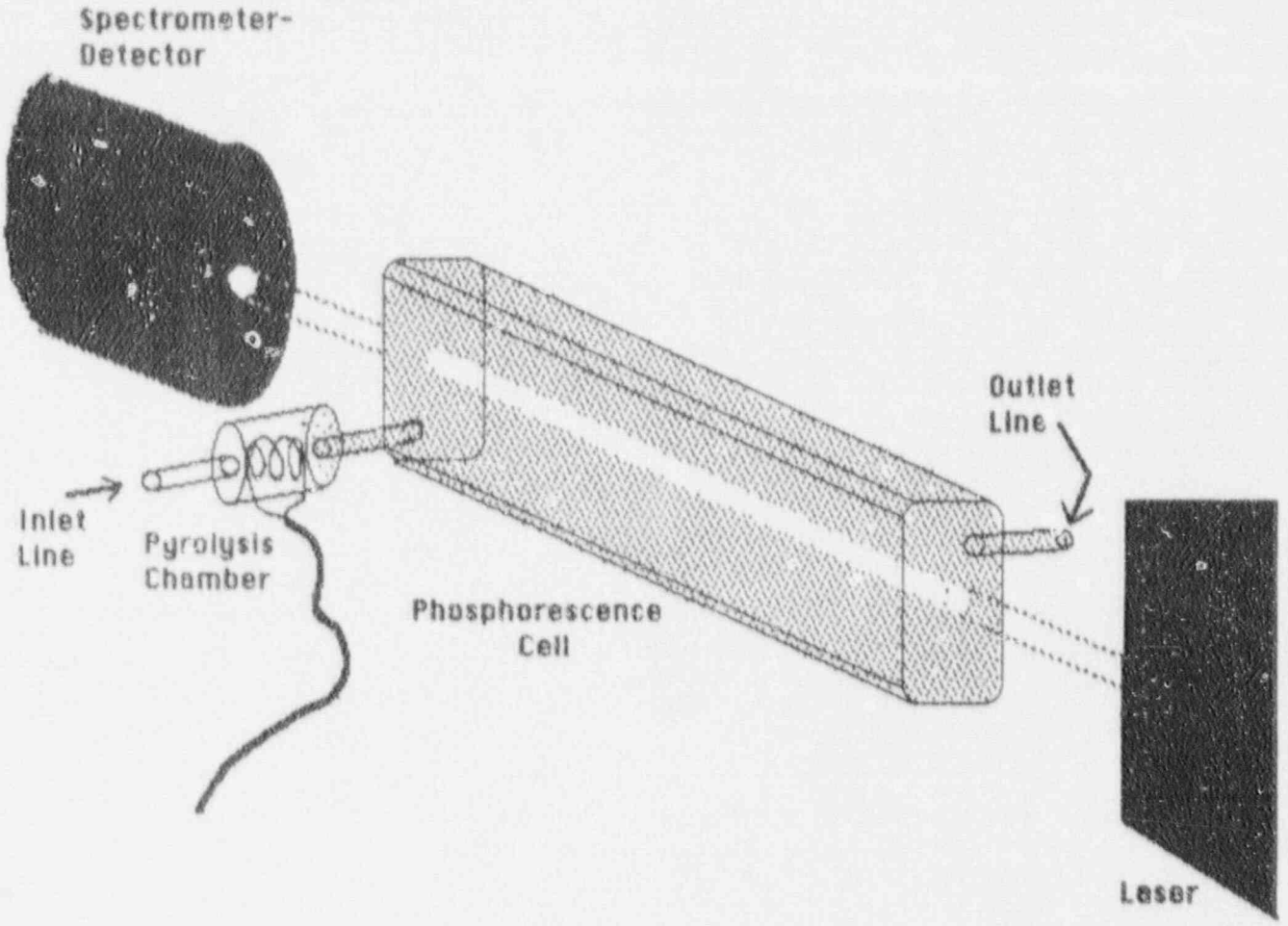

Figure 2. Phosphorescence cell, Laser, and associated apparatus.

Results and Discussion

Interaction of Methyl Iodide With Carbon

A typical curve for the passage of methyl iodide through a carbon bed is shown in Figure 3. After a brief delay lasting, at most, a few minutes, the methyl iodide is released in a broad peak with a long tail. The tailing is probably the result of the high internal porosity of the carbon, resulting in long diffusion paths in and out of the pores. This type of curve was observed only for used carbon or carbon subjected to special treatment. For untreated new carbon, which is impregnated with TEDA, the methyl iodide was quantitatively retained and none was detected in the effluent.

Comparison of various samples gave results that were difficult to correlate, and study of duplicate samples soon established that there were uncontrolled variables affecting the results. After some investigation, the humidity of the room air was found to be a major factor. This was not controlled in the original work, but it was found to vary over a wide range and to affect the results considerably. This was no surprise, once established, because humidity was known to be a factor in carbon performance. The implication of this effect is that the humidity decreases the residence time of the methyl iodide in the carbon and therefore allows less time for exchange or reaction. Standard methyl iodide retention tests are normally conducted at 95 percent relative humidity, which is much higher than the humidity encountered in any of these experiments, and so the residence time for methyl iodide is still shorter in the standard tests.

A series of experiments was then done to further evaluate the effect of humidity and organic vapors on methyl iodide retention.

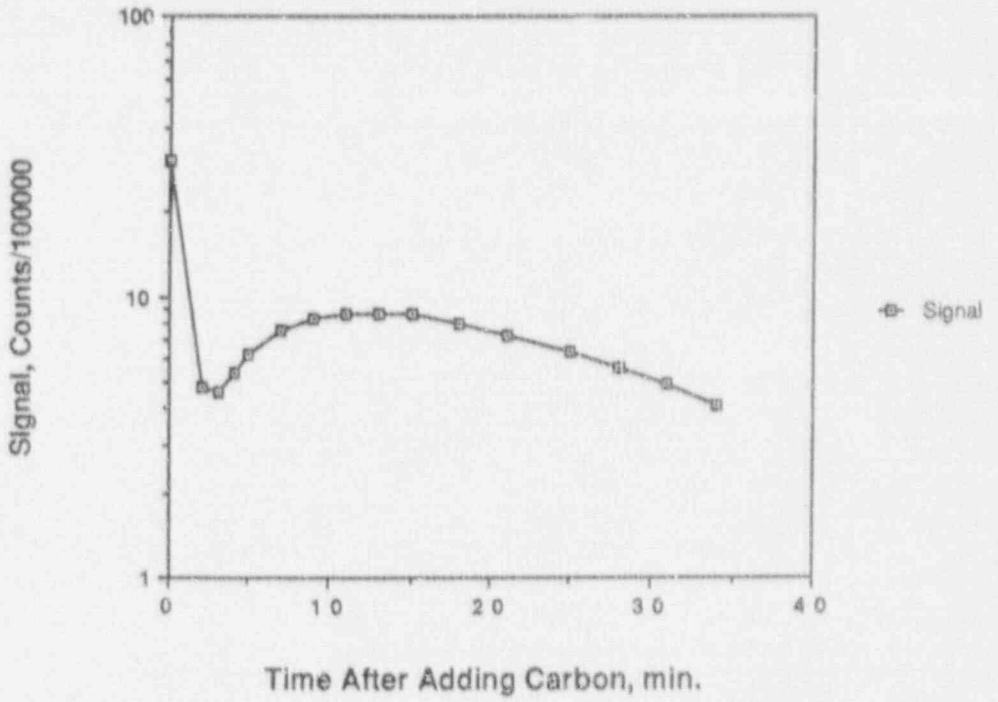

Figure 3. Typical methyl iodide curve.

In the first set of experiments, the air was not dehumidified, but carbon samples were dried before the experiment by overnight storage in a dessicator. The results clearly showed that the methyl iodide is more strongly held and is released more slowly from the dried carbon (Figure 4).

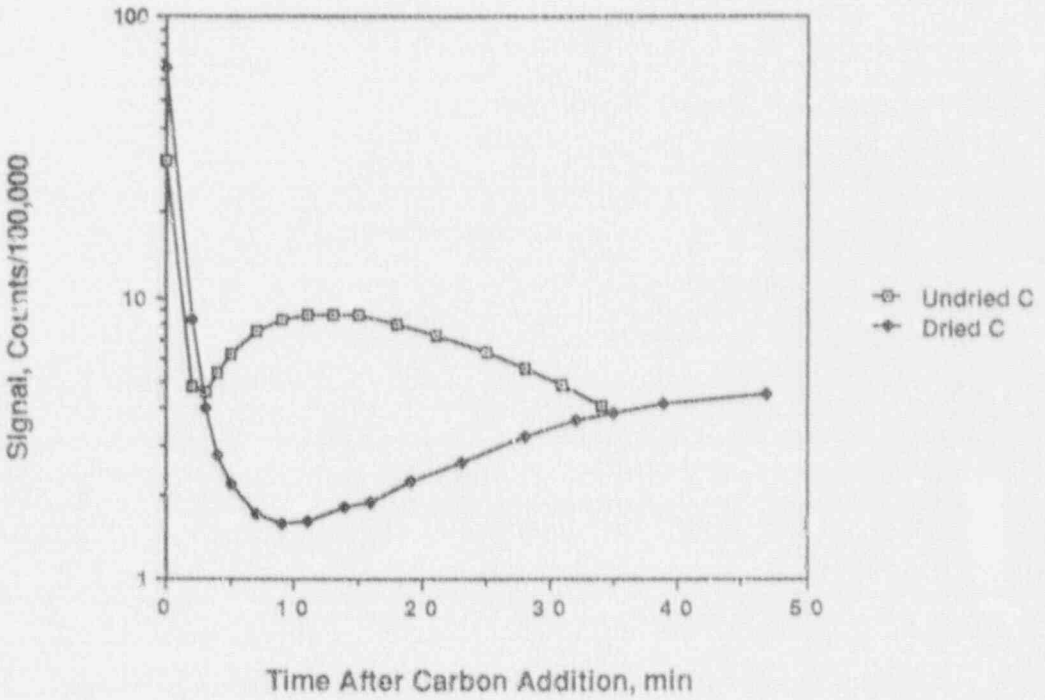

Figure 4. Dried and undried carbon compared.

In the second set of samples, a sample of relatively low service (nine months) was dried by overnight storage in a dessicator, and then a portion of this material was exposed to xylene vapor until it had taken up about 30 percent of its own weight of xylene. These two samples were then tested similarly. The results are shown in Figure 5. The results were striking. The sample loaded with xylene retained almost no methyl iodide; the other sample retained nearly all. Following this test, a sample of unused carbon was prepared with a similar xylene loading and tested. Although a substantial amount of the methyl iodide was retained, there was still a steady release that had not been observed in untreated new carbon (Figure 6).

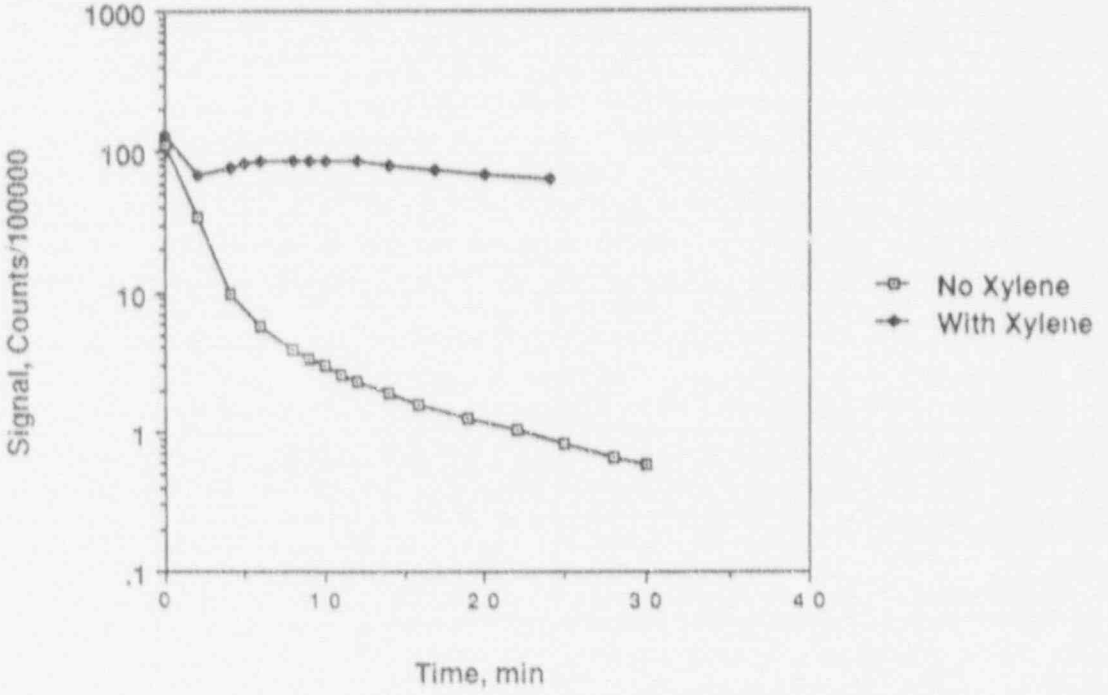

Figure 5. Effect of xylene loading on MI elution.

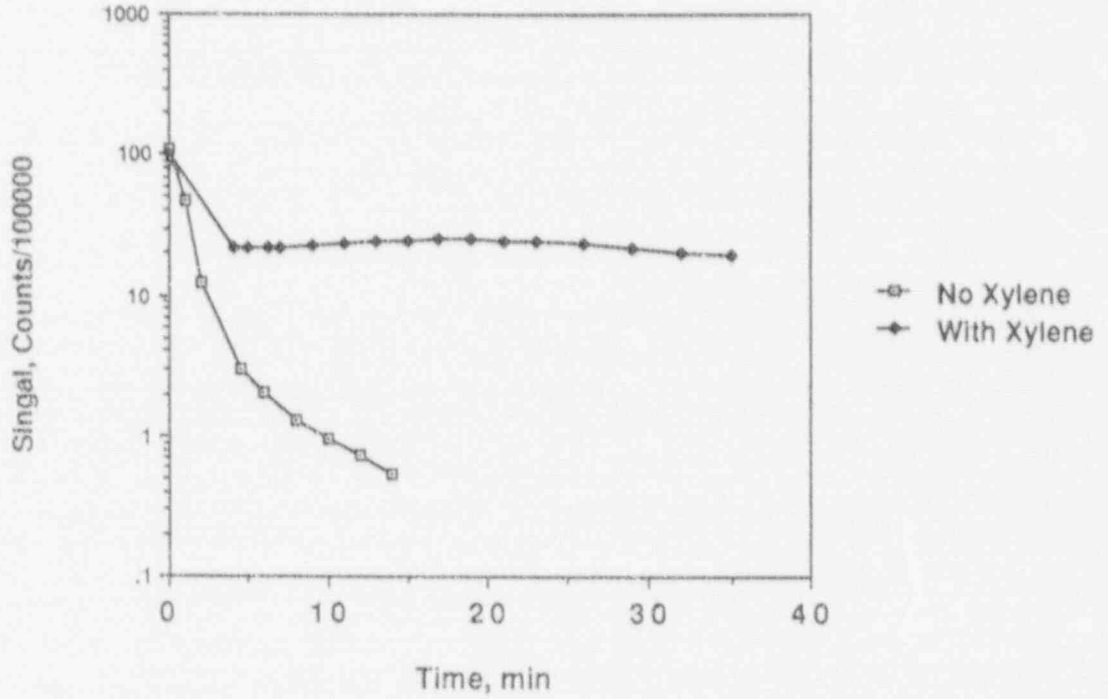

Figure 6. Effect of xylene on MI elution.

In a final set of samples, the effect of removing all humidity was observed. The results are shown in Figure 7. A carbon batch that had seen 29 months of service was tested under three different conditions: first, with no humidity control; second, with dried carbon but ordinary laboratory air; and, finally, with dried carbon and dried air. The results show the much longer residence of the methyl iodide in the carbon under dry conditions.

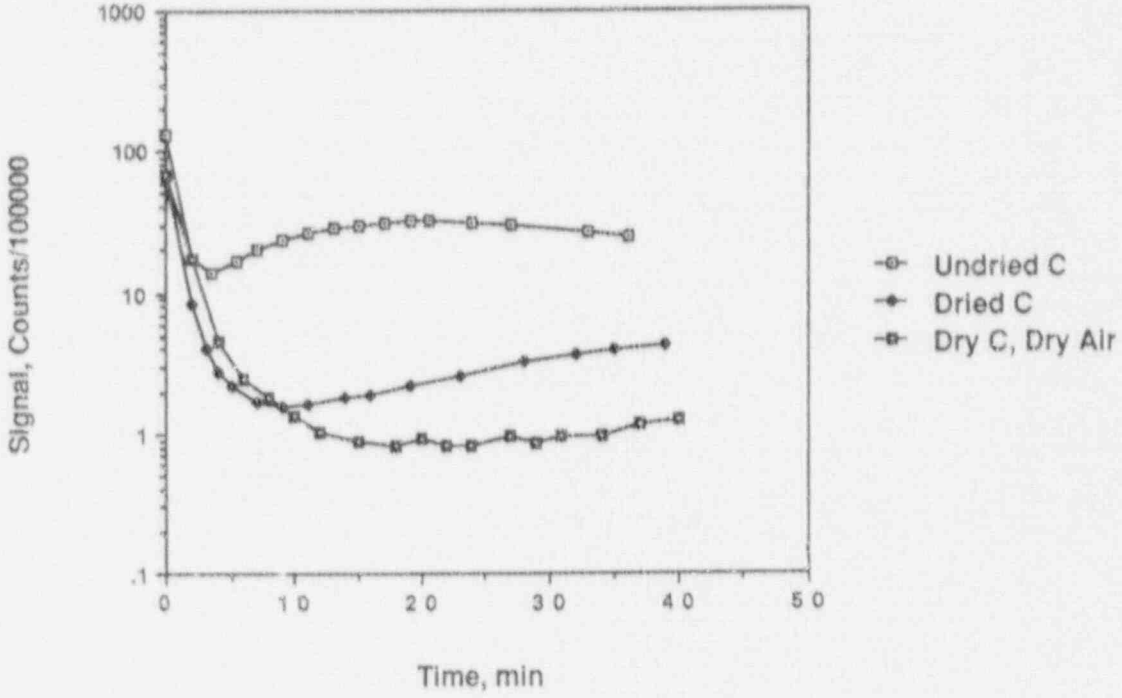

Figure 7. MI elution in dry air.

Humidity, temperature, and organic contamination have all been shown previously to affect the performance of carbon in retaining radioactive methyl iodide. Experiments of the type described here could be used to quantify these effects by establishing the residence times of the iodine in the carbon bed under the conditions of interest. Unfortunately, the equipment had to be dismantled before these experiments could be carried to that point. An improved system would include humidity and temperature control as well as equipment for injecting methyl iodide at a constant rate. With such a system, quantitative measurement of such factors as preconditioning and various organic contaminants could be made readily.

Methyl Iodide Retention as a Function of Iodide Content and Area

Retention of methyl iodide by the carbon used at the Savannah River Site (SRS) decreases steadily with time in service. This phenomenon was characterized by Evans.[1] Carbon samples with time in service ranging from 0 to 30 months were selected for this study and their methyl iodide (MI) retention was measured by the method previously described. Results are shown in Table 1. The anticipated wide variation of MI retention was observed.

The hypothesis was adopted that the variation in MI retention was the result of the chemical reaction (or perhaps the physical removal) of the iodide impregnant. The leach method was used to test for the presence of iodide. Using the iodide-selective electrode, the concentration of iodide in the solution could be measured continuously during the leaching process. A set of typical leaching curves is shown in Figure 8. As the result of a number of preliminary experiments, a leaching time of ten minutes was adopted as a standard. Using this value, we attempted to optimize several factors. The time was long enough to make any variation in the mixing of the sample and solution unimportant and also to leach most of the iodide into the solution. It was short enough to minimize effects of electrode drift and other causes of variability observed at long leach times. The results of the leach tests are shown in Table 1.

Table 1. **Leach, area, and methyl iodide retention data for the carbon samples studied.**

Sample	Area (M2/g)	Iodide Leach (ppm by weight)	AxIL	Methyl Iodide Retention	-LnI/Io
P3046	391	90	35,200	19	0.163
P5116	836	270	225,700	72	1.27
15732	849	110	93,390	51	0.713
K4047	380	190	72,200	32	0.386
(New)	1176	665	750,800	96	3.0
K6057	758	134	101,500	44	0.58
K2016	312	341	106,200	36	0.446
L3126	774	286	221,200	62	0.968
P2126	736	265	194,900	70	1.20
L3095	865	203	175,500	73	1.31
1850	292	115	33,600	12	0.127

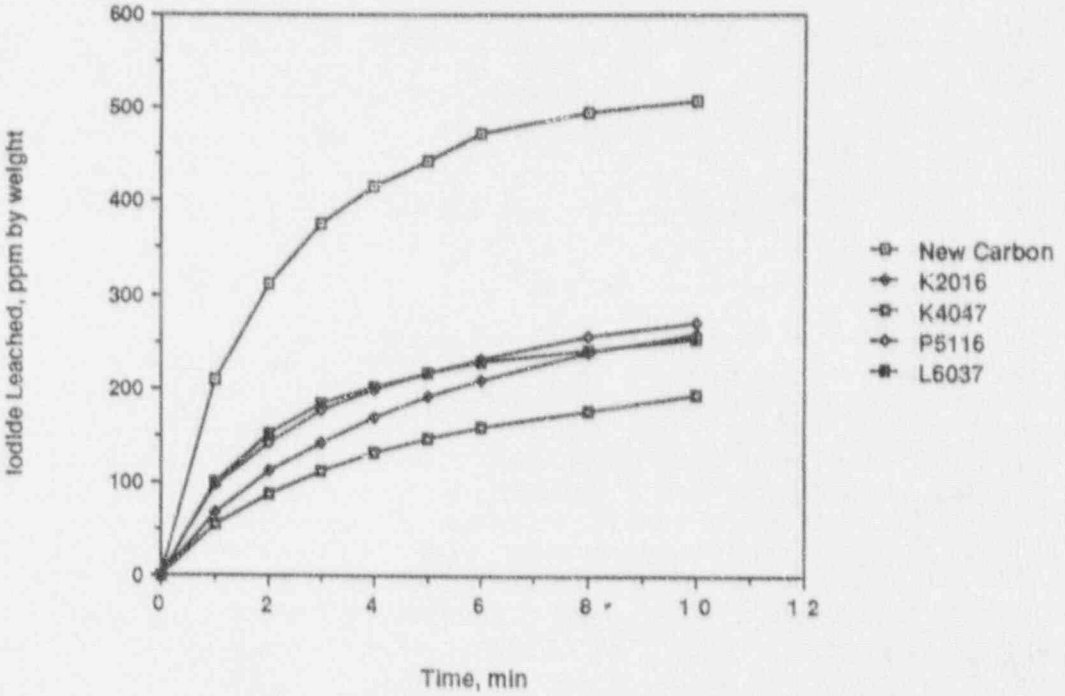

Figure 8. Representative iodide leach curves.

A plot of the leach data against the methyl iodide retention data showed a rough correlation (Figure 9). However, there was considerable scatter, and this was not resolved by repeating MI retention or iodide leaching measurements for the outliers.

Simultaneously with the leaching studies, surface area measurements of the carbon were undertaken. The carbon had a relatively high surface area of about 1000 square meters per gram as received. Most of this surface was in internal pores. Microscopy showed a highly convoluted fibrous structure derived from the original fibrous structure of the coconut shell. Scouting measurements with gas sorption for measuring surface area showed that the effective surface area of the carbon decreased by a factor of as much as three during service, even in samples outgassed at high temperature (350°C). Evidently, some part of the internal surface was blocked off by non-volatile substances entering the carbon structure during service.

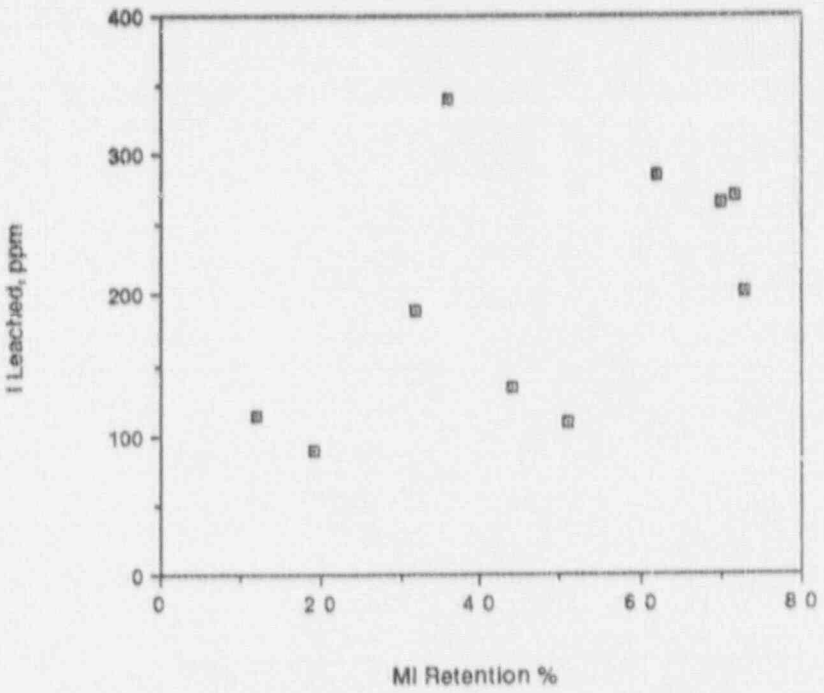

Figure 9. Iodide leached versus MI retention.

Carbon samples give a Type I adsorption isotherm because they are microporous. The absolute values of surface area analyses made using Type I isotherms has been questioned because the micropores are filled at the same time as the surface is covered with the adsorbate gas. In this work the absolute value of the surface area is not so important as consistency because the numbers were used only for relative comparisons.

As a result of the preliminary studies, a series of surface area measurements was undertaken. These showed significant changes in surface area among samples that had been in service, although the amount varied significantly between samples. The surface area data given in Table 1 correlate with the methyl iodide retention shown in Figure 10. This correlation is somewhat better. The data points shown are the average of two or more measurements. The carbon samples used in these measurements were so small that significant variation was found among individual samples.

At this point, a mathematical model of methyl iodide retention was developed and applied to the data. As a result of the studies described in the first part of this paper, it was learned that methyl iodide passes fairly quickly through the carbon compared to the time required for the methyl iodide analysis. It was also learned that retention of the radioactive isotope is the result of an exchange process. As Dietz(2) has confirmed, this follows the expected first order relationship with thickness, thus:

$$\mathrm{Ln}\,(I/I_0) = -Cx \qquad (1)$$

where I_0 is the amount of radioiodine entering the bed and I is the amount reaching the depth (x). If it is then assumed that there are two factors affecting the removal constant (C) and they are the surface area (A) of the carbon and the density (D) of active sites on the surface, then it is reasonable to write:

$$C = K\,A\,D \quad . \qquad (2)$$

A is directly measurable, but it is not obvious that all the surface area is equally important. The residence time of gas in the carbon bed is less than 0.2 seconds; consequently, diffusion into much of the interior through very small holes is too slow to be important. Using A directly in this equation infers that the area of the accessible surface is diminished during use in proportion to the change in the total surface measured by gas sorption. This must be considered a plausible assumption, especially in the light of the results.

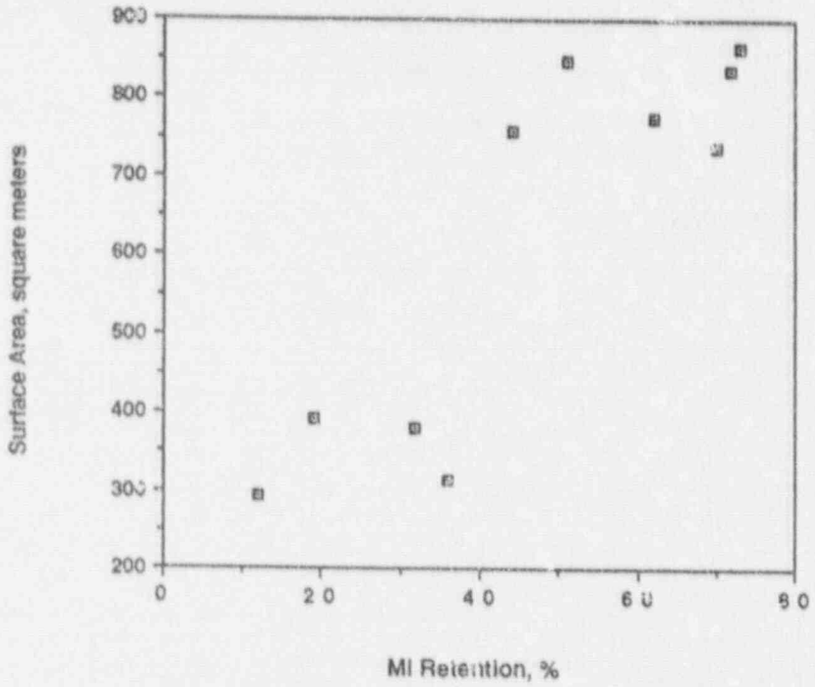

Figure 10. Surface area versus MI retention.

D (the density of active sites) is not directly measurable and can, in principal, also differ between inside and outside surfaces. It is presumably a function of, not only the amount of active iodide impregnant remaining on the surface, but also of the presence of other substances such as water and organic molecules sorbed on the carbon. In the methyl iodide retention test, humidity and temperature are carefully controlled, so it is possible to compare samples on a consistent basis.

D should be proportional to the amount of iodide on the carbon surface, and it should, in principle, be possible to measure this chemically. Oxidized iodine, or iodine chemically bound to the surface, is not expected to be effective in retaining radioiodine. The water leach is an attempt at such a measurement. The water leach test does not recover all the iodine. Even with new carbon, only about half the iodide originally added is recovered as iodide. Presumably, the remainder is inaccessible to the water because of surface tension in the small pores. Activation analysis shows that essentially all the iodide added is present in some form in all samples studied. However, the water-leach test should recover the most accessible iodide.

From the preceding, at constant bed thickness, humidity, and temperature, it might be expected that:

$$\mathrm{Ln}\,(I/I_0) = -k\,A\,D \qquad (3)$$

As Figure 11 shows, this is not a bad approximation to what is actually found. The data for new carbon were not included in the plot because it also has TEDA impregnant on it.

The results of this study suggest that the simpler methods of water leaching and surface area measurement might be used in place of methyl iodide retention to evaluate carbons of this type. However, the following limitations of these methods should be kept in mind.

- The effect of TEDA, where present, is not measured.
- Large quantities of extraneous materials such as organic vapors can cause the leach test to be an inadequate measure of quality.
- The effect has not yet been much studied at low service times, so the functional relationships in this region are still uncertain.

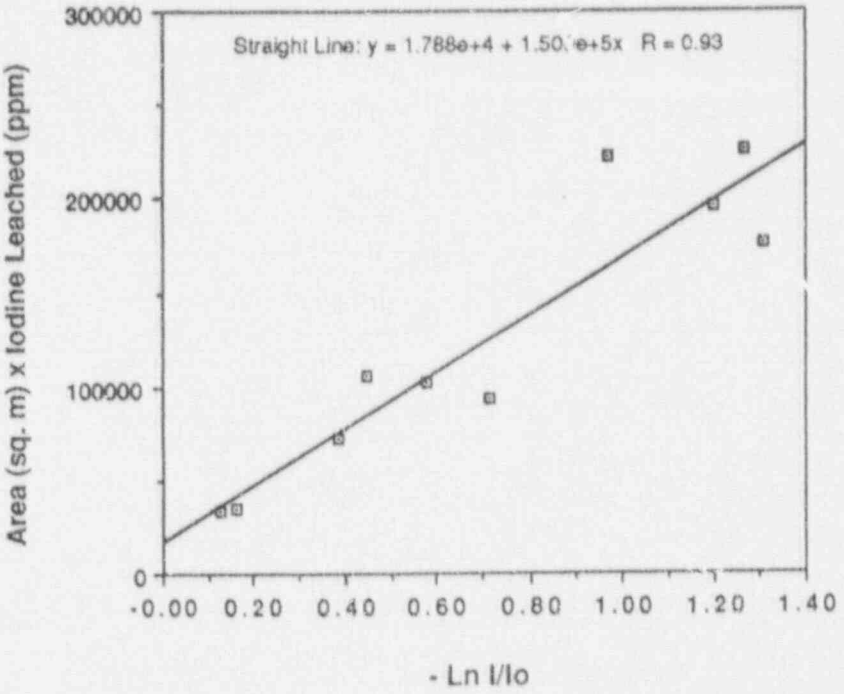

Figure 11. Fit of data to mathematical model.

References

1. Evans, A. G., "*Confinement of airborne radioactivity: final progress report January/December 1978*," DP-1542 (February 1980).

2. Deitz, V. R., "*Charcoal performance under accident conditions in light-water reactors*," NUREG/CR-3990 (March 1985).

DISCUSSION

KOVACH: I think if you used an unimpregnated carbon you would get very similar results. Whether a carbon is capable of moving methyl iodide is not demonstrated just by the absorption retentivity for stable methyl iodide.

HYDER: I didn't intend to propose it as such. I was more interested in developing a technique that was sensitive to iodine. After I started using it, I found that it could be used for looking at the effects of some substances on methyl iodide retention. But we are a long way from being able to correlate residence time, as it would be measured with the other parameters of the carbon.

KOVACH: What was the concentration of methyl iodide?

HYDER: Typically, we put about 50 microliters of methyl iodide into 5 liters of air.

KOVACH: Have you checked the velocity through your carbon bed?

HYDER: Yes, the velocity was carefully controlled. We regularly used a water displacement system in all experiments to measure velocity accurately. Velocity through the bed was about 8 cm^3/sec, or about 4 bed volumes per second. Methyl iodide desorption varied with carbon history.

FREEMAN: It is my understanding that the methyl iodide in your little evaporating bowl was methyl iodide-127. Therefore, the removal mechanism was just physical adsorption not isotopic exchange because there was no isotopic force to cause a change. Therefore, it doesn't make any difference whether TEDA or KI was on the carbon.

HYDER: Exactly, except the removal mechanism for TEDA is supposed to be that of chemical reaction, which would prevent release of methyl iodide.

FREEMAN: That is correct.

EVANS, A.G.: There has been some speculation that one of the reasons why both TEDA and some of your soluble iodine decrease is because the TEDA is reacting with the impregnated iodine. This might explain some of the apparent loss of materials.

HYDER: It is at the moment something of a mystery exactly what happens to the TEDA, but I can't rule it out. TEDA disappears from the carbon. I asked the plant to run some analyses for TEDA, but their chromatograph was tied up, so I had to defer solving this particular mystery.

GUEST: We use single impregnated carbons with a minimum of 5% TEDA on them. We had some samples of carbon taken out of our systems that had been in service up to three years. The worst loss of TEDA was 3.5 to 3.8% of the original 5%. I don't know what is happening that you are losing your TEDA so quickly. It seems surprising. It may be an analysis problem or the fact that the TEDA is reacting, as Mr. Kovach suggested.

HYDER: We find that we get a certain level of acidic gases going through the carbon during service. You might expect these to react with TEDA. The pH of the extract drops steadily during service and this may well have something to do with the loss of the TEDA. Therefore, the differences you noted may also result from differences in the contaminants in the two air streams.

MULCEY: What is the detection limit of your apparatus in terms of concentration of methyl iodide?

HYDER: Initial concentration, 50 µg/5 L; sensitivity was 3 or 4 orders of magnitude below this, depending on how low the light background could be made (by shedding out room light).

REMOVAL CHARACTERISTICS OF SOME ORGANIC IODINE FORMS BY SILVER IMPREGNATED ADSORBENTS

Y. Kobayashi
Japan Nuclear Fuel Service Company, Ltd.
2-2-2 Uchisaiwai-cho, Chiyoda-ku, Tokyo, 100 Japan

Y. Kondo, Y. Hirose
Hitachi Works, Hitachi, Ltd.
1-1-3 Saiwai-cho, Hitachi-shi, Ibaraki-ken, 317 Japan

T. Fukasawa
Energy Research Laboratory, Hitachi, Ltd.
1168 Moriyama-cho, Hitachi-shi, Ibaraki-ken, 316 Japan

Abstract

The removal characteristics of organic iodine forms, such as methyl-, ethyl-, i-propyl-, n-propyl-, i-buthyl-, n-buthyl-, and cyclohexyl-iodides were evaluated on silver impregnated adsorbents, such as silver silca gel and silver alumina.

The decontamination factor values were evaluated in regard of alkyl iodide species, nitrogen oxides concentration, temperature, preliminary iodine loading, linear gas velocity and adsorbent column length. The results obtained in this study revealed that silver silica gel and silver alumina were practically effective to remove organic iodine as well as inorganic iodine.

I. Introduction

For the past several years, various kinds of silver impregnated adsorbents have been investigated to remove iodine from off gas streams of spent nuclear fuel reprocessing plants. [1][2] Iodine forms considered previously were mainly elemental iodine and methyl iodide. Only qualitative evaluation was made on organic iodine forms other than methyl iodide [1] [3] and no quantitative evaluation was made on them. In this study, the removal efficiencies of the organic iodine forms were evaluated on silver impregnated silica gel (AgS) and alumina (AgA).

II. Experimental

Adsorbents

Table 1 shows the specifications of the adsorbents used in this study. AgS was made by Süd Chemie, GMBH and contained 12 wt% silver. AgA was made by Hitachi, Ltd. and contained 24 wt% silver.

Table 1 Specifications of the Iodine Adsorbents

	Carrier	Impregnated Material	Silver Content (wt %)	Adsorbent Size (mesh)
Silver Silica Gel	Silica Gel	$AgNO_3$	12	10~20
Silver Alumina	Activated Alumina	$AgNO_3$	24	10~20

Experimental method

Figure 1 shows the flow diagram of the experimental apparatus for evaluating the removal characteristics of the adsorbents. Carrier gas was air and the humidity in the gas stream was approximately 0.4 vol%. Gas chromatograph and spectrophotometer were used to determine the concentrations of the organic iodine and nitrogen oxides (NOx), respectively. The decontamination factor (DF) was calculated from the iodine concentrations at the inlet and the outlet of the adsorbent column. The detection limits of organic iodine forms were about 0.6 ppm and about 10 ppb using the flame ionization detector (FID) at the inlet and the electron capture detector (ECD) at the outlet, respectively.

The adsorbent column was cylindrical glass tube with an inner diameter of 10 mm and a height of 300 mm. The adsorbent was loaded in this column to get normally a height of 20 mm.

Table 2 shows the main experimental conditions. The organic iodine forms were six kinds of normal- and iso-alkyl iodides, and cyclohexlyl iodide. This study also evaluate the organic iodine removal efficiency of the adsorbents which adsorbed preliminarily an adequate amount of elemental iodine (I_2)[4], which considered that the I_2 was the main iodine forms to be treated at the off gas system. To minimize the analysis time three kinds of organic iodine were mixed at maximum and loaded to the adsorption column to maintain the total iodide concentration of about 50 ppm.

Ⅲ. Results and Discussion

Removal characteristics for the organic iodines

Figure 2 shows the dependency of the DF values for organic iodines on the preliminarily adsorbed amounts of elemental iodine on AgS and AgA.

The result shows that the DF values decreased with increasing preliminarily adsorbed I_2 amounts for each organic iodine. This tendency agrees with the reported results for elemental iodine [4].

In case of no preliminary adsorption, the DF values of over 10^3 could be obtained for the organic iodines except for methyl iodide. So methyl iodide was found to be the most difficult form to be removed.

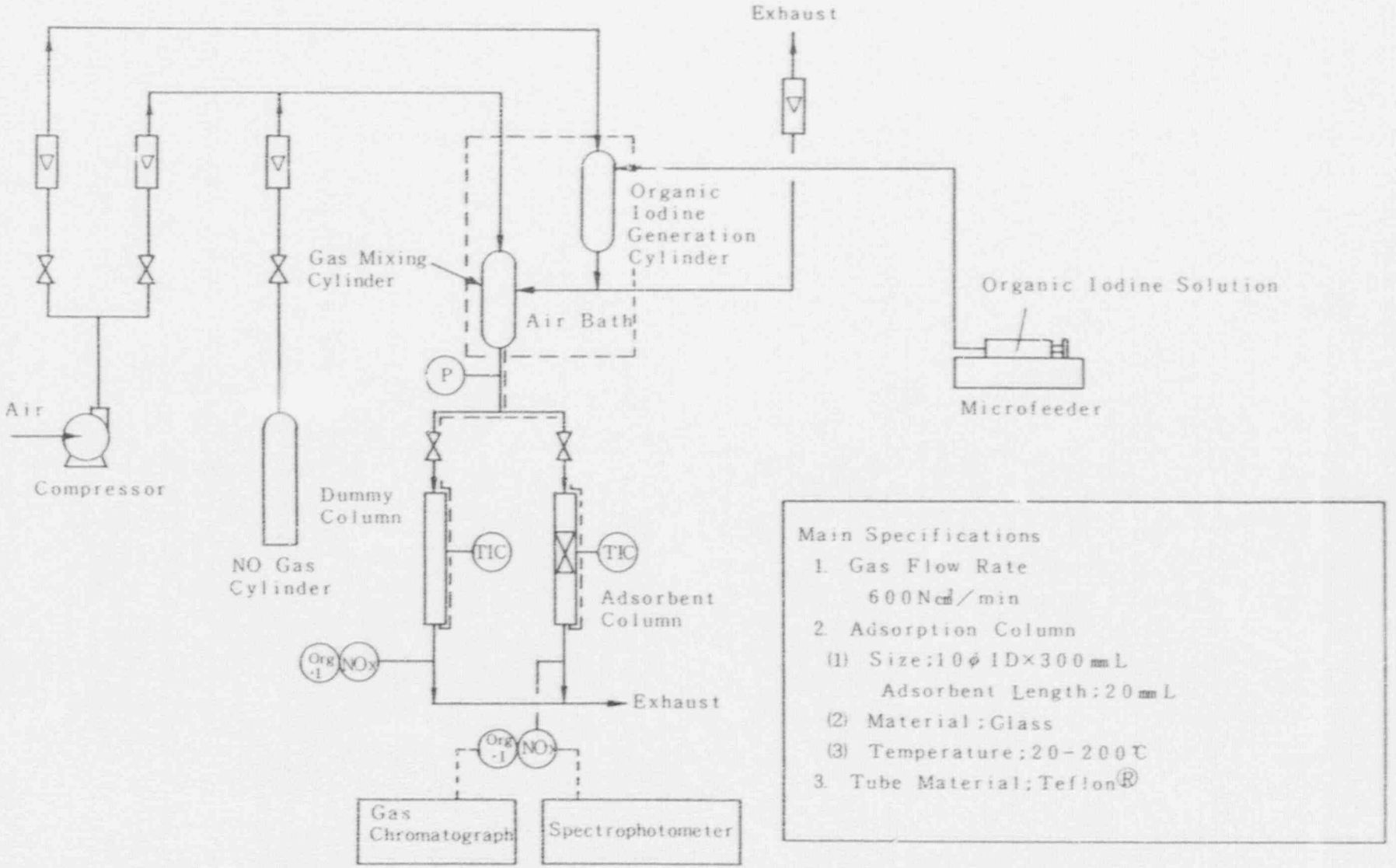

Figure 1 Flow Diagram of the Experimental Apparatus

Table 2 Experimental Conditions

Item	Conditions
Organic Iodine	Methyl Iodide Ethyl Iodide n-Butyl Iodide i-Butyl Iodide n-Propyl Iodide i-Propyl Iodide Cyclohexyl Iodide
Iodine Concentration (vol ppm)	1, 5, 20, 50
NOx Concentration (vol%)	0, 1.5
Temperature (°C)	50, 100, 150
Linear Gas Velocity (cm/s)	20, 50
Adsorbent Length (mm)	20, 50

Futhermore, AgA showed the higher DF values than AgS, which could be explained by the higher silver content (24 wt%) for AgA than that (12 wt%) for AgS and thus higher reaction ability of AgA.

Effect of temperature and NOx concentration

Figure 3 shows the dependency of the DF values on the temperature and the effect of the 1.5 vol% NOx on the DF values. For AgS, the DF values for every organic iodine were constant over 100 °C. For AgA, the DF values for isobutyl iodide and isopropyl iodide were constant over 50 °C and the DF value for methyl iodide gradually increased with temperature (50-150 °C). AgA and AgS had the same removal ability for organic iodines at 50-100 °C and AgA had the higher removal ability for methyl iodide at 150 °C.

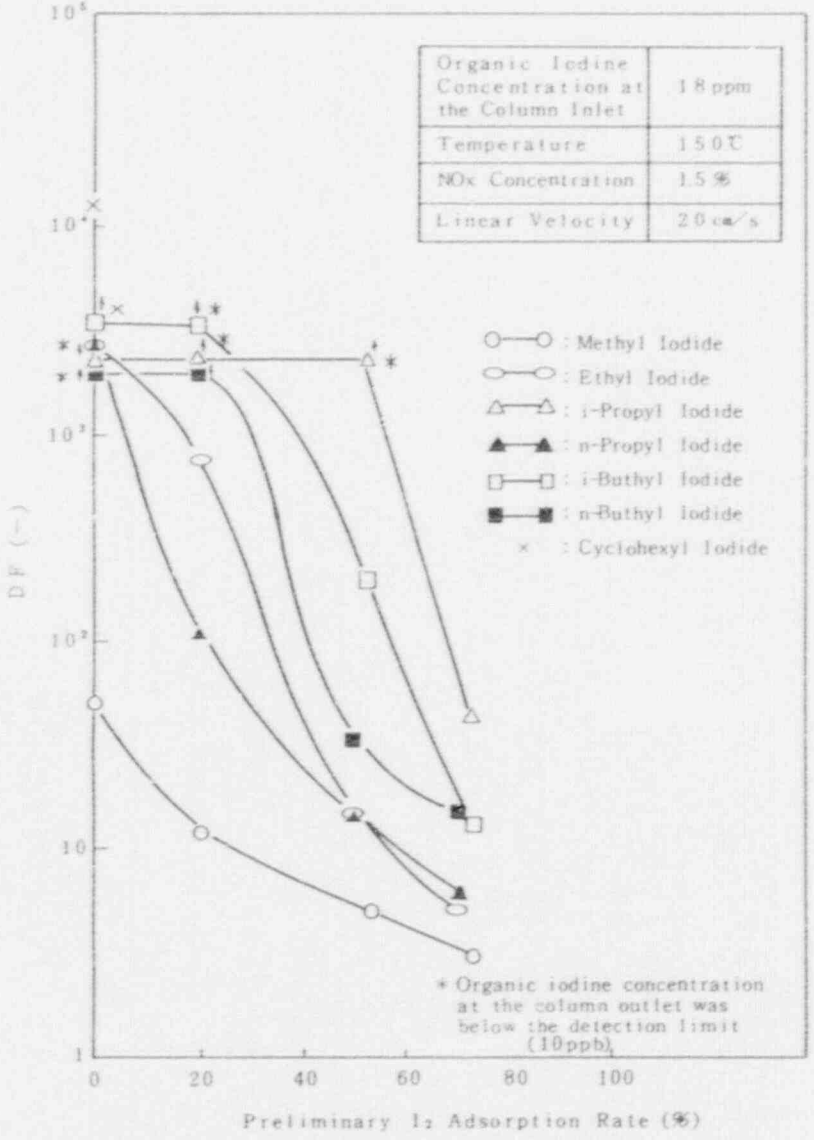

(a) Ag S

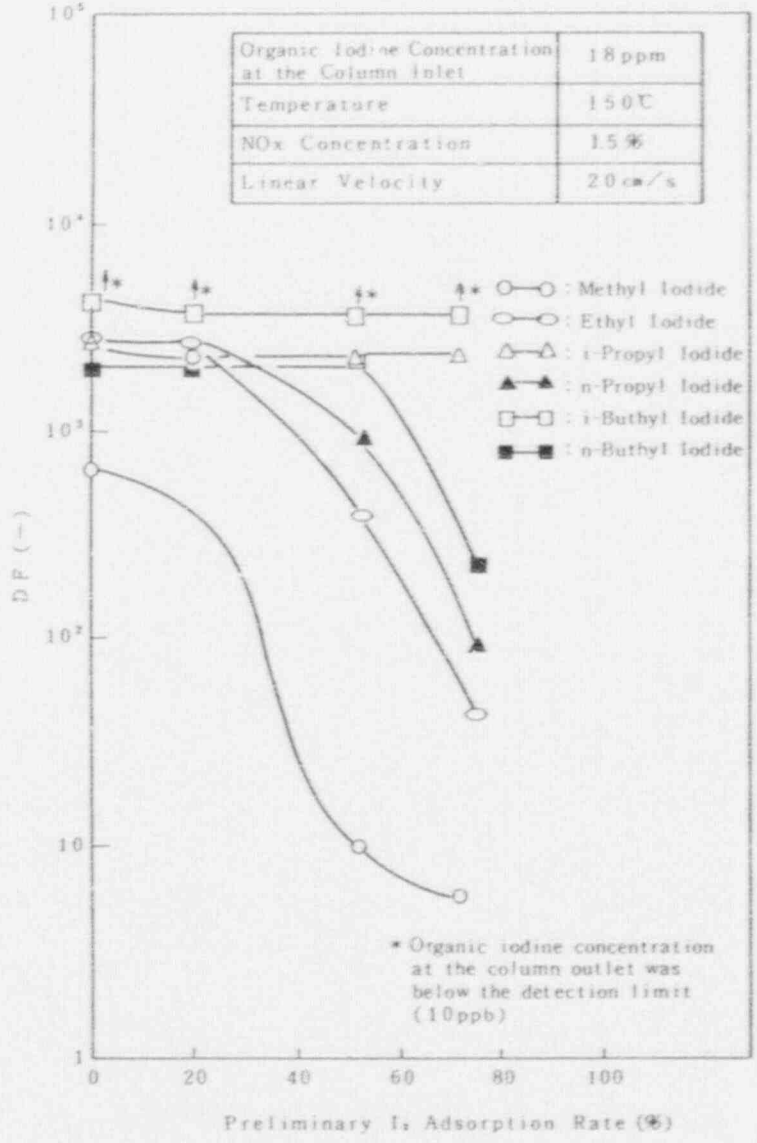

(b) Ag A

Figure 2 Effect of Preliminary I_2 Adsorption Rate on DF

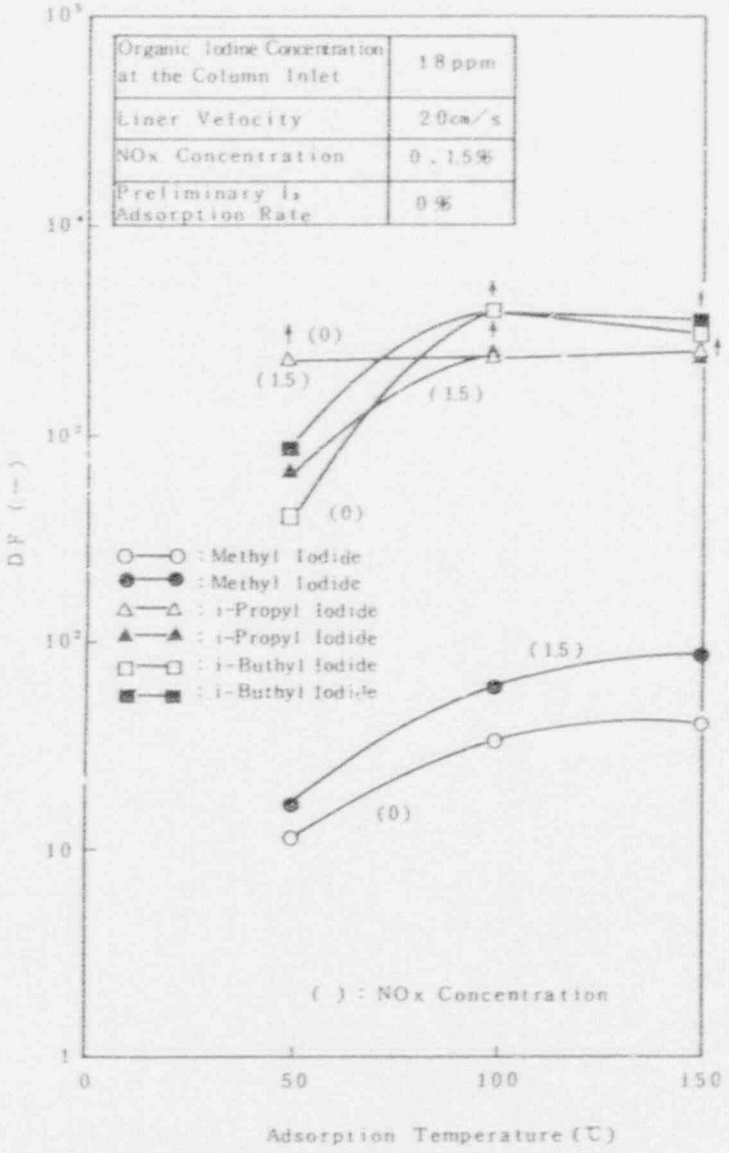

(a) AgS

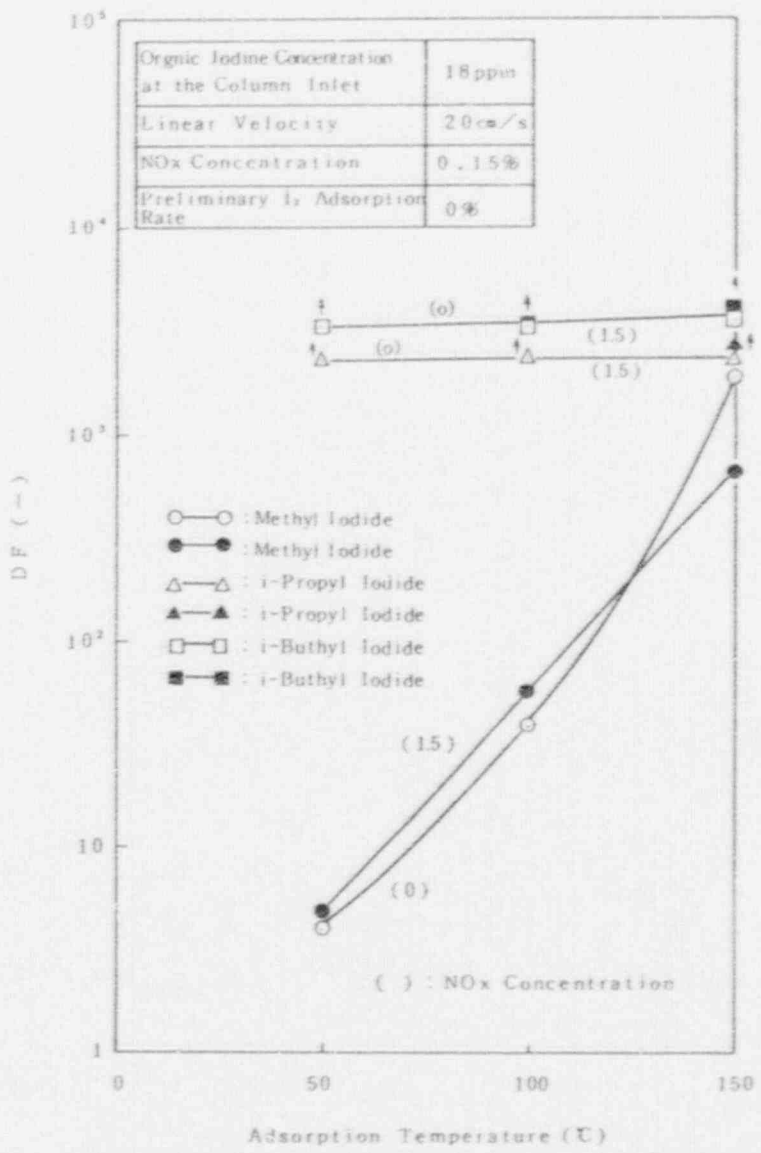

(b) AgA

Figure 3 Effect of Temperature on DF

1.5 vol% of NOx was found to have no adverse effect on removal of organic iodines.

Effect of organic iodine concentration

Figure 4 shows the dependency of the DF values for methyl iodide on its concentration. The DF values for methyl iodide slightly decreased with its concentration both in the presence and in the absence of NOx. The dependencey of iodine concentration was also investigated for isobytyl- and isopropyl-iodides, but their concentration of 1-20 ppm had no adverse effect on their DF values, which were over 10^3 in each case.

Examination of the removal characteristics for organic iodines

Table 3 shows the comparison of the DF values for seven kinds of organic iodines obtained in the same condition with AgS and AgA. Althouth table 3 shows the minimum DF values based on detection limits, their order of magnitude coincides with the tendency shown on figure 2. AgS and AgA could equally remove alkyl iodides, so far studied except for methyl iodide, with the DF values over 10^3 when temperature, NOx concentration, linear gas velocity and column length were 150 °C, 1.5 vol%, 20 cm/s and 20 mm, respectively.

For methyl iodide, the DF values of over 10^3 could be also obtained with longer adsorbent column (50 mm) and higher velocity (50 cm/s), however the DF values of 50 and 7.3×10^2 were obtained for AgS and AgA,

Table 3 DF for Organic Iodines by AgS and AgA

(Temperature ; 150 °C, NOx Concentration ; 1.5 vol%, Linear Velocity ; 20 cm/s, Adsorbent Length ; 20 mm)

Organic Iodine Form	AgS	AgA
Methyl Iodide	50 ($2.5 \times 10^{3*1}$)	7.3×10^2 ($2.8 \times 10^{3*1}$)
Ethyl Iodide	$> 2.6 \times 10^3$	$> 2.8 \times 10^3$
i-Propyl Iodide	$> 2.3 \times 10^3$	$> 2.7 \times 10^3$
n-Propyl Iodide	$> 2.7 \times 10^3$	$> 2.9 \times 10^3$
i-Buthyl Iodide	$> 3.5 \times 10^3$	$> 4.2 \times 10^3$
n-Buthyl Iodide	$> 1.8 \times 10^3$	$> 2.0 \times 10^3$
Cyclohexyl Iodide	$> 1.2 \times 10^3$	—

*1 Adsorbent Length 50 mm, Linear Velocity 50 cm/s.

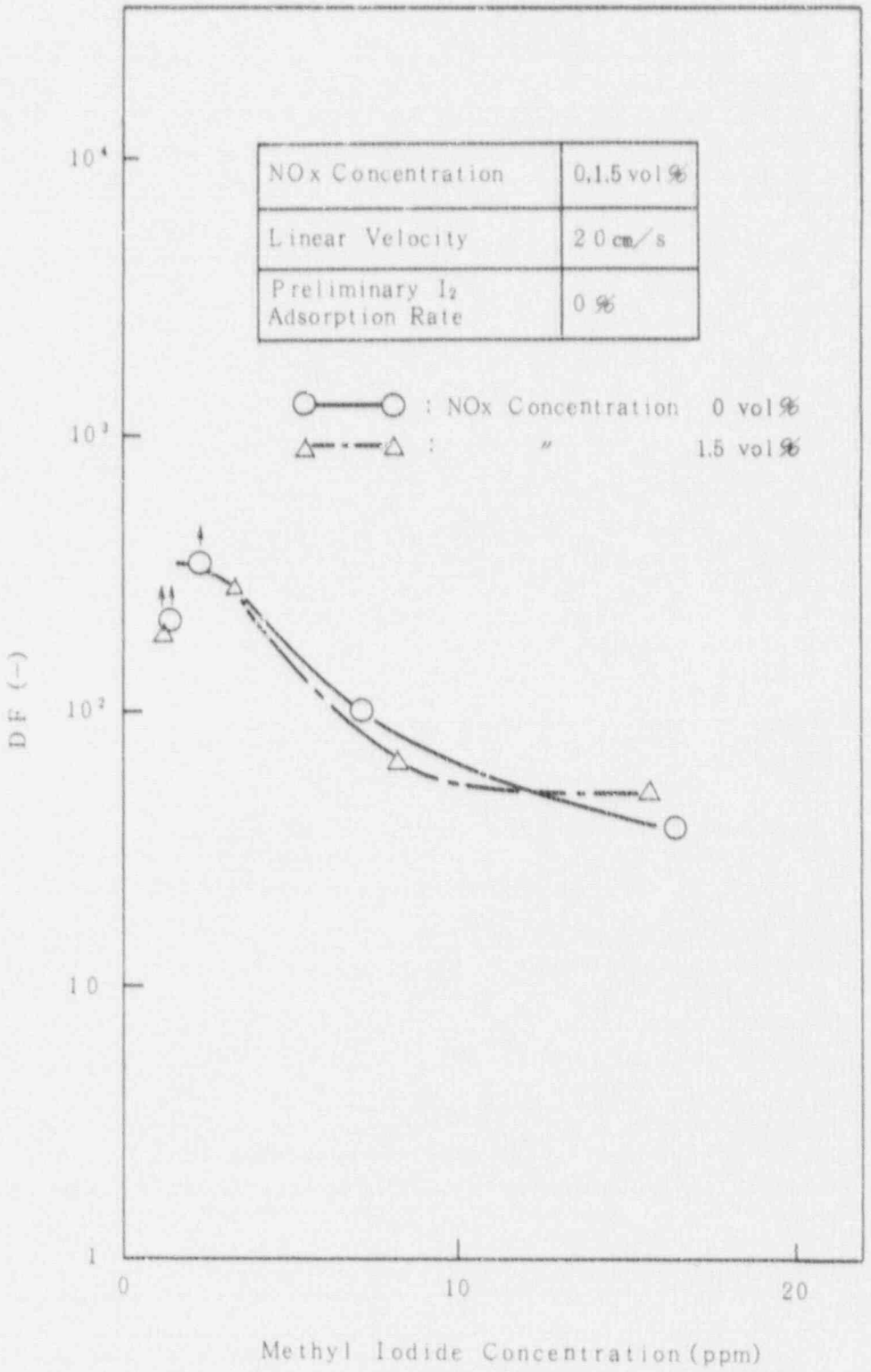

Figure 4 Effect of Methyl Iodide Concertration on DF (AgS, 150°C)

respectively, with shorter adsorbent column (20 mm) eventhough lower velocity (20 cm/s).

The results obtained in this study revealed that AgS and AgA were practically effective to remove organic iodines as well as inorganic iodine.

From figure 2 and table 3, cyclohexyl iodide shows the highest DF value and methyl iodide shows lowest value. Its order is as follows, cyclohexyl > isopropyl > isobuthyl > normalbuthyl > normalpropyl > ethyl > methyl.

As was reported previously [1], the reaction between alkyl iodide and silver impregnated adsorbent was considered to proceed as follows,

$$R^+\text{-}I^- + Ag^+ \rightarrow R^+ + AgI, \quad (1)$$

$$R^+ + NO_3^- \rightarrow R\text{-}NO_3, \quad (2)$$

where R^+, $R^+\text{-}I^-$ and $R\text{-}NO_3$ are carbonium ion, alkyl iodide and alkyl nitrate, respectively.

Reaction (1) easily proceeds with stable carbonium ion, so the order of the stability for each carbonium ion might be proportional to the adsorption reactivity for organic iodine and to the magnitude of the DF value. The stability for each carbonium ion can be evaluated experiencially and coincides the order of the DF value shown in figure 2 and table 3.

Thus the DF values for alkyl iodides could be qualitatively evaluated by the stability of the carbonium ion in alkyl iodides.

IV. Conclusions

The removal efficiency for organic iodine forms were evaluated on AgS and AgA which were chosen as adsorbents. Following conclusions were obtained.

1. The adsobents could remove the alkyl iodides with the DF values over 10^3 in a proper application.

2. 1.5 vol% of NOx had no adverse effect on the removal of alkyl iodides.

3. Temperature of 100-150°C had no effect on the removal of alkyl iodides by AgS and AgA except for methyl iodide removal by AgA. The DF value for methly iodide by AgA increased with temperature in this region.

4. Organic iodide concentration of 1-20 ppm had little effect on the removal of alkyl iodides.

5. The removal efficiencies obtained for different alkyl iodides could be explained by the stability of the carbonium ion.

6. Representing all organic iodides by Methyl iodide is sufficiently conservative manner to evaluate the removal efficiency of organic iodine by AgS and AgA.

References

(1) Wilhelm,J.G., et al., "Head-end iodine removal from a reprocessing plant with a solid sorbent." Proceedings 14th ERDA Air Cleaning Conference, CONF-760822, 1, 447 (1976).

(2) Hattori,S., et al., "Removal of iodine from off-gas of nucler fuel reprocessing plants with silver impregnated adsorbents." Proceedings 18th DOE Nuclear Airborne Waste Management and Air Cleaning Conference, CONF-840806, 2, 1343 (1984).

(3) Smith,S.R., and West,D.L., "Determination of volatile compounds of fission-product iodine.", Nuclear Applicatioins, 3, 43 (1967).

(4) Maurel,J.M., and Vigla,D., "Behaviour of a sorbent material (AC 6120) for iodine removal in the presence of nitrogen oxide." Proceedings 19th DOE/NRC Nuclear Air Cleaning Conference, CONF-860820 2, 730 (1986).

DISCUSSION

FURRER: I would like to know how you took the gaseous sample after your bed? Was it a cold trap or did you take the sample directly out of the flow?

KONDO: The outlet gas collected in a cold trap at a temperature of -10°C. The gas was absorbed in hexane and injected into a gas chromatograph to measure the average concentration of the outlet gas.

FURRER: I would like to make a comment. The unidentified peaks in your gas chromatogram are the reaction products from secondary and tertiary alkyd iodides with $AgNO_3$ to alkenes and alkanes. We found these results some years ago. The paper was published in the Monatshefte fur Clemie, 1976.

KOVACH: (1) You are dealing with two different processes here. One is a physical adsorption process and the other is the iodide-silver reaction. Have you assumed that your system was under complete equilibrium conditions as far as physical adsorption was concerned with all of your compounds and the sole effect was the iodine-silver reaction? (2) Do you expect the alkyl halides to be present in 10-50 ppm concentrations in a processing plant?

KONDO: (1) We have already confirmed that the main reaction is a chemical reaction with the silver nitrate impregnated adsorption materials. Below a temperature of 150°C, no desorption of iodine from AgS and AgA was observed using a nitrogen gas purge following I_2 loading. (ref. CONF-840408, 2:1343 (1984). (2) No, we do not expect alkyl halides in the 10-50 ppm range. We performed the experiment with iodide concentrations as high as several tens of ppms, because of the detection limit in the experiment. But we think that the decontamination factors obtained here can be extrapolated to low concentrations.

MULCEY: In your paper you refer to a global NO_x concentration, were the separate effects of NO and NO_2 investigated?

KONDO: No, they were not, but we measured the NO/NO_x ratio. It was from 0.3 to 0.6. No adverse effects were observed from a combined total NO_x concentration up to 1.5 volume percent.

CLOSING COMMENTS OF SESSION CO-CHAIRMAN EVANS

Let me summarize the four papers presented in today's session. In two papers dealing with activated charcoal, we learned of the natural weathering of carbon by exposure to flowing air and about the adverse effects of paint fumes and other air pollutants on carbon bed performance. In the remaining two papers, we learned of experimental materials under development as potential replacement for granular activated carbon in iodine adsorber beds.

SESSION 10

NUCLEAR CODES AND STANDARDS

Wednesday: August 15, 1990
Co-Chairmen: A. A. Weadock
B. B. Reinert

OPENING COMMENTS OF SESSION CO-CHAIRMAN WEADOCK

CHANGES IN ADSORBER TESTING AS A RESULT OF NRC GENERIC INFORMATION
J. J. Hayes, Jr.

US NRC REGULATORY GUIDANCE FOR ENGINEERED SAFETY FEATURE AIR CLEANING SYSTEMS
R. R. Bellamy

IAEA DECADAL ACTIVITIES IN THE FIELD OF RADIOACTIVE GASEOUS WASTE MANAGEMENT
G. R. Plumb

CLOSING COMMENTS OF SESSION CO-CHAIRMAN REINERT

OPENING COMMENTS OF SESSION CO-CHAIRMAN WEADOCK

The title and content of this session, Nuclear Codes and Standards, is not all-inclusive; we have already had several sessions this week dealing with the status and use of various industry codes and standards relating to nuclear air-cleaning.

The scope during this session will be a little different however, and will focus on the use and incorporation of these codes and standards into regulatory guidance; a topic of obvious practical interest and concern to our attendees.

Leading off the session will be two papers of specific interest to NRC licensees. The first paper details the impact of NRC-issued generic information on technical specification requirements and testing protocols for activated charcoal testing. Next, we will be hearing an update on the status and content of NRC Regulatory Guide 1.52, last revised in 1978. Our third and final paper takes a more global perspective and provides an overview of IAEA activities in the 1980s related to gaseous waste management.

CHANGES IN ADSORBER TESTING AS A RESULT OF NRC GENERIC INFORMATION

John J. Hayes, Jr.
U.S. Nuclear Regulatory Commission
Washington, D.C. 20555

Abstract

Before a nuclear power plant can be licensed by the Nuclear Regulatory Commission (NRC), it must demonstrate that, even in the event of a nuclear accident, the exposure to radiation of onsite and offsite individuals will remain within NRC regulations. One of the ways licensees limit such exposure is to incorporate into their plant design such engineered safety feature (ESF) systems as atmospheric cleanup systems. Typically such a system contains impregnated activated charcoal adsorbers which remove radioiodine. Licensees are required by their plant-specific technical specifications (TS) to demonstrate on a periodic basis that, at the end of its operating cycle, the charcoal is capable of removing radioiodine with an efficiency sufficient to ensure performance equivalent to that assumed in the plant's Final Safety Analysis Report.

Between the period 1985 and 1987, the NRC identified deficiencies in Method A of ASTM Standard D 3803-1979, which is utilized for the determining the capability of activated charcoal to remove radioiodine. These deficiencies were presented in NRC Information Notice 87-32 and in an EG&G report, EGG-CS-7653. A series of control room habitability surveys conducted at operating plants between September 1985 and December 1986 found that some licensees were testing activated charcoal at inappropriate conditions and that, for some plants, the acceptance criterion for adsorber penetration in the TS was lower than that credited in the staff's safety evaluation. In other cases, the acceptance criterion did not incorporate an adequate margin to account for charcoal degradation. The NRC issued these findings in Information Notice No. 86-76 and in NUREG/CR-4960.

The NRC conducted a study of operating nuclear power plants to determine what, if any, changes have been made to the technical specifications, test conditions, acceptance criterion for adsorber penetration and the test method for activated charcoal as a result of the issuance of NRC generic information in the form of Information Notices 86-76 and 87-32, NUREG/CR-4960, and EGG-CS-7653. The results of the study revealed that very few licensees have implemented the generic information and that few are contemplating utilizing it. Those that have utilized the information or are contemplating its use have not applied it in its entirety or accurately. The study also showed that the generic information needs to be applied to most ESF ventilation systems. Licensees continue to test their charcoal

with inappropriate test conditions, protocol, TS, and acceptance criterion for penetration. Given the lack of implementation of appropriate testing of the charcoal, concerns, identified in earlier NRC studies regarding the capability of the charcoal to perform its intended function at its assumed efficiency, remain unchanged.

I. Introduction

Before obtaining a license from the Nuclear Regulatory Commission (NRC), owners of nuclear power plants are required to demonstrate that, even in the event of a nuclear accident, individuals will not be exposed to any more radiation than is permitted by NRC regulations (1) 10 CFR Part 50, Appendix A, General Design Criterion 19 and (2) 10 CFR Part 100. One of the means of limiting such potential exposure is to incorporate into the plant's design such engineered safety feature (ESF) systems as atmospheric cleanup systems. A typical component of such a system is the impregnated activated charcoal adsorber. These adsorbers remove elemental and organic forms of radioiodine.

The operators of nuclear power plants (NRC licensees) are required by their plant-specific technical specifications (TS) to demonstrate, on a periodic basis, that the charcoal is capable of removing radioiodine with an efficiency sufficient to ensure performance equivalent to that assumed in the plant's Final Safety Analysis Report (FSAR). In 1983, the Committee on Nuclear Air & Gas Treatment (CONAGT) of the American Society of Mechanical Engineers (ASME) invited a number of laboratories to participate in a round robin testing program of activated charcoal. The results of the round robin revealed gross differences in the measured penetration when using test method A of the ASTM D 3803-1979[1] standard. These differences raised concerns within the NRC as to whether or not charcoal in the ESF ventilation system would perform with an efficiency equivalent to or greater than that assumed in the licensing of the plant and whether or not licensees were meeting their technical specifications. Therefore, the NRC contracted with EG&G, Idaho to conduct a program to evaluate the (1) results of the round robin, (2) ASTM test standard, and (3) laboratories testing the charcoal. In addition, EG&G was to conduct another round robin and, if it proved appropriate, to propose a revision to the test standard.

In April 1987, the results of EG&G's work were published in a technical evaluation report EGG-CS-7653[2]. This report's recommendations were directed toward the ASTM D 3803 standard, the testing laboratories, and the NRC. With respect to the standard, the report recommended sweeping revisions to the radioanalytical methods and substantial changes to the requirements for test procedures and instrumentation associated

with Method A of ASTM D 3803-1979. The report included a draft revision of the standard which incorporated these changes. The EG&G report stated that this revised standard, with its 16-hour pre-equilibration period, would increase the sensitivity and reliability of the standard to the detection of degradation of charcoal performance. In December 1989, the ASTM D-28 Committee essentially adopted this revised standard.

Addressing the charcoal testing laboratories, the report identified the need for laboratories to use standards as references in their analytical work and to maintain a well calibrated system by periodically testing internal reference charcoal and evaluating these results. A laboratory accreditation program was recommended. Finally, the report recommended that the NRC

1. Revise all TS to refer directly to the most recent revision of the ASTM D 3803 standard for all activated charcoal performance evaluations;

2. Revise all TS to an acceptance limit of 20 penetration (80% efficiency) for used charcoal and 3% for new charcoal when tested using the revised ASTM D 3803 standard; and

3. Reevaluate current activated charcoal adsorber designs and TS in light of the more "realistic" efficiencies obtained from the revised test method, particularly in the use of 2-inch-deep charcoal adsorbers in critical ventilation systems which might be subject to condensing water vapor or steam.

The report did note that the use of heaters in the ESF ventilation systems would allow the acceptance test to be conducted at 70% relative humidity and would reduce the inherent variability of the test. The report also noted that the recommended acceptance criterion of 20% penetration for used charcoal might be too permissive to ensure adequate radioiodine removal capability.

In July 1987, the NRC issued Information Notice No. 87-32[3] to inform NRC licensees of deficiencies in the testing of nuclear-grade activated charcoal. The information notice indicated that EGG-CS-7653 was published and placed in the Public Document Room. In addition, it also noted that there were problems with the capabilities of the testing laboratories and with the ASTM test method, neither of which had ever been verified. It further stated that testing laboratories could use the EG&G protocol (developed to address some of the test method's deficiencies) to perform charcoal tests until a revised D 3803 standard could be adopted. [As stated previously a revised D

3803 standard was approved in December 1989[4] and was issued in February 1990.]

During the period between September 1985 and December 1986 a series of control room habitability surveys were conducted at operating plants to determine whether the control room habitability systems would perform as they were described in licensee's response to TMI Action Item III.D.3.4, "Control Room Habitability." The results of the survey were reported in NUREG/CR-4960[5]. One finding in the report identified problems involving laboratory testing of charcoal and associated plant TS. Some licensees were testing activated charcoal at conditions that would overpredict the capability of the charcoal to remove radioiodine. Tests were being conducted at inappropriate temperatures (80 or 130 degrees Celsius instead of 30 degrees Celsius) and at an inappropriate relative humidity (at a relative humidity of 70% when the test should have been conducted at a relative humidity of 95% because the relative humidity of the air to the charcoal was not controlled to 70% or lower).

Another finding was that the acceptance criterion in the technical specifications for the penetration test was inappropriate because the criterion was

1. equal to or lower than that credited in the staff's safety evaluation; and/or

2. did not include the appropriate safety factor from Regulatory Guide 1.52[6] to ensure that, at the end of the unit's operating cycle, the charcoal would have a removal efficiency at least equal to that credited in the staff's safety evaluation.

Table 4.2 of NUREG/CR-4960 indicated that only 1 of 15 units surveyed performed their laboratory test of charcoal for the control room at an appropriate temperature of 30 degrees Celsius. In addition, licensees at only 4 of the 15 plants incorporated the appropriate safety factor in their TS.

Information Notice No. 86-76[7] told NRC licensees about the problem of testing the charcoal at an inappropriate temperature.

II. Purpose of the Study

This study was performed to determine whether NRC licensees, in response to the issuance of NRC generic information in the form of Information Notices 86-76 and 87-32 and reports NUREG/CR-4960 and EGG-CS-7653, had made changes to their

(1) test method, test laboratory, and/or test conditions;

(2) technical specifications; and

(3) acceptance criterion for penetration for the laboratory test; and

(4) whether changes should have been made in the above three areas.

A total of 80 nuclear units were invited to participate in this voluntary study. Responses to the study covered 37 nuclear units and 93 ESF ventilation systems.

The study was performed utilizing a survey. A survey form was developed for participation by licensees. The survey form, presented in Appendix A, was divided into an introductory section followed by four numbered sections (I-IV). The introductory section requested a system description including (1) system flowrate; (2) design value for the charcoal adsorber face velocity; (3) adsorber bed depth; (4) the adsorber efficiencies assumed in the latest licensee safety analysis submitted to the NRC and the submittal date; (5) whether the system utilized electrical heaters to limit relative humidity to 70% or less; and (6) the adsorber efficiency credited in the latest NRC safety evaluation and its issuance date. Section I of the survey requested information on the TS and some of the test conditions for the particular ESF system. Information requested included (A) the laboratory test method utilized; (B) test conditions such as temperature, relative humidity, acceptance criterion for the laboratory test either in terms of penetration or efficiency, pre-equilibration period, face velocity, and testing laboratory; and (C) additional clarifying comments. Section II of the survey form requested information from licensees planning to revise their TS and/or their test conditions or change their test laboratory. If they were planning revisions, they were asked to note the changes and to give clarifying comments, if appropriate. Section III of the survey form asked the licensees to indicate what changes had been made to the laboratory test method, test conditions, and/or TS since January 1, 1986. Again, the reasons for the changes and clarifying comments, if appropriate, were requested. Since the survey form only sought information on what licensees had changed <u>to</u> and not what they had changed <u>from</u>, discussions were held with licensee personnel to determine conditions that existed before the change. Section IV of the survey form, "Individual to Contact," gave the NRC staff information needed to arrange the discussion.

III. Results of the Study

Changes Incorporated and/or Contemplated

The 37 plants responding to the study reported that nine ESF ventilation systems (less than 10%) had made changes to either their TS, the test method, test conditions, or acceptance criterion for penetration as a result of either the EG&G work or the control room habitability work or the information notices associated with these efforts. The survey indicated that licensees were contemplating changes in slightly more than 20% of the ESF ventilation systems (21 of 93) as a result of NRC generic information.

The fact that so few have changed their TS, test method, or test protocol or are even contemplating a change, may be an indication that most of the charcoal in the ESF ventilation systems is presently being tested at appropriate conditions, with an appropriate test method and an appropriate acceptance criterion for penetration such that changes are not needed. Conversely, licensees may have chosen to ignore the generic information and maintain the "status quo." One could speculate that licensees were awaiting the ASTM D 3803 revision before implementing any change. Indeed, data from the study indicated that for 12 of the 21 systems for which changes are contemplated, licensees planned to evaluate the use of the revised ASTM D 3803 standard. However, no licensee to date has made the change to the 1989 revision. The test methods currently being used are distributed as follows:

ASTM D3803-1979/1986	68%
RDT-16-1T 1973	21%
RDT-16-1T 1977	11%

None of the units indicated that they had changed test laboratories as a result of the EG&G work and its associated information notice although at least one of the laboratories previously testing charcoal no longer performs such tests.

Need for Change

Before it could be determined whether the existing test method, test conditions, TS, and acceptance criterion for the penetration test were appropriate; the appropriate test conditions, test method, TS, and acceptance criterion for the penetration test had to be defined. The appropriate conditions came from the Information Notices 86-76 and 87-32, NUREG/CR-4960, EGG-CS-7653, and Regulatory Guide 1.52. The appropriate

test method was considered to be the revised ASTM D3803 standard or the EG&G protocol in EGG-CS-7653. The appropriate test conditions and acceptance criterion were defined as follows:

1. Temperature

   All charcoal was considered to be tested at an appropriate temperature if it was tested at 30 degrees Celsius.

2. Relative Humidity

   Systems without heaters which do not control relative humidity of the incoming air to 70% or less should be tested at 95% relative humidity. Systems with heaters which control the relative humidity of the air to 70% or less should be tested at 70% relative humidity.

3. Face Velocity

   Systems designed for a face velocity of 40 ft/min or less should be tested at 40 ft/min. Systems designed with a face velocity greater than 40 ft/min should be tested at the design velocity.

4. Acceptance Criterion for Penetration

   The acceptance criterion for penetration should be given, depending upon how the acceptance criterion is defined, as either:

   Allowable Penetration = (100% - Efficiency Credited in NRC Safety Evaluation)/Safety Factor,

   Safety Factor = 5 [for systems with heaters]
   = 7 [for systems without heaters]

   or

   Removal Efficiency = Efficiency Credited in NRC Safety Evaluation + 0.857 (100% - Efficiency Credited in NRC Safety Evaluation) [for systems without heaters]

   = Efficiency Credited in NRC Safety Evaluation + 0.8 (100% - Efficiency Credited in NRC Safety Evaluation) [for systems with heaters]

5. Pre-equilibration Period

The pre-equilibration period should be 16 hours.

All 93 ventilation systems were evaluated to determine whether the charcoal was tested in a manner to meet these five criteria. Only one system met all five. The remaining 92 systems were deficient in one or more of these criteria. Every system met at least one of the criteria. Table 1 provides information on the number of systems as a function of the number of inappropriate criteria.

Table 1 Number of Systems and Their Inappropriate Criteria.

Number of Inappropriate Criteria	Number of Systems
1	17
2	49
3	20
4	6

More than 80% of the ventilation systems (75 of 93) are deficient in two or more criteria. Table 2 indicates the number of systems with deficiencies in each criterion.

Table 2 Number of Systems with Deficiencies in a Given Criterion

Criterion	Number of Systems with Deficiencies
Pre-equilibration Period	66
Temperature	65
Acceptance Criterion for Penetration	46
Relative Humidity	16
Face Velocity	6

From Table 2 it can be observed that the majority of the deficiencies, almost 90%, occur in the pre-equilibration period, the test temperature, and the acceptance criterion for

penetration that determines whether the charcoal will perform its intended function. As noted previously, problems in these areas were identified in the NRC generic information documents. From the data collected in the study, it appears that the deficiencies still exist and that licensees have not made appropriate changes to their TS and/or their test conditions, nor are they, for the most part, planning changes.

It should be noted that of the 46 systems that had an inappropriate acceptance criterion for penetration, five systems had an acceptance criterion which was less than that assumed in the safety analysis or the safety evaluation while another 23 had an acceptance criterion which was equal to that assumed in the safety evaluation. Thus, almost 30% of the systems surveyed could restart, following a refueling outage, with charcoal with an efficiency less than or equal to that assumed in the safety evaluation.

It should be noted that one licensee's response in this study, involving nine ESF systems, indicated that while the plant-specific TS allow the charcoal to be tested at a temperature of 80 degrees Celsius, both an 80 degree and a 30 degree Celsius test are performed. The 30 degree test is used to determine acceptability of the charcoal. Discussions with the licensee indicated that they have replaced the charcoal on the basis of the 30 degree test results. However, for the purposes of this study, these nine units were classified as having an inappropriate test temperature criterion because their is no requirement for the licensee to utilize the 30 degree test.

The study also showed that some licensees test their charcoal at 25 degrees Celsius. This is because some licensees are testing in accordance with various versions of RDT 16-1T[8,9,10]. This test temperature was changed from 25 degrees Celsius to 30 degrees Celsius with the issuance of the 1977 version of RDT 16-1T. Since the 25 degree is still considered a realistic temperature for determination of charcoal capability, those systems which had their charcoal tested at 25 degrees were counted as having an appropriate temperature for the purposes of this study.

Changes Made

In assessing the changes that have been made, in some cases, licensees made changes that were inappropriate for the system involved and, in some cases, not enough changes were made. For example, four systems had their test temperature changed from 130 degrees Celsius to 80 degrees. Three systems did change their test temperature to 30 degrees Celsius, but the acceptance criterion for penetration was changed to an inappropriate value.

Those that did change the acceptance criterion for penetration did seem to implement it correctly.

Changes Contemplated

As with the ventilation systems for which changes have already been made, licensees contemplating changes show a mixed success in selecting appropriate changes. The previously mentioned licensee, who performs both the 80 degree and the 30 degree Celsius tests for nine ESF systems is considering adopting the 1989 revision of ASTM D 3803. That licensee would reduce the test temperature from 80 degrees Celsius to 30 degrees Celsius; change the pre-equilibration period to 16 hours; and reduce the acceptance criterion for allowable penetration (because of the 16 hour pre-equilibration period) to below that assumed for the safety analysis and the safety evaluation in all nine cases.

Two licensees were contemplating changes to three ESF ventilation systems which involved consideration of the use of the 1989 revision of ASTM D 3803 but the specific changes were not identified. Another licensee was considering a change to utilize the 1986 version of the ASTM D 3803 standard and an appropriate change to the acceptance criterion for allowable penetration from 10% to 1%, but the test temperature would not be changed to 30 degrees Celsius but rather to 80 degrees Celsius. Another licensee is contemplating changes to incorporate a 30 degree test for three ventilation systems but the pre-equilibration period would not be changed to 16 hours for the three and the acceptance criteria would remain unchanged and inappropriate for two of the systems.

IV. Conclusions

The NRC has issued generic information to its licensees in the form of reports and information notices on appropriate laboratory test protocol, test conditions, TS, and acceptance criterion for penetration. An NRC study revealed that very few licensees have implemented this information and that few are contemplating utilizing it. Those that have utilized the generic information or are contemplating its use, have not applied it in its entirety nor accurately. The results of the study also showed that the generic information is applicable to most ESF ventilation systems. Given the lack of implementation of appropriate test conditions, protocol, TS, and acceptance criterion for penetration, concerns, identified in earlier NRC studies regarding the capability of the charcoal to perform its intended function at its assumed efficiency, remain unchanged. The NRC is reviewing the results of this study.

Acknowledgements

The author wishes to acknowledge the cooperation of the NRC project managers who assisted him in the study and NRC licensees who provided the data for the study.

References

1. American Society for Testing and Materials, "Standard Test Methods for Radioiodine Testing of Nuclear-Grade Gas-phase Adsorbents," ANSI/ASTM D 3803-1979 (1980)

2. Scarpellino, C. D. and Sill, C. W., "Final Technical Evaluation Report for the NRC/INEL Activated Carbon Testing Program," EGG-CS-7653 (1987)

3. U.S. Nuclear Regulatory Commission, "Deficiencies in the Testing of Nuclear-grade Activated Charcoal," Information Notice No. 87-32 (1987)

4. American Society for Testing and Materials, "Standard Test Method for Nuclear-Grade Activated Carbon," ANSI/ASTM D 3803-1989 (1990)

5. Driscoll, J. W., "Control Room Habitability Survey of Licensed Commercial Nuclear Power Generating Stations," NUREG/CR-4960, . L-87-22 (1987)

6. U.S. Nuclear Regulatory Commission, "Design, Testing, and Maintenance Criteria for Post Accident Engineered-Safety-Feature Atmosphere Cleanup System Air Filtration and Adsorption Units of Light-Water-Cooled Nuclear Power Plants," Regulatory Guide 1.52, Revision 2 (1978)

7. U.S. Nuclear Regulatory Commission, "Problems Noted in Control Room Emergency Ventilation Systems," Information Notice No. 86-76 (1986)

8. U.S. Department of Energy, "Gas-Phase Adsorbents for Trapping Radioactive Iodine and Iodine Compounds," RDT M 16-1T (1971)

9. U.S. Department of Energy, "Gas-Phase Adsorbents for Trapping Radioactive Iodine and Iodine Compounds," RDT M 16-1T (1972)

10. U.S. Department of Energy, "Gas-Phase Adsorbents for Trapping Radioactive Iodine and Iodine Compounds," RDT M 16-1T (1973)

Appendix A Survey Form

You are requested to complete the following survey forms for your plant. The information in this survey will form the basis of a paper to be presented at the 21st DOE/NRC Nuclear Air Cleaning Conference entitled, "Changes in Adsorber Testing As a Result of NRC Guidance". Please complete one survey form for each engineered safety feature ventilation system at your facility. If you have two or more reactors on site and the units are identical in design and there are no differences between each Unit's Technical Specifications, then just indicate that the information for Unit X is also applicable to Unit Y e.g., McGuire Units 1/2. Otherwise, a separate survey form should be completed for each ESF ventilation system for each Unit. Presentation of an earlier draft of this survey form to utility personnel required 30 minutes to an hour per Unit to complete.

Please send your completed survey forms by June 22, 1990 by mail or FAX to:

Jack Hayes
U. S. Nuclear Regulatory Commission
Washington, D. C. 20555
FAX Numbers (301) 492-0259, 492-0260, 492-1137
FAX Verification Number (301) 492-0262

If there are any questions concerning the completion of the survey, please telephone the above at (301) 492-1456 between the hours of 6:45 A. M. and 4:30 P. M. Eastern Daylight time.

Your cooperation in this survey is greatly appreciated.

PLANT NAME _____

ENGINEERED SAFETY FEATURE VENTILATION SYSTEM (CIRCLE AND COMPLETE THE SURVEY FORM FOR EACH APPROPRIATE SYSTEM)

ANNULUS VENTILATION
CONTROL ROOM
STANDBY GAS TREATMENT SYSTEM
FUEL HANDLING BUILDING
CONTAINMENT/REACTOR BUILDING
AUXILIARY BUILDING
EQUIPMENT CUBICLES (MAY BE ECCS PUMP ROOMS)
OTHER (SPECIFY) _____

SYSTEM DESCRIPTION

1. FLOW RATE _____CFM

2. CHARCOAL FACE VELOCITY _____FT/MIN

3. CHARCOAL BED DEPTH _____INCHES

4. LATEST VALUE OF LICENSEE ASSUMED CHARCOAL ADSORBER REMOVAL EFFICIENCY IN DOSE ANALYSIS CALCULATION IN SUPPORT OF AMENDMENT REQUEST, OPERATING LICENSE, ETC., APPROVED BY THE NRC _____% DATE OF SUBMITTAL _____

5. ARE ELECTRICAL HEATERS USED TO REDUCE RELATIVE HUMIDITY TO 70% OR LESS? YES NO

6. CHARCOAL ADSORBER REMOVAL EFFICIENCY CREDITED IN LATEST NRC SAFETY EVALUATION _____%
DATE OF ISSUANCE IF DIFFERENT THAN ORIGINAL SAFETY EVALUATION ISSUED FOR THE OPERATING LICENSE _____

I. EXISTING TECHNICAL SPECIFICATIONS

A. CHARCOAL ADSORBER TEST METHOD (CIRCLE APPROPRIATE TEST METHOD)

ASTM D3803-1979 ASTM D3803-1986

ASTM D3803-1989 RDT M16-1T-1973

RDT M16-1T-1977 RDT M16-1T-1972

OTHER (SPECIFY) _____

B. TEST CONDITIONS

1. TEMPERATURE (CIRCLE)

25 C 30 C 80 C 130 C

OTHER (SPECIFY) _____

2. RELATIVE HUMIDITY (CIRCLE)

70% 95% OTHER(SPECIFY)_____

3. ACCEPTANCE CRITERIA (RESPOND TO a OR b BELOW ONLY)

a. ALLOWABLE PENETRATION (CIRCLE)

0.175% 0.2% 1.0% 5.0% 10.0%

OTHER (SPECIFY) _____

b. REMOVAL EFFICIENCY (CIRCLE)

99.825% 99.8% 99.0% 95.0%

90.0% OTHER (SPECIFY) _____

4. PREEQUILIBRATION PERIOD FOR USED CHARCOAL

_____ HOURS

5. FACE VELOCITY

_____ FT/MIN

6. TESTING LABORATORY

_____

C. ADDITIONAL CLARIFYING COMMENTS

_____
_____
_____
_____
_____

II. IF YOU ARE PLANNING TO REVISE YOUR TECHNICAL SPECIFICATIONS FOR THIS SYSTEM, COMPLETE THIS SECTION. OTHERWISE PROCEED TO SECTION III.

A. INDICATE REASON FOR REVISING THE TECHNICAL SPECIFICATIONS:

1. INTERLABORATORY COMPARISON RESULTS OF ASTM D3803 TEST METHOD ("FINAL EVALUATION REPORT FOR THE NRC/INEL ACTIVATED CARBON TESTING PROGRAM", EGG-CS-7653)

2. INFORMATION NOTICE 87-32, "DEFICIENCIES IN THE TESTING OF NUCLEAR-GRADE ACTIVATED CHARCOAL"

3. INFORMATION NOTICE 86-76, "PROBLEMS NOTED IN CONTROL ROOM EMERGENCY VENTILATION SYSTEMS"

4. NUREG/CR-4960, "CONTROL ROOM HABITABILITY SURVEY OF LICENSED COMMERCIAL NUCLEAR POWER GENERATING STATIONS"

5. O T H E R (P L E A S E S P E C I F Y)

_____
_____
_____
_____
_____
_____
_____

B. WHAT REVISIONS ARE YOU PLANNING TO MAKE?

1. CHANGING CHARCOAL ADSORBER TEST METHOD TO: (CIRCLE APPROPRIATE TEST METHOD)

ASTM D3803-1979 ASTM D3803-1986

ASTM D3803-1989 RDT M16-1T-1973

RDT M16-1T-1977 RDT M16-1T-1972

OTHER (SPECIFY) _____

2. CHANGING TEST CONDITIONS TO:

a. TEMPERATURE (CIRCLE)

25 C 30 C 80 C 130 C

OTHER(SPECIFY)_____ __

b. RELATIVE HUMIDITY (CIRCLE)

70% 95% OTHER (SPECIFY) _____

c. ACCEPTANCE CRITERIA (RESPOND TO 1 OR 2 BELOW ONLY)

1. ALLOWABLE PENETRATION (CIRCLE)

0.175% 0.2% 1.0% 5.0%
10.0% OTHER (SPECIFY) _____

2. REMOVAL EFFICIENCY (CIRCLE)

99.825% 99.8% 99.0%

95.0% 90.0%

OTHER (SPECIFY)_____

d. PREEQUILIBRATION PERIOD FOR USED CHARCOAL

_____ HOURS

e. FACE VELOCITY

_____ FT/MIN

C. ADDITIONAL CLARIFYING COMMENTS

_____
_____
_____
_____
_____

III. IF YOU REVISED YOUR TECHNICAL SPECIFICATIONS FOR THIS SYSTEM, SINCE 1/1/86, COMPLETE THIS SECTION. OTHERWISE, GO TO IV.

A. INDICATE REASON FOR REVISIONS.

___ 1. INTERLABORATORY COMPARISON RESULTS OF ASTM D3803 TEST METHOD ("FINAL EVALUATION REPORT FOR THE NRC/INEL ACTIVATED CARBON TESTING PROGRAM", EGG-CS-7653)

___ 2. INFORMATION NOTICE 87-32, "DEFICIENCIES IN THE TESTING OF NUCLEAR-GRADE ACTIVATED CHARCOAL"

___ 3. INFORMATION NOTICE 86-76, "PROBLEMS NOTED IN CONTROL ROOM EMERGENCY VENTILATION SYSTEMS"

___ 4. NUREG/CR-4960, "CONTROL ROOM HABITABILITY SURVEY OF LICENSED COMMERCIAL NUCLEAR POWER GENERATING STATIONS"

___ 5. O T H E R (P L E A S E S P E C I F Y)

_____
_____
_____
_____
_____

B. WHAT REVISIONS WERE MADE?

1. CHARCOAL ADSORBER TEST METHOD CHANGED TO: (CIRCLE APPROPRIATE TEST METHOD)

ASTM D3803-1979 ASTM D3803-1986

ASTM D3803-1989 RDT M16-1T-1973

RDT M16-1T-1977 RDT M16-1T-1972

OTHER (SPECIFY) _____

2. TEST CONDITIONS CHANGED TO:

a. TEMPERATURE (CIRCLE)

25 C 30 C 80 C 130 C

OTHER (SPECIFY)_____

b. RELATIVE HUMIDITY (CIRCLE)

70% 95% OTHER (SPECIFY) _____

c. ACCEPTANCE CRITERIA (RESPOND TO 1 OR 2 BELOW ONLY)

1. ALLOWABLE PENETRATION (CIRCLE)

0.175% 0.2% 1.0% 5.0%

10.0% OTHER (SPECIFY) _____

2. REMOVAL EFFICIENCY (CIRCLE)

99.825% 99.8% 99.0%

95.0% 90.0%

OTHER (SPECIFY) _____

d. PREEQUILIBRATION PERIOD FOR USED CHARCOAL

_____ HOURS

e. FACE VELOCITY

_____ FT/MIN

C. ADDITIONAL CLARIFYING COMMENTS

_____

_____

_____

_____

_____

_____

IV. INDIVIDUAL TO CONTACT

NAME _____

TITLE _____

TELEPHONE NUMBER ( ) _____

TIME REQUIRED TO COMPLETE FORM (HOURS PER UNIT) _____

DISCUSSION

ORNBERG: We dealt with a number of different plants and have seen the variation in all the tech. specs. across all the systems. There is a great deal of confusion out there. I guess one of the questions I hear from many of the plants is that they are not sure where this should start; who should start first in this change. It is obvious that many of the technical specifications go back to the early and mid 1970s, and that there was even more confusion back then. We know a lot more now. My first question is, can or should the NRC do something with regard to a generic technical specification change? Every time I have been involved in discussions people shudder at that thought. If you are a single licensee and proposing something that even smells of a generic technical specification change, there is some ominous cloud that hangs over the discussion at that point. Can you elaborate on that or describe the process that you have to go through with a generic technical specification change?

HAYES, J.: I am most familiar with the Westinghouse process for a generic technical specification change which involves the technical specification upgrade program. I think the review is supposed to be completed sometime in October of this year. Westinghouse owners group made a submittal that is being reviewed. I believe North Anna is the plant undergoing the initial review. In answer to your question whether the NRC should be initiating generic technical specification changes, one of the problems I have had and the licensees have had, is that the technical specifications are not specific enough in this area. In other words, it does not spell out the test conditions, the acceptance criteria, or the method to be utilized. What I have suggested to licensees is that they come forward and request technical specification changes. I do not believe they would have to come forward on a generic basis to go through the CR GR process. I think they could do this on an individual basis without going through the CR GR process and be successful.

ORNBERG: You would be looking at 100 different plants going through this individual process. There would be confusion among the utilities concerning test conditions. It seems to me more efficient for the NRC to send a letter to all of them to suggest technical specification changes and explain to all the utilities that this type of change is looked upon favorably by the NRC. That would initiate the process.

HAYES, J.: The results of this study became available two weeks ago. When passed up to the management chain for review, the ultimate boss for Regulatory Guide projects, Jim Partlow, had this question, "What are we willing to do about this." You may be right, we may be coming out with a generic letter with respect to this item. Obviously, we have a potential for a creditability problem. We have designed systems for certain efficiency and we have assumed that efficiency in our accident evaluations. If charcoal is not capable of performing at that level, we have to correct the situation.

USNRC REGULATORY GUIDANCE FOR ENGINEERED SAFETY FEATURE AIR CLEANING SYSTEMS

Dr. Ronald R. Bellamy
U. S. Nuclear Regulatory Commission
475 Allendale Road
King of Prussia, Pennsylvania 19406

Abstract

The need for clear, technically appropriate, and easily implementable guidance for the design, testing, and maintenance of nuclear air cleaning systems has long been recognized. Numerous industry consensus standards have been issued and revised over the last 30 years. Guidance has also been published by the U. S. Nuclear Regulatory Commission in the form of regulations, regulatory guides, standard review plans, NUREG documents, and information notices. This paper will summarize the latest revisions to these documents and emphasize Regulatory Guide 1.52, "Design, Testing, and Maintenance Criteria for Post-Accident Engineered-Safety-Feature Atmosphere Cleanup System Air Filtration and Adsorption Units of Light-Water-Cooled Nuclear Power Plants," which was last revised in 1978. The USNRC has undertaken a project to revise this regulatory guide, and the status of that revision is highlighted.

Introduction

One of the primary means for the U. S. Nuclear Regulatory Commission to distribute guidance is by publishing regulatory guides. Regulatory guides are documents issued by the NRC staff to describe and make available to the public methods acceptable to the NRC staff of implementing specific parts of the Commission's regulations, to delineate techniques used by the staff in evaluating specific problems or postulated accidents, or to provide guidance to applicants. It is important to note that regulatory guides are not substitutes for regulations, and compliance with them is not required. Methods and solutions different from those set forth in regulatory guides will be acceptable if they provide a basis for the findings requisite to the issuance or continuance of a permit or license by the NRC. However, regulatory guides are considered to be of sufficient importance that safety analysis reports are required to contain sections detailing the degree of compliance with applicable regulatory guides. In short, a regulatory guide is one acceptable means of satisfying the NRC's regulations, and this means has been endorsed by the NRC staff.

Comments and suggestions for improvements in all regulatory guides are encouraged at all times. Guides will be revised, as appropriate, to accommodate comments and to reflect new information or experience. Once reviewed and concurred in by the NRC staff, new and revised regulatory guides are reviewed by the NRC's Committee to Review Generic Requirements (CRGR) to ensure that backfit issues are appropriately considered, and by the Advisory Committee on Reactor Safeguards. They will be noted in the Federal Register, and public comments will be explicitly solicited. Comments should be sent to the Secretary of the Commission, U. S. Nuclear Regulatory Commission, Washington, D.C., 20555, Attention: Docketing and Services Branch.

Anyone desiring a single copy of issued regulatory guides should request it in writing to the U. S. Nuclear Regulatory Commission, Washington, D. C. 20555, Attention: Director, Division of Document Control. You may also request placement on automatic distribution for single copies of future guides in any one of ten specific divisions of guides (power reactors, research and test reactors, fuels and material facilities, environmental and siting, materials and plant production, products, transportation, occupational health, antitrust review, and siting). Issued guides may be reproduced.

Engineered Safety Feature Air Cleaning Regulatory Guides

Regulatory Guide 1.52, "Design, Testing and Maintenance Criteria for Post-Accident Engineered Safety Feature Atmosphere Cleanup System Air Filtration and Adsorption Units of Light-Water-Cooled Nuclear Power Plants," is the applicable regulatory guide for engineered safety feature (ESF) air cleaning systems. It was first issued in June 1973. Revision 1 was issued for comment in July 1976, and incorporation of these comments resulted in the issuance of Revision 2 in March 1978. There have been no revisions of the Regulatory Guide since that time. This Guide has proven to be an extremely useful and important document. It is referenced in numerous plant technical specifications and in so doing, becomes a part of the facility license and an enforceable regulation. Most importantly, it has been used as a vehicle to reference numerous industry consensus standards, and emphasize the importance of these standards. Standards and other documents referenced have included:

1. ERDA 76-21, "Nuclear Air Cleaning Handbook"
2. ANSI/ASME N509, "Nuclear Power Plant Air Cleaning Units and Components"
3. ANSI/ASME N510, "Testing of Nuclear Air Treatment Systems"
4. ASTM D3803, "Standard Test Methods for Radioiodine Testing of Nuclear-Grade Gas-Phase Adsorbents"
5. ASTM D4069, "Standards Specification for Impregnated Activated Carbon Used to Remove Gaseous Radioiodine from Gas Streams"

The Need to Revise Regulatory Guide 1.52

The above-referenced documents have been issued in numerous revisions since the last revision of Regulatory Guide 1.52 was issued in 1978. Unfortunately, the Regulatory Guide in some cases refers to specific editions of these documents, and in some cases the Regulatory Guide does not refer to any specific editions. This has caused significant confusion over the last 10 years. Plant technical specifications referring to specific editions of the Regulatory Guide lock the licensee into outdated, inferior documents that must be satisfied. Although this has been acknowledged by the regulatory authorities, no documented position on what guidance to use has been issued. The dilemmas become compounded now that the ASME Committee on Nuclear Air and Gas Treatment has issued (and revised) ASME/ANSI AG-1, "Code on Nuclear Air and Gas Treatment." The need to revise Regulatory Guide 1.52 has been recognized since 1980, and a revision was initiated twice, but never completed. In the summer of 1988, a decision was made to allocate the necessary resources to revise the

Guide, and that effort is ongoing. A number of internal drafts have been generated, and internal comments incorporated. Progress, nonetheless, has not been as fast as anticipated. A draft is not yet available for public comments, although a working paper is in the final stages of development, and is anticipated to be ready in the fall of 1990. When issued, it will be noted in the Federal Register, and public comments will be solicited and welcomed.

Planned Changes

Regulatory Guide 1.52 refers to a significant number of documents, many of which are industry consensus codes and standards. It is a major goal of the upcoming revision to Regulatory Guide 1.52 to refer to the latest issue of each of these documents. This will improve the usefulness of this regulatory guide as a regulatory document and, as importantly, as a vehicle to provide endorsed guidance to the users of the guide, the operators of commercial nuclear power plants, the designers of air cleaning systems, corporations who perform in-place testing, and consultants.

A. Carbon Testing Procedures and Criteria

Committee D28 of the American Society for Testing and Materials is recognized as containing technical expertise with respect to nuclear grade active carbon. ASTM D3803-89 will be referenced as the appropriate testing procedures for radioiodine removal by activated carbon. This is a revised document that incorporates industry comments. In addition, ASTM D4069-90 will be referenced as the appropriate acceptance criteria for laboratory testing of new activated carbon. This revised version of ASTM D4069 conforms to ASTM D3803-89, and although not yet issued, ASTM Society ballots are due August 31, 1990. No negative ballots are anticipated, and ASTM D4069-90 should be available shortly thereafter.

B. Water Sprays and Carbon Wetting Phenomena

The original version of Regulatory Guide 1.52 suggested the use of water sprays on the carbon sections of filter systems to ensure fire extinguishing capability. Revisions 1 and 2 of the Guide acknowledged the possibility of inadvertent activation of the sprays, and discussed other means of adsorbent cooling. Proposed Revision 3 to the Guide substantially augments and expands this discussion. The Guide will clearly indicate that wetting of impregnated activated carbon should be avoided because it establishes conditions for rapid chemical corrosion between the impregnants and stainless steel structural material supporting the charcoal beds. For example, inadvertent actuation of water spray systems or deluge systems may result in the rapid disintegration of stainless steel screens unless the wetted charcoal is removed promptly and replaced with dry material. Thus, water spray or deluge systems should not be used for adsorbent cooling purposes because of the severe corrosion problems which result; however, water deluge systems may be used for fire extinguishment if licensees are aware of the potential implications of system actuation.

Further, the Guide will include provisions for removal of a sample of used carbon and laboratory testing following detection of, or evidence of, penetration or intrusion of water (or other foreign material) into any portion of an ESF atmosphere cleanup system.

C. DOP Toxicity

The potential risk to humans from intake is addressed in Revision 3 to Regulatory Guide 1.52. DOP, an acronym for dioctyl phthalate or di-2-ethylhexyl-phthalate (DEHP), is the standard challenge aerosol used in the testing of HEPA filters. DOP has been considered to be a substance of low toxicity by all routes of human intake. The National Cancer Institute has conducted carcinogenesis bioassay tests on DOP; preliminary findings showed DOP to be potentially carcinogenic in mice and rats but the reports made no determination of risk to humans. At such time as definitive recommendations are made by the National Institute for Occupational Safety and Health (NIOSH), specific guidance on the use of DOP will be issued through the Office of Nuclear Reactor Regulation and through Regional Administrators.

D. Carbon Impregnants

In all revisions to the Guide, activated carbon is assumed as the sorbent material for radioiodine removal. There has not been any specific discussions on the impregnant used to improve radioiodine removal efficiency at high humidities. Typical impregnants used are iodide - or amine - compounds. It has been suggested that the use of potassium iodide-impregnated carbon in primary containment recirculating ESF atmosphere cleanup systems may result in the release of free nonradioactive iodine which could interact by isotopic exchange with the relatively stable Cs131I deposited on containment surfaces in a design basis accident (DBA), making free 131I available in the containment atmosphere and increasing the airborne radioactive iodine fraction. While the existence of such conditions in a DBA has not been conclusively demonstrated, licensees should consider the use of carbons coimpregnated with potassium iodide and a tertiary amine to prevent the potential release of free iodine from the carbon impregnant and to minimize the potential for the formation of airborne radioactive iodine within containment.

E. Department of Defense Qualified Products List

The basic specifications for HEPA filters are contained in two military specifications, MIL-F-51068, "Filter, Particulate, High Efficiency, Fire-Resistant," and MIL-F-51079, "Filter Medium, Fire-Resistant, High-Efficiency." Part of the requirements of these specifications concern listing on the Department of Defense Qualified Products List for HEPA filters installed in commercial nuclear power stations. These requirements need not apply if the manufacturer maintains a quality assurance program consistent with the requirements of Appendix B, "Quality Assurance Criteria for Nuclear Power Plants and Fuel Reprocessing Plants" to 10 CFR Part 50. Therefore, licensees and manufacturers are being given an option for implementing quality assurance for HEPA filters: either have the manufacturer of the filters maintain an Appendix B QA program, or purchase filters listed

on the Qualified Products List. It is important to note, however, that for all activities affecting the safety-related functions of HEPA filters, Appendix B applies.

There are no changes planned to the reference for USDOE filter test facilities.

F. Carbon Testing Definitions

To ensure that there is no misunderstanding on testing required for new activated carbon, proposed Revision 3 to Regulatory Guide 1.52 will clearly specify that each original or replacement batch or lot of impregnated activated carbon used in the adsorber section should meet the requirements for adsorbent contained in Section 5 of ANSI/ASME N509 and in ASTM D4069. In ASTM D4069, a test performed "only for qualifications purposes" should be interpreted to mean a test that establishes the suitability of a manufacturer's product for a generic application, normally a one-time test establishing typical performance of the product. Tests not specifically identified as being performed only for qualification purposes should be interpreted as "batch tests." "Batch tests" are tests to be made on each production batch of product to establish suitability for a specific application.

The definition of batch and lot of activated carbon are taken from ANSI/ASME N509. A "batch of activated carbon" or a "batch of impregnated activated carbon" is the maximum quantity of adsorbent (not to exceed 10 cubic meters) manufactured from the same base material, processed throughout its manufacturing cycle in the same equipment and under the same manufacturing procedures, which can be homogenized at one time in one blending device and for which certified results of appropriate tests of physical and chemical properties are available. This constitutes a "batch" to be presented for radioactive and/or other specified tests under conditions within tolerances specified. A "lot of activated carbon" or a "lot of impregnated activated carbon" is that quantity of adsorbent consisting of one or more batches of the same type and grade, each of which meets the specified performance, physical and chemical requirements, and is shipped to the same purchaser by the same manufacturer for the same job requirement.

G. Allowable Repairs

It is not unusual for leak tests of installed HEPA or carbon banks to fail to satisfy the leak test conditions in the technical specifications. There are repairs that are not acceptable, and repairs that are allowable. HEPA filter banks in ESF atmosphere cleanup systems which fail to satisfy the appropriate leak test conditions should be examined to determine the location and cause of leaks. Repairs, such as alignment of filter frames and tightening of filter hold-down bolts, may be made; however, repair of defective, damaged or torn filter media by patching or use of caulking materials is not permissible in ESF atmosphere cleanup systems and such filters should be replaced and not repaired. HEPA filters that fail to satisfy test conditions should be replaced with qualified filters. After repairs or filter replacement, the ESF atmosphere cleanup system should be retested in accordance with Section 10 of ANSI/ASME N510.

The above process should be repeated as necessary, until the system combined penetration and leakage (bypass) is less than 0.05%.

Adsorber banks which fail to satisfy the appropriate leak test conditions should be examined to determine the location and cause of leaks. Repairs, such as alignment of adsorber cells, tightening of adsorber cell hold-down bolts, or tightening of test canister fixtures, may be made; however, the use of silicone sealants or any other temporary patching material on adsorbers, filters, housings, mounting frames, or ducts should not be allowed. After repairs or adjustments have been made, the adsorber banks should be retested in accordance with Section 11 of ANSI/ASME N510. The above process should be repeated as necessary, until the adsorber bank combined penetration and leakage (bypass) is less than 0.05%.

H. Injection Location for Refrigerant Gas

Numerous questions have arisen with respect to the effect of refrigerant gas on HEPA filters. This question is important when the refrigerant is injected upstream of the HEPAs, in order to obtain adequate mixing or for other space considerations. Revision 3 to Regulatory Guide 1.52 will indicate that it is acceptable to inject a refrigerant gas upstream of a bank of HEPA filters in order to test a bank of adsorbers since it has been shown that prefilters and HEPA filters in the duct have no effect on the refrigerant test gas and that refrigerant gases have no adverse effect on HEPA filters.

I. Frequency of In-Place Testing

Guidance on when leak testing is required has, in the past, indicated that such testing should be performed: (1) initially, (2) at least once per 18 months thereafter, (3) following painting, fire, or chemical release in any ventilation zone communicating with the system, and also for adsorber banks after removal of an adsorber sample for laboratory testing if the integrity of the adsorber system is affected. This guidance will be supplemented in Revision 3 to Regulatory Guide 1.52. Testing will continue to be required initially and once per 18 months, but the 18 month criteria will include "or once per refueling outage." The requirement for testing after painting, fire, or chemical release will include additional guidance to indicate that this testing need be done only if communication with the system occurred in such a manner that the HEPA filters or carbon adsorbers could become adversely affected by the fumes, chemicals, or foreign materials. Testing will also specifically be required (1) after each partial or complete replacement of a HEPA filter bank or of a carbon adsorber in an adsorber section or bank, (2) following detection of, or evidence of, penetration or intrusion of water or other foreign material into any portion of an ESF atmosphere cleanup system, and (3) for adsorber banks following removal of an adsorber sample for laboratory testing if the integrity of the adsorber section is affected.

J. Activated Carbon Decontamination Efficiencies

A major point of discussion with respect to the upcoming revision to the Guide concerns what laboratory tests are required for used carbon, what is the acceptant criteria, and what credit can be assigned (decontamination efficiencies) for accident analyses. Specific test methods in ASTM D3803 will be referenced, with maximum methyl iodide penetrations based on ASTM experience. More specificity will be included in terms of bed depths and relative humidity control.

Summary

The basic document that has been issued by the U. S. Nuclear Regulatory Commission to disseminate approved guidance concerning engineered safety feature air filtration systems is Regulatory Guide 1.52. This guide was originally issued in 1973, and has been revised twice since that time. The latest revision is dated March 1978. Since that time, numerous industry consensus standards have been revised a number of times, and since these consensus standards are referenced quite heavily in Regulatory Guide 1.52, it is clear that this Guide is in need of revision. The USNRC has undertaken a project to revise this Guide that, after two years of effort and internal review, has resulted in a document ready for public comment. It is anticipated this proposed revision will be issued for public comment in the fall of 1990. Although the major change will be to refer to the latest available industry guidance, other clarifications such as the effect of carbon wetting, toxicity of DOP, allowable repairs, frequency of in-place testing, and laboratory activated carbon testing criteria, will also be made.

The USNRC recognizes the importance of Regulatory Guide 1.52, and its impact on the safe operation of nuclear power stations. Public comments will be welcomed, and will be considered prior to the issuance of a final revision.

DISCUSSION

KUMAR: You referred to the efficiencies in Regulatory Guide 1.52. I have a suggestion. Jack Hayes said that with heaters the safety factor is 7 but without heaters it is 5. The safety factor should be linked to a relative humidity that may be obtained with or without heaters. In our case, Davis-Besse, we never see more than 70% relative humidity even without heaters. That does not mean that efficiency will be down without heaters.

BELLAMY: If a licensee could justify to us that their system would never be above 70% relative humidity, i.e., would have the equivalent of heaters, it would be a factor we would consider in our analysis.

EDWARDS: There is no relation between AQA program (10CFR60,B" or NQA-1) and QPL testing. What basis does the NRC have in implying such a mutually exclusive relationship? i.e., that using NQA-1 to manufacture a filter will guarantee that the filter will meet QPL requirements. A clean room filter can be manufacturer to NQA-1.

BELLAMY: The criterion we have used all these years is 10CFR50, Appendix B, Quality Assurance Program. If licensees desire to continue to use that program to qualify their HEPA filters in advance of installation, that is acceptable. The QPL is referenced in two military specifications, and in N510-1978 and N510-1979. A number of us have witnessed these tests at Edgewood and other places and it is the staff's opinion that the program is equivalent to having the manufacturer of the HEPA filters implement an effective Appendix B Quality Assurance Program. That does not eliminate your right, either as a purchaser of a HEPA filter or as a user of a HEPA filter, to visit the manufacturer and conduct an independent QA check.

EDWARDS: A QA program does not do the same thing as a QPL test program. It is entirely different.

BELLAMY: I think that the differences are considered not to be sufficient to affect the performance of the HEPA filter once it is installed in the plant. That is the conclusion that we made.

JACOX: You mentioned, correctly, that in earlier versions of Regulatory Guide 1.52 you referenced specific editions of documents and cited others without a specific edition designation. You did not state what you will be doing in the new edition. Would you comment on that?

BELLAMY: Revision 3 of the Regulatory Guide will specifically reference dates and titles of documents. There has always been a concern on the part of the NRC staff on how to reference consensus standards. I am aware that some consensus standards point out that the latest issued version of a document is acceptable for use. The staff is not comfortable with that and we will continue to reference specific editions of documents.

JACOX: Will that be 100% rather than partial as it is now?

BELLAMY: Yes, that is the goal. If we miss any, let us when you get it.

PATEL: Does proposed Regulatory Guide 1.52 Rev. 3 eliminate the in-place testing of (1) downstream HEPA filters and (2) HEPA charcoal testing following painting, chemical release, or a fire?

BELLAMY: It will not be eliminated.

PATEL: How about testing the downstream HEPA filter?

BELLAMY: It will not eliminate the requirement for testing.

MILLER: I am interested in how you will handle references to consensus standards ASME N509 and AG-1?

BELLAMY: That question came up yesterday morning in another panel. At that time, I said I would address it here. The Regulatory Guide, as now drafted, will reference the latest issues of ASME N509 and N510. There is no mention of AG-1 in that document at the present time. Because this is an on-going project and because we have had many different staff people working on it at different times both at Headquarters and at the Regional Office, the question of referencing AG-1 has not come up yet. By the time we get comments on the proposed revision and resolve all the comments as we are required to do, and conduct our cost benefit analysis, additional sections in AG-1 will have been issued and then there would be an opportunity to reference AG-1.

FRANKLIN: I am referring to the question asked by Mr. Edwards. The 10CFR50 QA Program is not a performance test. It is only an assurance that the manufacturer will reproduce a product to a specification. A QPL program includes a performance test that assures that the product will meet certain performance criteria. I cannot understand how you can connect the two. When you qualify for a QPL designation in order to assure customers that they are getting a qualified filter, the manufacturer has to have a 10CFR QA Program. In either case, a QA program would have to be in place. I think you are saying that if you follow MIL-51068 specifications you don't need to conduct a performance test.

BELLAMY: In my preprint you will find that there are requirements applied in addition to Appendix B, Quality Assurance Program. To say that all you have to do is satisfy Appendix B QA and you then have an acceptable HEPA filter is not what I implied. Your comment is well taken. There is further discussion on this matter in the paper.

IAEA DECADAL ACTIVITIES IN THE FIELD OF RADIOACTIVE GASEOUS WASTE MANAGEMENT

G. R. Plumb
Waste Management Section
Division of Nuclear Fuel Cycle and Waste Management
International Atomic Energy Agency
Vienna, Austria

Abstract

The IAEA has long recognised that gaseous waste management is vital in the design and safe operation of all nuclear facilities such that in the decade of the 1980's the IAEA programme covered the important aspects of the entire field. The activities reviewed in this paper were marked at the outset by a comprehensive international symposium on the subject in February 1980 organised by the IAEA jointly with the Nuclear Energy Agency of the OECD when the detailed state-of-the-art was established in 43 papers. In the interim, experts have been convened in IAEA sponsored meetings to result in sixteen technical documents which included summaries of three substantial Co-ordinated Research Programmes.

Early IAEA activities paid particular attention to management of gas radionuclides which from a matured nuclear industry, could be judged to build-up to long-term sources of irradiation for regional and global populations. The radionuclides of long half-life and capable of widespread dispersion were krypton-85, tritium, carbon-14 and iodine-129. Detailed international studies into capture and retention of the radionuclides initiated in the mid-1970's, had been pursued and enlarged to offer practicable industrial application for the more significant wastes by the mid-1980's.

Mid-term ongoing activities in handling and retention of gaseous radionuclides arising from abnormal operations in nuclear power plants were given much emphasis following the Chernobyl accident. An important Co-ordinated Research Programme on retention of airborne nuclides in nuclear facilities during accident conditions was completed in 1988 leading to an Advisory Group Meeting extending technology to manage the more complex and severe accident conditions at Nuclear Power Plants. The impending technical report is aimed to assist the many Member States presently undertaking decisions on gas treatments for the controlled venting of LWR containments in severe accidents.

In the latter years the IAEA activities included detailed examinations of the design and operation of gas cleaning systems for the range of nuclear facilities. Technical reports on gaseous waste management were issued relating to high-level liquid waste conditioning plants (including control of semi-volatiles), nuclear power plants, low- and intermediate- level radioactive materials handling facilities and radioactive waste incinerators. Notably, there is a comprehensive guide on the practice of particulate filtration throughout nuclear operations, which is awaiting early publication to update an equivalent much-used 1970 report.

I. Introduction

The status of IAEA activities in gaseous waste management and the forward programme were examined at the beginning of the decade in a paper to an international symposium at IAEA Headquarters in Vienna organised jointly with OECD/NEA[1]. The previous IAEA forum dealing specifically with the field was twelve years earlier in New York in cooperation with USAEC and Harvard University[2].

Activities in nuclear gas cleaning technology described at the 1980 Symposium were greatly influenced by the watershed requirements for increased demands for safety efficiency and reliability following the Three Mile Island accident. In turn activities in the latter years were given greatly increased emphasis due to the Chernobyl accident. Priority will no doubt continue to be devoted to treatment of releases from nuclear power plants where the potential extreme source terms under accident conditions present major challenge to gas cleaning systems and demand highest standards of environmental protection.

In the early 1980's, much attention was paid by the IAEA to managing the discharge to the environment of the gaseous radionuclides which owing to build up in the environment from expanding nuclear programmes could be judged to constitute long term sources of irradiation to regional and global populations. The principal radionuclides involved are krypton-85, tritium, carbon-14 and iodine-129, each having long half-life and the capability of widespread dispersion. Excepting for the former, each is intimately involved in life cycle processes. The emissions of the volatile radionuclides were the subject of very broad debate across the international scene and some national regulations were being framed to specify quantitative emission limits for ^{85}Kr and ^{129}I.

International programmes mainly concerning research and development into methods of capture and retention of the radionuclides had been initiated in the mid 1970's, pursued and enlarged to offer industrial application by the mid-1980's. Emphasis had been placed by the IAEA on noble gases, tritium and iodine with reports covering the management strategy and developments in technology to aid in control of routine discharges in compliance with the principles of ALARA for the range of nuclear facilities.

From the mid-1980's, IAEA activities in the gaseous waste management area became directed towards improvement of particulate filtration and radioiodine removal equipment. A Co-ordinated Research Programme (CRP) comparing test methods for particulate filters was followed by another CRP on retention of iodine and other airborne radionuclides under abnormal and accident conditions. Related assessments were also carried out by expert groups and technical reports were issued with early completion of a comprehensive guide into particulate filtration in nuclear facilities outstanding to update a notable 1970 report[3].

During the late 1980's the IAEA activities also included examinations of the design and operation of gas cleaning plants across the range of nuclear facilities with documents on the especial problem of control of semivolatiles in high-level liquid waste vitrification plants, gas cleaning in low- and intermediate-level materials handling and radioactive waste incineration with the specific challenging treatment of the emissions. Gas treatment technology for nuclear power plants however received particular emphasis in a recent Technical Reports Series document with another to be published soon to cover the abnormal operations contributing to the information supporting vital decisions in many Member States on controlled venting of reactor containments under severe accident conditions.

II. Gas Treatment Studies

Krypton-85 Retention

IAEA activities on this fission product noble gas radioisotope (half-life 10.8 y, beta-0.25 MeV, gamma-0.002 MeV) in the nuclear fuel cycle were focused and substantially completed with the early issue of a Technical Reports Series entitled Separation, Storage and Disposal of Krypton-85[4].

Nearly all the inert isotope is discharged to the atmosphere in reprocessing and the growth of nuclear power as then envisaged led to corresponding concern that the accumulation in the atmosphere and the consequent global impact would increase greatly without the commercial scale application of techniques for separation and retention.

The report quantified the emission sources, concentrating on the major arisings in fuel reprocessing but also considered reactor off-gases. The methods and concepts for immobilisation, storage and disposal were reviewed with regard to the radiological hazards. It was concluded that economic commercial scale retention and disposal required further R&D to adapt ordinary cryogenic separation technologies. Advanced concepts including ion implantation process into metallic matrices were developed and demonstrated for safe decay storage.

The Member States with legislation specifically limiting ^{85}Kr emissions (making retention required in large scale reprocessing) are not currently engaged in such reprocessing operations. Present operating or early commercial reprocessing plants do not have routine ^{85}Kr separation and immobilisation units installed. Some further development and design remains outstanding before change in industrial practice can be realised.

Tritium Removal and Handling

In the context of the IAEA programme commenced in the late 1970's attention to the isotope was directed to concentration and separation techniques for tritiated effluents.

Tritium (half-life 12.3 y, beta-0.006 MeV) is formed in reactors through ternary fission and neutron activation of deuterim, lithium and boron in coolants, canning or control components. Tritiated water contamination of effluents is caused particularly from heavy water reactors and reprocessing plants unless especial measures are taken.

The Technical Reports Series document reviewing the need for controls and the technologies available was published in 1981[5]. Continued developments in separation equipment recovery operations and immobilisation process designs were recommended. Techniques for on-line monitoring were not regarded as entirely satisfactory. Subsequent review of strategy and techniques based on the ongoing national and international programmes was recommended. The final report on the Co-ordinated Research Programme on the Handling of Tritium Contaminated Effluents and Waste was published in 1984[6].

Present operating or early large scale commercial reprocessing plants have not applied the voloxidation or isotope enrichment process examined in the first report. The process options based on recycle of tritiated liquid streams in reprocessing to confine the isotope in highly active head-end and HLW acid recovery operations have been importantly progressed for some plants. However, many drawbacks foreseen in the IAEA reports have been confirmed so that the advances in tritium management in reprocessing plants to achieve isolation and immobilisation of this radionuclide have not progressed to commercial application.

Iodine Removal and Treatment

The management of radioiodine was evaluated by IAEA expert groups in two main directions namely the control of short-lived isotopes principally ^{131}I (half-life 8 d) of concern in reactors and the control of long-lived ^{129}I (half-life 1.7×10^7 y) of concern in emissions from reprocessing plants.

Activities relating to the management of were reported first in 1980[7] where methods and scenarios applicable in normal and emergency situations were examined by a Technical Committee. Management of ^{129}I in operations at reprocessing plants was also reviewed considering the technical means of retention, immobilisation, storage and disposal with regard to the radiological hazards. Subsequently the subjects of treatment, conditioning and disposal of ^{129}I including the aspects of management in the contents of unreprocessed spent fuel were reported some seven years later in an IAEA technical report[8]. This took into account the advances in options and the detailed radiological studies in the interim. Control of gaseous emissions through technologies which can be applied to reprocessing dissolver operations was examined. Adsorption or absorption methods were recommended to control doses from gaseous emissions to local populations to safe levels. Alkaline scrubbing of dissolver off-gases was concluded to be an effective gas treatment dependent upon the rigorous limitation of organic material in the dissolving process. The organics limitation in turn influences the recycle of recovered nitric acid and the management modes to be adopted for ^{3}H control.

Semivolatiles Treatment

The contaminants in gaseous effluents from nuclear facilities usually consist of particulates and gases. However, under some circumstances semivolatiles may arise and not be adequately trapped by common devices. These include isotopes of selenium, technetium, ruthenium, antimony, tellurium and caesium. A technical report considered the arisings and control in fuel cycle facilities under normal conditions[9]. Ruthenium was shown to be the most important semivolatile contaminant arising under acidic oxidizing conditions in highly active reprocessing stages and within high-level liquid waste solidification plants. Ruthenium volatilization phenomena were reviewed corresponding to low temperatures involved in high-level liquid waste evaporation and to high temperatures corresponding to subsequent calcination and vitrification. Experience was examined in detail on ruthenium control in gas treatment processes for high-level waste treatment plants.

III. Examinations of Gas Cleaning Systems

High-Level Liquid Waste Conditioning

Member States have undertaken substantial research and development programmes to achieve the removal of volatilised fiss products occurring in nitrogen oxide laden off-gases during the immobilisation of high-level liquid wastes. A Technical Committee reviewed the design and performance of the typical systems and equipment used in the advanced high-level waste treatment plants to lead to publication of a technical report in 1988[10].

Facilities Handling Low- and Intermediate- Level Radioactive Materials

The number of developing Member States constructing new facilities for production and processing of radioisotopes is increasing, making important the provision of the latest comprehensive information on design and operation of suitable off-gas cleaning and ventilation systems. The Technical Reports Series representing the results of an Advisory Group Meeting was published in 1988[11].

Radioactive Waste Incinerators

Treating combustible wastes by incineration potentially leads to the highest volumetric reduction, at the same time converting the waste to inorganic stable residues which may be easily immobilised for geological disposal. The overall advantages of the process are however often not achieved in problematic installations. Secondary wastes including liquid effluents from gas treatment and filters, maintenance and decommissioning wastes arising owing to corrosive off-gas conditions may require to be taken into account.

The incinerator may have to burn a wide range of wastes of variable composition (eg. low or high PVC content, halogen, nitrate or sulphur constituents) so that the selection of incinerator/-off-gas treatment combination has proved complex. To provide essential comprehensive guidance especially for developing Member States, the IAEA sponsored a Technical Committee Meeting in 1984 which was concluded in an appropriately detailed Technical Reports Series in 1989[12].

Testing and Monitoring

A Technical Reports Series reviewing methods, techniques and equipment for testing and monitoring of particulate filters, iodine sorption systems and noble gas delay systems in nuclear power plants was issued in 1984[13]. Most test methods were applied only to the nuclear power plants but many methods were applicable to corresponding systems in other nuclear facilities. No international consensus was determined regarding the use of a particular method as standard or regarding distinction of criteria between accident and normal conditions. Test methods were regarded as requiring development to become capable of demonstrating compliance with accident criteria.

A Co-ordinated Research Programme (CRP) on Comparison of Test Methods for High Efficiency Particulate Air Filters (HEPA) was initiated in 1982[14]. Continuing concern regarding difficulties in assessing the HEPA performance and iodine adsorbers during accident conditions led to the initiation of a further CRP on Retention of Iodine and Other Radionuclides in Nuclear Facilities during Abnormal Conditions. Large components of the programme running from 1983-1988 were necessarily concerned with development of appropriate sensitive test methods for HEPA filters and iodine adsorbers under high temperature, humidity and radiation[15]. Comparison of results from existing HEPA tests under ambient conditions on filter media from a single source with efficiencies less than 99.99% showed no contradictions. Rig methods were developed to indicate that HEPA performance levels for a glass fibre filter material were maintained up to 300°C. Beyond that stage commencement of reduced performance and physical deterioration was observed. The high temperature testing was based on silica or metallic aerosols and further development was proposed.

Particulate Filtration in Nuclear Facilities

Removal of particulate radioactive material by fibrous filters from the atmospheric exhaust is an essential feature of virtually all nuclear installations. A Technical Committee Meeting was held in 1988 to produce a comprehensive 'state-of-the-art' guide to design background, operation, installation, maintenance and testing of nuclear air cleaning filters. Particular emphasis is placed on High Efficiency Particulate Air filters (HEPA) because of the great utility, although other equipment types are given thorough coverage. The immediately impending technical report[16] will succeed the important report on air filters for nuclear facilities widely used since 1970[3].

Design of Systems at Nuclear Power Plants for Normal and Abnormal Conditions

An expert review of the design principles of off-gas cleaning systems for nuclear power plants (NPP) was commenced at an Advisory Group Meeting in 1983 and was concluded in a Technical Reports Series in 1987[17].

Because of the large inventory of fission products in the fuel ($5x10^9$ GBq/GW(e) y) and increasingly demanding airborne radionuclide release limits by Member States, air and process off-gas cleaning technologies were progressing rapidly. Recovery efficiencies were improved whilst at the same time meeting concerns following the TMI accident requiring smaller probabilities of malfunction. The report identified and quantified airborne arisings, reviewed status and trends in design for normal operation and design basis accidents and gave comprehensive guidelines for design of off-gas and air cleaning component and systems for NPP's. Aerosol filtration operations, iodine retention processes and noble gas delay systems were examined for LWR's and other types of reactors.

The trends of the decade necessitating successful handling of airborne radionuclides during even the least probable but most severe reactor accidents were reflected, when following the IAEA CRP on extending gas treatment technology[18], an Advisory Group Meeting was held late 1989. The objective of the last of the series of activities in the decade was a critical review of the design strategies and complex interfaces for the successful mitigation of the consequences from airborne radionuclides in the spectrum of abnormal operations up to severe accidents for NPP's. The report will be completed in the present year.

Conclusions

The IAEA activities in the field of gaseous radioactive waste management continued through the 1980's at the high-level reached from 1978 on. Resurgent emphasis arose initially largely from two directions: firstly from the aftermath of the accident at Three Mile Island with demand for new and improved systems of increased safety, reliability and efficiency particularly in abnormal operations and; secondly from the environmental assessments of the early 1970's which highlighted the relative radiological impacts of the long-lived ubiquitous gaseous fission products ^{3}H, ^{85}Kr, and ^{129}I which are emitted in normal operations from power reactors and reprocessing facilities.

Activities related to the latter were backed by development, essentially leading by the mid-decade to practicable industrial scale systems for retention of ^{129}I which have impacts judged to be the most significant. The activities related to the former were further reinforced by the aftermath of Chernobyl particularly in mitigation measures for controlled venting of power reactor containments in severe accidents. Limited IAEA activities in this direction continue into the next decade and with some development of

gaseous radioactive waste treatment systems to attain increased reliability and efficiency in accident conditions.

Nuclear gas cleaning technology was successfully established during the 1950's and fundamental changes and innovations have since remained steadily progressive. Normal development by manufacturers has been successful in maintaining the status of some equipment, the HEPA filter representing a notable example. The extension of related IAEA activities in the next decade beyond the objective of more robust, passive systems based on present technology may depend upon unforeseen innovations linked with development of new reactor concepts.

References

(1) INTERNATIONAL ATOMIC ENERGY AGENCY, Management of Gaseous Wastes from Nuclear Facilities, Proc. IAEA-OECD/NEA Symp., IAEA, Vienna (1980).

(2) INTERNATIONAL ATOMIC ENERGY AGENCY, Treatment of Airborne Radioactive Wastes, Proc. IAEA Symp. New York, IAEA, Vienna (1968).

(3) INTERNATIONAL ATOMIC ENERGY AGENCY, Air Filters for Use at Nuclear Facilities, TRS Technical Reports Series No. 122, IAEA, Vienna (1970).

(4) INTERNATIONAL ATOMIC ENERGY AGENCY, Separation, Storage and Disposal of Krypton-85, Technical Reports Series No. 199, IAEA, Vienna (1980).

(5) INTERNATIONAL ATOMIC ENERGY AGENCY, Handling of Tritium-bearing Wastes, Technical Reports Series No. 203, IAEA, Vienna (1981).

(6) INTERNATIONAL ATOMIC ENERGY AGENCY, Management of Tritium at Nuclear Facilities, Final Report of CRP on Handling of tritium contaminated effluents and wastes, Technical Reports Series No. 248, IAEA, Vienna (1984).

(7) INTERNATIONAL ATOMIC ENERGY AGENCY, Radioiodine Removal in Nuclear Facilities: Methods and Techniques for Normal and Emergency Situations, Technical Reports Series No. 201, IAEA, Vienna (1980).

(8) INTERNATIONAL ATOMIC ENERGY AGENCY, Treatment, Conditioning and Disposal of Iodine-129, Technical Reports Series No. 276, IAEA, Vienna (1987).

(9) INTERNATIONAL ATOMIC ENERGY AGENCY, Control of Semivolatile Radionuclides in Gaseous Effluents at Nuclear Facilities, Technical Reports Series No. 220, IAEA, Vienna (1982).

(10) INTERNATIONAL ATOMIC ENERGY AGENCY, Design and Operation of Off-gas Cleaning Systems at High Level Liquid Waste Conditioning Facilities, Technical Reports Series No. 291, IAEA, Vienna (1988).

(11) INTERNATIONAL ATOMIC ENERGY AGENCY, Design and Operation of Off-gas Cleaning and Ventilation Systems in Facilities Handling Low- and Intermediate- Level Radioactive Material, Technical Reports Series No. 292, IAEA, Vienna (1988).

(12) INTERNATIONAL ATOMIC ENERGY AGENCY, Treatment of Off-gas from Radioactive Waste Incinerators, Technical Reports Series No. 302, IAEA, Vienna (1989).

(13) INTERNATIONAL ATOMIC ENERGY AGENCY, Testing and Monitoring of Off-gas Cleanup Systems at Nuclear Facilities, Technical Reports Series No. 243, IAEA, Vienna (1984).

(14) INTERNATIONAL ATOMIC ENERGY AGENCY, Comparison of High Efficiency Particulate Filter Testing Methods, Final Report of CRP, IAEA-TECDOC-355 IAEA, Vienna (1985).

(15) INTERNATIONAL ATOMIC ENERGY AGENCY, Retention of Iodine and Other Airborne Radionuclides in Nuclear Facilities during Abnormal and Accident Conditions, Final Report of CRP, TECDOC-521 IAEA, Vienna (1989).

(16) INTERNATIONAL ATOMIC ENERGY AGENCY, Particulate Filtration in Nuclear Facilities, Technical Reports No. (to be published in 1990).

(17) INTERNATIONAL ATOMIC ENERGY AGENCY, Design of Off-gas and Air Cleaning Systems at Nuclear Power Plants, Technical Reports Series No. 274, IAEA, Vienna (1987).

(18) INTERNATIONAL ATOMIC ENERGY AGENCY, Handling and Retention of Airborne Radionuclides at Nuclear Power Plants during abnormal operations, Technical Reports Series No. (to be published in 1990).

CLOSING COMMENTS OF SESSION CO-CHAIRMAN REINERT

From John's paper I think I learned that not everybody has a timely response to guidance and I don't think that is unique to the NRC. All of us know that it exists in almost every area. The important thing that Ron Bellamy told me is he was going to have a draft out by Labor Day. The Guide doesn't apply to me at DOE but I am going to hold him to it. However, if you noticed he didn't say 1990, just "Labor Day". From Jeff Plumb I learned that the IAEA are prolific compared to some of the other agencies. In some ways, that is good but I hope DOE, in particular, doesn't do things like that in the way of standards. We have enough trouble going with the ones they have given us.

SESSION 11

MODELING

Wednesday: August 15, 1990
Co-Chairmen: R. R. Bellamy
J. Pearson

C A I R E

– A REAL– TIME

FEEDBACK SYSTEM

FOR

EMERGENCY RESPONSE –

H. Braun
Federal Ministry for the Environment,
Nature Conservation and Nuclear Safety,
Husarenstr. 30, D-5300 Bonn, FRG

H.D. Brenk, H. de Witt
Brenk Systems Planing
Heinrichsallee 38, D-5100 Aachen, FRG

ABSTRACT

In cases of nuclear emergencies it is the primary task of emergency response forces and decision making authorities to act properly. Whatever the specific reason for the contingency may be, a quick and most accurate estimate of the radiation exposure in consequence of the emergency must be made. This is a necessary prerequisite for decisions on protective measures and off-site emergency management.

With respect to this fact and the recent experience of the Chernobyl accident, remote monitoring systems have increased their importance as an inherent part of environmental surveillance installations in the FRG and in other countries. The existing systems in Germany are designed to cover both, routine operation and emergency situations. They provide site specific meteorological data, gross effluent dose rates, and dose rate measurements at on-site and approximately 30 off-site locations in the vicinity of a plant. Based on such telemetric surveillance net-

works an advanced automatic on line system named CAIRE (Computer AIded Re:ponse to Emergencies) has been developed as a real time emergency response tool for nuclear facilities. This tool is designed to provide decision makers with most relevant radiation exposure data of the population at risk.

All dose assessment models currently used in cases of emergencies are associated with appreciable uncertainties. Due to error propagation these uncertainties may lead to increasing divergence between model calculations and reality with increasing duration of the event if the calculations are not controlled by environmental measurements.

In order to minimize this deficiency CAIRE allows the continuous feed-back of current measurements of environmental impacts into diagnostic calculations for bringing measurements and calculations into best correspondence.

This is the main advantage of CAIRE compared to conventional emergency systems and it results in both, a consistent actual interpretation of a bulk of single measurements of dose rates and/or activity concentrations, and a more realistic set of model parameters. Subsequently these parameters are used as input data for the evaluation of actual dose commitments and projections of them by means of real-time calculation.

A second advantage is a more realistic assessment of the source term if in-plant dose rate measurements are not available due to emissions out of leckages, e.g. In such cases the assessment of the source term can be based on off-plant dose rate measurements located on the ground within a source distance between 200 and 300 m.

A further advantage: CAIRE can also be operated as a simulator for personnel training and emergency response exercises.

The development phase of CAIRE has already been finished. CAIRE is now in an operational status and available for applications in emergency planning and response.

1. BASIC PROBLEMS OF DECISION MAKERS

In cases of nuclear emergencies it is the primary task of emergency response forces and decision making authorities to act properly. Whatever the specific reason for the incident or the accident may be, quick and most accurate analyses of the actual and future exposure situation in the endangered area must be made. This is an unalterable prerequisite for appropriate protective measures in due course.

With respect to this, model calculations have the advantage to supply consistent interpretations of possible radiation impacts in consequence of an emergency. Thus they do be able to improve decision making significantly. The use of model calculations as a basis for decision making processes, however, is not sacisfactory. This is the case for two reasons. First, their assessment certainties are limited, and, second, the results of model calculations can only be relevant for decision making if they are supplied in real-time.

If we assume a bandwidth of about one order of magnitude to differenciate between various possible protection measures, such as

- sheltering
- ingestion of iodine tablets,

or

- evacuation,

the assessment certainty of model calculations must be significantly smaller.

This requirement, however, cannot be obtained by model calculations alone.

On the one hand this is caused by the limited assessment certainties of partial models of Fig. 1. On the other hand, due to error propagation the assessment certainty of model calculations may principally decline with increasing duration of the emergency. Hence, the deviation between model calculations and reality may grow uncontrolled. This is the case for each model calculation if it is not made conform to the true situation from time to time.

With respect to the partial models, Fig. 1 shows the greatest uncertainty for the assessment of source terms (up to 4 orders of magnitude). This uncertainty is not in contradiction to the variability of real emissions caused by the nuclear accidents in Harrisburg, Windscale and Chernobyl, cf Tab. 1.

Table 1: Bandwidth of real emissions during nuclear accidents

Released Total Activity (Bq)	I-131	Cs-137
Harrisburg (a)	6.3×10^{11}	very small amounts
Windscale (b)	7.4×10^{14}	2.2×10^{13}
Chernobyl (b)	1.7×10^{18}	8.9×10^{16}

(a) Facility with containment

(b) Facility without containment

CONVENTIONAL WAY OF DOSE PROJECTIONS

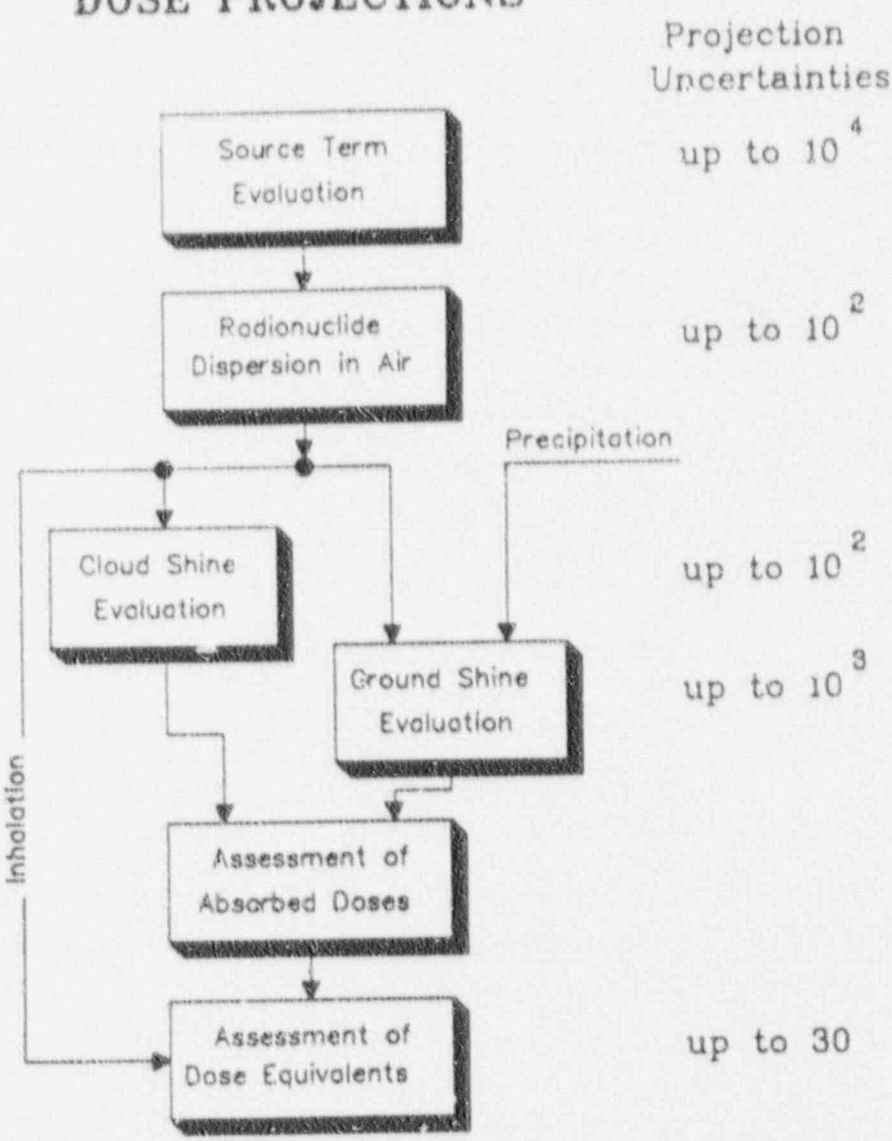

Fig.: 1

Uncertainties involved in dose assessments for the early phase after nuclear accidents

BS

In contrast to this, the inherent uncertainties of the other partial models, for atmospheric dispersion and deposition as well as for the dose evaluation models, are of lower importance.

Because of the deficiencies of model calculations explained above, one may conclude to base decisions preferably on measurements of dose rates and activity concentrations both, in air and on the ground.

But even this is not satisfactory. In fact, measurements are free of greater uncertainties. Their decisive disadvantage, however, is the fact that they are only available after activity has been released to the environment. Difficulties in decision making processes are also raised by the fact that measurements are only available at discrete, possibly less representative points. Additionally, the measurements are not necessarily synchronized, and usually comprehend only single exposure pathways. Moreover, in cases of superposition of several radiological effects it is difficult to accomplish equivocal associations.

Thus, an optimal real-time evaluation of a growing amount of measurements, differnet in their physical character and taken at various locations and time periods is hardly possible without support of interpolating model calculations. This is especially true with respect to the psychological stress to which decision makers may be exposed in real emergency situations.

Apart from the real-time problem, the advantages and disadvantages of model calculations and measurements are essentially complementary. It is self-suggesting, therefore, to merge the two decision aids in such a way that the deficiencies of each aid are compensated and all available information is used in the best way possible.

This combination can be realized by a systematic and continous feedback of actual measurements into diagnostic model calculations in order to bring calculations and measurements in best correspondence, and to supply consistent information about the actual exposure situation in the endangered area. Additionally, this procedure also forms the best bases for further projections of the radiological situation.

As mentioned before already, decision makers do not wait. Therefore, all decision relevant information have to be supplied in real-time, i.e. before any decision is necessary and before significant changes of the radiological situation may accur.

2. DEVELOPMENT OF CAIRE

2.1 Introduction

In order to meet the main objectives (feedback and real-time) explained above an advanced emergency guidance system for real-time applications and personnel training, named CAIRE (Computer AIded Response to Emergencies), has been developed. It is an emergency response tool originally based on a feedback procedure in connection with telemetric networks. It can also be operated, however, with the aid of field team measurements and a combination of both.

The main tasks of CAIRE are diagnoses and projections of radiation exposure, guidance of field teams and personnel training for exercise purposes. These objectives have been realized in two steps:

First, in a feasibility study [1] it was shown that on-line model-based consistent interpretation of surveillance measurements by feeback of them into model calculations is possible in real-time. Appropriate numerical tools had been developed to meet the objectives of sufficiently fast convergence of the adaption procedures, and the accomplishment of considerable reduction of uncertainties in emergency dose projections, cf. [2], [3].

All calculation procedures developed within the scope of the feasibility study mentioned above, however, necessitated an expensive high capacity computer to remain them within the obligatory real-time period of 10 minutes. This was a serious deficiency with respect to practical application of the system in monitoring networks.

Therefore, a second step of development was iniciated in order to meet the following principal objectives:

- evaluation of an operable feedback system

  and

- optimization of the existing software and hardware to accomplish real-time and economic requirements.

2.2 Realization of Feedback

Refering to the explanation of feedback in chapter 1, CAIRE has a special software modul, where the integration of measurements of activity concentrations, dose rates and/or ground contaminations into model calculations takes place, cf Fig. 2. Key element of this modul is the iterative adaption procedure being illustrated by the control circle in Fig. 2: Starting with initial values of model parameters for each time step, the system systematically adapts the calculations of absorbed doses to the corresponding measurements. This is done by variation of the model parameters until the difference between calculated and measured values becomes a minimum. The variations are automatically executed on the basis of a particular variation strategy considering the rank of sensitivity of each parameter. This strategy distinguishes between the assessment of the source term and the determination of other dispersion and deposition parameters.

First, the source term can be assessed by detecting gamma rays at monitoring stations near the plant within 200 m to 300 m of

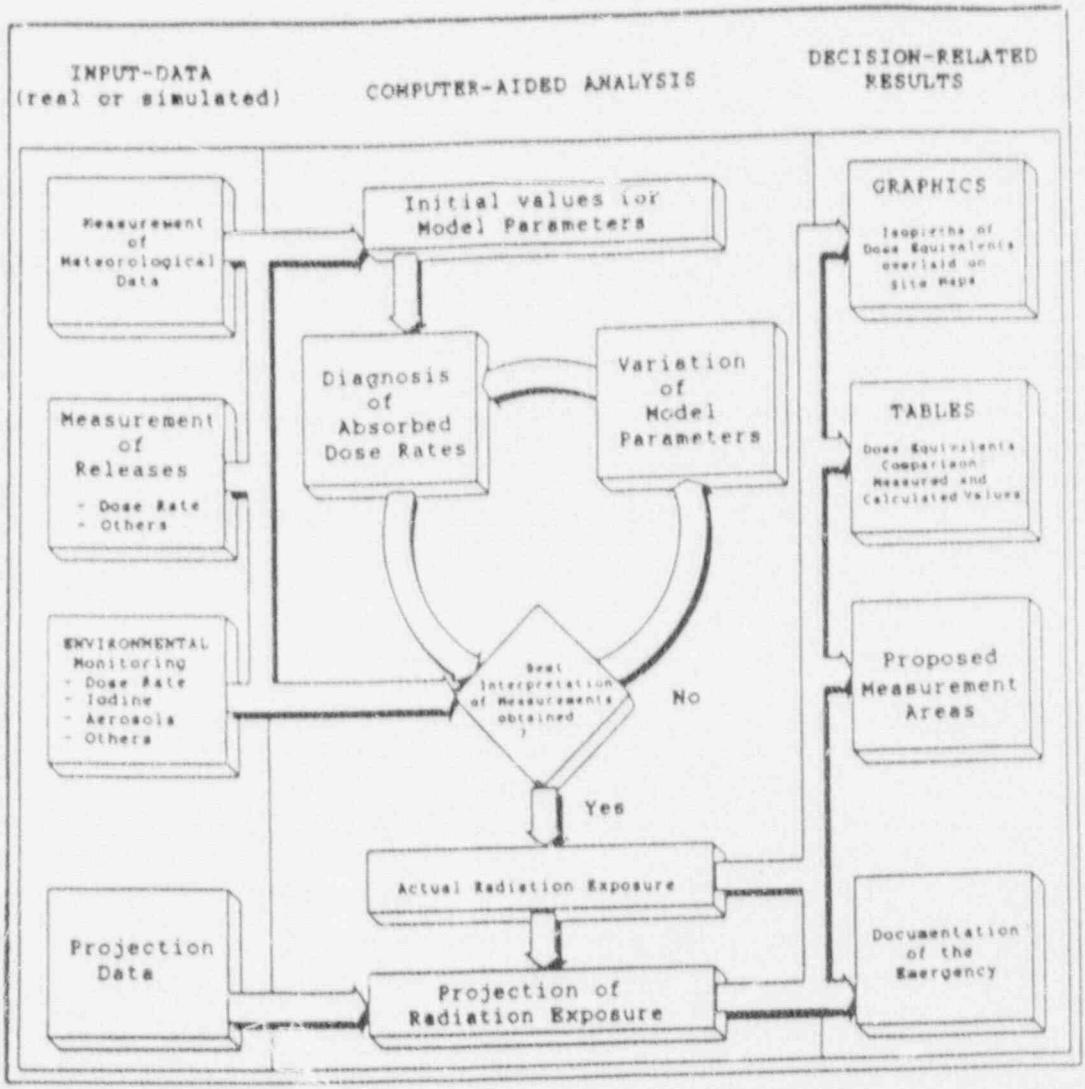

Fig.: 2 Logical scheme of CAIRE

distance. This assessment is independent of the meteorological dispersion model used and the current weather situation, because the mean free path way of the decisive photons in air is in the range of hundred meters.

Our numerical experience shows, that 5 stations in a source distance of 200 m to 300 m are enough to determine the source term within an accuracy of one order of magnitude.

In a second step of the variation strategy the rest of the model parameters is evaluated by adapting the calculated values of dose rates and activity concentrations to the corresponding measurement values. In doing so the strategy also ensures that physical contradictions with respect to the finally selected set of parameters are avoided.

The adaption procedure is repeated each time step and results in both, a consistent actual interpretation of a bulk of single measurements, and a more realistic set of model parameters, including the source term. Subsequently these parameters are used to evaluate actual dose commitments of population at risk. Based on this dose projections can be calculated.

The outputs of these calculations are supplied in form of color graphics, tables and guidance information for field teams. Additionally, all emergency data are stored for perpetuation of evidence, and later investigations.

2.3 Realization of Real-Time

The accomplishment of real-time calculations was possible under the following main conditions:

- choice of an analytical puff-trajectory dispersion model for describing the time-deperdent activity concentration in air and subsequent ground deposition,

- analytical approximation of the necessary time and volume integrations to evaluate gamma - submersion doses,

- use of parallel processors, called transputers, for enlarging the computation capacity.

For the selection of an instationary air dispersion and deposition model allowing for changing weather conditions a lot of more or less co' lex, numerical dispersion models were available which could pri...ipally be applied in this connection. The requirement, however, to keep the computational time within the permissible scope of 10 minutes, severely restricted the number of convenient models. Therefore a quasi-instationary analytical Gaussian puff-type dispersion model is used as a reasonable approximation to solve the problem. This model has been developed by GEISS et. al., cf. [4] and [5]. Its analytical character allows relatively short computation times.

A further condition to realize the real-time calculations in CAIRE was a substancial reduction of computing time for the evaluation of the cloud shine factor. This aim was obtained, first, by quasi-analytical integration over a cloud configuration being maximally combined by 50 single Gaussian puffs.

Second, for the integration over the exposure time a procedure has been developed allowing the evaluation by using 3 to 7 bases, generally. The resulting accuracy for this procedure lies between 10 and 20 %.

Compared to the former conventional numerical solution of the volume and time integral the new procedure allowed an acceleration of computing time of about 4 orders of magnitude.

Even this enormous reduction of computing time was not sufficient to supply all necessary calculations, tables and graphics in real-time. Therefore a third condition concerning the hardware had to be satisfied.

A realization on main frames was out of question because of their expensiveness and relatively low availability due to their multi-user operation systems and the obligatory long distance data transmissions.

A solution of the problem on a micro computer in connection with a net of transputers, however, had the advantage, to be reasonably prized and shows high availability. Beyond this, the complete system of software and hardware forms a complete self-contained unit which can be individually designed for each user.

In order to take sufficient profit of the application of transputers it was necessary to considerably parallelize the calculation procedures. This leads to a further advantage of transputer applications. As the data processes are not bound to certain individual transputers, it is possible to enlarge the transputer net with the objective of accelerating the calculation or the graphic processes in order to keep them within real-time.

The application of transputers resulted in an additional decrease of the computation time of about one order of magnitude so that, over all, 5 orders of magnitude have been obtained to meet the real-time requirements of CAIRE.

3. FINAL REMARKS

Complex decision making processes in emergency situations, with most of the decision makers under extreme psychological stress and pressure of time, can significantly be improved by support of real-time feedback systems. This is the case, first, because systematic feedback of actual measurements into the analytical calculations ensures more accurate diagnoses of the actual exposure situation in the endangered area, and hence form the best possible basis for dose projections. Second, the results of the analyses of the system are available within time periods sufficiently short to contribute to reducing the load of time pressure to decision makers.

These improvements have been accomplished for the first time in the advanced emergency guidance system CAIRE, which can also be used for personnel training. The system is operable now and can either be directly connected to telemetric networks being installed around nuclear power plants or adapted to the proceedings of mobile field teams or a combination of both. It checks and processes all input data both, on-site and off-site, and supplies all decision-related results in a sufficiently condensed user-orientated manner.

For the time being CAIRE shows good performance for cases of simple orographic terrain up to source distances of about 30 km. In cases of more complex orography the dispersion model used has to be completed, at least by a wind field model in order to consider the influence of hills, mountains and valleys. This increases the number calculations and thus the computation time substancially. Appropriate performance tests are under way.

References

[1] de WITT, H.; BRENK, H.D.; KRUSCHEL, K.-P.; KNAUP, A.G.

OLDES - ein KFÜ-integrierbares System zur Diagnose und Prognose der Strahlenexposition bei erhöhten Emissionen aus kerntechnischen Anlagen

BS-Report No. BS 8205/1, Aachen, Dez. 1985, ISBN 3-924329-10-9

or BMU-1986-135, Der Bundesminister für Umwelt, Naturschutz und Reaktorsicherheit, Schriftenreihe Reaktorsicherheit und Strahlenschutz, ISSN 0724-3316

[2] BRENK, H.D.; de WITT, H.; KNAUP, A.G.; KRUSCHEL,K.-P.

OLDES - An Advanced Real-Time Emergency Response Tool for Nuclear Facilities

Paper presented at the Joint OECD (NEA)/CEC Workshop on Recent Advances in Reactor Accident Consequence Assessment, Volume II, p. 310, Rome 25/29 January 1988

[3] de WITT, H.; BRENK, H.D.; KNAUP, A.G.; KRUSCHEL, K.-P.

Real-Time Emergency Computations for Nuclear Installations

Paper presented at the CEC-2nd International Real Time Workshop in Luxembourg, 16th - 19th May 1989, Volume 2, p.101

[4] GEISS, H.

Ausbreitung von Schadstoffen in der Atmosphäre

KTG-Seminar Band 1, Verlag TÜV-Rheinland, Köln 1983, ISBN-3-88585-127-X

and

Anwendung von einfachen und weiterentwickelten Gaußmodellen

Atomwirtschaft, Juli/August 1983

[5] STRAKA, J.; GEISS, H.; VOGT, K.J.

Diffusion of Waste Air Puffs and Plumes under Changing Weather Conditions

Contributions to Atmospheric Physics, Vol. 54, Nr. 2, May 1981

DISCUSSION

BELLAMY: I would like to ask Mr. Braun if a copy of this computer simulated code would be available to us here in the United States, and if so how would we go about getting hold of a copy of it?

BRAUN: Principally the computer code is available in the United States. If there is real interest on your side, please, directly address either to me or Brenk Systems Planning, Heinrichsallee 38, D-5100 Aachen, FRG.

DORON: I want to ask about the meteorology. You mentioned that the model is useful after about 30 kilometers. Do you have provisions to enter a changing meteorology in the region or do you only have one meteorological station to represent the whole area?

BRAUN: I think the validity of the model for source distances greater than 30 km is a misunderstanding on your side. I mentioned that the meteorological dispersion model is a Gaussion-Puff-Trajectory model. The model is used in correspondence with the monitoring network around the nuclear power plants, usually up to source distances of 30 km. It is not a regional dispersion model.

With respect to your question concerning the meteorology: the model allows for changing weather conditions. In cases of simple flat terrain one meteorological station may be sufficient. For more complex terrain more than one station can be incorporated in windfield calculations.

DORON: So you have to use a model to get the wind field? You cannot enter meteorological data from different points in the field?

BRAUN: Meteorological data from more than one meteorological station can be incorporated in wind field evaluations. The number of available meteorological data depends on the site where the system CAIRE is used.

SCHOLTEN: I am sure that is a good program, but you need a very complicated computer system for CAIRE and also input from outside. Would it not be better to have a simpler code so that you can use a P.C. system that you can find in any average working office?

BRAUN: First: the system CAIRE does not need any main frame computer. It simply runs on a P.C. extended by transputers.

Second: the measurement input from outside is supplied by already existing telemetric networks. Thus the code is used, in a first step, for diagnostic purposes, i.e., the diagnostic calculations incorporate all measurements from various locations and various time intervals to interpret them in a comprehensive form with respect to the value of object, the equivalent dose. In this way it is made sure that the calculations reflect the real actual exposure situation as exactly as possible. Among others, this procedure allows to evaluate the source term only on the bases of emission measurements. This is important for otherwise undetected airborne leakage from the plant. This would hardly be possible with such a simple instrument you mentioned.

SCHOLTEN: In the Netherlands we have simpler codes. You rely on a technical system.

BRAUN: For decision makers the correct analyses of the actual and future exposure situations of the public is much more important than simple codes.

SCHOLTEN: The point I am making is that your decision makers have to rely on sophisticated computers. Isn't it better to have simple codes that can be run on any kind of office computer?

BRAUN: What would your reaction be if the results of your simple code are completely different from the actual measurement in the field. A more sophisticated code with feedback technique, like CAIRE, is designed to make sure that this situation cannot happen.

KINETIC MODELLING OF THE PURGING OF ACTIVATED CARBON AFTER SHORT TERM METHYL IODIDE LOADING

V. Friedrich
Institute of Isotopes
of the Hungarian Academy of Sciences
H-1525 Budapest, P.O.Box 77.
Hungary

and

I. Lux
Central Research Institute for Physics
of the Hungarian Academy of Sciences
H-1125 Budapest, Konkoly Th. M. ut 29-33.
Hungary

Abstract

A bimolecular reaction model containing the physico-chemical parameters of the adsorption and desorption was developed earlier to describe the kinetics of methyl iodide retention by activated carbon adsorber. Both theoretical model and experimental investigations postulated constant upstream methyl iodide concentration till the maximum break-through.

The work reported here includes the extension of the theoretical model to the general case when the concentration of the challenging gas may change in time. The effect of short term loading followed by purging with air, and an impulse-like increase in upstream gas concentration has been simulated.

The case of short term loading and subsequent purging has been experimentally studied to validate the model. The investigations were carried out on non-impregnated activated carbon. A 4 cm deep carbon bed had been challenged by methyl iodide for 30, 90,120 and 180 min and then purged with air, downstream methyl iodide concentration had been measured continuously. The main characteristics of the observed downstream concentration curves (time and slope of break-through, time and amplitude of maximum values) showed acceptable agreement with those predicted by the model.

I. Introduction

Physical adsorption plays an important role in the retention of gases and vapours by activated carbons even if the performance of the carbon was improved by special impregnants (eg. KI or TEDA for the removal of methyl iodide). It is, therefore, important to understand and model the physico-chemical processes resulting in the retention of airborne contaminants. During the last two decades investigations have been performed on the dynamic character of gas adsorption on granular carbon adsorbents[1,2,3], experimental studies of the influence of various parameters have also been reported[4,5,6]. Experimental investigations have examined charcoal performance for long term operation and within a wide range of conditions including those likely to be encountered following an accident[7,8]. However, such experiments are limited in time and range of parameters, and therefore predictive models can be useful when assessing long term and post- accident behavior.

A bimolecular reaction model containing the physico-chemical parameters of the adsorption and desorption has been developed to describe the kinetics of methyl iodide retention on activated carbon[9,10]. Both theoretical model and experimental investigations postulated constant methyl iodide loading till the maximum break-through. The work reported here includes the extension of the model to such cases when the concentration of the challenging gas changes in time, for example after a short loading period falls to zero, and the adsorbent is then purged with air. This case has been investigated experimentally and the results were compared with the model calculations. The model can also be used to simulate adsorber performance when more subsequent impulse-like inlet concentration changes occur, the results of such calculations are also presented.

II. Theoretical Model

Assuming that the adsorption mechanism can be represented by the reversible processes of adsorption and desorption, a bimolecular reaction model was developed to describe the kinetics of adsorption on activated carbon[9,10]. At constant inlet gas concentrations, an analytical solution was found for low inlet concentrations and a cascade-type numerical method was used for calculations at higher inlet concentrations.

Considering that the condition of constant inlet concentration represents a special case of the adsorption process it was necessary to develop the model for the general case when any change in inlet concentration (whether increase or decrease) may occur.

Let E(z,t) be the concentration of the adsorbed gas molecules at the point z (measured from the inlet point of the adsorption column) and the time t. Furthermore let G(z,t) be the concentration of the propagating gas molecules at z and t and A(z,t) be the density of the active (adsorbing) sites. The evolution of the system is governed by the following relations:

$$\frac{\partial}{\partial t}E(z,t) = k_F G(z,t)A(z,t) - k_B E(z,t) \qquad (1)$$

describes the adsorption-desorption process where k_F and k_B are the respective rate constants. The conservation of the adsorbing sites is expressed as

$$A(z,t) + E(z,t) = A_o \qquad (2)$$

where A_o is the density of the adsorber sites in the absence of adsorbed gas molecules. The system is initially (at t=0)

$$G(0,t) = E(z,0) = 0 \qquad (3)$$

whereas the incoming gas-concentration is fixed as

$$G(0,t) = G_o(t) \qquad t > 0 \tag{4}$$

Finally the conservation of the gas molecules within the column is described by the equation

$$\int_0^z [E(z',t)+G(z',t)]dz' = v \int_0^t [G_o(t') - G(z,t')]\, dt' \tag{5}$$

where v is the velocity of the gas-flow in the column. The l.h.s. of Eq.(5) gives the quantity of gas molecules residing within the section of the column between 0 and z at the time t, whereas the r.h.s. expresses the difference of the gas-quantities entering and leaving the same section.

Differentiation of Eq.(5) yields:

$$\frac{\partial}{\partial t}[E(z,t)+G(z,t)] = -v \frac{\partial}{\partial t} G(z,t) \tag{6}$$

Transforming the coordinates as

$$x = k_F A_o z/v \;,\; y = k_B(t-z/v) \tag{7}$$

and introducing the functions F(x,y) by the relation

$$E(z,t) = A_o \int_0^{k_B(t-z/v)} F(x,y')\, dy' \tag{8}$$

Eqs. (1) through (6) transform to

$$\frac{k_F}{k_B} G(z,t) = \alpha(y) - \int_0^{k_F A_o z/v} F(x',y)\, dx' \tag{9}$$

and

$$F(x,y) = \alpha(y) - \int_0^x F(x',y)\, dx' - [1+\alpha(y)] \int_0^y F(x,y')\, dy' + \int_0^x \alpha(y-x'+x') F(x',y')\, dx' \int_0^y F(x,y')\, dy' \tag{10}$$

w[illegible]

$$\alpha(y, \quad , \quad \frac{}{k_B} \tag{11}$$

the inlet gas concentration. Eqs. (8) through (10) describe the change in space and time of the concentrations in the column. For x=0 and for y=0 Eq.(10) can be solved analytically, e.g.

$$F(x,0) = \alpha(0)\, e^{-x} \tag{12}$$

while in the general case the solution obtained numerically as follows.

The independent variables x and y are discretized as

$x_i = i.(2\Delta x)$ $\quad i=0,1,....N_x$
$y_j = j.(2\Delta y)$ $\quad j=0,1,....N_y$

The following auxiliary quantities are defined:

$$A_{ij} = 1 + \alpha(y_j) \cdot \int_0^{x_i} F(x',y_j)\, dx' \tag{13}$$

$$B_{ij} = 1 - \int_0^{y_j} F(x_i,y')\, dy' \tag{14}$$

Approximating the integrals in Eqs. (10), (13) and (14) by the simple trapezoidal rule and neglecting the term $\Delta x\, \Delta y\, F_{i+1,j}^2$ we have

$$A_{i+1,j} = A_{ij} - \Delta x\, (F_{i+1,j}+F_{ij}) \tag{15}$$

$$B_{i+1,j-1} = B_{i,j-1} - \Delta y\, (F_{i+1,j} + F_{i+1,j-1}) \tag{16}$$

and

$$F_{i+1,j} = [(A_{ij} - \Delta x F_{ij})\, (B_{i+1,j-1} - \Delta y\, F_{i+1,j-1}) - 1] \,/\, [\Delta y\, (A_{ij} - \Delta x\, F_{ij}) + \Delta x\, (B_{i+1,j-1} - \Delta y\, F_{i+1,j-1}) + 1] \tag{17}$$

Eq.(17) is solved successively for every i at a given j value and repeatedly for increasing j's. The initial values F(i,0) and F(0,j) follow from Eq.(12) and the corresponding analytical solution for F(0,y).

In the case of stepwise change in the inlet concentration, i.e. if

$$\alpha(y) = \alpha_k \qquad y_{k-1} < y \le y_k \tag{18}$$

$k=1,2,...$

it can be easily seen that the function F(0,y) changes its values stepwise as

$$F(0,y_k+0) = \alpha_{k+1} + \frac{1+\alpha_{k+1}}{1+\alpha_k}\, [F(0,y_k-0) - \alpha_k] \tag{19}$$

whereas at the time of constant inlet concentration α_k the function evolves as

$$F(0,y) = \exp[-(1+\alpha_k)\, (y-y_{k-1})]\, F(0,y_{k-1}) \tag{20}$$

if $y_{k-1} < y \le y_k$

Thus Eqs. (12), (15), (16), (17), (19) and (20) define a complete iterative solution of Eq.(10) and Eqs.(8) and (9) serve for the reconstruction of the concentrations of interest in case of stepwise variation of the inlet gas concentration.

III. Experimental

The investigations were carried out in a laboratory test apparatus described in Ref. 10. The test bed was filled with Norit RB 1.5 type non-impregnated activated carbon. The challenging gas was methyl iodide vapour, generated by evaporating liquid methyl iodide at controlled temperature and diluted by controlled air flow. The concentration of methyl iodide in the challenging mixture was 3.5×10^{-7} mol cm^{-3}. The temperature of the methyl iodide-air mixture was 50°C, relative humidity was 50%, the temperature of the test bed was also 50°C. The bed depth was 4 cm, diameter 2 cm, face velocity of the air-methyl iodide mixture 3 cm s^{-1}. The carbon was preconditioned at the above temperature and humidity up to constant weight (about 1 hour). After the desired loading period the carbon was purged with air of the same flow rate. The downstream concentration of methyl iodide was continuously measured by gas chromatograph during loading and purging.

IV. Results and Discussion

Results of the theoretical model

As it is shown in section II, Eqs. (8) through (10) describe the gas concentration at any time and in any section of the adsorption column. From practical point of view the concentration at the end of the column (ie. the break-through) is of most interest, therefore the functioning of the model is demonstrated by calculating break-through curves in some typical cases. A computer code based on Eqs. (12) through (20) and the following set of parameters were used for the calculations:

$k_F = 4.0 \times 10^{3}$ cm^{3}mol^{-1}s^{-1}
$k_B = 8.0 \times 10^{-4}$ s^{-1}
$A_0 = 4.0 \times 10^{-3}$ mol cm^{-3}
$v = 3$ cm s^{-1}
$z = 4$ cm

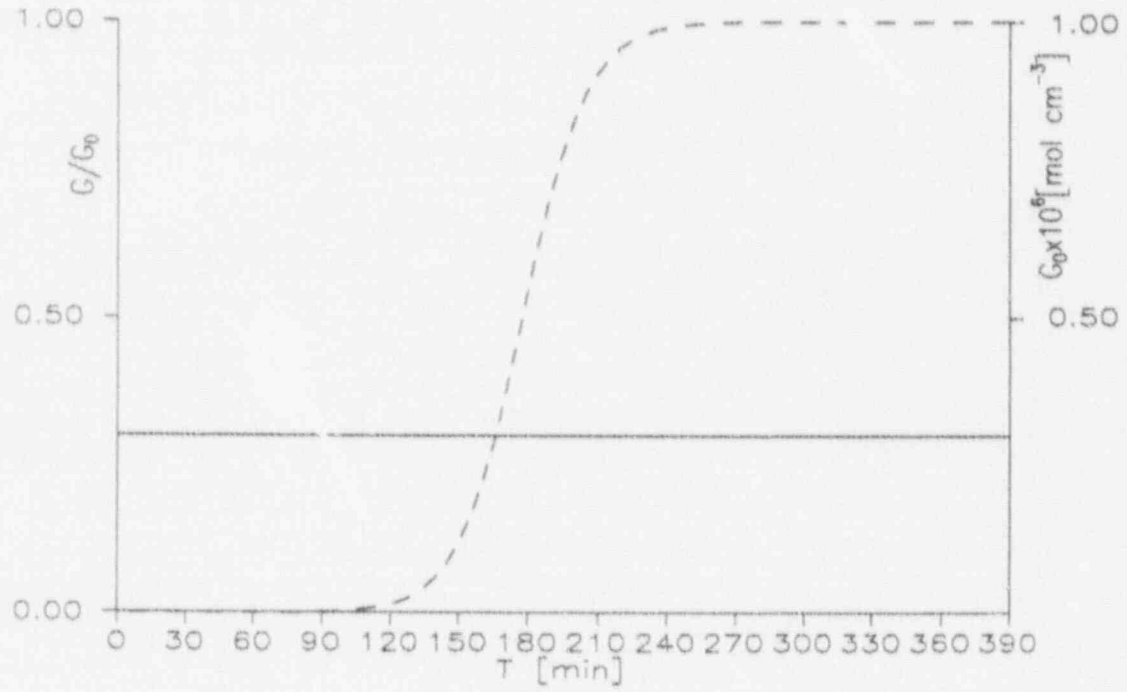

Figure 1. Calculated break-through at constant methyl iodide loading. Solid line: concentration of the challenging methyl iodide vs. time. Dashed line: downstream concentration of methyl iodide vs. time

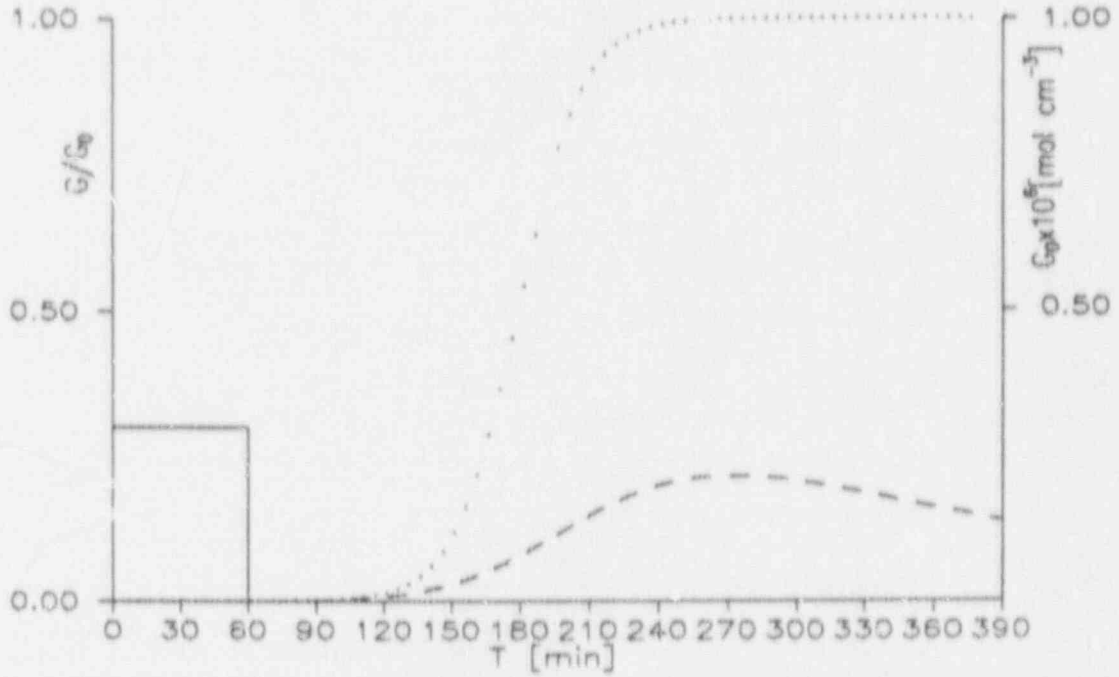

Figure 2. Calculated break-through at 60 min methyl iodide loading followed by purging with air. Solid line: concentration of the challenging methyl iodide vs. time. Dashed line: downstream concentration of methyl iodide vs. time. Dotted line: break-through at constant upstream concentration (see Fig.1).

The first special case is when the adsorption column is challenged by gas of constant concentration. The result of this process, shown in Fig.1, is the well-known break-through curve, determined by the above parameters and the inlet gas concentration[10]

The second typical case is when the adsorber is being loaded during a certain time period and then purged with the carrier gas (eg. air). As it is shown in Fig.2, this process results in the delayed elution of the previously adsorbed gas (dashed line). The delay time, the maximum value and the duration of the discharge depends on the physico-chemical parameters, the concentration of the challenging gas and the loading time (in the given example 3.0×10^{-7} mol cm^{-3} and 60 min, respectively, see solid line). The dotted line shows the break-through if the loading was not interrupted at 60 min.

In the third case the adsorber is continuously challenged and there is an impulse-like increase in the inlet gas concentration for a short time period. It can be seen in Fig.3 that the impulse-like loading of the adsorber does not have a significant immediate effect on the downstream concentration (ie. does not immediately influence the performance of the adsorber) but results in a sooner break-through (see dashed line) compared with the break-through in the case of constant inlet concentration (dotted line).

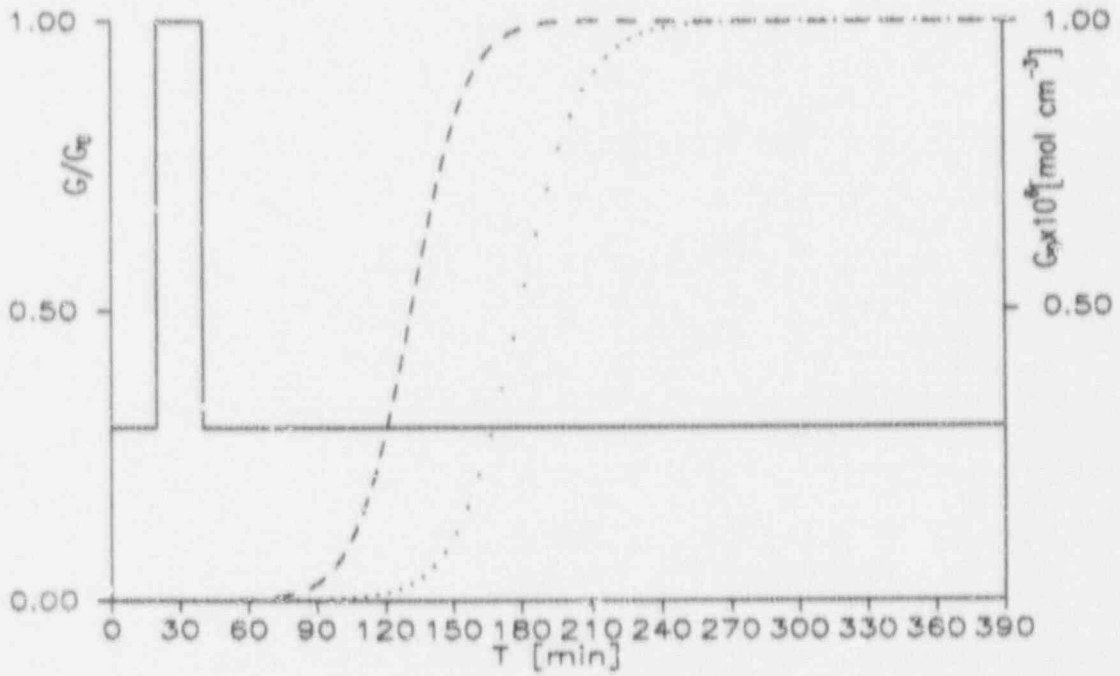

Figure 3. Calculated break-through at constant methyl iodide loading with an impulse-like increase in upstream concentration between 20 and 40 min. Solid line: concentration of the challenging methyl iodide vs. time. Dashed line: downstream concentration of methyl iodide vs. time. Dotted line:break- through at constant upstream concentration (see Fig.1).

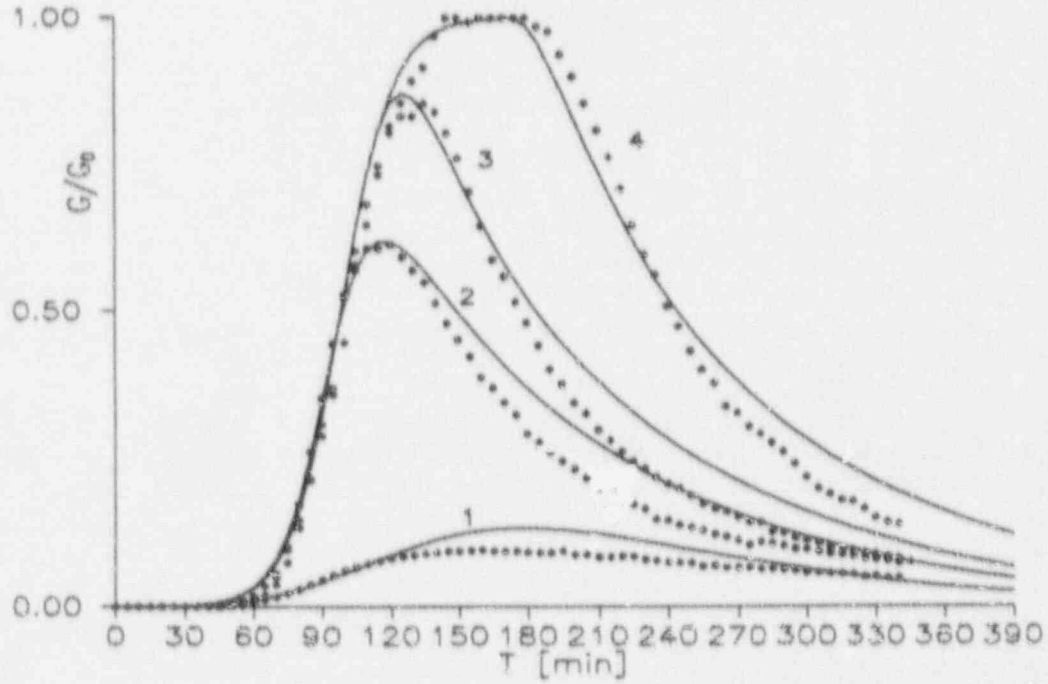

Figure 4. Calculated (solid line) and measured (dotted line) downstream concentrations of methyl iodide at 30, 90, 120 and 150 min methyl iodide loading (curves No. 1, 2, 3 and 4, respectively).

It is to be remarked that the extent and character of the effect (eg. whether just a sooner break through or a peak-type change in the downstream concentration or the combination of both) depends on the time point, duration and amplitude of the inlet concentration impulse.

Comparison of the model with the experimental results

In the course of the experiments the carbon bed was challenged by methyl iodide vapour till a certain time and purged with air afterwards. This procedure corresponds to the second case discussed in the previous section.

The results of the experiments and the corresponding model calculations are shown in Fig.4.

Curves No. 1, 2, 3 and 4 show the downstream methyl iodide concentration during 30, 90, 120 and 180 min loading and subsequent purging, respectively. The dotted lines are measured concentrations divided by the inlet concentration (G/G_0), whereas the solid lines show calculated curves. When calculating the theoretical curves the following procedure was performed:

The values of parameters v, z and G_0 were those set in the experiments (3 $cm\,s^{-1}$, 4 cm, 3.5×10^{-7} $mol\,cm^{-3}$, respectively). A_0 was experimentally determined by measuring adsorption isotherms and using the Langmuir equation for the calculation (a more detailed description of this method can be found in Ref.10). The value of A_0 determined in this way is 2.5×10^{-3} $mol^{-1}cm^{3}$. The values of k_F and k_B were then determined by fitting the iterative solution of Eqs. (6) through (10) on each measured curve, using the method of least squares. Finally, the curves shown in Fig.4 were calculated using the averages of the four k_F and k_B values, respectively:

$$k_F = 4.0\pm0.8 \times 10^{3}\ cm^{3}mol^{-1}s^{-1}$$
$$k_B = 9.0\pm1.0 \times 10^{-4}\ s^{-1}$$

When comparing the measured downstream concentration curves with those calculated by the model it can be established that the model acceptably reproduces the main characteristics of the observed concentration curves (ie. the time and slope of break-through, the time and amplitude of the maximum value), taking into account the experimental error of k_F, k_B, A_0 and G_0. A significant deviation can be observed between the measured and calculated curves at longer purging time, namely the elution of the adsorbed methyl iodide occurs faster than predicted by the model. This deviation exceeds the experimental error and needs further investigation, which may involve the extension of the model with some other processes (eg. pore diffusion, capillary condensation).

V. Summary and Conclusions

A former bimolecular reaction model describing the adsorption kinetics of methyl iodide on activated carbon[10] has been extended to the general case when the concentration of the challenging gas changes in time. It is shown that the model can be used to predict the performance of charcoal adsorbers at constant upstream gas concentrations and also when the concentration changes in time. The effect of short term loading followed by purging with air and an impulse-like increase in upstream concentration has been simulated. In the practice the former case corresponds to the conditions during and after an accident, the letter case simulates an increased, short term adsorber loading due to temporary abnormal plant operation.

The case of short term loading and subsequent purging has been experimentally studied to validate the model. The acceptable agreement of the experimental results and model calculations shows that the model can be used to predict adsorber performance. The deviation observed between the measured and predicted data indicates the need for further development of the model.

Acknowledgement

The authors wish to thank Mr. J. Hargittay for his experimental work and discussions and Mr. O. Lécz for excellent computer work.

References

1. Deitz, V.R. and Jonas, L.A., "Catalytic trapping of methyl iodide by beds of impregnated charcoal", Nucl. Technol., 37, 59 (1978)
2. Jonas, L.A., Deitz, V.R. and Romans, J.B., "Desorption kinetics of methyl iodide from impregnated charcoal", Nucl. Technol., 48, 77 (1980)
3. Grubner, O. and Burgess, W.A., "Calculation of adsorption break- through curves in air cleaning and sampling devices", Environmental Science Technology, Vol.15, 1346 (1981)
4. Deuber, H., Gerlach, K., "Laboratory tests of activated carbon for methyl iodide retention: influence of various parameters", IAEA Seminar on the testing and operating of off-gas cleaning systems at nuclear facilities, Karlsruhe, 3-7 May 1982, IAEA-SR-72/34
5. Shiomi, H., Yuusa, Y., Tani, A., Ohki, M. and Nakagawa, T., "A parametric study of removal efficiency of impregnated activated charcoal and silver zeolite for radioactive methyl iodide" Proc. 17th DOE Nuclear Air Cleaning Conference, Vol.1, 199 (1983)
6. Billinge, B.H.M. and Broadbent, D., "The effects of temperature and humidity on the ageing of TEDA impregnated charcoals", Proc. 20th DOE/NRC Nuclear Air Cleaning Conference, Vol.1, 572 (1989)
7. Vikis, A.C., Wren, J.C., Moore, C.J. Fluke, R.J., "Long-term desorption of 131-I from KI-impregnated charcoals loaded with CH_3I, under simulated post-LOCA conditions", Proc. 18th DOE Nuclear Air Cleaning Conference, Vol.1, 65 (1985)
8. Wren, J.C. and Moore, C.J., "Long-term desorption of CH_3I from a TEDA-impregnated charcoal bed under post-LOCA conditions" Proc. 20th DOE/NRC Nuclear Air Cleaning Conference, Vol.2, 1117 (1989)
9. Friedrich, V., Lux, I., "Theoretical and experimental study of the adsorption of radioactive gases on continuous flow columns" J.Radioanal.Nucl.Chem., Letters 93, 5, 309 (1985)
10. Friedrich, V., "Kinetic studies of the retention of radioactive gases by activated carbon adsorbers", Proc. 20th DOE/NRC Nuclear Air Cleaning Conference, Vol.1, 512 (1989)

MATHEMATICAL MODELS FOR CHANGES IN HEPA FILTER PRESSURE DROP CAUSED BY HIGH AIR HUMIDITY *

[1]C. I. Ricketts, [1]M. Schneider, and J. G. Wilhelm

Kernforschungszentrum Karlsruhe GmbH
Laboratorium für Aerosolphysik und Filtertechnik II
Postfach 3640, D-7500 Karlsruhe 1
Federal Republic of Germany

[1]Consultant

Abstract

Possible high air humidities resulting from an accident in a nuclear installation threaten the integrity of HEPA filter units in the facility air cleaning systems. Field surveys indicate that filter units continue to be exposed to adverse humidities in routine service despite the development of moisture countermeasures.

One of the detrimental consequences of exposure to high air humidity is an increase in filter pressure drop. Reported failures due to a tearing of the filter medium partly result from elevated structural loadings imposed by Δp increases. The extent to which filter Δp varies with airstream conditions can be used to help calculate safety margins for filter units during normal and upset operations as well as during postulated accidents involving high air humidity.

Studies of humidity-related changes in pressure drop were carried out to help explain structural failures in routine service and to obtain the empirical data needed to numerically model flow dynamics in air cleaning systems under accident conditions. Tests were performed on full-scale filter units under fog conditions and on samples of filter media at humidities up to 99% RH.

Test results show that typical changes in Δp can be mathematically modeled by a number of time functions having coefficients that can only be determined empirically. Regression analysis is used to establish the coefficients for specific filter units and dust loadings tested under the operating conditions of interest. Comparison of measured and calculated increases in pressure drop for clean filter units under fog conditions show that good agreement can be obtained with coefficients determined as relatively simple functions of the airstream velocity and liquid water content.

---

* Work performed under the auspices of the Federal Ministry for the Environment, Nature Conservation and Nuclear Safety under Contract No. SR 290/1.

I. Introduction

Ventilation and air-cleaning systems provide for the thermal comfort and the health safety of working personnel in industrial and laboratory facilities that contain hazardous or toxic radioactive materials. The air cleaning systems (ACSs) also help to prevent the release of contaminated airborne particulates and gases to the surrounding environment. The required extremely good particle removal efficiencies at relatively low pressure drops are made possible by the use of High Efficiency Particulate Air (HEPA) filter units[1,2].

Particularly in power reactor facilities, minimum system airflows are required - in order to maintain pressure differentials between confinement zones[3], to remove the decay heat from iodine adsorbers[4], as well as to cool electrical equipment[5]. To ensure that airborne radioactive particles do not escape containment barriers, it is also crucial that the HEPA filter units remain free of leaks.

The presence of liquid water within the matrix of typical glass fiber HEPA filter media can not only reduce system airflow to below the design minimum but can also lead to tears in the filter medium itself. As a consequence, iodine desorption, pressure differential inversions, or the failure of ACS controls or electrical components become possible. Not to mention potentially large decreases in HEPA filter removal efficiency. The end result can be an escape of airborne radioactivity to less contaminated areas or to the environment.

Moisture Countermeasures and Their Shortcomings

Since the adverse effects of moisture on filter performance could quickly lead to a loss of containment, liquid water is one of the more stringent possible challenges from which HEPA filter units in nuclear service must be protected. This protection is based not only on the treatment of the airstream to prevent filter exposure to moisture, but also on the use of moisture-resistant construction materials to minimize the detrimental effects of inadvertent exposure. Airstream humidity can be reduced to a safe level upstream of HEPA filters by the use of droplet separators and air heaters[3]. Water repellant filter media[6] and qualification tests in standards for new filter units[7,8] are intended to inhibit failure should filters nevertheless become wet for brief periods of time.

The realizations of these countermeasures, however, have not entirely eliminated incidents of filter malfunction or failure related to moisture[9-12]. This indicates that filter units are still being exposed to sensible moisture and that filter construction materials, the medium in particular, remain yet sensitive to its effects. Reported exposures and subsequent failures, most of which occurred during normal operations, can have several of a variety of possible causes.

The potential sources of moisture within the containment boundaries are numerous. The inlet air itself, the reactor coolant, fire sprinkler or containment spray-injection systems, and even ground water[3] are among these. In addition to equipment failures,

cases of filter exposure to liquid water have been attributed to errors in the design, the installation, the operation, as well as the maintenance of air cleaning systems or ACS components[3,13-16]. Uncertain is whether reported incidents could be related to regulatory guides that do not specify minimum performance characteristics for mandated droplet separators[8] or those that do not require them at all[17], for ACSs in service during normal operations.

Once liquid water appears at filter units, performance degradations intended to have been essentially eliminated by water repellancy treatments and filter qualification standards can occur nonetheless. For instance, filter medium water repellancy can be significantly reduced by dust loading[18-20], creasing[12,21], gamma radiation exposure[19], and aging[21] of the filter medium. All factors to be taken into account with nuclear grade filter units.

It is not unreasonable to question whether current moisture-resistance qualification tests for new, clean filter units[7,8], sufficiently simulate the moisture-induced stresses that can eventually occur in aged, dust-loaded filters, during the service conditions for which failures have been reported. With the exception of the recent realization of commercial high-strength units in Germany[22], user requests for HEPA filters with greater moisture resistance[23] seem to be going unheeded. Revisions of current filter unit standards to reflect improvements in performance should accompany any adoption of better filters.

Though the inherent fragility of glass fiber filter media in a wet condition can be overcome by a reinforcing scrim, this improvement is not yet to be found in widespread use. Nor does it give the appearance of finding recognition in filter unit qualification standards any time soon. Similarly, measures to prevent the detrimental, moisture-induced loosening of the filter pack have not been implemented in general practice, nor is their potential benefit reflected in filter standards. Means for promoting the drainage of water from the filter medium remain largely uninvestigated as to their viability in mitigating deteriorations in the performance of filter units accidentally subjected to fog.

Additionally open to question are the reliability and performance of conventional filter units during emergencies such as a LOCA or fire suppression actions - situations that would involve the release of large quantities of steam or water into containment areas. Minimum performance characteristics for mandated droplet separators in standby gas treatment systems are not always specified in regulatory guides[8], for example. As active components, which require external power and control systems, heaters are more likely to fail during an emergency than passive ones. The effectiveness of demisters and heaters in protecting aged, dust-loaded filter units has yet to be experimentally proven under transient conditions involving condensing steam.

For the above reasons it is worthwhile to reevaluate the processes underlying the potential escape of radioactive materials caused by filter unit exposure to humid airflows.

Potential Cause-and-Effect Relationships That Could Lead to a Loss of Containment Due to Humid Airflows

The sequences of phenomena that can occur between initial humidity exposure and an eventual release of airborne radioactive substances are illustrated schematically in Fig. 1. The incorporation of liquid water into the filter medium from the airstream, results from any one or combination of three mass transfer processes. The subsequent effects can include penetration of filter units by liquid water or detrimental changes in the filtration characteristics of an intact filter medium. An increase in filter unit pressure drop, accompanied by simultaneous decreases in filter medium tensile strength and pack rigidity, threatens the folded filter medium with irreversible structural damage. The effect with the greatest potential ramification is the increase in filter unit Δp.

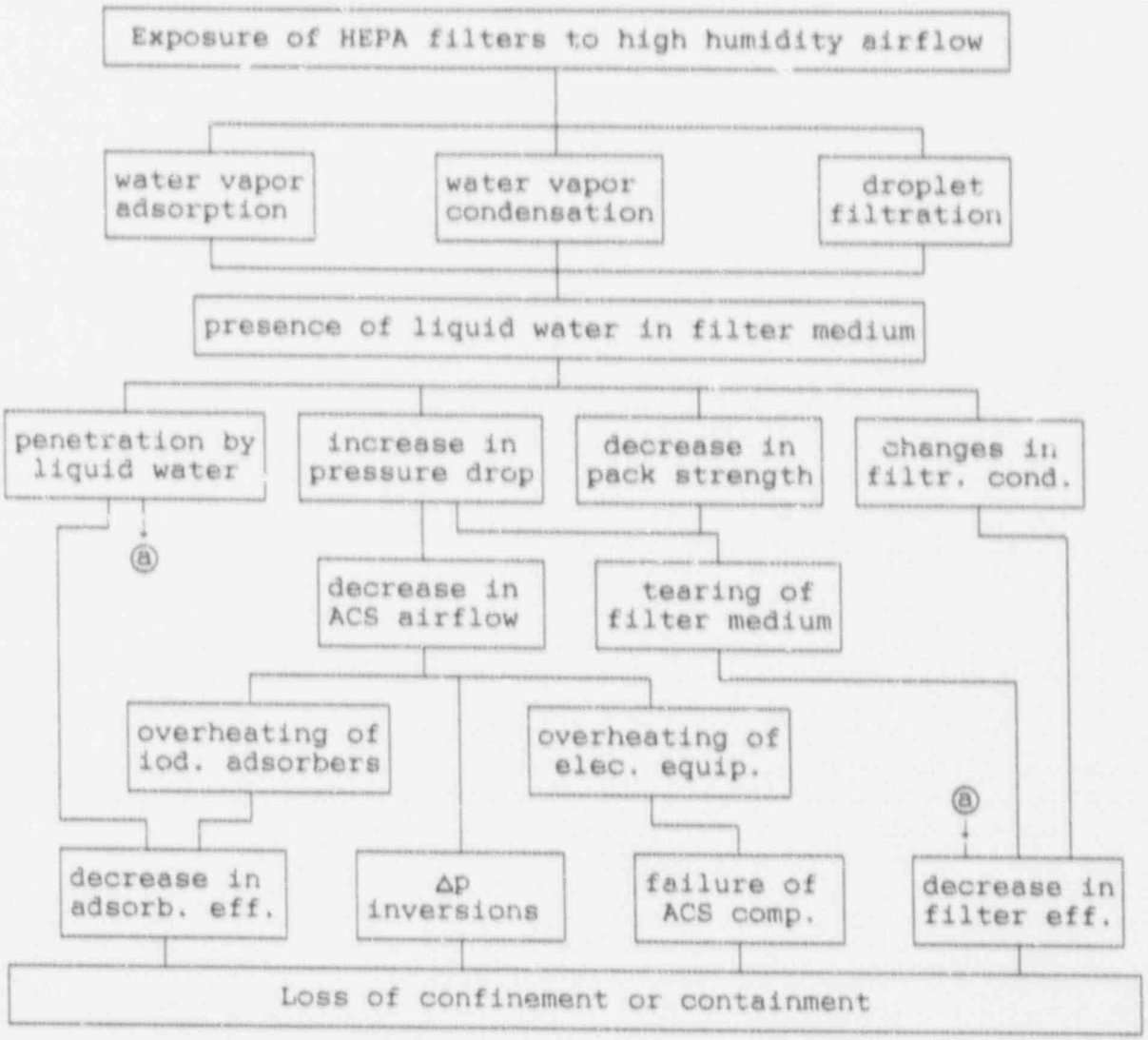

Fig. 1: Sequences of phenomena that can lead to a release of radioactivity caused by filter exposure to high humidity airflow.

Increase in Flow Resistance Due to Humid Airflow

In humid air, the extent of increases in the flow resistance of HEPA filter media is influenced primarily by the amount of liquid water incorporated, as well as by the chemical composition, amount, and size distribution of any captured dust particles present. How quickly water is transfered into the filter medium and the characteristics of any dust loading present will play important roles in the rate of increase in flow resistance. The airstream temperature can also be decisive at $\varphi \leq 100\%$ RH for filters loaded with fine dusts. Filter medium and airstream parameters with significant influence on the rate and the extent of change in filter medium Δp and liquid water content (LWC) are summarized in Fig. 2.

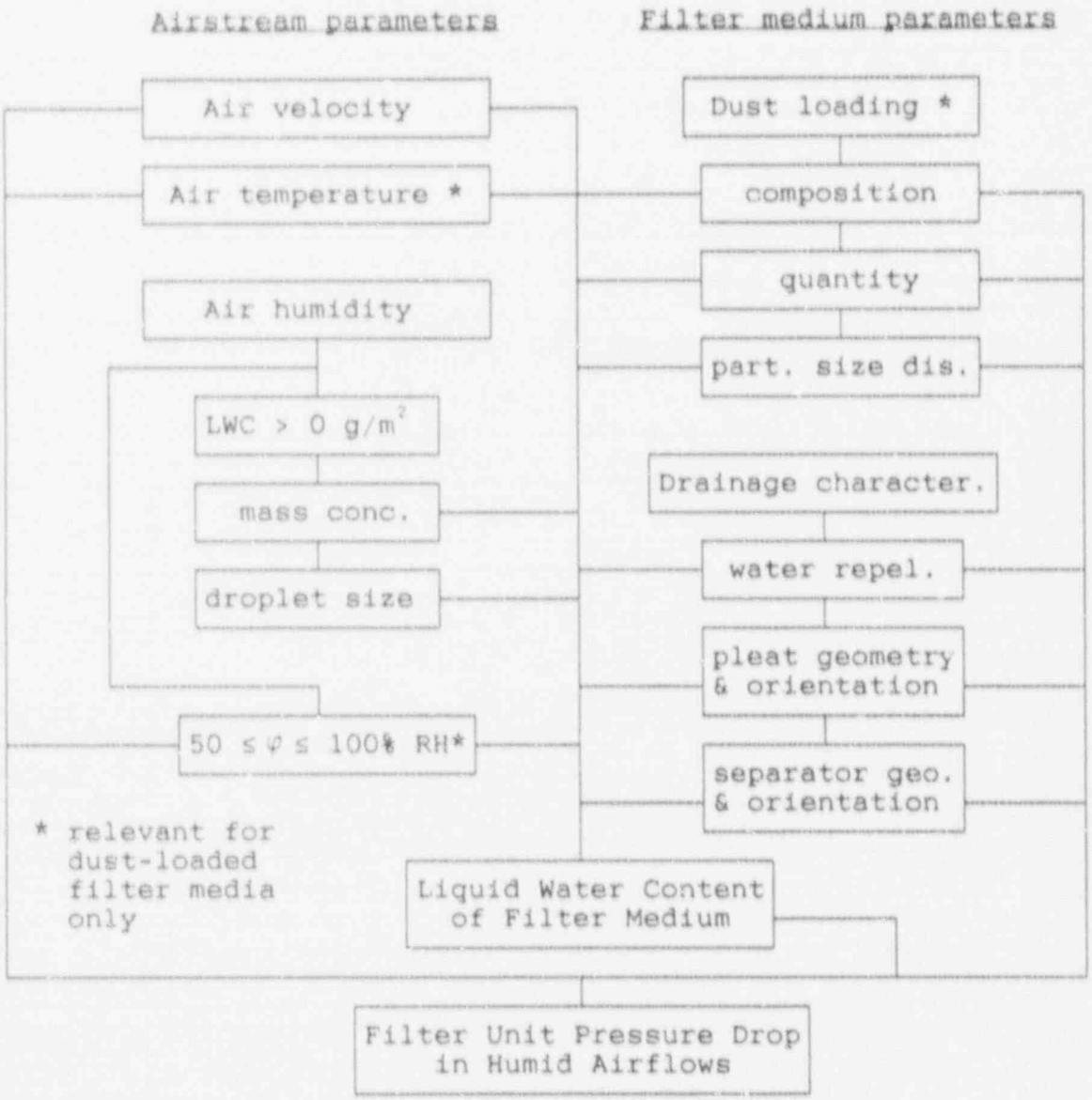

Fig. 2: Parameters with significant influence on the Δp and the filter medium LWC of HEPA filter units in humid airflows.

Many of the parameters listed influence filter pressure drop independently of filter medium LWC. Those that affect filter medium LWC or the structure of captured dust deposits can have additional effects on filter Δp. In dry air for example, the characteristics of the aerosol particulates help determine the structure of the dust loading on the upstream surface and within the fiber matrix. The velocity, temperature, and the relative humidity of airstreams can influence the dust structure or the filter medium LWC, both of which in turn affect pressure drop. Under fog conditions, filter medium drainage characteristics influence not only the blockage of the upstream surface by drainage water but also the liquid water content.

The challenge to filter units posed by moisture-related decreases in airflow. Air velocity will not necessarily remain constant as a result of HEPA filter exposure to high humidity. It can sink, depending upon the extent of the blowers' capability to maintain constant delivery with the increasing filter pressure drop. During a LOCA, expanding steam could elevate airflows through ACSs in spite of increases in filter Δp[18].

Flows diminished to levels below the controlled operating range of the air cleaning system are not necessarily harmless, as is evident in Fig. 3. Should the level of airflow approach zero, the maximum blower Δp at no air delivery would appear across the water clogged filters. The path $\Delta p_F(Q_h)$, which filter Δp follows as the humid airflow through the ACS sinks, depends on the system and blower characteristic curves $\Delta p_S(Q_d)$ and $\Delta p_B(Q)$. The airstream and filter medium parameters that affect filter pressure drop determine how quickly and how far this path is traversed. Comparatively, the paths in dry air $\Delta p_F(Q_d)$, are straight lines. The max. damper Δp is Δp_{Dmax}.

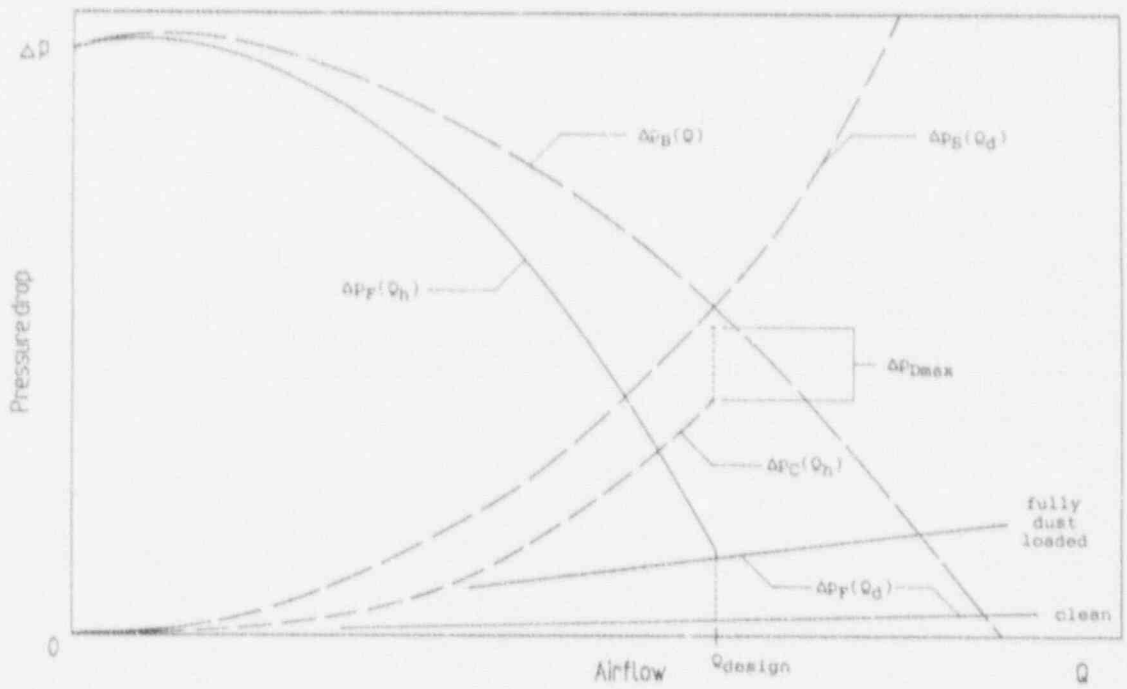

Fig. 3: Path for rise of filter Δp with increasing filter flow resistance and decreasing ACS flow due to high air humdity.

The latent potential of the blowers for producing destructive pressure drops across filter units being clogged with water is worthy of closer examination. It is only after the control damper reaches the fully-open position, in an attempt to maintain constant flow conditions, that the system airflow begins to be reduced by the filters' clogging. As the flow level sinks, two phenomena act to enable filter unit pressure drop Δp_F, to rise significantly. The sum of the pressure drops across the ACS components other than the HEPA filters and the damper, Δp_C, will decrease. Simultaneously, the static pressure delivered by the blowers Δp_B, will increase. The overloading of filters with dust could cause the same effects, though at much slower rates. The kinetics of increases in Δp_F due to soot loading during a fire could take place just a quickly as those possible during water loading.

That the potential maximum pressure drop across the filters is essentially $\Delta p_{B_{max}}$ can be expressed mathematically as follows. For airflows reduced by increases in filter flow resistance, the relationship between the three functions is given by

$$\Delta p_F(Q_h) = \Delta p_B(Q) - \Delta p_C(Q_h) - \Delta p_D(Q), \qquad (Q < Q_{design}). \qquad (1)$$

(the $\Delta p_D(Q)$ term is $\nearrow 0$)

As

$$\lim_{Q \to 0} \Delta p_B(Q) = \Delta p_{B_{max}}$$

and

$$\lim_{Q \to 0} \Delta p_C(Q_h) = 0$$

then

$$\lim_{Q \to 0} \Delta p_F(Q_h) = \Delta p_{B_{max}} .$$

In order to protect filters from this challenge, with a safety factor of two for example, the burst strength of filter units in a wet condition, at the end of service, should be at at least twice that of $\Delta p_{B_{max}}$. This can provide a rough estimate for the minimum pressure drop which should be required in moisture resistance tests for the qualification of new filter units as nuclear grade.

The challenge to filter units posed by elevated flows of humid air. The above evaluation does not, however, take into account any filter pressure drops > $\Delta p_{B_{max}}$ that could result from increased flows driven by the expanding steam of a LOCA[24]. Maximum values for these cases are scenario dependent and would best be determined by numerically modeling the resulting flow transients within the ACS. Computer codes being developed to this end[25] require as input, functions that describe changes in filter Δp with time for various airstream and filter unit parameters. Of particular interest are those summarized in Fig. 2. The primary reason for investigating the influence of

these parameters on filter Δp is for purposes of safety analysis. The elimination of moisture related filter malfunction or failure is the end objective.

Evaluation of prior investigations. To be found in the literature are differing, partly contradictory trends for the extents and rates of change in the flow resistance of test filters exposed to moisture laden air[26]. This can be attributed to the difficulties encountered in the accurate measurement and control of high airstream humidities. An additional contributing factor is the sensitivity of filter pressure drop to small changes in humid air states close to and above saturation. Frequently the humidities of the test airstreams were not measured. Differences in test air temperatures, as well as in the characteristics of the filter media and the dust loadings of the filter units investigated, contribute to seemingly inconsistent results. A cross comparison of results for tests performed with decreasing airflows are not possible for the many cases where the characteristic curve of the employed blower was not denoted. The lack of data suitable for modelling purposes is, however, mostly due to the fact that parametric studies have not been the principal objectives of past investigations.

In the preparation of tests performed for the development of mathematical models, two major conclusions were drawn from results found in the literature. One was the necessity for instrumentation and control systems to accurately measure and to closely regulate airstream humidity. The second was the need to perform tests using the filter units and the dust loadings typical for the air cleaning systems of interest.

II. Experimental Work

To study the behavior of HEPA filter units or media under high humidity conditions requires rather sophisticated test facilities built specifically for this purpose. Experiments were performed with two test rigs at Kernforschungszentrum Karlsruhe (KfK), one for filter units, the other for samples of filter media. In each case, careful attention was paid to the accurate measurement and control of airstream humidity, temperature, and velocity.

Tests of Filter Units in Super-Saturated Airstreams

Full-scale filter units were tested under super-saturated conditions in the TAIFUN facility. Descriptions of the test filters, procedures, and results have been described in detail elsewhere, together with that of the rig itself[27].

Test on Samples of Filter Media at Air Humidities up to 99% RH

Preliminary tests showed parametric investigations on dust-loaded units at humidities up to saturation to be impractical for a number of reasons. These included the limited number of dust-loaded filters available and the different degrees of loading among them. An

additional factor was the thermal inertia of the test rig which made precisely achieving the desired relative humidity a process too demanding for the test time available.

A smaller rig was therefore constructed for testing samples of filter media removed from full-scale filter units. Only in this way could the available dust-loaded filters be cost effectively investigated to the extent necessary for a useful parametric study. For air humidities up to saturation, it is the filter medium that accounts for the greatest proportion of the total filter unit flow resistance. Results of tests on specimens alone can be used to calculate the pressure drop of filter units containing the folded filter medium[28].

LÜFTER test rig. Variations in the pressure drop of filter media specimens were investigated using the laboratory test rig LÜFTER, shown schematically in Fig. 4 and photographically in Fig. 5. The airstream is recirculated through the test section by a sliding vane compressor driven by a 0.75-kW electric motor. A throttle valve at the compressor inlet limits the airflow to 6 m^3/h. Carbon particulates worn from the compressor vanes are removed by a .20- x .20- x .29-m HEPA filter at the compressor discharge.

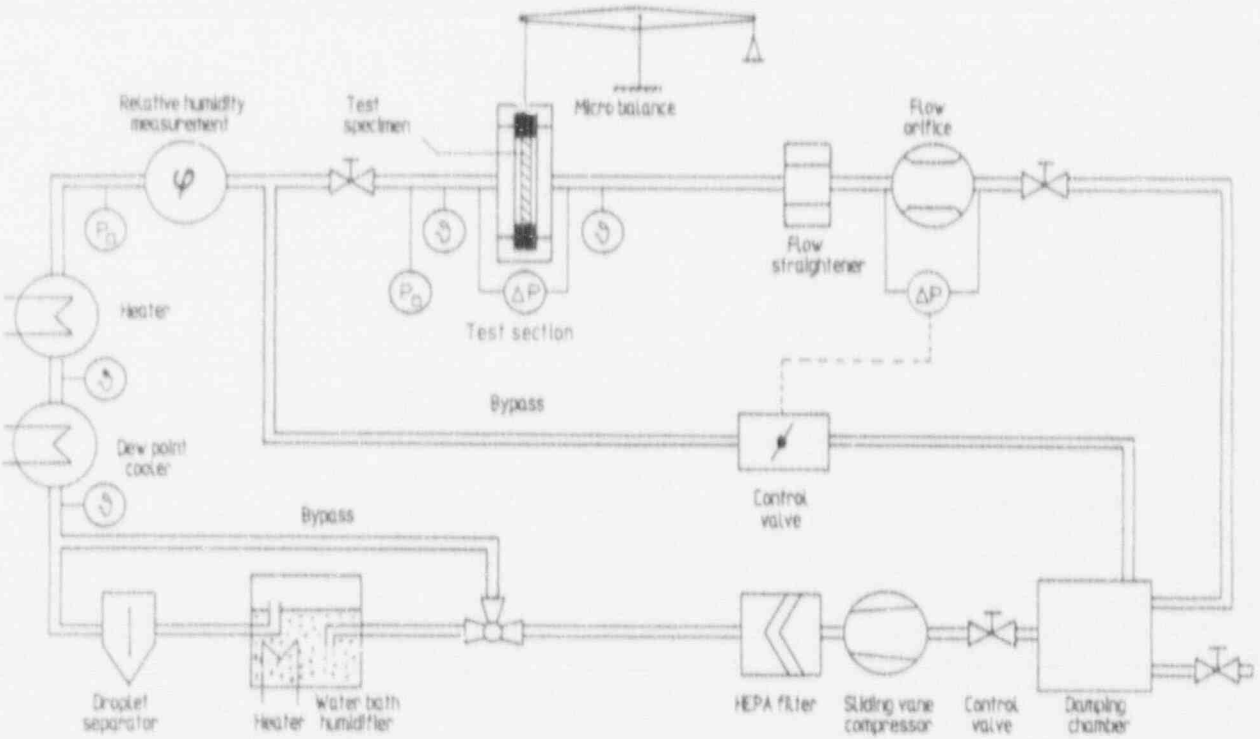

Fig. 4: Schematic diagram of the laboratory test rig LÜFTER.

The clean air is humidified by bubbling it 0.4 m through a 20-l water bath maintained at some 2°C above the air dew-point temperature set for the test. A downstream perforated plate serves as a droplet separator to minimize the carryover of liquid water. The water-saturated air exits the cooler at the set dew-point temperature and enters a heat exchanger where it is heated up to the desired dry-bulb temperature. The fine adjustment and regulation of the airstream dry-

bulb and dew-point temperatures allows the air relative humidity to be accurately set and maintained.

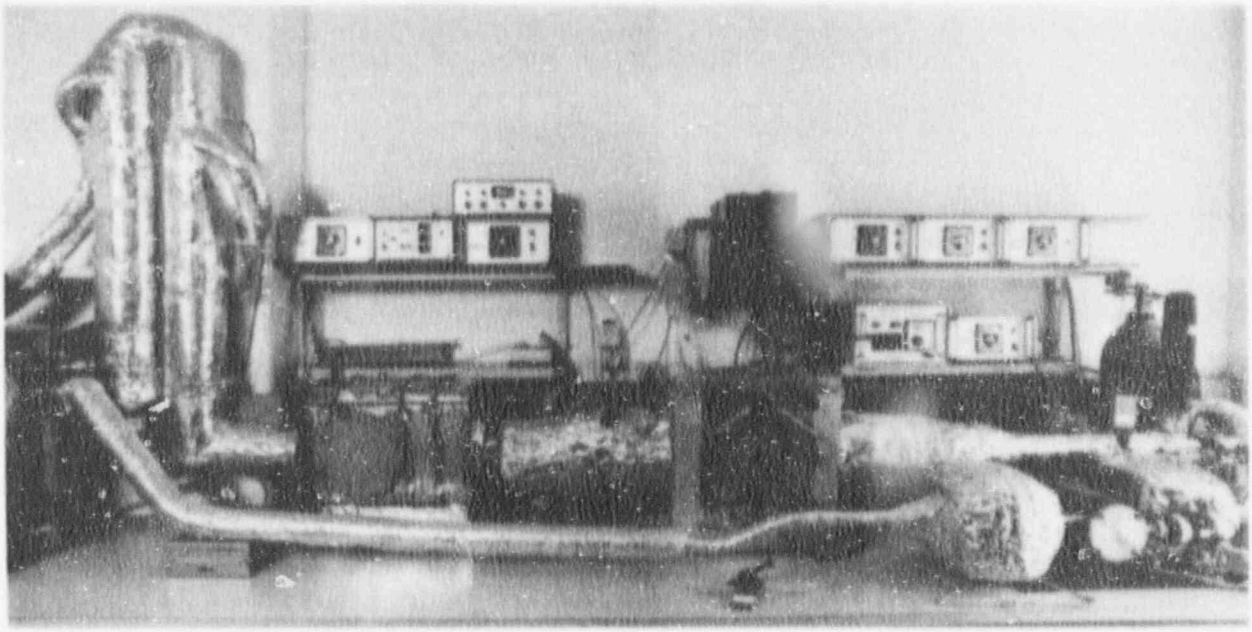

Fig. 5: Photo of LÜFTER test rig.

The air relative humidity is measured psychrometrically upstream of the junction that divides the airflow between the bypass and the test section. Aged four-wire, 100-Ω RTD probes connected to a precision ohmmeter sense the wet- and dry-bulb temperatures. Only 5 to 25% of the 6-m^3/h airflow required for the humidity measurement is directed to the test section, illustrated in Fig. 6. The remainder is routed through the bypass to a control valve which serves to keep the airflow through the test section constant.

Parameters sampled at the test section include the pressure drop of the test specimen as well as the dry-bulb temperature and absolute pressure of the airstream. The liquid water content of the 108-mm dia. test specimen can be gravimetrically established with a microbalance during intermittent interruption of the airflow to the test section. An orifice plate downstream of the test section is used to measure the airflow and to provide feedback to the control valve via a pressure transducer.

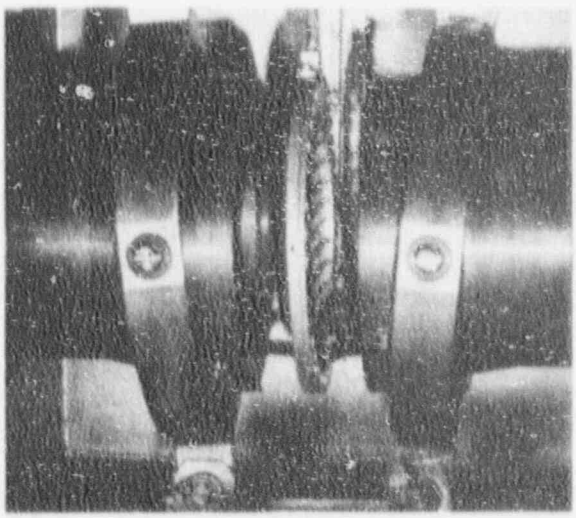

Fig. 6: View inside test section.

The airflows of the test section and the bypass are fed into a 16-l pulsation damping chamber before returning to the compressor. A third inlet provides makeup air to compensate for any leaks in the system which is operated in an overpressure mode. With the exception

of the compressor and its discharge filter, all components and connecting ductwork are wrapped with regulated heating elements and insulation. The performance characteristics for the test rig, the measurement instrumentation, and the control systems are summarized in Table I.

Table I: Performance characteristics of the LÜFTER test rig.

Test parameter	Operating range	Measurement uncertainty	Control tolerance
at test section			
Airflow (m^3/h)	0 - 1.7	± 0.003	± 0.006
Air temperature (°C)	20 - 80	± 0.05	± 0.1
Air humidity (% RH)	40 - 99	± 0.5	± 1.0
Overpressure (kPa)	0 - 20	-	-
for test sample			
Superf. vel. (cm/s)	0 - 5	± 0.01	± 0.02
Pressure drop (kPa)	0 - 15	± 0.01	-
LWC (g/m^3)	1 - 500	± 0.1	-
X-sect. area (cm^2)	92	-	-

Test specimens and test procedures. Filter units purchased from several manufacturers on the open market were sources for clean samples. Test specimens loaded with fine particle dusts came from commercial filter units after normal service in uncontaminated laboratory air cleaning systems at KfK. Specimen dust loadings lay between 0.1 and 4 g/m^2 for pressure drops in the range of 290 to 800 Pa at 2.5 cm/s, 25°C and φ < 40% RH. The dry weight of samples was determined after conditioning in an oven for 24 h at 50°C and an absolute pressure of 5 kPa.

Kinetic tests were run after a 30 to 60-min conditioning of the airstream to achieve the desired at the test temperature and airflow. Specimens were spanned between the halves of a ring-shaped holder before being mounted in the test section. During mounting, the test section was blocked off from the test air and open to the ambient enviroment at < 50% RH. Tests began with the opening of the valve upstream of the test section. The change in specimen Δp with time was recorded for up to 4 ' of exposure at constant temperature, relative humidity, and flow. Tests were ended and the specimen weighed once an approximate maximum or minimum equilibrium value of pressure drop was attained.

Typical test results.

The test results of Figs. 7 - 9 show some typical effects of three important airstream parameters on the relative Δp increase of dust-loaded specimens having an initial Δp of 500 Pa at 2.5 cm/s in dry air. In general, both the rate and the extent of the Δp increase grow with greater values of relative humidity above 70% as seen in Fig. 7. No significant change in pressure drop was evident at < 70% RH and 25°C. The increase in Δp_{max} with rising constant relative humidities was nonlinear above 90% RH.

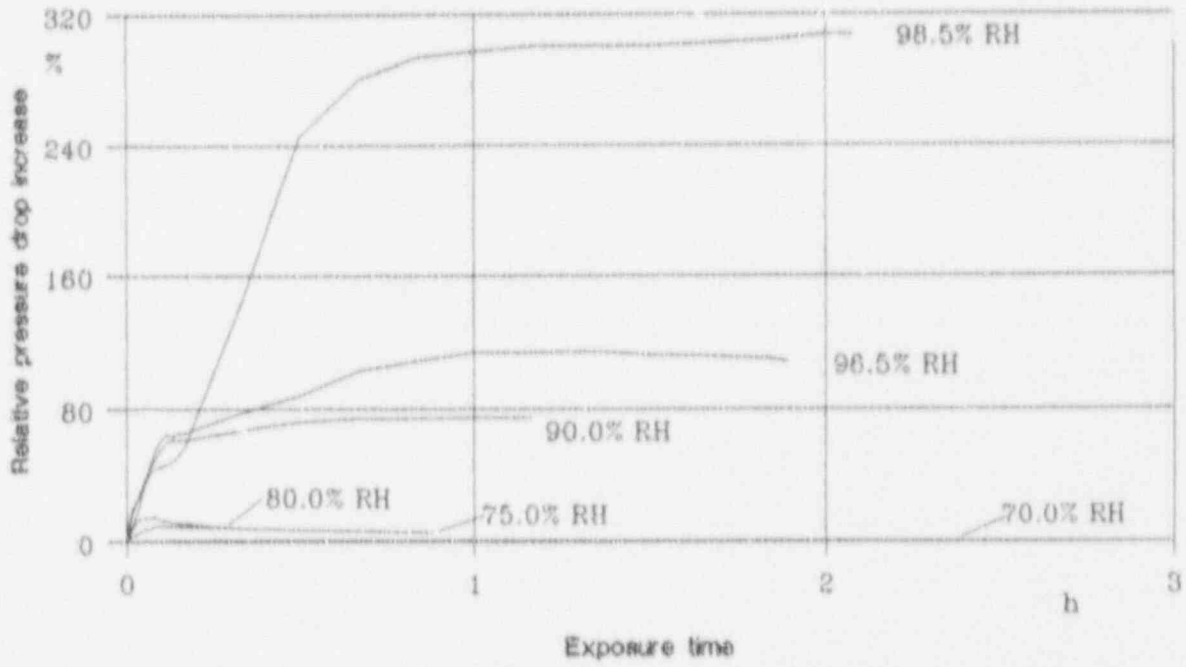

Fig. 7: Influence of air relative humidity on the rate and extent of the relative Δp increase for a dust-loaded HEPA filter medium at 25°C and 2.5 cm/s.

For the given test conditions, Fig. 8 shows that a 20% increase at 25°C, changes at 50°C to a decrease of about the same magnitude. The equilibrium value at 75°C is an even lower ~44%. This indicates that temperature can play a decisive role in the structural loading of filter units at high relative humidities up to saturation. The threat to filter integrity can decrease with increasing temperature. This indicates another potential benefit in the use of air heaters, in addition to that of lowering airstream relative humidity. The mechanisms triggered by this temperature effect are not yet established.

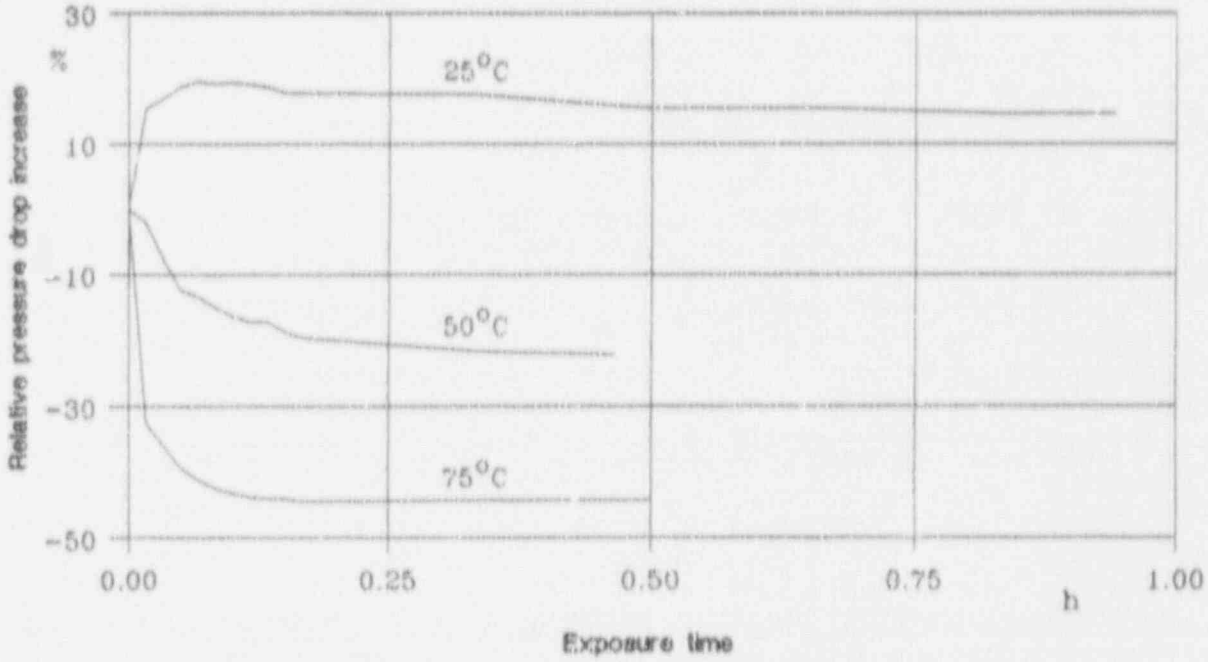

Fig. 8: Influence of temperature on the rate and extent of the relative Δp increase for a dust-loaded HEPA filter medium at 94% RH and 2.5 cm/s.

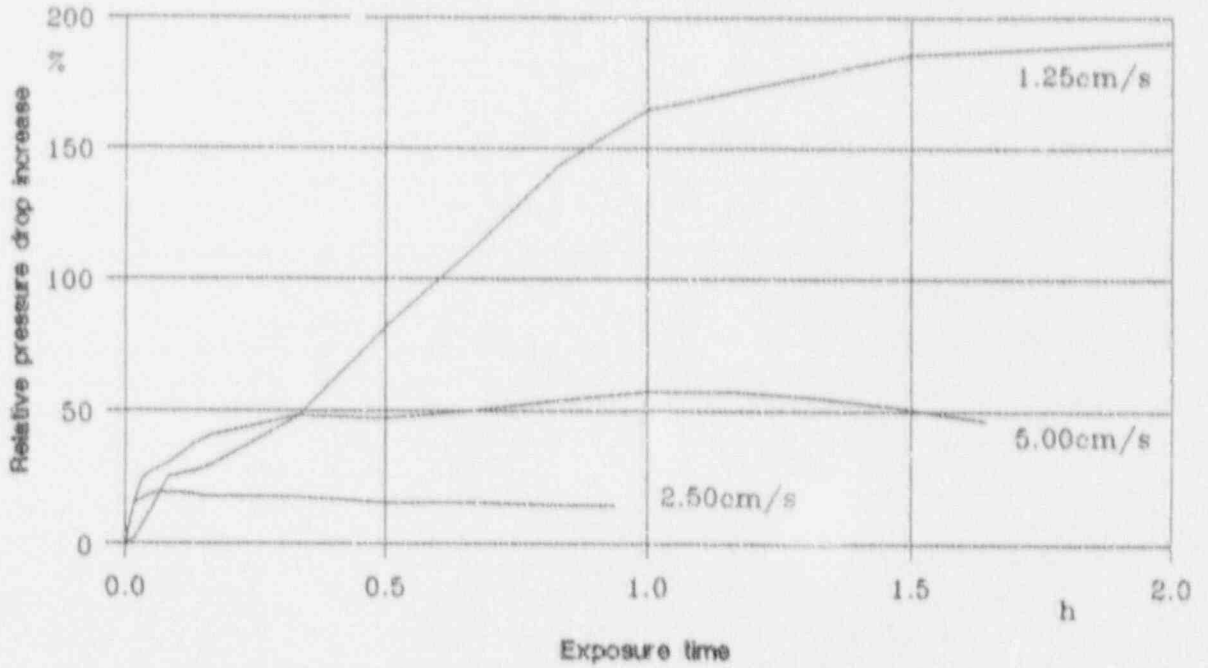

Fig. 9: Influence of filtration velocity on the rate and extent of the relative Δp increase for a dust-loaded HEPA filter medium at 25°C and 94% RH.

The curves of Fig. 9 indicate that filtration velocities less than design values can produce Δp increases greater than those for V = 2.5 cm/s. This phenomenon poses an additional threat to filters in ACSs where airflows have been reduced to lower than design values by the effects of high air relative humidity. It has not been observed in tests of dust-loaded filters in super-saturated airstreams.

III. Mathematical Models for Changes in HEPA Filter Pressure Drop

Results for tests performed at constant flow indicate that humidity-related variations in filter pressure drop with time can be approximated well by the functions illustrated in Fig. 10 and summarized in Table II. Whether the pressure drop changes significantly and whether a decrease or an increase occurs, depends on both the airstream parameters and the characteristics of the filter medium. Decreases have been observed for filter units or media loaded with fine particulate dust in service and tested at $\vartheta > 50°C$ and air humidities up to 99% RH, for example. All, clean filter units or media showed negligible changes up to saturation, as did some dust-loaded ones for certain combinations of temperature and relative humidity.

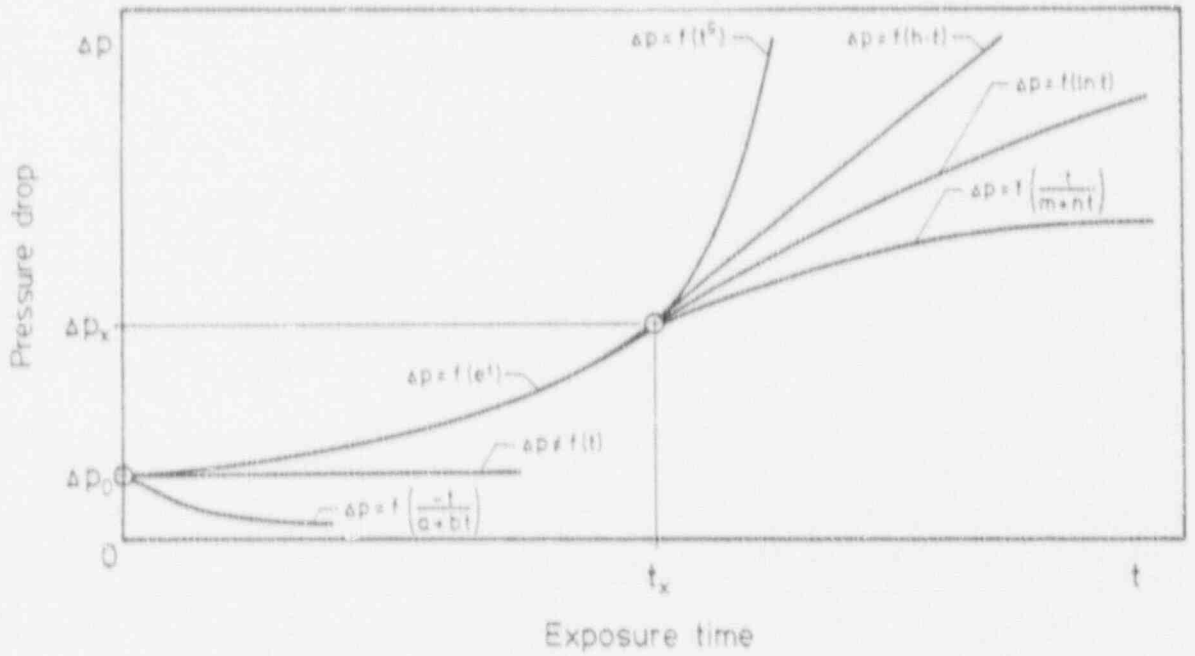

Fig. 10: Time functions observed for the changes in pressure drop of HEPA filter units or media exposed to humid airflows.

Based on visual appearance, functions similar in form to those of Table II appear among curves published by other investigators who tested with constant airflows[29-32].

Table II: Summary of currently established time functions for the variation of HEPA filter pressure drop due to high air humidity.

Type of Time Function	Functional Relationship Δp =	Airstream conditions $20 \leq \vartheta \leq 80$ °C, $60 \leq \varphi < 100\%$ RH, filter units		$20 \leq \vartheta \leq 50$ °C, $0.5 \leq LWC \leq 10$ g/m³, filter units	
		clean	loaded	clean	loaded
$-\frac{t}{a + bt}$	$\Delta p_0 - \left(\frac{t}{a + bt}\right)$	–	yes	–	–
$\Delta p \neq f(t)$	Δp_0	yes	yes	–	–
e^t	$\Delta p_0 \exp(c_1 t^{c_2})$	–	yes	yes	yes
t^g	$\Delta p_x + g_1 t^{g_2}$	–	–	yes	–
t	$\Delta p_x + ht$	–	yes	–	yes
$\ln t$	$\Delta p_x + k_1 \ln k_2 t$	–	yes	yes	yes
$\frac{t}{m + nt}$	$\Delta p_x + \left(\frac{t}{m + nt}\right)$	–	yes	–	–

Filter units in super-saturated airstreams.

Significant increases, initially of the exponential form to be expected[33], were invariably observed for filter units in super-saturated airflows[27]. The rise in Δp under fog conditions could be modelled by e^t up to a transition pressure drop Δp_x, - regardless of filter unit manufacturer, design, pleat orientation to the airflow, dust loading, or the test air conditions. Above Δp_x, the curves exhibited one of several other functional forms.

With clean filters, an extremely steep increase of the form t^g occurred shortly before failure for minipleat types from most manufacturers and for deep-pleat units from several suppliers. This was also typical for all deep-pleat units in the sizes 305 x 305 x 292 mm and 610 x 610 x 150 mm from 3 manufacturers.

Characteristic of a few deep-pleat filters slightly loaded with dust, was a linear range, possibly an extended transition into an $ln(t)$ function, interrupted by structural failure. Otherwise, the form of $ln(t)$ was found to be typical for both conventional and high strength deep-pleat units - clean and dust-loaded - as well as for all dust-loaded minipleat filters.

Samples of Filter Media and Filter Units for Air Humidities ≤ 99% RH

Filter units or media with the most variety and combinations of time functions were those loaded with dust and exposed to air relative humidities between 50 and 99%. Observed exclusively in this

group were the functions of $-t/(a+bt)$ and $+t/(m+nt)$, an indication of adsorption phenomena. For relative humidities high enough to influence pressure drop, the airstream temperature determined the sign. A third, less frequent initial function was e^t, followed by either $+t/(m+nt)$ or $ln(t)$, and occasionally both. The linear ht function was also evident in some cases in a transition stage between the other types. Mathematical models for dust-loaded filters are still being refined and will be published in more detail later[34].

Determination of the Empirical Coefficients

Once the relevant functional forms have been identified by least-squares fitting, the next step is to determine the coefficients necessary to make them useful. Summarized in Table III are the known airstream parameters with primary influence on coefficient values. Though this tabulation can be considered neither complete nor universal, it provides an initial general reference. The filter parameters of Fig. 2 will also greatly influence the coefficients. Hence, they can only be determined empirically. This requires that a number of filters or samples of filter media be evaluated in tests within the range of the operating conditions of interest.

Table III: Summary of currently established empirical time function coefficients and airstream parameters of influence.

Coefficient of Table II	Airstream conditions $20 \leq \vartheta \leq 80$ °C $60 \leq \varphi < 100\%$ RH	 $20 \leq \vartheta \leq 50$ °C $0.5 \leq$ LWC ≤ 10 g/m³
a	$f(\vartheta, \varphi, V)$	-
b	$f(\vartheta, \varphi, V)$	-
c_1	$f(\vartheta, \varphi, V)$	f(LWC, V, ϑ)
c_2	$f(\vartheta, \varphi, V)$	f(LWC, V, ϑ)
g_1	-	f(LWC, V)
g_2	-	
h	$\frac{d}{dt}\Delta p(t)$ for $t > t_x$	
k_1	$f(\Delta p_x)$	$f(\Delta p_x)$
k_2	$f(t_x)$	$f(t_x)$
m	$f(\vartheta, \varphi, V)$	-
n	$f(\vartheta, \varphi, V)$	-
Δp_x	$f(\vartheta, \varphi, V)$	f(LWC, V, ϑ)
t_x	$f(\Delta p(t)$ for $t < t_x, \Delta p_x)$	

To obtain such coefficients for evaluation, ten new filter units from one production lot were tested under steady-state conditions at ϑ = 20°C, LWCs between 1.2 and 10 g/m³, and average filtration velocities V, from 54 - 216 m/h. For

$$\Delta p(t) = \Delta p_0 \exp (c_1 t^{c_2}) \quad , \quad t < t_x$$

and

$$\Delta p(t) = \Delta p_x + k_1 \ln k_2 t \quad , \quad t \geq t_x$$

the empirical coefficients and their respective coefficients of determination R^2, or standard deviations σ, were

$$c_1 = 1.08 \cdot 10^{-2} (\mathrm{LWC} \cdot \mathrm{V}) - 1.19 \cdot 10^{-1} \qquad (R^2 = 0.98),$$

$$c_2 = 1.38 = \frac{\sum_{i=1}^{10} c_{2i}}{10} \qquad \text{(values ranged from 1.13 – 1.95)} \quad (\sigma = 0.25),$$

$$k_1 = 1.32\, \Delta p_x + 1.25 \cdot 10^{-2} \qquad (R^2 = 0.91),$$

$$k_2 = \frac{1}{t_x},$$

$$\Delta p_x = 1.16 \cdot 10^{-1}\, \mathrm{LWC} + 8.20 \cdot 10^{-3}\, \mathrm{V} + 3.75 \cdot 10^{-2} \qquad (R^2 = 0.97),$$

and

$$t_x = \left[\frac{1}{c_1} \ln \left[\frac{\Delta p_x}{\Delta p_0}\right]\right]^{1/c_2}$$

As shown by four typical curves in Fig. 11 the calculated values fit the measured ones reasonably well. The relative simplicity of the models, as well as the ease with which the empirical coefficients can be determined from test results[35], should encourage further investigations in this area. With the experience gained, it is possible to show that the information necessary for these particular models could have been obtained by 5 or 6 filter tests and a judicious selection of the test conditions. The greatest disadvantage of such models lies in their validity for only a single production lot of filter units.

Mathematical models such as these have applications other than that of being able to predict pressure drop increases in terms of particular airstream parameters. For example, an equation similar to that for Δp_x was established to predict the pressure drop at structural failure Δp_d, for the filter units. Measured values for the 10 tests deviated from

$$\Delta p_d = 7.71 \cdot 10^{-3}\, \mathrm{V} + 1.60 \cdot 10^{-1}\, \mathrm{LWC} + 2.84 \qquad (R^2 = 0.86)$$

by not more than 12%. An empirical expression for the exposure time until failure was also developed in terms of V and LWC using the above functions and coefficients.

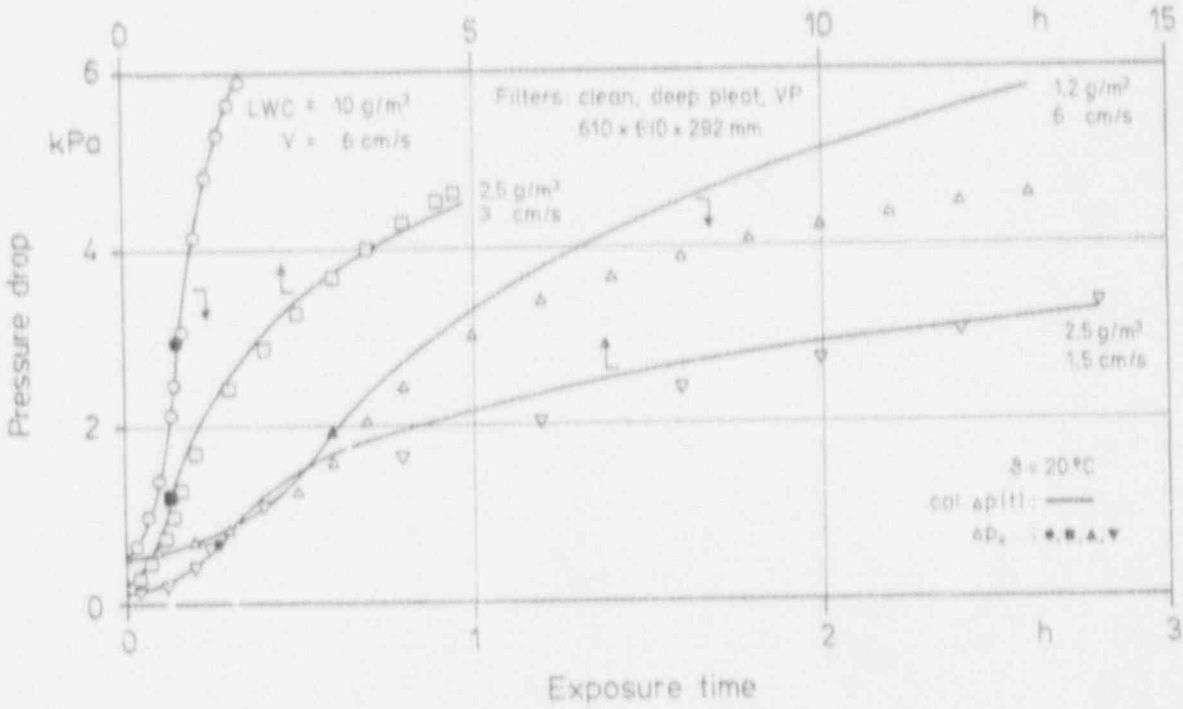

Fig. 11: Comparison of measured and calculated pressure drop increases for clean, deep-pleat, 610- x 610- x 292-mm filters at 20°C under fog conditions.

IV. Summary and Conclusions

Surveys of the literature indicate that the development of measures to counter the effects of high air humidity have not eliminated incidents of moisture-related HEPA filter failure or air cleaning system malfunction. Prevention of similar events in the future will depend on the possible causes being forthrightly addressed. Included among these are the nonuse or the shortcomings of available countermeasures - in particular insufficiently stringent performance standards for new, clean nuclear-grade filter units in humid air. Regulatory guides that do not take full advantage of potential countermeasure technology may also in part be responsible. Improved field surveys and incident reporting systems would be required to more definitively attribute reported failure events to their respective causes.

Current safety concepts, which essentially rely on countermeasures intended to prevent filter exposure to moisture, should include back-up provisions sufficient enough to at least prevent filter structural failure in humid airflow. That the maximum blower static pressure could in principle appear across water-clogged HEPA filter units additionally underscores the need to consider revision

of filter unit wet-strength qualification standards. Based on established failure mechanisms, the stabilization of the filter pack and the use of filter media with increased wet strength could help eliminate structural failure in humid airflow. The reliability of filter units in dry air would thereby also be increased.

The results of the parameteric studies reported on here indicate that pressure drop increases for clean filters exposed to fog at steady-state conditions can be modeled well by relatively simple functions of the exposure time and several airstream parameters. Pressure drop increases for clean water-repellent filter media were insignificant up to saturation. Models for dust-loaded filter units in humid airflows are still in development.

The principal drawback of such models is their particularly strong dependence on the characteristics of the filter units and any captured particulates involved. Accordingly, safety analysts will be forced either to obtain empirical data for the specific cases of interest or to choose conservative values from those that otherwise become available.

The observed decreases in Δp of dust-loaded filters for elevated temperatures above 40 - 50°C offer a potential benefit in lowering the structural loads on filter units at air humidities up to saturation. They also point to a further advantage in the use of heaters. Under fog conditions, however, no positive effect was evident for the filter units and temperatures (up to 50°C) investigated.

V. Future Tasks

For the future, a number of research needs become apparent not only for model development and verification but also with regard to protecting filter units from moisture-related failure.

The models currently under development will be valid only for steady-state operating conditions. Flow, humidity, or temperature transients can affect the transfer of water into the filter medium or the captured-dust structure, and hence filter Δp. Models for Δp increases with varying airstream conditions remain to be delt with.

The observed overproportional increases in Δp of dust-loaded samples for $V = 1.25$ cm/s, together with the potential increases in filter Δp with decreasing system airflow seem particularly threatening to filter unit integrity. Since each can contribute to filter failure in normal service, their potentially interactive, individual effects need be investigated in combination. The utilization of simplified or scale-model air cleaning systems will be required in such an endeavor.

With respect to severe accident conditions, the effectiveness of currently employed droplet separators and heaters in protecting aged, dust-loaded filters from condensing steam need to be verified, particularly during the transient temperature, humidity, and flow conditions of a major LOCA.

VI. Acknowledgements

The authors wish to acknowledge the invaluable contribution of Mr. E. Demmer for the design, construction, and operation of the LÜFTER test rig. The effort of Dr. V. Rüdinger in obtaining funding and guiding the research effort into its final stages is also greatly appreciated.

VII. References

(1) Tillery, M.I,
High Efficiency Air Filtration;
in: Filtration Principles and Practices,
Matteson, M.J. and Orr, C.: Eds., 2nd ed.;
Marcel Decker Inc., New York, 1987.

(2) IES-RP-CC-001-86
Recommended Practice for HEPA Filters;
Institute of Environmental Sciences,
Mt. Prospect, IL 60056, 1986.

(3) Burchsted, C.A., Fuller, A.B. and Kahn, J.E.
Nuclear Air Cleaning Handbook;
ERDA 76-21
Oak Ridge National Laboratory, Oak Ridge, TN, 1976.

(4) ANSI / ASME N509 - 1980
Nuclear Power Plant Air Cleaning Units and Components;
ASME, New York 10017, 1980.

(5) Nicolaysen, E., Carey, K.E. and Wollak, J.J.
Standardization of Air Cleaning Systems
for Nuclear Powerplants;
CONF 760 822 (1977) p. 761 ff.

(6) MIL-F-51079D
Military Specification
Filter Medium, Fire-Resistant, High-Efficiency;
U.S. Government Printing Office, Wash., D.C., 1985.

(7) MIL-F-51068F
Military Specification
Filter, Particulate, High-Efficiency, Fire Resistant;
U.S. Government Printing Office, Wash., D.C., 1986.

(8) DIN 25 414
Lüftungstechnische Anlagen in Kernkraftwerken;
Beuth Verlag GmbH, Berlin 30, 1990.

(9) Bender, H.
Personal communication;
PHDR Versuchsanlage, Karlstein, FRG, 4.86.

(10) Frigerio, N.A. and Stowe, R.S.
Plutonium and Uranium Emission Experience in U.S. Nuclear Facilities Using HEPA Filtration;
in: Proceedings of Seminar on High Efficiency Aerosol Filtration in the Nuclear Industry;
Aix-en-Provence, France, Nov., 1976,
Commission of the European Communities, Luxembourg, 1977
p. 457 ff.

(11) Lillyman, E. and Bristow, H.A.S.
Some Experience in HEPA Filtration at DERE and AWRE;
in: Proceedings of Seminar on High Efficiency Aerosol Filtration in the Nuclear Industry;
Aix-en-Provence, France, Nov., 1976,
Commission of the European Communities, Luxembourg, 1977,
p. 483 ff.

(12) Ricketts, C.I., Rüdinger, V. and Wilhelm, J.G.
HEPA Filter Behavior Under High Humidity Airflows;
CONF 860 820 (1987), p. 319 ff.

(13) Moeller, D.W.
Problems in Nuclear Air-Cleaning Systems;
Nuclear Safety 16 (4) (1975) p. 469 ff.

(14) Moeller, D.W.
Failures in Air-Monitoring, Air-Cleaning, and Ventilation Systems in Commercial Nuclear Power Plants
(Jan. 1, 1975 - June 30, 1978);
Nuclear Safety 20 (2) (1979) p. 176 ff.

(15) Moeller, D.W. and Sun, L-S.C.
Failures in Air-Monitoring, Air-Cleaning, and Ventilation Systems in Commercial Nuclear Power Plants, 1978-1981;
Nuclear Safety 24 (3) (1983) p. 352 ff.

(16) Muhlheim, M.D.
Technical Note: AEOD/E410
Operational Experiences Involving Standby Gas Treatment Systems that Illustrate Potential Common-Cause Failure or Degradation Mechanisms;
Nuclear Safety 26 (5) (1985) p. 648 f.

(17) Regulatory Guide 1.140, Revision 1
Design, Testing, and Maintenance Criteria for Normal Ventilation Exhaust System Air Filtration and Adsorption Units of Light-Water-Cooled Nuclear Reactor Power Plants;
Office of Standards Development,
USNRC, Wash., D.C., 1979.

(18) Peters, A.H. et al.
Applications of Moisture Separators and
Particulate Filters in Reactor Containment;
TID-4500, USAEC DP-812,
Savannah River Laboratory, Aiken, SC, 1962.

(19) Jones, L.R.
Effects of Radiation on
Reactor Confinement System Materials;
CONF 720 823 (1972) p. 655 ff.

(20) Johnson, J.S. et al.
The Effects of Age on the Structural Integrity of
HEPA Filters;
CONF 880 822 (1989) p. 366 ff.

(21) Robinson, K.S. et al.
In-Service Aging Effects on HEPA Filters;
in: Gaseous Effluent Treatment in Nuclear Installations;
Fraser, G. and Luykx, L., Eds.,
Graham & Trotman, London, 1986, p. 60 ff.

(22) Rüdinger, V., Ricketts, C.I. and Wilhelm, J.G
High Strength HEPA Filters For Nuclear Applications;
Nuclear Technology, to be published in Oct. 1990.

(23) Carbaugh, E.H.
Survey of HEPA Filter Applications and
Experience at Department of Energy Sites;
NTIS, UC-70, PNL-4020,
Pacific Northwest Laboratories, Richland, WA, 1981.

(24) Durant, W.S. et al.
Activity Confinement System of the Savannah River
Plant Reactors;
TID-4500, DP-1071
Savannah River Laboratory, Aiken, SC, 1966.

(25) Neuberger, M. and Schlehuber, F.
Störfallbeanspruchung innerhalb von Lüftungsanlagen;
in: Projekt Reaktor Sicherheit, Jahresbericht 1989,
KfK-4450/89, Kernforschungszentrum Karlsruhe (1990).

(26) Rüdinger, V., Ricketts, C.I. and Wilhelm, J.G.
Limits of HEPA Filter Application Under High-Humidity
Conditions;
CONF 840 806 (1985) p. 1058 ff.

(27) Ricketts, C.I., Rüdinger, V. and Wilhelm, J.G.
The Flow Resistance of HEPA Filters in Supersaturated
Airstreams;
CONF 880 822 (1989) p. 668 ff.

(28) Schlehuber, F.
HEPAFIL - ein Programm zur Berechnung der Strömungsgrößen am Schwebstoffilter;
KfK-4773,
Kernforschungszentrum Karlsruhe, FRG, 1990.

(29) Jones, L.R.
HEPA Filter Performance Following Service and Radiation Exposure;
CONF 740 807 (1974) p. 565 ff.

(30) Nitteberg, L.J. and Smith, R.K.
Humidity Test Report
NPR High-Effiency Filter Bid Evaluation;
TID-7677 (1963) p. 575 ff.

(31) Stratmann, J.
Bericht eines Großverbrauchers von Schwebstoffiltern der Klasse S;
in: Proceedings of Seminar on High Efficiency Aerosol Filtration in the Nuclear Industry;
Air-en-Provence, France, Nov., 1976,
Commission of the European Communities, Luxembourg, 1977.
p. 411 ff.

(32) Schwalbe, H.C.
Redevelopment of the Savannah River Laboratory Moisture Resistance Test for Filter Paper;
CONF 680 821 (1968) p. 80 ff.

(33) Lathrache, R.
Stationäre und instationäre Partikelabscheidung in Faserfiltern;
Wiss. Z. Techn. Univ. Dresden 29 (6) (1980) p. 1337 ff.

(34) Ricketts, C.I.
Das Verhalten von Schwebstoffiltern der Klasse S unter Durchströmung mit Luft hoher Feuchte;
Dissertation, Universität Karlsruhe, to be published in 1991.

(35) SAS User's Guide: Statistics, Ver. 5 Ed.,
SAS Institute, Cary, NC (1985) p. 711 ff.

DISCUSSION

KOVACH: On the fourth or fifth slide you were showing temperature effects at constant relative humidity. Was this a used filter?

RICKETTS: The tests were performed on small samples of filter media removed from filter units after normal service in an air cleaning system at Kernforschungszentrum Karlsruhe.

KOVACH: A clarification, you were coming in at 94% R.H. and that you were superheating. Therefore the humidity would be lower at higher temperature. Or did you maintained 94% R.H. all the way through.

RICKETTS: These were results from three different tests. Each test was conducted at a different temperature but the relative humidity was identical for each test.

KOVACH: Is the velocity that you gave a normalized velocity under standard conditions or the velocity at actual temperature?

RICKETTS: That is the velocity at the actual temperature.

KOVACH: If you normalized velocity there would have been significantly different velocities through the media.

RICKETTS: No, I gave the velocity in the media.

OPTIMIZATION OF AIR DUCTS FOR NUCLEAR REACTOR POWER GENERATION STATION

Katsumi Hirao
Nuclear Power Design Division
Nuclear Power Construction Department
Tokyo Electric Power Company
Tokyo, Japan

Hirokazu Yoshino
Plant & System Planning Section
Plant & System Planning Department
Nuclear Energy Group
Toshiba Corporation
Yokohama, Japan

Takayuki Sonoda
Nuclear Power Plant Engineering Department
Hitachi, Works
Hitachi Ltd.
Hitachi, Japan

Abstract

In the optimization study on the heating, ventilating and air conditioning system in Nuclear Reactor Power Generation Station, proper arrangement of air ducts has been studied using the experimental and analytical investigation from a viewpoint of duct arrangement optimization. This study consists of two parts. Part I is optimization of air ducts in the corridors and Part II is optimization of air duct in each room.

In part I , from viewpoints of confinement of radioactive materials in facilities having possible radioactive contamination and improvement of thermal environment for workers, we have studied air ducts system in which fresh air is supplied to corridors and heat removal and ventilation for each room are performed by transfering air from the corridors, instead of current ducts system with supply duct to each room. Hereafter we call this air ducts system as "substitution of corridors for air ducts". Surveying plant characteristics in 1350 MWe class Advanced Boiling Water Reactor Power Station, hypothetic test building, that is one floor model which consists of a corridor and twenty-one (21) rooms is established. Air temperature and air flow distribution in the corridor and each room in the above test building are examined, using a similar model and a thermal fluid computer analysis program. From the test results, temperature in the corridor rises in proportion to a distance from supply outlet, rising rate of the temperature has certain value and items to be considered for application of substitution of corridors for ducts to a actual plant are obtained.

Futhermore, conceptual design of substitution of corridors for ducts is conducted for reactor area in a Advanced Boiling Water Reactor Power Station, using design method obtained in this study. As a result, reduction of air ducts and space for duct arrangement and improvement of environment in corridors are obtained.

In part II , the condenser room with complex configuration and

large space, and the electrical equipment room with simple space are selected for model areas. Experimental investigation with the one-tenth reduced scale model and analytical investigation with a three-dimensional thermal hydraulic analysis method are performed to understand the flow and the temperature characteristics in both rooms.

In the investigation of the condenser room, the measured temperature data in an actual plant in the plant operation mode are compared and evaluated with the measured data at the experiment and the result of the analysis. The optimized duct arrangement was proposed from the temperature distribution and the flow distribution point of view by selecting six (6) duct patterns as a parameter. In addition, three (3) cases were selected for analysis from the six (6) cases of experiments, and three-dimensional thermal hydraulic analysis have been carried out, and verified the conformity with the actual plant data. As a result, based on the obtained ventilation type, the optimization of air-duct in the condenser room are established.

In the investigation of the electrical equipment room, experimental investigation is done for the conditions of duct patterns (layouts of supply and exhaust ducts) and several thermal parameters. The experiment was done for twenty-seven (27) cases under each condition. The thermal parameters are the configuration of rooms, that of heat generators in each room and the heat generation density in each room. And the optimization of air-duct arrangement is estalished in accordance with room conditions and the method of selection for duct arrangement design is estalished. Now, analytical investigation method verified by comparing with experimental data in typical cases.

Based on these studies, experimental and analytical investigation (using a three-dimensional thermal hydraulic analysis) technique has been established, and the effective design method for duct arrangement of HVAC design has been verified for Boiling Water Reactor Power Station. The air-duct arrangements optimized in this study are applied to an Advanced Boiling Water Reactor Power Station in trial and reduction of the air-duct quantity is confirmed.

Optimization of Air Ducts in the Corridors (Part I)

I. Introdution

In our current design, ventilation and air conditioning for nuclear power stations have been performed by supply and exhaust ducts installed in each room. But recently, corridors where operators pass frequently are required to have improved thermal environment for operators. Additionally, as building volume of a nuclear power plant is reduced from a stand point of rationalization, each system and equipment should also be reduced in the amount of the materials. We have proposed an air duct ventilation system as "substitution of corridors for air ducts" in order to respond above requirements. As substitution of corridors for air ducts is assumed, temperature distribution in corridors should be evaluated quantatively, because it is expected that supply air temperature to each room is different due to air temperature distribution in a corridor. From this point of view, we made a scale model which can easily change heat load and so

on as parameters, and studied the tendency of temperature distribution in a corridor through experiments and computer analyses.

II. Method of Study

Before the study of design method for "substitution of corridors for air ducts", shapes and heat loads in reactor area and radioactive waste disposal area of a 1350 MWe class Advanced Boiling Water Reactor Power Station are surveyed. Results of the survey are shown in Table 1. From the results of the survey, a model of nuclear power plant is established as shown in Figure 1.

Table 1 Plant data for ventilation system design

Items	Reactor Area (R/A)	Rad. Waste Area (Rw/A)
Shapes of Corridors	Blind Alley (3 Floors) Loop (1 Floors)	Blind Alley (3 Floors) Loop (1 Floors)
Length of Corridors	About 160 m/Floor	About 160 m/Floor
Widths of Corridors	Average of Narrow Corridors 2.4 m Average of Wide Corridors 8.6 m	Average of Narrow Corridors 1.8 m Average of Wide Corridors 6.6 m
Height of Corridors	5.9 m (2.3 ~7.7 m)	6.1 m (4.5 ~7.6 m)
Shape of Rooms	Square 84 % Others 16 %	Square 100 %
Number of Rooms	Average 18 Rooms/Floor	Average 14 Rooms/Floor
Area of Rooms	Average 37 m²/Room	Average 71 m²/Room
Volume of Rooms	Average 228 m³/Room	Average 449 m³/Room
Heat Load of Equipment in Corridors	Maximum 19200 W	Maximum 19200 W
Heat Load of Lighting in Corridors	Average 14.9 W/m² (10.2 ~19.7 W/m²)	Average 18.1 W/m² (14.0 ~19.0 W/m²)
Heat Load of Equipment in Rooms	Maximum 15200 W	Maximum 15200 W
Heat Load of Lighting in Rooms	Average 11.7 W/m² (9.3 ~15.0 W/m²)	Average 14.7 W/m² (13.7 ~15.9 W/m²)
Thickness of Wall	0.72 m ± 0.42 m (Drywell 2.0~2.5 m)	0.9 m ± 0.1 m
Size of Hatchway	Maximum 8.9 m × 6.0 m	Maximum 2.0 m × 3.0 m

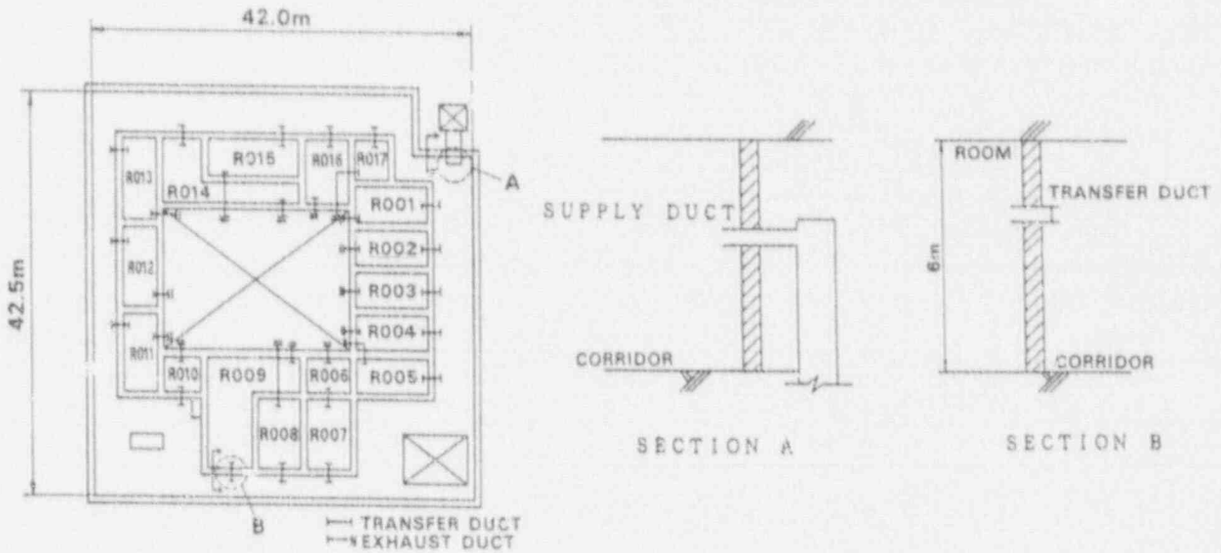

Figure 1 Typical floor model in a nuclear power plant

This hypothetical test building is designed to imitate typical floor in the nuclear power station, and it consists of a circular corridor and rooms surrounded by the corridor. On the floor, a hatchway is installed considering the effect of the lower level floor. Fresh air over this floor is supplied from the corridor corner into the corridor. Openings (transfer ducts) are installed in the partition wall between the corridor and each room, and the exhaust ducts are installed in each room. Air for each room is supplied from the corridor via transfer duct. Therefore, the supply air temperature for each room has a relation with the position of the transfer duct which is installed in the partition wall.

Scale model tests and computer analyses shown below, are carried out for a primary purpose of understanding the tendency of the air temperature distribution in the corridor.

III. Tests and Analyses

Method of Scale Model Tests

In this scale model test, a similar model reduced to a scale of one-tenth hypothetical test building size (See Figure 1, the model size is approximately 4m x 4m x 1m) is adopted. The similarity rules applied to the test and the reduction ratio are listd in Table 2. Similarity rule of velocity is calculated by allowing the archimedes number to agree between the actual device the model in Equation (1). These rules are typical in such a similar model test. (1)(2)(3)

$$\text{Archimedes Number} = \frac{\text{Buoyancy Force}}{\text{Inertial Force}} = \frac{\rho g \beta \Delta\theta l^3}{\rho l^2 u^2} = \frac{g \beta \Delta\theta l}{u^2} \qquad (1)$$

[$\Delta\theta$: Differential temperature l : Representative length u : Air velocity ρ : Density
β : Unit volume expansion g : Gravitational acceleration]

Table 2 Similarity rules

Item	Similarity Rule and Reduction Ratio
Velocity	$nu = n\theta^{1/2} \cdot nl^{1/2} = (1/10)^{1/2}$
Heat Load	$nQ_H = n\theta^{3/2} \cdot nl^{5/2} = (1/10)^{5/2} = 3.16 \times 10^{-3}$
Flow Rate	$nV = nl^2 \cdot nu = (1/10)^{5/2} = 3.16 \times 10^{-3}$
Thermal Resistance	$nr = nu^{-1} \left(\frac{1}{\alpha_N \gamma_N} + 1 \right) - \frac{1}{\alpha_M \gamma_N}$

nu: Reduction Ratio of Air Velocity
$n\theta$: Reduction Ratio of Differential Temperature
nl: Reduction Ratio of Representative Length
nQ_H: Reduction Ratio of Heat Load
nV: Reduction Ratio of Air Flow Rate
nr: Reduction Ratio of Thermal Resistance
α_M: Heat Transfer Coefficient (Actuality)
α_N: Heat Transfer Coefficient (Scale Model)
γ_N: Thermal Resistance (Actuality)

In scale model tests, it is usual to use one-room model and heat loads from walls are simulated by plate heaters or regarded as an adiabatic system. In this scale model test, the mulit-room model is considered and heat load from the wall is simulated by using wall material having thermal conductivity calculated based on the reduction ratio of thermal resistance.

Conceptual flow diagram of model test is shown in Figure 2.

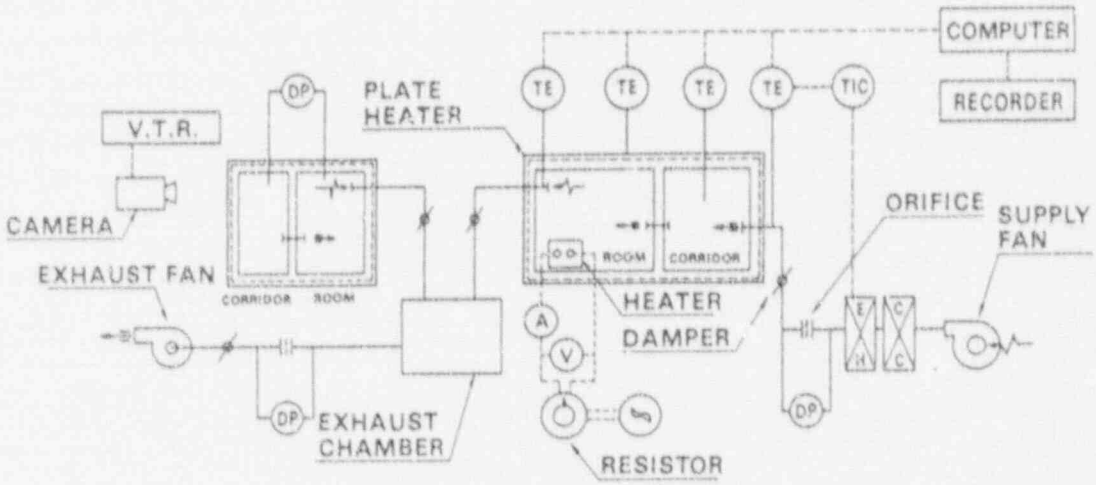

Figure 2 Conceptual flow diagram of model test

About two hundred fifty thermocouples are installed in the model in order to measure the air temperature distribution in the corridor.

Method of Thermal Fluid Computer Simulation

In this analysis, non-compressive viscosity fluid model is used as air flow since the air flow velocity in this study is sufficiently lower than the sound speed and there is no factor of causing a significant turbulent flow except a flow near the duct outlet. The buoyant force effect and the vortex viscosity effect by turbulent flow are analyzed by approximation of Boussinesq and Zero(0) equation model. These flows are given by the following equations (2),(3) and (4). The number of meshes is 2023 (17x17x7). The individual physical property values are the same as those of the scale model tests.

$$\frac{\partial u_j}{\partial x_j} = 0 \tag{2}$$

$$\frac{\partial u_i}{\partial t} + \frac{\partial}{\partial x_j}(u_i u_j) = -\frac{1}{\rho_0}\frac{\partial P}{\partial x_i} + \frac{\partial}{\partial x_j}\left((\nu_0 + \varepsilon_M)\frac{\partial u_i}{\partial x_j}\right) + \frac{\rho_{(T)}}{\rho_0}\vec{g} \tag{3}$$

$$\rho_{(T)} = \rho_0 \{1 - \beta (T - T_0)\}$$

$$\frac{\partial h}{\partial t} + \frac{\partial}{\partial x_j}(h\, u_j) = \frac{\partial}{\partial x_j}\left((\alpha_0 + \varepsilon_H)\frac{\partial T}{\partial x_j}\right) + \dot{Q} \tag{4}$$

u: Velocity h: Enthalpy ν_0: Viscosity
P: Pressure T: Temperature α_0: Thermal Diffusivity
g: Gravitational Acceleration
ε_M: Eddy Viscossity ε_H: Eddy Diffusivity

Conditions for Tests and Analyses

In the tests and analyses, the measurement of air temperature and air flow distribution in the model was carried out using the heat load as a parameter. This parameter is the thermal distribution in the model (Table 3 and 4). Table 3 divides the heat load over the floor in the model into three cases. We refer to the case of small load as "Case a ", the average case as "Case b ", and the large case as "Case c " in accordance with plant data for ventilation system (Table 1). Case c is divided into the case of small heat load from equipment in the corridor and the case of great heat load from equipment in the corridor. In table 4, we refer to the case where the heat load from the equipment in the room becomes larger as the room is closer to the air supply outlet in the corridor as "Heat Load Distribution 1", the reverse case as "Heat Load Distribution 3", and the flat case as "Heat Load Distribution 2".

Table 3 Heat load parameter

	Heat Load in the Model (W)				
	Total Heat Load	Corridor		Rooms	
		Equipment	Walls, Lighting	Equipment	Walls, Lighting
Heat Load a	32560	0	14830	8840	8840
Heat Load b	65010	5700	21740	28730	8840
Heat Load c-1	97460	9420	26160	53040	8840
Heat Load c-2		26150	26160	36210	8840

Table 4 Heat load distribution in the model

	Heat Load (W)											
Room Number	Heat Load a Distribution			Heat Load b Distribution			Heat Load c-1 Distribution			Heat Load c-2 Distribution		
	1	2	3	1	2	3	1	2	3	1	2	3
R001		520		5750	1690	0		3120		7220	2130	
R002		520		5100	1690	0		3120		6450	2130	
R003		520		4470	1690	0		3120		5640	2130	
R004		520		3830	1690	0		3120		4840	2130	
R005		520		3190	1690	0		3120		4030	2130	
R006		520		2550	1690	0		3120		3220	2130	
R007		520		1920	1690	0		3120		2410	2130	
R008		520		1280	1690	0		3120		1600	2130	
R009		520		640	1690	640		3120		800	2130	
R010		520		0	1690	1280		3120		0	2130	
R011		520		0	1690	1920		3120		0	2130	
R012		520		0	1690	2550		3120		0	2130	
R013		520		0	1690	3190		3120		0	2130	
R014		520		0	1690	3830		3120		0	2130	
R015		520		0	1690	4470		3120		0	2130	
R016		520		0	1690	5100		3120		0	2130	
R017		520		0	1690	5750		3120		0	2130	

IV. Result and Evaluation

Results

As one result of these model tests, Figure 3 shows the relationship between the distance from the outlet in the corridor and the air temperature of the corridor. In Case a/2(heat load a and distribution 2) and b/2, the standard deviation by the primary approximation is calculated for 100m and 160m distances from the outlet in the corridor, as the temperature rise rate is nearly linear. These standard deviations are shown in Table 5. This Table shows that the standard deviations for 100m distance from the corridor outlet has better coincidence.

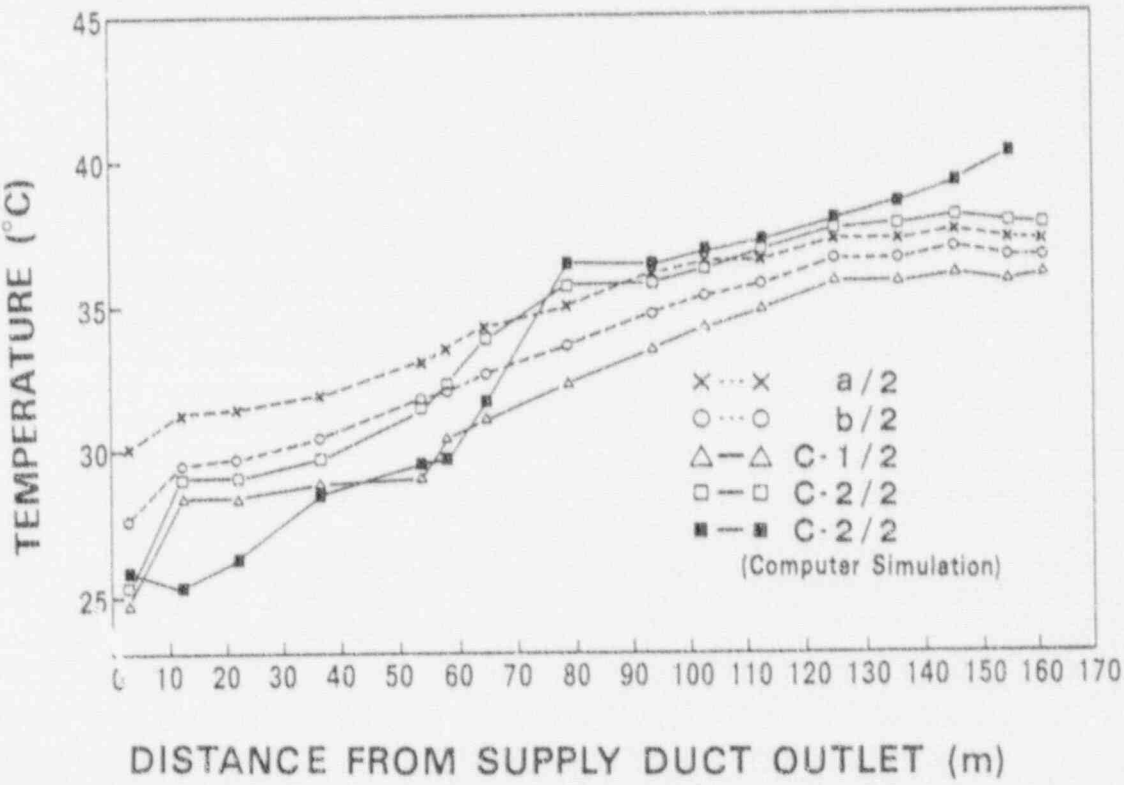

Figure 3 Air temperature in corridor

Table 5 Standard deviation of the primary approximation for air temperature in corridor

	Case a/2		Case b/2	
	From outlet to 100m	From outlet to 160m	From outlet to 100m	From outlet to 160m
Standard deviation of the primary approximation	0.31	0.66	0.31	0.71

Therefor, Table 6 shows the result in which the primary approximation of each case is performed up to 100m long from the outlet. If Case c-1 and c-2 are excluded in this table as these cases are based on large heat load in plant data for ventilation system (Table 1), the temperature rise in the corridor is about 0.06 C/m.

Table 6 Temperature rise in corridor in each case

	Heat Load Distribution 1	Heat Load Distribution 2	Heat Load Distribution 3
Heat Load a		Tc=28.4+0.0694 X σ = 0.31	
Heat Load b	Tc=28.9+0.0762 X σ = 0.32 Tc=30.7+0.0578 X * σ = 0.37	Tc=29.9+0.0647 X σ = 0.31	Tc=26.9+0.0654 X σ = 0.61
Heat Load c-1		Tc=26.0+0.0796 X σ = 0.89	
Heat Load c-2	Tc=30.5+0.0918 X * σ = 0.93	Tc=26.4+0.105 X σ = 0.94	

Tc : Air Temperature in Corridor (℃) X : Distance from Outlet (m) * : Looped Corridor

As a typical result of the computer analyses, the output for Case c-2/2 as well as comparison with the model tests is shown in Figure 3. The average difference between the air temperature by computer analysis and by model test is 0.35 C. The air temperature has good coincidence between computer analysis and model test as the standard deviation is +1.7 C. Figure 4 shows sectional air flow distribution in the corridor for computer analysis and model test on Case b/2. The air flow in the same direction as supply air flow over the floor, reverse air flow to the outlet along the roof, and so on, direction and velocity have good coincidence between computer analyses and model tests. Therefor, we can judge that the tendency of temperature rise in the model tests is the same as that of computer analyses.

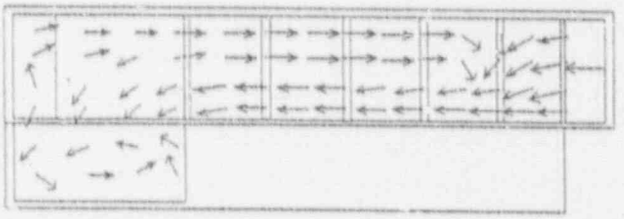

Model Test (Case b/2)

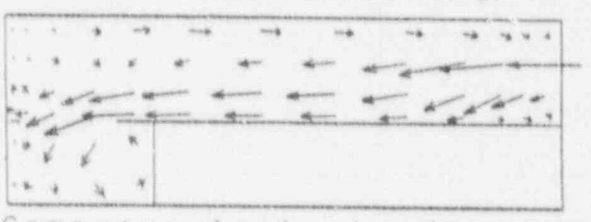

Computer Analysis (Case b/2)

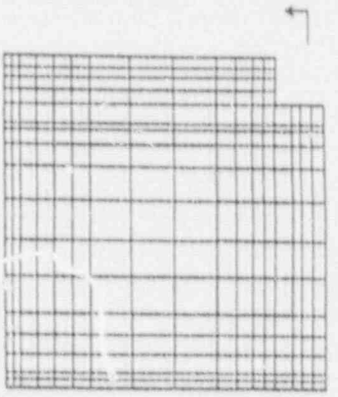

Mesh for Computer Analysis (Plan)

Figure 4 Comparison of air flow pattern between model test and computer analysis

Summary of Design Method

On the basis of the above results and the other data on air flow distribution and so on, we have established the design method of "substitution of corridors for air ducts". The design method is summarized as follows:

1) Distance from a supply outlet in the corridor to a transfer duct of each room is to be within 100m.
2) Temperature rise in the corridor is expected to be 0.06 C/m.
3) Air flow velocity at the outlet in the corridor should be selected about 10 m/sec. to make the temperature in the corridor uniform.
4) When a large opening is installed in the floor, the outlet in the corridor should be installed apart from it as far as possible.

Conceptual Design

The conceptual design of the ventilation system, "substitution of corridors for ducts" is conducted for the reactor area of the 1350 MWe class Advanced Boiling Water Reactor Power Station, using the knowledge obtained in this study. The amount of duct reduction is shown in Table 7. About 30 % of total ducts are reduced. And an improvement of environment in corridors of about 10 C temperature is obtained.

Table 7 Comparison of duct amount

	This System	Current System	Ratio
Supply Ducts	16	53	0.30
Exhust Ducts	48	45	1.07
Transfer Ducts	8	2	4.00
Total	72	100	0.72

Optimization of Air-duct in each room (Part II)

I. Introduction

The optimization of air-duct in each room is performed by comparing and evaluating the experimental investigation with the one-tenth reduced scale model and analytical investigation with a three-dimensional thermal hydraulic analysis method.

The study was performed through the following three (3) steps.

STEP 1. A room with complex configuration and a room with simple space (which can be applied to general design) are selected for model areas.

In case of the model room which is simulated complex configuration, the measured temperature data in an actual plant in some plant operation modes are compared and evaluated with the measured data at the experiment and the result of analysis.

STEP 2. Various cases of duct patterns and conditions in the both rooms are compared and evaluated with experiment and analysis. And the optimized duct layouts are selected.

STEP 3. The scope of application of optimized duct patterns is evaluated, and the optimized duct arrangements of this study are applied, in trial, to an Advanced Boiling Water Reactor Power Station and effects are estimated.

II. Method of study

Selection of model areas

For evaluations of the optimization of air-duct in each room, model areas, which are performed experiment and analysis, are selected from the view point of complex area and generalized area for duct arrangements.

Temperature data are measured in an actual plant, and are used for the experimental and analytical investigation for the model area.

The model areas are two types considering the followings.

a) The area which requires investigations for general design, because the complex air flow is expected and the large three dimensional air flow including up and down flow may occur.
b) The area for general design, because the configuration in the room is simple and flow and temperature distributions are easily definable.

The condenser room and the electrical equipment room are selected as the rooms corresponding to above a) and b).

Method of experiment and analysis

Experiment In case of the experimental investigation of the room with different room average and supply temperatures, the Archimedes Number (eq.(5)) must be kept equal between the model and actuality, which is the similarity rule derived from the buoyancy force and inertia force.

$$Ar = \frac{Fb}{Fi} = \frac{g \ \beta \ \Delta\theta \ l}{u^2} \quad (5)$$

Ar : Archimedes Number
Fb : buoyancy force = $\rho \ g \ \beta \ \Delta\theta \ l^3$
Fi : inertial force = $\rho \ l^2 \ u^2$
ρ : density
g : gravitational acceleration
β : unit volume expansion
$\Delta\theta$: differential temperature
l : representative length
u : air velocity

From the similarity rule, each experimental parameter is set for the one-tenth reduced scale model.

An experimental device is composed as figure 5 and set as the condenser room model. The electrical equipment room model is composed as the part of the condenser room model.

The temperature and flow characteritics are measured in the experiment and compared with the measured temperature data in an actual plant and the result of the analysis.

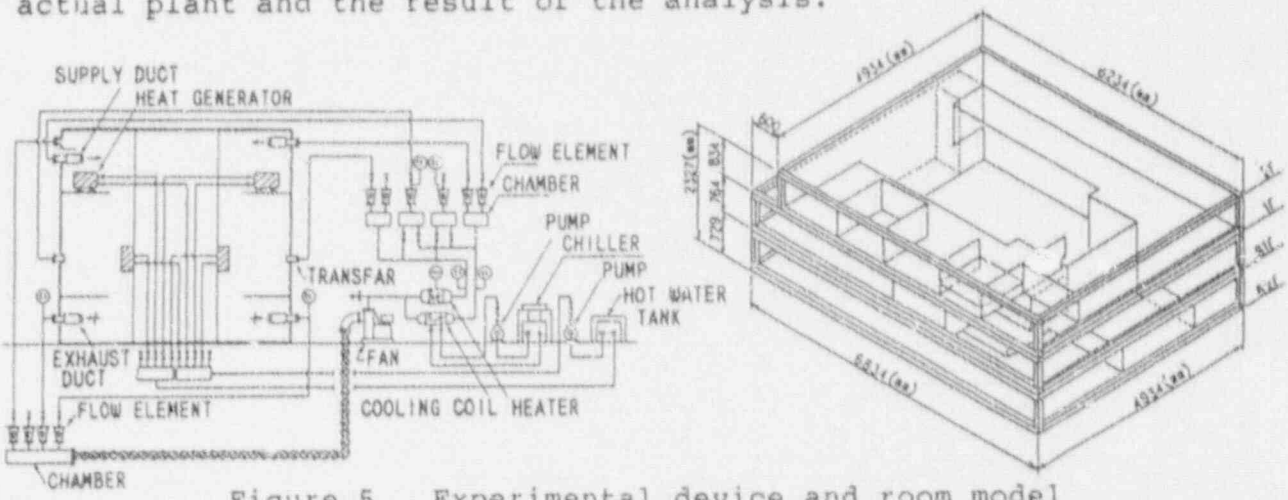

Figure 5 Experimental device and room model

Analysis In the analysis of this study, three-dimensional thermal hydraulic analytical code for non-compressible viscosity fluid is used which treats the thermal convection caused by two forces (buoyancy force and inertial force). Figure 6 indicates the analysis model for the condenser room.

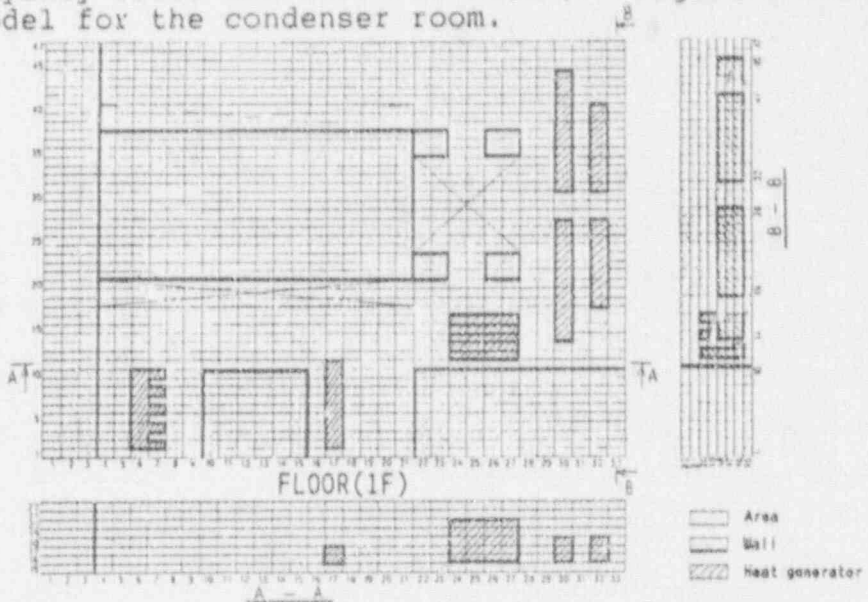

Figure 6 Analysis model for condenser room

III. Optimization of air-duct in condenser room

Experimental condition

Using the condenser room model reduced to one-tenth scale of 1350MWe Advanced Boiling Water Reactor Power Station (ABWR) (see Figure 6), following experiments are performed.

a) Experiment for confirming the temperature distribution of the condenser room of 1100MWe plant ducting using the 1/10 ABWR model. (Case A)

b) Experiments for applying the optimized air duct in the condenser room of 1350MWe plant. (Case B, C)

The basical patterns of duct arrangements are two types. One is that supply ducts are located at upper area (1F) and exhaust ducts are located at lower area (B2F) (Case B). The other is opposite to the above case (Case C). Each case has three (3) duct patterns as shown in Table 8. These are the cases of changing and reducing the supply and exhaust ducts.

Table 8 Experimental conditions of condenser room case

<Experimental case>

Experimental case	Duct Pattern (1F / B1F / B2F)	Note
Case B-1		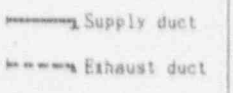 Supply duct Exhaust duct
Case B-2	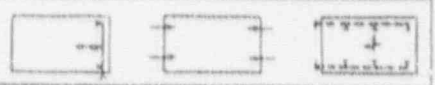	
Case B-3	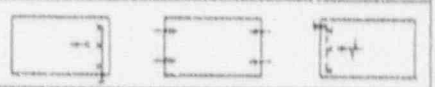	
Case C-1	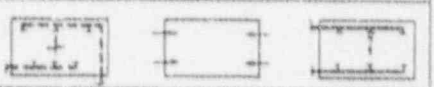	
Case C-2	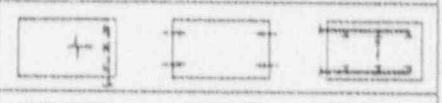	
Case C-3	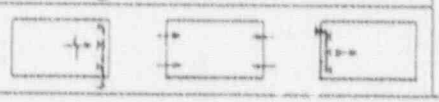	

<Common>

	Actual	Model	Note
1. Length(㎜)	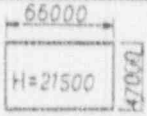	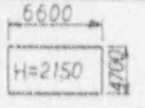	nℓ =1/10 nQ =1/350 nV =3.06×10⁻²
2. Heat load(W)	825,580	2,360	
(1) B2F Piping	339,540	971	
(2) B1F Piping	83,720	238	
(3) 1F Piping	287,210	820	
Heater	80,230	232	
SJAE	34,880	99	
3. Velocity(m/s)	(5.0)	(1.5)	
Supply	6.0	1.8	
Transfar	4.0	1.2	
4. Air flow rate(㎥/h)	(122,100)	(374)	
Supply	64,200	197	
Transfar	57,900	177	

Experiment and analysis

Experiment Figure 7 indicates the measured temperature data of experiment (Case A) and the actual plant.

The tendency of temperature distribution seems nearly equal.

Figure 8 indicate the results of measured temperature of each experiment based on table 8 for selecting the optimized air duct.

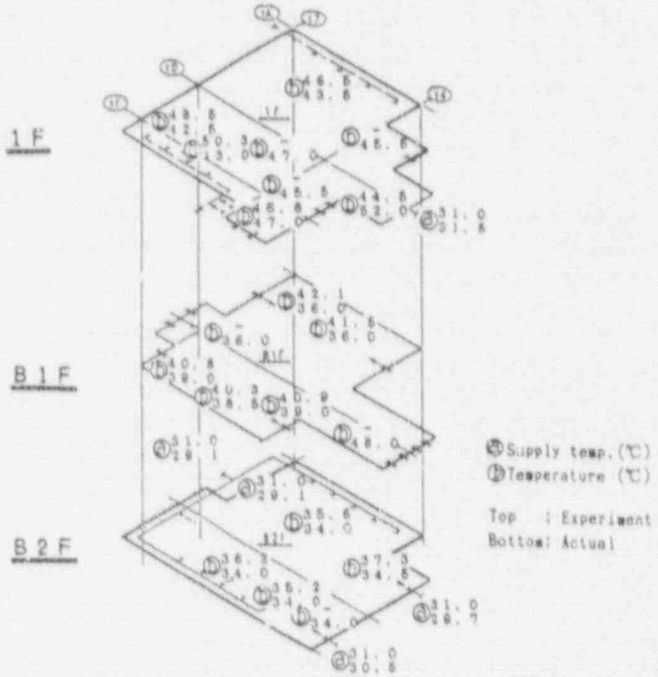

Figure 7 Result of the temperature measured in the experiment (Case A)

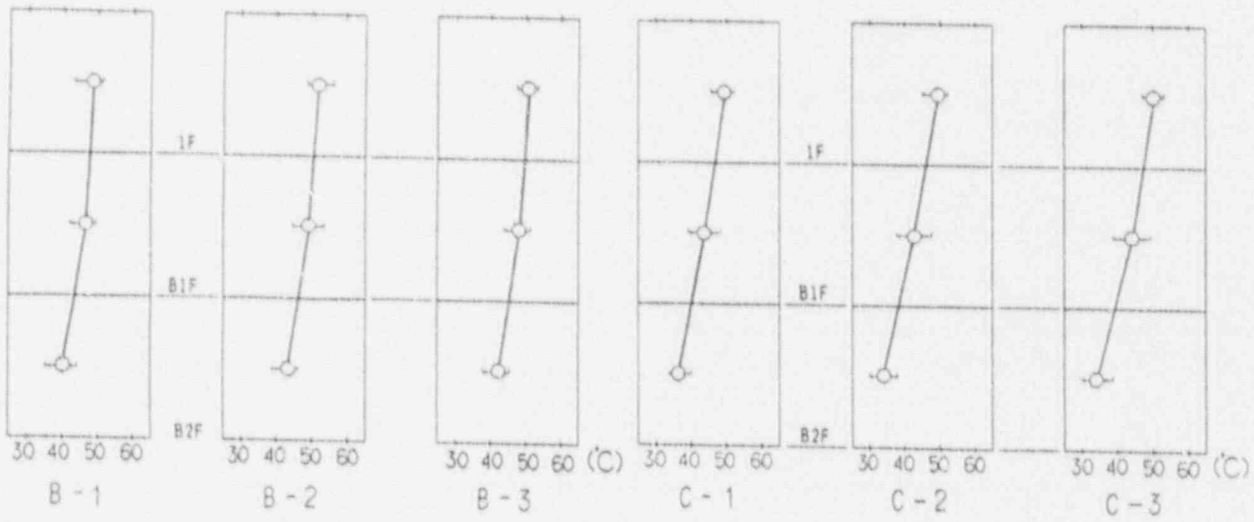

Figure 8 Temperature distribution of each experiment (Case B, C)

From the result of experiments, the dependence of duct patterns on temperature distribution is confirmed as follows.

a) The upper supply and lower exhaust method (Case B) is largely influenced by supply duct and less influenced by exhaust duct. The upper exhaust and lower supply method (Case C) is little influenced by supply duct and largely influenced by exhaust duct.
That is to say, ducts of upper area have larger effect.

b) The upper supply and lower exhaust method (Case B) is more gentle slope in temperature.
That is to say, the ventilation method case B matches for complex and large space.

From the above, the followings are concluded as the guideline for adoption of optimized air duct in the condenser room.

i) The duct arrangement with the upper supply (1F) and lower exhaust (B2F) method has the gentle slope in temperature from upper to lower space.

ii) Minimized exhaust duct is possible because of the small dependence on temperature distribution in lower space.

iii) Supply ducts must be routed in upper space.

Analysis Using the analysis model (see figure 6), analytical investigation is performed to evaluate measured data of the experiment and to determine the duct arrangement in condenser room.

Figure 9 indicates the temperature data from measurement of experiment and result of analysis. The tendency of analized temperature distribution is nearly equal to the data of experiment. The analized direction of air flow has same tendency to the experimental data measured by tuft method.

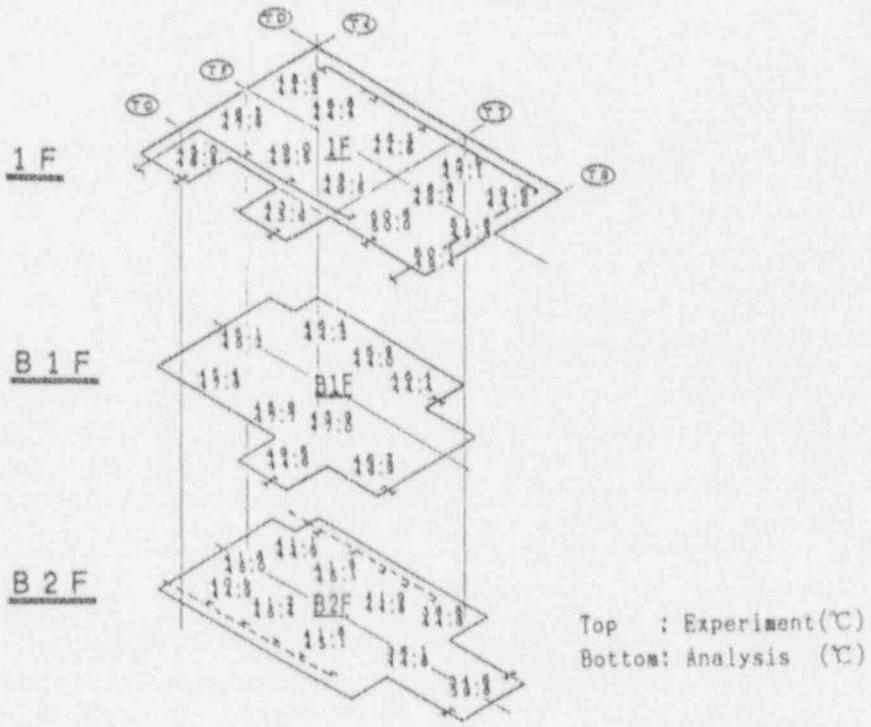

Figure 9 Temperature distribution of experiment/analysis

As the next step, to study a rationalized exhaust ducts design based on the guideline i), ii), iii) above, two analytical cases of pattern A and B are investigated which are considered as reduced exhaust ducts.

Figure 10 indicates the result of analysis. The temperature distribution is nearly equal in both cases, and these duct patterns are applicable to the condenser room.

Table 9 Duct patterns for analysis

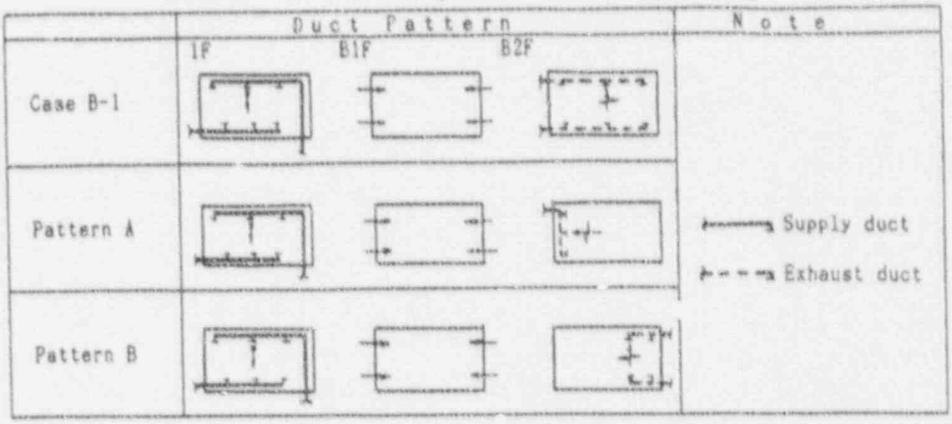

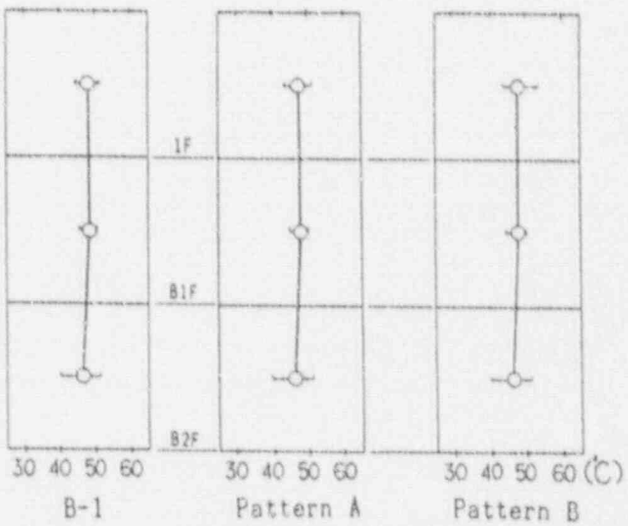

Figure 10 Temperature distribution for cases A, B with reduced exhaust ducts

Conclusion Experimental and analytical investigations are performed for some optimized air ducts in the condenser room, and from the view points of reduction of the air ducts and temperature and flow distribution, the two most optimized air duct systems have been established.

IV. Optimization of air-duct in the electrical equipment room

Experimental condition

In the investigation of the electrical equipment room, experiment is done for conditions of duct patterns (layout of supply and exhaust ducts) and several thermal parameters. The thermal parameters are the configuration and layouts of heat generators and the heat generation density in the room. The experiment is consist of twenty-seven (27) cases shown in Table 10 and 11.

Table 10 Experimental configurations

m_1	Duct pattern	note
①	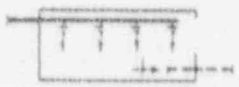	Supply duct type
②	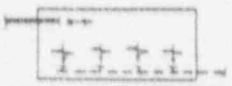	Exhaust duct type
③	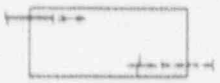	Ductless type

m_2	Configuration of heat generator	Note
①	Concentration 	
②	Dispersion 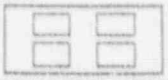	
③	Concontration 	Large type
④	Concentration 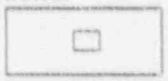	Small type
⑤	Dispersion 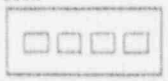	Small type

m_3	Heat load	Heat density
①	139,500 W	66W/㎡
②	41,800 W	20W/㎡
③	13,950 W	6.6W/㎡

Table 11 Experimental conditions

<Common>

	Actual	Model	Note
1.Length(㎜)	26700 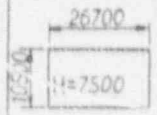 H=7500	2900 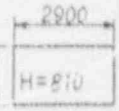 H=810	n ℓ=1/9.2 n Q=1/400 n V=2.92×10⁻²
2.Velocity(m/s)	6	1.7	

<Experimental case>

Experimental code (m_1 – m_2 – m_3)	Actual Heat load (W)	Actual Flow rate (㎥/h)	Model Heat load (W)	Model Flow rate (㎥/h)
① – ① – ①	139,500	19,000	349	55
② – ① – ①	139,500	19,000	349	55
③ – ① – ①	139,500	19,000	349	55
① – ② – ①	139,500	19,000	349	55
② – ② – ①	139,500	19,000	349	55
③ – ② – ①	139,500	19,000	349	55
①–①(②, ④)–②	41,800	5,700	105	17
②–①(③, ④)–②	41,800	5,700	105	17
③–①(③, ④)–②	41,800	5,700	105	17
①–②(⑤)–②	41,800	5,700	105	17
②–②(⑤)–②	41,800	5,700	105	17
③–②(⑤)–②	41,800	5,700	105	17
① – ① – ③	13,950	1,900	35	5.5
② – ① – ③	13,950	1,900	35	5.5
③ – ① – ③	13,950	1,900	35	5.5
① – ② – ③	13,950	1,900	35	5.5
② – ② – ③	13,950	1,900	35	5.5
③ – ② – ③	13,950	1,900	35	5.5

(Eighteen (18) points of temperature measurement are installed nine (9) horizontally times two (2) vertically.)

Experiment and analysis

Experiment Figure 11 indicates frequency of temperature appearance within eighteen (18) points measurement.

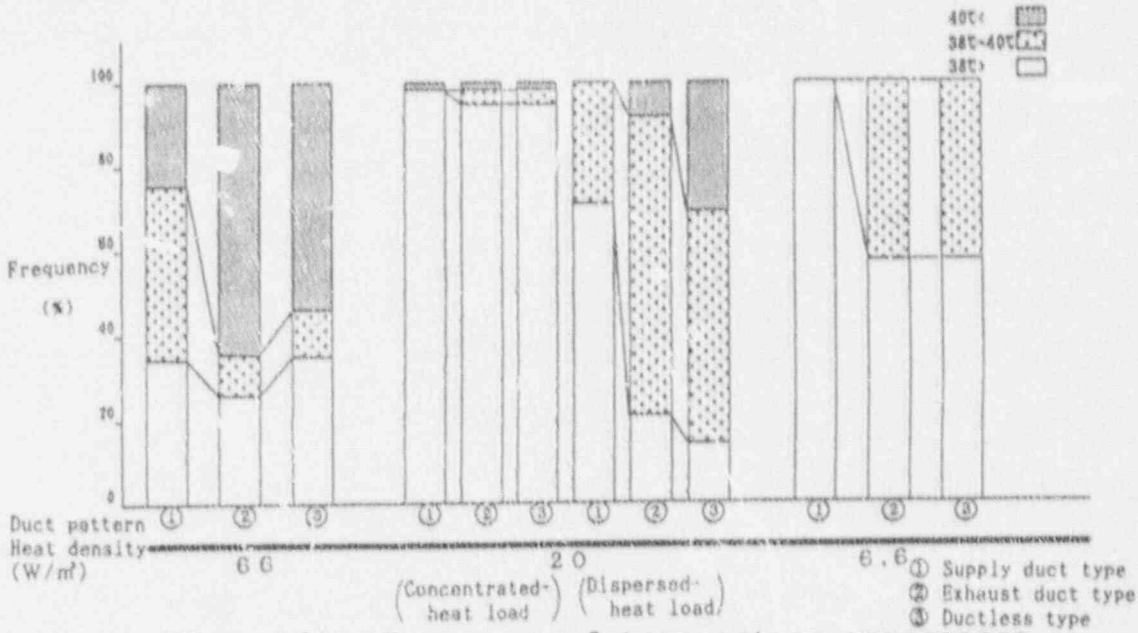

Figure 11 Frequency of temperature appearance in each experimental condition

From the experimental investigation, the followings are concluded as the guideline for application of duct design to ventilate the simply configurated room such as the electrical equipment room.

a) The room with large heat generation density must have supply ducts with several air outlets in both cases of concentrated or dispersed heat generation.

b) The room with medium heat generation density must have supply ducts with several air outlets in case of dispersed heat generation.

c) The room with low heat generation density can be ventilated by ductless type.

Analysis Analytical investigation is performed for selected typical cases and compared with experimental temperature data. The tendency of temperature distribution is nearly equal.

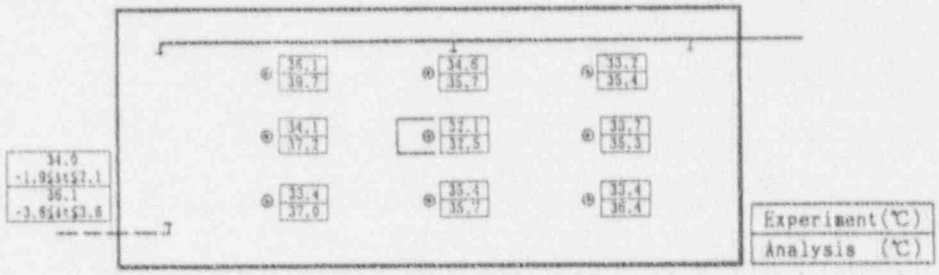

Figure 12 Temperature distribution of experiment/analysis

Conclusion As a result of experiment and analysis, the guideline for air duct optimization in a typical room such as the electrical equipment room is established as shown in figure 13.

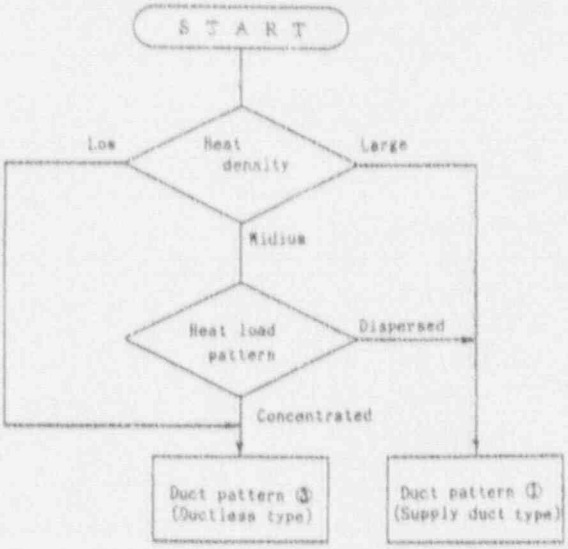

Figure 13 Flow diagram of selection of optimized air duct

V. Summary

Optimized duct arrangement

In this study, experimental and analytical investigations are performed, and for the condenser room with large complex configuration and the electrical equipment room with simple configuration, optimized air duct arrangements are proposed.

For the optimized air duct in the condenser room, the ventilation method with upper supply and lower exhaust duct arrangement is proposed from the view point of reduction of the air duct and temperature and flow distribution.

For the optimized air duct in the electrical equipment room, the optimized duct configurations are proposed in accordance with heat load conditions in the room.

Conceptual design for actual plant

A conceptual design based on the optimized air duct arrangement is carried out for 1350MWe Advanced Boiling Water Reactor Power Station. The effect of reduction of air duct is shown in table 12.

Table 12 Effect of reduction of air duct

		This study ①	Previous design ②	Ratio ①/②
Condenser room	Supply duct	49	49	
	Exhaust duct	25	51	
	Total	74	100	0.74
Electrical equipment room	Supply duct	56	68	
	Exhaust duct	20	32	
	Total	76	100	0.76

Conclusion

The design method for optimization of air ducts has been established by a series of model tests and computer analyses, and the conceptual design has been conducted for 1350 MWe class ABWR power station. As a result, it is confirmed that reduced ducts and space as well as improved environment in corridors are implemented.

Acknowledgements

The assistance of Shin-Nippon Air Conditioning Engineering Co.,Ltd., Hitachi Plant Engineering & construction Co.,Ltd. and Nuclear Engineering Lab. Toshiba Co. during this study is gratefully acknowledged.

References

1. I. Emori and D. J. Schuring, "Theory and Application of Model Test", Gihou-Dou, Tokyo, 1979.
2. T. Shoda and T. Tsuchiya, "Modeling Criteria for the Room Air Motion", Transactions of the Society of Heating, Air-Conditioning and Sanitary Engineers of Japan No.17, Oct, 1981.
3. N. Kobayashi, "Model Experiment for Room Air Distriution", Heating, Air-Conditioning and Sanitary,58-3, 1984.

ALTERNATIVES TO CURRENT PROCEDURES USED TO ESTIMATE CONCENTRATIONS IN BUILDING WAKES

J. V. Ramsdell, Jr.
Atmospheric Sciences Department
Pacific Northwest Laboratory
Richland, Washington

Abstract

This paper discusses a new model for estimating concentrations in building wakes and offers alternative guidance for evaluating the consequences of releases from nuclear facilities. The new model accounts for about 57% of the variability in concentrations observed in wakes. Models suggested in current guidance account for less than 10% of the variability. The alternative guidance demonstrates application of the new model. It covers ground-level releases, roof-top vent and short-stack releases, and elevated releases. It also includes a procedure for accounting for uncertainty in building-wake diffusion estimates.

Introduction

The Nuclear Regulatory Commission provides licensees with guidance on acceptable methods for implementing the Commission's regulations. Regulatory Guides 1.3, 1.4, and 1.5 deal with the problem of estimating diffusion in building wakes simply.[1],[2],[3] Regulatory Guides 1.111 and 1.145 modify the earlier guidance to include use of onsite meteorological data and account for enhanced diffusion at low wind speeds.[4],[5] This paper describes new methods for estimating diffusion in wakes. It offers an alternative to the guidance in Regulatory Guide 1.145, and it compares diffusion estimates made with the alternative to estimates made with the Regulatory Guide procedures.

Regulatory Guide 1.145 recommends treating all releases from buildings as ground-level releases and basing wake diffusion estimates on three equations. These equations are

$$X = Q/[U(\pi\sigma_y\sigma_z + A/2)] \quad (1)$$

$$X = Q/(3\pi U\sigma_y\sigma_z) \quad (2)$$

and

$$X = Q/(\pi U\Sigma_y\sigma_z). \quad (3)$$

where X = concentration at the plume centerline
Q = release rate
U = wind speed at a height of 10 m
σ_y, σ_z = horizontal and vertical diffusion coefficients, respectively
A = projected area of the building, and
Σ_y = a modified horizontal diffusion coefficient.

Equation (1) is a standard building-wake model. It underestimates concentrations near the release point. Equation (2) gives concentrations that are a factor of 3 lower than those predicted for the center of a plume in the absence of a building wake. Thus, Equation (2) limits the credit that may be taken for additional diffusion in a wake. Equation (3) is a ground-level diffusion model in which a modified horizontal diffusion coefficient accounts for increased diffusion resulting from wind meander during low speed conditions. The modification is an empirical correction that depends on wind speed, atmospheric stability, and distance. It includes the effects of building wakes implicitly because it is based on data collected in building-wake experiments.

These equations are used in a two-step procedure. In the first step, Equations (1) and (2) estimate concentrations in the wake. The larger of the concentrations is saved for the second step where it is compared with the concentration estimated using Equation (3). The final concentration estimate is the lower value.

Diffusion in Wakes

Comparisons of concentrations measured in building-wake diffusion experiments with model predictions show that building-wake models do not describe variations of concentrations associated with changes in atmospheric conditions.[6] Figure 1 compares model predictions of centerline concentrations in the wakes with concentrations measured between 8 to 400 m from the release point. At these distances, wake effects should dominate diffusion. On the average, the models predict concentrations that are of the right order of magnitude, but they clearly don't predict the variations.

Further analysis shows that the primary problem with the models is the way in which they account for the effects of wind speed on diffusion. Variation of the ratio between predicted and observed concentrations with wind speed provides a clear indication of the problem. If the model were correct, the ratio would be independent of wind speed because the model includes wind speed as a factor. However, this isn't the case; the ratio is very much a function of wind speed.

Multiple linear regression of observed concentrations on distance, projected building area, wind speed, and stability provides insight to the proper relationship between centerline concentrations in building wakes and wind speed. It also provides a means of determining the predictability of centerline concentrations in building wakes. The regression yields

$$X/Q = \frac{85\ S^{0.47}\ U^{0.72}}{x^{1.1}\ A^{1.2}} \qquad (4)$$

where X/Q = normalized concentration at the plume centerline (s/m^3)
S = numerical equivalent of the Pasquill-Gifford stability class, 1 = A, 2 = B, etc.
U = wind speed (m/s) at 10 m upwind of the building
x = distance from the release point (m), and
A = minimum projected area of the building.

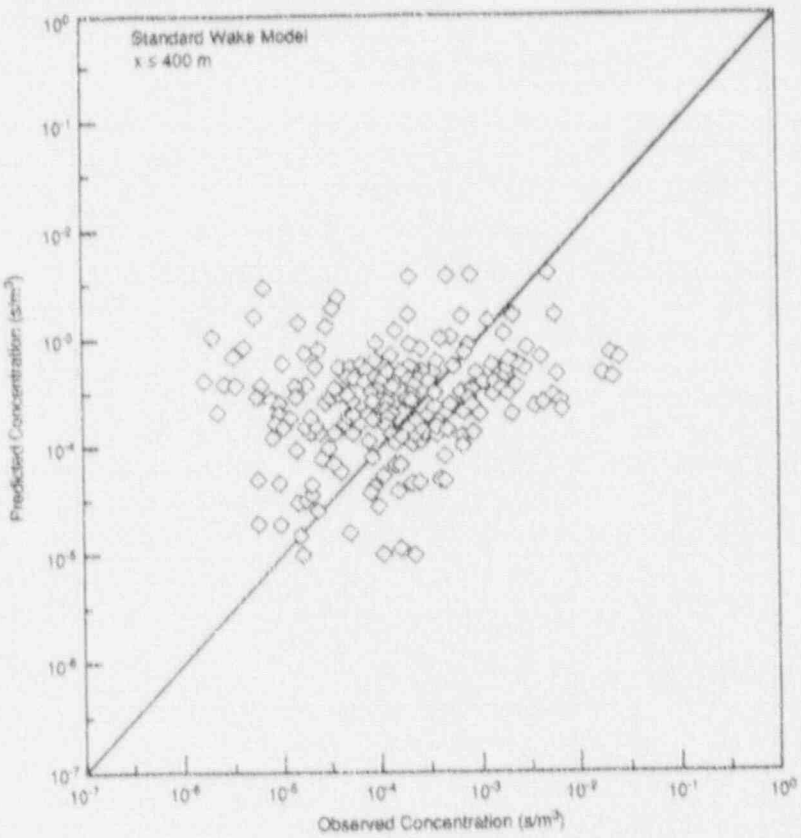

Figure 1 Comparison of centerline concentrations predicted by a standard wake diffusion model with centerline concentrations observed in wakes to a distance of 400 m.

Figure 2 compares the concentrations estimated using Equation (4) with centerline concentrations measured in field experiments. The regression model is significantly better than the regulatory guide models. It accounts for about 65% of the variation in the observed concentrations. The standard wake model accounts for less than 10% of the variation.

A regression model can be expected to perform better than the standard model, but the difference is greater than would be expected. Use of the regression model was recommended as an interim measure until models more firmly based on physical principles could be developed.[6] Regression models provide reasonable predictions when applied within the limits of the data, but extrapolation beyond these limits is always subject to question.

Ramsdell derives theoretical expressions for building-wake diffusion coefficients that may be used in the usual Gaussian diffusion models.[7] These expressions assume that diffusion and travel time are directly related. A relationship between concentration and distance follows from the Galilean transformation $x = Ut$ where t is the travel time. Without repeating the details of the derivation, wake diffusion coefficients may be estimated by

$$\Sigma_{wy}^2 = \sigma_y^2 + \sigma_{yw}^2 \qquad (5)$$

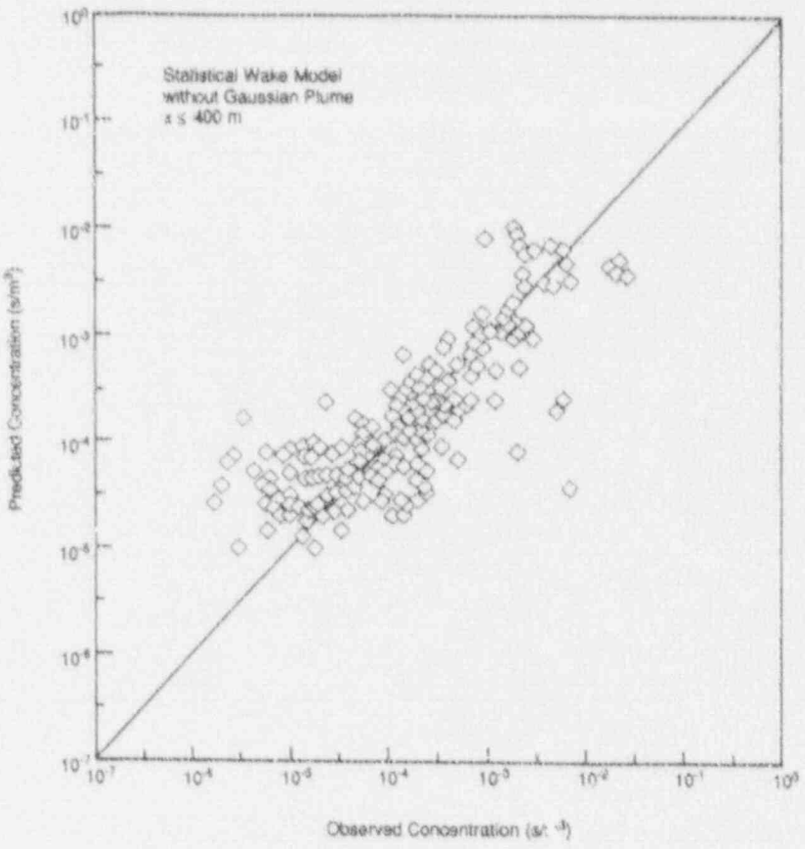

Figure 2 Comparison of centerline concentrations predicted by a regression model with centerline concentrations observed in wakes to a distance of 400 m.

and

$$\Sigma_{wz}^2 = \sigma_z^2 + \sigma_{zw}^2 \tag{6}$$

where Σ_{wy}, Σ_{wz} = diffusion coefficients to be used in Gaussian models
σ_y, σ_z = diffusion coefficients resulting from background turbulence, and
σ_{yw}, σ_{zw} = diffusion coefficient increment caused by turbulence in the building wake.

Assume that the standard methods of estimating σ_y and σ_z are acceptable and consider σ_{yw} and σ_{zw}.

The wake diffusion increments are

$$\sigma_{yw}^2 = \frac{kA^{1/2}}{0.0076U^2}\left[1 - \left(1 + \frac{0.0869x}{A^{1/2}}\right)\exp\left(\frac{0.0869x}{A^{1/2}}\right)\right] \tag{7}$$

and

$$\sigma_{zw}^2 = \frac{kA^{1/2}}{0.0076U^2S^2}\left[1 - \left(1 + \frac{0.0869Sx}{A^{1/2}}\right)\exp\left(\frac{0.0869Sx}{A^{1/2}}\right)\right] \tag{8}$$

where S is a stability parameter ranging from about 1 for extremely unstable atmospheric conditions to 2.5 in extremely stable conditions. The k in Equations (7) and (8) represents a combination of several terms in the theoretical model that can't be evaluated easily with readily available meteorological data. It is treated as a dimensional constant.

Figure 3 compares centerline concentrations to a distance of 400 m predicted with a Gaussian model with σ_{ys} and σ_{zs} given by Equations (7) and (8) with $k = 1\ m^2/s^2$. For the moment, σ_y and σ_z are assumed to be negligible. Clearly, the theoretical model is an improvement over the regulatory guide models and is nearly as good as the regression model. It accounts for about 57% of the variability in observed concentrations. However, it is biased in that it slightly underpredicts the centerline concentrations. If $k = 0.91\ m^2/s^2$ were used, the model would be unbiased. Addition of the normal diffusion components reduces the concentrations estimated by the theoretical model. Setting $k = 0.5\ m^2/s^2$ compensates for this reduction.

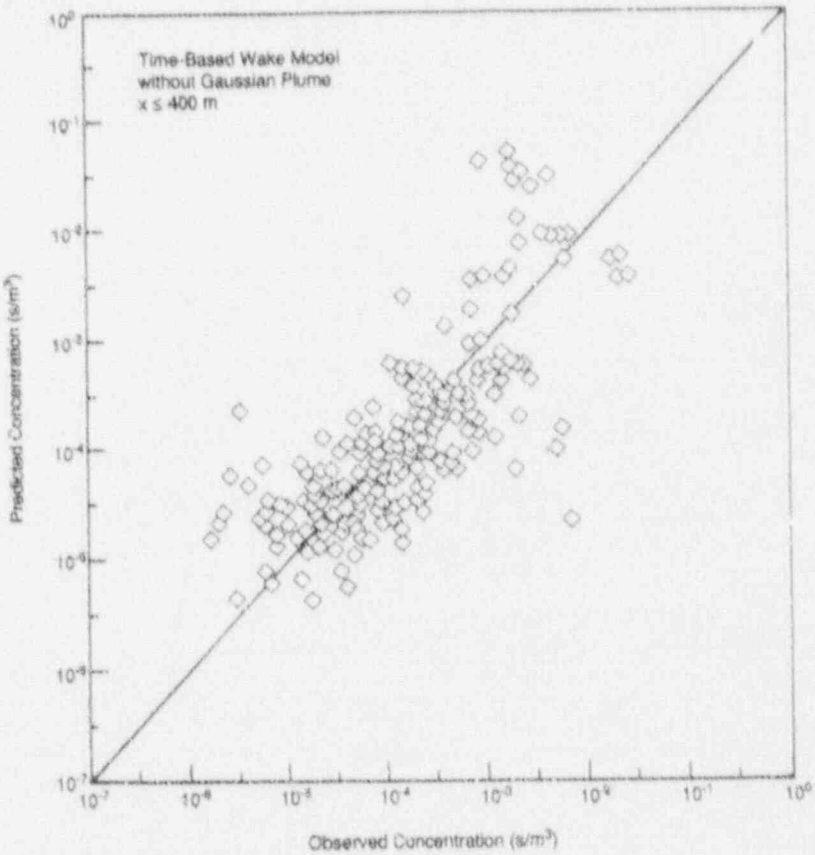

Figure 3 Comparison of centerline concentrations predicted by a model with time-based wake diffusion coefficients observed in wakes to a distance of 400 m.

Alternative Guidance

The following procedures offer an alternative to the procedures recommended in Regulatory Guide 1.145. They implement the wake diffusion model just described. They also incorporate features to prevent unrealistically high concentration predictions near the release point.

Ground-Level Releases

The starting point for the alternative guidance is a slightly modified version of the standard Gaussian plume model for ground-level releases. The modifications account for initial dilution of the effluent before release and for diffusion in wakes. It is

$$X = Q/(F_0 + \pi U \Sigma_{wy} \Sigma_{wz}) \qquad (9)$$

where F_0 is the flow at the release point and Σ_{wy} and Σ_{wz} are defined by Equations (5), (6), (7), and (8) with $k = 0.5$ m^2/s^2. The flow keeps Equation (9) from predicting concentrations that exceed the concentration at the release point. This is important when the release point is a vent or short stack. The flow may be set to zero, if desired.

With diffusion coefficients defined by Equations (7) and (8), Equation (9) naturally achieves the goals of the two-step Regulatory Guide 1.145 procedure. The wake diffusion increments approach zero as the distance from the release point decreases. They increase to a maximum value determined by the building area as distance increases, and they increase as the wind speed decreases. It is not necessary to limit the wake correction near the source or to make a correction for meander at low wind speeds.

Figure 4 compares centerline concentrations predicted using Equation (9) for distances between 8 and 1200 m with observed concentrations. For this example, diffusion coefficients from the XOQDOQ and PAVAN computer codes[8],[9] represent the normal diffusion, and F_0 is 0. The model accounts for about 55% of the concentration variations and is slightly biased toward overprediction.

Under most atmospheric conditions, the alternative procedure predicts concentrations that are lower than the Regulatory Guide 1.145 procedure predictions. Figure 5 compares concentrations predicted using Equation (9) and predictions made using the Regulatory Guide 1.145 procedure. Equation (9) gives lower concentrations near the release point and carries the wake effects farther downwind. However, both curves show regions near the source where the building wake enhances diffusion. They also approach a common curve at long distances where the initial effects of the building are not significant.

Near the source, the difference in concentration predictions of the two procedures is primarily a function of atmospheric conditions. Table 1 shows ratios of concentrations predicted 400 m downwind of a 2000-m^2 building using the two procedures as a function of wind speed and stability. Ratios greater than 1.0 show those combinations of atmospheric conditions for which Equation (9) gives lower concentrations. For most combinations, the ratio is between 1.0 and 5.0. The largest reductions in concentrations occur in low, wind, stable

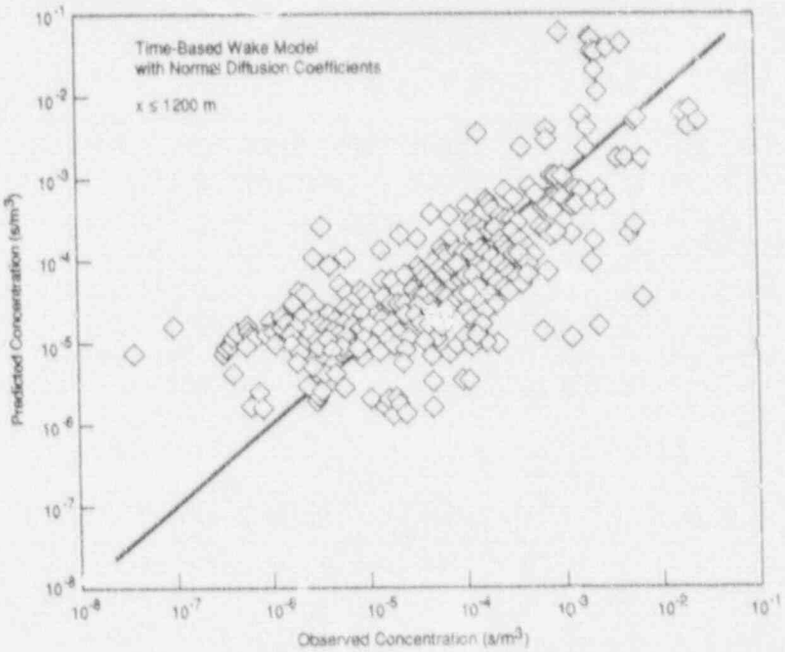

Figure 4 Comparison of centerline concentrations predicted by a model with time-based wake diffusion coefficients which include normal and wake components to a distance of 1200 m.

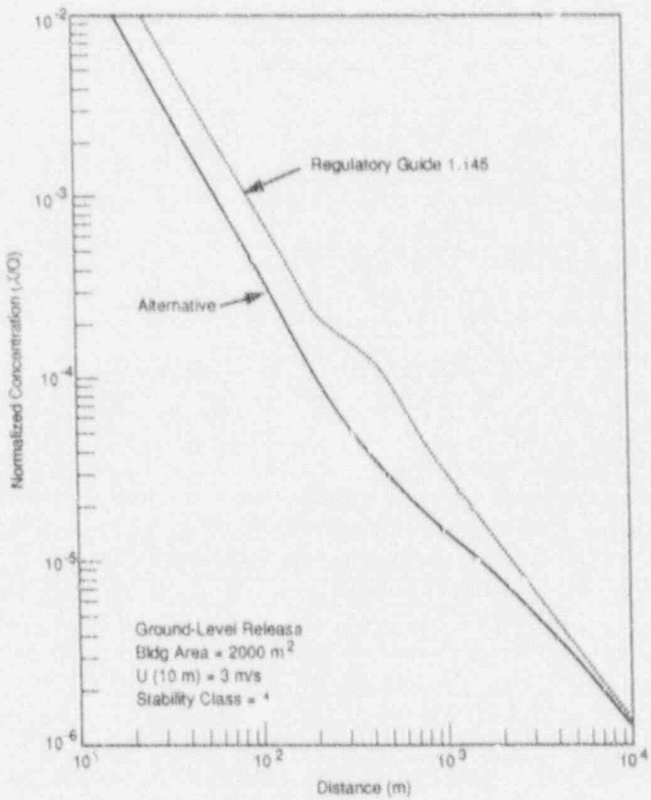

Figure 5 Comparison of normalized concentrations estimated using the Regulatory Guide 1.145 procedure and the new wake model.

Table 1 X/Q reduction factor (regulatory guide/alternative).

Wind Speed (m/s)	Pasquill-Gifford Stability Class						
	A	B	C	D	E	F	G
1.8	2.02	3.36	5.00	6.62	8.02	13.25	20.21
3.6	1.23	1.52	1.87	2.54	3.06	4.68	10.41
5.8	1.06	1.13	1.21	1.36	1.46	2.01	4.19
8.5	1.00	1.00	1.00	0.97	0.93	1.13	2.16
11.2	0.98	0.95	0.91	0.83	0.73	0.80	1.41
14.3	0.97	0.93	0.87	0.75	0.62	0.63	1.00

conditions. In these conditions, the reduction may exceed a factor of 10. Finally, during high wind speed conditions, Equation (9) predicts concentrations that are higher than the concentrations predicted by the regulatory guide procedure.

The ratios in Table 1 show the differences in concentration predictions between the two procedures for specific sets of atmospheric conditions. The impact of these differences on diffusion estimates at a specific site depends on the frequency of occurrence of each combination of wind speed and stability. Figure 6 shows cumulative frequency distributions for normalized concentrations predicted using

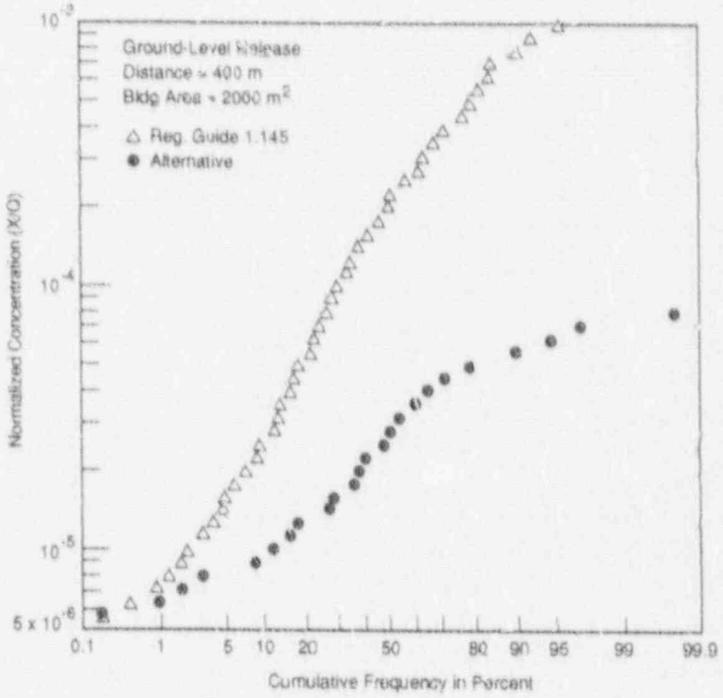

Figure 6 Comparison of annual cumulative frequency distributions for normalized concentrations estimated using the Regulatory guide 1.145 procedure and the new wake model.

Equations (9) and the regulatory guide procedure. The distributions are based on a joint frequency distribution for wind speed and stability for Hanford.

Two features in the figure deserve comment. First, the range of concentrations predicted by the regulatory guide procedure is much larger than the range predicted by Equation (9). However, recall that the regulatory guide procedure did not do well in predicting the variation of concentrations measured in building-wake diffusion experiments. Second, the slope of the curve for the concentrations predicted using Equation (9) flattens when the cumulative frequency exceeds about 90%. As a result, differences between the concentrations exceeded 10, 5, and 1% of the time are small.

Elevated Releases and Fumigation

Regulatory Guide 1.145 defines elevated releases as releases occurring from points that are more than two and one-half times the height of adjacent structures. For elevated releases, it suggests using

$$X = \frac{Q}{\pi U \sigma_y \sigma_z} \exp(h_e^2/2\sigma_z^2) \qquad (10)$$

to compute ground-level concentrations, where U is the wind at release height, h_e is the effective release height, and all other symbols are as previously defined. Transitional meteorological conditions that typically occur in morning and near bodies of water are treated separately using a "fumigation" model. This model, which assumes rapid downward mixing of material, is

$$X = Q/[(2\pi)^{1/2} U_1 \sigma_y h_e]. \qquad (11)$$

The wind speed, U_1, in Equation (11) is a layer-average speed that may be assumed to be 2 m/s in the absence of better information.

The only suggested change to this guidance is the addition of an optional F_e term to the denominators of Equations (10) and (11). This is not a fundamental change to the equations. It only reflects a recognition that the maximum concentration in the plume may be no greater than the concentration at the release point.

Elevated-Vent and Short-Stack Releases

Regulatory Guide 1.145 treats releases from points lower than two and one-half times the height of adjacent structures as ground-level releases. However, Regulatory Guide 1.111 provides somewhat different guidance. It considers releases from roof-top vents and short stacks as a separate class of releases. What has been refered to as a "split-h" approach is used in estimating concentrations for this class of releases. It is an empirical method of accounting for a frequently observed phenomenon in which plumes from short stacks alternate between being entrained in a building wake and escaping from the wake. Conceptually, the "split-h" approach is as applicable to evaluating the consequences of accidental releases as it is to evaluating the consequences of routine releases.

The "split-h" procedure divides the releases into three groups based on the ratio between the vertical velocity of the release and the wind speed at the release height. If the vertical velocity of a release is less than or equal to the wind speed (ratio <= 1), the release is assumed to be at ground level in the wake of the building. If the ratio is greater than 5, the release is assumed to be an elevated release. In either of these cases, the concentration is computed using the equation appropriate for the release assumption. A mixed-release mode is assumed if the ratio is between 1 and 5. In a mixed-release mode, concentrations are computed by averaging concentrations estimated with elevated and ground-level plume equations.

Weights given to the ground-level and elevated plume concentrations depend on the ratio between the vertical velocity and the wind speed. If the weight assigned to the ground-level concentration is E_t, then the weight given to the elevated concentration is $1 - E_t$. Regulatory Guide 1.111 computes E_t from

$$E_t = 2.58 - 1.58W_o/U \quad \text{for} \quad 1 < W_o/U < 1.5 \tag{12}$$

and

$$E_t = 0.3 - 0.06W_o/U \quad \text{for} \quad 1.5 < W_o/U < 5 \tag{13}$$

where W_o is the vertical velocity at the release point. Building-wake diffusion data of Johnson et al.[18] provide the basis for the numerical constants in Equations (12) and (13).

Using the "split-h" procedure with the ground-level and elevated plume models suggested in the regulatory guides results in lower concentration predictions than are estimated with the ground-level model. That is not necessarily the case when the procedure is used with the ground-level diffusion model represented by Equation (9). Table 2 compares 50% and 95% normalized concentrations predicted using hourly meteorological data from the Hanford Site for 1987. The example assumes a projected building of 2000 m^2. In addition, for the roof-top release, it assumes a release height of 40 m, an F_o of 10 m^3/s, and a W_o of 10 m/s.

Table 2 Comparison of X/Q predictions made by the Regulatory Guide 1.145 and alternative procedures using 1987 hourly meteorological data from the Hanford Site.

	Distance	RG 1.145	Alternative Procedure	
			Ground-Level	Roof-Top
50% X/Q	400 m	2.2E-4(a)	2.8E-5	1.2E-5
	1600 m	3.2E-5	8.0E-6	1.1E-5
	6400 m	5.4E-6	3.0E-6	3.5E-6
95% X/Q	400 m	9.6E-4	6.4E-5	6.4E-5
	1600 m	1.8E-4	1.8E-5	7.2E-5
	6400 m	5.0E-5	1.0E-5	1.8E-5

(a) E-4 = 10^{-4}

Concentrations estimated using the alternative procedures are lower than those estimated using the current procedures. However, with the alternative procedures, ground-level releases do not always give lower concentrations than roof-top releases. Near the source, the concentrations from roof-top releases are lower than concentrations from ground-level releases. The situation changes as the distance from the source increases. Even with the "split-h" procedure and a nominal vertical velocity of 10 m/s, the roof-top releases tend to give larger concentrations than ground-level releases.

Uncertainty

The new wake diffusion models account for more of the variability in observed concentrations than the model in the current guidance. However, the scatter of the data in Figure 4 clearly shows that there is still a significant amount of uncertainty in building-wake concentration estimates. This remaining uncertainty must be considered in evaluating the consequences of potential releases. This section discusses one method of combining the model concentration estimates with uncertainty to get a cumulative frequency distribution.

Mathematically, the problem is to find the probability that the concentration in a wake at some distance x will exceed a threshold value, X_0. This probability can be represented as $P(X > X_0)$. It may be estimated from the distribution of meteorological conditions and uncertainty using

$$P(X > X_0) = \sum_M [P(X/X_s > X_0/X_s)\ P(M)] \qquad (14)$$

where X_s is the model estimate of the concentration at distance x given meteorological conditions M with a probability P(M). If M represents a specitic wind speed, wind direction, and stability combination, P(M) is a probability from the normal joint frequency distribution used with the current guidance.

Figure 7 characterizes the uncertainty remaining in diffusion estimates in complementary cumulative distributions of the ratio of X/X_s. The x axis in this figure is the ratio between observed and predicted concentrations, and the y axis is the probability that this ratio will be exceeded. The solid line in the figure represents a complementary cumulative distribution function that approximately fits the distribution of ratios for ground-level releases when Equation (9) is used to estimate concentrations. This figure may be used to estimate $P(X/X_s > X_0/X_s)$. For example, if X_0/Q is 1.0E-4 and X_s/Q is 6.5E-5 then X_0/X_s is 1.54. The figure shows that the probability of exceeding 1.54 is about 0.39 (39%).

Table 3 shows computation of the probability of X/Q exceeding 1.0E-4 for the ground-level release example in Figure 6. The first column in the table gives a frequency band, and the second column gives an approximate X_s/Q for the band. The third column gives the ratio used as input to Figure 7. The last column is the product of the probability of X/Q exceeding 1.0E-4 given X_s/Q (column 4) and the probability of occurrence of the meteorological conditions associated with X_s/Q (column 5). The total at the bottom of the last column is the probability that X/Q will exceed 1.0E-4. Table 2 shows that the

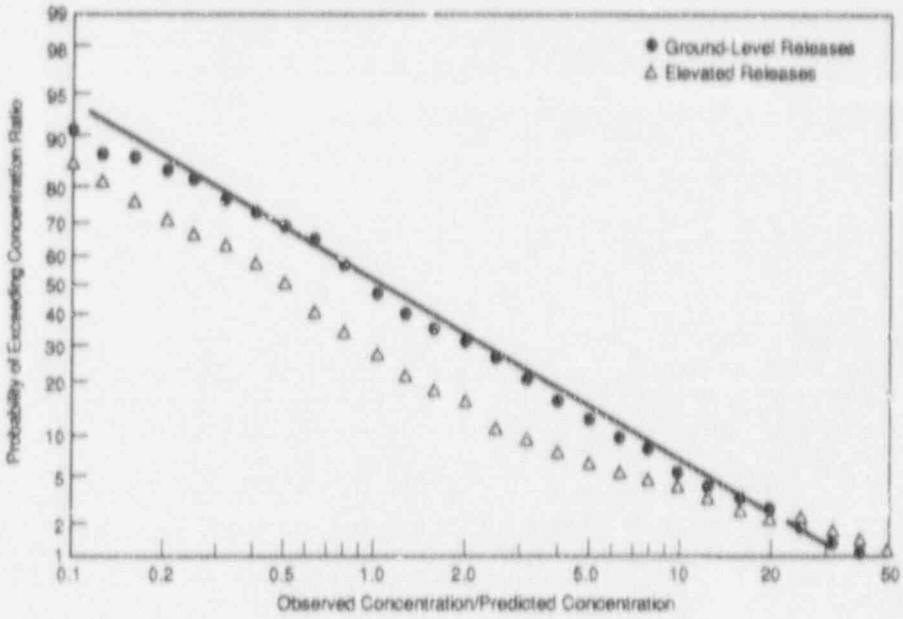

Figure 7 Uncertainty estimates for the new wake models.

Table 3 Computation of the probability that the normalized concentration (X/Q) will exceed 1.0E-4.

	$X_{s/q}$	X_o/X_s	$P(X/X_s>X_o/X_s)$	P(M)	
> 99%	8.0E-5	1.25	0.45	0.01	0.005
95 - 99%	7.0E-5	1.43	0.41	0.04	0.016
90 - 95%	6.2E-5	1.61	0.38	0.05	0.019
80 - 90%	5.4E-5	1.85	0.34	0.10	0.034
70 - 80%	4.7E-5	2.13	0.31	0.10	0.031
60 - 70%	4.0E-5	2.50	0.27	0.10	0.027
50 - 60%	3.3E-5	3.03	0.24	0.10	0.024
40 - 50%	2.5E-5	4.00	0.18	0.10	0.018
30 - 40%	1.9E-5	5.26	0.14	0.10	0.014
20 - 30%	1.5E-5	6.67	0.11	0.10	0.011
10 - 20%	1.1E-5	9.09	0.08	0.10	0.008
< 10%	8.3E-6	12.05	0.05	0.10	0.005
					0.212

95% X/Q is about 6.5E-5. However, the computation in Table 3 shows that the probability of X/Q exceeding 1.0E-4 is greater than 20% when uncertainty is considered.

The solid line in Figure 8 shows the results of repeating the calculation in Equation (14) for a number of threshold concentrations. After adding uncertainty to the model concentration predictions, the 95% concentration is approximately 4.0E-4. This value is a factor of about 6 higher than the 95% concentration estimated by the new wake diffusion model, and it is a factor of 2.4 lower than estimated by the current procedure.

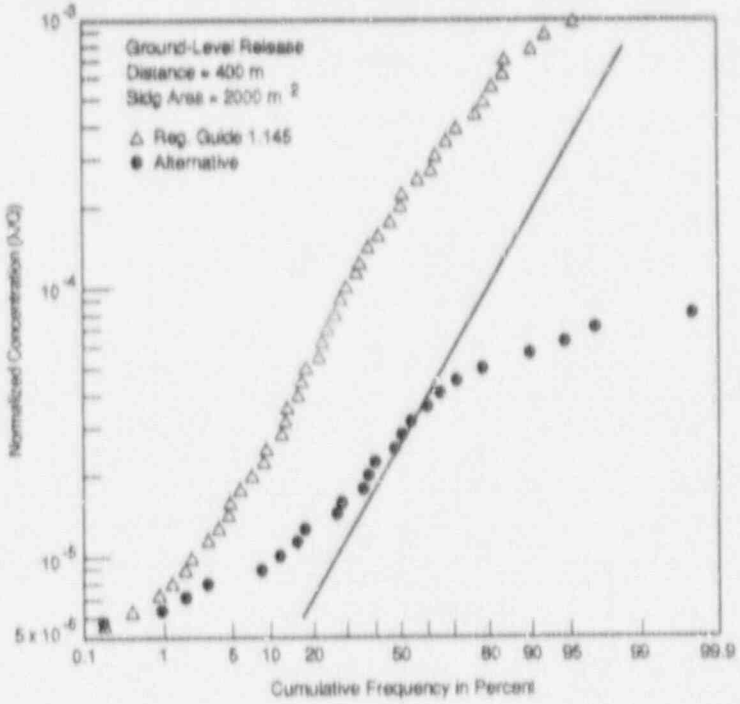

Figure 8 Same as Figure 6, with an additional curve that accounts for the uncertainty in predictions made by the new wake model.

Conclusions

This paper discusses a new model for estimating concentrations in building wakes and offers alternative guidance for evaluating the consequences of releases from nuclear facilities. The new model accounts for about 57% of the variability in concentrations observed in wakes. Models suggested in current guidance account for less than 10% of the variability. The proposed guidance demonstrates application of the new model. It covers ground-level releases, roof-top vent and short-stack releases, and elevated releases. It also includes a procedure for accounting for uncertainty in building wake diffusion estimates.

As an example, the paper shows application of the proposed guidance to a 2000-m^2 building using meteorological data at Hanford. In the example, changing from the procedures recommended in Regulatory Guide 1.145 to those suggested as an alternative reduces the 95% X/Q used for evaluation of accident consequences by a factor of about 2.4 at 400 m.

Acceptance of the alternative guidance discussed in the paper would impact current thinking related to diffusion in wakes in several ways. The most significant change is in the concept of worst-case meteorology.

Under current guidance, worst-case meteorology is synonymous with low wind speeds and stable atmospheric conditions. Frequently this means F stability and a 1 m/s wind speed. However, worst-case meteorological conditions exist only in reference to specific diffusion

models. With the new building-wake model and proposed guidance, the worst-case meteorological conditions depend on release mode and distance from the release point. Near the building, the worst-case conditions are moderate to high wind speeds. These speeds generally occur during near-neutral stability. For a specific application, the worst-case conditions should be determined from the model and a representative joint frequency distribution.

Diffusion models recommended in current guidance estimate high concentrations at low wind speeds, and these estimates are sensitive to small changes in wind speed. As a result, the wind speed classes in joint frequency distributions have fine resolution for low wind speeds and coarse resolution at high speeds. Diffusion models in the proposed alternative guidance estimate high concentrations at high wind speeds. Fine wind speed resolution at low speeds in joint frequency distributions does not make a significant contribution to the concentrations of interest. With these models, uniform wind speed classes are a better alternative than varying from fine to coarse resolution. Of course, the problem of class sizes can be avoided by using hourly meteorological data directly for diffusion estimates. The computations, which lead to Figure 6, were made with hourly data (8760 observations) and took less than 2 min on a personal computer.

The suggested alternative guidance includes use of the "split-h" procedure from Regulatory Guide 1.111 for releases from roof-top vents and short stacks. With the models in the current guidance, use of the "split-h" procedure would result in reduction of the predicted consequences of roof-top vent and short-stack releases. With the models proposed in the alternative guidance, use of the procedure can result in increases in predicted concentrations at some distances. The result of the example presented in Table 2 demonstrates this.

Acknowledgments

This work was performed for the U.S. Nuclear Regulatory Commission, Office of Nuclear Regulatory Research by the Pacific Northwest Laboratory under NRC FIN B-2929-0. Battelle Memorial Institute operates the Pacific Northwest Laboratory for the U.S. Department of Energy under Contract DE-AC06-76RLO 1830.

References

1. U.S. Nuclear Regulatory Commission. Assumptions Used for Evaluating the Potential Radiological Consequences of a Loss of Coolant Accident for Boiling Water Reactors. Regulatory Guide 1.3. Rev. 2. U.S. Nuclear Regulatory Commission, Washington, D.C. (1974).

2. U.S. Nuclear Regulatory Commission. Assumptions Used for Evaluating the Potential Radiological Consequences of a Loss of Coolant Accident for Pressurized Water Reactors. Regulatory Guide 1.4. Rev. 2. U.S. Nuclear Regulatory Commission, Washington, D.C. (1974).

3. U.S. Nuclear Regulatory Commission. Assumptions Used for Evaluating the Potential Radiological Consequences of a Steam Line Break Accident for Boiling Water Reactors. Regulatory Guide 1.5. U.S. Nuclear Regulatory Commission, Washington, D.C. (1971).

4. U.S. Nuclear Regulatory Commission. Methods for Estimating Atmospheric Transport and Dispersion of Gaseous Effluents in Routine Releases from Light-Water-Cooled Reactors. Regulatory Guide 1.111. Rev. 1. U.S. Nuclear Regulatory Commission, Washington, D.C. (1977).

5. U.S. Nuclear Regulatory Commission. Atmospheric Dispersion Models for Potential Accident Consequence Assessments at Nuclear Power Plants. Regulatory Guide 1.145. Rev. 1. U.S Nuclear Regulatory Commission, Washington, D.C. (1983).

6. Ramsdell, J. V. Atmospheric Diffusion for Control Room Habitability Assessments. NUREG/CR-5055. U.S. Nuclear Regulatory Commission, Washington, D.C. (1988).

7. Ramsdell, J. V. "Diffusion in Building Wakes for Ground-Level Releases." PNL-SA-17611, Pacific Northwest Laboratory, Richland, Washington (1990). (To be published in an Urban Atmospheres edition of Atmospheric Environment fall of 1990)

8. Sagendorf, J. F., Goll, J. T. and Sandusky, W. F. XOQDOQ: Computer Program for the Meteorological Evaluation of Routine Effluent Releases at Nuclear Power Stations. NUREG/CR-2919. U.S. Nuclear Regulatory Commission, Washington, D.C. (1982).

9. Bander, T. J. PAVAN: An Atmospheric Dispersion Program for Evaluating Design Basis Accidental Releases of Radioactive Materials from Nuclear Power Stations. NUREG/CR-2858. U.S. Nuclear Regulatory Commission, Washington, D.C. (1982).

10. Johnson, W. B., Shelar, E., Ruff, R. E., Singh, H. B., and Salas, L. Gas Tracer Study of Roof-Vent Effluent Diffusion at Millstone Nuclear Power Station. AIF/NESP-007b. Atomic Industrial Forum, Washington, D.C. (1975).

DISCUSSION

DORON: Did you consider for a specific site the effects of changes in wind direction as well as wind speed. At a specific site, when the building has a certain configuration, changing may give different results for the same location.

RAMSDELL: If I were to use this model for a specific site, I would definitely put in a directionally dependent area. However, for the analysis that I have presented, I assumed the cross-sectional building areas used for licensing the commercial power plants. The cross-sectional areas used for the three INEL facilities were given to me by people at INEL. The model was very much overpredicting the concentrations at Diablo Canyon until we got the right building area. After that, we were very close. An area of 1600 sq. meters was used in licensing Diablo Canyon. When their meteorologists went back to the drawings, they found that the area was more typically 7000 sq. meters. Putting that area into the model reduced the bias by about a factor of 7. For Diablo Canyon, we are predicting about 80% of the variation in centerline concentrations. This is a particularly difficult site because we only used experimental data for one distance. Therefore, we don't have the normal distance dependence to assist in getting a high correlation; we only have the variation in meteorological conditions.

LAGUS: When you have an extended source of variable aspect, don't you have a problem modeling wakes using a Gaussian plume which is exact only for a point source?

RAMSDELL: Two approaches to modeling an extended source in a wake came to mind immediately. The first is to use the expressions given in the paper to estimate wake diffusion coefficients and use these coefficients in a line source model. The other approach is to model the source as a line of point sources having equal release rates.

CLOSING COMMENTS OF SESSION CO-CHAIRMAN BELLAMY

This session has had five papers associated with mathematical modeling. We have discussed computer simulated models for emergency response to accidents, for purging activated carbon after a short term insult of methyliodide (which I would characterize as an accident), heard about HEPA filter performance, talked about the optimization of air duct design, and we have heard about some new mathematical models for meteorological considerations. It demonstrates the importance of being able to analyze situations mathematically and, as pointed out by a number of the questions and comments, the importance of being able to consider the use of personal computers and the ease of using computer codes in the future for our work.

SESSION 12

FILTERS

Wednesday: August 15, 1990
Co-Chairmen: H. Gilbert
R. Dorman

OPENING COMMENTS OF SESSION CO-CHAIRMAN GILBERT

HIGH EFFICIENCY STEEL FILTERS FOR NUCLEAR AIR CLEANING
W. Bergman, J. Conner, G. Larsen, R. Lopez, C. Turner, G. Vahla, C. Violet, K. Williams

A PERMANENTLY MAGNETIZED HIGH GRADIENT MAGNETIC FILTER FOR GLOVE-BOX CLEANING AND INCREASING HEPA FILTER LIFE
J. H. P. Watson, C. H. Boorman

BEHAVIOR OF THE POLYGONAL HEPA FILTER EXPOSED TO WATER DROPLETS CARRIED BY THE OFFGAS FLOW
K. Jannakos, G. Potgeter, W. Legner

EFFICIENCY AND MASS LOADING CHARACTERISTICS OF A TYPICAL HEPA FILTER MEDIA MATERIAL
V. J. Novick, P. J. Higgins, B. Dierkschiede, C. Abrahamson, W. B. Richardson

AEROSOL PENETRATION INSIDE HEPA FILTRATION MEDIA
P. Letourneau, Ph. Mulcey, J. Vendel

CLOSING COMMENTS OF SESSION CO-CHAIRMAN DORMAN

OPENING COMMENTS OF SESSION CO-CHAIRMAN GILBERT

This is the second conference session on filters and particulate air cleaning. The objective of this session, as well as the earlier session, is to improve air cleaning technology.

We have five interesting papers. In addition to improving our techniques and our products, we might try also to improve the economy of air cleaning in terms of conserving both time and funding. Sometimes I think the concept of economy has been downgraded even if not forgotten. We must strive to upgrade particulate filtration, not only in efficiency, but with due regard to its practical design for the operation being filtered.

HIGH EFFICIENCY STEEL FILTERS FOR NUCLEAR AIR CLEANING*

W. Bergman, J. Conner, G. Larsen, R. Lopez,
C. Turner, G. Vahla, C. Violet, and K. Williams
Lawrence Livermore National Laboratory
P. O. Box 5505 Livermore, CA 94550

Abstract

We have, in cooperation with industry, developed high-efficiency filters made from sintered stainless-steel fibers for use in several air-cleaning applications in the nuclear industry. These filters were developed to overcome the failure modes in present high-efficiency particulate air (HEPA) filters. HEPA filters are made from glass paper and glue, and they may fail when they get hot or wet and when they are overpressured.

In developing our steel filters, we first evaluated the commercially available stainless-steel filter media made from sintered powder and sintered fiber. The sintered-fiber media performed much better than sintered-powder media, and the best media had the smallest fiber diameter.

Using the best media, we then built prototype filters for venting compressed gases and evaluated them in our automated filter tester.

I. Introduction

HEPA filters have provided the nuclear industry with the best available technology for nearly 40 years in preventing the release of radioactive particles into the environment. Although improvements were made in the reliability and performance over this time, the present HEPA filter used in the nuclear industry is quite similar to the original unit that was made by gluing folded filter paper into a wooden frame. The most significant improvement was the replacement of the cellulose filter paper with glass fiber filter paper in the late 1950s to make the filter fire-resistant. This change was prompted by a fire at the Rocky Flats Plant in 1957, when some of the combustible HEPA filters burned. An excellent review of the history of HEPA filters in the nuclear industry is given by Gilbert.[1]

The reliability of HEPA filters has been criticized in recent years because of increasing concern with environmental protection and the recent disclosure of serious contaminants at several Department of Energy (DOE) facilities. Much of the criticism of HEPA filters is based on the potential structural damage to the filter. Our investigation of high-efficiency steel filters was motivated by our desire to reduce this failure potential.

*This work performed under the auspices of the U.S. Department of Energy by Lawrence Livermore National Laboratory under Contract No. W-7405-ENG-48.

HEPA Structural Damage

HEPA filters may suffer structural damage under extreme conditions of temperature, humidity, air flow or shock wave, and particle deposits. The failure of HEPA filters under these conditions is not surprising since HEPA filters are essentially delicate, weak structures made by gluing folded paper into a frame. These failure modes can be avoided by providing adequate design features in the off-gas system.

High Air Flow or Shock Wave. HEPA filters will be structurally damaged when they are subjected to high air-flow conditions that may occur during tornadoes or explosive shocks.(2)

High Temperature. When HEPA filters are exposed to hot exhaust, they can suffer severe reductions in strength and structural integrity. These HEPA failures depend strongly on the material and the design of the filter, in addition to the temperature and time of exposure.(3-6) Visible structural damage, such as media tears and distortions, are usually seen when HEPA filters are exposed to temperatures above 250°C. Above 175°C (350°F), the binder that holds the filter paper together begins to burn off, leaving a filter medium that can be easily blown apart.(5-6) Although all HEPA filters used in nuclear facilities are required to be qualified and labeled by Underwriters Laboratories as fire-resistant,(7) these tests do not simulate real failure modes, where high-temperature exposure is followed by mechanical stresses.

Since HEPA filters are not generally installed in high-temperature process streams, they experience high-temperature exposure only during accident conditions. Under these conditions, the HEPA filter blow-out is due to more than just the high temperature.

High Humidity. Recent studies have shown that HEPA filters can suffer severe structural damage and may even blow out under high humidity conditions.(8-11) The accumulation of water in the HEPA filter leads to an increase in the differential pressure and a decrease in the filter pack stability and the media's tensile strength. The increased mechanical load on the filter, coupled with the decreased strength, can lead to structural failures.

Heavy Particle Deposits. Particle deposits on HEPA filters increase the mechanical load on the filters and can lead to mechanical failure in the same fashion as discussed for high humidity. The use of an efficient, cleanable prefilter can prevent this problem.

Combination of Conditions. The combination of the previous conditions can lead to an accelerated destruction of HEPA filters. Swedish studies have shown that high humidity at 100°C causes a HEPA filter to "fail due to its own weight or in a minimal stream of air.(10)" Another example is the case of high humidity and heavy particle loading. In this case, the particle deposits increase the water adsorption in the filter and can lead to filter blow-out.

The potential for HEPA filter blow-out following high-temperature exposure is very high if the HEPA is subjected to any additional stress. The HEPA medium is structurally weak since the binder holding the filter paper together is burned off.

In addition, the entire filter pack is loosely supported in the filter frame.[4,6] Any subsequent exposure that exerts a mechanical strain on the filter can cause the HEPA pack to blow out of the filter housing. In some instances a water spray was used to put out fires in HEPA filters, which caused the filters to blow out of their frames.

Steel Filters Do Not Suffer Structural Damage

The high-efficiency steel filters described in this report do not suffer from the type of structural damage described for the glass-paper filters. This follows from the intrinsic strength of the steel and the welded construction of the filter. The steel media consist of fibers or powder held together in a mat by diffusion bonding and are far stronger than glass-paper media. Welding the steel media into a steel housing yields a high-strength filter that will not have structural damage under extreme conditions of high temperature, humidity, air flow or shock wave, and particle deposits.

The use of steel filters in nuclear air cleaning applications is not new. Cleanable stainless steel filters were used as prefilters to extend the life of HEPA filters in hot off-gas systems such as in waste calciners [13] and in waste incinerators [14]. These filters had high pressure drops (over 8 inches w.g. at 4 feet per minute air velocity) and low efficiencies (about 65%) when clean. The pressure drop and efficiency increased as particles built up on the filter. Dillmann et al [15,16] described the use of 2 µm stainless steel fibers to make deep bed filters for use as vent filters in nuclear power reactors. The deep bed filters had efficiencies comparable to the glass HEPA filters but were much larger and could not be cleaned. Klein and Goossens [17] showed major improvements in filter efficiency with decreasing diameter of the steel fibers from 12 to 4 µm. However, the efficiencies were far below HEPA grade. They also showed that deposits of methylene blue aerosols could be efficiently cleaned from a cylindrical filter by washing with a water spray. Recently, Randhahn et al [18] described a stainless steel filter that had efficiencies comparable to a HEPA filter. However, no pressure drop data was given for a comparison to HEPA filters. Dillmann et al [19] showed that sintered metal filters made from fibers performed much better than those made from metal powder. The pleated cylindrical filters made from 2 µm fibers had efficiencies of 99.8% for uranin particles and a pressure drop of 5.6 inches of water at 58.9 cfm.

II. Steel Filter Media Evaluation

We evaluated the commercially available steel filter media made from sintered powder and sintered fiber. The large variety of filter media that we evaluated is illustrated by the electron micrographs shown in Figs. 1–5. Figure 1 shows the surface of a sintered-powder filter from Pall Trinity (PMM-M020) at 2X magnification. The cross section of this filter is shown in Fig. 2. Figure 3 shows the surface of a sintered-fiber filter from Bakaert (3AL3) at 2X magnification, while Fig. 4 shows the cross section of the filter. The structure of sintered-metal filters can also be rather complex, as illustrated by the four magnifications of a Memtec filter (XS44) in Fig. 5. Our objective was to screen samples of the filter media and select the most promising candidate for use in fabricating steel filters. The screening process consisted of measuring the aerosol penetration and the pressure drop across each filter at several flow rates.

General Procedure

Figure 6 is a schematic of the test apparatus used in our screening tests. We used a variety of aerosols such as dioctyl sebacate (DOS), sodium chloride, and silica to challenge the filters. The concentration of particles was measured as a function of particle size by using one of two laser particle counters from Particle Measuring Systems, Inc. One laser particle counter (4SLAS-32) had a sample flow rate of 0.3 l/m and measured particles from 0.065 to 1.0 µm over 32 channels. The other counter, (LPC-HS-Special) had a sample flow rate of 2.8 l/m and measured particles from 0.07 to 0.5 µm over 16 channels. The two particle counters were used interchangeably in our study. We determined the aerosol penetration as a function of particle size from the ratio of the downstream to upstream concentrations for each particle size range. Before measuring the upstream particle concentration, we first diluted the sample, using one to three stages of TSI diluters to prevent counting more than one particle at a time in the laser counter. A typical dilution ratio was 1000:1 in our tests. To prevent premature plugging of the filter, the upstream aerosols were directed to a dump while the concentrations were measured. The concentration of particles downstream from the filter was measured after the aerosols were directed to the filter.

Figure 7 shows the measured concentration of DOS aerosols generated by a Laskin nozzle in a typical steel-filter screening test. This figure shows the upstream, downstream, and background concentrations as functions of particle size. The background measurement represents the downstream sample with the aerosol generator turned off. We took background measurements to verify that there were no leaks present.

The filter penetration was computed from the ratio of the downstream to upstream particle concentrations and the results are plotted in Fig. 8. This penetration curve represents the fraction of DOS particles passing through a sample of Pall sintered-fiber media (FH025-HEPA) at a face velocity of 6.2 cm/s. The pressure drop at this face velocity was 190 mm of water. This filter had the best performance of those tested in our evaluation.

Sintered-Fiber Filters Are Better Than Sintered-Powder Filters

We evaluated a large number of different filter media from Pall Trinity, Memtec, Michigan Dynamics, Bakaert, and Mott to find the best ones. Our studies showed that for equivalent sized powder and fiber, the powder filters always had a higher particle penetration and a higher pressure drop than the fiber filters. Figure 9 illustrates this point with two filters from Pall Trinity: a sintered powder filter (PMM-M050) made from 5.0 µm steel powder and a sintered fiber filter (PMF-FH050) made from 5 µm steel fiber. Both filters were evaluated at a face velocity of 1.25 cm/s. The powder filter has a maximum particle penetration of 0.95 and a pressure drop of 7.4 mm water. In contrast, the fiber filter has a maximum particle penetration of 0.017 and a pressure drop of 0.9 mm of water.

The higher filter penetration and higher pressure drop for the sintered-powder media compared to the sintered-fiber media is due to the filter structure. Figure 10 shows electron micrographs of metallurgical samples of the sintered-fiber (10A) and sintered-powder (10B). The more open structure of the sintered-fiber filter has less air resistance than the more closed structure of the sintered-powder filter. This accounts for the lower pressure drop in the sintered-fiber filter. The

more open structure of the sintered-fiber filters also increase the residence time of the particles inside the filter. This increased residence time increases the particle capture due to Brownian motion and hence decreases the filter penetration.

Filters With Thinner Fibers Are Better

Another major finding from our screening tests is that sintered-fiber filters made from thinner fibers have better performance than those made with thicker fibers. Figure 11 shows the penetration of two different Pall sintered-fiber filters at a face velocity of 3.7 cm/s. The filter made with 5 μm diameter fiber (PMF-FH050) has a much higher penetration than the filter with 2.5μm diameter fiber (PMF-FH025). One of the most efficient media from our screening tests was a Pall filter made with 2.0 μm diameter fiber (PMF-FH025-HEPA).

Steel Filter Media Have Similar Penetration but Higher Pressure Drop Compared to Glass HEPA Media

Our filter penetration measurements demonstrated that the Pall steel filter with 2.0 μm fibers (FH025-HEPA) had a particle penetration similar to the glass HEPA filter, but more than three times the pressure drop. Figure 12 shows the DOS penetration for the steel-fiber media and the glass HEPA media when tested at 3.5 cm/s face velocity. The pressure drops across the steel and glass media are 9.9 and 2.9 mm of water, respectively. Thus, a steel HEPA filter would require more than three times as much filter area to have penetration and pressure drop similar to the glass HEPA filter. This would result in a very expensive filter.

III. Development and Evaluation of Prototype Steel Filters

We then used the results of our screening test to develop prototype filters for applications as venting filters for pressurized gas systems. The increased air resistance of the steel filters compared to the glass filters is not important in those venting applications. Figure 13 shows a prototype filter from Memtec that we evaluated for our application as a vent filter. This filter was cut in half to expose the two-stage concentric-cylinder design. The exhaust flow enters the large opening in the bottom, passes through the outer cylindrical filter and the inner filter, and finally exits through the small opening on top. This filter design represents a compromise between minimum filter penetration and minimum cost.

We evaluated the prototype vent filter in our automated filter tester shown in Fig. 14. This figure shows the filter being inserted into the filter chuck of the test apparatus. The basic components of the tester are similar to those shown schematically in Fig. 6. The DOS aerosols are generated with a Laskin nozzle generator. The results of the penetration measurements for the filter are shown in Fig. 15. This filter has a maximum penetration of $1.2X10^{-7}$ at 0.1μm particle diameter and 3.0 cfm flow rate. The pressure drop is 1.36 m of water (1.94 psi).

A more complex prototype filter from Pall Trinity is shown in Fig. 16. This filter also has a two-stage concentric design but has the filter media pleated into a cylindrical configuration. Figure 16 shows the housing with the two filter stages separated from each other. The results of our penetration measurement are shown in Fig. 17. We see that this filter has a maximum penetration of $3.2X10^{-8}$ at 0.1 μm particle diameter and 2.0 cfm flow rate. The pressure drop at these conditions is 107

mm of water. Although this filter with the pleated cylinder design has a lower penetration and pressure drop, it also costs several times more than a filter with the flat cylinder design.

Another prototype filter that we developed is shown in Fig. 18. This filter is a single-stage filter with a pleated-cylinder design and is made from a combination of sintered fiber (FH025) and sintered powder (M010). The results of our penetration test are shown in Fig. 19. This filter has a maximum penetration of $1.6X10^{-3}$ at 0.09μm particle diameter and 6.0 cfm flow rate. The pressure drop at this flow rate is 295 mm of water.

IV. Conclusion

We have developed high-efficiency steel filters for use in nuclear air-cleaning applications to avoid the structural damage that occurs with the glass-paper HEPA filters. However, the steel filter media have the same penetration but more than three times the pressure drop as glass-paper HEPA filters. The steel filters at this time are, therefore, restricted to applications that are not sensitive to air-flow resistance. They can be used in exhaust vents for a pressurized gas system or in any compressed gas line. These filters can also be used in many other applications where glass-paper HEPA filters are used, if the filter capacity is downgraded. However, under these conditions, the steel filter is much larger and far more expensive than the comparable glass-paper HEPA filter. Figure 20 shows that the steel filter is much larger than a glass-paper HEPA filter with similar penetration and pressure-drop characteristics.

References

1. Gilbert, H. G., "The high-efficiency filter in nuclear air cleaning" in Proceedings of the 19th DOE/NRC Nuclear Air Cleaning Conference, Seattle,WA, 18–21 August 1986, CONF-860820, pp 933–946 (1987).

2. Gregory, W. S., Martin, R. A., Smith, P. R., and Fenton, D. E., "Response of HEPA filters to simulated accident conditions" in Proceedings of the 17th DOE/NRC Nuclear Air Cleaning Conference, Denver, CO, 2–5 August 1982, CONF-820833, pp 1061–1068 (1983).

3. Pratt, R. P. and Green, B. L., "Performance testing of HEPA filters under hot dynamic conditions" in Proceedings of the 18th DOE/NRC Nuclear Air Cleaning Conference, Baltimore, MD, 12–16 August 1984, CONF-840806, pp 1107–1127 (1984).

4. Pratt, R., "The performance of filters under hot dynamic conditions" in Proceedings of the European Conference on Gaseous Effluent Treatment in Nuclear Installations, Luxembourg, 14–18 October 1985, Fraser and Luykx, Eds., Graham & Trotman, pp 824–836 (1986).

5. Briand, A., Laborde, J. C., and Mulcey, P., "Limits of HEPA filters operation under high-temperature conditions" in Proceedings of the 19th DOE/NRC Nuclear Air Cleaning Conference, Seattle, WA, 18–21 August 1986, CONF-860820, pp 890–904 (1987).

6. Ensinger, U., Rudinger, V., Wilhelm, J. G., "Efficiency of HEPA filters at elevated temperatures: investigations with the TiO_2 test method," in Proceedings of the 20th DOE/NRC Nuclear Air Cleaning Conference, Boston, MA, 22-25 August 1988 (1989).

7. Underwriters Laboratory, test UL-586, "Test performance of high-efficiency particulate, air filter units," 7 April 1977.

8. Rudinger, V., Ricketts, C. I., and Wilhelm, J. G., "Limits of HEPA filter application under high humidity conditions," in Proceedings of the 18th DOE/NRC Nuclear Airborne Waste Management and Air Cleaning Conference, Baltimore, MD, 12-16 August 1984, CONF-840806, pp 1058-1084 (1985).

9. Ricketts, C. I., Rudinger, V., and Wilhelm, J. G., "HEPA filter behavior under high humidity airflows" in Proceedings of the 19th DOE/NRC Nuclear Air Cleaning Conference, Seattle, WA, 18-21 August 1986, CONF-860820, pp 319-352 (1987).

10. Normann, B., "The effects of high relative humidities on HEPA filter media," in Proceedings of the 19th DOE/NRC Nuclear Air Cleaning Conference, Seattle, WA, 18-21 August 1986, CONF-860820, pp 300-318 (1987).

11. Ricketts, C. I., Rudinger, V., and Wilhelm, J. G., "The flow resistance of HEPA filters in supersaturated airstreams" in Proceedings of the 20th DOE/NRC Nuclear Air Cleaning Conference, Boston, MA, 22-25 August 1988, CONF-880822, pp 668-694 (1989).

12. Rudinger, V., Ricketts, C. I., Wilhelm, J. G., and Alken, W., "Development of glass fiber HEPA filters of high structural strength on the basis of the establishment of the failure mechanisms," in Proceedings of the 19th DOE/NRC Nuclear Air Cleaning Conference, Seattle, WA, 18-21 August 1986, CONF-860820, pp 947-966 (1987).

13. Schurr, G.A. "Cleanable sintered metal filters in hot off-gas systems" in proceedings of the 16th DOE Nuclear Air Cleaning Conference, 20-23 October 1980, San Diego, CA, CONF-801038, pp 708-718, (February 1981).

14. Kirstein, B.E. Paplawsky, W.J., Pence, D.T., and Hedahl, T.G., "High efficiency particulate removal with sintered metal filters" in Proceedings of 17th DOE Nuclear Air Cleaning Conference, 20-23 October 1980, San Diego, CA, CONF-801038, pp 719-744, (February, 1981).

15. Dillmann, H.G., and Pasler, H. "Experimental investigations of aerosol filtration with deep bed fiber filters" in Proceedings of 17th DOE Nuclear Air Cleaning Conference, Denver, CO, 2-5 August 1982, CONF-820833, pp 1160-1174, (February, 1983).

16. Dillmann, H.G. and Pasler, H. "A filter concept to control airborne particulate releases due to severe reactor aaccidents and implementation using stainless-steel fiber filters" in 18th DOE Nuclear Airborne Waste Management and Air Cleaning Conference, 12-16 August, 1984, Baltimore, MD, CONF-840806, pp 1417-1428., (March, 1985).

17. Klein, M. and Goossens, W.R. A. "Aerosol filtration with metallic fibrous filters" in Proceedings of 17th DOE Nuclear Air Cleaning Conference, Denver, CO, 2-5 August, 1982, CONF-820833, pp. 504-522, (February, 1983).

18. Randhahn, H., Gotlinsky, B., and Tousi, S., "The development of all metal filters for use in the nuclear industry" in 20th DOE/NRC Nuclear Air Cleaning Conference, Boston, MA, 22-25 August 1988, CONF-880822, pp 726-748, (May, 1989).

19. Dillmann, H.G., Bier, W., Linder, G., and Schubert, K., "Measurements of removal efficiencies performed on powder metal and fiber metal cartridges to be used in uranium enrichment facilities and glovebox exhaust ducts" in Proceedings of the 19th DOE/NRC Nuclear Air Cleaning Conference, Seattle WA, 18-21 August 1986, CONF-860820, pp 392-407 (May, 1987)

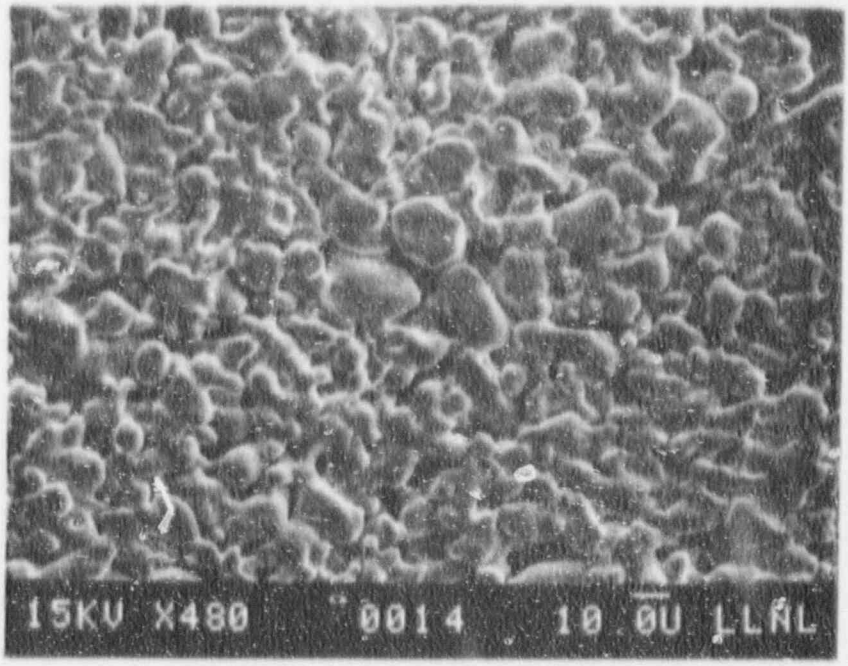

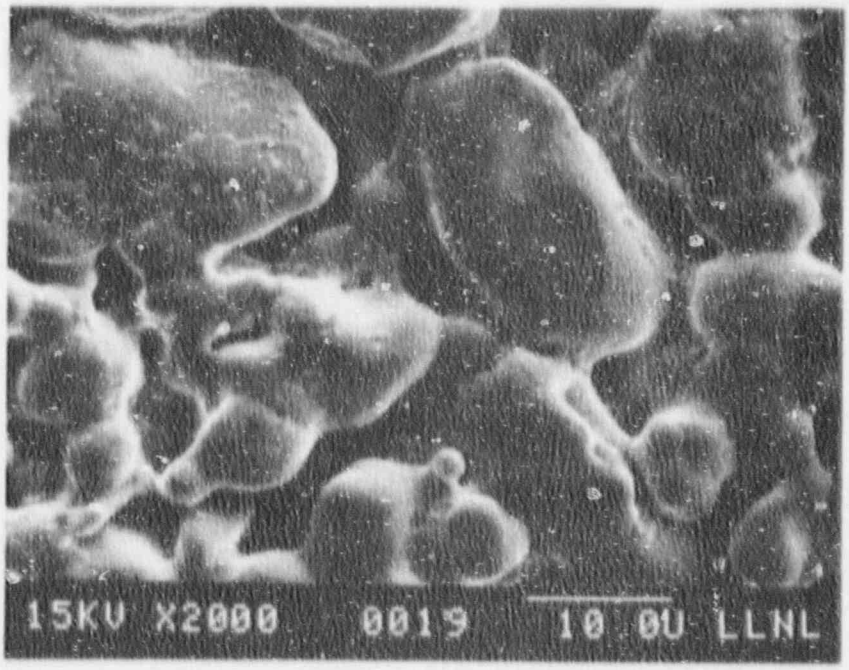

PALL M020

Figure 1 Electron micrographs of the surface of a sintered-powder filter (Pall M020) at increasing magnification.

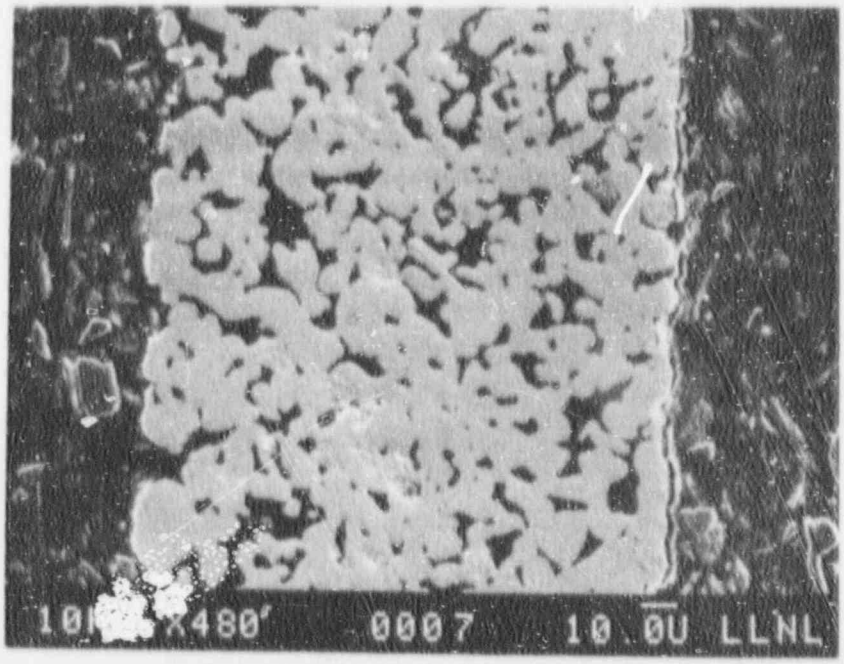

PALL M020

Figure 2 Electron micrograph of a cross section of a sintered-powder filter (Pall M020).

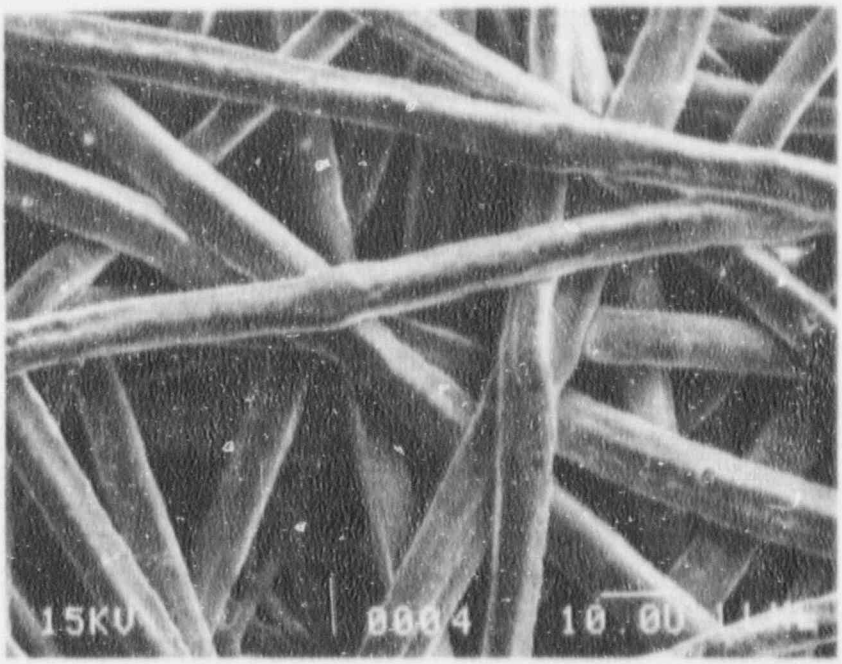

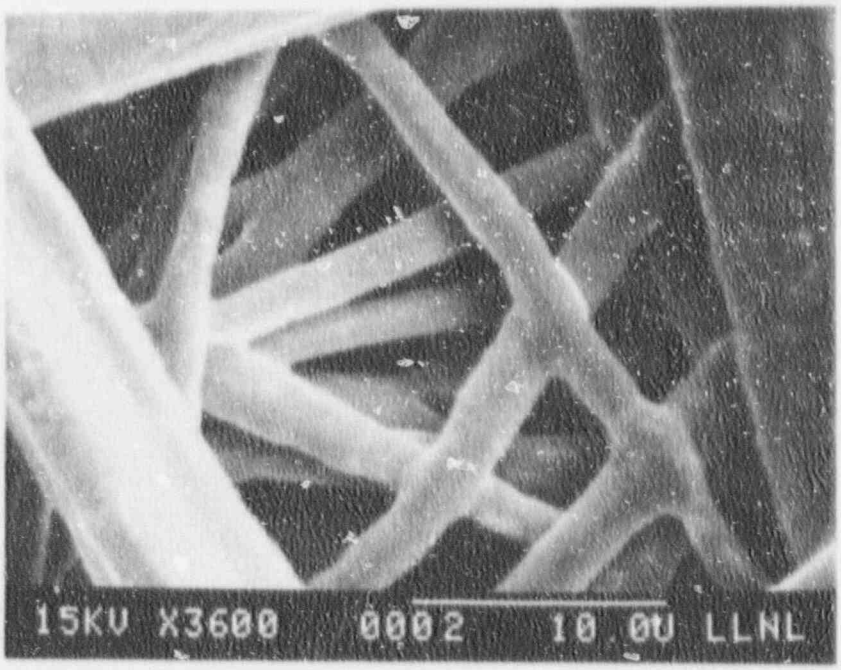

Bakaert 3AL3

Figure 3 Electron micrographs of the surface of a sintered-fiber filter (Bakaert 3AL3) at increasing magnification.

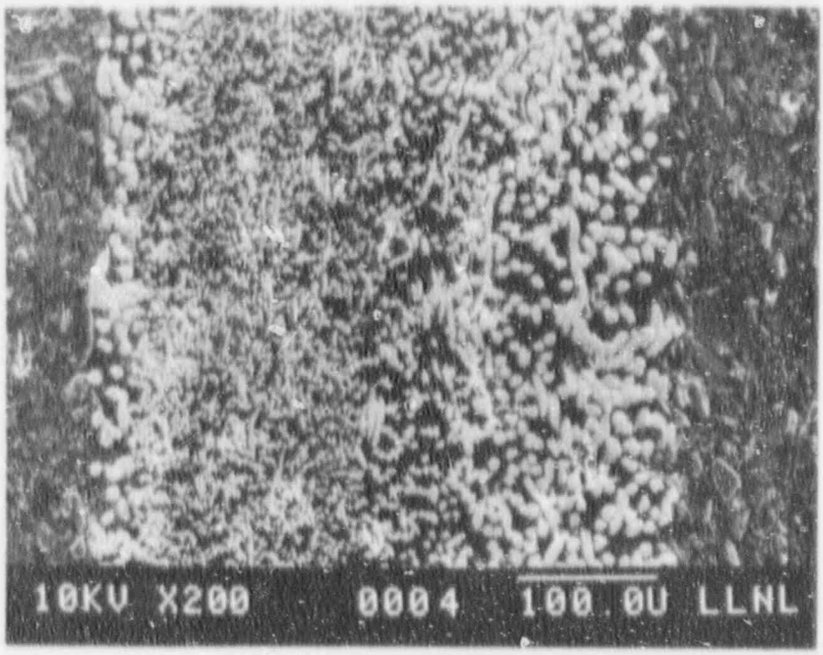

Bakaert 3AL3

Figure 4 Electron micrograph of a cross section of a sintered-fiber filter (Bakaert 3AL3).

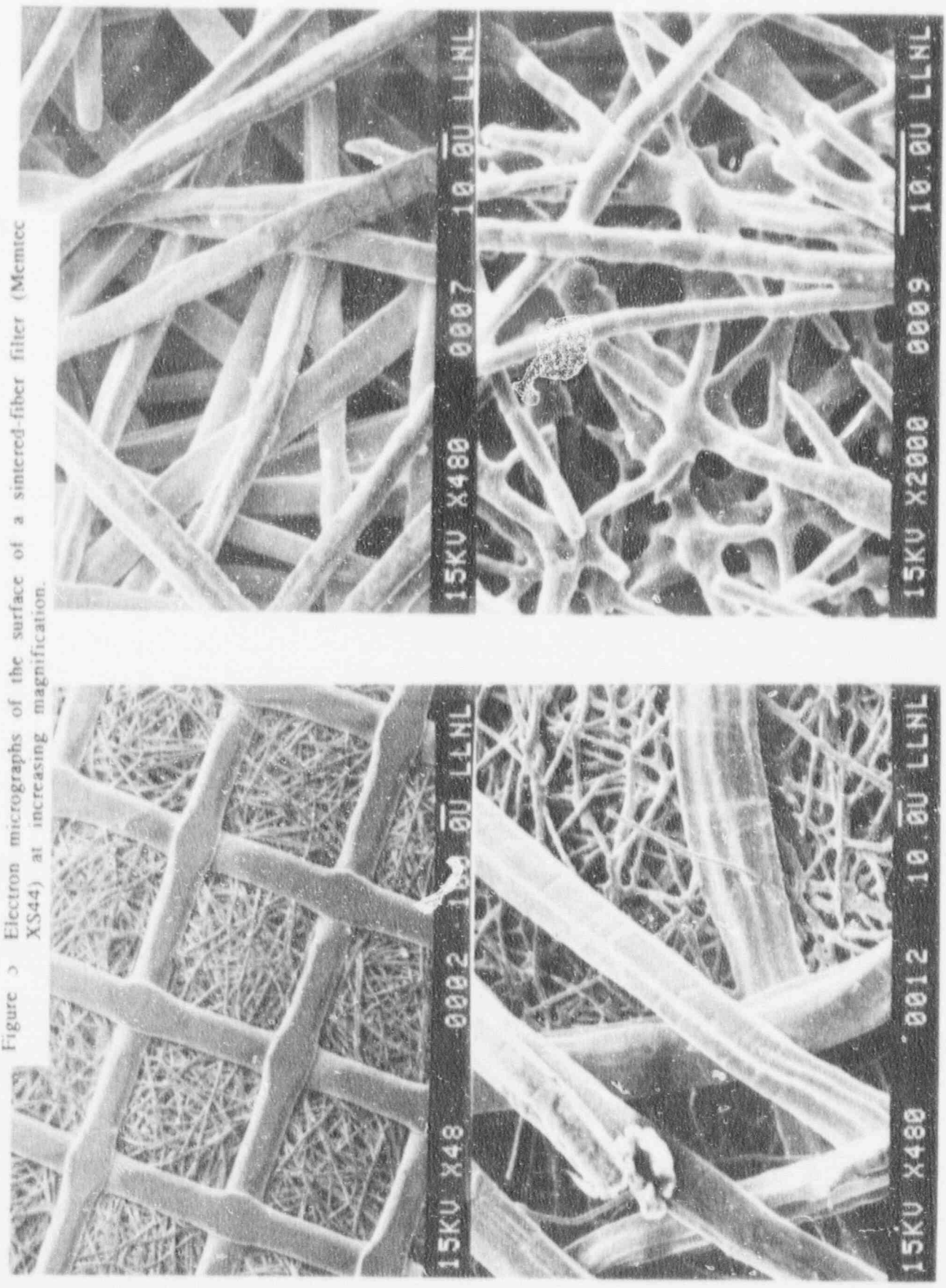

Figure 3 Electron micrographs of the surface of a sintered-fiber filter (Memtec XS44) at increasing magnification.

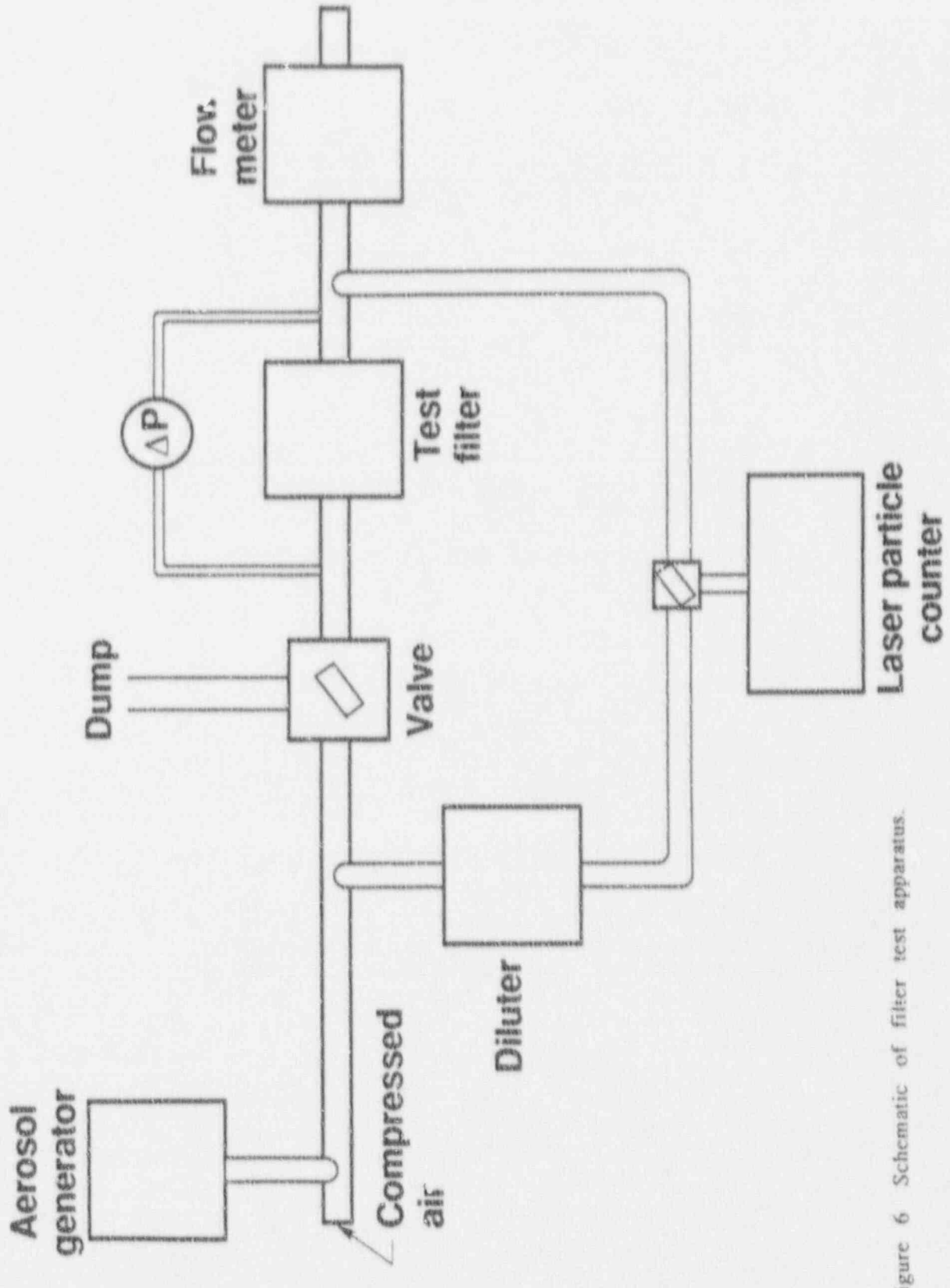

Figure 6 Schematic of filter test apparatus.

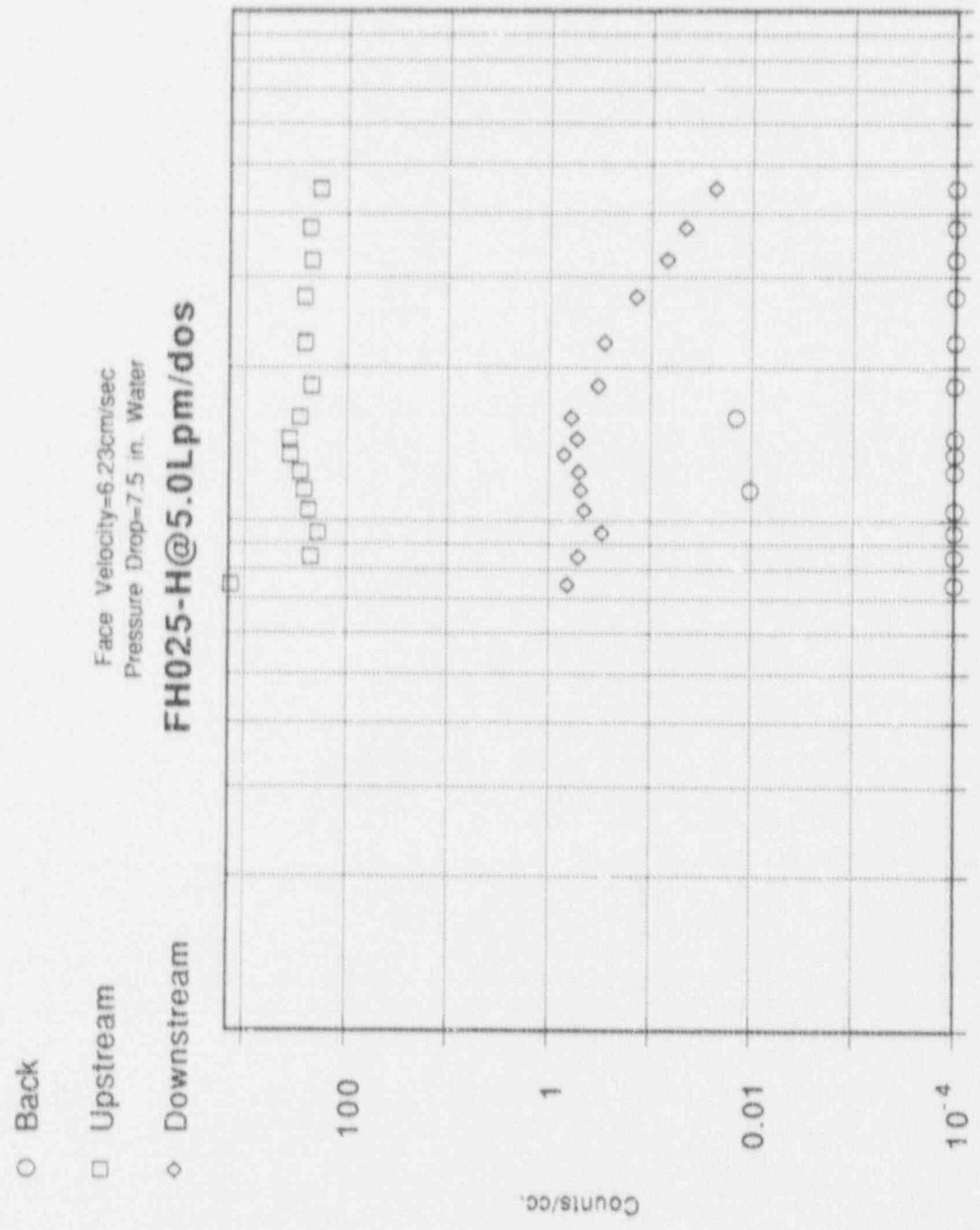

Figure 7 Concentration of DOS particles measured upstream and downstream of the filter.

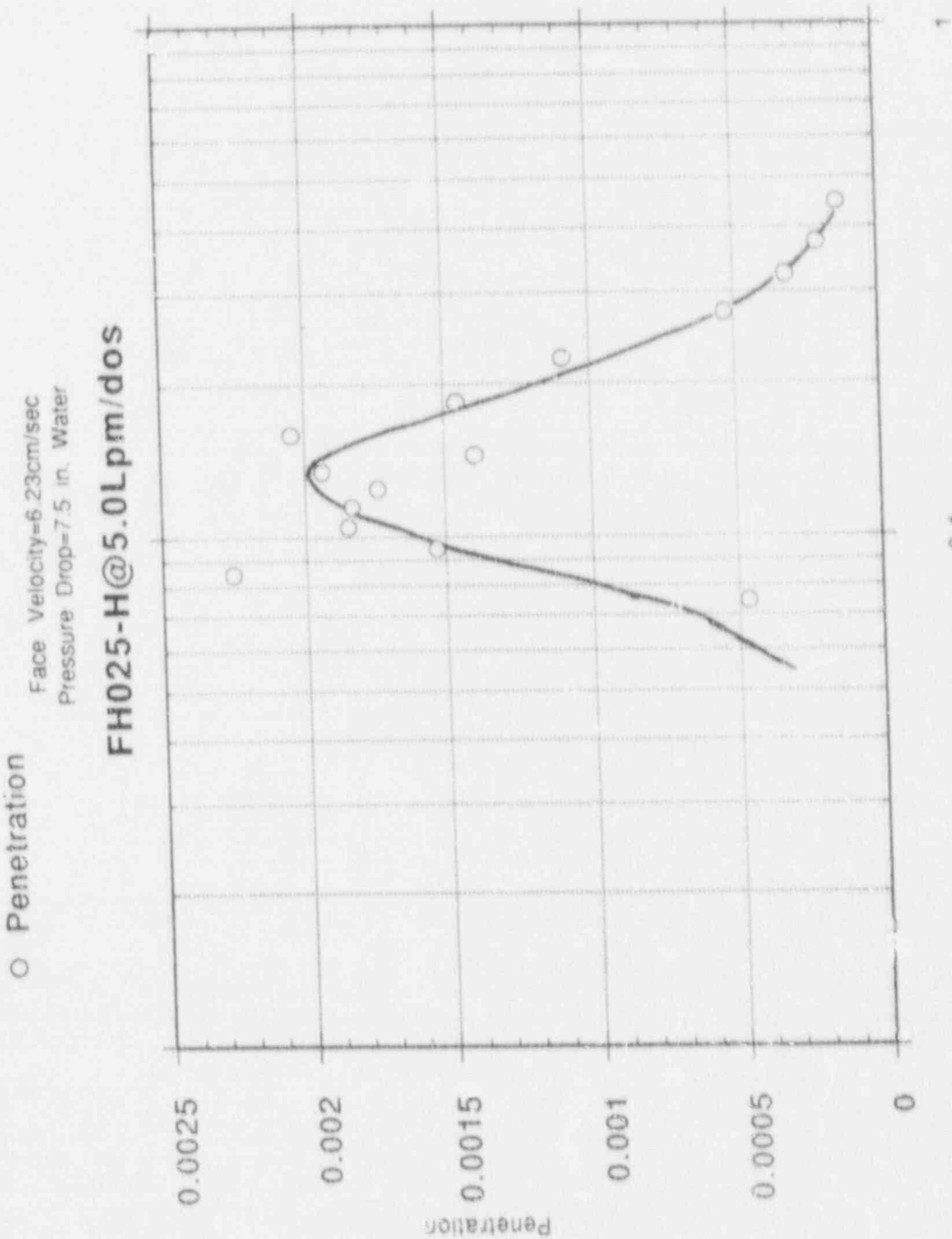

Figure 8 Filter penetration of a sintered-fiber medi. FH025-HEPA.

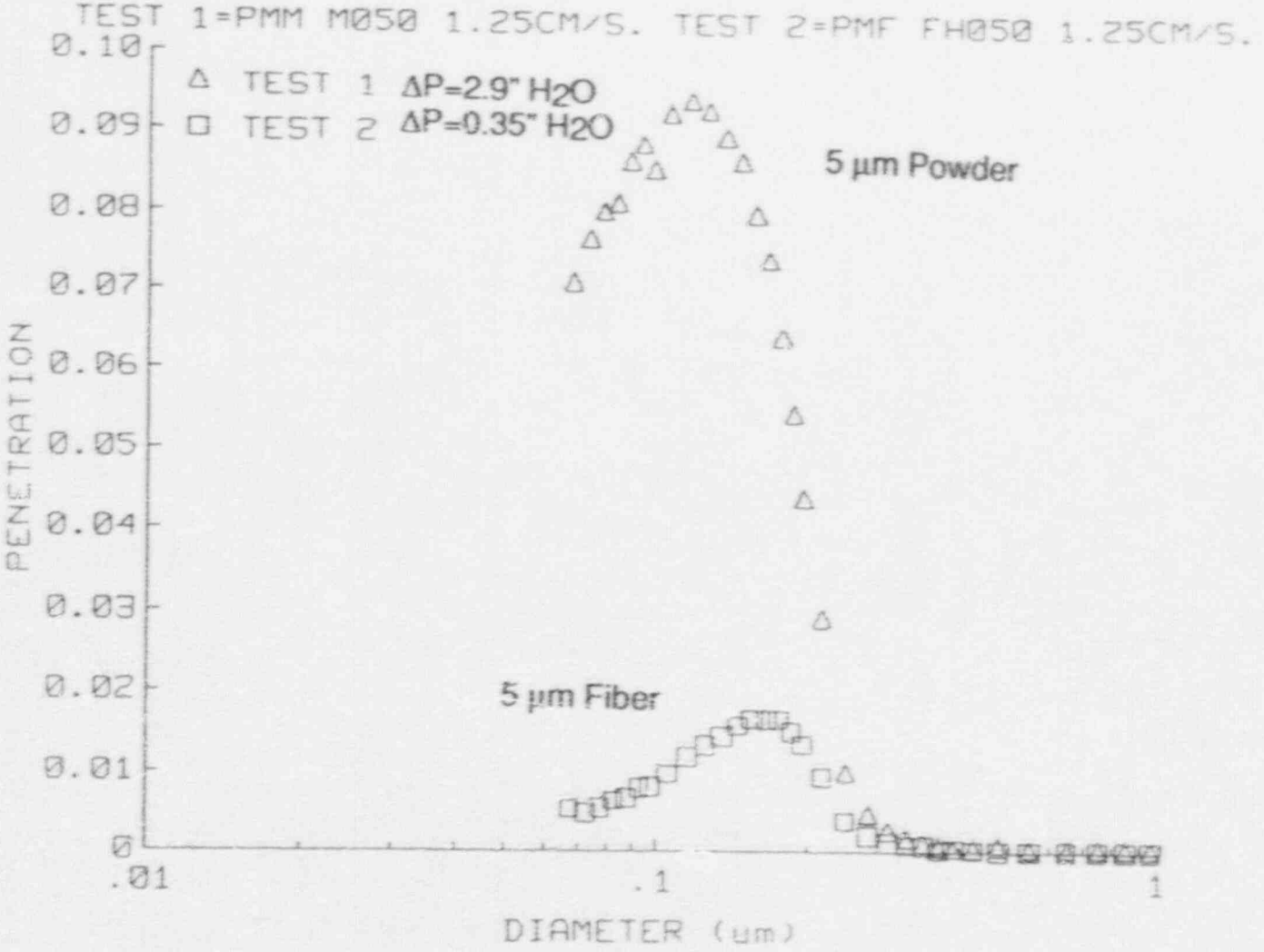

Figure 9 Sintered-fiber filters have lower particle penetration than sintered-powder filters.

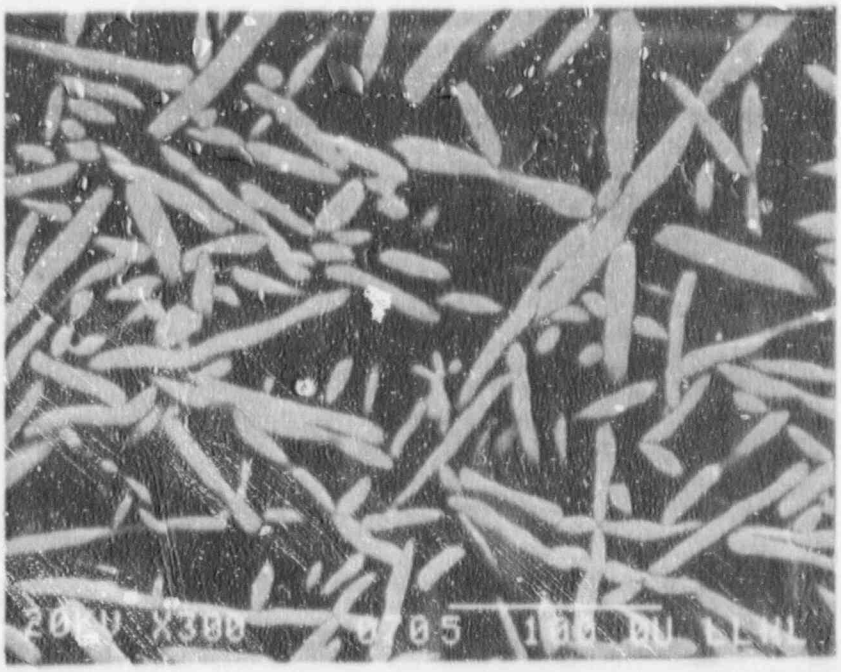

10A Sintered Fiber

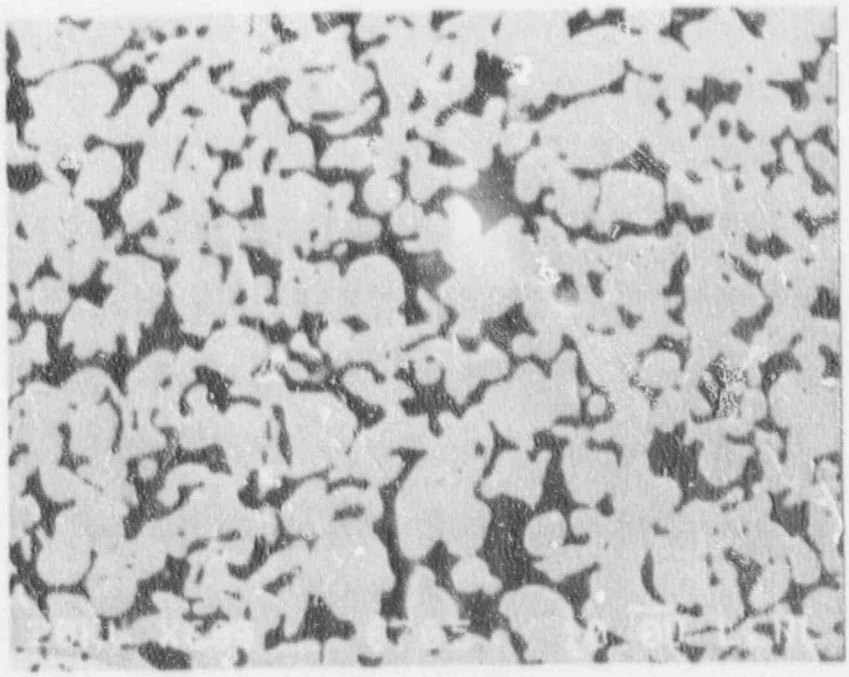

10B Sintered Powder

Figure 10 Electron micrographs of metallurgical samples of sintered-fiber (10A) and sintered-powder (10B) filters.

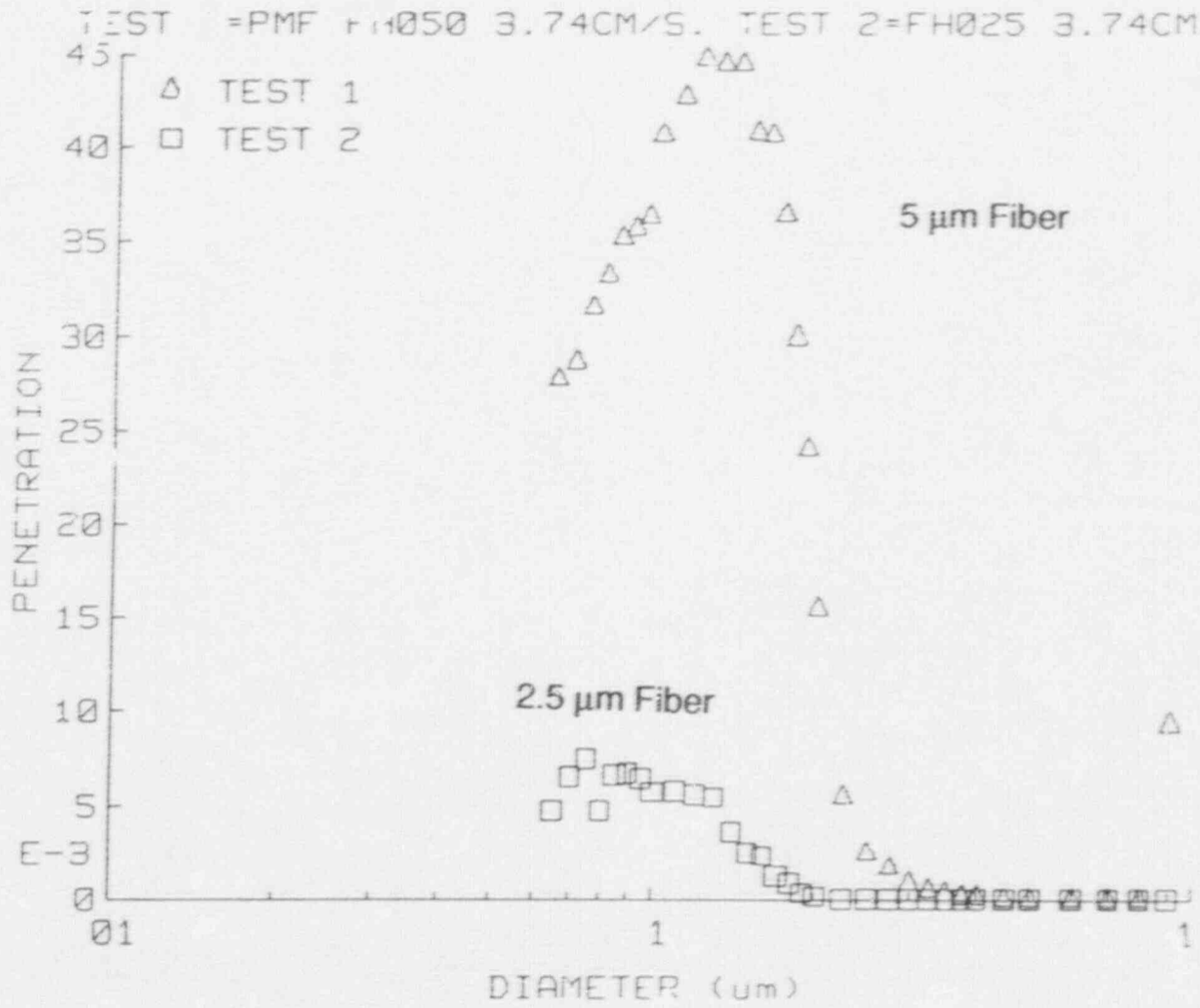

Figure 11 Particle penetration decreases with decreasing fiber diameter.

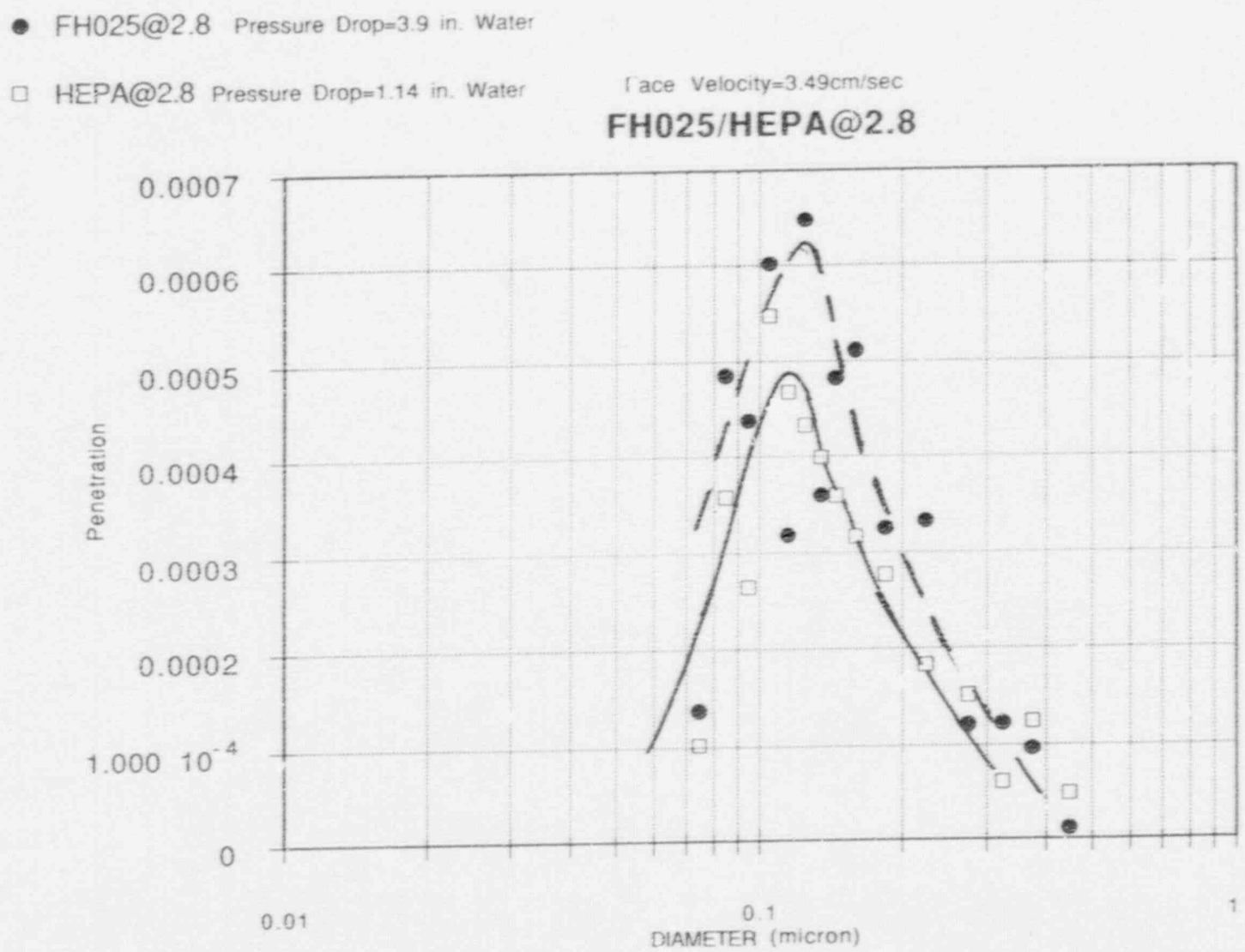

Figure 12 Steel filter media have similar penetration, but 3.4 times the pressure drop of glass-paper HEPA media.

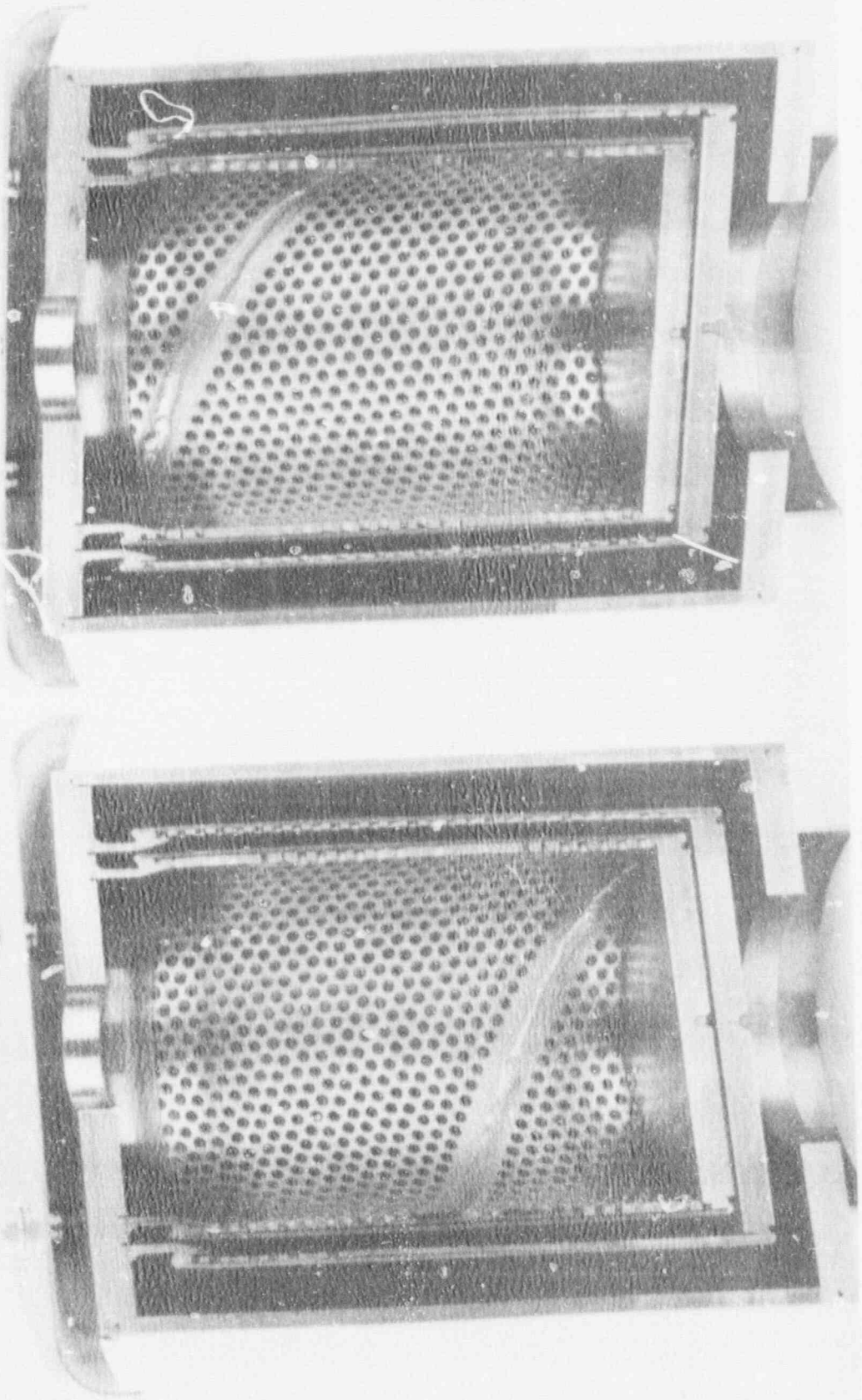

Figure 13 Prototype Memtec steel filter with two-stage concentric-cylinder design. Media not pleated.

Figure 14 Operator installing prototype steel filter in LLNL automated filter tester.

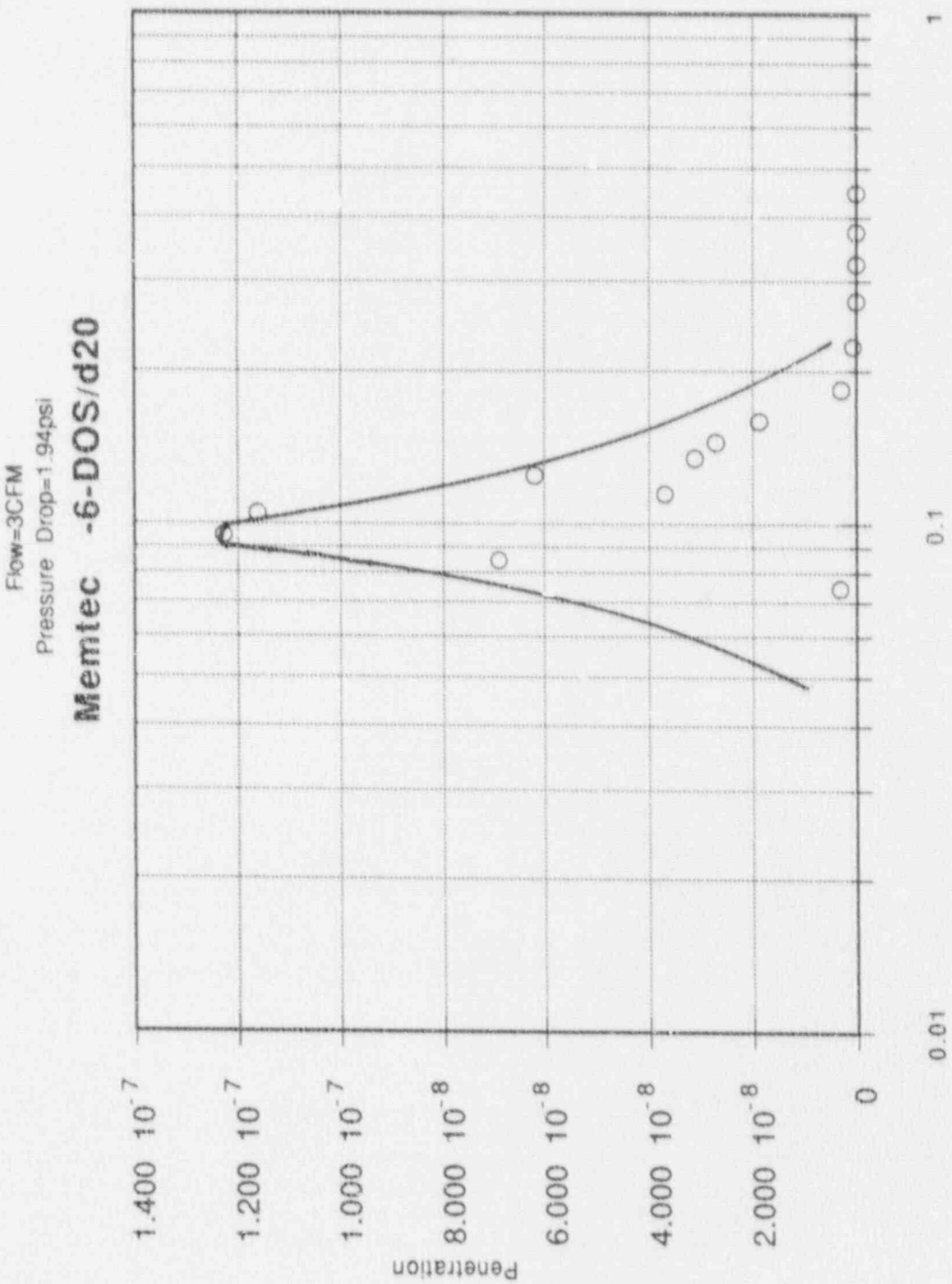

Figure 15 Aerosol penetration through prototype Memtec filter shown in Fig. 13 at 3 cfm. Pressure drop is 1.94 psi.

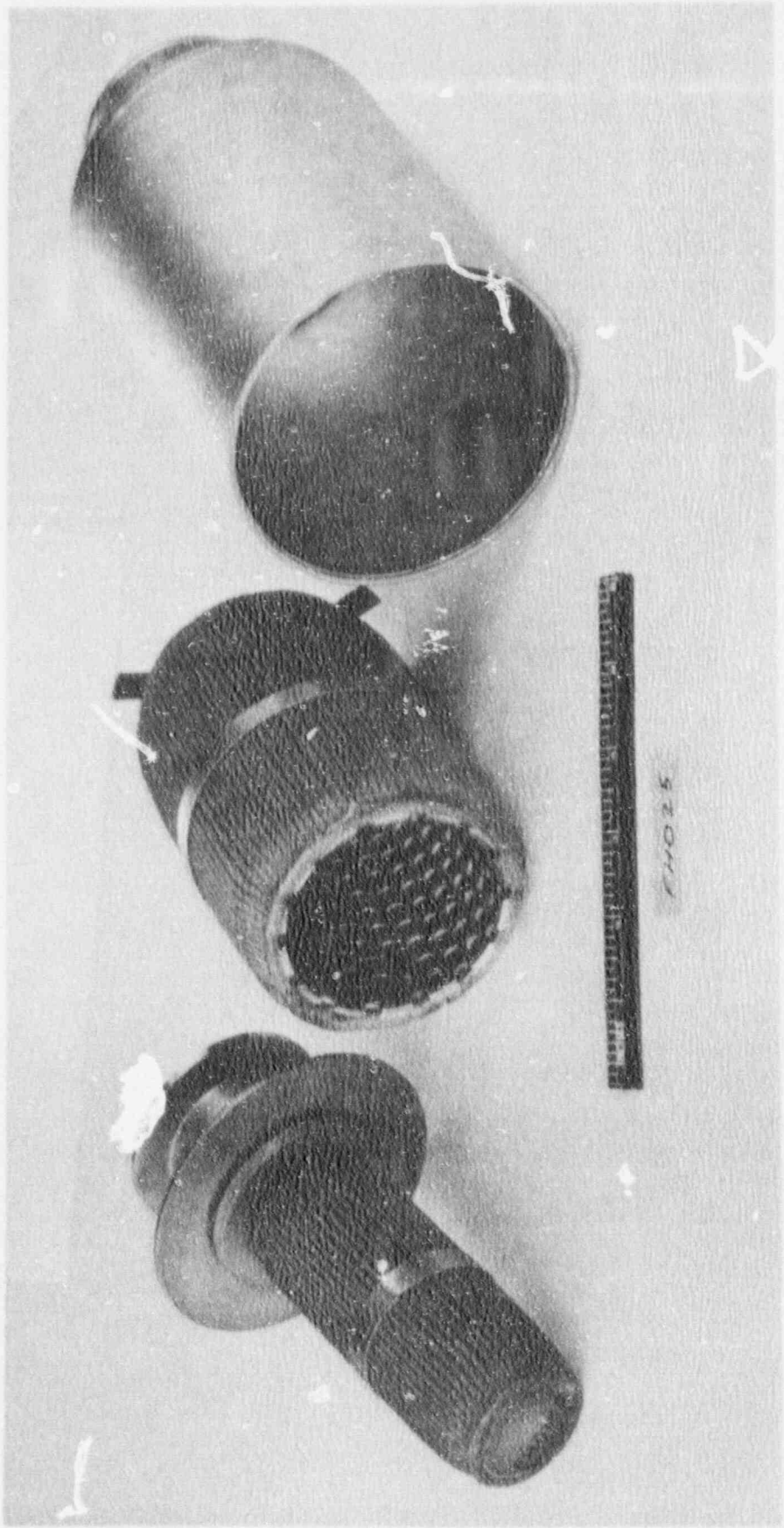

Figure 16 Prototype Pall steel filter with two cylindrical filter stages shown disassembled (pleated media).

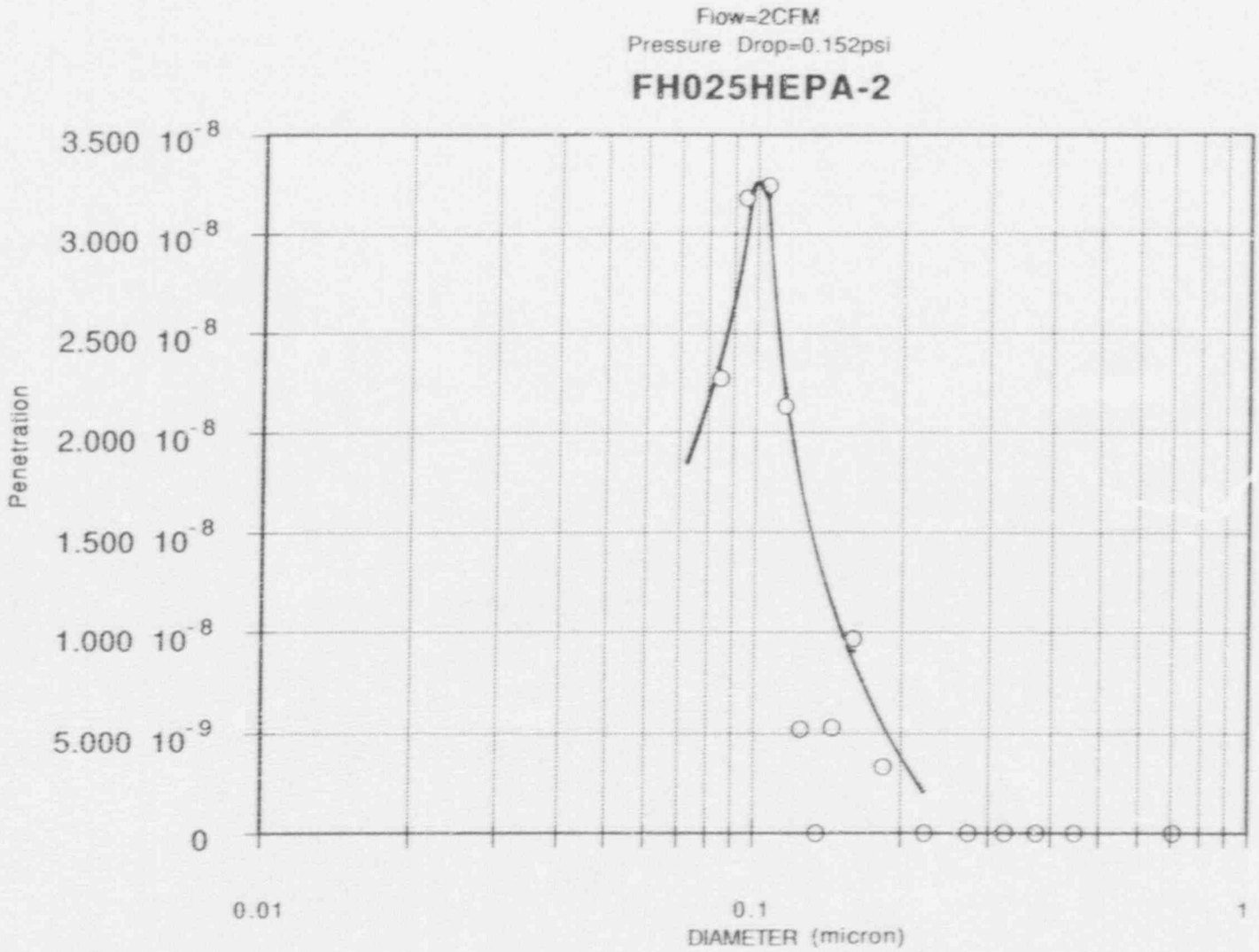

Figure 17 Aerosol penetration through prototype Pall filter shown in Fig. 16 at 2 cfm. Pressure drop is 0.15 psi.

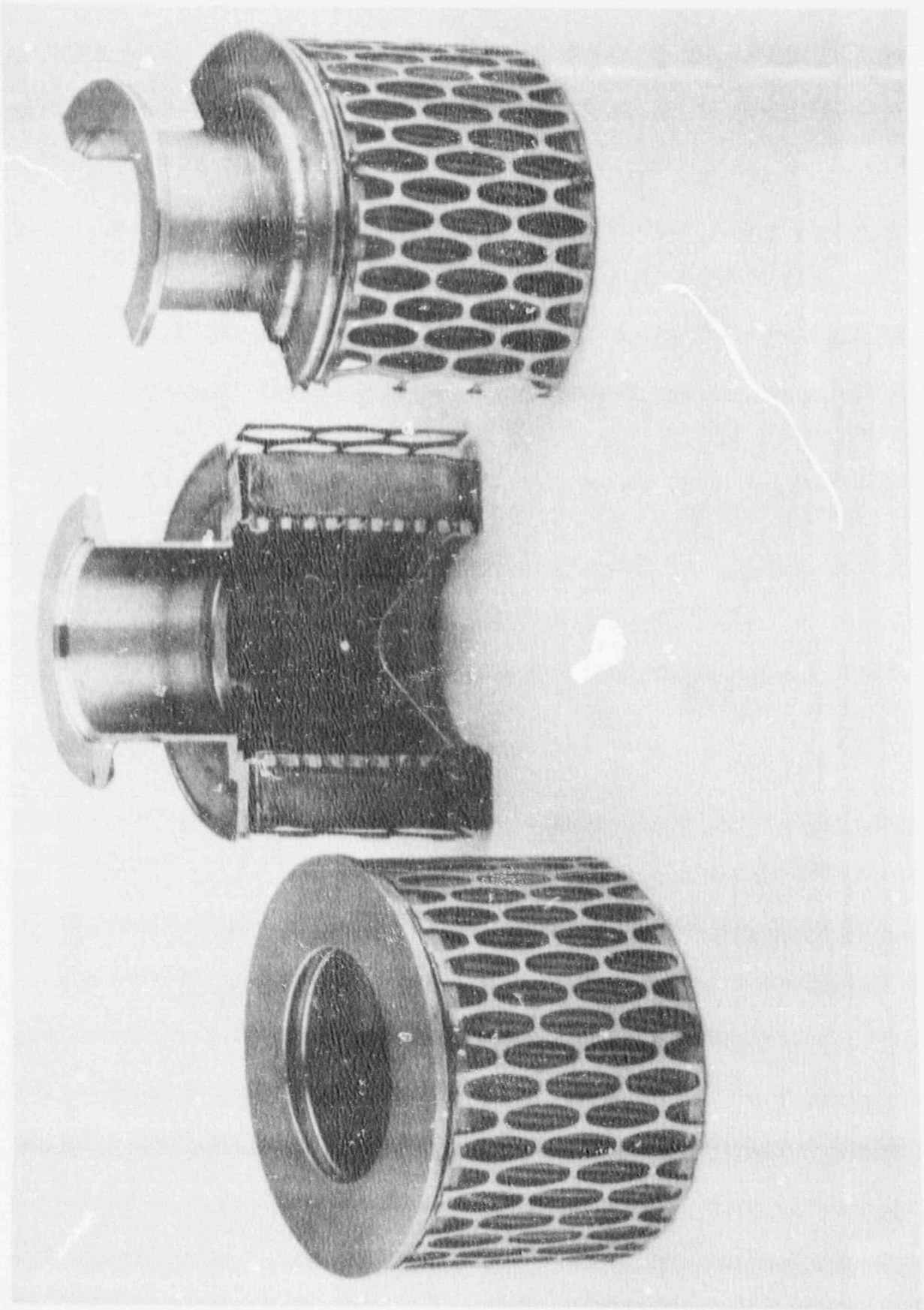

Figure 18 Prototype Pall filter with a single-stage pleated-cylinder design.

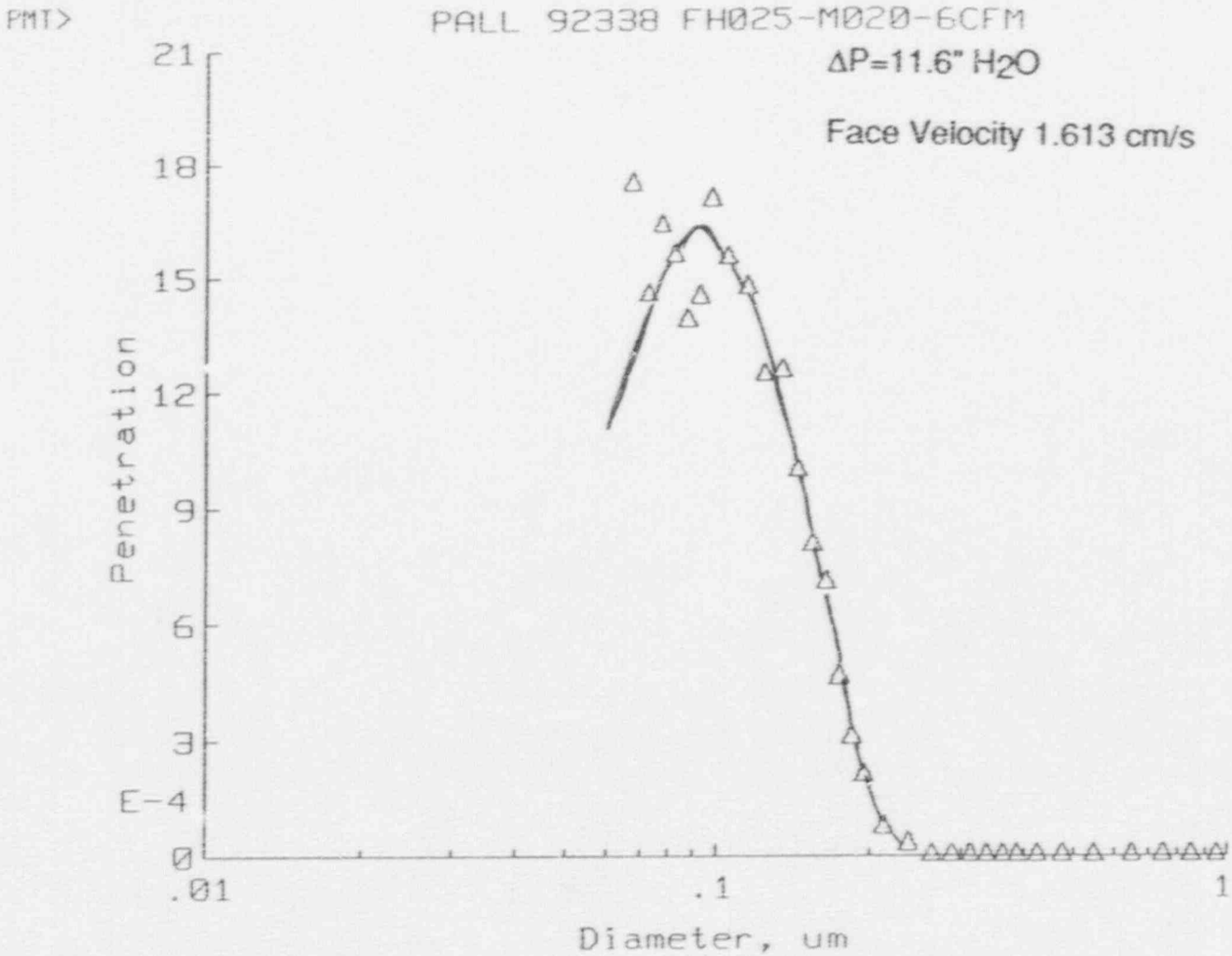

Figure 19 Filter penetration of prototype filter in Fig. 18 at 6 cfm. Pressure drop is 11.6 in. of water.

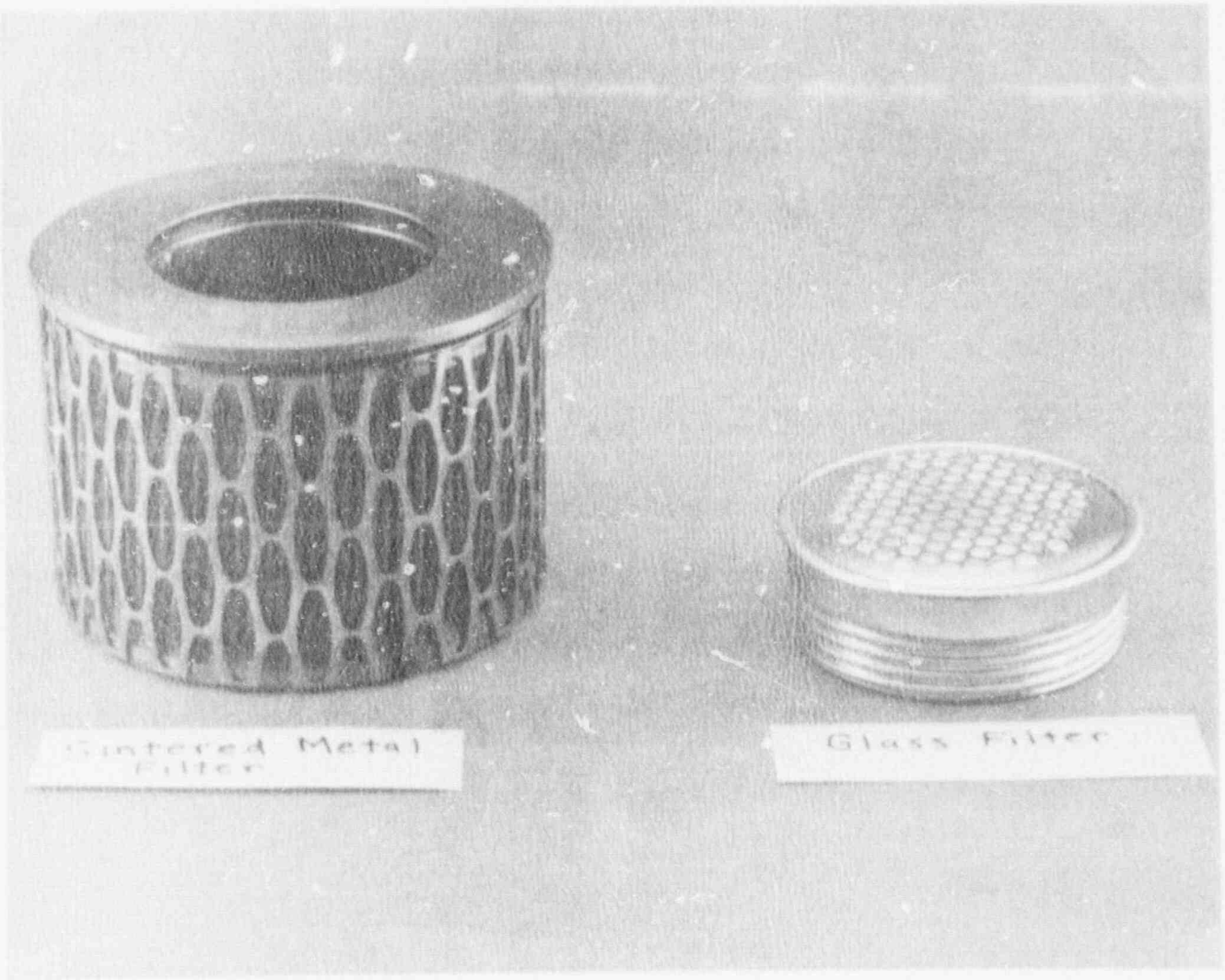

Figure 20 Photograph showing that the prototype steel filter is much larger than the glass-paper HEPA filter.

DISCUSSION

SEIBERT: You stated that typical ventilation systems would not tolerate high resistance to flow. You also said that you had reduced the four-fold difference in resistance between regular HEPA filters and steel filters to a two-fold difference. Although steel filters have higher mechanical integrity than typical HEPA filters, installations can have redundancy by installing two or three stages. Would that change your conclusion?

BERGMAN: Figure 12 of the paper shows that the steel HEPA media has 3.4 times the air resistance of the standard glass HEPA media. This higher pressure drop would not be acceptable in most ventilation systems. Although it is true that those installations having three stages of standard glass HEPA filters have about the same pressure drop as a single stage steel HEPA filter, the multiple filter installations also have much higher efficiencies. Until both the pressure drop and the efficiency of steel HEPA filter become comparable to the glass HEPA filter, the steel HEPA filter will not generally be suitable for use in ventilation systems. However, in applications where the glass HEPA filter is subject to severe structural failure, the steel HEPA filter may be acceptable in spite of the higher air resistance.

MORRIS: If you had the Midas touch and you could convert a glass material to stainless steel, would you expect to get a better efficiency from the glass? If not, why?

BERGMAN: There will be no difference between a glass fiber and a metal fiber filter. The glass fiber filter may have a slightly better performance because of added electrostatic attractive forces that do not exist with a steel fiber filter. However, this increase would be very small for the glass fiber filter because it still conducts electricity.

MORRIS: You would expect the stainless steel filter to come up to the same efficiency level? There is no reason you can think of why it shouldn't?

BERGMAN: No, not one reason.

MORRIS: Is there any way of using electrostatics for your benefit? Could you charge the particles and get a better filter?

BERGMAN: Electrostatics will not be beneficial in steel filters because they conduct electricity. We had previously looked at applying electrostatics to glass fiber filters and published several papers in previous Proceedings of this conference. Although electrostatics showed remarkable improvements in filter performance, they were not well received in the nuclear industry because of increased complexity and lower reliability.

A PERMANENTLY MAGNETISED HIGH GRADIENT MAGNETIC FILTER FOR GLOVE-BOX CLEANING AND INCREASING HEPA FILTER LIFE

Dr J.H.P. Watson and Dr C.H. Doorman
Institute of Cryogenics
University of Southampton
Southampton SO9 5NH
England

Introduction

The purpose of this paper is to describe the structure and testing of a permanently magnetised magnetic filter on simulants for radioactive material. The experimental work was carried out at British Nuclear Fuels plc, Sellafield, England and in CEN/SCK, Mol, Belgium using Cr powder which is a good magnetic simulant for PuO_2. The basis of the use of such a filter in the nuclear industry relies on the fact that much of the radioactive material is paramagnetic, as shown in Table 1.

Material	Origin	Susceptibility (SI)
U	Magnox fuel	3.9 (10^{-4})
Pu	Research Labs	6.3 (10^{-4})
UO_2	Oxide Fuel (AGR, PWR, BWR, LMFBR)	1.2 (10^{-3})
PuO_2	LMFBR fuel	3.7 (10^{-4})
Zr	PWR, BWR fuel	1.1 (10^{-4})
Insoluble Fission Products		
Mo	Irradiated Fuel	1.2 (10^{-4})
Ru	from all types of	4.6 (10^{-5})
Rh	reactor	1.7 (10^{-4})
Pd		8.2 (10^{-4})
Tc		3.9 (10^{-4})

Table 1 Magnetic volume susceptibility data (SI units) for materials occurring in the nuclear industry.

In the last twenty years a separation technique has been developed which allows weakly paramagnetic particles of colloidal size to be separated from fluid which passes through the separator. This method is called high gradient magnetic separation (HGMS) and is accomplished by magnetising a fine ferromagnetic wire matrix by an externally applied magnetic field. The wires of the matrix attract the paramagnetic particles which are also magnetised by the applied magnetic field. The technology of HGMS is used throughout the world to purify kaolin clay. In the United States this industry is centred in Georgia. Many of the applications of this technology in the minerals industry have been discussed by Svoboda[1].

While modern technology allows the generation of high magnetic fields and which have been used in many applications, there remain a significant number of applications where the magnet or solenoid, providing the magnetic field, would be difficult, if not impossible, to accomodate. This paper describes a new approach to this problem, by using a magnetically hysteretic material to construct the ferromagnetic matrix, it has been possible to provide a magnetic field in the region of the matrix and also have a residual magnetisation within the matrix. This provides extremely compact magnetic separation systems. There are some subtle

differences between this separation system and conventional HGMS which makes the radial feed system, with all its advantages, almost mandatory for hysteretic HGMS.

The permanently magnetised magnetic filters described in this paper have the following important features: (1) No external magnet is required. (2) No external power is required. (3) Small in size and portable. (4) Easily interchangeable. (5) Can be cleaned without demagnetising.

Two uses have been proposed for such a filter:

(A) As a cleanable pre-filter in front of an absolute filter in order to reduce the load on the absolute filter and thereby increase its useful life. This reduces greatly reduces the absolute filter storage cost.

(B) To improve housekeeping in a glove-box by preventing the spread of fine PuO_2 through the box by constantly circulating the air or part of the air through the filter. By adopting this measure operator exposure could be reduced.

Magnetic interaction of a particle and a magnetic fibre

The theoretical model assumes a flow of paramagnetic particles carried by a fluid past a magnetised wire. We assume that the wire is ferromagnetic and hysteretic. The magnetic field in which the wire sits is the internal demagnetising field H_i of the whole assembly of hysteretic wires which have been magnetised to saturation after which the external applied field is reduced to zero. This leaves the residual demagnetising field as the magnetic field in which the wires and the paramagnetic particles sit. In this situation

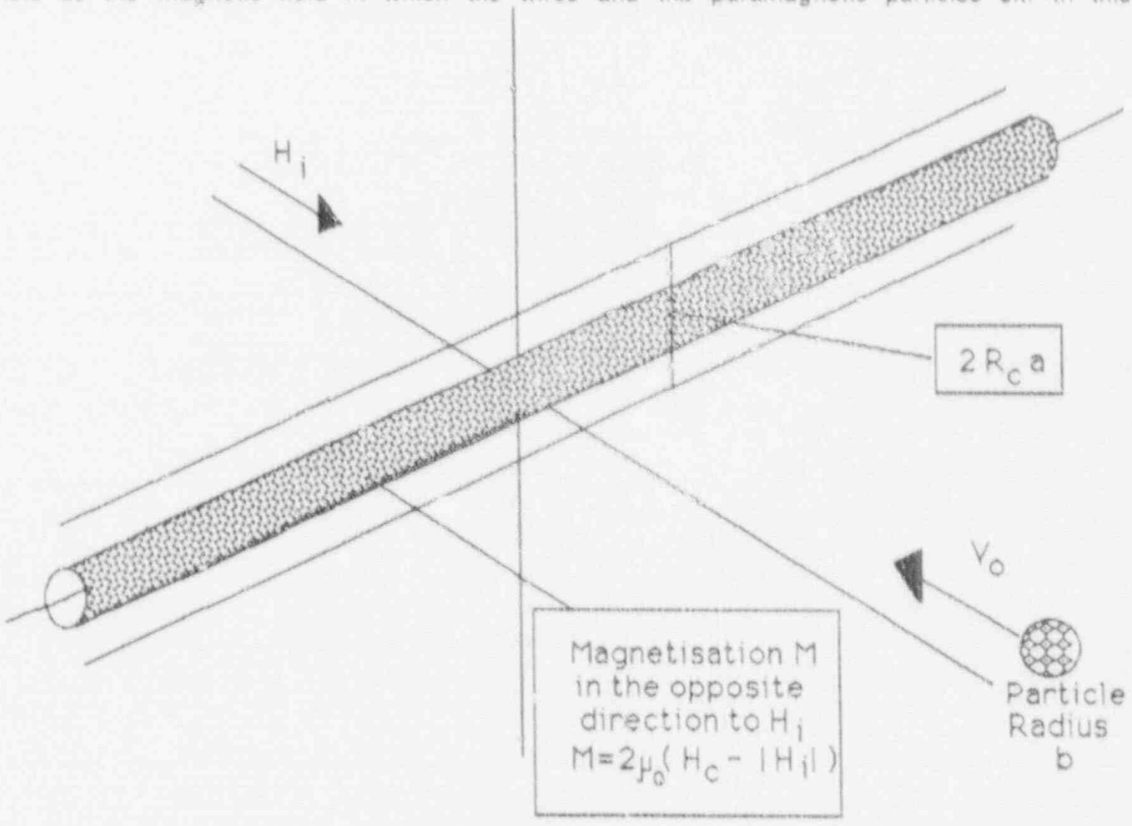

Fig 1 Shows the particle of radius b carried by a fluid of background velocity V_o moving parallel to the x-axis along which a magnetic field H_i is applied. It is necessary to determine the capture cross-section $2R_c a$, as shown. R_c is referred to as the capture radius.

the magnetisation M of the wire is in the **opposite** direction to the local magnetic field H_i and is given by $M = 2\mu_o(H_c - |H_i|)$ where H_c is the coercive force and $\mu_o = 4\pi(10^{-7})$H/m, the permeability of free space. It is assumed that the wire is perpendicular in direction to this local field. From this following the methods by Watson[2] and more recently by Lawson, Simons and Treat[3] and Simons and Treat[4], the equations of motion can be calculated and the capture cross-section $2R_c a$ for the particle can be calculated. Here R_c is termed the capture radius and a is the wire radius. The geometical significance of the capture cross-section is illustrated in Fig 1.

The equations of motion determining the particle trajectories show and, in consquence, the capture of particles by a fibre, in are background magnetic field H_i, are determined by three parameters;

i) V_m / V_o

where V_m is the 'magnetic velocity' containing all the important magnetic parameters in the system,

and V_o is the flow velocity. V_m is given by;

$$V_m = (2/9)\chi b^2 MH_i / \eta a \qquad (1)$$

where χ is the difference in susceptibility between the fluid of viscocity η and the particle of radius b. M is the magnetisation of the ferromagnetic wires of radius a and H_i is the local magnetic field, which for the case of the permanently magnetised matrix is referred to as the internal field H_i. Then using the expression given above for the wire magnetisation M, equation (1) becomes

$$V_m = (4/9)\chi b^2 \mu_o (H_c - |H_i|)|H_i| / \eta a \qquad (1a)$$

V_m is maximised with respect to H_i when $|H_i| = H_c/2$.

(ii) The short range parameter K, given by;

$$K = M/2\mu_o H_i = \{ H_c/|H_i| \} - 1 \qquad (2)$$

If the wire is not magnetically saturated then $K = 1$. If V_m is maximised then $K = 1$, as the capture radius R_c depends on V_m / V_o and on K, the maximum in R_c does not necessarily occur at $|H_i| = H_c/2$.

iii) Stoke's number, N_{st}:

$$N_{st} = (2/9)\rho_p b^2 V_o / \eta a = (Re/9)(\rho_p / \rho_L)(b^2 / a^2) \qquad (3)$$

ρ_p and ρ_L are the particle density and the fluid density, respectively, Re is the wire Reynolds number where $Re = 2\rho_L V_o a / \eta$. The efficiency of capture by the fibre can be adjusted by changing these parameters.

In the case of a permanently magnetised filter the optimisation of these parameters is crucial. To understand why this is so some background is necessary. In HGMS weakly magnetic particles are captured by the combination of high fields and high field gradients. This is possible through the use of large electromagnets, or superconducting magnets so large values of V_m can be obtained. However there are some disadvantages which must be considered. One of these concerns the short range term, K, and the fact that for a soft ferromagnet with low hysteresis K can only have a values between 0 and 1. In the case of a permanently magnetised filter the magnetic field is significantly smaller than that experienced in HGMS, however, because of magnetic hysteresis, it is possible to create values of K much greater than unity. Consequently, the optimisation of the field and magnetisation is crucially important. Given this optimisation, magnetic particles passing the filter elements will be captured if they are inside the capture radius R_c of that element.

The magnitude of R_c can be determined from V_m, V_o and K. It is possible to build a model relating relating K to R_c for various V_m / V_o ratios. Fig 2 shows a graph of the capture radius as a function of the ratio of magnetic velocity to flow velocity. This graph has been obtained from data calculated by Watson[5]. These values were calculated for the case where dependence on the Stokes number is small and negligible.

It is interesting to look at the differences between conventional HGMS and HGMS with hysteretic

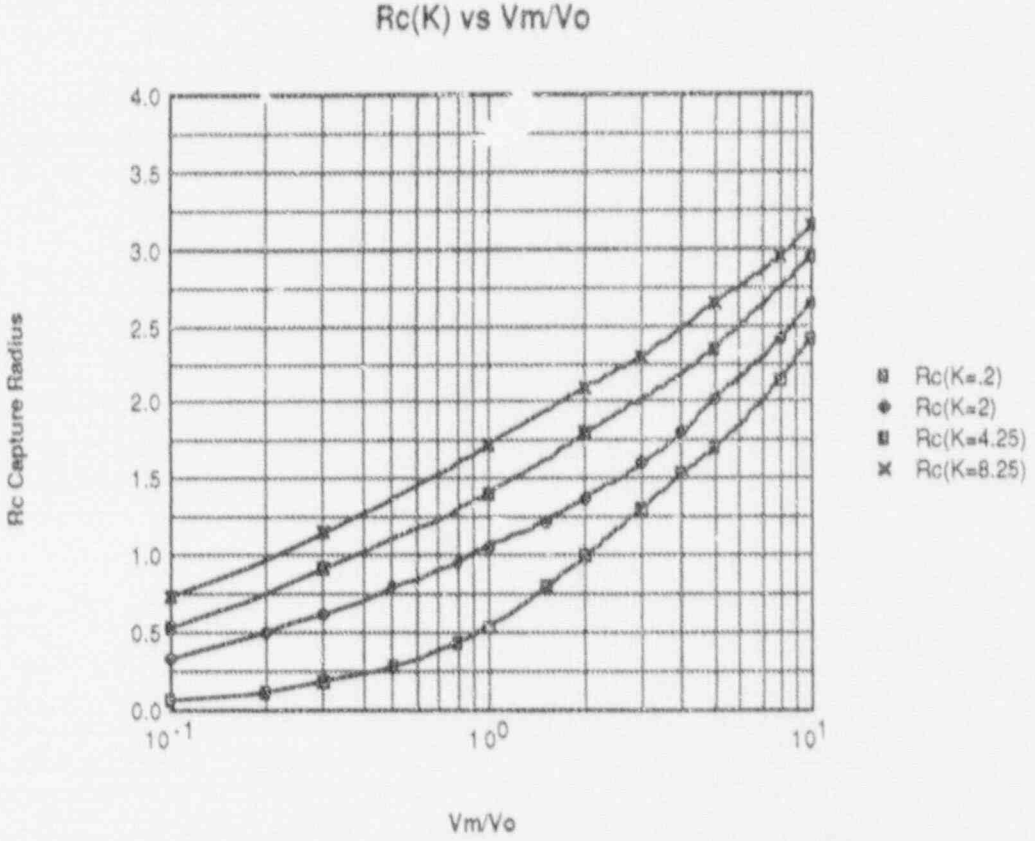

Fig 2 Shows R_c versus V_m / V_o for various values of the parameter K. For normal soft ferromagnetic material K can never be greater than 1, but for hysteretic material values of K>>1 are possible.

materials. In conventional HGMS, the surface of the wire becomes divided into four regions, two of the regions are attractive to paramgnetic material and two repulsive to paramagnetic material. In hysteretic HGMS, the attractive regions become repulsive and vice versa. This has been discussed previously by Boorman, Watson and Bahaj[6].

The development of this model requires an understanding of the filtration applications envisaged for the system. A prototype filter has been constructed incorporating a roll of expanded ferromagnetic metal mesh, as shown in Fig.3. The mesh is an hysteretic ferromagnetic but it is also flexible with a coercive force of 300 Oersted. Chromindur is a product of Telcon Metals Ltd, Manor Royal, Crawley, England.

The matrix was magnetised parallel to the surface of the sheets in the roll, and also parallel to the filter axis. The applied field was then reduced to zero, and, due to the hysteretic nature of the Chromindur, the filter remained magnetised with an internal field strength H_i of 14881 Am^{-1}. The magnetisation of those legs perpendicular to the field, on which most magnetic capture will occur due to the large field gradients

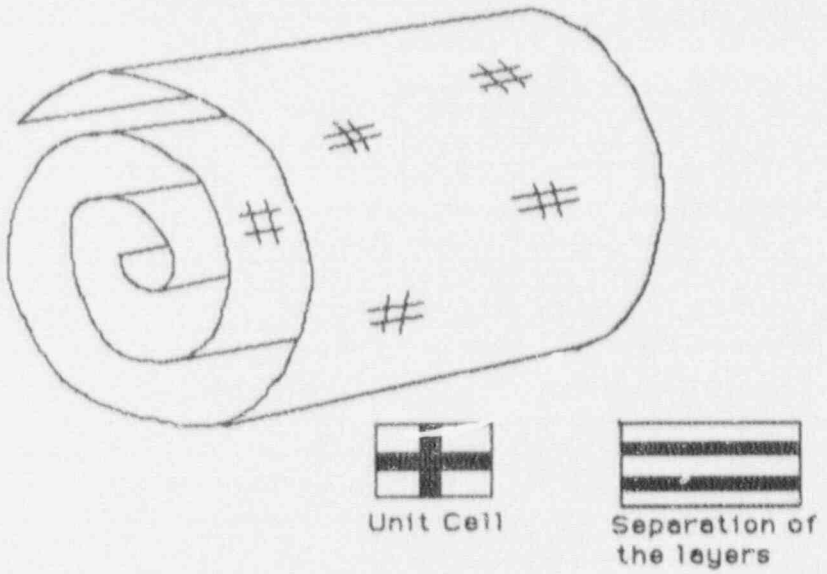

Fig 3a Structure of the prototype filter showing a role of chromindur expanded metal mesh. This is wound on the inlet tube so the flow is radially outwards through 76 layers of mesh. A cross-section through the filter is shown. The unit cell is the repeated unit generating the two dimensional sheet. The separation of the layers is 0.4 mm

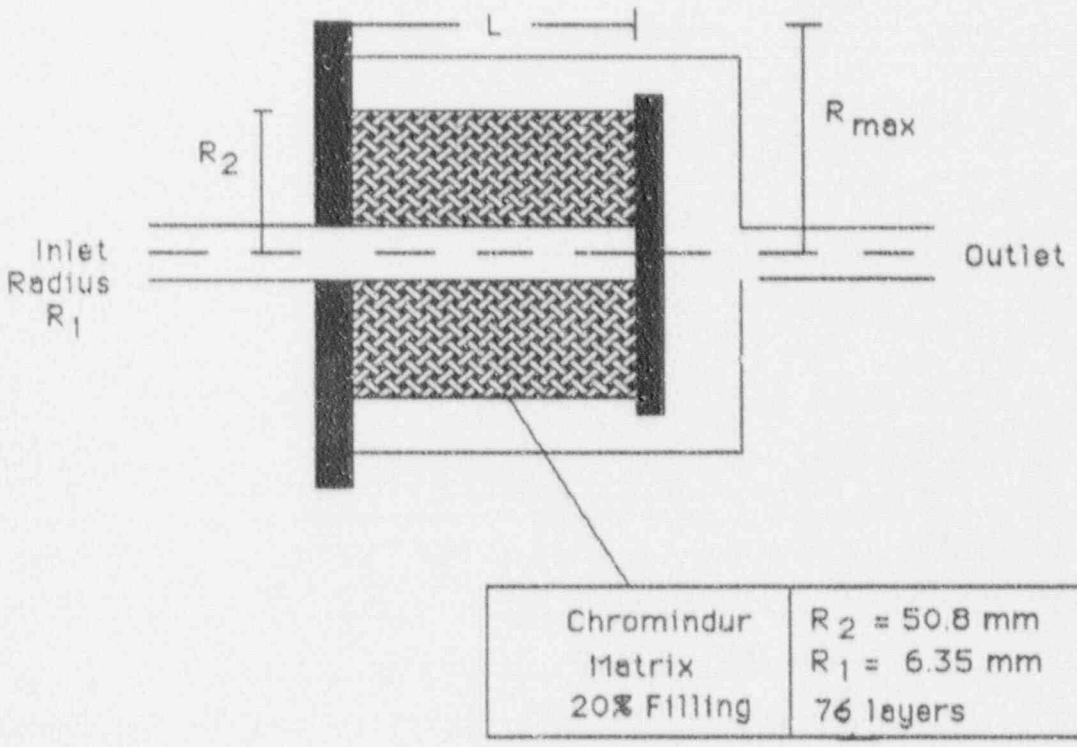

Fig 3b Shows a section through the filter. The original filter had a length L=25.4 mm. The matrix is wound on the central perforated tube. The gas flow is radially outwards. The separation between the layers is 0.4 mm and the thickness of the sheet is 0.2 mm. The chromindur is magnetised in the plane of the sheets that is parallel to the axis of symmetry.

present, will be 17980 Am^{-1}. For fibres of radius, a = 0.2 mm, and particles of radius, b = 0.5 microns, with a susceptibility of 5 x 10^{-5} (S.I. units), the resulting magnetic velocity will be 0.0018 mm/sec. In this case a value of V_m / V_o = 0.03 would be suitable, i.e. a flow velocity of 0.06 mm/sec. The corresponding value of K will be 2.55.
A reasonable approximation to these parameters (for the case V_m / V_o = 0.03) is:

$$R_c = a + b.K \qquad (4)$$

where a = 0.0094 and ba = 0.048. The capture radius for the filter elements in this case will therefore be 0.132. Assuming a 7% filling factor, the total volume of the matrix is 1.4 x 10^{-5} m^3. As already mentioned, the mass loading envisaged for the filter is about 0.04gm/m^3. Nesset and Finch[7] introduced a quantity called the loading number which has been modified to incorporate interparticle frictional forces and this loading number has been used to calculate the total mass that can be theoretically captured by the filter. Using this approximation the total mass captured by the filter has been calculated to be 283 grams. If the loading is 0.04gm/m^3, and assuming a 60% packing factor for the material built up on the wires, this means the total processed volume will be 4,126 m^3, and, at a flow rate of 0.0036 m^3/hr (assuming an inlet flow area to the filter of 0.001m^2) the overall lifetime of the filter will be 1.15 million hours!! It should be realised that this is a small prototype filter. Practical filters will need to process somewhere in the region of 10 m^3/hr if they are to be useful.

In a filter of this structure with conventional HGMS, with the field applied parallel to the sheets of Chromindur, the particles would be captured into the holes in the mesh so a radial feed system would certain to block as the suspension must pass through the holes so an axial feed would be appropiate here. On the contrary, for hysteretic HGMS the particles are attraced to the mesh leaving the holes clear which makes a radial feed ideal[6].

Experimental work at British Nuclear Fuels plc, Sellafield

Experimental arrangements

In order to test this filter in an 'in-situ' environment it was sealed and attached to a glove box at British Nuclear Fuels plc. The arrangement is shown in Fig.4.

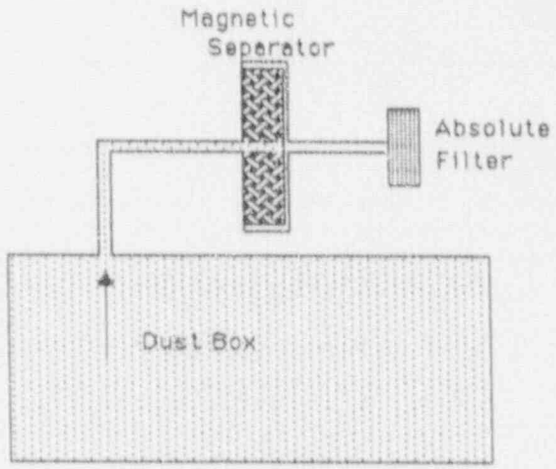

Fig 4 Arrangement of the glove box test rig at Sellafield. A Cr powder simulant was used in these tests.

Chromium powder was suspended inside the glovebox and circulated through the filter. The filtered air then passed through a second filter which contained a glass microfibre filter (to detect any particles that may have passed through the magnetic filter). This second filter was both weighed, visually inspected and replaced after every hour of operation. The pressure drop across the microfibre filter was recorded throughout the test while the pressure drop across the magnetic filter was recorded from the forty-sixth hour of the test. The pressure within the glove box was kept approximately constant between the levels of negative one inch and negative six inches water gauge, by the use of the vacuum pump and a compressed air line. The chromium dust was suspended by hand through the glove ports and by the use of the compressed air line. The flow rate through the filter was kept at 300 cm^3/min.

Results

(1) Loading of the filter

The loading on the filter was maintained at between 0.5 and 0.8 grams per hour throughout the test. Throughout the test, last 96 hours, no breakthrough was detected by the microfibre filter. It was estimated that the total amount of Cr powder that passed into the filter was 50 grams ($\pm$ 10 grams)

(2) Washing the filter

The filter was washed using a solution of manganese chloride. The susceptibility of this solution had been measured and adjusted to match that of the Cr powder. Hence it was hoped that it would be possible to wash out the majority of the Cr powder. The solution was passed through the filter continuously for several hours. The filter was then removed and shaken before being replaced in the flow stream. A total of 25 grams of Cr was removed from the filter in this way.

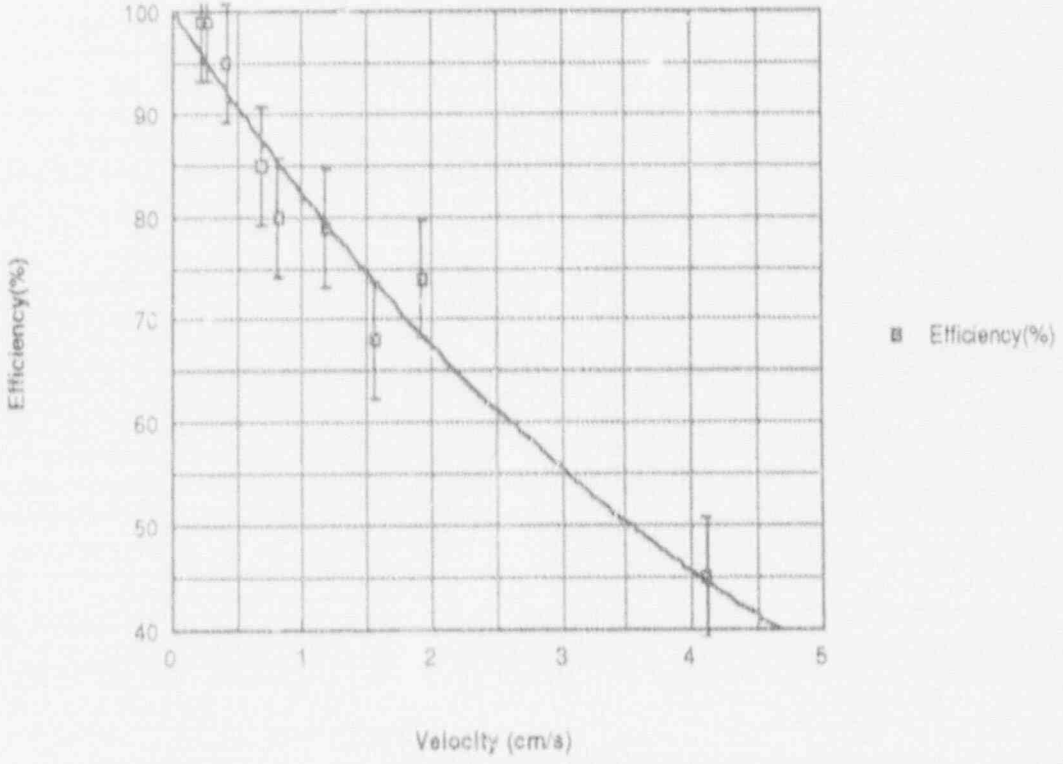

Fig 5 Filter efficiency for Cr powder as a function of the average velocity. The flow rate in litre/hr, for this filter, can be obtained by multiplying the velocity by 36.36

Experimental testing of the prototype filter at CEN/SCK, Mol , Belgium

The performance of the magnetic filter was tested at Mol in Belgium using an APS 33 Aerodynamic Particle sizer. Chromium powder simulants were used in place of the radioactive UO_2 or PuO_2, since the filter was required for further research after this testing was complete. The powder, after being acid washed to ensure purity from ferromagnetic contamination, was mixed with water and then atomised to produce a fine spray. This spray was then heated and passed over a bed of silica gel to remove any moisture before passing through the magnetic filter.

Initially a low mass loading was used to test the efficiency of the filter at various flow rates. Comparisons could then be made with the results obtained using non-magnetic aerosols.

At a flow rate of 8 litres/hour (0.22 cm/s) the filter was found to be exceedingly efficient. Over a four hour run the efficiency of the filter was greater than 99%. Similar results were obtained at 10 litres/hour (0.27cm/s). However, as can be seen from Fig 5, the efficiency fell as the flow velocity was increased. For this filter the flow rate in litre/hr can be obtained by multiplying the velocity in cm/s by 36.36.

These results are very encouraging. However they are interesting to compare with the efficiency of mechanical capture acting alone within the filter as a function of particle size. A series of tests were carried out at Mol in which non-magnetic aerosols were passed through the filter. Fig 6 provides a comparison of the capture of the magnetic and the non-magnetic particles for particle diameters of 0.5 micron, 1.0 micron and 2.0 microns. Above two microns diameter the mechanical capture is very strong but, at the smaller sizes, the capture due to magnetic forces considerably increases the capture of the particles.

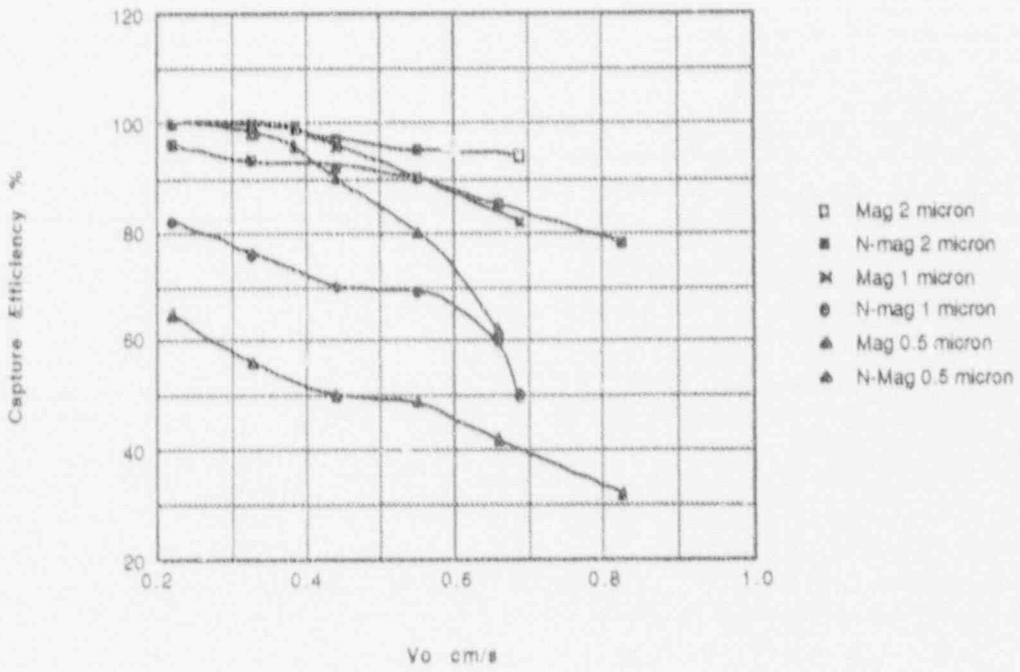

Fig 6 Filter efficiency for various magnetic and non-magnetic particles of various sizes with the test filter at various flow velocities.

Conclusions and Future Program

Although there has been no detailed comparison of the capture radius with the experimental results, the theoretical model has suggested a number of important factors which have been incorporated into the

separator design, namely:

1. The matrix material should have high coercive force and high remanence while remaining highly ductile and malleable.
2. The internal field H_i within the structure is highly dependent on the overall shape of the matrix. The shape can be changed to optimise the capture radius.
3. The material held on the matrix wires in hysteretic HGMS is on the opposite quadrants to conventional HGMS. Confirmation of this experimentally illustrated the value of radial feed in hysteretic HGMS.
4. Although not discussed in detail in this paper, a complete solution to the calculation of the capture radius, including magnetic, drag and gravitational forces has been achieved[7]. This model also includes a frictional term acting between the particles of the captured material. The effect of gravity on the capture and retention of low density weakly magnetic particles in a magnetic field, created by a highly coercive material, are small. On the other hand for high density particles gravity is important and retention remains small unless the inter-particle friction is high.

Experimental results have been obtained with the filter under various flow conditions using chromium metal powder as a magnetic simulant for PuO_2. At low flow rates the capture efficiency was 100%. About 30gm. of chromium was recovered from the filter and while this was collected using radial flow the pressure drop across the filter was constant. The theoretical capacity of the filter was near 200gm. At higher flow velocity the efficiency drops as theory suggests. When a comparison is made between the material passing through the separator and a theoretical expression given by Watson[2] it is found the filter is consistently more efficient than theory predicts, however the predicted scaling with the quantities used in the theory appears successful allowing the perfomance of different filter designs to be calculated with reasonable confidence. The next step is to work with PuO_2 rather than a simulant.

Using the results from the prototype filter an algorithm was constructed to predict the efficiencies expected from various sized filters operating over a range of flow rates varying from 1 m^3/hr to 100 m^3/hr. While the filter dimensions become very large at the higher flow rates, the algorithm suggests that reasonably sized units can be constructed with high extraction efficiencies at moderate flow rates.

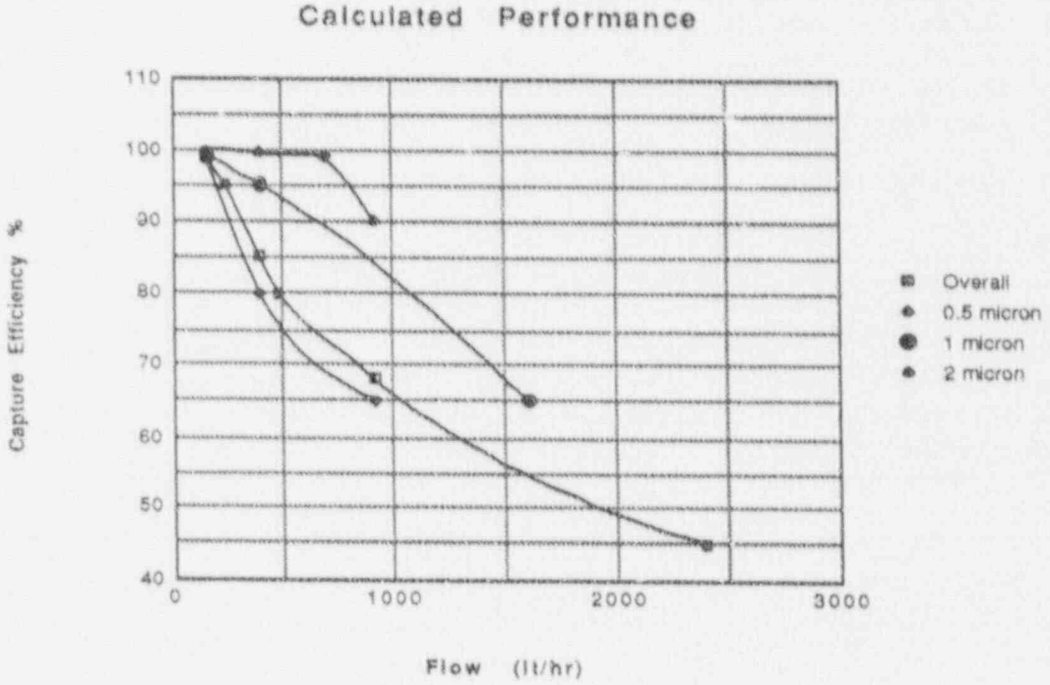

Fig 7 The projected perfomance of the proposed filter based on the results obtained using chromium metal powder as a simulant for PuO_2. The total capacity of the filter is in excess of 530 gm. of material.

A suitable compromise is for a filter with same inner and outer radii as the filter used in this work which allows an overall dimension R_{max}, as shown in Fig 3b, to be less than 6in., a requirement for glove box posting. A test a filter with L=406.4 mm, R_1=6.35 mm, R_2=50.8 mm and with R_{max}< 6 in. or 152.4mm has been built. There are to be 74 layers 0.4 mm apart.

This filter will start tests at British Nuclear Fuels plc, Sellafield in the last part of 1990 on PuO_2.

Acknowledgement

The authors wish thank N.A.T.O. for providing travel and subsistence under their 'Double-Jump' programme and for help, advice and hospitality from Warren Baxter, R.G.G. Holmes of British Nuclear Fuels plc, from J.P. de Worm and Michel Klein of SCK, Mol and from Malcolm Sanders and his colleagues of Atomic Energy Authority, Winfrith. The authors are very grateful John A. Williams formerly of BNF plc for his advice and for the suggested uses of this separator, to Blair Emory for his efforts to find a test site for the filter in the United States and finally, to Rodney Major of Telcon Metals who provided a lot of encouragement, some financial support for one of us (CHB) and for supplying the prototype filter without which we could not have carried out this research.

References

1. Svoboda, J. "Magnetic Methods for the Treatment of Minerals." Developments in Mineral Processing. Fuerstenau ed. 1987 Elsevier. Amsterdam.

2. Watson, J. H. P. Magnetic Filtration. J.Appl.Phys. 44(No. 9, September): 4209 - 4213, 1973.

3. Lawson, W. F., W. H. Simons and R. P. Treat. The dynamics of a particle attracted by a magnetized wire. J.Appl. Phys. 48(No. 8, August): 3213-3224, 1977.

4. Simons, W. H. and R. P. Treat. Particle trajectories in a lattice of parallel magnetized fibers. J.Appl. Phys. 51((1), January): 578-588, 1980.

5. Watson, J. H. P. High-Capacity, High-Intensity Magnetic Separators using Low Magnetic Field. Sixth International Conference on Magnet Technology, MT-6. 1: 308 -314, 1977.

6. Boorman, C. H., J. H. P. Watson and A. S. Bahaj. Magnetic Filtration Studies using a permanently Magnetised matrix. IEEE Trans. Magn. MAG-23(No. 5, September): 2755 - 2579, 1987.

7. Boorman, C.H. 'The theory and application of permanently magnetised materials to fine particle processing' Ph.D. Thesis, Institute of Cryogenics, University of Southampton, Southampton, U.K., 1987.

DISCUSSION

HANSON: I am curious if you tried reversing the polarity on the filters to see if it would cause the contamination to fall off? Is that practical?

WATSON: What we did to remove material was to simply wash the filter in a liquid. If you use a liquid, the viscosity is considerable higher than air and you can wash the material out because of the very much higher drag on the particles. It is very difficult to change magnetic properties.

BEHAVIOR OF THE POLYGONAL HEPA FILTER EXPOSED TO WATER DROPLETS CARRIED BY THE OFFGAS FLOW

K. Jannakos, G. Potgeter, W. Legner
Kernforschungszentrum Karlsruhe GmbH
Postfach 3640, D-7500 Karlsruhe
Federal Republic of Germany

Abstract

A polygonal HEPA filter element has been developed and tested with a view to cleaning the dissolver offgas from reprocessing plants. It is likewise suited to filter process offgases generated in other plants.

Due to its high dew point (about 30°C) the dissolver offgas, before being directed into the HEPA filter, is heated with a gas heater to approx. 100°C so that condensation in the pipework upstream of the filter and in the filter proper is avoided. In case of failure of the heater the offgas may undergo condensation upstream of the HEPA filter until it is bypassed to a standby heater or a standby filter system. Consequently, the filter may be loaded with water droplets. Therefore, experiments have been performed with a view to estimating the behavior of the polygonal filter element when exposed to condensate droplets in a real plant.

According to the experiments performed so far it can be anticipated that in case of failure of the heater the amount of condensate produced until bypassing to a standby system will not damage a new or little loaded polygonal filter element.

The experiments will be carried on with the goal of investigating the behavior of a heavily loaded polygonal filter element exposed to water droplets.

Introduction

The polygonal HEPA filter has been developed to filter process offgases from nuclear facilities, especially to filter dissolver offgases originating in reprocessing operations. The dissolver offgas is normally treated in scrub columns before it is passed through the filter system. When entering the filter system it is wet saturated at a temperature of about 30°C. In the filter system it is precleaned in a demister, then heated to approx. 100-150°C in a gas heater, and only then passed through the HEPA filter. Therefore, before the gas enters the HEPA filter, its relative humidity is <4 %. This prevents condensate droplets from developing in the gas pipework or in the filter proper.

In case of failure of the heater the offgas may cool down to room temperature until it is bypassed to the standby filter system and the standby heater, respectively, and considerable amounts of condensate may be produced which are present as droplets in the offgas. For instance, during cooling down of the offgas from 30°C to 20 °C in the state of saturation 13 g of condensate per kg of dry air are produced. Some of the condensate droplets will reach the HEPA filter where most of them will be removed.

Objective of Testing

It was proposed to study the behavior of the polygonal HEPA filter exposed to water droplets carried by the offgas stream. Above all it was to be found out

whether and, if applicable, after which duration the filter is damaged by exposure to droplets.

Description of the Polygonal HEPA Filter

The polygonal HEPA filter element (Figure 1) was presented at the "Nuclear Air Cleaning Conferences" 1986 and 1988 (1, 2) .To help better understand the results and the differences in design and face flow as compared to the usual rectangular filter element a brief description of the polygonal filter element will be given below.

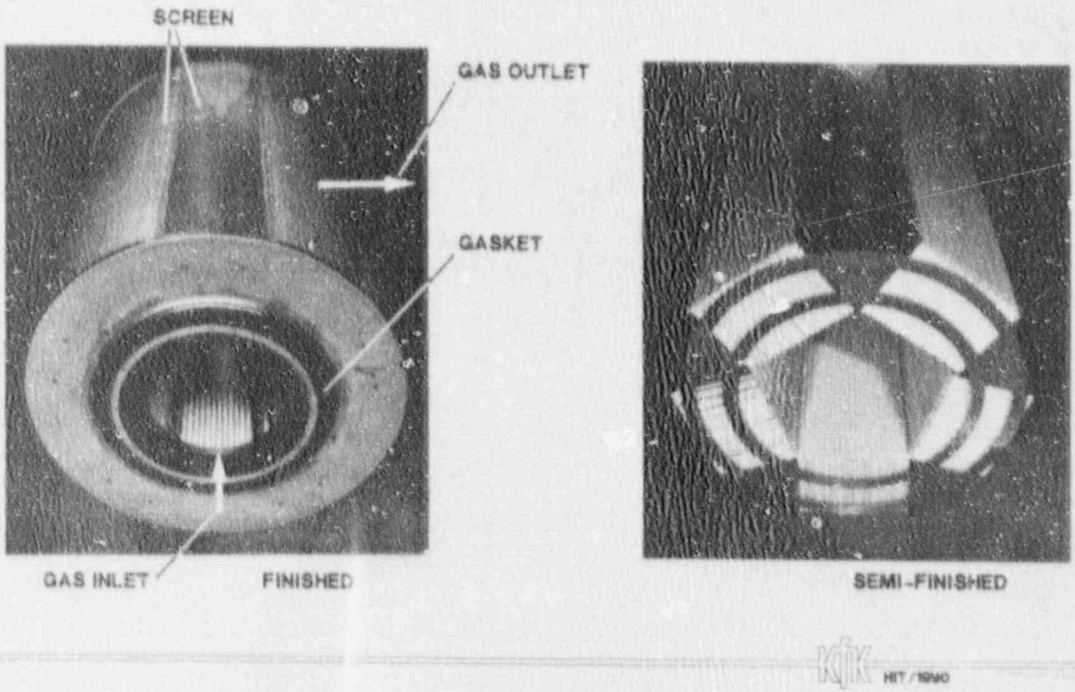

FIG. : 1 POLYGONAL FILTER ELEMENT (HEPA) VIEWED FROM THE BOTTOM

The polygonal filter element is an annular filter; the filter element is cylinder shaped. The filter medium (fiber glass paper) mounted endlessly with only one pasting line on the perimeter is compartmentalized into five filter chambers with equally wide inner and outer surfaces using V-shaped spacers. The filter elements used in the various tests have a protective strip made of fiber glass provided between the filter medium and the spacer edge. A slotted sheet metal is installed between the inner space and the filter medium. The slots are 10 mm in length and 0.7 mm in width. The slotted sheet metal serves to protect the filter medium and to guarantee radial flow through it. The polygonal filter elements can be manufactured with or without slotted sheet metal.

The offgas flows from the bottom through the circular cross-section in axial direction into the interior and then in radial direction through the filter medium towards the outside. The circular cross-section of face flow is much smaller than the face flow area of the filter ring and has been dimensioned in such a way that at nominal gas flow in the non-loaded condition the pressure loss of the filter element is approx. 0.3 kPa. The maximum admissible operating temperature is 160°C.

Based on test results the mechanical structure of the filter element was optimized so that the axial strain of the stainless steel filter frame does not exert an influence on the filter medium at operating temperatures up to 180°C.

Test Facilities

For investigating the behavior of the polygonal filter element exposed to water droplets, two test benches were used: VERBE, in which a 72° sector (1/5 of the polygonal filter element) was investigated, and REFIFI, which allowed the entire filter element to be tested. A short description of the test benches and of the results obtained will be given below.

VERBE Test Bench

The VERBE test bench (Figure 2) has been designed in such a manner that 1/5 of the polygonal filter element (one filter chamber) can be tested. The flow conditions at the filter medium correspond to those encountered when the polygonal filter element is installed in a standard filter housing. It was possible to choose any value for the lateral contact pressure of the filter medium. In the experiments the same contact pressure was chosen as for the standard filter element. The attachment of the filter medium at the top and bottom edges corresponded to that of the polygonal filter element. Experiments were performed with and without slotted sheet metal. The water droplets were injected about 80 cm upstream of the gas inlet of the filter element using a two-fluid nozzle. According to information from the manufacturer of the nozzles the mean droplet diameter under the conditions set for the experiments and with a rate of H_2O injection of 6 kg/h is 18.5 µm, whereas it is 19,9 µm for 12 kg/h and 17,4 µm for 18 kg/h.

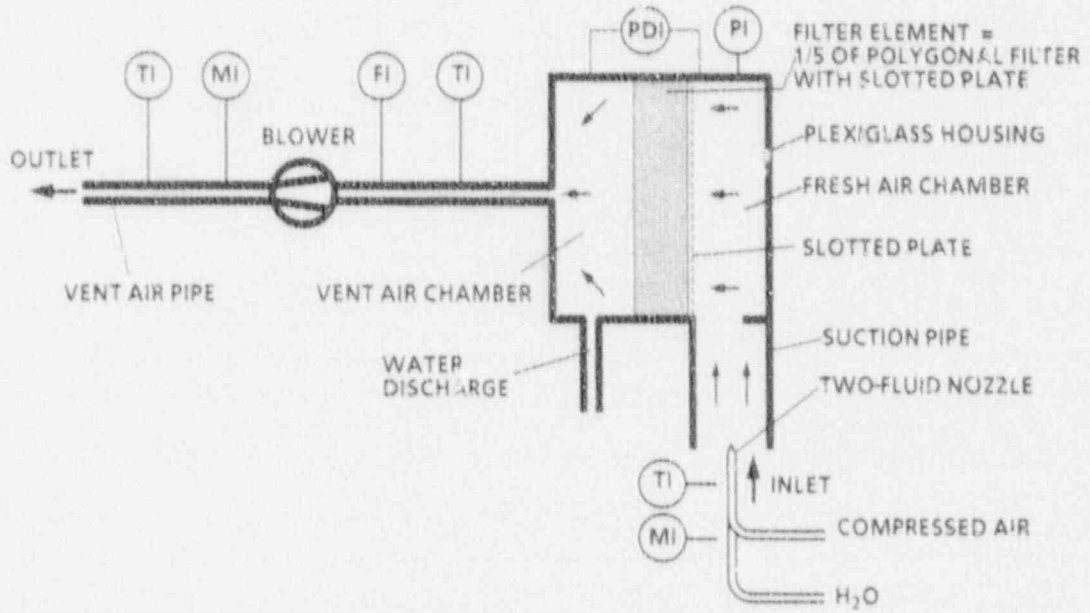

Fig.: 2 VERBE: DEVICE FOR TESTING THE HEPA POLYGONAL FILTER ELEMENT DURING EXPOSURE TO WATER DROPLETES

The quantities of air and water were set prior to the test and kept constant during the test. The air taken in was ambient air. Therefore, the relative humidity of the air taken in was not always constant during the test. The following parameters were measured.

- the pressure differential immediately at the filter element;
- the discharging quantity of water downstream of the filter;
- the temperature and the relative humidity upstream of and downstream of the filter.

Most parts of the VERBE test bench were made of plexiglass in order to be able to observe the flow conditions and the behavior of the filter medium during the test.

Test Conditions

All the tests started with the dry filter element. The dimensions of the filter element were equal to the dimensions of a filter chamber (=1/5) of the polygonal filter element. They were 730 mm in height, 180 mm in width, 120 mm in depth. About ten tests each were performed with one filter element. In every case ambient air was taken in at about 21 °C. The relative humidity of the air taken in was not constant but varied during the test series between 21 % and 57 %. The water injected was likewise at ambient temperature and the quantity was always larger than necessary in order to achieve saturation of the air taken in. A test lasted about six hours. Two tests were performed which lasted 70 hours.

Test Results

A total of 30 tests were carried out at different offgas flow rates (600 m^3/h = nominal gas flow rate, 800 and 1000 m^3/h) with different quantities of water injected : 7, 16 and 28 g per m^3 of air taken in. Three filter elements were used in the tests.

General phenomenological consideration of the behavior of the filter element. All the tests were similar in their course. However, the data measured differed and depended on the quantity of water injected, the gas flow and the condition (dry or wet) of the filter element. After water injection had started the water droplets were entrained by the air taken in and carried to the filter medium. The whole quantity of water injected arrived at the upstream side of the filter. It was not possible to determine the droplet size and distribution immediately upstream of the filter inlet side.

After a certain interval depending on the quantity of water injected - between 5 and 50 minutes in the test - some of the droplets injected and retained on the filter medium started to flow downwards at the inlet side of the filter element. At the inlet of the filter element the water was entrained by the air taken in and returned to the surface of the medium. Then the quantity of water flowing downward increased so that the flow developed into a spout from the filter inlet towards the filter medium. During that time interval the pressure differential at the filter element increased steeply. At the downstream side of the filter element water droplets were visible at some points after development of the spout; they run towards the bottom of the filter element along the edges of the spacers. Then the downstream side of the filter element became completely saturated with water and the spout stopped to exist. The quantity of water measured at that point in time at the downstream side of the filter element was larger than the quantity of water injected. Subsequently, the conditions prevailing at the filter element were

steady state. After the downstream side of the filter element had been fully wetted it was observed that during the entire test very few single droplets were entrained by the gass flow at the edges of the spacer.

Data measured. Figure 3 shows a typical plot of the differential pressure immediately at the filter element with 600 m^3/h gas flow rate and different quantities of water present in the offgas as entrained droplets. With the quantities of water getting larger in the offgas the differential pressure rose and the time from the start of water injection up to attainment of the maximum differential pressure became shorter. When the water injection was stopped the pressure differential dropped within about twenty minutes to nearly the original value measured before the onset of water injection.

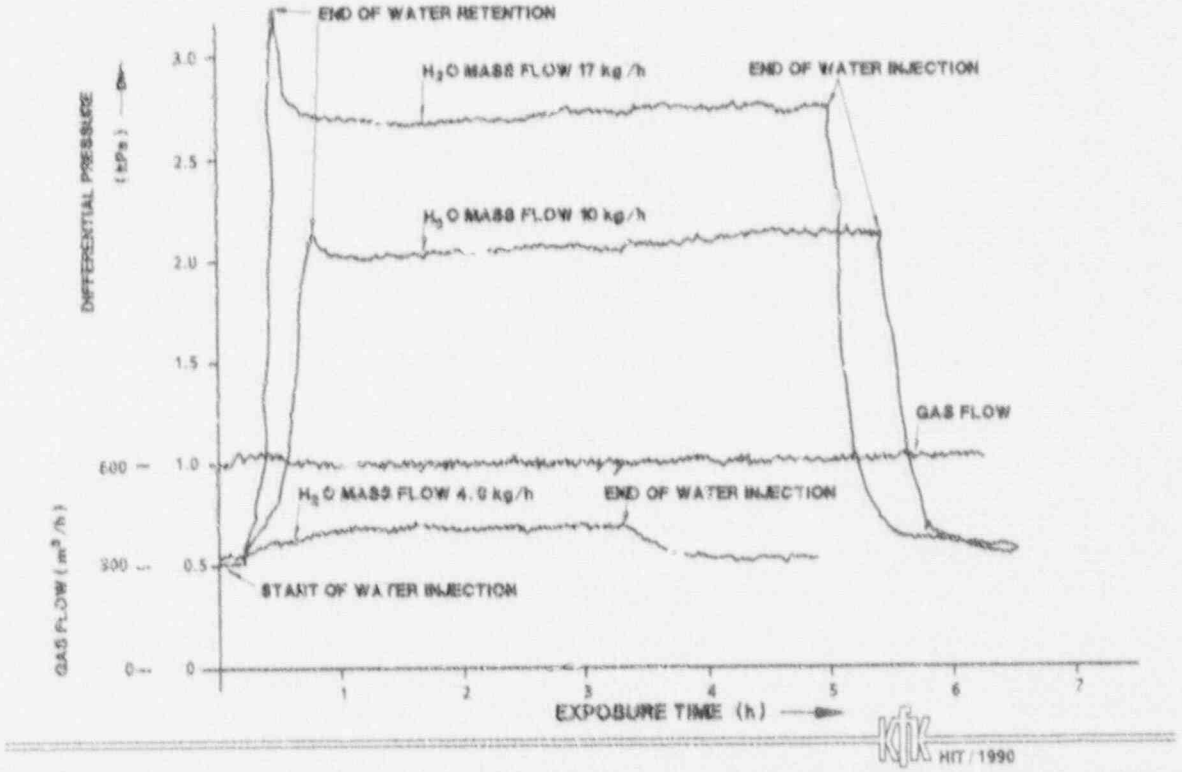

FIG. 3 DIFFERENTIAL PRESSURE BEHAVIOR AT THE POLYGONAL FILTER ELEMENT WITH VARIOUS WATER VOLUMES INJECTED

As already mentioned, the differential pressure depends likewise on the condition of the filter element. Figure 4 shows the plot of the differential pressure in a filter element which had been exposed to 10 kg/h water droplets in the dry condition at room temperature (21 °C) and at 600 m^3/h gas flow rate; the water injection had been intentionally interrupted after 4.7 hours and was restarted after another 70 minutes by injecting the same quantity of water. The maximum differential pressure prior to interruption of water injection was 2.2 kPa, but after restart of water injection only 1.5 kPa.

The steep rise in the pressure differential shortly after the onset of water injection is probably attributable to the water repelling effect of the dry filter medium. The water droplets are retained at the filter medium and pushed inside by the gas in the grooves of the spacer towards the spacer edge where they run down to the filter bottom. Only when the filter medium has been saturated with water it becomes permeable to the arriving water droplets. A constant value of the differential pressure is then established which is obviously dependent on the value of

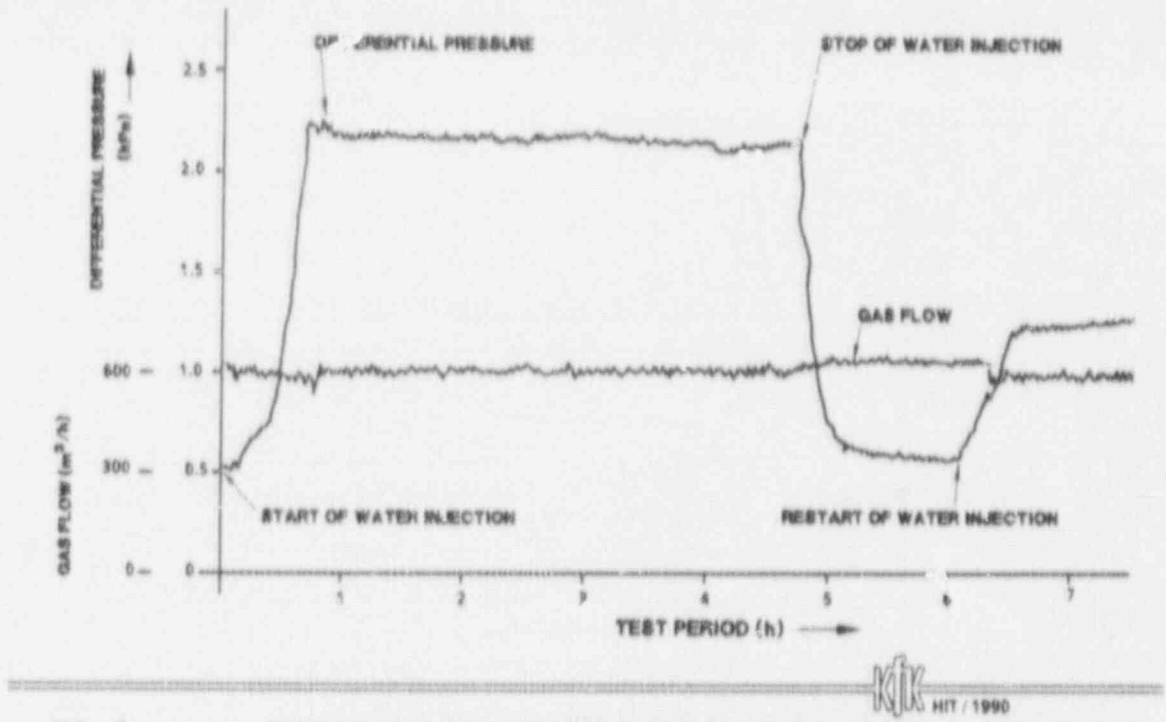

FIG. 4 DIFFERENTIAL PRESSURE BEHAVIOR AT THE POLYGONAL FILTER ELEMENT DURING WATER INJECTION IN THE INTAKE AIR

saturation with water of the filter medium (i.e. the quantity of water contained in the wet filter medium). The value of saturation with water probably depends on the condition of the filter element prior to water injection. This is the only plausible explanation of the differenrent values of differential pressures plotted in Figure 4.

Figure 5 shows a typical plot of the quantity of H_2O at the downstream side of the filter element during testing at 600 m^3/h gas flow rate and 10 kg/h of water injected. The quantity of water corresponding to the difference between the water injected and the water measured at the downstream side of the filter element was consumed mainly to saturate the intake air.

The entrainment of individual water droplets at the downstream side of the filter element was well visible. With small quantities of water hardly visible droplets were entrained by the offgas flow. The larger the quantity of injected water became the more frequently water droplets were entrained by the offgas flow.

Condition of the filter elements after testing: The average duration of a test with water injection was six hours. In addition, two tests of about 72 hours duration were performed without interruption. As already mentioned, also tests involving larger gas flows and quantities of water injected were performed in order to be able to estimate the limit of operation of the polygonal filter element. The maximum differential pressure applied was 6.5 kPa; it was achieved at 1000 m^3/h gas flow rate and 16 kg/h water injected.

As the tested filter elements were examined for their condition at the end of each test, subsequently dried and used again in the following test, one filter element underwent test operation of up to sixteen days duration and during that time interval it was exposed to water droplets for a total of about 100 hours with

interruptions between the single tests. At the end of testing none of the three filter elements tested exhibited visible damage.

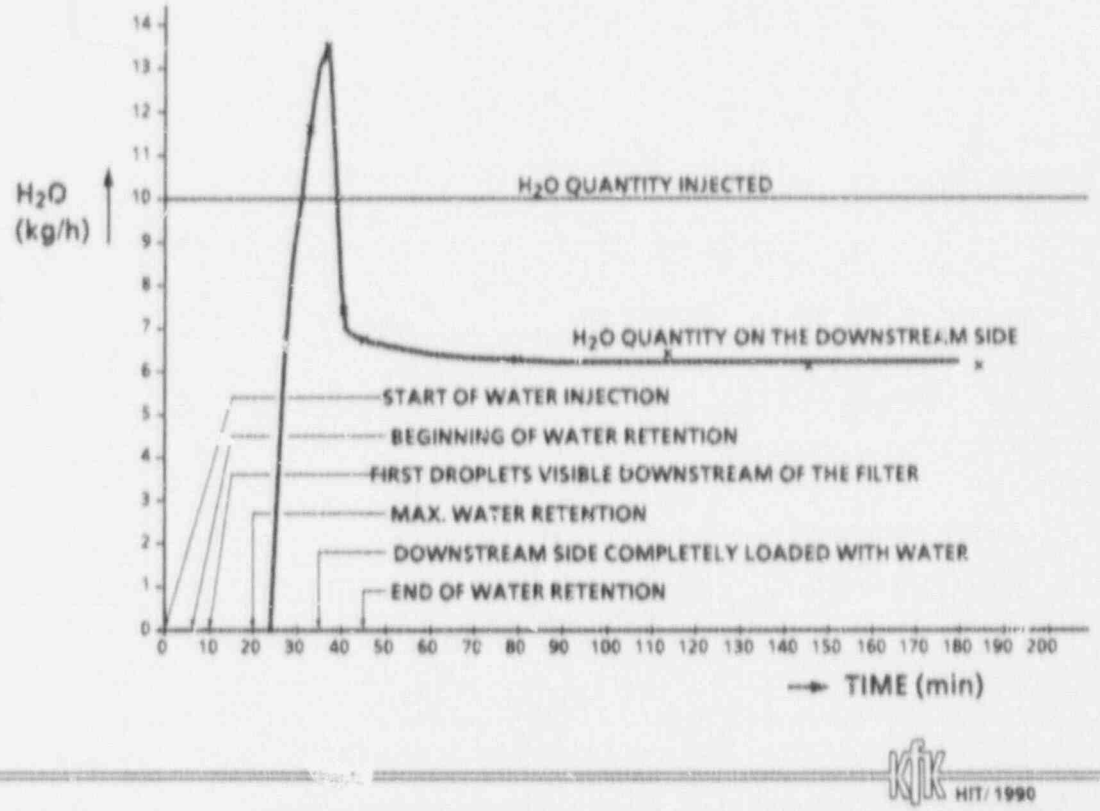

FIG. 5 H_2O QUANTITY ON THE DOWNSTREAM SIDE OF THE FILTER

REFIFI Test Bench

The REFIFI test bench (Figure 6) consists of a standard filter housing for the polygonal filter and the respective measurement and water injection devices, as shown in Figure 6.

The intake pipe into which the water was injected is 203 mm in inner diameter. The water was injected at about 6 m distance from the filter housing. The inner diameter of the filter housing is 790 mm and the diameter at the inlet of the filter element is 205 mm. A complete polygonal filter was installed for testing. The tests were performed at 3000 m^3/h nominal gas volume flow rate. Tests were performed in the vent air and circulated air modes of operation.

In the vent air mode of operation it was found that the filter element remained dry despite the water injected. Consequently, no rise in the differential pressure was measured, not even over several hours of test operation with water injection. Most of the water injected accumulated in the bottom part of the housing due to cross-sectional widening in the filter housing and coagulation taking place in the pipework which probably had increased the droplet size. The remainder of the water did not suffice to saturate the intake air; for instance, of 30 kg/h

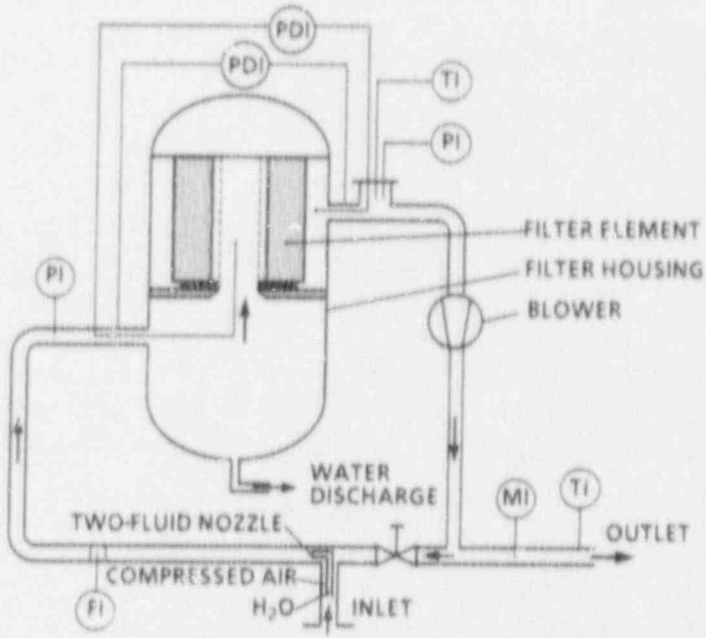

Fig.: 6 REFIFI: DEVICE FOR TESTING THE HEPA POLYGONAL FILTER ELEMENT

of water injected 24 kg/h accumulated in the bottom part of the housing. Therefore, the tests in the vent air mode of operation have not been continued.

In the circulated mode of operation the circulating gas was wet saturated (100 % relative humidity plus water droplets). The gas temperature was 44°C, the gas volume flow rate was 3000 m^3/h, and the quantity of water injected was 18 kg/h. 8 kg/h of water injected accumulated in the bottom part of the housing. The remainder (10 kg/h) certainly arrived at the filter element as droplets or vapor. Figure 7 is a plot of the differential pressure directly at the filter element. It differs from a plot derived from the tests in the VERBE test bench; see Figure 3. The maximum differential pressure is attained only after about seven hours.

Taking into account the results obtained with the VERBE test bench the following conclusions can be drawn regarding the events in the REFIFI test bench.

- The quantity of water arriving as droplets at the filter element was small.
- Saturation of the filter medium with water took several hours (approx. 6) because only after saturation of the filter medium with water the steady-state differential pressure was attained.
- Likewise, it took several hours until water could run down at the downstream side of the filter.

After 80 hours of test operation with water injection the filter element was dismounted and examined for possible damage by application of the oil mist test. No damage was found. Three tests were carried out under similar test conditions and with similar test values.

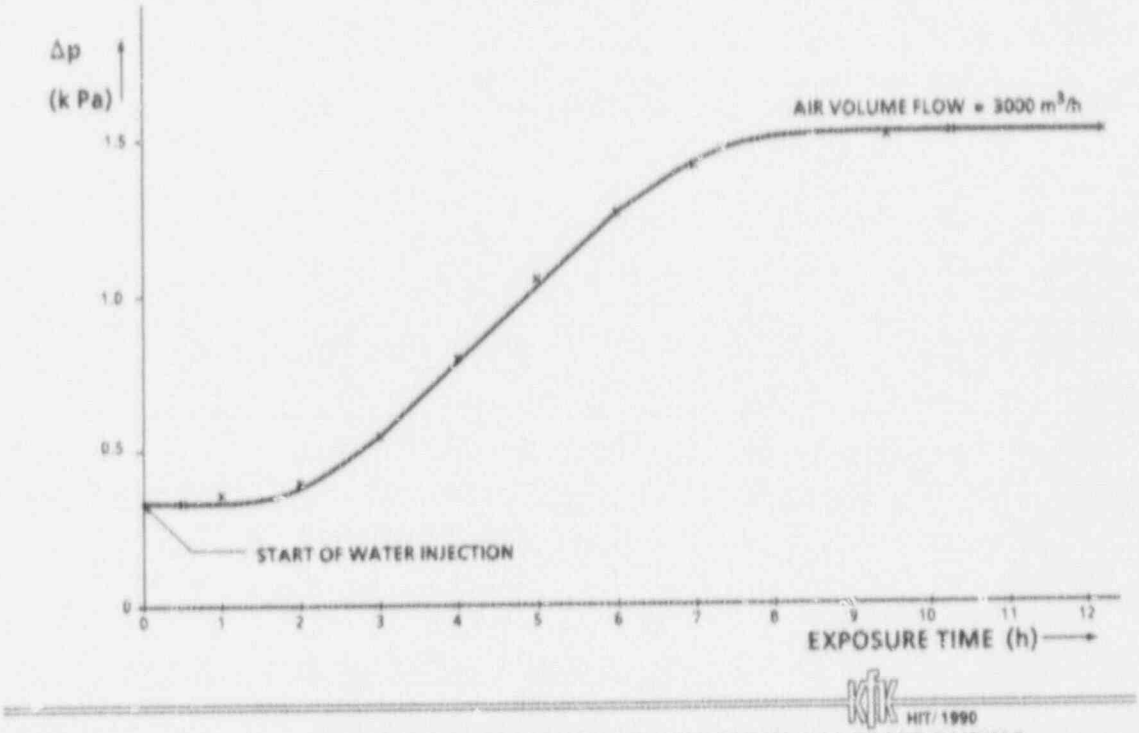

FIG.: 7 DIFFERENTIAL PRESSURE AT THE POLYGONAL FILTER DURING WATER INJECTION

In order to find out how a damaged polygonal filter element could look like a polygonal filter element was installed in the REFIFI test bench in which only 1/5, i.e. only one filter chamber, was provided with filter medium. The rest of filter chambers were tightly sealed with sheet metal. This filter element was tested while exposed to a wet saturated gas flow at a rate of 3000 m^3/h (corresponding to 5 times the nominal gas flow rate). The maximum differential pressure at the filter element was 5.1 kPa. After about 4 hours the filter element was dismounted and inspected. Several tears at the edge of pleating of the filter medium were detected at the downstream side of the filter element; see Figure 8.

Assessment of the Polygonal Filter Element

The experiments were performed with a view to assessing whether after failure of the gas heater installed upstream of the polygonal filter element damage to the latter must be expected to occur by droplets before a standby filter section or a standby heater can start operation (estimated maximum duration until connection to standby systems 1 - 2 hours).

It was not possible and, actually, not intended to simulate exactly the operating conditions prevailing in an offgas system installed, above all as regards the amount of condensate, the droplet size, and the droplet size distribution.

On the basis of the tests performed with quantities of water smaller or larger than calculated to be present in an accident occurring in a real plant it can be anticipated that a polygonal filter element not loaded or little loaded will not be damaged under accident conditions.

The behavior of a loaded filter element will be studied in a later test series.

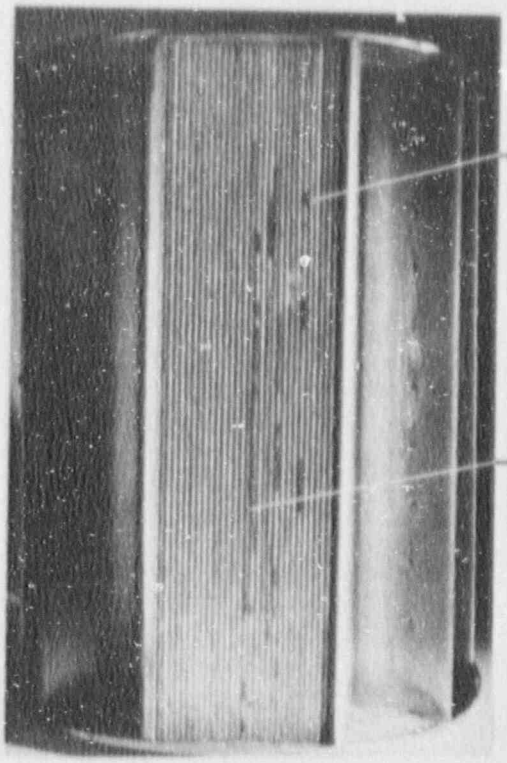

KfK HIT / 1990

FIG. 8 POLYGONAL FILTER ELEMENT AFTER EXPOSURE TO WATER DROPLETS
POLYGONFILTERELEMENT NACH DER BEAUFSCHLAGUNG MIT WASSERTROPFEN

References

/1/ K. Jannakos, J. Furrer, G. Potgeter, H. Mock: Advanced Filters for Nuclear Facilities and Filter Conditioning for Disposal.
Proceedings of the 20th DOE/NRC Nuclear Air Cleaning Conference, Vol.2, 1055 (1988).

/2/ K. Jannakos, W.J. Becka, G. Potgeter, J. Furrer: Development at the Karlsruhe Nuclear Research Center (KfK) of Remotely Operated Filter Housings and Filter Elements for Reprocessing Plants,
Proceedings of the 19th DOE/NRC Nuclear Air Cleaning Conference, Vol. 1, 426 (1986)

EFFICIENCY AND MASS LOADING CHARACTERISTICS OF A TYPICAL HEPA FILTER MEDIA MATERIAL

V.J. Novick, P.J. Higgins, B. Dierkschiede,
C. Abrahamson and W.B. Richardson
Engineering Physics Division
Argonne National Laboratory
Argonne, Illinois

and

P.R. Monson and P.G. Ellison
Westinghouse Savannah River Company
Aiken, South Carolina

Abstract

The particle removal efficiency of the HEPA filter material used at the Savannah River Site was measured as a function of monodisperse particle diameter and two gas filtration velocities. The results indicate that the material meets or exceeds the minimum specified efficiency of 99.97% for all particle diameters at both normal and minimum operating flow conditions encountered at the Savannah River site.

The pressure drop across the HEPA filter material used at the Savannah River site was measured as a function of particle mass loading for various aerosol size distributions. The pressure drop was found to increase linearly with the particle mass loaded onto the filters, as long as the particles were completely dry. The slope of the curve was found to be dependent on the particle diameter and velocity of the aerosol. The linear behavior between the initial pressure drop (clean filter) and the final pressure drop (loaded filter) implies that the filtration mechanism is dominated by the particle cake that rapidly forms on the front surface of the HEPA filter. This behavior is consistent with the high filtration efficiency of the material.

Introduction

An Airborne Activity Confinement System (AACS) is used in each of the reactors at the Savannah River site to provide for the capture and confinement of accidentally released radioisotopes. Figure 1 presents a schematic description of the AACS.[1] The purpose of the moisture separator (first filter) is to remove the water droplets and any other large aerosol particles before they can be deposited in the High Efficiency Particulate Air (HEPA) filter. The HEPA filter is designed to remove all particles from the gas stream with efficiencies of at least 99.97%.[2] The final component of the filter compartment is a carbon bed. The purpose of the carbon bed is to remove more than 99.9% of the elemental iodine vapors from the exhaust gas.[3]

The purpose of this research was to characterize the HEPA filter media material. This work consisted of three major tasks. The first task was to determine the filtration efficiency spectrum for solid particles as a function of particle diameter. The second task was to measure the pressure drop characteristics of the HEPA filter material as a function of the aerosol mass loading. Particle size effects were studied by using different particle size fil[illegible]ion efficiency spectrum for solid particles as a function of particle diameter. The third task was to provide a theoretical foundation that will allow the experiment results from the mass loading tests to be generalized. An experimental apparatus was set

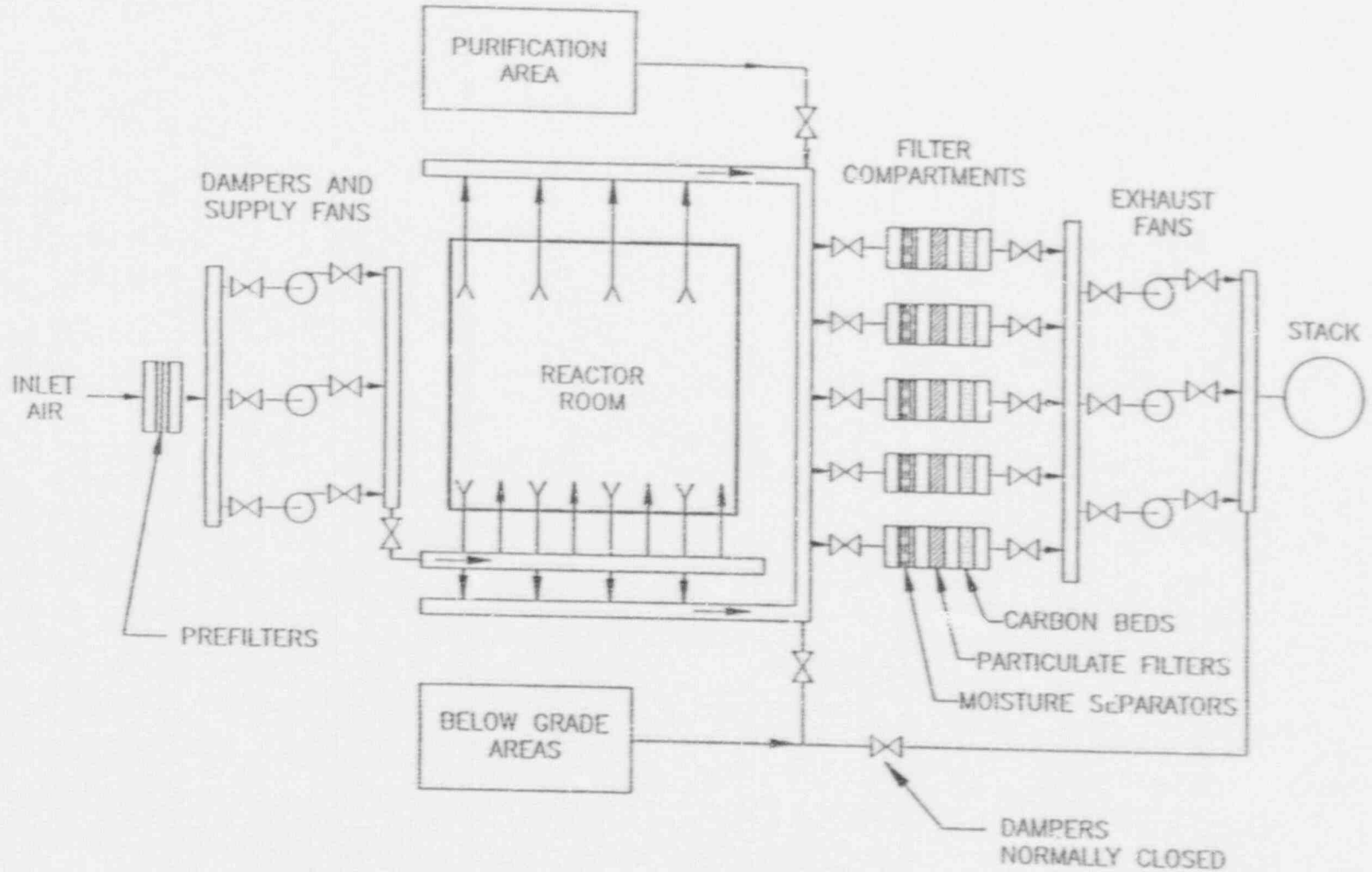

Figure 1. Schematic of the Airborne Activity Confinement System (AACS)

up based on filter characterization work discussed in the literature.[5,6] Sodium chloride was chosen as the challenge aerosol based on a number of considerations. Sodium chloride is highly soluble in water, it is non-toxic, and it allows a precise means of analysis by conductivity. Sodium chloride particles produced by atomization are non-spherically shaped. In comparison to spherical particles, they may simulate more closely the shape of particles likely to be produced in the Savannah River Reactor. The filter media was chosen to be identical with the Savannah River filter material. However, the filter size was chosen to be 47 mm in diameter in order to facilitate laboratory handling and analysis and to minimize the total mass of particles that are needed to be aerosolized. To account for the difference in filtration area, the gas flow rate was scaled such that the velocity through the filter medium was the same for both plant filters and laboratory filters. The gas viscosity is expected to be similar to that encountered at Savannah River by using air at 25°C. The particle size is an experimental variable since there is uncertainty in the particle size distribution that may be released into the AACS.

Experimental Set-up for Efficiency Tests

Figure 2 illustrates the experimental apparatus used for the efficiency tests. The experimental set-up consists of two main systems, aerosol generation and aerosol sampling. The aerosol generation system consists of an aerosol nebulizer, a dryer to dry the wet aerosol and a neutralizer to reduce the electrical charge on the aerosol to a Boltzmann equilibrium. The aerosol sampling system consists of a mixing chamber and the aerosol sampling devices.

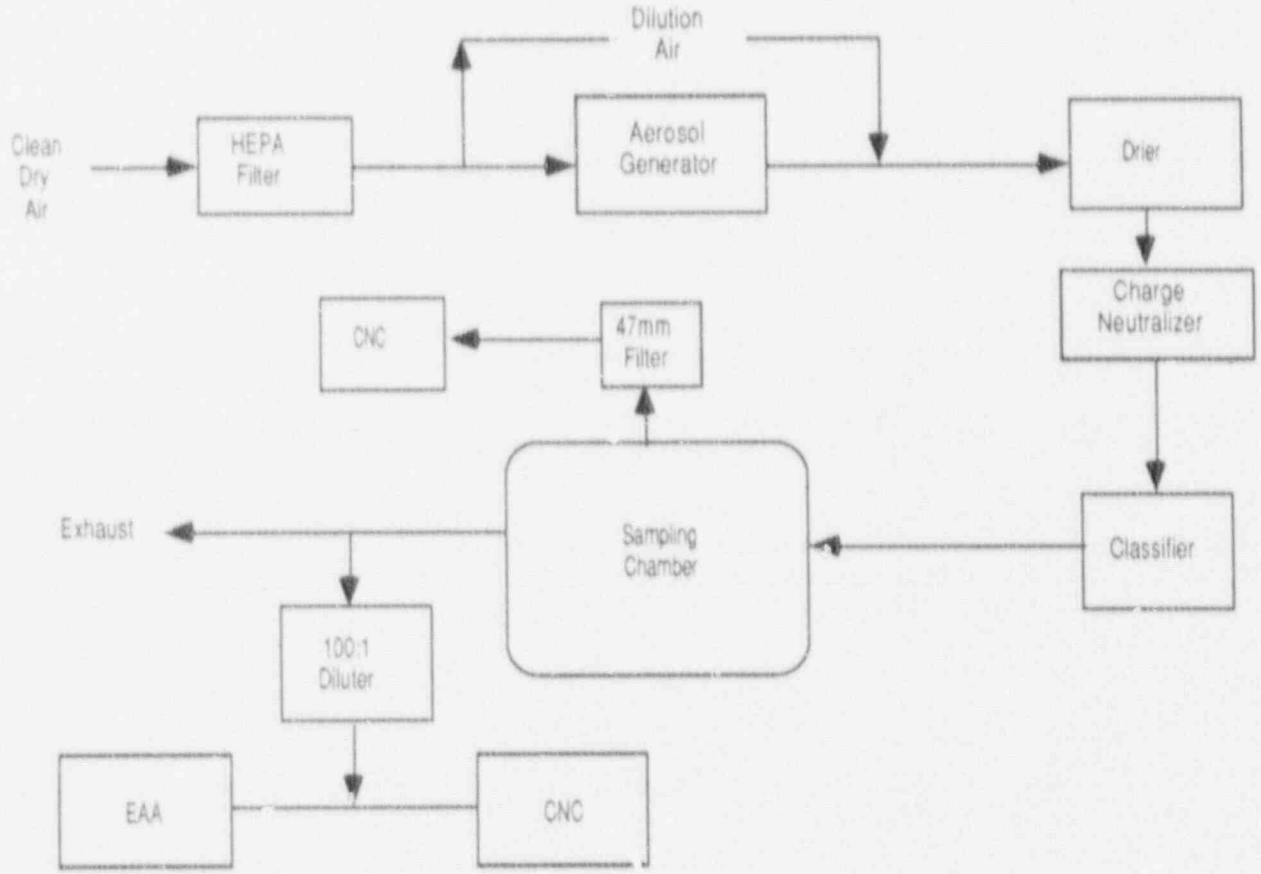

Figure 2. Experimental Configuration for Efficiency Tests

Typically, filter efficiency spectra are obtained using monodisperse challenge aerosols. In addition, the characterization of the filter efficiency using monodisperse particles would be more useful for later code input for calculating probable scenario dependent releases. A proven method of generating monodisperse aerosols is to use an electrostatic classifier.[7,8] The classifier used in this work is the Model 3071, manufactured by TSI Inc. of St. Paul, Minnesota, capable of producing monodisperse particles ranging from 0.01 μm to 1 μm in diameter.

Data was acquired during the efficiency test, by simultaneously using condensation nucleus counters (CNC's) to measure the filtered and unfiltered particle concentrations from the sampling chamber. The CNC used to measure the unfiltered particle concentration (TSI Model 3020) has an internal mass flow controller, factory set to sample the aerosol at a rate of 0.30 liters/min. The instrument has two particle counting modes, providing a dynamic measurement range of 10^{-2} to 10^{7} particles/cm^3. The CNC used to measure the filtered particle concentration (TSI Model 3760) operates in only the single-particle mode. Aerosol flow through this CNC is controlled by a critical orifice and an external vacuum pump, providing a constant gas flow rate of 1.415 liters/min. The range of particle concentrations measurable by the Model 3760 extends from 10^{-3} to 10^{3} particles/cm^3. For particle concentrations below 10^{3} particles/cm^3, the two CNC's simultaneously measured the same aerosol concentration to within 15%.

Efficiency Test Results

Flowrates and voltages on the Electrostatic Classifier were adjusted to provide at least eight different monodisperse particle diameters, ranging from 0.05 μm to 0.5 μm, as challenge aerosol for the filters. The penetration of particles through the filter was measured for each minute by dividing the downstream particle concentration by the upstream particle concentration. The removal efficiency for a given particle size was found by averaging the penetration values over at least 15 minutes and subtracting the average penetration from one. The penetration as a function of time over the 15 minute measurement was observed to be fairly constant, decreasing by only 10% to 20%. This slow decrease in penetration is typically observed as the particle cake forms on the filter's surface.

The filtration efficiency was measured at two different gas velocities. The velocity of 2.98 cm/s through the filter media is typical of normal operating flow rates of the AACS. The velocity of 0.89 cm/s was tested in order to determine the efficiency for the minimum operating flow rate conditions of the AACS.

Figures 3a and 3b show the average number penetration as a function of particle size for the two filtration velocities. Figure 3a shows that for a filtration velocity of 0.89 cm/s the maximum penetration occurs near 0.3 μm. This maximum penetration corresponds to a minimum filtration efficiency of 99.99886%. As expected from filtration theory, the efficiency is seen to increase for both larger and smaller particle sizes. This is because the mechanism of filtration for smaller particles is diffusion, which varies inversely with particle size. For particles larger than that producing minimum efficiency, impaction and interception with the fibers increase directly as function of particle size.

For the higher filtration velocity of 2.98 cm/s, the overall penetration increased approximately by a factor of ten and shifted toward smaller particle diameters. In this case, the maximum penetration occurred at approximately 0.15 μm, corresponding to a filtration efficiency of 99.9727%. Two additional points are included on this graph. When the efficiency for 0.12 μm particles was first measured, it was noticed that this point did not fall on a smooth curve joining the other points. The efficiency

measurement was repeated for this particle size and this time the point did fall very close to the curve defined by the other data points. To investigate repeatability, another test was rerun at 0.199 µm. This time the second measurement was consistent with the first and with the majority of the other data points. Since no procedural error was evident, the error in the first measurement at 0.12 µm was attributed to filter variation. Out of 10 total filters tested at 2.98 cm/s, only this one produced results inconsistent with the others. No inconsistencies were observed at 0.89 cm/s.

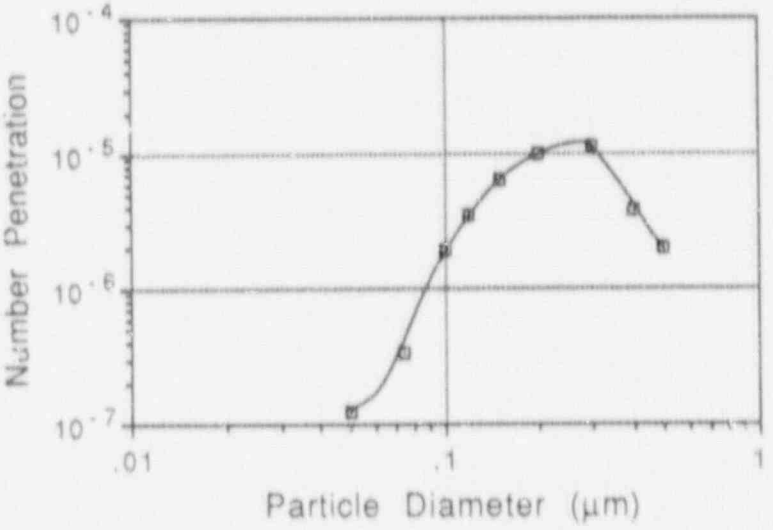

Figure 3a. Number Penetration Versus Particle Diameter for Monodisperse NaCl Aerosols Using an Electrostatic Classifier, Filtration Velocity = 0.89 cm/s

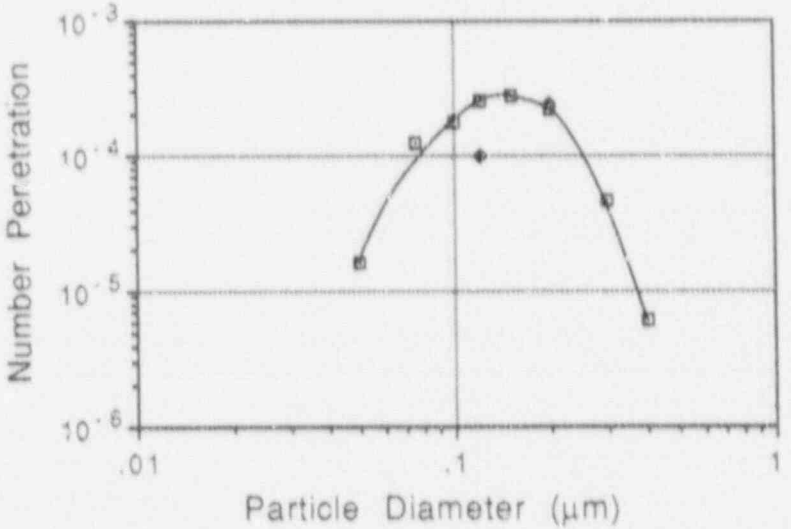

Figure 3b. Number Penetration Versus Particle Diameter for Monodisperse NaCl Aerosol Using an Electrostatic Classifier, Filtration Velocity = 2.98 cm/s

Due to the high collection efficiency of the filter material, it is postulated that there will be a rapid formation of a particle cake on the surface of the filter. Therefore, it is expected that the pressure drop behavior of this filter material as it is loaded with a mass of particles, will follow that predicted by particle cake theory.

Theory

A general model describing the increase in pressure drop as a function of mass loading can be found in a variety of sources[9,10]. For high levels of particle mass loadings on filters, it is generally accepted that the total pressure drop across the filter can be written as the sum of the pressure drop across the clean filter plus the pressure drop across the filter cake due to particle loading.

$$\Delta P = \Delta P_0 + \Delta P_p \qquad (1)$$

For the range of pressure drops under consideration in these tests, the gas flow through the filter is laminar, allowing equation (1) to be rewritten in terms of the gas velocity.

$$\Delta P = K_1 V + K_2 V M/A \qquad (2)$$

where

V = gas velocity through the media

M/A = particle mass loading per unit area.

The constant K_1 depends on the filter structural properties such as the porosity and thickness of the filter. K_2 is a constant for a given set of particle and cake parameters such as the particle size and cake porosity. This simple model assumes that the particles are solid. Liquid droplets are more difficult to model due to factors such as the wetability of the filter media and the surface tension and viscosity of the liquid. Obviously there is no cake formation with liquid droplets.

The value of K_1 for the filter material tested in this work can be found by measuring the clean filter pressure drop as a function of gas velocity. Figure 4 plots the data and fits a straight line through the data for velocities up to 5 cm/s. The slope of this line is K_1. The value of K_1 is given as 7.97×10^2 g/cm^2 s. The value of K_2 can be determined both theoretically and experimentally. The theoretical analysis first assumes that the layer of particles forming the cake is comprised of isolated spheres far enough apart so the flow around one sphere does not interfere with the flow around a neighboring sphere (i.e., the porosity of the cake, e, approaches one) and that the Reynold's number, is less than one, then Stoke's Law can be applied to determine K_2.

$$K_{2Stokes} = (18\,\mu)/(CD^2\,\rho_p) \qquad (3)$$

where

μ = gas viscosity

ρ_p = particle density

D = particle diameter

C is the Cunningham slip correction factor given as:

$$C = 1 + \lambda/D\ [2.514 + 0.80 \exp(-0.55\ D/\lambda)] \quad (4)$$

where λ is the mean free path of the gas. For air molecules at standard conditions the mean free path, λ, is 0.066 μm.

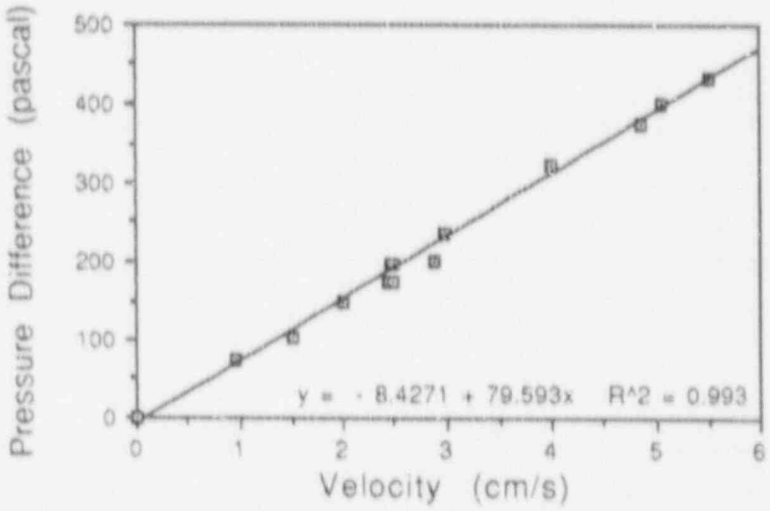

Figure 4. Filtration Velocity Versus Pressure Difference for Clean 47mm HEPA Filter

In real situations the spheres touch causing the flow around each sphere to be affected by its neighboring spheres, hence the porosity no longer approaches 1. In order to account for the effect that porosity has on pressure difference, a resistance factor, R, is defined which allows for a real solution of K_2:

$$K_2 = RK_{2Stokes} \quad (5)$$

At least two different researchers have developed methods of defining resistance factor R[11]. The work of Kozeny and Carman led to a semi-empirical equation that determines the resistance factor to be:

$$R = 2\ K_{ck}\ (1 - e)/e^3 \quad (6)$$

where e is defined as the porosity of the filter cake and the empirical constant K_{ck} is equal to 4.8 for spheres and 5.0 for irregular shapes. Leith and Allen[10] state that Equation (6) should not be used if $e > 0.7$.

Alternatively, Rudnick and First[12] developed an equation for R derived from theory and thus does not have an empirical constant as in Equation (6). This equation is given as:

$$R = [3 + 2(1 - e)^{5/3}] / [3 - 4.5\ (1 - e)^{1/3} + 4.5\ (1 - e)^{5/3} - 3(1 - e)^2] \quad (7)$$

Both methods of determining R require a knowledge of the porosity of the particle cake. However, the porosity can only be determined with experimental measurements of the thickness of the deposited cake and the total mass of particles in the cake. R can also be

calculated directly from the experimental data without a thickness measurement by combining Equations (1),(2),(3) and (5) to give:

$$R = AC\rho_p D^2 (\Delta P - \Delta P_o)/18\,\mu V M \qquad (8)$$

Both theoretical and experimental values for the resistance factor R will be discussed in the section describing the results of the filter mass loading tests.

Experimental Set-up for the Mass Loading Tests

The sampling chamber allowed for three 47mm filters, a cascade impactor and a Tapered-Element Oscillating Microbalance (TEOM) to simultaneously sample the aerosol stream. Simultaneous measurements of the aerosol particle mass collected by each port, as determined by the average between a gravimetric analysis and conductivity analysis, indicate that the maximum difference between any two ports is 1.1% while the average difference is 0.5%.

To investigate the role particle diameter plays in the mass ing vs. pressure drop on the HEPA filters, a series of tests were designed to load the ters to given values of pressure difference with particle size distributions of different mass median diameters. The different particle size distributions were obtained by using two different nebulizers, changing the solution concentration of NaCl solute and varying the gas velocity through the nebulizer. The polydisperse aerosols used in the mass loading tests were sized before and after each test with a seven-stage inertial cascade impactor.

The basic concept of the experiment remained the same as in the efficiency work. Clean, dry air was supplied to an aerosol nebulizer producing a distribution of droplets. The droplets were then dried and neutralized and the solid aerosol particles were collected for analysis. There were a number of improvements in the experimental set-up relative to the efficiency apparatus. A schematic diagram of the equipment used for these tests is given in Figure 5. Connecting transport tubing was shortened and as many components as possible were mounted vertically to minimize particle losses due to settling. An impinger was added after the Retec nebulizers to remove large droplets that were the major factor in forming occasional plugs in the transport tubing. Another impinger/mixing chamber was added just before the sampling chamber for all tests. This impinger removed any large resuspended agglomerates, allowing better control over the sampled particle size during the course of the experiments. The chamber also provided a number of additional ports where dilution air could be added and the pressure and humidity measured.

Mass Loading Test Results

The first series of tests duplicated the aerosol generation and filter collection parameters for two mass loading tests in order to show that the experiments were reproducible and to quantify the amount of error inherent in the experiments. Measurements were made by collecting aerosols on a 47mm filter until a desired pressure drop was observed across the filter. The mass on each filter was determined by an analytic balance and by measuring the conductivity of the solution used to wash the filter. Measurements were typically taken at pressure differences of 500, 1000, 1500 and 2000 Pascal (2, 4, 6, and 8 inches of water) above the initial pressure drop through the clean filter. Supplementary measurements were obtained with a Tapered Element Oscillating Microbalance (TEOM), a real time mass collection device. Problems with the

reliability and reproducibility of the TEOM in the larger size ranges, limited its usefulness in these experiments.

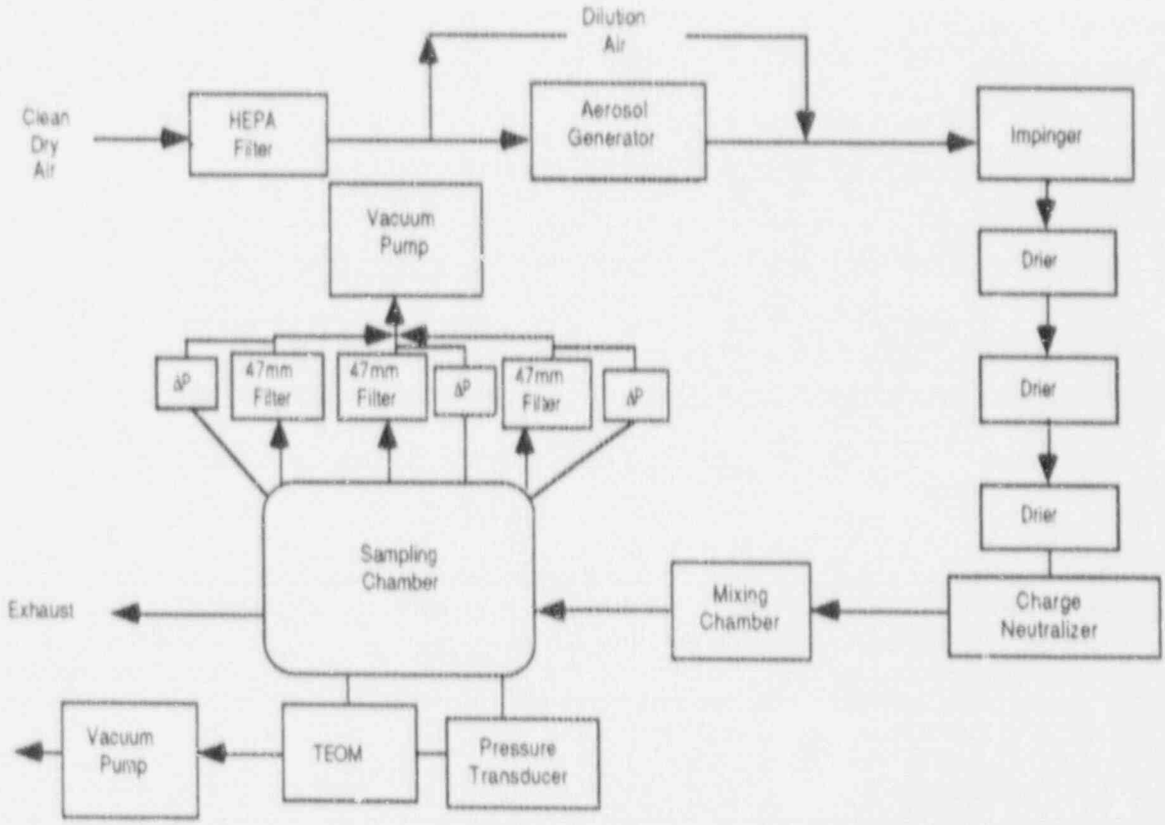

Figure 5. Experimental Configuration for Pressure Difference Versus Mass Loading Tests

However, as Figure 6 indicates the TEOM was able to confirm the essentially linear behavior of the mass loading as a function of pressure drop. This justifies fitting the 47mm filter data with a linear least squares fitting routine. Four sets of 47mm filter data were collected for the TSI generator using a 10% NaCl solution concentration. These tests are overlaid with data taken from Novick and Higgins[13] and shown in Figure 7. The particle sizes measured for these four tests are shown 20% larger than those measured for the Novick and Higgins test for the same generation and sampling conditions. This difference is most probably due to the improved transport properties of the redesigned experimental system. Note that the reproducibility in particle size, determined by the average between cascade impactor measurements just before and after each mass loading test, between the four tests is excellent. The spread in the data for this particular generator, solution concentration and flow rate (TSI, 10% NaCl and 2.45 cm/s) is approximately ± 7% from the average of all of the data points.

Figure 8 presents the data from four sets of 47mm filter tests compared with the Novick and Higgins results for the Retec generator with a 10% NaCl solution concentration at a filter media velocity of 2.45 cm/s. Again the particle size distribution transported by the new system is larger than that measured in the Novick and Higgins test. The spread in the data for this set of conditions is approximately ± 12%. Both of these measures of the scatter in experimental data is consistent with the error expected from an analysis of the uncertainty in each of the measuring devices. Some of the error may be attributed to particle size differences between tests.

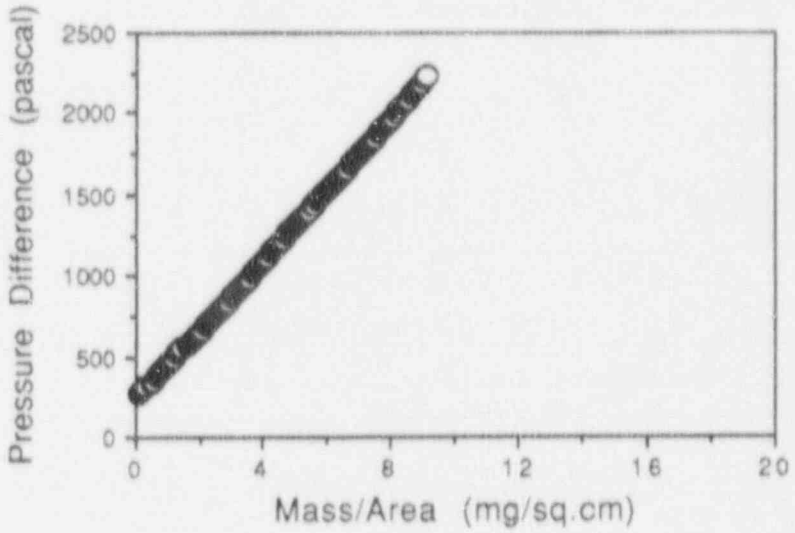

Figure 6. Example of Linear Increase of Mass Loading with Pressure Drop Using the TEOM

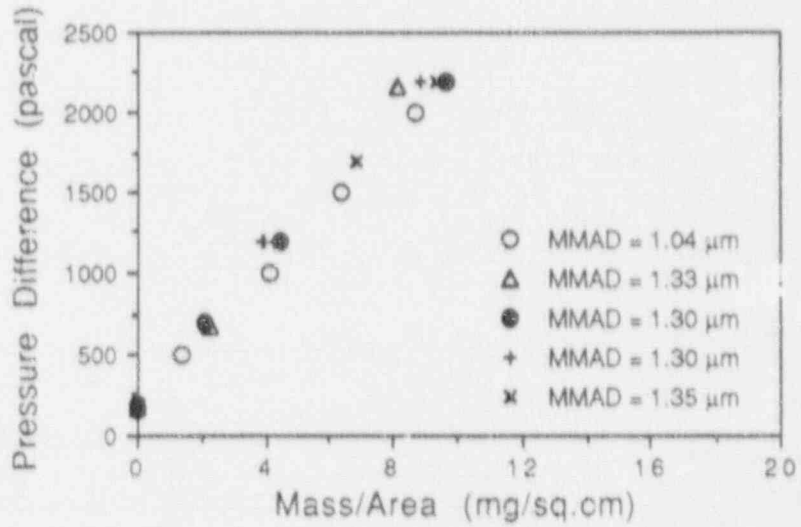

Figure 7. Tests Comparing the Pressure Difference Versus Mass Loading Using the TSI Atomizer with a 10% Solution (Velocity = 2.45 cm/s)

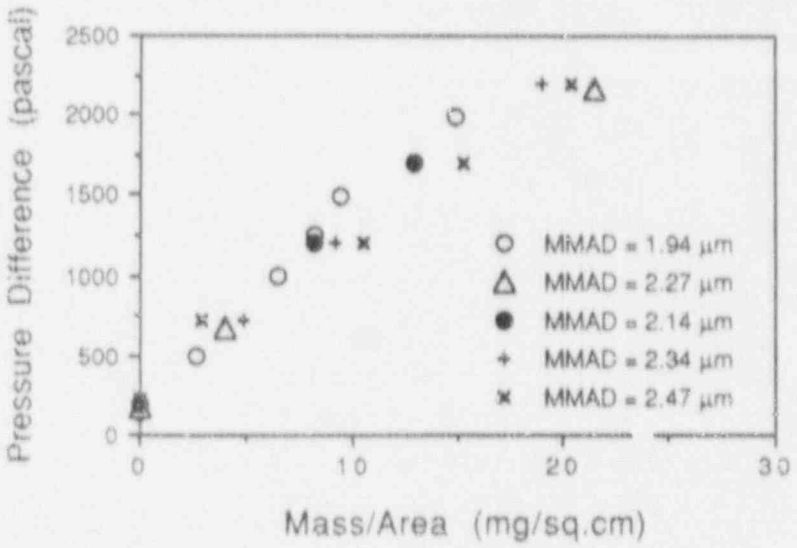

Figure 8. Tests Comparing the Pressure Difference Versus Mass Loading Using the Retec Nebulizer with 10% Solution (Velocity = 2.45 cm/s)

Figures 9 through 12 present examples of the data obtained for each test using a different particle size distribution. In all, nine different particle size distributions were measured. As stated earlier, the TEOM confirms the essentially linear behavior of the mass loading as a function of pressure drop. Therefore, each data set was fit with a linear function using the standard least squares routine contained in the Cricket Graph software. The particle size tests were limited at the low end by the time required to obtain a pressure drop of 2000 Pascal (8 inches of water) across the filter. For the smallest size tested, MMD = 0.66 µm, a continuous collection time of 14 hours was required. The large particle size limit was determined by the transport efficiency through the experimental system. Increasing the solution concentration beyond 10% with the Retec generator resulted in no increase in particle size distribution.

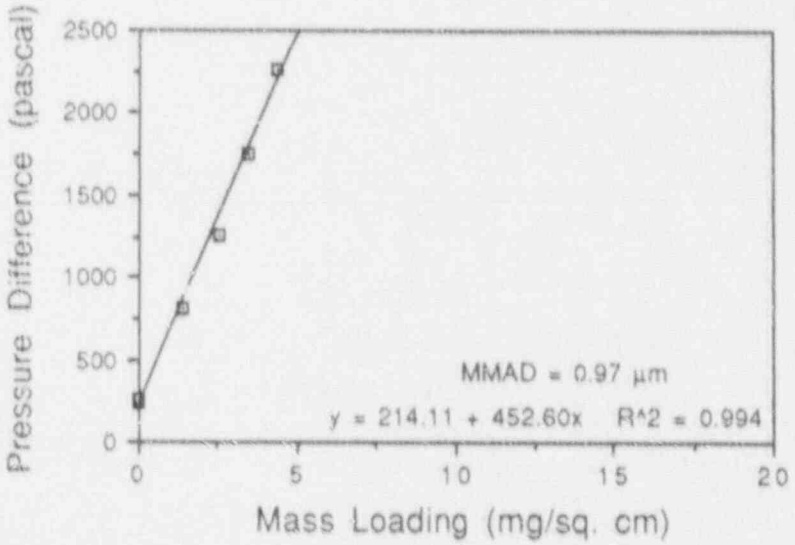

Figure 9. Pressure Difference Versus Mass Loading for a Particle Size Distribution with a MMD = 0.66 µm (TSI Atomizer, 2% Solution, V = 3 cm/s)

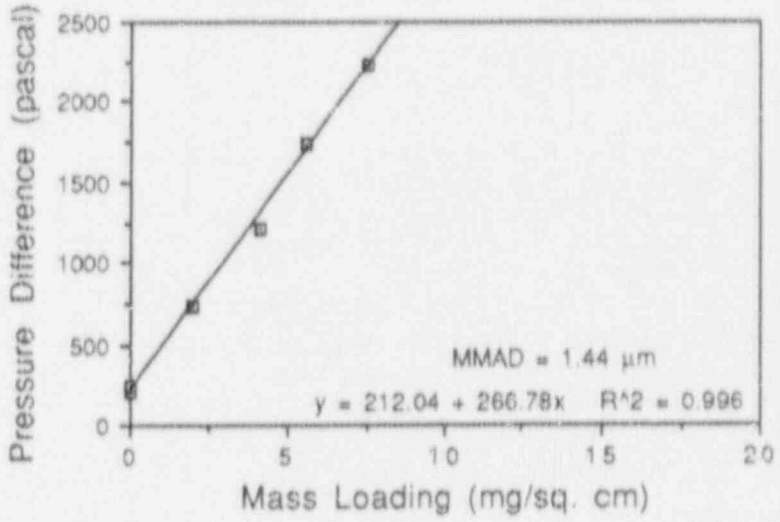

Figure 10. Pressure Difference Versus Mass Loading for a Particle Size Distribution with a MMD = 0.99 µm (TSI Atomizer, 15% Solution, V = 3 cm/s)

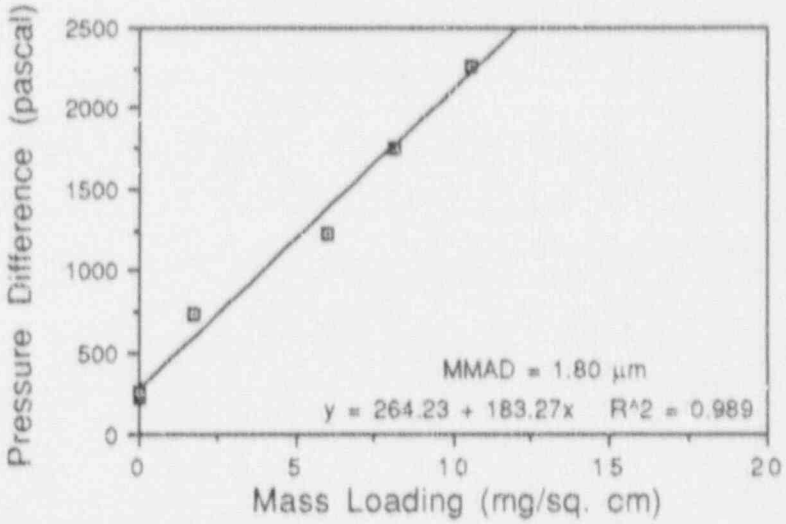

Figure 11. Pressure Difference Versus Mass Loading for a Particle Size Distribution with a MMD = 1.23 µm (Retec Generator, 10% Solution, V = 3 cm/s)

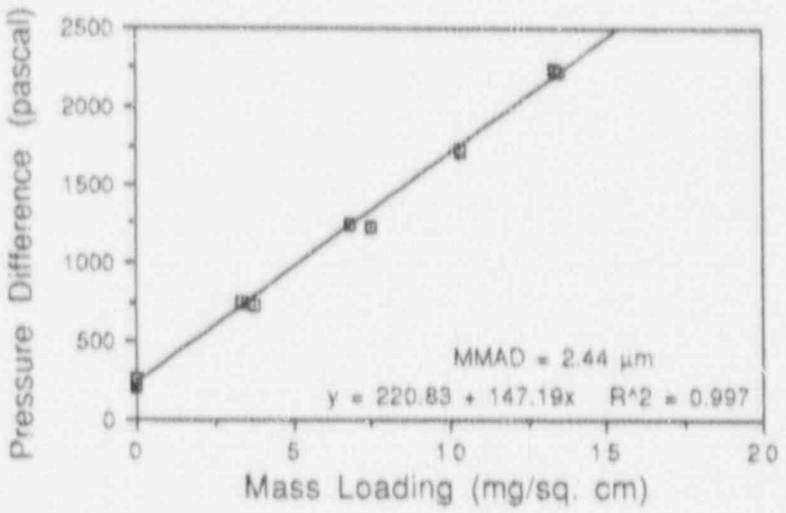

Figure 12. Pressure Difference Versus Mass Loading for a Particle Size distribution with a MMD = 1.69 µm (Retec Generator, 10% Solution and 4% Solution, V = 3 cm/s)

Clearly, Figures 9 through 12 show that varying amounts of aerosol material can be collected on the filter for a given increase in pressure difference. As discussed previously, it is common practice to define the specific resistance of a filter as the increase in pressure difference for a given amount of mass per unit filter area at a given velocity, so that comparisons between filters can be made. In this work, the measured specific resistance ranges from 3.9×10^5 s^{-1} to 1.4×10^6 s^{-1} for particle mass median diameters ranging from 1.7 µm to 0.7 µm. Comparisons between the specific resistance for particles in this size range, can be made with other researchers.

Rudnick and First[12] tested Arizona road dust on four woven fabric filters and measured specific resistances between 5.5×10^5 s^{-1} and 1.0×10^6 s^{-1}. Apparently, the particle size distribution was only measured once from a portion of the dust batch and not for each experiment. The particle size is given as an area median of 0.5 µm with an approximate standard deviation of 1.73. This would mean that the nominal mass median particle diameter for the Arizona road dust experiments was 0.68 µm, which is within the range of particle size tested in this work using NaCl. Note that the measured specific resistance of the road dust is also within the range measured for the NaCl.

Durham and Harrington[14] also measured the specific resistance for three types of glass fiber filters using fly ash. Specific resistances ranging between 4.3×10^4 s^{-1} to 7×10^4 s^{-1} at a relative humidity of 30%. The particle size in these experiments was also only measured once from the fly ash batch by dispersing a small quantity in a liquid and using a Coulter counter. The resulting measured mass mean diameter was 4 µm. Optical measurements of the particle size were made for every test, but the authors only reported that the range of particle size remained between 1 µm and 25 µm throughout the tests.

Specific resistances can also be calculated from the data given by McCormack[15]. These mass loading tests were conducted with a variety of HEPA filters, of which the type designated 1 appears to be the same as the Savannah HEPA filter. The test aerosol was generated by burning sodium in air with steam added in some tests, to increase the

relative humidity from aerosol 40% to near 60%. The calculated values of the specific resistance ranged from 8.7 x 10^4 s^{-1} to 6.4 x 10^5 s^{-1}. In general, the larger values occurred at higher humidities and lower flowrates. The particle size measured in these tests ranged from 6.8 µm to 1.4 µm, averaging 3 µm for the mass median aerodynamic diameter. However, the particle size was not measured for every test. Clearly, the larger fly ash and sodium hydroxide particles have lower values for the specific resistance compared to the smaller NaCl or Arizona road dust.

Examination of Figures 9 through 12 show a similar relationship between the slope of the line which is the specific resistance, K_2, and the mass median particle diameter representative of the aerosol distribution. Figure 13 presents a graphic presentation of all the mass loading data from tests denoting the relationship between the mass loading per unit area per unit pressure difference (i.e., the inverse slope) and the mass median particle diameter. Clearly, the specific resistance decreases as the particle diameter is increased.

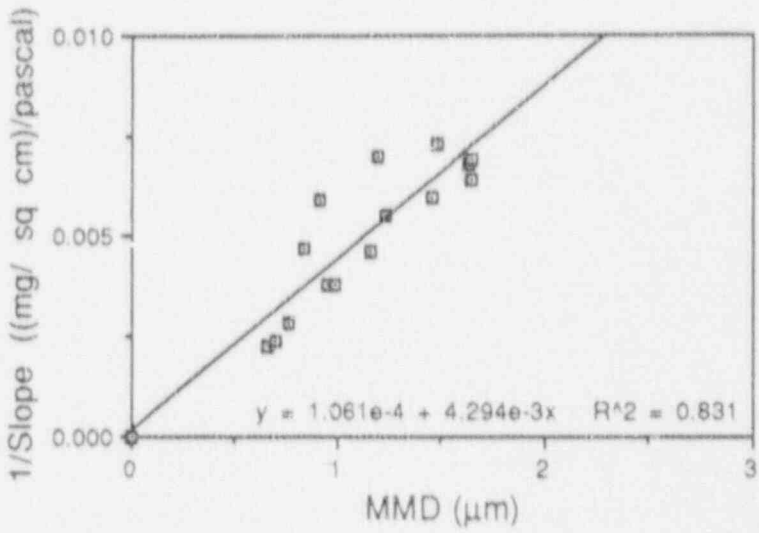

Figure 13. Mass Loading Per Unit Area Per Unit Pressure Difference Versus Particle Size for All Data with V = 3 cm/s

In order to compare experimental results with theoretical predictions, thickness measurements were taken of the particle cake for a number of tests. The porosity of the cake can be calculated from the thickness and cross sectional area of the cake and knowledge of the density of the solid particles.

For all data, where thickness was measured, the porosity averaged 0.7 with a standard deviation of almost 50%. The calculated resistance factor based on the the porosity of each test, R, however, has a standard deviation on the order of 200%, from an average of 21, clearly indicating that either a better method for determining R is required or that R has a functional dependence on some experimental parameter. On the other hand, using Equation (8) for the same data set, the average value of R_{exp} is 6.8 with a standard deviation of 35%.

Another method of determining R, that is instructive, is to take the slope, K_2 of each of the pressure drop vs. mass loading curves. This slope is essentially an average of the $(\Delta P - \Delta P_0)/(M/A)$ measurements for that particular velocity and particle size. Dividing the slope by the velocity and plotting the results as a function of the inverse of the particle diameter squared, is a convenient method of combining all of the data on one graph. The slope of this line should simply equal R times some constants as indicated from Equation (8). However, Figure 14 shows that the data clearly has a y-intercept, indicating that R is also a function of the particle size. The slope from Figure 14 defines R to be

$$R = 3.06 + 7.56 \times 10^7 \rho_p \, CD^2 \qquad (9)$$

The density and particle size are in cgs units. This method of determining R has a standard deviation of only 20% which is much closer to that expected from the analysis of errors in the experiment.

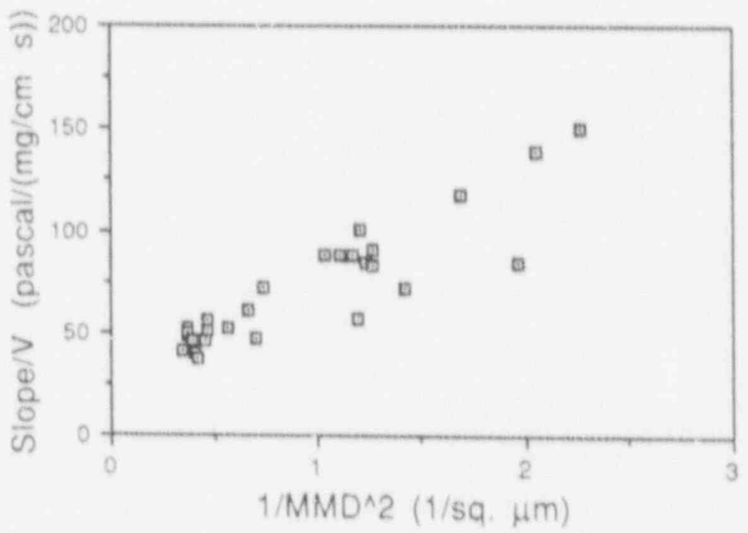

Figure 14. Slope/V as Determined by the $\Delta P/V(M/A)$ From the Mass Loading Versus Dp Curves, as a Function of Particle Size

Conclusions

The HEPA filter media is at least 99.99886% efficient for all dry particles sizes traveling with a gas whose velocity is 0.89 cm/s. The media is at least 99.9727% efficient for particle dusts at a velocity of 2.98 cm/s. These measured efficiencies meet or exceed current specifications. Efficiency spectra were determined for both flow rates allowing the release to the environment to be calculated for a given particle size distribution.

The resistance factor, R, was shown to be dependent on the mass median particle diameter for polydisperse aerosol distributions. This contradicts the assumption that the resistance factor, itself, is independent of particle size. However, as particle diameter decreases, the resistance factor does indeed become a constant according to Equation (9).

Combining Equation (9) and Equation (8) allows the mass loading per unit area to be predicted for a given increase in pressure differences across the filter, a given velocity and known or estimated mass median particle diameter.

$$M/A = (\Delta P - \Delta P_o)\, C\rho_p D^2 / 18\, V \mu\, (3.06 + 7.56 \times 10^7 \rho_p\, CD^2) \qquad (10)$$

Equation (10) also uses cgs units for all terms. This equation accounts for variations in particle diameter, particle density, gas viscosity and gas velocity. Therefore, it can be generalized to a wide variety of filtration scenarios within certain limitations.

One limitation is that the model described by Equation (10) is only good for dry, solid particles. Wet soluble particles appear to produce an exponential increase in pressure drop as the aerosol mass is increased in the filter. This effect was also seen by McCormack[15] using sodium hydroxide-aerosols. It is probable that insoluble particles with a liquid coating also exhibit non-linear behavior. However, Durham and Harrington[15] Ariman and Helfritch[16] showed that for some combination of aerosol and filter materials, the specific resistance of a filter cake decreased as the relative humidity was increased from 20% to 60% and from 20% to 80% respectively. This effect has not been quantified or incorporated into the model.

Another limitation is the extension of Equation (10) to other materials and shapes. Based on the agreement between Rudnick's data for Arizona road dust and this work with NaCl, in measuring the porosity of the particle cake, Equation (10) should be applicable to a wide variety of materials that are relatively non-sticky. In addition, based on the observation by Kozeny and Carmen of a 4% difference between spherical and irregularly shaped particles, Equation (10) should be applicable to most particles with aspect ratios near unity. Flakes and needles would probably have significantly different porosities and hence different values for the resistance factor. Finally, there may be limitations on the applicable particle size range of equation (10). Very small particles with high adhesive coefficients may cause variations in the cake porosity in a manner similar to the 'sticky' particles mentioned earlier. Also, particles with a size corresponding to the minimum efficiency of the filter material may cause an initial non-linear increase in pressure differential as a function of mass loading.

In general, the highly efficient collection capabilities of this filter media, cause a particle cake to be formed very rapidly on the surface of the filter. Measurements indicate that this cake forms in the first few minutes of aerosol collection. This phenomena allows the use of Equation (10) for predicting mass loadings on the Savannah River HEPA filter material.

Acknowledgement

The authors would like to acknowledge the U.S. Department of Energy, Nuclear Energy Group, for supporting this work under Contract No. W-31-109-ENG-38.

References

1. Petry, S.F., et al, L-Area Ventilation Tests - 1984, SRL Report DPST-85-336, March 1985.

2. Savannah River Plant Specifications DPSOP 40-2, Spec.4.

3. Tinnes, S.P., and Petry, S.F., System Analysis Airborne Activity Confinement System of the Savannah River Production Reactors, SRL Report DPSTSY-100-10, March 1986.

4. Lurant, W.S., et al, Activity Confinement System of the Savannah River Reactors, SRL Report DP-1071, August 1966.

5. Lee, K.W., and Liu, B.Y.H., "Experimental Study of Aerosol Filtration by Fibrous Filters," Aerosol Science and Technology 1:35-46 (1982).

6. Liu , B.Y.U., Pui, D.Y.H., and Rubow,K.L., "Characteristic of Air Sampling Filter Media," Aerosols in the Mining and Industrial Work Environment, Marple, V.A., and Liu, B.Y.H., Editors, Ann Arbor, Michigan, (1983).

7. Berglund, R.N., and Liu, B.Y.H., "Generation of Monodisperse Aerosol Standards," Environ. Sci. Tech. 7:147-152, (1973).

8. Knutson, E.O., and Whitby, K.T., "Accurate Measurement of Aerosol Electric Mobility Moments," J. Aerosol Sci. 6:453-460, (1975).

9. Wark, K., and Warner, C.F., Air Pollution, Harper and Row, New York (1981).

10. Leith, D., and Allen, R.W.K., in Progress in Filtration and Separation 4 (R.J. Wakeman Ed.) Elsevier, New York (1986).

11. Wakeman, R.J. Progress in Filtration and Separation 4 (R.J. Wakeman Ed.) Elsevier, New York (1986).

12. Rudnick, S.N., and First, M.W., "Specific Resistance (K2) of Filter Dust Cakes: Comparison of Theory and Experiments," in the Third Symposium on Fabric Filters for Particulate Collection EPA-600/7-789-087 (June 1978).

13. Novick V.J., and Higgins, P.J., Westinghouse Savannah River Report WSRC-RP-89-793 (1989).

14. Durham, J.F., and Harrington, R.E., "Influence of Relative Humidity on Filtration Resistance and Efficiency of Fabric Dust Filters," Filtration and Separation, July/August (1971).

15. McCormack, J.D., Hilliard, R.K., and Barreca, J.R., "Loading Capacity of Various Filters for Sodium Oxide/Hydroxide Aerosols," 15th DOE Nuclear Air Cleaning Conference CONF 780819 (1979).

16. Ariman, T., and Helfritch, D.J., "How Relative Humidity Cuts Pressure Drop in Fabric Filters," Filtration and Separation 14: 127-130 (1977),.

AEROSOL PENETRATION INSIDE HEPA FILTRATION MEDIA

P. Letourneau, Ph. Mulcey, J. Vendel
Commissariat à l'Energie Atomique
IPSN/DPT/SPIN/SEIP
CEN/Saclay - 91191 Gif-sur-Yvette Cédex, France

Abstract

Attemps made to modelize changes in HEPA filter pressure drop as a function of such parameters as the amount of aerosol collected, which also take account of filtering medium characteristics, those of the filtered aerosol and the filtration velocity, have always been limited by a lack of knowledge of the distribution of particles within the medium.

For the last few years, a method, developed over 25 years ago to study the distribution of Radon daughters within filter media made of cellulose fibers, has been reused and applied to radioactive and fluorescent aerosols penetration studies. This method enables determination of aerosol distribution on the surface and inside the filter medium by peeling away successive layers using an adhesive tape and measuring the specific amounts removed each time.

Knowledge of aerosol penetration within the filter has revealed that, for a given aerosol, particle distribution inside the filter rapidly decreased exponentially and that fixation on the filter's front surface rapidly superseded penetration inside the medium.

The deposit profiles thus measured have made it possible to propose a model for determining the rate of filter pressure drop increase - based on the model proposed by Bergman - that closely agrees with experimental results.

I. Introduction

Work has been underway for several years in our laboratory in order to modelize the removal efficiency and presure drop of HEPA filter media, as a function of such parameters as: aerosol particle size distribution and concentration, filtration velocity, rate of clogging, ...

This paper concerns the work conducted to modelize filter pressure drop change during clogging.

The first part of this paper will be concerned with the test installation and the characteristics of the test aerosol (uranine) and those of the filtering media (D. 306 Bernard-Dumas).

The second part will deal with experimental results. The latter involves the following:
- measurements of the change in pressure drop as a function of the surface mass of the filtered aerosol at various filtration velocities,

- aerosol distribution within and on the surface of the filter medium.

The last part of the document will deal with modelling, and in particular, the incorporation of the penetration profiles in the pressure drop calculation model developed by Bergman[2].

II. The test facility

II.1. Description

The test facility is shown in simplified form in figure 1.

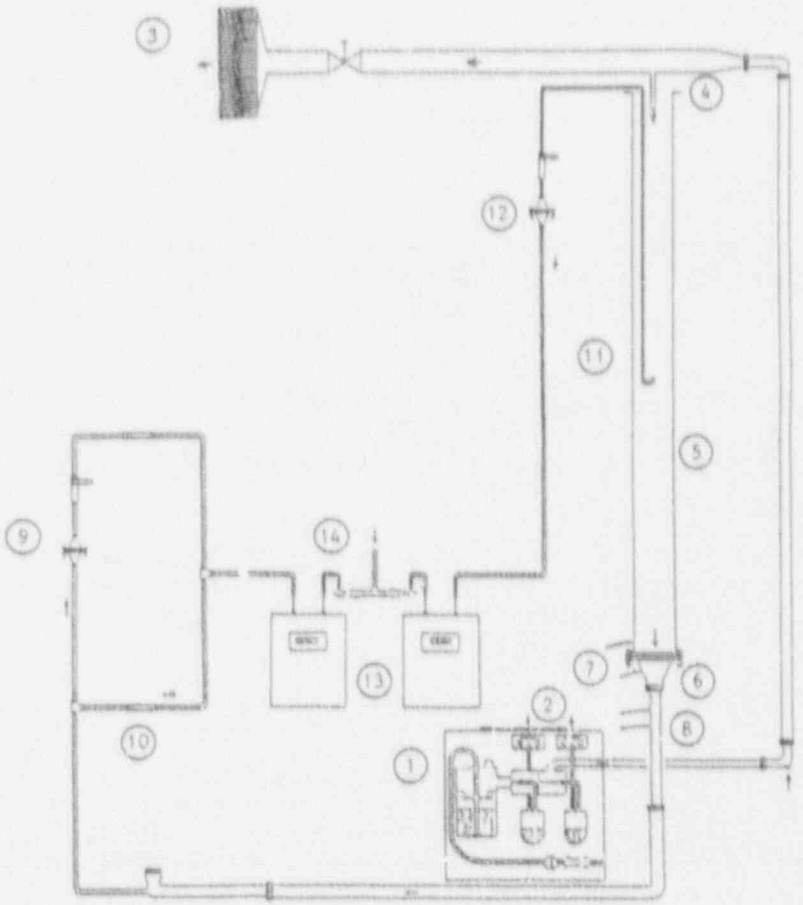

1 Uranine aerosol generator
2 Cartridge filters
3 Exhaust HEPA filter
4 Aerosol injection
5 Main duct
6 Filter holder
7 Pressure drop controller
8 Venturi flowmeter
9 Downstream filter holder
10 By-pass
11 Sampling probe
12 Upstream filter holder
13 Pneumatic gas meters
14 Air ejectors

Figure 1 Schematic diagram of the test facility

The aerosol produced by the uranine generator (n° 1 in drawing) is partly or totally injected in the main duct (n° 5) used to convey the air flow corresponding to the filtration velocity selected. Samples taken upstream (n° 12) and downstream (n° 9) from the filter tested (n° 6) are used to evaluate the volume concentration upstream and the removal efficiency of the filter tested.

Filter pressure drop is continuously monitored (n° 7) and the filtered air flow is kept constant during the test via a venturi system (n° 8).

II.2. Test aerosol

Tests were made using uranine aerosol (soda fluorescein) produced by a standardised NF X 44011 generator. The characteristics of the fluorescent aerosol thus produced are as follows:

type: fluorescein (sodium salt)

shape: spherical

density: 1,500 kg/m^3

number median diameter: 0.08 µm

mass median diameter: 0.15 µm

geometric standard deviation: 1.6

aerosol generator output: 25 to 30 mg/h

II.3. Filtering media

The filter media used are HEPA type media made of glass fiber. Their characteristics are as follows:

Supplier: Bernard-Dumas (France)

Product n°: D 306

Thickness: 475 µm

GSM: 67.4 g/m^2

Proportion occupied by fibers: 7.38 10^{-2} (in volume)

Shape: plane filter disks of actual filtration diameter of 10.8 cm

These characteristics are averages determined on the basis of 14 samples.

III. Experimental results

III.1. Initial filter pressure drop

Figure 2 shows the change in filter pressure drop (ΔP) as a function of filtration velocity (Um).

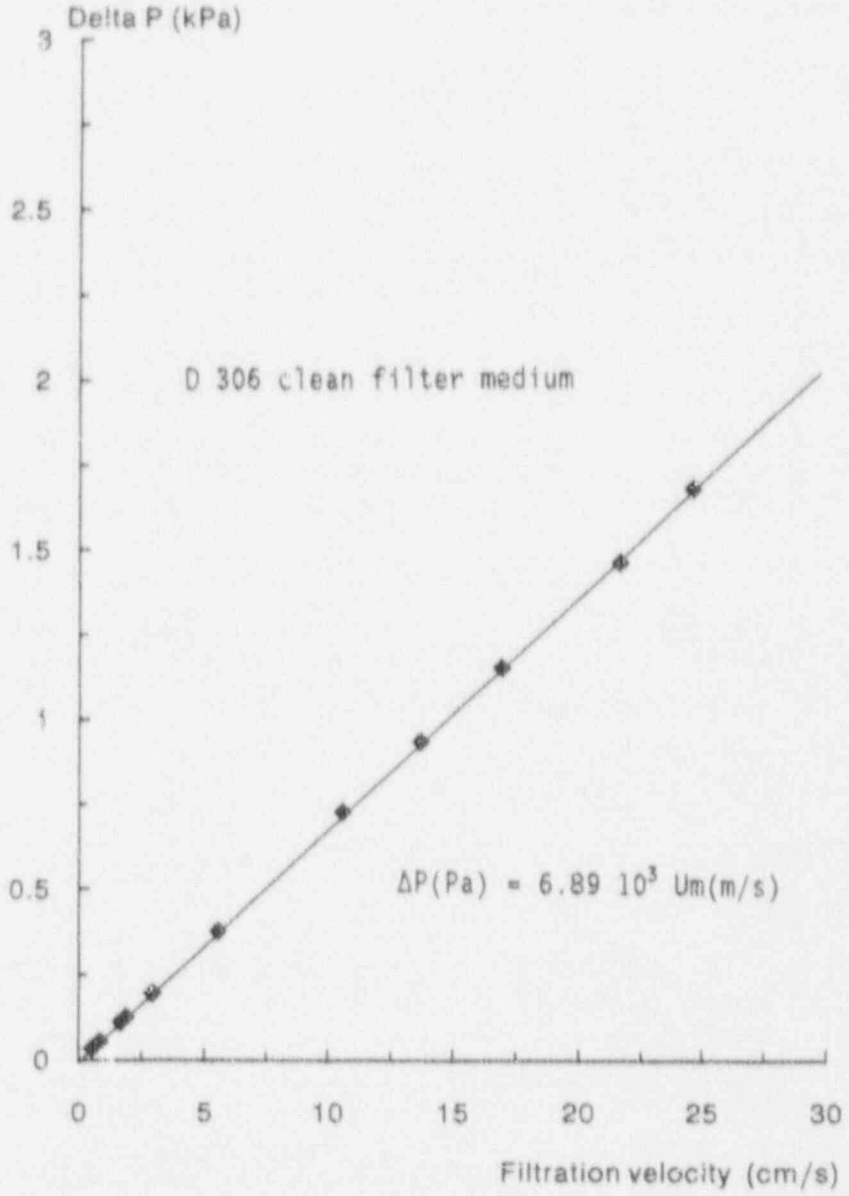

Figure 2 Change in pressure drop of clean D 306 medium versus filtration velocity

The average result obtained from 13 filters led to the following formula:

$$\Delta P = 6.89\ 10^3\ Um \qquad (1)$$

where ΔP is expressed in Pa and Um in $m.s^{-1}$

III.2. Change in filter pressure drop during clogging

The graphs of D 306 filter pressure drop variation as a function of the amount of aerosol filtered per effective unit of filter surface are shown in figure 3. The filtration velocities selected are respectively: 3, 5, 10, 20 and 30 cm/sec.

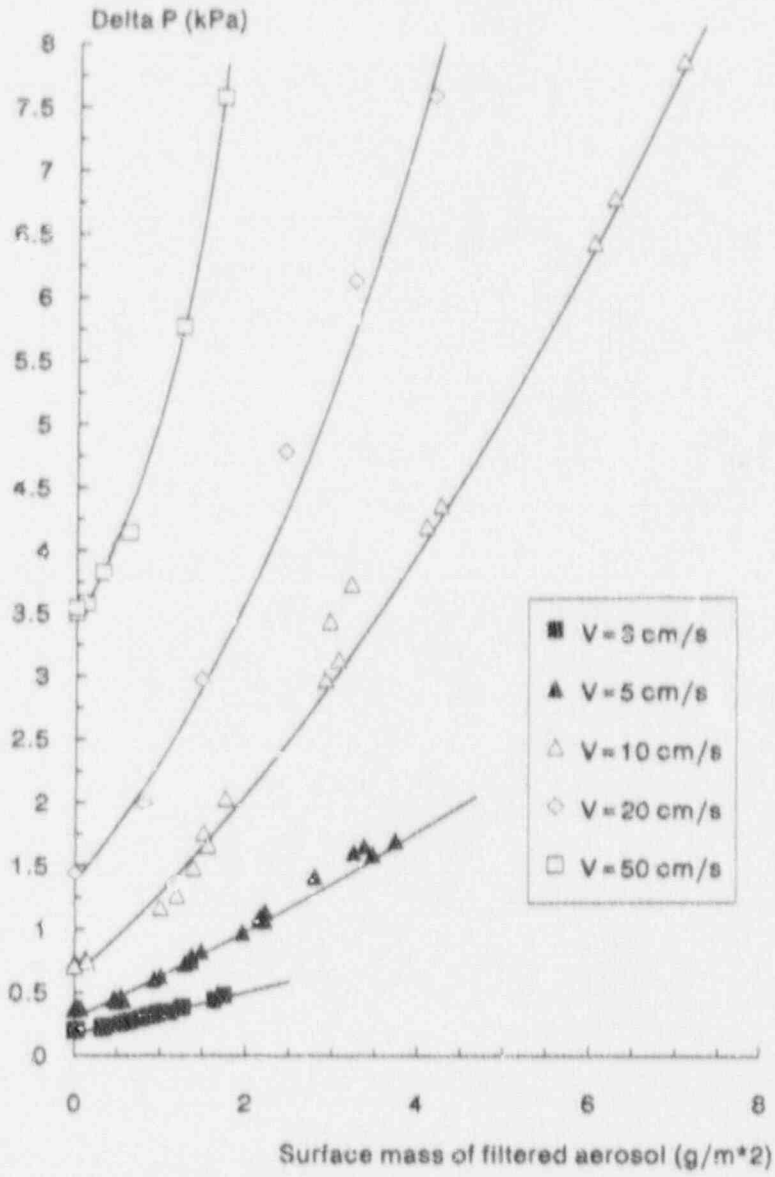

Figure 3 Changes in pressure drop of loaded D 306 media versus surface mass of filtered aerosol for different filtration velocities

III.3. Profiles of aerosol particle penetration inside filtering media

III.3.1. Peeling method

The method consists in using an adhesive tape sample of known surface area to collect a fraction of the filter's thickness, and to repeat this operation until no filter medium remains.

If operation is performed very repititively, the operator succeeds in obtaining a constant number of samples. Fourteen peelings were consistently made in this study, of a mean thickness of 34 μm.

III.3.2. Penetration within the filter medium

The results obtained allow the general penetration rate to be determined. The first peeling was ignored due to its considerable dependence on the total amount collected (filter surface accumulation).

It was revealed that the penetration profile is uniform at low velocities and has two distinct slopes as filtration velocities increase, and that the second part of the graph significantly depends on the filtration velocity. This is shown in figure 4.

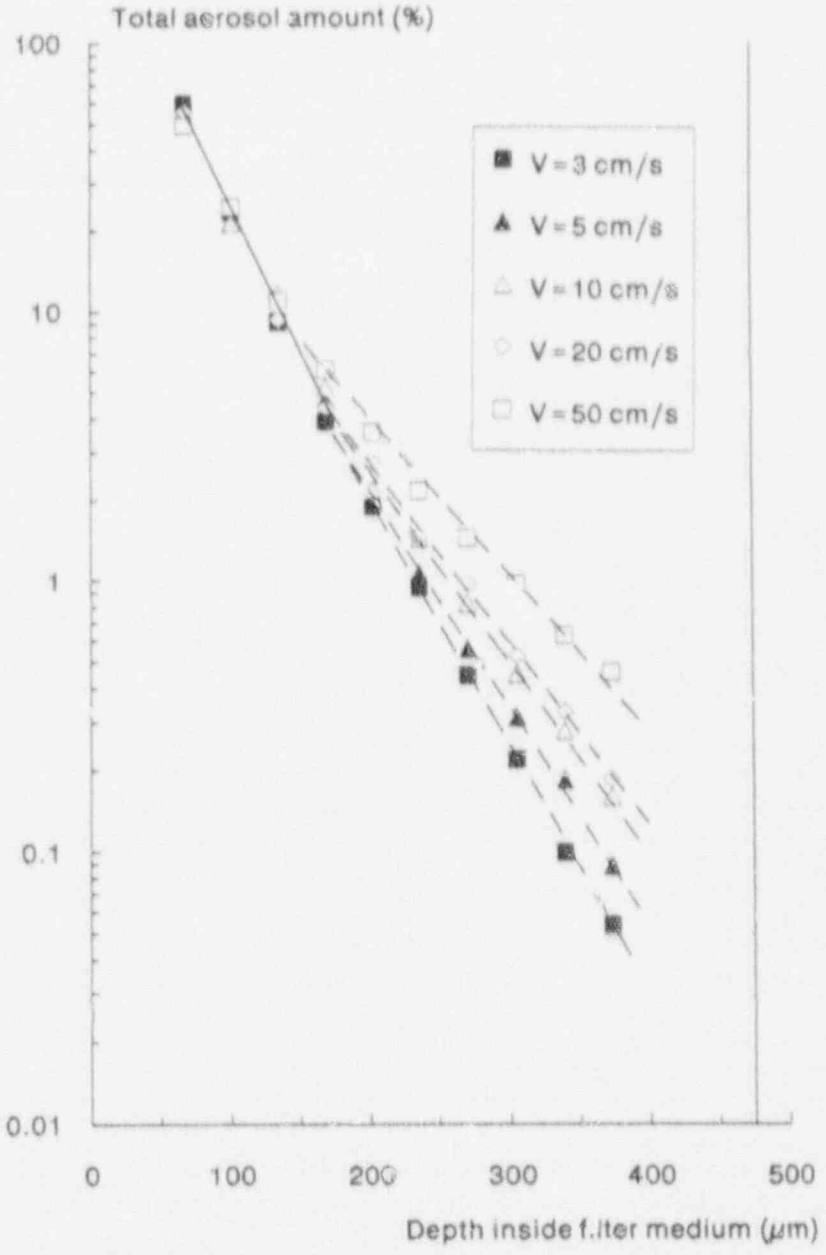

Figure 4 Distribution profiles versus deposition depth for different filtration velocities (D 306 media)

In this figure, the amount of fluorescent material removed on peels 2 to 14 is expressed as a percentage of the total amount collected on these peels.

III.3.3. Aerosol deposit on the filter's front surface

Penetration profiles are only slightly affected by the amount of aerosol filtered, as may be seen in figure 5. However, the amounts deposited on the upstream filter surface, and collected by the first peeling, depend greatly on this value, as shown in figure 6, in which the percentage of fluorescent material collected by the first peeling as compared to the total surface mass of deposited aerosol was plotted at various filtration velocities.

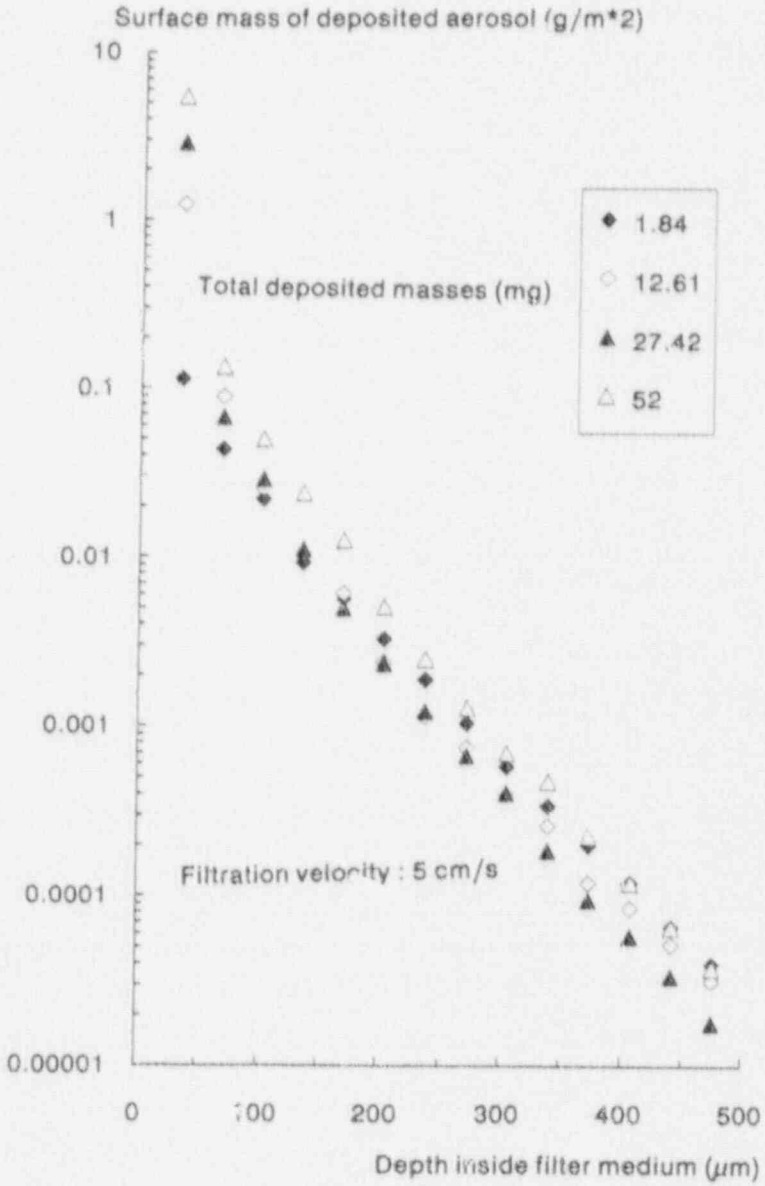

Figure 5 Surface mass of deposited aerosol versus deposition depth for different filtered masses
(Um = 5 cm/s)

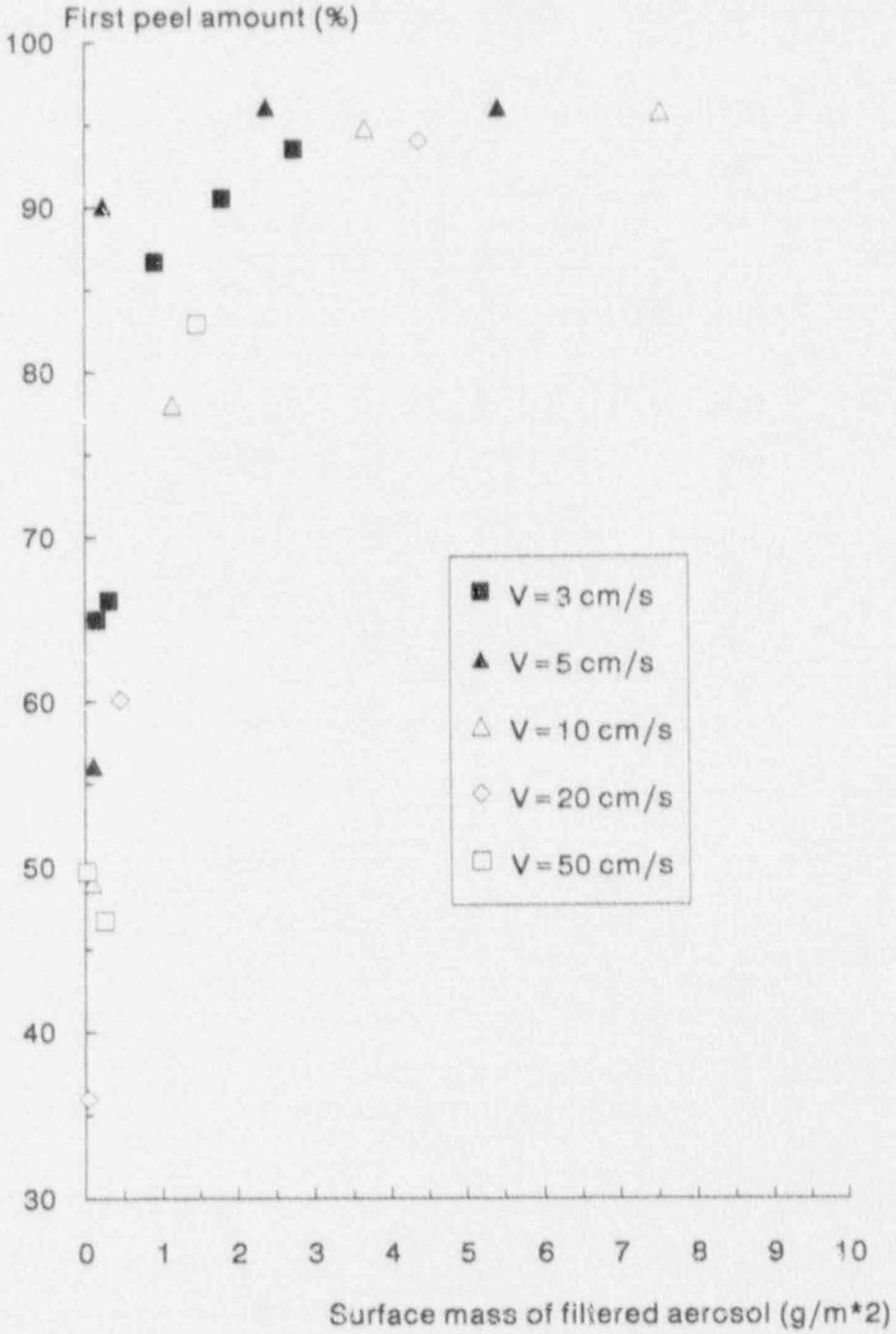

Figure 6 Changes in surface deposition versus surface mass of filtered aerosol for different filtration velocities

This figure shows that the amount of aerosol penetrating inside the filter medium decreases rapidly and becomes almost insignificant when the total surface mass of filtered aerosol is greater than approximately 2.5 g/m^2. Beyond this value, filtration by the aerosols deposited on the upstream surface of the filter becomes the dominating mechanism.

IV. Modelling

IV.1. Pressure drop characteristics of a new filter

The formula developed by Davies[1]:

$$\Delta P = 16\ \mu\ Um\ Z\ \frac{\alpha_F^{3/2}}{R^{*2}} \qquad (2)$$

adequately describes the change in pressure drop (ΔP) of a filtering medium as a function of filtration velocity (Um). In this formula:

μ is the dynamic viscosity of the gas
α_F is the fraction of the filter volume occupied by the fibers
R^* is an equivalent fiber radius
Z is the thickness of the medium.

Using the characteristics measured for the D 306 medium (see II.3), we were able to determine an equivalent fiber radius of 0.63 μm.

IV.2. Pressure drop modelling of a clogged filter

In order to account for the change in pressure drop of the filter medium, Bergman[2] proposed extending Davies model by assuming that the deposit of particles of radius r inside the medium was equivalent to adding a new group of fibers. Formula 2 is modified as follows:

$$\Delta P = 16\ \mu\ Um\ Z\ \left(\frac{\alpha_F}{R^{*2}} + \frac{\alpha_p}{r^2}\right)^{1/2} \left(\frac{\alpha_F}{R^*} + \frac{\alpha_p}{r}\right) \qquad (3)$$

in which α_p is the fraction of the filter volume corresponding to the particles.

Although determining α_F poses no major difficulty, since the structure of a filter medium may be assumed to be homogeneous to a large degree, the same is not true for α_p.

Attemps to apply this formula for HEPA filters[3] have revealed considerable differences between the model and experimental results.

Since one of the main reasons of these differences was attributed to the assumption that aerosol particles were uniformly distributed within the filter medium, the method of using representative profiles to calculate α_p was applied.

If the filter medium is considered to be a series of disks of thickness dx, its total pressure drop may be expressed as follows:

$$\Delta P = \int_0^Z 16\ \mu\ Um\ \left(\frac{\alpha_F}{R^{*2}} + \frac{\alpha_p(x)}{r^2}\right)^{1/2} \left(\frac{\alpha_F}{R^*} + \frac{\alpha_p(x)}{r}\right) dx \qquad (4)$$

In this formula, α_p is a function of the thickness.

Since aerosol distribution inside the filter medium decreases exponentially, it can easily be shown that α_p can be expressed as follows:

$$\alpha_p(x) = \frac{m}{s} \cdot \frac{k\ e^{-kx}}{\rho(1 - e^{-kZ})} \qquad (5)$$

in which:

m/s is the surface mass of the aerosol collected
ρ is the density of the particles
k is the mean penetration factor in the filter medium.

Using formula (4) with α_p determined by formula (5), results in:

$$\Delta P = \frac{16\ \mu\ Um\ \alpha_F^{1/2}}{R^*\ k} \left\{ \left\{ \frac{2\ \alpha_F\ r}{3\ R^{*2}} \cdot \left[(1+\beta)^{3/2} - (1+\beta e^{-kZ})^{3/2} \right] + \frac{\alpha_F}{R^*} \left\{ 2 \left[(1+\beta)^{1/2} - (1+\beta e^{-kZ})^{1/2} \right] + \log \left\{ \frac{\left[(1+\beta)^{1/2} - 1 \right] \left[(1+\beta e^{-kZ})^{1/2} + 1 \right]}{\left[(1+\beta)^{1/2} + 1 \right] \left[(1+\beta e^{-kZ})^{1/2} - 1 \right]} \right\} \right\} \right\} \qquad (6)$$

with $\beta = \frac{k\ R^{*2}}{\rho\ \alpha_F\ r^2} \cdot \frac{m}{s}$

An average value of factor k ($k = 2.69\ 10^4\ m^{-1}$) obtained from figure 5, which shows that for the first part of the graph - that for which deposits (and therefore their effect on pressure drop) are the greatest - k is almost independent of filtration velocity.

Results are indicated in figure 7 and 8, in which the change in pressure drop noted at filtration velocity ($\Delta P/Um$) is expressed as a function of the surface mass of filtered aerosol.

It can be seen in this figure that the experimental points corresponding to the various filtration velocities agree closely with the graph derived from formula (6).

The improved model satisfactorily describes the behaviour of the filter pressure drop during clogging with uranine aerosol even for surface mass of filtered aerosol of more than 2.5 $g.m^{-2}$ - i.e for a total amount of aerosol deposited on the filter surface of more than 90%.

mechanism from fibers to cake filtration seems to have no consequence on the pressure drop modelling.

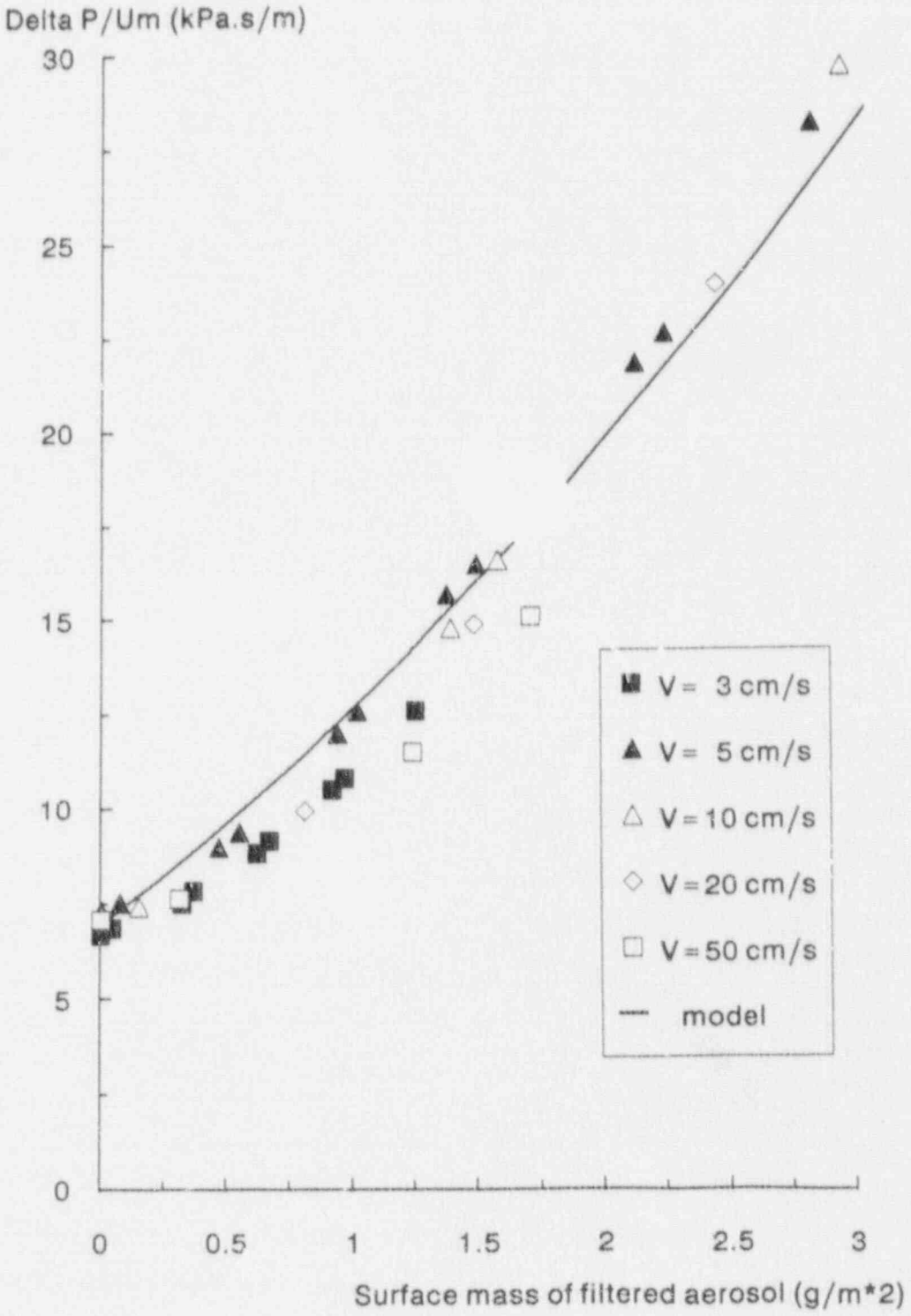

Figure 7 Changes in pressure drop with clogging : comparison of the improved model with experimental results (m/s < 3 $g.m^{-2}$)

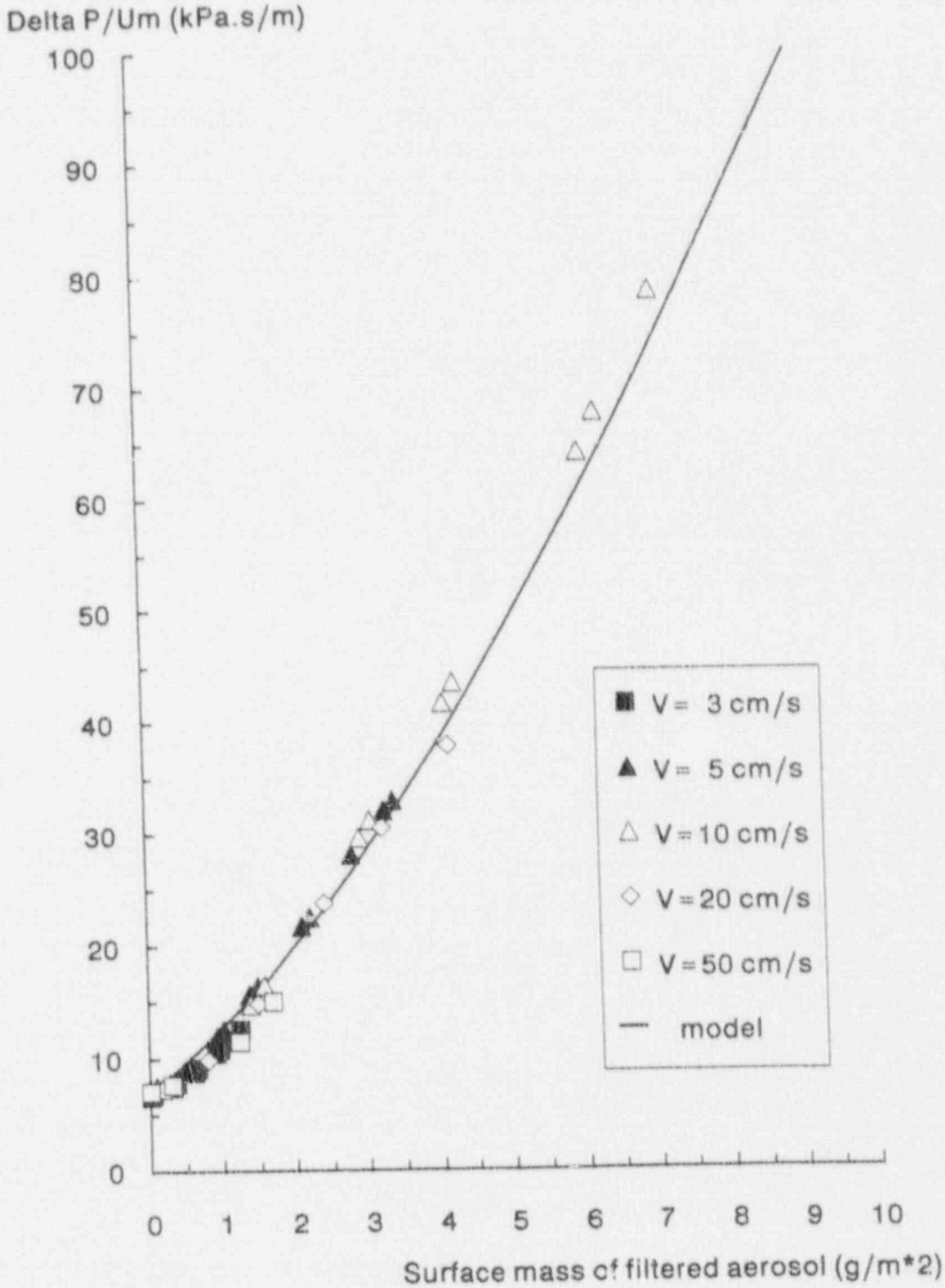

Figure 8 Changes in pressure drop with clogging : comparison of the improved model with experimental results ($m/s < 10\ g.m^{-2}$)

V. Conclusions

Determining the change in pressure drop for HEPA filters as a function of the amount of aerosol collected has been the subject of many studies but none have resulted in a satisfactory model since the distribution of the aerosol particles inside the filter medium was not accounted for. Using an adhesive tape peeling method provided the data required to describe particle penetration in the filter medium and enabled it to be shown that particles deposited on the filter surface rapidly become the most important factor.

The use of actual profiles of penetration within the filter medium makes it possible to adequately describe the change in filter pressure drop, regardless of filtration velocity.

Moreover, the description of the evolution of the filter pressure drop during clogging seems not to be affected by the change from fibers to cake filtration.

Acknowledgements

The authors take great pleasure in acknowledging the help of P. Journot from the Laboratory of Process Engineering, University of Chambéry (France) in carrying out all the analytical part of this study.

References

(1) Davies, C.N., Air Filtration, Academic Press, New York (1973)

(2) Bergman, W., Taylor, R.D., Miller, H.H., Biermann, A.H., Hebard, H.D., da Roza, R.A. and Lum, B.Y. Enhanced filtration program at LLNL. A progress report - 15th DOE Nuclear Air Cleaning Conference, CONF-780819, Boston, 1978

(3) Letourneau, P., Mulcey, Ph. and Vendel, J. Prediction of HEPA filter pressure drop and removal efficiency during dust loading, 20th DOE/NRC Nuclear Air Cleaning Conference, CONF-880822, 1988

CLOSING COMMENTS OF SESSION CO-CHAIRMAN DOMAN

Dr. Bergman: Improved metal filters by fabrication of metal fibers into filter medium. Test data indicate HEPA efficiency but with somewhat higher pressure drop.

Dr. Watson: Long interested in magnetic separation, describes a new approach by constructing a ferro-magnetic matrix. The filters described have important features such as requiring no external magnet or power, are smaller and portable, and can be cleaned without demagnetizing.

Dr. Jannakos: Tests at Kernfornschungszentrum Karlsruhe of a polygonal filter designed to withstand water droplets expected from an accident involving coolant, show effective resistance to damage. This finding parallels U.S. data where filters show similar resistance to water damage.

Dr. Novick: Pressure drop across HEPA filter material has been measured as a function of loading for various particle size distributions. Results show that for dry particles 1) there is a linear increase of pressure drop with mass, 2) small particles cause more rapid rise of resistance than those of larger distributions. The authors consider that the linear increase of pressure drop with mass loading is caused by the particle cake which forms on the filter surface. Maximum penetration through the filter material was found in the 0.15 to 0.3 μ region, depending on filtration velocity.

Dr. Mulcey: Tests made using hetero-dispersed aerosols of 0.15 μ mass median and the HEPA filter material showed a rapid exponential decrease of particle concentration inside the filter. The authors state that deposition on the front surface of the filter quickly supersedes penetration in depth. Their model of a clogged filter describes the change in pressure drop with loading by the aerosol even when surface loading accounts for more than 90%.

That concludes this afternoon's session. We thank the authors for their interesting presentations and you, the audience, for participating.

SESSION 13

SAFETY

Wednesday: August 15, 1990
Co-Chairmen: H. P. Wichmann
J. P. Mercier

OPENING COMMENTS OF SESSION CO-CHAIRMAN WICHMANN

IMPACTS OF THE FILTER CLOGGING ON THE BEHAVIOUR OF A VENTILATION NETWORK IN THE EVENT OF FIRE
J. C. Laborde, M. C. Lopez, M. Pourprix, J. Savornin, J. Teissier

BEHAVIOR OF RUTHENIUM IN THE CASE OF SHUTDOWN OF THE COOLING SYSTEM OF HLLW STORAGE TANKS
M. Philippe, J. P. Mercier, J. P. Gué

POOL FIRES IN A LARGE SCALE VENTILATION SYSTEM
P. R. Smith, I. H. Leslie, W. S. Gregory, B. White

CONTINUOUS AIR MONITOR FOR ALPHA-EMITTING AEROSOL PARTICLES
A. R. McFarland, J. C. Rodgers, C. A. Ortiz, D. C. Nelson

MEASUREMENT SYSTEM FOR ALPHA AND BETA AEROSOLS WITH WIDE DYNAMIC RANGE AND KRYPTON-85 MASKING
H. P. Wichmann, H. Tiggemann, H.-J. Kreiner

OPENING COMMENTS OF SESSION CO-CHAIRMAN WICHMANN

Five papers devoted to safety will be presented in this session. Fire is one of the events which may have severe consequences in a nuclear plant. In such an accident, it is important to understand the behavior of the ventilation network because it is one of the containment barrier for the plant. The first paper will present the impact of filter clogging on the behavior of the ventilation network in the event of a fire. In nuclear reprocessing plants, high activity wastes are stored waiting vitrification. Due to the high heating power of the fission projects, they must be cooled. The second paper will present original observations concerning the behavior of ruthenium in case of a hypothetical shutdown of the cooling system for a high activity waste storage facility. The third paper, like the first one, is related to a fire accident and will present the effects on a large scale ventilation system. The fourth and fifth papers will deal with monitoring systems for aerosols. The fourth paper discusses a continuous air monitor for alpha-emitting aerosol particles. The fifth paper describes a measurement system for alpha and beta aerosols with a wide dynamic range and krypton-85 masking. I think these are very significant presentations at the Nuclear Air Cleaning Conference because much of our interest is concerned with how to maintain and improved safety at nuclear plants.

IMPACTS OF THE FILTER CLOGGING ON THE BEHAVIOUR OF A VENTILATION NETWORK IN THE EVENT OF FIRE

J.C. Laborde*, M.C. Lopez**, M. Pourprix*, J. Savornin***, J. Teissier***
Commissariat à l'Energie Atomique, IPSN
*DPT/SPIN/SEIP
CEN/Saclay - 91191 Gif-sur-Yvette Cédex, France
**DPT/SPIN/SEIP/LESI
CEN/Grenoble - B.P. 85 X, 38041 Grenoble Cédex, France
***DAS/STAS/SPI
CEN/FAR - B.P. 6, 92265 Fontenay-aux-Roses Cédex, France

Abstract

One of the main roles of ventilation in a nuclear plant is to maintain dynamic containment during normal or accidental operating conditions. Among the incidents likely to affect a nuclear installation, fire is one of those which, coming from the safety standpoint, requires the greatest attention because it is one of the most probable risks. The consequences of a fire have to be analysed not only in the room where it breaks out, but also for the entire ventilation network. To evaluate these consequences and develop strategies against fire, the Commissariat à l'Energie Atomique (CEA) uses several test rigs and calculation codes by which the impact of a fire upon the sensitive points of a network can be determined.

Research and development studies currently under way give priority to the clogging of High Efficiency Particulate Air (HEPA) filters. Beginning with polymer fires in a 85 m^3 ventilated room, the influence of filter clogging on the characteristic parameters of the associated ventilated network (pressure in room, extraction flow, ...) is highlighted. The resultant modelling study following these experiments reveals that coupling of a ventilation code with a fire code cannot be disassociated from the development of a filter clogging model. This paper also gives the first experimental results relative to the determination of the variation, according to time and mass of deposited aerosols, of the air flow resistance of a filter clogged by aerosols derived from combustion of standard polymers used in the nuclear industry (methyl acrylate polymer, polyvinyl chloride). A methodology to extend the results obtained on our clogging test rig to any ventilation network is then described.

I. Introduction

Fire in a nuclear plant is an accident event which must be taken into consideration during the building design phase since it is one of the most probable risks. Studying fires and their consequences is complicated due to the diversity of the causes and parameters related to fire spreading. As a consequence, it can easily be conceived that thermal challenges will, in almost cases, be associated with other challenges such as the release of gases and aerosols, pressure stresses and vapour condensation.

The effect of these phenomena on the behaviour of ventilation systems and associated air cleaning components must be studied in order to evaluate if containment is maintained during the fire.

The Commissariat à l'Energie Atomique initiated a research and development programme several years ago in view of specifying fire prevention and fighting strategies. This programme involves the implementation of experiments and calculation codes designed to control the fire and its consequences from the source term until release to the environment.

One of the critical factors with respect to the fire safety strategy is the presence of aerosols, which is generally difficult to take into consideration. However, the behaviour of High Efficiency Particulate Air filters (HEPA filters) is closely dependent on the accumulation of aerosols which can rapidly clog these filters and decrease the capacities of the ventilation system.

This paper demonstrates, on the basis of polymer fires created in a ventilated room and the modelling of the associated ventilation system behaviour, the importance of the risk of HEPA filter clogging. Some results concerning clogging according to the aerosols formed during fires are also given.

II. Description of experimental and calculation means

In order to study, under full scale conditions, the spread of fires in confined areas and their consequences on the behaviour of ventilation systems, two experimental facilities (BEATRICE and MELANIE) and a ventilation code (SIMEVENT) are currently used.

II.1. BEATRICE test rig (figure 1)

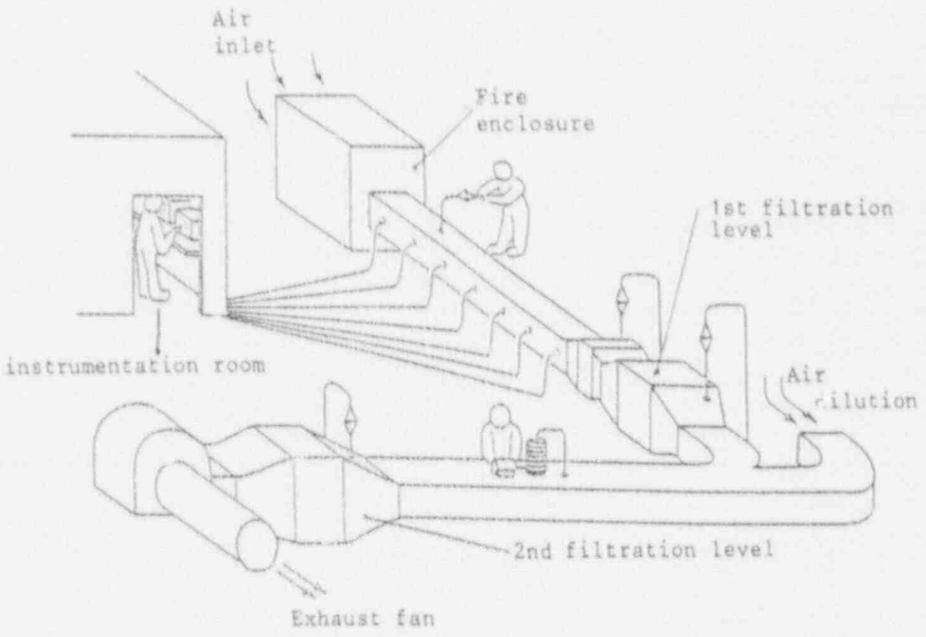

Figure 1 BEATRICE test rig

Initially designed to determine the characteristics of fire of dust deposits in ventilation ducts and their effect on the behaviour of air cleaning systems[1], the BEATRICE test facility was modified in order to create fires involving various materials in a small ventilated enclosure.

This test facility consists of a 2 m^3 volume made of stainless steel where the combustible materials are located, and an exhaust circuit consisting of 2 m long rectangular straight sections (450 x 300 mm^2). It comprises two HEPA filter stages which simulate the two filtration levels (before and after air dilution) usually recommended in nuclear plants.

A fan, located downstream from the circuit, provides the air exhaust flow (3,400 m^3/h under rated conditions).

Sampling and measuring points are located along the exhaust circuit in order to determine the following parameters:

- temperature of air and of duct wall,
- air flow rate,
- HEPA filter pressure drop,
- size distribution and concentration of the aerosols formed.

II.2. MELANIE test facility (figure 2)

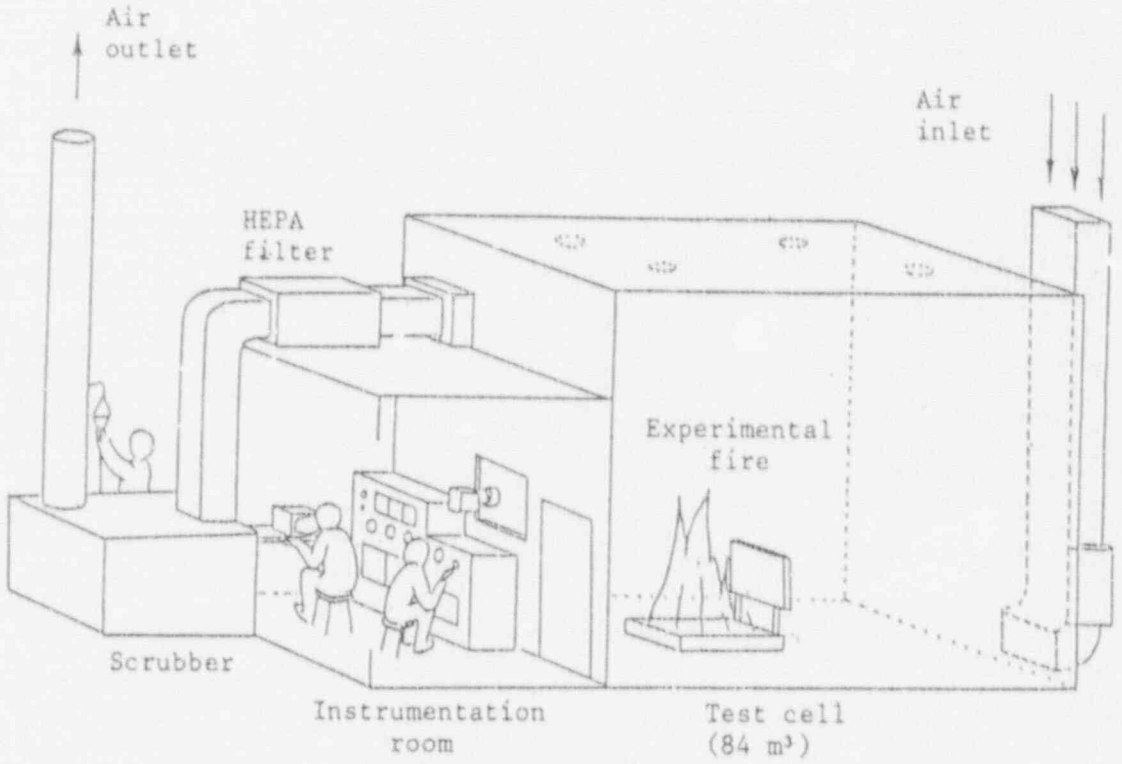

Figure 2 MELANIE test facility

Test enclosure

The test enclosure is a room with concrete walls of an approximate volume of 85 m^3. Another adjoining room is coupled to the test enclosure and serves as the control and instrumentation room. Between these two rooms, a rectangular window made of tempered glass enables the test to be filmed and observed.

The combustible materials are located in the centre of the test enclosure in a stainless steel tray (90 x 70 x 10 cm^3) on a metal frame (43 cm high) associated to a weighing system.

Associated ventilation network

It consists of the following:

. An air supply system, which includes:
- an air intake duct which can be thermally insulated,
- a fan,
- an air flow control damper,
- low or high position air intake, through 0.4 x 0.6 m^2 grids.

. An exhaust system, which includes:
- an exhaust duct located in the room, equipped with high or low 0.4 x 0.8 m intake grids,
- a fire damper,
- a filter housing equipped with HEPA filter,
- a scrubber,
- a fan,
- an exhaust stack.

Instrumentation

The test facility is equipped with instrumentation connected to a data acquisition system which provides the following informations:
- air temperature at various points in the room and in the exhaust duct,
- thermal flux,
- air intake and exhaust flow rates,
- pressure at various points of the system,
- gaseous effluents composition (gases and aerosols),
- combustible weight loss,
- contamination transfer coefficients from the source term to the exhaust HEPA filter.

II.2. The SIMEVENT ventilation code[2]

The SIMEVENT ventilation code is used to evaluate the behaviour of a complex ventilation network submitted to various disturbances of mechanical and/or thermal origin. The code is based on the division of the system in nodes linked by branches. A node represents a point of the system whose temperature and pressure can be considered as uniform. A branch is a part of the system limited by two nodes and fully defined by the relation $\Delta P = f(Q)$ which expresses the pressure difference (ΔP) as a function of the flow rate (Q) in the branch.

For a given accident situation, the code makes it possible to calculate the new values of pressure and temperature at the nodes and the flow rates in the branches. It can then be seen whether the simulated incident causes undesirable effects with respect to safety (reversal of air flow, room overpressure, etc).

To evaluate the consequences of a fire in a room, a fire description code must be used to be coupled with SIMEVENT. Two complementary methods were used to achieve this coupling:

- the use of SIMEVENT with a fire software programme based on a simplified model of the change in temperature of a room subjected to fire,
- the use of SIMEVENT with the FLAMME code[3], which makes it possible to precisely describe the fire in the room using a zone model.

Using SIMEVENT with the simplified model is a fast preliminary approach to solving the problem, which may then be more precisely analysed, if necessary, with SIMEVENT and FLAMME together.

A semi-empirical correlation which calculates the gas temperature in the upper layer of a room as a function of the fire heat release rate, the ventilation flow rate, the ambient temperature, and the room's physical and size characteristics was developed by Alvares, Foote and Pagni at the Lawrence Livermore National Laboratory[4].

Given the following:

Q_c : fire heat release rate (kW)

C_{pa} : gas specific heat capacity ($kJ.kg^{-1}.K^{-1}$)

T_a : ambient temperature (k)

T : upper layer temperature (K)

m_a : mass ventilation flow rate ($kg.s^{-1}$)

A : room surface area (m^2)

h : effective heat transfer coefficient ($kW.m^{-2}.k^{-1}$)

$$h = \sqrt{\frac{k_m \rho_m C_{pm}}{t}} \quad \text{if } t \leq t_p$$

$$h = \frac{k_m}{e} \quad \text{if } t > t_p$$

k_m : wall specific heat conductivity ($kW.m^{-1}.K^{-1}$)

C_{pm} : wall specific heat capacity ($kJ.kg^{-1}.K^{-1}$)

ρ_m : wall density ($kg.m^{-3}$)

e : wall thickness (m)

t_p : wall thermal penetration time (s) $t_p = \left(\frac{\rho_m C_{pm}}{k_m}\right)\left(\frac{e}{2}\right)^2$

t : time (s)

The upper layer temperature rise above ambient is calculated as follows:

$$\frac{T - T_a}{T_a} = 0.63 \left(\frac{Q_c}{m_a C_{Pa} T_a}\right)^{0.72} \left(\frac{hA}{m_a C_{Pa}}\right)^{-0.36}$$

This formula constitutes the simplified model used with SIMEVENT.

III. Experimental evaluation of the effects of polymer fires

III.1. Test conditions

The characteristics of the two polymer fires are indicated in table 1.

Table 1

Combustible Material	Type	Methyl Acrylate Polymer (PMMA) + 250 ml of ethyl alcohol	PMMA + Polyvinyl Chloride (PVC) + 250 ml of ethyl alcohol
	Weight (kg)	10.200	10.530 of PMMA + 1 of PVC
Ventilation Parameters	Air supply (m^3/h)	upper part 2,480	upper part 1,800
	Exhaust (m^3/h)	lower part 3,930	lower part 3,950
	ΔP room (daPa)	- 12.5	- 12

Note:

- the room is initially set at a negative pressure.
- the difference between the air supply and exhaust flow rates is due to leakage from the outside,
- the 250 ml of alcohol are used to ignite the combustible material.

III.2. Typical results

We are mainly interested in the effects of the presence of aerosols whose characteristics are indicated in table 2[5].

Table 2

	10.200 kg PMMA fire	11.530 kg PMMA + PVC fire
Aerodynamic mass median diameter (μm)	1.03	1.3
Geometric standard deviation	3.5	2.8
Mean concentration (mg/m^3)	108	138
Weight of aerosols deposited in the room (g)	20	25
Weight of residue (ashes) (g)	0	215
Weight collected on the exhaust HEPA filter (g)	150	190

As shown in figure 3, these aerosols involve the HEPA filter clogging which results in a significant increase of the pressure drop and a decrease in the exhaust flow rate. This phenomenon occurs even though the weight of the aerosols deposited on the filter is low (200 grams approximately) and only represents 2% of the initial combustible material weight.

Filter clogging causes the room pressure drop to increase (see figure 3c). It must therefore be considered one of the most important factors to be taken into consideration, since an over-pressure in the room may result in the spreading of contamination to the outside.

The duration of fire never exceeds 1 h, the most important change in paramaters occurs during the first 30 min.

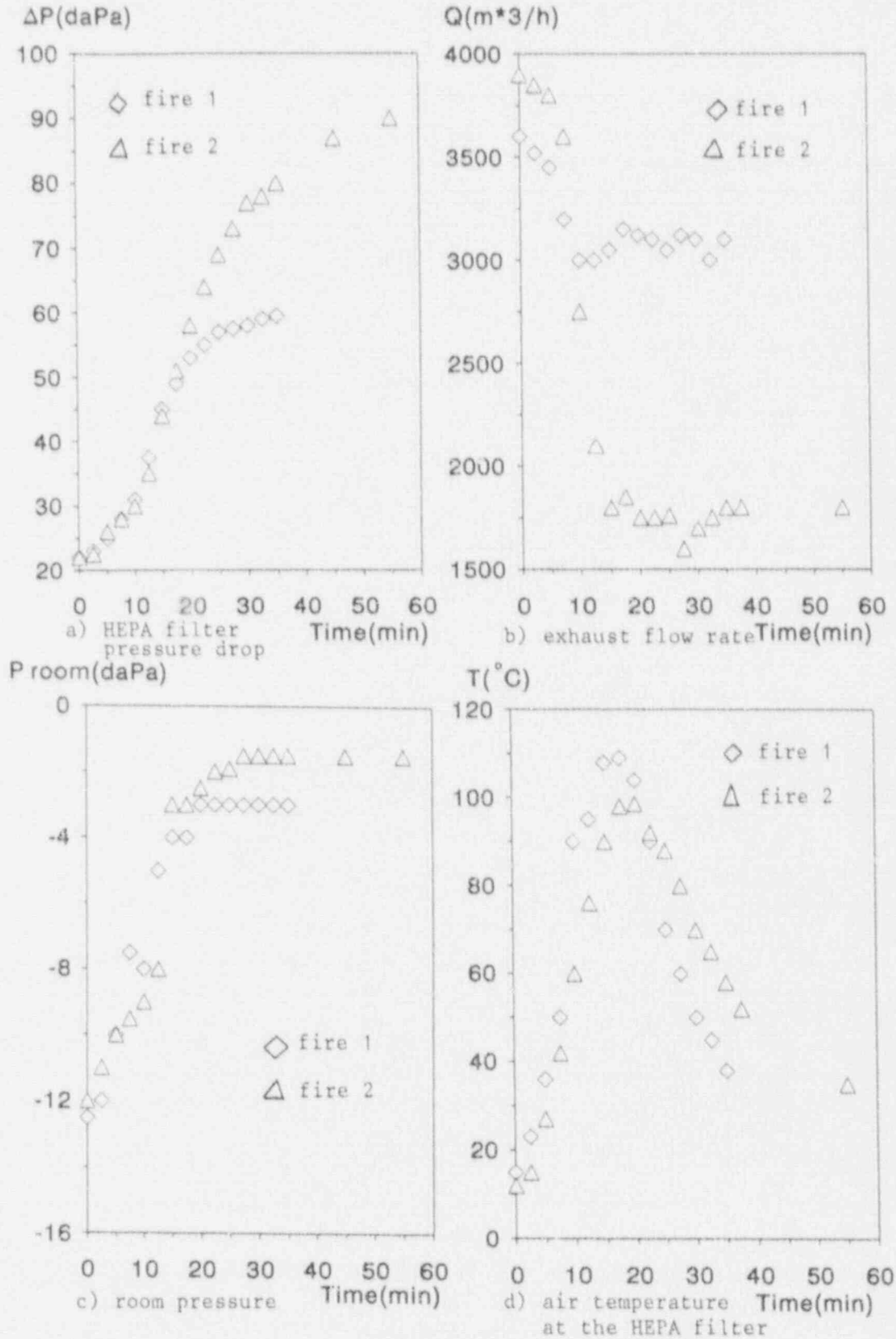

Figure 3 Evolution of characteristics values during the fires

IV. Modelling the effects of polymer fires[6]

The SIMEVENT modelling diagram of the MELANIE test facilty is shown in figure 4.

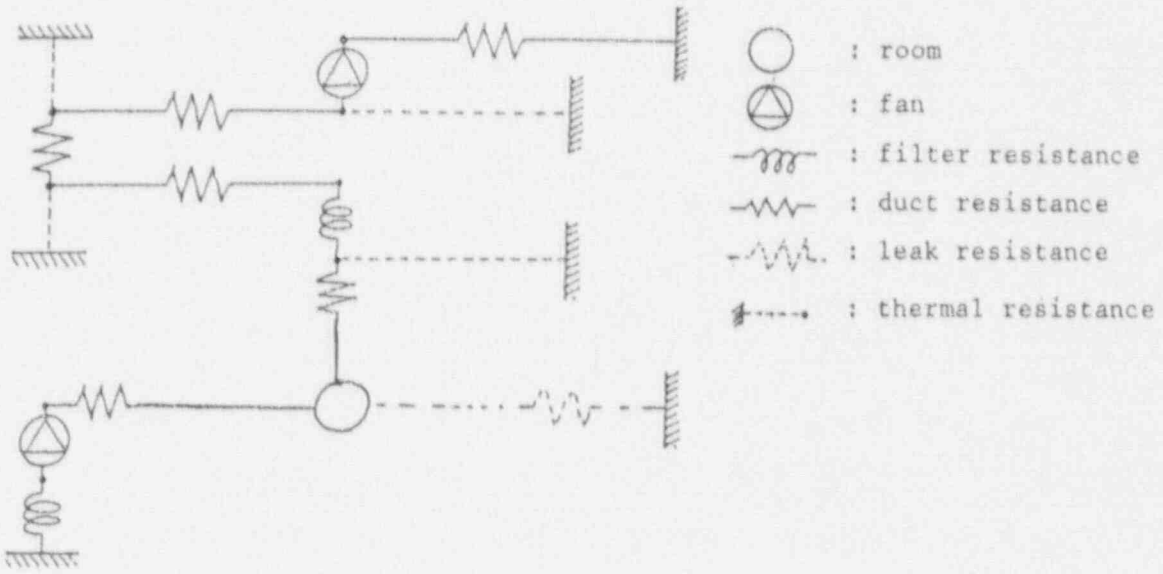

Figure 4 MELANIE modelling diagram

The code was initially used to describe the fire on the basis of the simplified model, i.e. by only considering the fire in terms of temperature evolution.

We note a rather bad fitting between the results provided by the code and those derived from the experiment, in particular with respect to exhaust flow rate (see figures 5a and 5b), room pressure and pressure upstream from the HEPA filter (see figures 5c and 5d). The differences are attributed to the filter clogging which is not taken into account in the code.

The filter clogging was therefore included in SIMEVENT, using the experimental data collected on MELANIE, in the form of "filter resistance" calculated as follows:

$$\Delta P = \frac{R_F \, \mu}{\mu_o} \, Q_V$$

This formula is expressed in SIMEVENT using the "GAINE" model

GAINE (N1, N2) = R_F, 0

ΔP : filter pressure drop (Pa) between N1 and N2

μ, μ_o : dynamic viscosity of air under experimental and standard conditions respectively (Poiseuille)

Q_v : volumetric flow rate at the filter (m^3/s)

R_F : filter resistance (kg/m^4s)

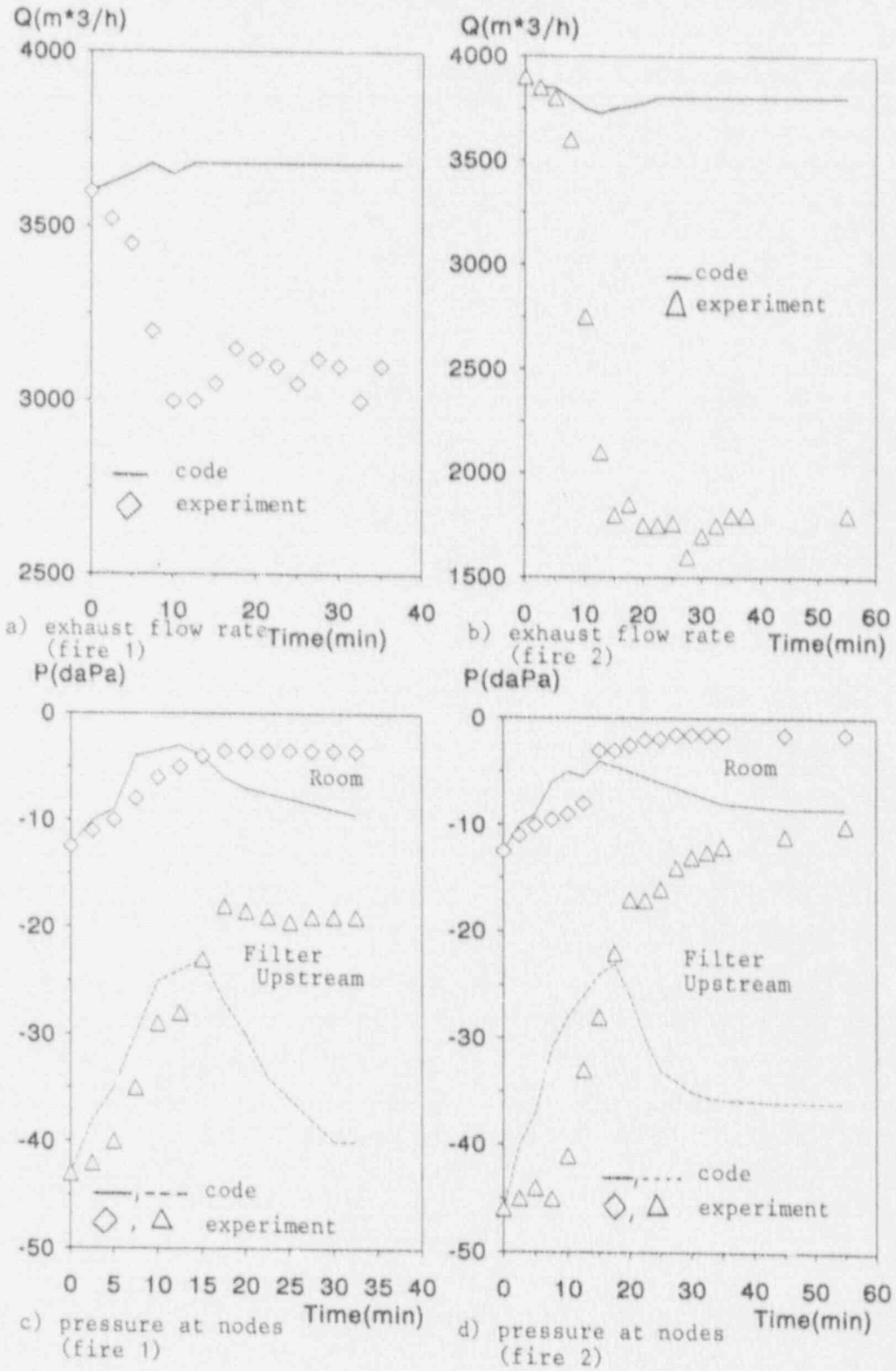

Figure 5 Comparison Code - Experiment without clogging model

Calculations can now be seen to better correlate with experiments (figure 6).

It results from this comparison that to evaluate the consequences of a fire on a ventilation network, the "Ventilation Fire" code used must include a module accounting for filter clogging.

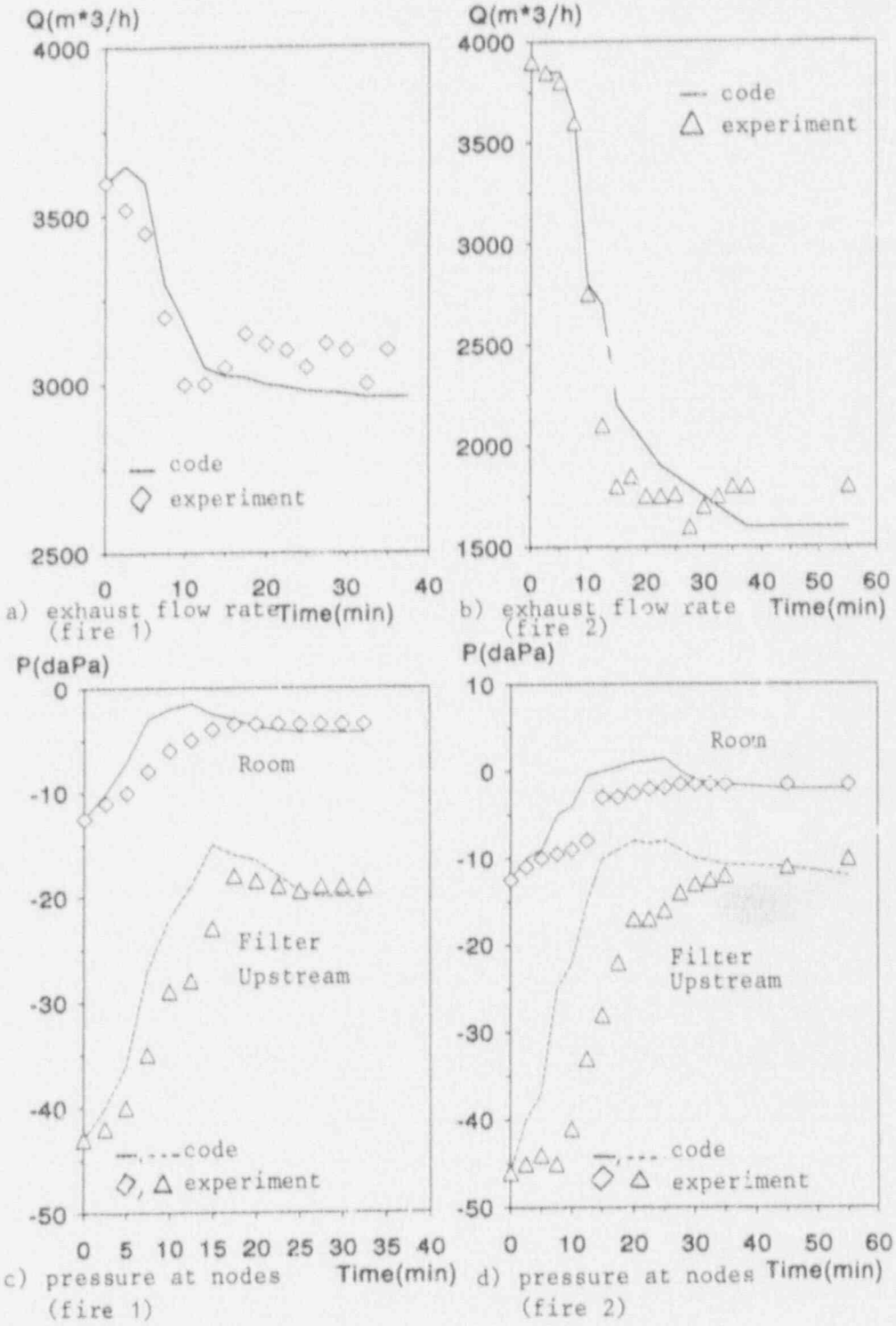

Figure 6 Comparison Code - Experiment with clogging model

V. Air flow resistance of a clogged filter

Generally speaking, there are very few models or basic experimental data concerning HEPA filter clogging. Furthermore, these data are provided by experiments using test aerosols (atmospheric particulates, ASHRAE particulates, etc) which are not representative of the aerosols actually formed during fires.

A study was therefore carried out using the BEATRICE test facility in order to acquire data concerning the clogging of filters with respect to aerosols formed during fires involving typical materials used in the nuclear industry. These materials are polymers (PMMA and PVC) used essentially to manufacture glove boxes.

Table 3 indicates some tests conditions and includes the weights of the aerosols deposited on the HEPA filters whose degree of clogging is to be evaluated.

Table 3

Test n°	Material	Amount of unburnt material (kg)	Amount of burnt material Q (kg)	Weight of aerosols deposited of the HEPA filters M (g)	M/Q (%)
1	2 kg PMMA	-	2	24.5	1.2
2	4 kg PMMA	-	4	54.0	1.3
3	6 kg PMMA	-	6	89.8	1.5
4*	2 kg transparent PVC + 1 kg PMMA	1.320	1.680	78.3	4.7
5*	2 kg opaque PVC + 1 kg PMMA	1.450	1.550	73.9	4.8
6*	4 kg transparent PVC + 2 kg PMMA	3.430	2.570	98.5	3.8
7*	4 kg opaque PVC + 2 kg PMMA	2.470	3.530	214.7	6.1

* It is assumed in tests n° 4, 5, 6 and 7 that the PMMA initially introduced was completely consumed and that unburnt material entirely resulted from the PVC.

The following values were measured continuously during these tests:

- air temperature and flow rate
- mass concentration of aerosols
- pressure drop

} at HEPA filter

The air resistance of the clogged filter (R_F) specified in section IV may be found using these values.

The graphs in figure 7 represent the variation of R_F as a function of time and aerosol mass deposited on the HEPA filter.

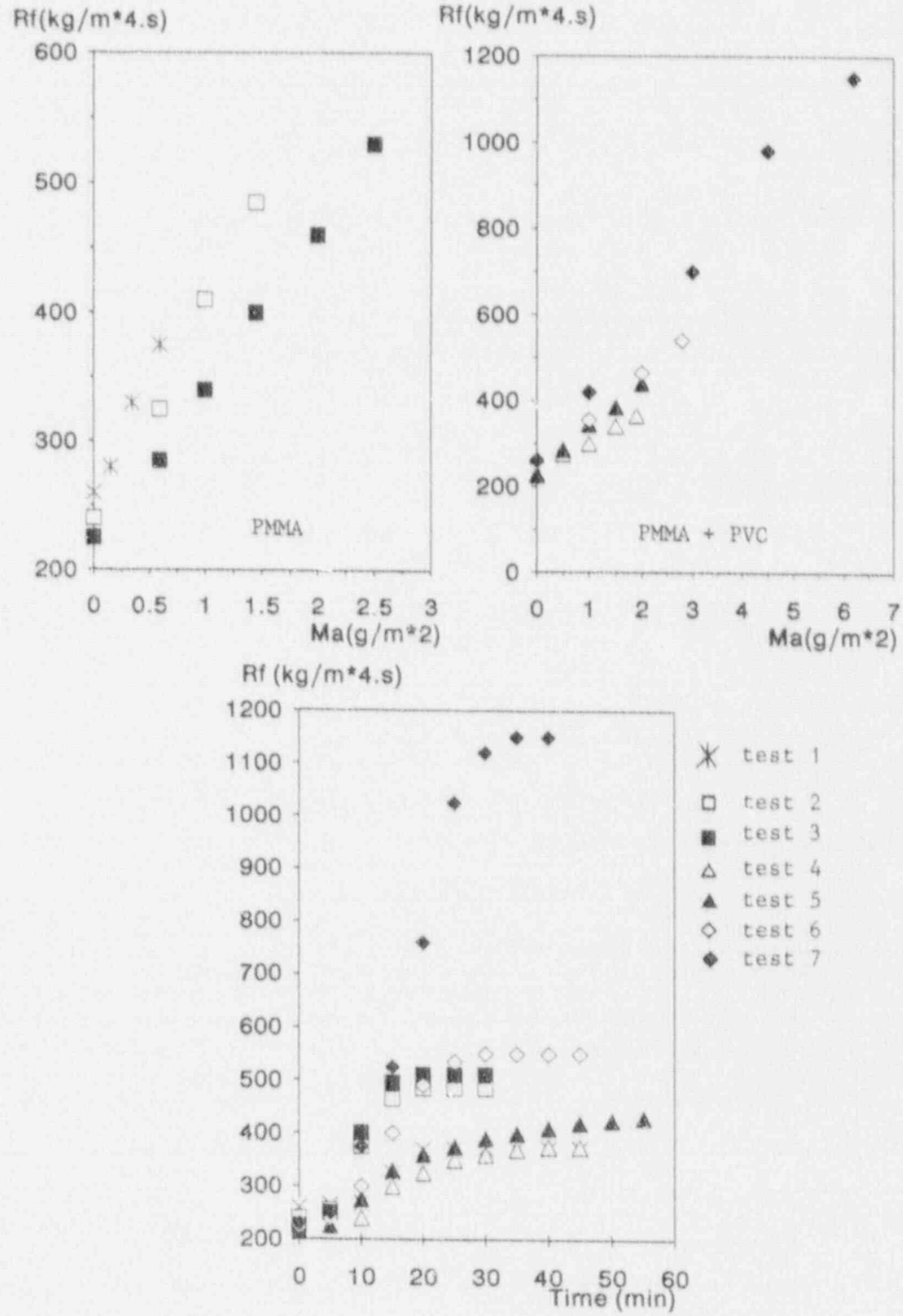

Figure 7 Variation of R_F as a function of time and mass of filtered aerosols

We can see that the resistance of the clogged filter varies linearly with the weight of the aerosols deposited on the HEPA filter, over the range from 0 to 10 g/m^2 tests.

A relatively small amount of aerosol causes large increases in air flow resistance considering the nature of these aerosols (i.e. solid and/or liquid particulates depending on condensation phenomena). Fires resulting from PMMA + PVC mixtures clog filters more rapidly than fires from pure PMMA.

Since the type of material is an important factor, other tests are currently being made involving other materials in view of elaborating a data bank of their respective clogging potential.

The following method is proposed to apply the results provided by BEATRICE to evaluating the behaviour, during a fire, of a given ventilation network modelled using SIMEVENT coupled with a fire code.

Basic data

a) Fire source term

It is characterized by the size distribution and the mass flow rate (Q_a) of the aerosols deposited on the HEPA filter. Integrating the $Q_a = f(t)$ graph provides the weight (M_d) of the aerosols deposited on the HEPA filter.

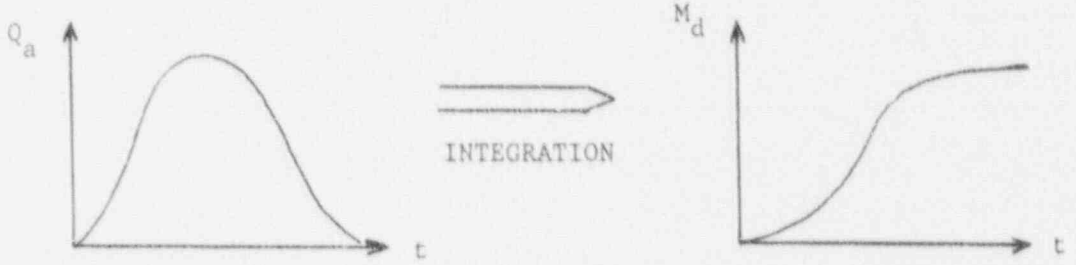

b) Resistance of a clogged filter

The results provided by the tests on BEATRICE will lead to typical graphs indicating the clogged filter resistance evolution $R_F = f(M_d)$ for various materials.

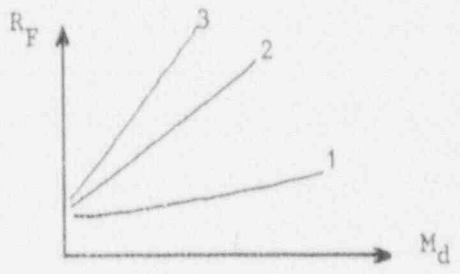

c) Modelling the system using the SIMEVENT code and a fire code

GAINE (N1, N2) = R_F, 0

Instruction describing the air flow resistance of the filter.

Methodology

* at t = 0 $M_d = 0$ $R_F = R_{F0}$

* at $t_1 = \Delta t$

Given the basic data:

1 → $M_d\ (t_1) = M_{d1}$

2 → $R_F(t_1) = R_{F1}$

3 → new system state (flow rate, pressure, etc)

* at $t_2 = \Delta 2\ t$

1 → $M_d(t_2) = M_{d2}$

2 → $R_F(t_2) = R_{F2}$

3 → new system state (flow rate, pressure, etc) and so on...

The above methodology would be easier to implement numerically if an analytical model describing the variation in the air resistance of a clogged filter was available. A basic study is currently underway to develop such a model on the basic of laboratory experiments involving test aerosols[7].

VI. Conclusion

This study shows that among the many phenomena involved in a fire, the risk of HEPA filter clogging is one of the factors that should be carefully evaluated.

Considering the complexity of the clogging mechanisms, many experiments must be conducted to acquire the basic data that could be incorporated in the codes describing the effects of a fire on the behaviour of ventilation networks.

The two main phenomena associated with filter clogging are the decrease in the air exhaust flow rate which may result in room overpressure, and the damage of the HEPA filter.

References

(1) Briand, A., Laborde, J.C., Mulcey, Ph., Savornin, Ph., Teissier, J.
Analysis and consequences of fire inside the ventilation ducts of a nuclear facility.
ASHRAE Conference, HVAC for Nuclear Facilities, Vancouver 1989

(2) Martin, G., Mulcey, Ph., Perdriau, Ph., Pruchon, Ph., Raboin, S.
Simulation of ventilation networks: presentation of the safety code PIAF complementary with fluid mechanics codes.
19th DOE/NRC Nuclear Air Cleaning Conference, Seattle 1986

(3) Duverger de Cuy, G., Malet, J.C.,
Calculating the consequences of a kerosene pool fire: the FLAMME computer code.
Interaction of Fire and Explosion with Ventilation Systems in Nuclear Facilities, Los Alamos 1983

(4) Alvares, N.J., Foote, K.L., Pagni, P.J.
Temperature correlation for forced ventilated compartment fires.
1st International Symposium on Fire Safety Science, Gaithersburg 1985

(5) Briand, A., Burghoffer, P., Laborde, J.C., Lopez, M.C., Pourprix, M.
Caractérisation et conséquences de feux de polymères en local ventilé - Evaluation des transferts de contamination.
CEA report, ARD 3220-2, december 1989

(6) Laborde, J.C., Martin, G.
Application du code SIMEVENT couplé à un modèle estimateur d'incendie.
CEA report, ARD 3220-3, december 1989

(7) Letourneau, P., Mulcey, Ph., Vendel, J.
Aerosol penetration inside HEPA filtration media.
21st Nuclear Air Cleaning Conference, San Diego 1990

BEHAVIOR OF RUTHENIUM IN THE CASE OF SHUTDOWN OF THE COOLING SYSTEM OF HLLW STORAGE TANKS

M. Philippe[1], J.P. Mercier[2] and J.P. Gué[1]

[1]Division du Cycle de Combustible
[2]Institut de Protection et Sûreté Nucléaire

Commissariat à l'Energie Atomique
Centre d'Etudes Nucléaires
Boîte Postale 6
92265 FONTENAY AUX ROSES
France

Abstract

The consequences of the failure of the cooling system of fission product storage tanks over a variable period were investigated as part of the safety analysis of the La Hague spent fuel reprocessing plant. Due to the considerable heat release, induced by the fission products, an prolonged shutdown of the tank cooling system could cause the progressive evaporation of the solutions to dryness, and culminate in the formation of volatile species of ruthenium and their release in the tank venting circuit.

To determine the fraction of ruthenium likely to be transferred from the storage tanks in volatile or aerosol form during the failure, evaporation tests were conducted by evaporating samples of actual nitric acid solutions of fission products, obtained on the laboratory scale after the reprocessing of several kilograms of MOX fuels irradiated to 30,000 MWday•t^{-1}. A distillation apparatus was designed to operate with small-volume solution samples, reproducing the heating conditions existing in the reprocessing plant within a storage tank for fission products.

The main conclusions drawn from these experiments are as follows:

- ruthenium is only volatilized in the final phase of evaporation, just before desiccation,
- for a final temperature limited to 160 °C, the total fraction of volatilized ruthenium reaches 12%,
- in the presence of H_2O, HNO_3, NO_x and O_2, the volatilized ruthenium recombines mainly in the form of ruthenium nitrosyl nitrates, or decomposes into ruthenium oxide (probably RuO_2) on the walls of the apparatus.

Assuming a heating power density of 10 W/liter of concentrate, and a perfectly adiabatic storage system, the minimum time required to reach dryness can be estimated at 90 h, allowing substantial time to take action to restore a cooling source. It is probable that, in an industrial storage tank, the heat losses from the tank and the offgas discharge ducts will cause recondensation and internal reflux, which will commensurately delay dryness and the release of the ruthenium from the solution.

1 Introduction

The problems raised by ruthenium in the radioactive offgases of a spent fuel reprocessing plant derive mainly from its complex chemistry and its high specific activity (essentially due to ^{106}Ru), since this fission product can in fact volatilize significantly during the evaporation or solidification of high-level liquid wastes.

Most of the ruthenium solubilized in dissolution is found in the raffinates of the first extraction cycles, which are then concentrated to a volume of 300 liters/t of uranium reprocessed, and then stored for at least one year before vitrification. These concentrates exhibit very high radioactivity and, due to a considerable heat release (about 10 W•liter^{-1} for a PWR fuel irradiated to 33,000 MWday•t^{-1} and cooled for three years before reprocessing), the tanks in which they are stored have to be cooled permanently.

The cooling systems are designed and maintained to perform their function with a very high level of reliability, so that a tank cooling system failure is extremely improbable. The analysis of the consequences of such an occurrence was nevertheless conducted as part of the safety analysis of the La Hague reprocessing plant, especially in order to determine the time interval after which a substantial release of radioactive materials could take place, and to evaluate the effectiveness of the emergency measures taken in such a situation. Due to the high activities present in the tanks, self-heating of the fission product concentrates, following a prolonged cooling system shutdown, could in fact culminate in their progressive evaporation up to desiccation, with these phases likely to cause the formation of volatile species of ruthenium liable to be released in the tank venting circuit. The evaluation of the activity transfer to the offgas system hence demands the knowledge of the fraction of ruthenium likely to escape from the storage tanks in volatile or aerosol form during the cooling shutdown. To do this, tests designed to simulate the progressive evaporation of a fission product solution in representative conditions were conducted on the laboratory scale with real concentrates, complying in particular with the heating power induced by the fission products.

2 Parameters affecting the volatilization of ruthenium in a cooling accident

The bibliography concerning ruthenium is extremely rich, but the tests conducted are sometimes not very systematic, and usually performed with synthetic solutions [1]. Among the factors governing the volatilization of ruthenium during effluent concentration operations, the following are generally distinguished.

- Solution concentrations in nitric acid and nitrates: while the effect of nitrates is less well understood, the volatility of ruthenium in nitric acid medium generally becomes high between 8 and 13 M, with volatile RuO_4 being formed by oxidation of the ruthenium nitrosyl complexes in solution.

- The presence of reducing agents: these products inhibit or delay the formation of RuO_4. They may be formed by radiolysis of the medium (HNO_2, H_2O_2), or introduced in the different steps of the process (TBP entrained in raffinates, denitration with formol).

- Solution storage time: the equilibrium of the different chemical species of ruthenium present in the concentrates is often slow to be established, and depends on the age of the solution. Storage also influences radiolysis in solution (production yield of certain species, degradation rate of organic compounds).

- Temperature: during evaporation, the oxidation kinetics of the ruthenium complexes depends directly on the temperature buildup profile. At higher temperatures, thermal decomposition of the ruthenium/nitrosyl complexes may also cause the formation of volatile RuO_4.

The large number of parameters involved precludes any precise and reliable prediction of the behavior of ruthenium during an FP tank cooling system shutdown. This nevertheless shows that the simulation tests are only significant if conducted with real solutions containing all the chemical elements likely to alter the behavior of the ruthenium, and in thermal conditions as close as possible to reality, especially the heating power released by the FP. This parameter will be preponderant, because it conditions the temperature buildup profile, the change in acidity of the solution, and the time required to reach dryness.

3 Experimental

The tests were conducted in a hot cell in order to:

- determine the liquid/vapor equilibrium curves of a real FP solution, to associate the change in temperature with that of the acidity of the concentrate in the subsequent tests,
- simulate the progressive vaporization of an FP concentrate to dryness, without taking any sample from the apparatus, to avoid disturbing the behavior of the different FP and to be able to compile their balances at the end of the operation.

Source of concentrates

The fission product concentrates used for these tests were obtained from the laboratory reprocessing of six MOX fuel rods containing 5% plutonium, irradiated to 30,000 MWday•t^{-1}. The raffinates of the first extraction cycle were concentrated to 300 l•t^{-1} with continuous denitration by the addition of formaldehyde.

The concentrate was then stored for six months for ageing before conducting the ruthenium volatilization tests. The composition of the FP concentrate is shown in Table 1. The activities are updated to the date of the tests, or after a cooling time of 1550 days (4·2 years).

Table 1

Composition of fission product concentrate

volume	315 l•t^{-1}	
chemical composition:		
• [HNO_3] M	1·8	
• [NO_3^-] M	8·1	
• [Mo] g•l^{-1}	2·4	
• [Zr] g•l^{-1}	6·6	
• [Fe] g•l^{-1}	13·6	
• [PO_4^{3-}] g•l^{-1}	0·24	
• [Ru] M	≈0·04	
β/γ activity:	TBq•m^{-3}	Ci•l^{-1}
• $^{144}Ce + ^{144}Pr$	5,032	136·0
• ^{125}Sb	118	3·2
• $^{106}Ru + ^{106}Rh$	4,603	124·4
• ^{134}Cs	3,718	100·5
• ^{137}Cs	11,255	304·2
• ^{154}Eu	725	19·6
total β/γ	25,452	687·9
total α activity	3,800	102·7
calculated residual power (W•l^{-1}):		
• α	3·57	
• β/γ	3·04	
• total	6·61	

Apparatus and procedure

The experimental rigs employed are shown in Figures 1 and 2. These systems were designed to operate with small volumes of concentrate (400 cm^3) and reproduce the actual heating conditions existing in a storage tank with a capacity of several tens of cubic meters.

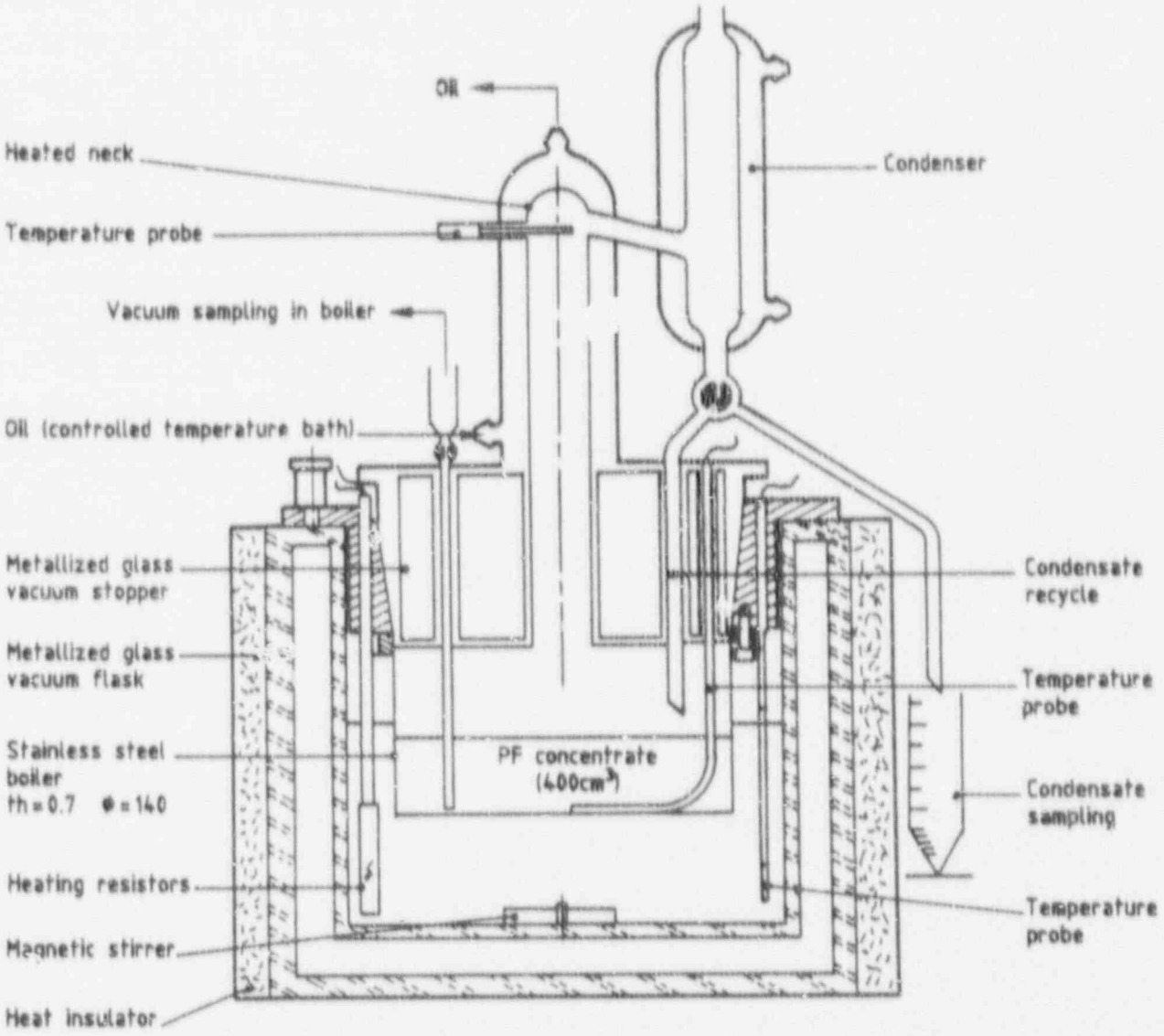

Figure 1 Apparatus used to determine liquid/vapor equilibrium curves

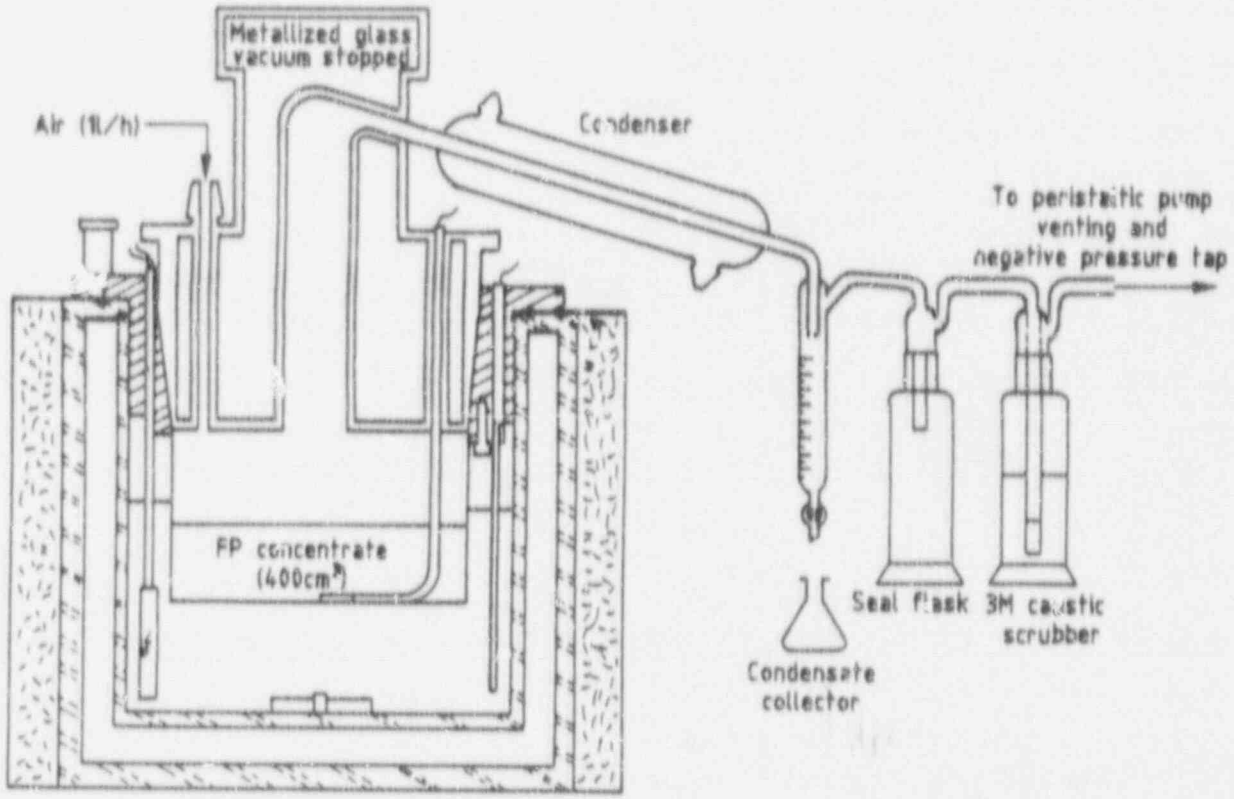

Figure 2 Apparatus used for the test of evaporation to dryness

Given the low heating power densities involved, the apparatus was fully insulated by a double wall of silver-plated glass under vacuum. The boiler tank was of stainless steel. Its cylindrical shape helped to keep the boiling surface area constant and to limit the variation in the heating surface area during evaporation. Heating was provided by oil circulation avoiding local overheating at the boiler wall. The heating power was adjusted in accordance with the heat balance. The heat really absorbed by the solution at any time was equal to the difference between the amount of heat supplied to the system and that lost to the exterior and absorbed by the apparatus. The determination of the mass of water and of the coefficient of thermal conductivity of the system as a function of temperature thus helps to calculate the total energy to be supplied to the system at any time to obtain the desired effective heating power.

During the tests, the heating power used was about 8 ±1·6 W (or a power density of 20 ±4 W/l of initial concentrate), and the heat losses reached up to nearly 80% of the total quantity of heat supplied at the end of evaporation.

The system used to determine the liquid/vapor equilibrium curves and shown in Figure 1 is distinguished by the heating of the neck to prevent partial liquid reflux in this zone. The method employed was direct distillation with recycle. Return of the condensate to the boiler ensured a fixed composition and equilibrium temperature in the fraction of solution remaining in the boiler. When equilibrium was reached, the distillate and concentrate were simultaneously sampled, and a larger fraction of the condensate withdrawn. The acidity and temperature of the concentrate then rose progressively until a new equilibrium was reached.

In the second system employed for the progressive vaporization of the concentrate and shown in Figure 2, the heating of the neck was eliminated, but the neck remained insulated by a double wall of silvered glass under vacuum. Only the condensate samples were taken periodically during the test. To avoid overpressures and vapor losses to the exterior, and also to take account of the air circulation in the storage tanks, the apparatus was placed under a slight air blanket (1 l•h^{-1}). The ruthenium volatilized in the test was trapped by a caustic scrubber.

4 Experimental results and discussion

4.1 Variation in acidity and temperature during vaporization of FP concentrates

The rough liquid/vapor equilibrium curves obtained with these FP concentrates are shown in Figure 3. These curves are compared with those of a water/nitric acid system.

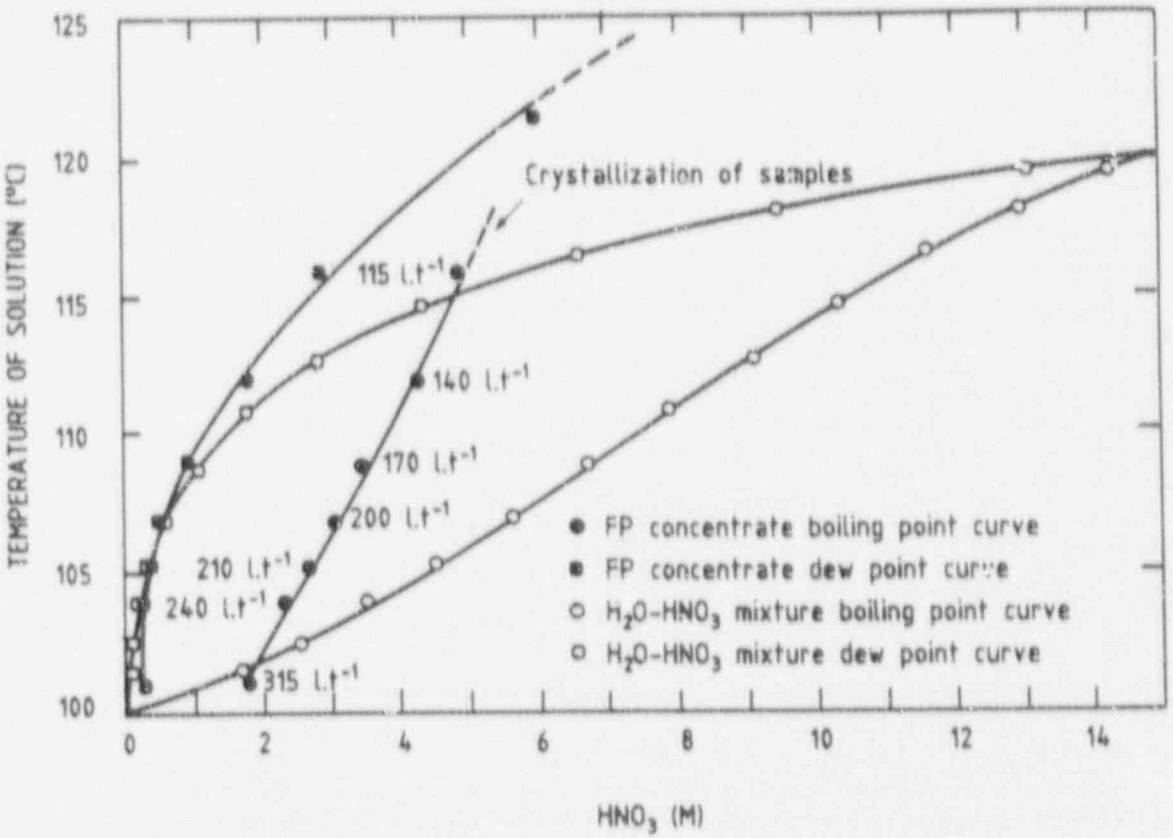

Figure 3 Liquid/vapor equilibrium curves of FP concentrate

As may have been expected, these two systems are quite different. For the same aqueous phase acidity, the boiling point is much higher for a solution containing saline nitrates than for an aqueous nitric acid solution. This is explained by the decrease in the partial pressure of the water due to the salts, causing a rise in the boiling point of the solution.

Above an acidity of 5 M (temperature 116 °C), the nitrate concentration is such that it is impossible to take any samples, because they crystallize at ambient temperature. From 130 °C, NO_x is also formed, indicating incipient decomposition of the nitrates. The acid balances that can be determined from the distillates are hence in excess, and no longer serve to estimate the real acidity of the boiler, and the

evaluation of the real volume of the liquid phase is also increasingly difficult due to the growing formation of precipitates. However, concentration was continued to dryness. The final acidity of the condensate was 11.5 M for a boiler temperature of over 150 °C, a much higher temperature than that corresponding to the azeotrope of the water/nitric acid mixture (120 °C).

The first data finally provided by this test can be summarized as follows.

- Variation in the acidity/temperature pair during vaporization is only significant for nitric acid concentrations of 5 M or less.
- The final temperature during the precipitate dryness phase is about 150 °C.
- Incipient decomposition of the nitrates is observed, and the concomitant appearance of NO_x from 130 °C.

4.2 Behavior of ruthenium during vaporization in the desiccation of FP concentrates

The experiment was conducted this time in a single step, without any samples taken from the boiler. Dryness was reached in 70 h (t = 0 corresponding to the equilibrium temperature of the FP tanks, or 60 °C). This interval was increased by the existence of an internal reflux estimated at 30% of the total flow rate of the vapors leaving the solution. After dryness, the residues were kept at 160 °C (experimental limitation) for nearly 20 h.

The cumulative volume of distillate collected and the change in the concentration of the solution are shown as a function of time in Figure 4. Dryness was reached at a concentration equivalent to 22 l·t^{-1}.

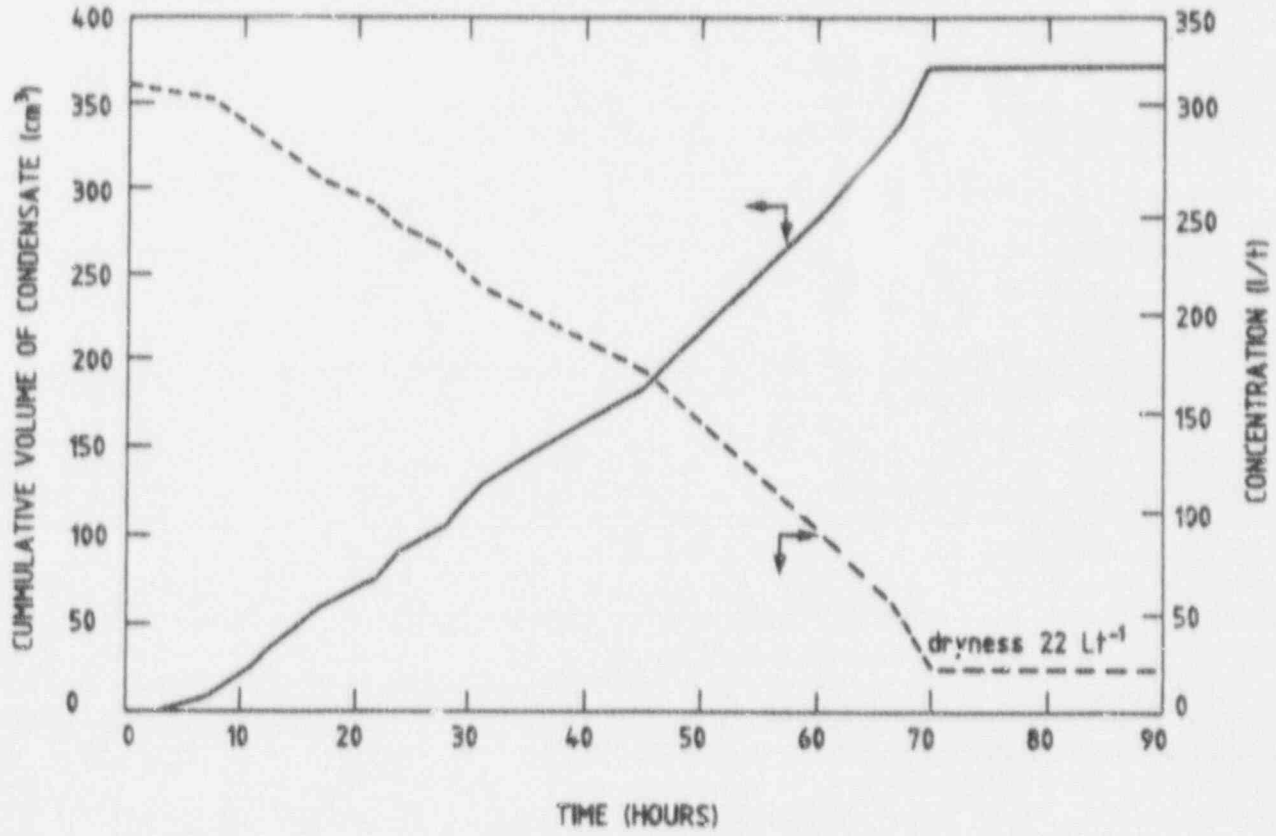

Figure 4 Cumulative volume of condensate and concentration as a function of time

The temperature buildup profiles of the solution and the heating bath are shown as a function of time in Figure 5. During the first 50 h, the solution temperature stabilized at around 102 to 103 °C. It then increased rapidly up to 150 °C before reaching desiccation.

Figure 6 shows the change in activity of the condensate, and in the total percentage of acid distilled as a function of time. As above, it can be observed that:

- the acidity of the condensate rises suddenly after the distillation of about 75% of the volume of initial solution, to reach a plateau at around 11·5 M,
- the amount of acid recovered in the condensate is more than 20% higher than the number of initial moles (partial recombination of NO_x produced by destruction of the nitrates).

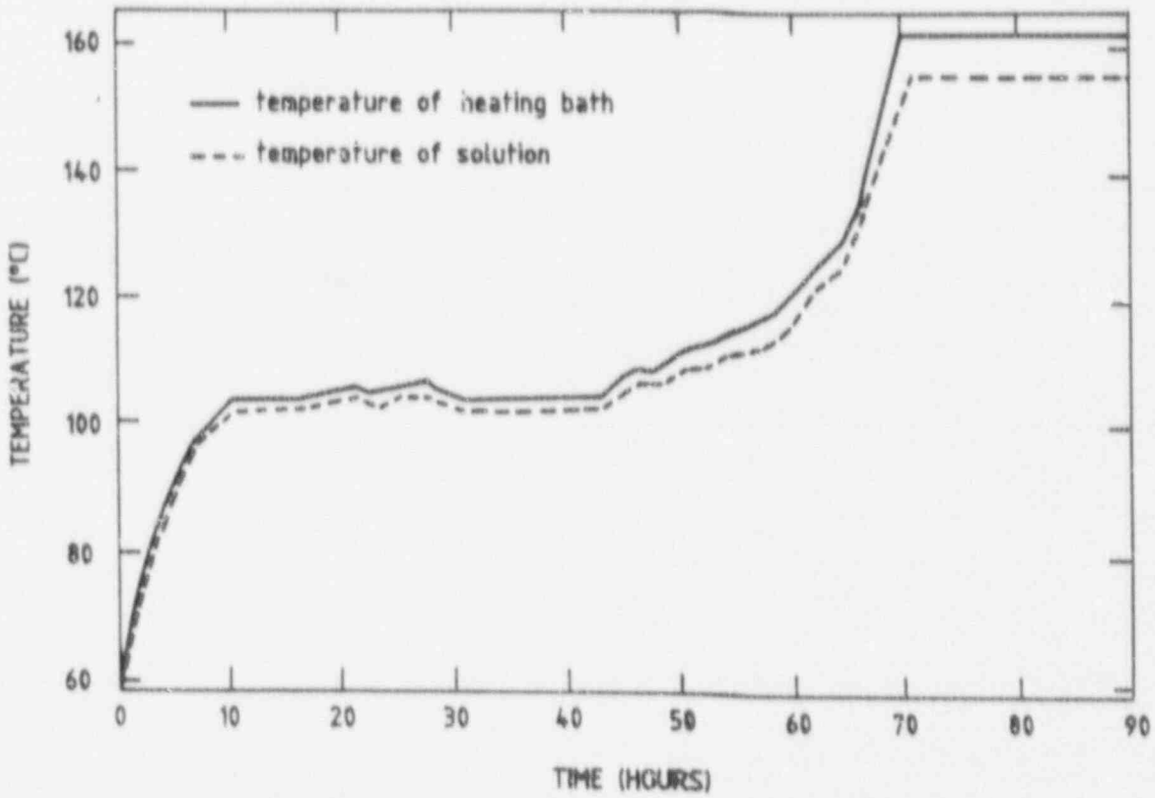

Figure 5 Temperature rise as a function of time

Figure 7 compares the variation in time of the ^{106}Ru fraction recovered in the distillates with those of ^{137}Cs and of the α emitters considered as non-volatile (fractions expressed with respect to the initial activities in the concentrates). Note that the behavior of the other FP measured (^{134}Cs and ^{144}Ce) is identical to that of ^{137}Cs throughout evaporation.

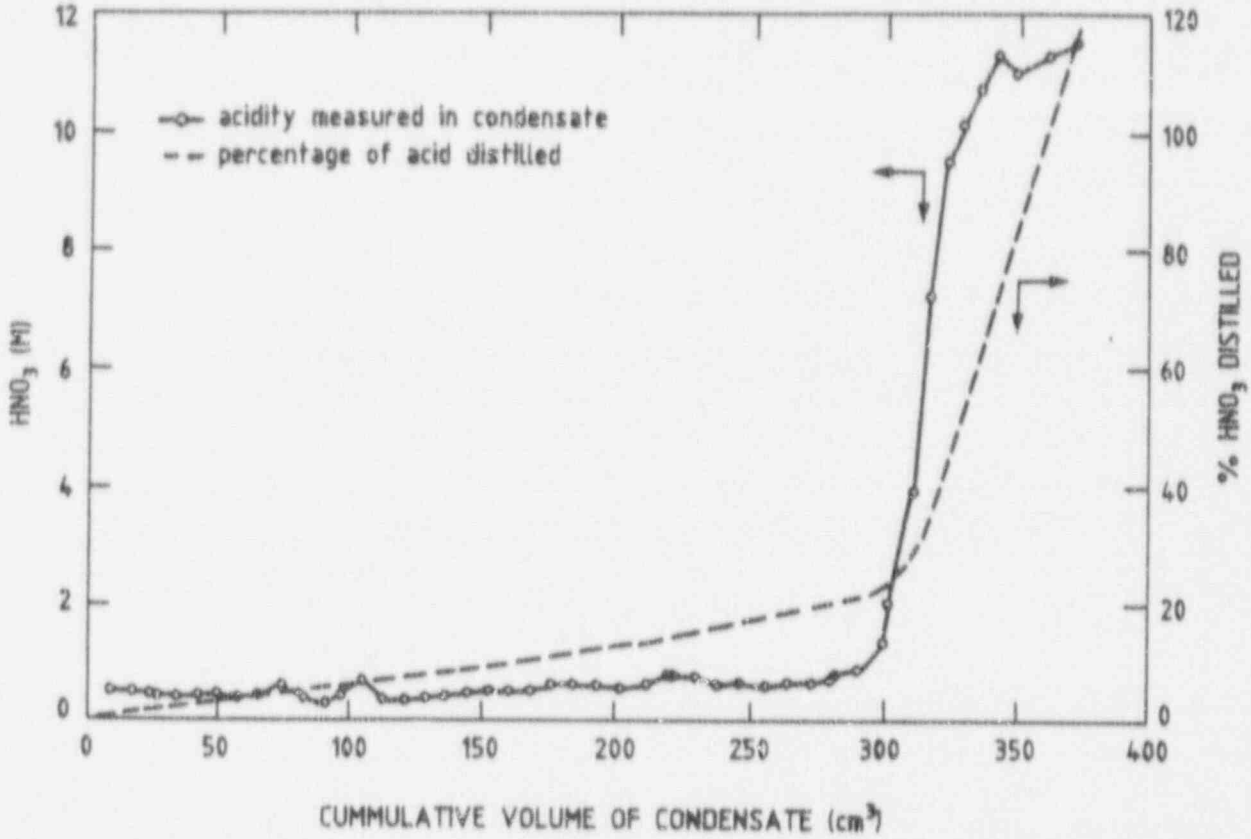

Figure 6 Condensate activity as a function of distilled volume

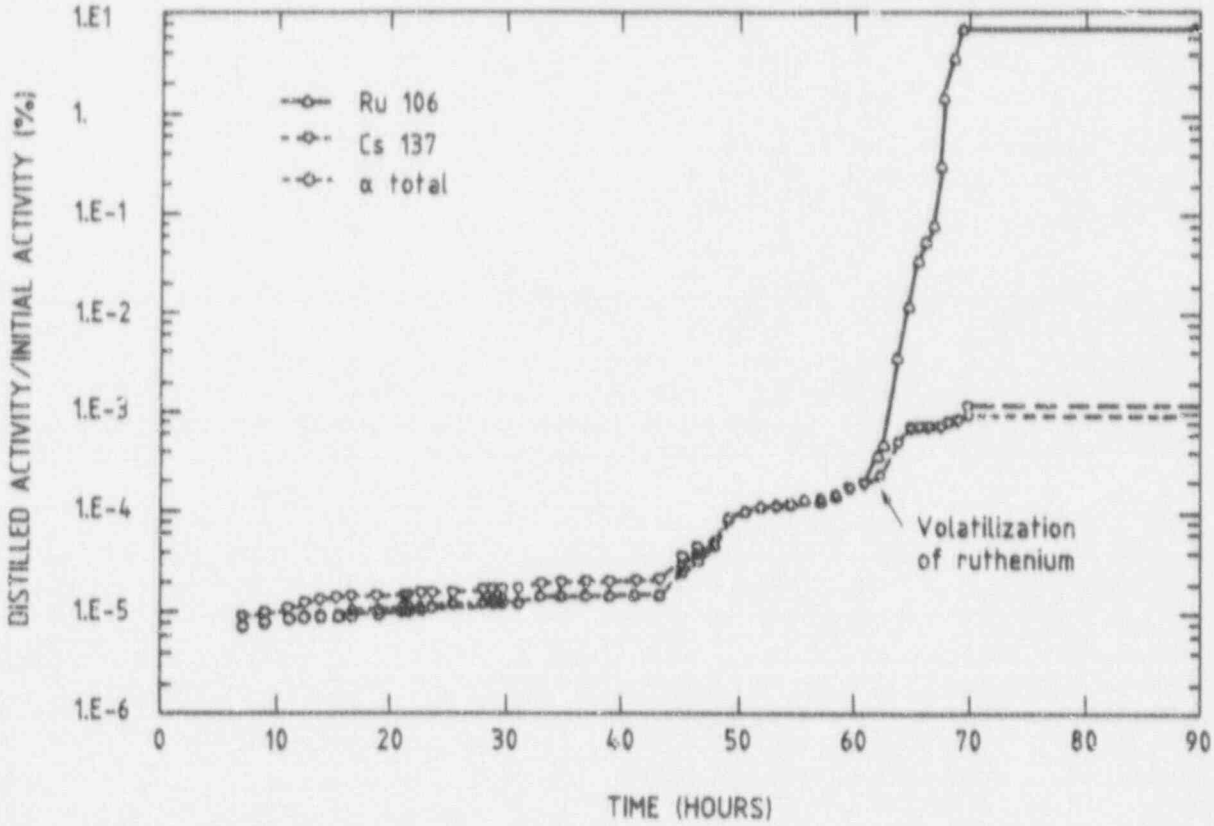

Figure 7 Percentage of distilled activity as a function of time

These curves finally show that ruthenium is volatilized after 60 h (brown coloration of the condensates), together with a sudden increase in acidity of the condensate pointed out above. This volatilization is effective from:

- a concentration of 85 $l \cdot r^{-1}$,
- a solution temperature of 119 °C,
- acidity of about 6 M in the boiler.

The ruthenium thus leaves in the final evaporation phase corresponding to the formation and the desiccation of the residues, thus confirming the results of previous studies conducted on simulated FP solutions [2,3].

Table 2 shows the final balance of ruthenium and of the main radioisotopes transferred from the tank during vaporization. The fractions of activity recovered in the condensate, the caustic trap and the evaporator rinse solution (neck and condenser) are expressed with respect to the initial activities of the concentrate.

Table 2

Balance of main radioisotopes transferred from the tank

		activity recovered (% of initial activity)					
radioisotope	initial activity GBq (Ci)	in solution in the condensate	in the caustic trap	in the apparatus rinse solution	in precipitate form	total distilled	
^{106}Ru	921 (24·9)	7·09	$2{\cdot}4 \cdot 10^{-4}$	3·33	1·68	12·1	
^{137}Cs	4503 (121·7)	$1{\cdot}12 \cdot 10^{-3}$	$7 \cdot 10^{-5}$	$2{\cdot}6 \cdot 10^{-4}$	-	$1{\cdot}45 \cdot 10^{-3}$	
α emitters	1520 (41·08)	$9{\cdot}1 \cdot 10^{-4}$	-	$2{\cdot}2 \cdot 10^{-4}$	-	$1{\cdot}13 \cdot 10^{-3}$	

Most of the volatilized ruthenium is found in the condensate (7% of total Ru) and not in the caustic trap ($\approx 10^{-4}$%). The share due to droplet entrainment is very small, representing a maximum of 0·01% of the total amount volatilized.

Visible/UV spectrophotometry (Figure 8)was used to confirm that the species solubilized in the condensate and the rinse solution were mainly in the form of complexes of ruthenium nitrosyl nitrates [5]. It can therefore be assumed that RuO_4, or possibly other volatile species of the RuNO type, such as those reported by Klein *et al* [4] are instantaneously recombined in the condenser in the presence of H_2O, HNO_3, NO_x and O_2 to form the foregoing complexes. These observations are confirmed by the sudden drop in the nitrous acid content in the condensates, observed from the onset of ruthenium volatilization (Figure 9).

The apparent volatilization rate constant, determined assuming a first-order kinetics, is $5{\cdot}3 \cdot 10^{-4}$ min^{-1} between 140 and 160°C. This figure is higher than the constant determined in 9 to 13 M boiling nitric acid medium for similar Ru concentrations [6,7]. The very clear influence of the nitrates and of the temperature on the ruthenium volatilization process is hence confirmed in these ranges close to dryness.

At the end of the experiment, the walls of the tank and the neck appear to be covered by a black deposit, insoluble in nitric acid. These fine particles, averaging 7 µm in size (measured by sedimentation), represent about 15% of the total quantity of ruthenium volatilized. This implies that part of the volatilized RuO_4 is thermally decomposed by the reaction:

$$RuO_4 \longrightarrow RuO_2 \downarrow + O_2$$

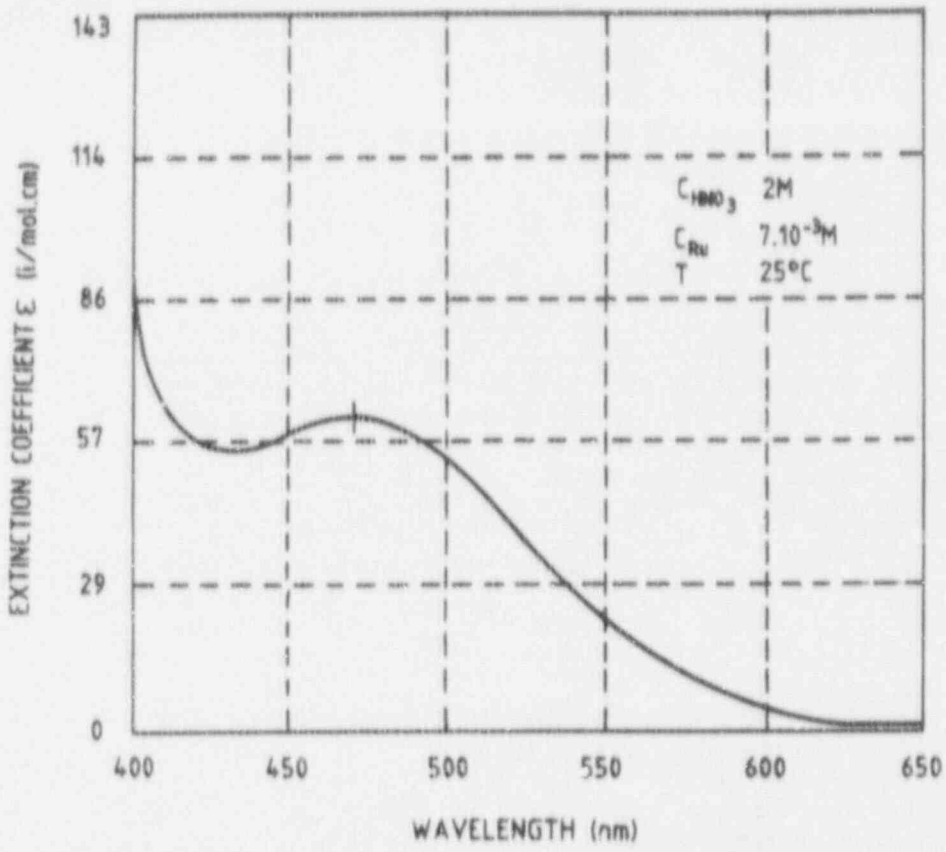

Figure 8 Absorption spectrum of ruthenium in condensate

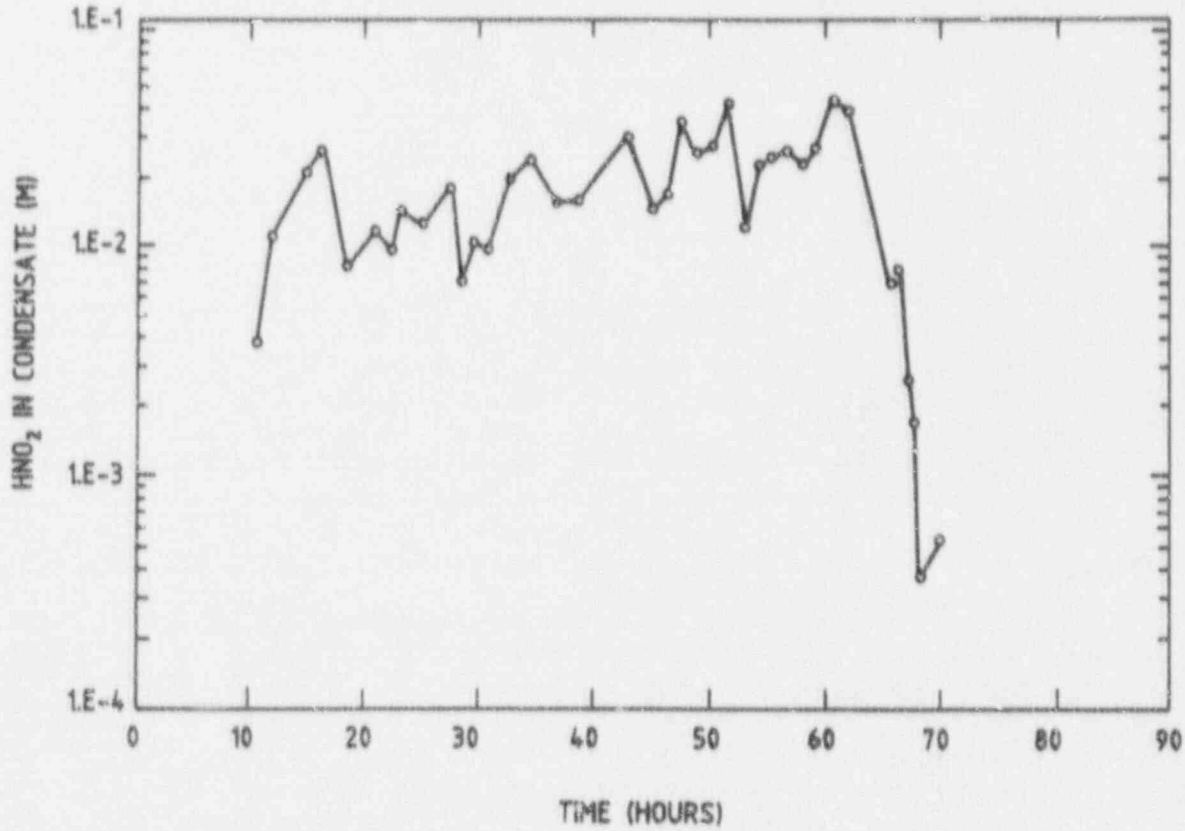

Figure 9 Nitrous acid measured in distillate as a function of time

or could have reacted with the NO_x present in the apparatus according to reactions of the following type [8]:

$$RuO_4 + 2NO \Leftrightarrow RuO_2 \downarrow + 2NO_2$$
$$RuO_4 + 4NO_2 \Leftrightarrow RuO_2 \downarrow + 2N_2O_5$$

However, ruthenium dioxide was not formally identified.

These experiments finally serve to distinguish three phases in the ruthenium release process.

- The boiling phase in which ruthenium transfer from the tank is slight and only occurs through the formation of aerosols entrained by the vapor with the other fission products.
- The phase approaching dryness, when the ruthenium begins to oxidize or to decompose locally, and when the transfer of radioactivity by volatilization of this element predominates over transfer in the form of aerosols with the other fission products.
- The final drying and calcination phase, in which the volatilized RuO_4 is decomposed on the tank walls or reacts with the NO_x probably to form solid RuO_2. These fine particles, given the extremely small gas flow rate, tend to redeposit on the apparatus walls.

5 Industrial scaling up

These tests finally demonstrated that the risk of ruthenium volatilization, in the case of the prolonged shutdown of the FP tank cooling system, would only exist in the ultimate phase of evaporation approaching dryness. During this final phase, the quantities of ruthenium likely to be transferred to the stack of the plant will depend on local conditions (temperature, NO_x, scavenging air, wall surface area) and especially on the holdup of the lines and the rate of aerosol entrainment.

Consequently, the time required to vaporize the concentrates completely will determine the maximum time allowed to the reprocessing plant operators to take remedial action. Based on the distillation rates measured experimentally, and assuming a heating power density of 10 $W \cdot l^{-1}$, this period could be about 90 h (including 5 h of rise to boiling point). In these conditions, volatilization of the ruthenium would only become effective after the 75th hour, leaving substantial time to restore a cooling source.

It is also probable that, in an industrial storage unit, the heat losses in the ducts of the offgas discharge system will cause local condensation and hence internal reflux in the storage tanks, which will commensurately delay the release of the ruthenium from the solution.

It is in fact very unlikely that complete evaporation of the stored solutions could occur, rather leaving the possibility of an equilibrium established between the power released by the FP and the heat losses of the tank and its vents.

It is nonetheless the operator's duty to minimize the scavenging air flow rate in the tanks, because this could shift the liquid/vapor equilibrium and accordingly accelerate the evaporation rate of the solution.

6 Conclusions

The experiments described in this document were conducted in order to analyze a prolonged accidental shutdown of storage tanks for fission product solutions in a spent fuel reprocessing plant. These tests, performed on a real FP solution, demonstrated very clearly that the volatile species of ruthenium are only formed in the ultimate phase of evaporation, close to dryness. During this phase, the transfer of activity by the volatilization of this element will prevail over simple contamination by aerosols. These volatile species nevertheless prove to be highly unstable, and could recombine mainly in the form of soluble complexes of ruthenium nitrosyl nitrates, or decompose, probably to RuO_2, depending on local conditions. These experiments also demonstrated that, on the industrial scale, the minimum time

available before the release of the ruthenium from the solution would be more than three days, leaving the plant operators substantial time to restore a cooling source.

References

[1] J.D. Christian, Process behavior and control of ruthenium and cesium
ANS AICHE Meeting, 5/6 August 1976

[2] C.E. May, B.J. Newby, K.L. Rohde and B.D. Withers, Fission product ruthenium volatility in a high-temperature process
IDO-14439, July 1958

[3] A. Ortins de Bettencourt and A. Jouan, Volatility of ruthenium during vitrification of fission products, 1 Distillation of nitric acid solutions and calcination of the concentrates
CEA R-3663 (I), January 1969 (in French)

[4] M. Klein, C. Weyers and W.R.A. Goossens, Volatilization and trapping of ruthenium in high-temperature processes
Paper 4-5 to 17th US DOE Air Cleaning Conference, 2/5 August 1982

[5] J.M. Fletcher, Nitrosyl ruthenium nitrato complexes in aqueous nitric acid
J.Inorg.Nucl.Chem., **12** 154-173 (1959)

[6] A. Sasahira and F. Kawamura, Short Note, Formation rate of ruthenium tetroxide during nitric acid distillation
J.Nucl.Sci.Technol., **25** (7) 603-606 (1988)

[7] T. Sato, Volatilization behaviour of ruthenium from boiling nitric acid
J.Radioanal.Nucl.Chem., **129** (1) 77-84 (1989)

[8] R.D. Brittain and D.L. Hildenbrand, Gas phase reactions of ruthenium tetroxide with nitrogen oxides
DOE/SR/00001-T120, Final Report, 5 April 1985

POOL FIRES IN A LARGE SCALE VENTILATION SYSTEM

by

P.R. Smith and I.H. Leslie
New Mexico State University

and

W.S. Gregory and B. White
Los Alamos National Laboratory

Abstract

A series of pool fire experiments was carried out in the Large Scale Flow Facility of the Mechanical Engineering Department at New Mexico State University. The various experiments burned alcohol, hydraulic cutting oil, kerosene, and a mixture of kerosene and tributylphosphate. Gas temperature and wall temperature measurements as a function of time were made throughout the $23.3m^3$ burn compartment and the ducts of the ventilation system. The mass of the smoke particulate deposited upon the ventilation system $0.61m \times 0.61m$ HEPA filter for the hydraulic oil, kerosene, and kerosene-tributylphosphate mixture fires was measured using an in situ null balance. Significant increases in filter resistance were observed for all three fuels for burning time periods ranging from 10 to 30 minutes. This was found to be highly dependent upon initial ventilation system flow rate, fuel type, and flow configuration.

The experimental results were compared to simulated results predicted by the Los Alamos National Laboratory FIRAC computer code. In general, the experimental and the computer results were in reasonable agreement, despite the fact that the fire compartment for the experiments was an insulated steel tank with 0.32cm walls, while the compartment model FIRIN of FIRAC assumes 0.31m thick concrete walls. This difference in configuration apparently caused FIRAC to consistently underpredict the measured temperatures in the fire compartment. The predicted deposition of soot proved to be insensitive to ventilation system flow rate, but the measured values showed flow rate dependence. However, predicted soot deposition was of the same order of magnitude as measured soot deposition.

Introduction

In this paper we describe the results of a series of pool fire experiments carried out in the Large Scale Flow Facility (LSFF) at New Mexico State University (NMSU), a full scale ventilation system similar to those found in nuclear facilities. The fuels used were methyl alcohol, kerosene, a "non-flammable" cutting oil, and a mixture of kerosene and tributylphosphate (TBP). The purpose of these pool fire experiments was to study the transport of the heat and smoke generated through the ventilation system to further verify the FIRAC[1] computer code developed by Los Alamos National Laboratory (LANL) through the use of realistic fuels and ventilation system configurations. In particular this series of experiments was intended to test the FIRIN compartment fire module of the FIRAC computer code.

The FIRIN module was developed by Pacific Northwest Laboratories (PNL) and was integrated into the FIRAC code to describe the combustion process[1] in a single compartment. The FIRIN module uses a zonal model that couples the hot and cold layers within the compartment. The module provides the capability of simulating pool or crib fires and predicts temperatures within the compartment and heat transfer through the compartment walls. Although FIRIN has other capabilities, such as prediction of oxygen concentration, changes in mass flow rates, etc., only temperature predictions were emphasized in this series of tests.

A secondary purpose of the experiments was to evaluate the prediction of soot produced and mass accumulated on the exhaust High Efficiency Particulate Air (HEPA) filter. The Experiments test both FIRIN's soot predictive capabilities and FIRAC's transport and filter plugging predictions.

Description of the Experiments

The LSFF is a laboratory of the Mechanical Engineering Department of NMSU located in Las Cruces, New Mexico. Figure 1 is a schematic of the full scale model ventilation system which consists of two room sized volumes connected by steel ducting. The model ventilation system is housed within a large prestressed concrete building which provides environmental control. The system is designed to accomodate thermal, pressure and aerosol inputs. Thermal input can be from a natural gas fired duct heater rated at 92000 kcal/h or by burning pool or crib fires in one of the simulated rooms. Pressure pulses are limited to a 140 kPa overpressure.

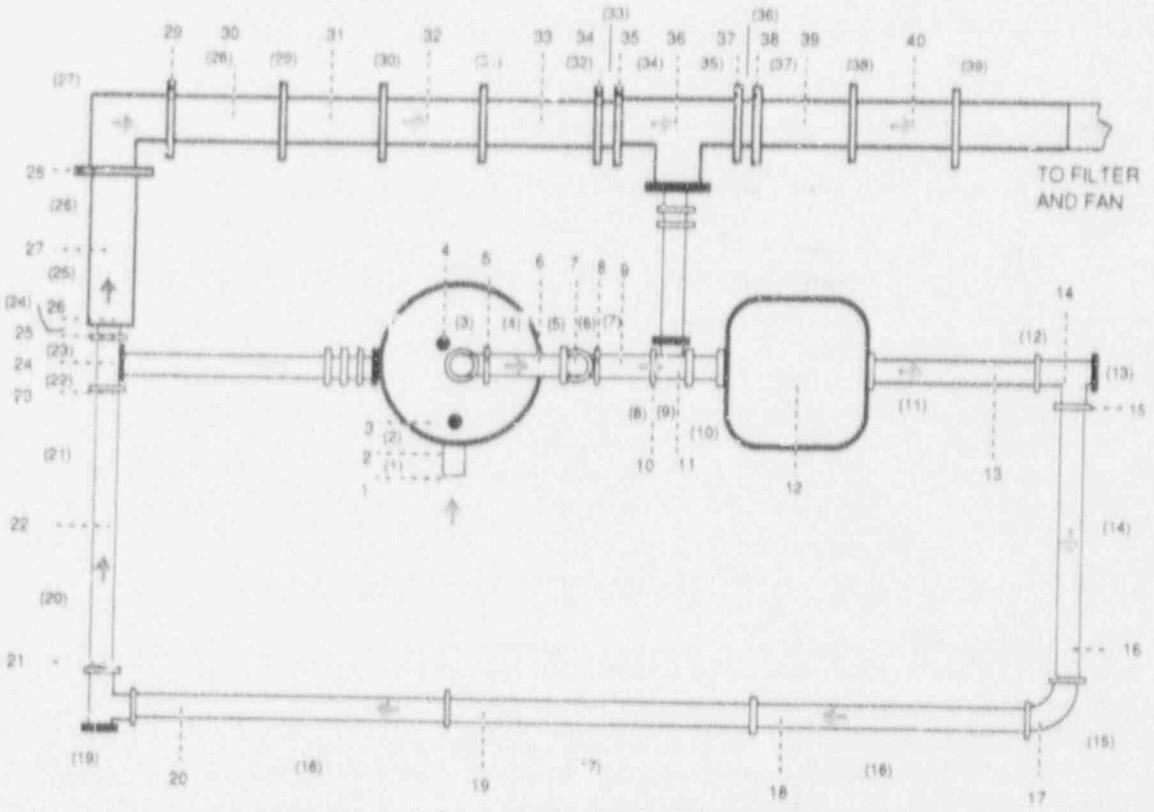

Figure 1 Schematic of Full Scale Ventilation System, Config.1

The arrangement of ducts and rooms of the ventilation system is shown in Figure 1. Schedule 20 pipe, 30.5cm in diameter, is used for a by-pass loop around the two rooms. The remainder of the ducting was fabricated from 0.64cm steel plate and has a flow cross-section which is 0.6m by 0.6m square. For a detailed description of the ventilation system see reference 2. The pool fire experiments reported in this paper used various configurations of the system, depending upon the fuel burned; these configurations will be described as each experiment is described.

Temperature measurements throughout the ventilation system were made with type J thermocouples. Wall temperatures were made using thermocouples peened into the steel walls. Gas temperatures at the centerlines of ducts and rooms were measured with shielded thermocou-

ples. Flow rate through the ventilation system, generated by a centrifugal blower (capable of a maximum flow rate of 5000cfm) located at the outlet of the ventilation system, was measured 30 duct diameters downstream of the fan outlet with a pitot tube connected to two Validyne DP103 pressure transducers (±0.01psid range). Pressure drop across the exhaust HEPA filter located upstream of the blower was measured using a Validyne DP7 pressure transducer (±1.0psid range). Temperatures, flow rate, and pressure drop across the HEPA filter were recorded at set time intervals using an HP 9845B data acquisition system. Burn times were measured with a stop watch.

The mass gained by the exhaust HEPA filter during the burn experiments was measured by a null balance system connected directly to the filter. This system had a least count of about 4g. See reference 2 for details.

All the pool fires were burned in a pan 0.615m above the bottom of the cylindrical tank shown in Figure 1. The pan has dimensions 0.33m wide, 1m long and 0.152m deep. The cylindrical tank is 2.74m in diameter and has a volume of 24.3m^3 with a nominal height of 4.1m. The walls of the tank are 0.635mm in thickness. The tank has openings at the top and bottom centerline and on the side 1.27m from the bottom. All these openings are 0.307m in diameter.

Table 1 lists the heights of the cylindrical tank centerline thermocouples above the bottom of the tank. Notice that thermocouple CT4 is actually located in the 0.307m pipe extending upward from the top opening of the tank.

Table 1 Location of Cylindrical Tank Centerline Thermocouples

Thermocouple No.	Height, m
CT1	0.85
CT2	2.41
CT3	3.95
CT4	4.54

Kerosene Pool Fires

Two flow configurations were used for the kerosene tests. The first configuration is shown in Figure 1. The flow enters the bottom of the cylindrical tank and follows the path through the ventilation system shown by the arrows. The second configuration is pictured in Figure 2. In this configuration, the bottom opening of the cylindrical tank is closed and the flow enters the tank from the top opening and flows out the side opening and along the path through the ventilation system, as indicated by the arrows. The total length of each flow path is about 70m.

Five experiments were run, each burning 5 liters of kerosene: two in configuration 1 (Figure 1) at 500cfm and 1000cfm flow rate; and three in configuration 2 (Figure 2) at 1000cfm, 1200cfm and 1700cfm flow rate. These experiments are summarized in Table 2 as tests KER03 through KER07.

Table 2 Kerosene Burn Tests

Test No.	Configuration	Nominal Flow Rate, cfm	Burn Time, min.	Filter ΔP Increase cm H_2O	Filter Mass Gain, g
KER03	1	500	12.80	4.57	137
KER04	1	1000	13.79	3.31	156
KER05	2	1000	5.30	3.56	61*
KER06	2	1700	6.93	4.32	106
KER07	2	1200	10.45	2.04	82

* Fire went out with about 1 liter of kerosene left in pan.

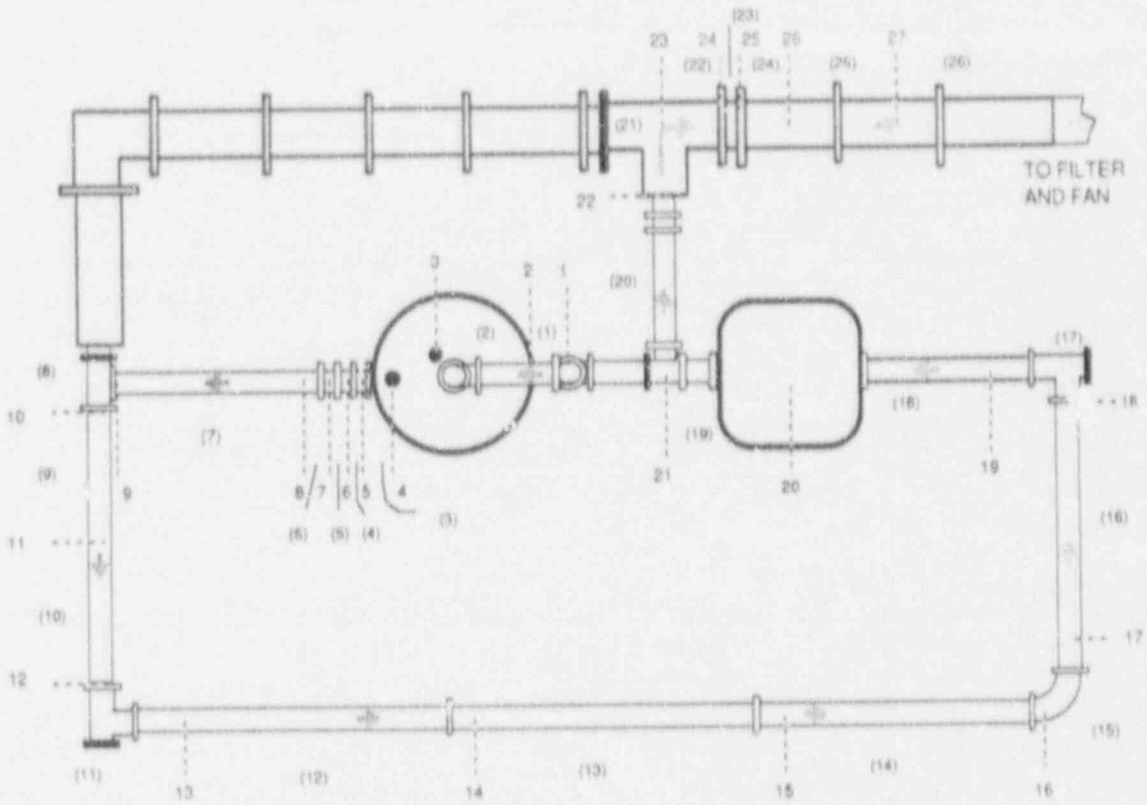

Figure 2 Ventilation System Configuration 2

Methyl Alcohol Burn Tests

The configuration of the ventilation system for the methyl alcohol burn tests (called configuration 3) is shown in Figure 3. The air enters the bottom of the cylindrical tank, exits the top and flows through the system as shown by the arrows. The total length of the flow path is about 20m. Four tests were run: two without insulation on the cylindrical burn tank, and two with a nominal 7.62cm blanket of fiberglass insulation over the entire surface of the tank. The conduction coefficient of the insulation was 0.04 $W/m^2 - K$. Table 3 summarizes the methyl alcohol burn tests, tests FUEL05 through FUEL08.

Table 3 Methyl Alcohol Burn Tests

Test No.	Insulation	Amnt.of Fuel, ℓ	Nom. Flow Rate, cfm	Meas. Flow Rate, cfm	Burn Time, min.	Fltr.Mass Gain, g
FUEL05	No	15	600	542	29.05	19.0*
FUEL06	No	15	1000	1008	31.14	-37.6**
FUEL07	Yes	15	1000	992	31.39	-23.9**
FUEL08	Yes	15	600	599	30.51	21.3*

*A large amount of condensation took place, so weight gain was probably water.

**Weight loss apparently due to drying of the filter during test.

Notice that all the alcohol burn tests used 15 liters of methyl alcohol and that two nominal flow rates were used: 600cfm and 1000cfm.

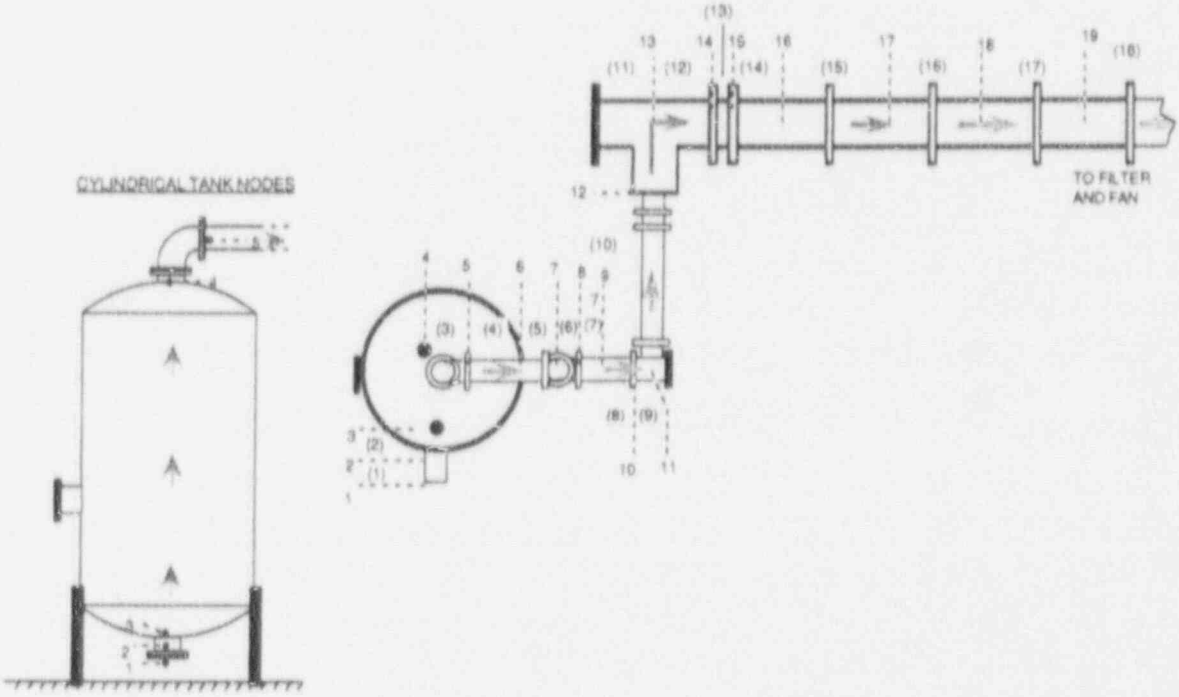

Figure 3 Ventilation System Configuration 3

Cutting Oil Burn Tests

Two burn tests were run with Rectorseal Dark Thread Cutting Oil. Configuration 3 (Figure 3) was used for both tests, one at a nominal flow rate of 600 cfm and one at 1000 cfm. The cylindrical burn tank was insulated, as described above, for both tests. Table 4 summarizes these as tests FUEL09 and FUEL10.

Table 4 Cutting Oil Burn Tests

Test No.	Insulation	Amnt.of Fuel, ℓ	Nom.Flow Rate, cfm	Meas.Flow Rate, cfm	Burn Time, min.	Fltr.ΔP Incr., cm H_2O	Fltr.Mass Gain, g
FUEL09	Yes	4	1000	1032	30.27	9.02	333.3
FUEL10	Yes	5	600	613	27.30	8.51	328.3

Kerosene-TBP Burn Tests

A mixture of 70.6% (by volume) kerosene and 29.4% TBP (3.0 liters of kerosene and 1.25 liters of TBP) was burned using configuration 3 (Figure 3) of the ventilation system. Three nominal flow rates were used: 600 cfm, 800 cfm, and 1000 cfm. The cylinderical burn tank was insulated, as described above, for all three tests. Table 5 summarizes the tests as tests FUEL11 through FUEL13.

Table 5 Kerosene-TBP Burn Tests

Test No.	Insulation	Amnt.of Fuel,	Nom.Flow Rate, cfm	Meas.Flow Rate, cfm	Burn Time, min.	Fltr.ΔP Incr., cm H_2O	Fltr.Mass Gain, g
FUEL11	Yes	4.25	600	1018	13.49	8.84	424.8
FUEL12	Yes	4.25	600	605	15.19	1.78	314.3
FUEL13	Yes	4.25	800	848	15.32	1.52	338.6

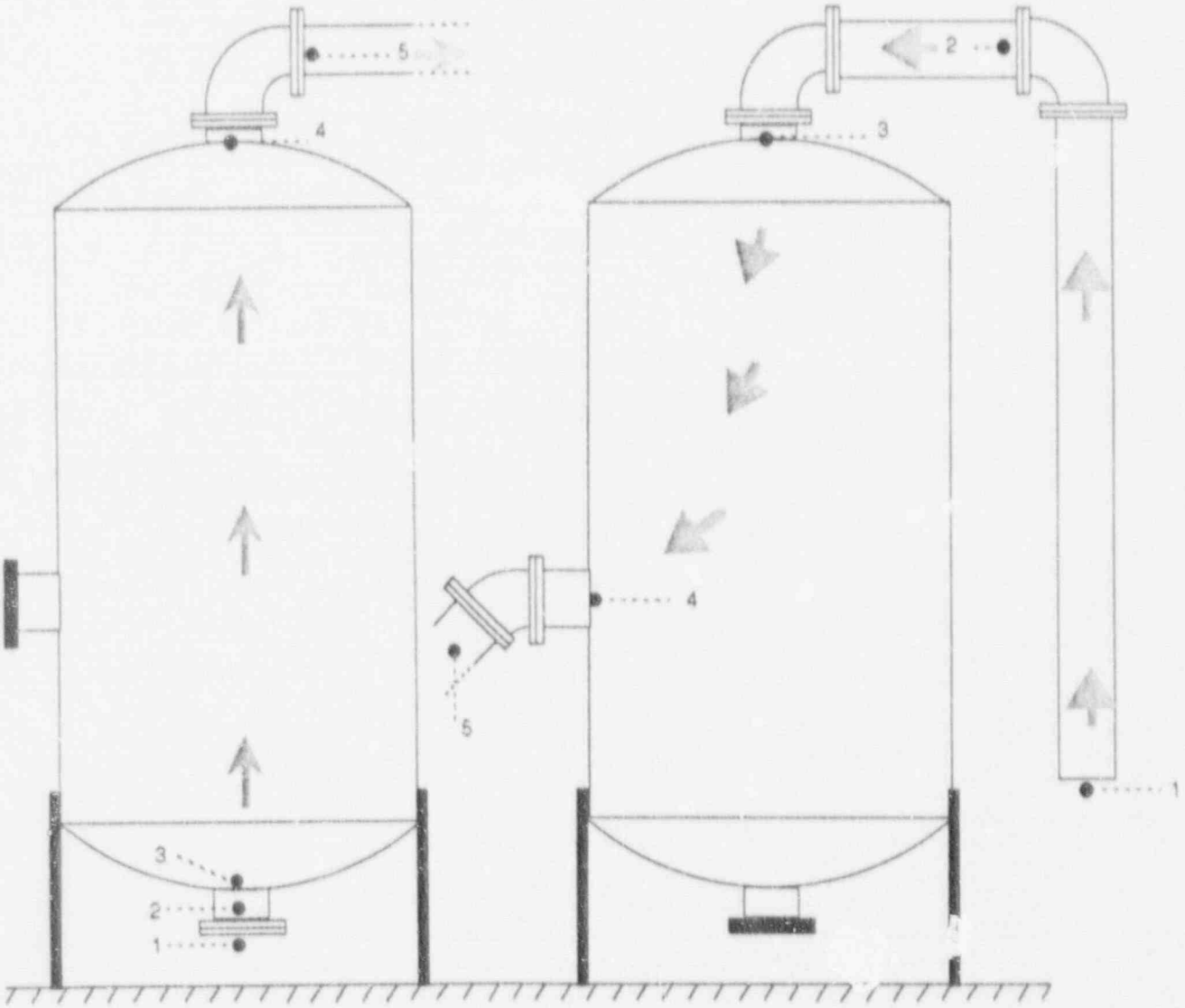

Figure 4 Burn Tank-Configuration 1

Figure 5 Burn Tank Configuration 2

Results and Discussion

In the following sections we discuss the experimental results and compare them to the results of the FIRAC computer simulations in the case of kerosene and kerosene plus TBP.

Kerosene Burn Tests Compared to FIRAC Simulation

The FIRAC node locations are shown in Figures 4 and 5. Figure 4 shows (for configuration 1) that nodes 1, 2, and 3 represent the characteristics of the incoming air flow, while nodes 4 and 5 model the exhaust flow from the burn tank for tests KER03 and 04. Figure 5 shows (for configuration 2) nodes 1, 2, and 3 characterizing the incoming air flow and nodes 4 and 5 modeling the exhaust flow from the burn tank for tests KER06 and 07. Downstream nodes for both configurations are shown in Figures 1 and 2.

Four plots are presented from FIRAC output for tests KER03, KER04, KER06, and KER07. KER05 was neglected because the fire terminated before all the fuel was consumed. Each plot presents the hot layer temperature predicted by FIRAC compared with tank CT measured temperatures. Other information such as hot layer height, O_2, CO_2, CO, and smoke concentration, fuel burning rate, pressures at branches, volumetric flow rates at branches, etc. can be found in reference 3.

Figures 6 through 9 give the comparisions of the FIRAC predicted hot layer temperature and the temperatures measured in the experiments at the four tank centerline locations. KER03 (Figure 6) has a flow rate of 500cfm entering the bottom of the tank. This low flow rate causes the hot layer to extend down to the floor. The measured tank temperatures peak at about 475°F (246 °C) while the FIRAC temperatures peak at about 375°F (190.6°C).

FIRAC predictions for KER04 are shown in Figure 7. The flow rate for KER04 was 1000cfm. The effect of this higher flow rate was manifested by a hot layer extending to approximately 2.5m above the floor, i.e. the higher flow rate pushed the hot layer up. The FIRAC temperature predictions decreased from those predicted in KER03 (135°C compared to 190.6°C). However, the experimental temperatures increased (274°C compared to 246°C for KER03). The underprediction of temperatures was also true for nodes throughout the remainder of the ventilation system[3].

Tests KER06 and 07 were performed with configuration 2. Configuration 2 has the fresh air entering the top of the burn tank and exiting the side of the tank about 2.4m above the tank bottom. This configuration did not allow use of the flow rates of 500cfm and 1000cfm. Instead, KER06 had a flow rate of 1700cfm and KER07, 1200cfm. Below these flow rates the burning caused instabilities that blew out the pool fire.

Figure 8 gives the tank temperature results for KER06. The hot layer in this case extended to the floor of the burn tank and the temperature of the hot layer exhibited an initial spike up to approximately 340°F (171°C) but then dropped back to a range of 225-250°F (107-121°C). Only CT4, at the top of the tank, compared favorably with the FIRAC prediction. However, the hottest temperatures experimentally were in the lower part of the tank, e.g. 770°F (410°C) measured compared to 340°F (171°C) predicted. As a result of these underpredictions in the burn tank, FIRAC also underpredicted the temperatures downstream in the rest of the ventilation system[3].

The FIRAC comparison to the experimental results for KER07 is shown in Figure 9. The results are very similar to those for KER06, except the peak temperatures are slightly lower.

A comparison of the predicted mass gain on the HEPA filter and that measured during the experiments is shown in Table 6. Table 6 indicates that the predicted deposition was of the same order of magnitude as the measured deposition. However, the predicted results are not sensitive to the two flow configurations or two flow rates used for the experiments.

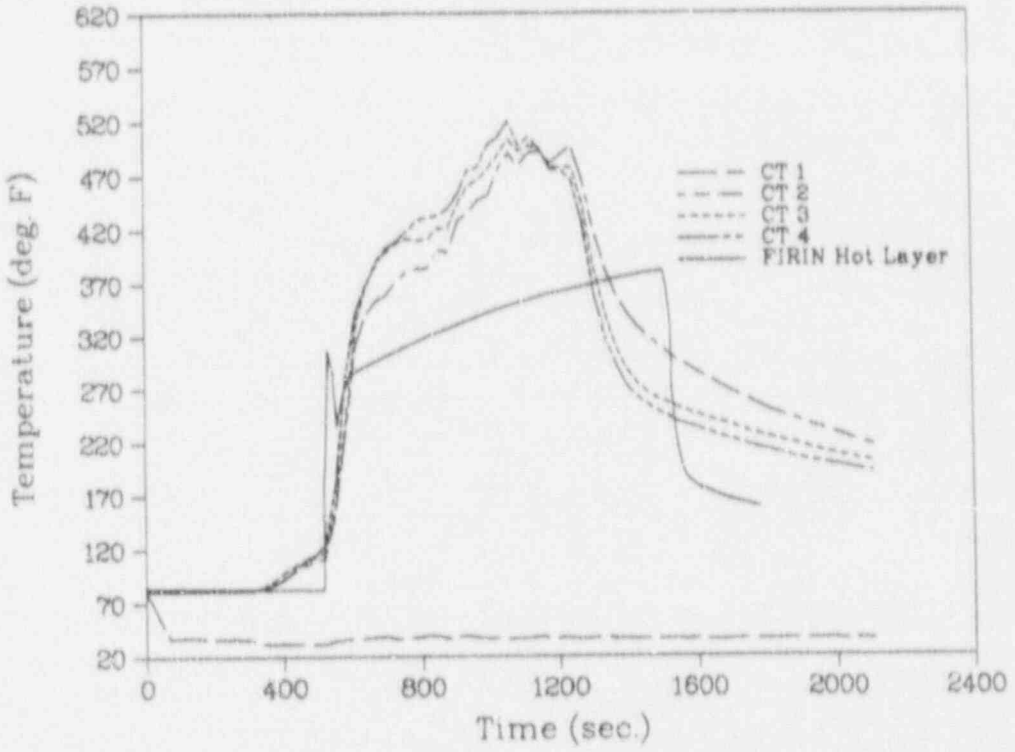

Figure 6 Kerosene Burn Test KER03 Tank Centerline Temperatures, Q=500cfm, Config.1

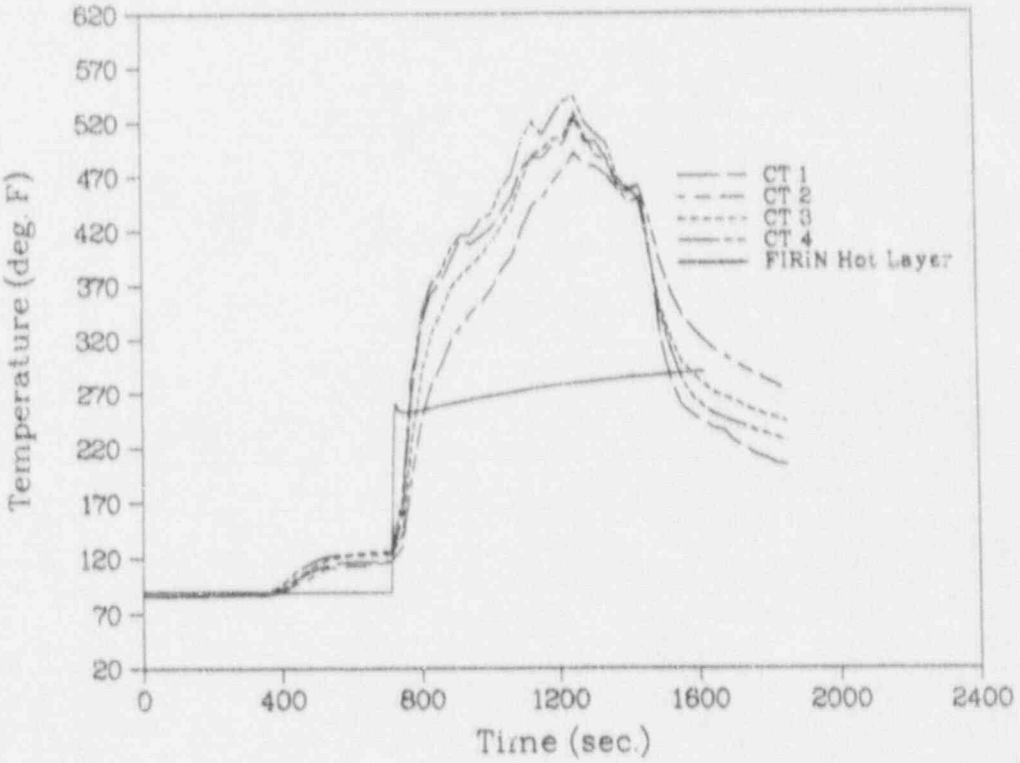

Figure 7 Kerosene Burn Test KER04 Tank Centerline Temperatures, Q=1000cfm, Config.1

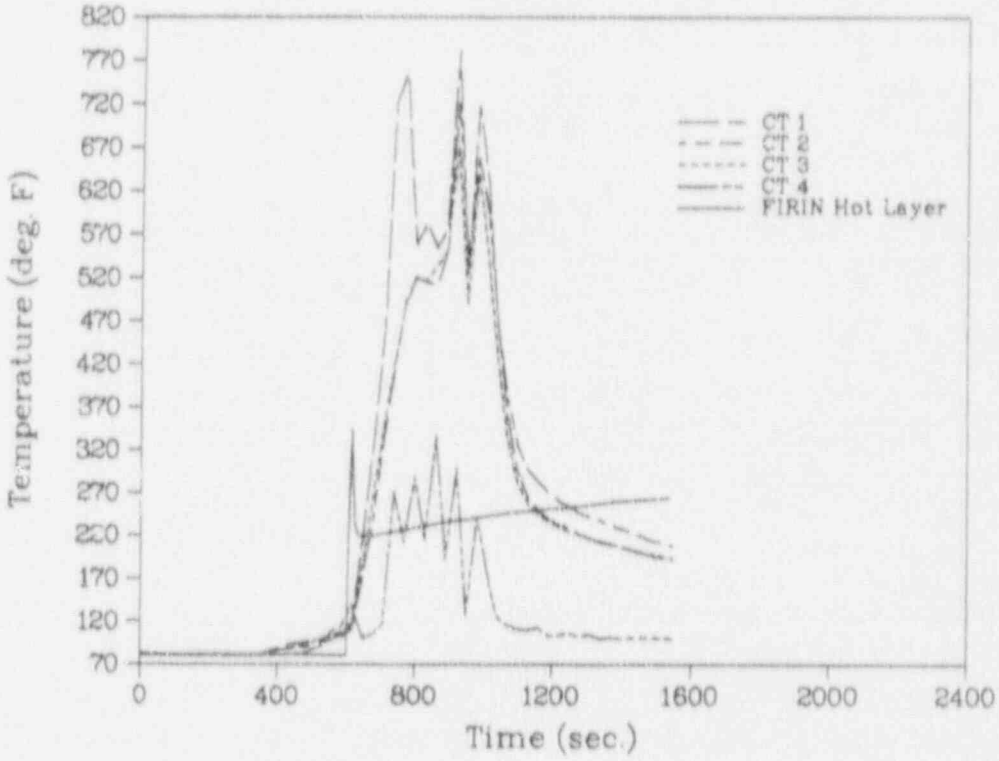

Figure 8 Kerosene Burn Test KER06 Tank Centerline Temperatures, Q=1700cfm, Config.2

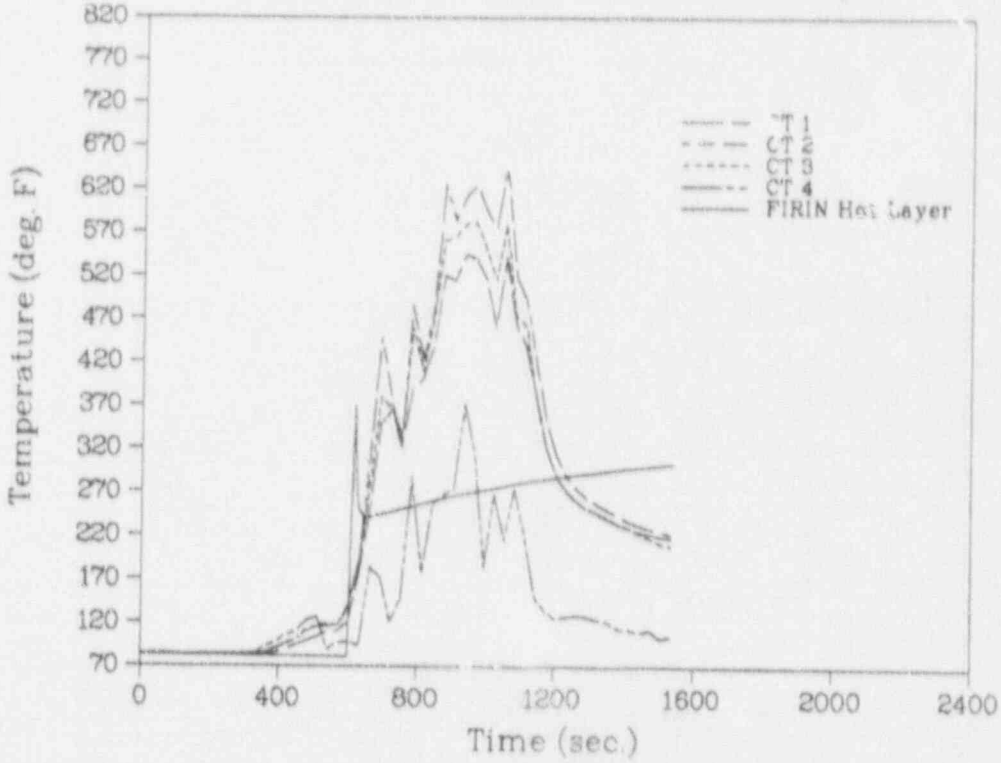

Figure 9 Kerosene Burn Test KER07 Tank Centerline Temperatures, Q=1200cfm, Config.2

Table 6 Soot Deposition on HEPA Filter for Kerosene Burn Tests

Test No.	Measured Mass Gain, g	Predicted Mass Gain, g
KER03	137	102.2
KER04	156	*
KER06	106	~ 100
KER07	82	~ 100

* Unconverged solution from FIRAC analysis.

Methyl Alcohol Burn Tests

One possible explanation for FIRAC's underprediction of the temperatures in the burn tank was that the FIRIN module assumed a 0.31m thick concrete wall, while the experiments were carried out in a tank with a 0.32cm thick steel wall. To quickly check this difference experimentally it was decided to run a series of experiments (using Configuration 3, Figure 3) with and without insulation on the steel burn tank. Mythl alcohol was chosen as the fuel to eliminate soot production. The resulting burn tank centerline temperatures for the four tests are shown in Figures 10 through 13. Complete results for these experiments are available in reference 4. Notice that the tests FUEL05 and FUEL08 are identical except for the wall insulation in the latter case. Both had flow rates of 600cfm and burned 15ℓ of alcohol. In Figures 10 and 13 we see that the burn tank centerline temperatures are nearly identical for these two experiments. However, the maximum interior wall temperature for FUEL05 (uninsulated case) was about 40°C lower than the maximum interior wall temperature for FUEL08 (insulated case)[4]. Similar results were obtained for tests FUEL06 and FUEL07 (Figures 11 and 12), the 1000cfm flow rate case. Thus, it appears experimentally that the bulk gas temperature within the burn tank is not overly sensitive to the wall insulation characteristics. Unfortunately, we were not able to easily change the thermal mass characteristics of the wall.

Cutting Oil Burn Tests

Figures 14 and 15 give the burn tank centerline temperatures measured for tests FUEL09 and FUEL10, respectively. Notice that the maximum temperatures attained were essentially the same (225°C) in both experiments as were the amounts of mass gained by the HEPA filter (see Table 4), although FUEL09 had a flow rate of 1000cfm while FUEL10 had a flow rate of 600cfm. It may be that FUEL09 had not yet reached its maximum temperature by the time its fuel was expended (note the increasing temperature just before burn out). For more extensive results see reference 4. No comparison to FIRAC predictions were possible since cutting oil was not included amoung the available FIRIN fuels.

Kerosene-TBP Burn Tests

Figures 16, 17, and 18 give the burn tank centerline temperatures for the kerosene-TBP mixture burn tests. The flow rates were 1000cfm, 600cfm, and 800cfm, respectively. Notice in all three cases the hot layer temperature predicted by FIRAC is lower than the measured maximum temperature by about 100°C, but that FIRAC predicted a longer burn time (i.e. the amount of energy release was comparable between simulation and experiment). Table 7 compares the measured and predicted mass gain of the HEPA filter. FIRAC predicts an essentially constant

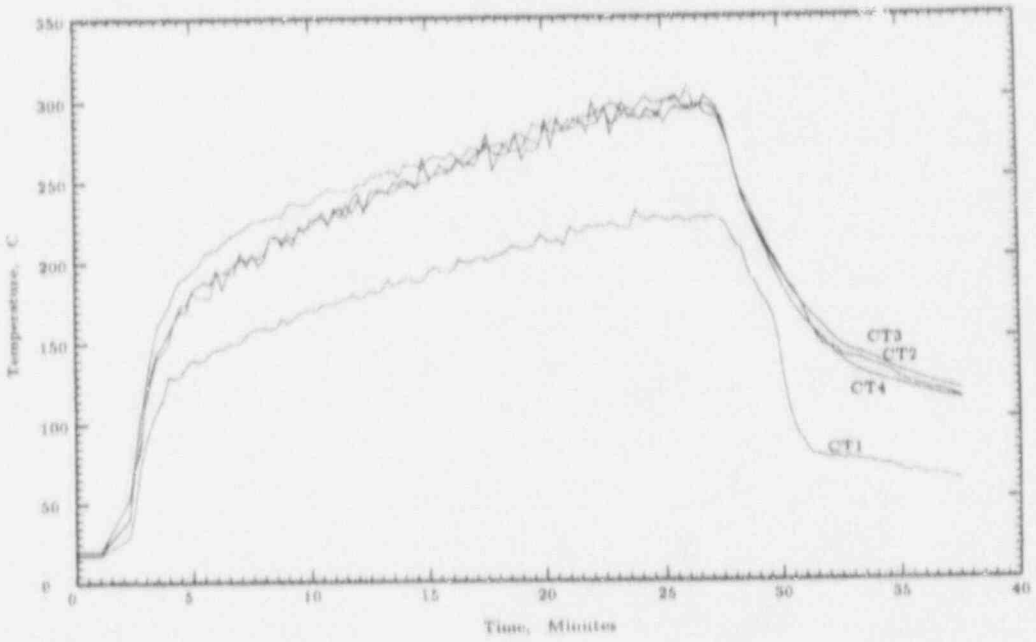

Figure 10 Alcohol Burn Test FUEL05 Tank Centerline Temperatures, Q=600cfm, Conf.3

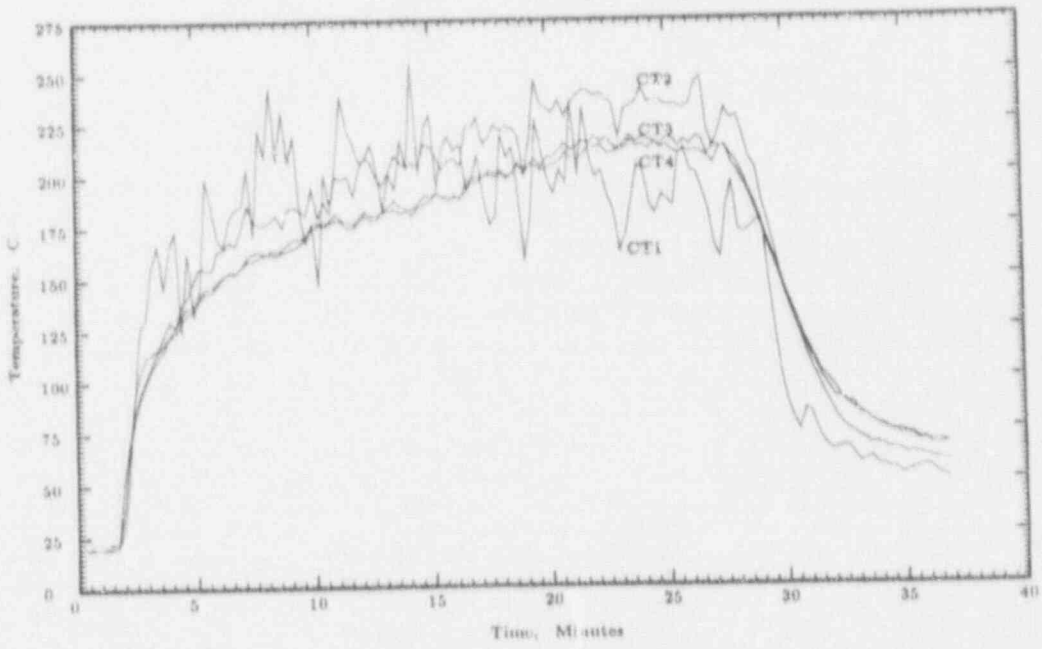

Figure 11 Alcohol Burn Test FUEL06 Tank Centerline Temperatures, Q=1000cfm, Conf.3

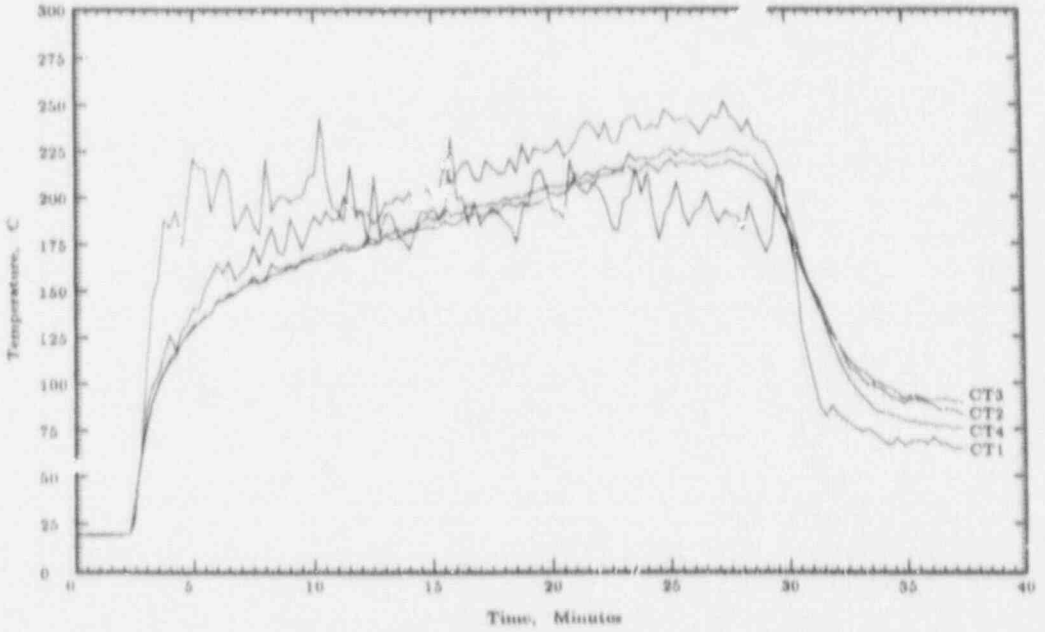

Figure 12 Alcohol Burn Test FUEL07 Tank Centerline Temperatures, Q=1000cfm, Conf.3

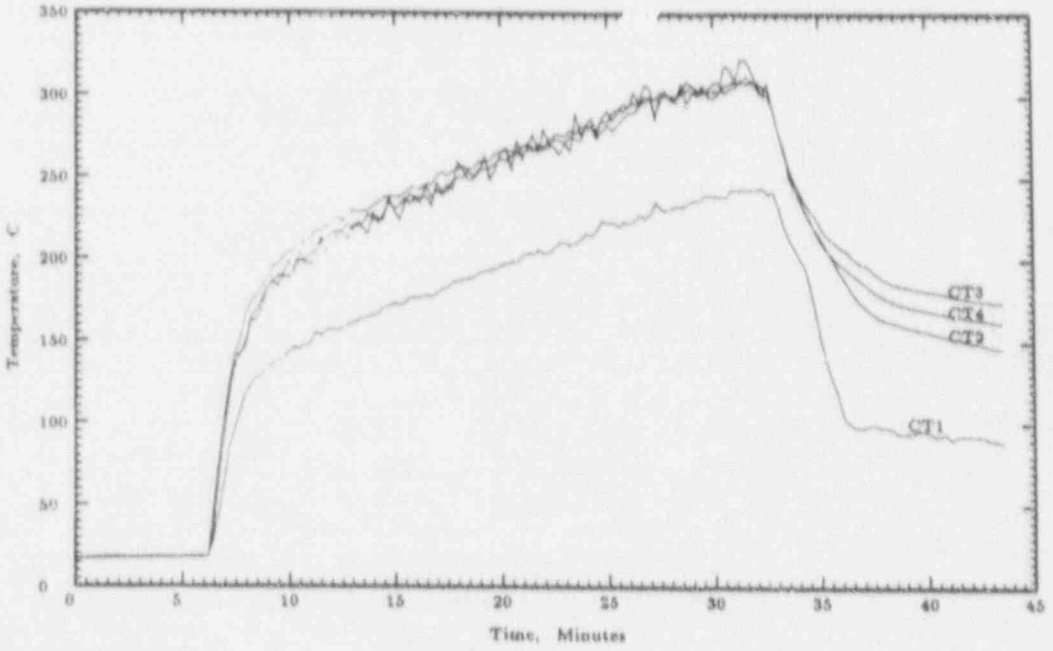

Figure 13 Alcohol Burn Test FUEL08 Tank Centerline Temperatures, Q=600cfm, Conf.3

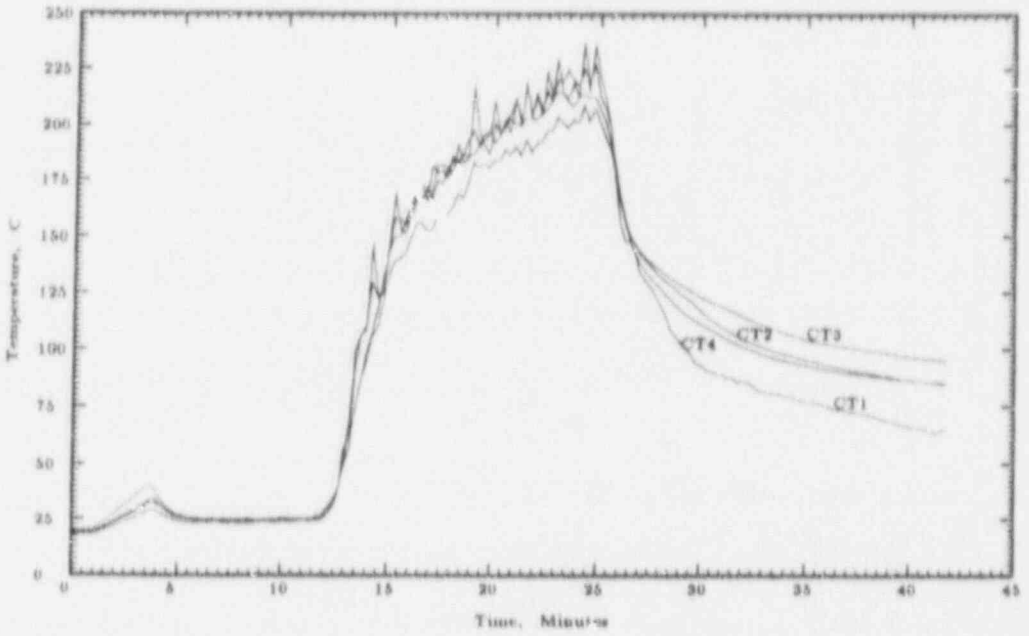

Figure 14 Cutting Oil Burn Test FUEL09 Tank Centerline Temperatures, Q=1000cfm, Config.3

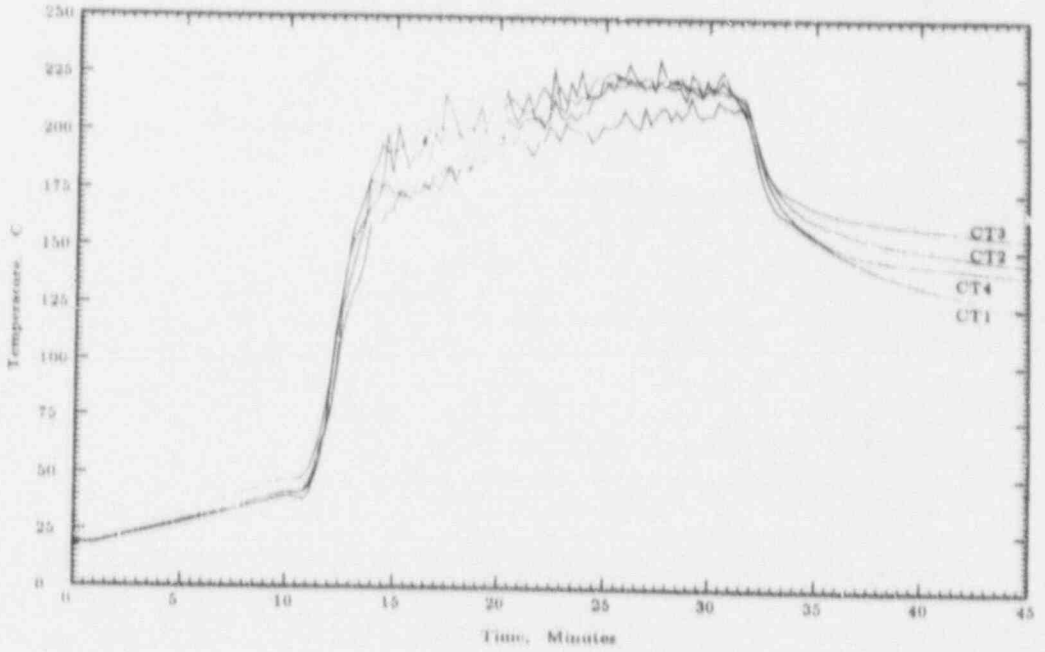

Figure 15 Cutting Oil Burn Test FUEL10 Tank Centerline Temperatures, Q=600cfm, Config.3

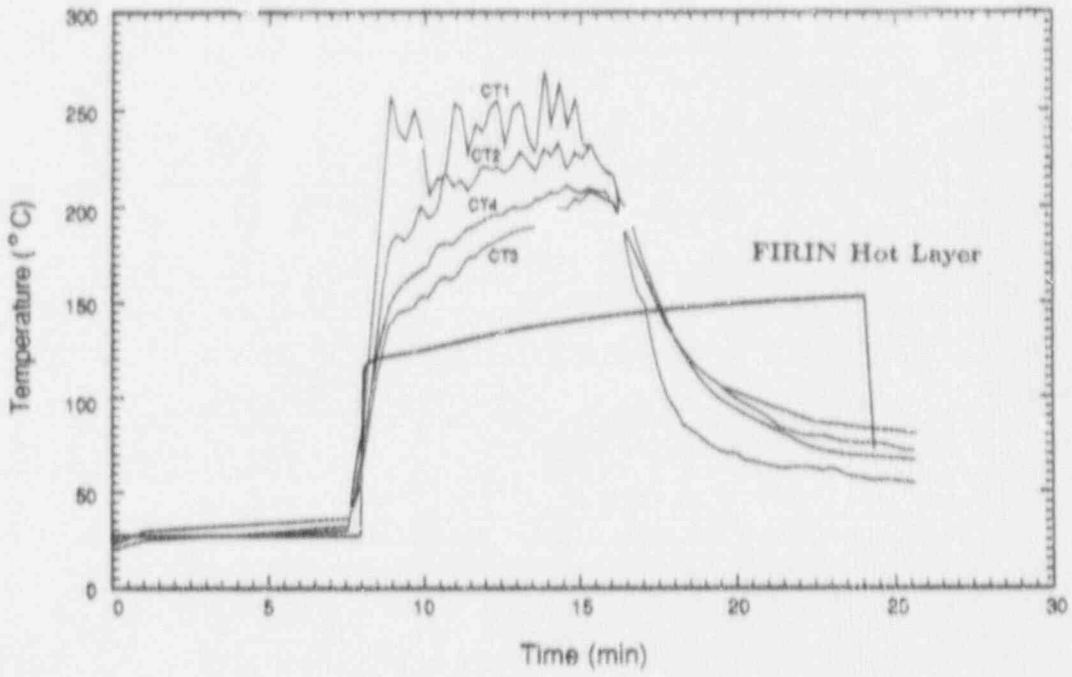

Figure 16 Kero-TBP Burn Test FUEL11 Tank Centerline Temperatures, Q=1000cfm, Config.3

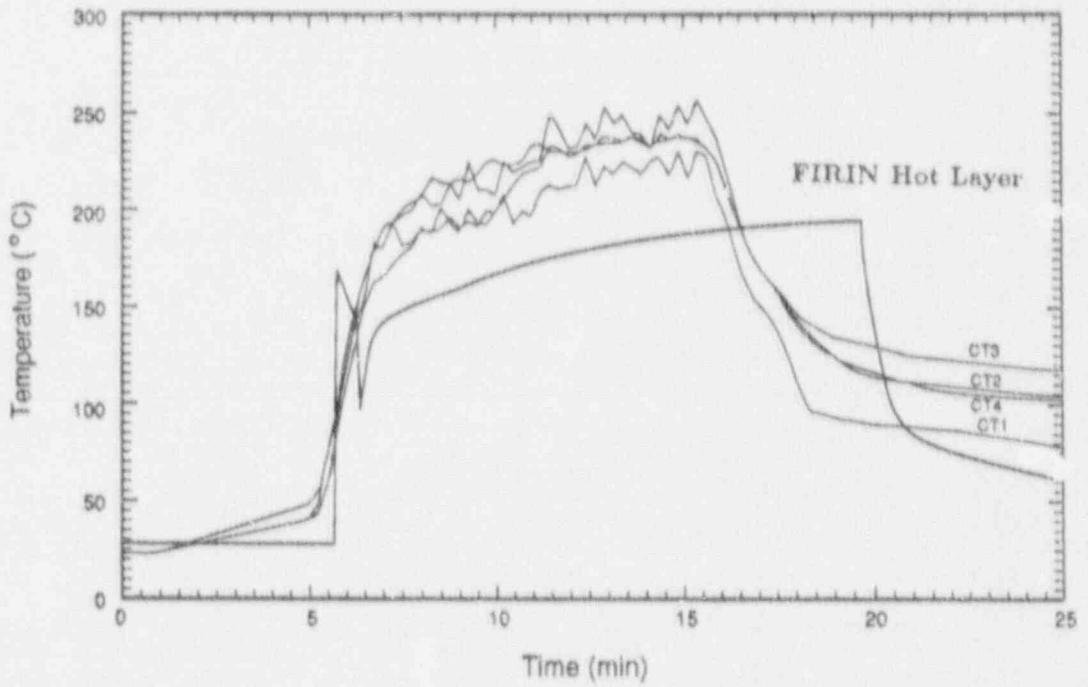

Figure 17 Kero-TBP Burn Test FUEL12 Tank Centerline Temperatures, Q=600cfm, Config.3

mass gain with flow rate (about 300g), while the measured values increase with flow rate. It appears that the predicted soot generation rate is insensitive to flow rate.

Table 7 Soot Deposition on HEPA Filter, Kerosene-TBP Burn Tests

Test No.	Flow Rate, cfm	Measured Mass Gain, g	Predicted Mass Gain, g
FUEL12	600	314.3	303.4
FUEL13	800	338.6	303.1
FUEL11	1000	424.8	297.3

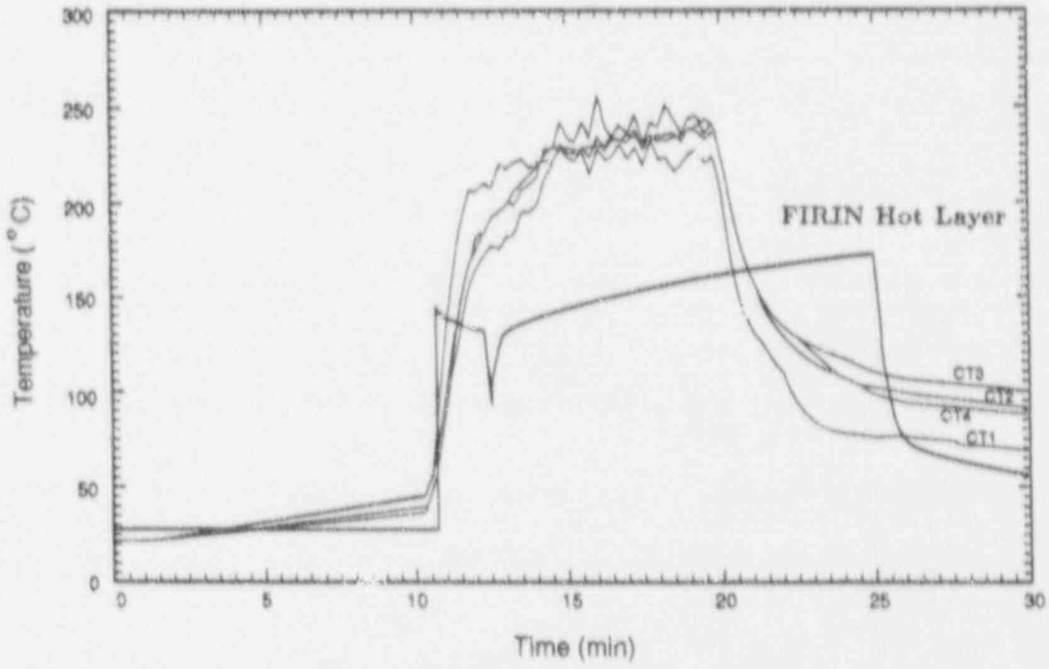

Figure 18 Kero-TBP Burn Test FUEL13 Tank Centerline Temperatures, Q=800cfm, Config.3

Filter Loading and Filter Resistance

The measured values of the mass of soot deposited upon the exhaust HEPA filter are given in Tables 2, 4, and 5 for Kerosene, cutting oil, and kerosene-TBP, respectively. Notice from Table 2 and 5 that the amount of soot deposition goes up directly as the flow rate. In Table 4, the 1000cfm case and 600cfm case seem to have the same mass gain, but notice that the amount of fuel burned in the 1000cfm case was 4ℓ, while in the 600cfm case the amount of fuel burned was 5ℓ. Hence, in general we can say that the amount of soot mass gain increases directly with flow rate.

Notice that the maximum gain at 1000cfm for Kerosene-TBP was 424.8g, for cutting oil, 333.3g and for kerosene, 156g. Even allowing for a 20% increase (i.e. to 399g) in the cutting oil soot since this burn had 1ℓ less fuel than the kerosene and kerosene-TBP burns, it is apparent that the Kerosene-TBP produced more soot. We can not compare the kerosene case, because its flow path (configuration 1) was about three times longer than the other two cases (configuration 3) and duct wall deposition probably greatly reduced the soot load of the air stream before it reached the HEPA filter.

Examination of Tables 2, 4, and 5 show that in all cases but one (KER04, Table 2), the resistance of the HEPA filter (indicated by an increase in the filter pressure drop) increased as the mass loading (i.e. the higher the mass loading the larger the increase in pressure drop).

Conclusions and Recommendations

FIRAC predicts the proper trends for the burn compartment temperature, but significantly underpredicts the maximum temperature. This may be due to the FIRIN module's use of a 0.61m thick concrete wall, while the experimental burn room had a 0.32cm thick steel wall. Further investigation of the effects of thermal upon the combustion process appears to be in order. Additionally, it is apparent that a zonal fire model has difficulty simulating a reverse flow situation (configuration 2) due to the large flow instabilities that occur for design flow rates.

Firac predicts the right order of magnitude for the mass of soot deposited upon the HEPA filter, but it does not show a dependence upon mass flow rate that is present in the experimental results. The cause for this should be investigated.

There appears to a direct dependence of HEPA filter resistance increase with mass loading upon the filter.

Mass loading upon the filter depends upon the fuel burned, the burning rate, and the distance of the fire from the filter.

Acknowledgements

We are grateful to John Corkran and Derek Jones for their careful performance of the experiments reported in this paper.

References

1. Nichols, B.D. and Gregory, W.S., "FIRAC User's Manual: A Computer Code to Simulate Fire Accidents in Nuclear Facilities", Los Alamos National Laboratory Report LA-10678-M, NUREG/CR-4561 (April 1986).

2. Nichols, B.D., Gregory, W.S., Fenton, D.L., and Smith, P.R., "Fire-Accident Analysis Code (FIRAC) Verification", Proc., 19th DOE/NRC Nuclear Air Cleaning Conference, Seattle, 18-21 August, 1986.

3. Gregory, W.S., White, B.W., Smith, P.R., and Leslie, I.H., "FIRAC Code Predictions of Kerosene Pool Fire Tests", Los Alamos National Laboratory Report, in press.

4. Smith, P.R., Leslie, I.H., "Pool Fire Experiments with Mythl Alcohol and Cutting Oil", Progress Report, New Mexico State University, Submitted to Los Alamos National Laboratory, February 19, 1990.

CONTINUOUS AIR MONITOR FOR ALPHA-EMITTING AEROSOL PARTICLES

A.R. McFarland[1], J.C. Rodgers[2], C.A. Ortiz[1] and D.C. Nelson[2].
[1]Department of Mechanical Engineering, Texas A&M University, College Station, TX 77843
[2]HSE-1, Los Alamos National Laboratory, Los Alamos, NM 87545
[3]MEE-9, Los Alamos National Laboratory, Los Alamos, NM 87545

Abstract

A new alpha CAM sampler is being developed for use in detecting the presence of alpha-emitting aerosol particles. The effort involves design, fabrication and evaluation of systems for the collection of aerosol and for the processing of data to speciate and quantify the alpha emitters of interest. At the present time we have a prototype of the aerosol sampling system and we have performed wind tunnel tests to characterize the performance of the device for different particle sizes, wind speeds, flow rates and internal design parameters. The results presented herein deal with the aerosol sampling aspects of the new CAM sampler. Work on the data processing, display and alarm functions is being done in parallel with the particle sampling work and will be reported separately at a later date.

Wind tunnel tests show that ≈50% of 10 μm aerodynamic equivalent diameter (AED) particles penetrate the flow system from the ambient air to the collection filter when the flow rate is 57 L/min (2 cfm) and the wind speed is 1 m/s. The coefficient of variation of deposits of 10 μm AED aerosol particles on the collection filter is 7%. An inlet fractionator for removing high mobility background aerosol particles has been designed and successfully tested. The results show that it is possible to strip 95% of freshly formed radon daughters and 33% of partially aged radon daughters from the aerosol sample. This approach offers the opportunity to improve the signal-to-noise ratio in the alpha energy spectrum region of interest thereby enhancing the performance of background compensation algorithms.

I. Background

Alpha continuous air monitors (CAMs) are used in the nuclear industry to detect the presence of transuranic (TRU) alpha-emitting aerosol particles. In principal, a steady flow of air is drawn into the CAM sampler and the aerosol particles are deposited on a collection substrate where the radioactivity energy spectrum is continuously monitored. Generally the particles are separated from air by filtration, although inertial impaction has also been used for collection (Tait, 1956; Alexander, 1966). In the case of a filter collector, the detector is placed parallel to the filter at a distance of approximately 5 mm from the filter face. Typically, with an inertial impactor sample deposition takes place on a substrate located over the detector.

Ideally, each radioisotope has a unique alpha energy signature which should render the speciation and quantification process straightforward. However, there are several practical limitations

which manifest themselves in obscuring the true results. First, in the case of filter detectors, the air gap causes a distortion of the low-energy tails of the alpha peaks leading to severe overlap, which suggests that CAM samplers should incorporate designs which reduce the gap to as small a value as practical. There is a limitation which must be taken into account since, if the gap is reduced below a certain level, there will be inadvertent losses of aerosol particles on the internal sampler walls in the filter/detector region. In a unique device for dealing with this problem, Kaifer et al. (1986) separated the sampling and readout functions of a CAM and collected the aerosol at ambient pressure and performed the analysis under vacuum in order to improve the resolution of the energy spectra. Due to the additional complexity and high cost of implementation, a vacuum readout approach was not considered in the present design.

Second, in the case of inertial impactors, the mechanics of operation preclude the collection of particles with sizes ≤ 0.5 µm which, for certain types of aerosol release mechanisms, can cause a failure to detect over half of the alpha-emitting aerosol particles present since, in some sampling situations, the mass median aerosol size is <0.5 µm AED (Kirchner, 1966; Elder et al., 1974). Also, inertial impactors have an inherent tendency to cause large particles to rebound from the collection surface and be carried away with the exhaust air stream. Greasing the collection surface will reduce the problem, however, the grease layer will cause additional distortion of the energy spectrum.

Third, the presence of alpha emitting background radionuclides (radon and thoron progeny) can cause difficulty in recognition of TRUs at concentrations far above regulatory alarm levels. For example, Pu-239 emits alpha radiation with an energy of 5.15 MeV and RaA/ThC emits at 6.0 MeV. Thus, the Pu region of interest in the alpha energy spectrum lies in the low energy tails of the natural background peaks. At the alarm level concentration for Pu-239 given in U.S. DOE Order 5480.11, the typical CAM sampler will register about 15 cpm from the TRU and may detect an order or two of magnitude greater count rate in the same region of interest after 8 hours of sampling due to the tailing of the energy spectra of the radon/thoron progeny. The most common approach to dealing with this problem is to employ a numerical algorithm to subtract an estimation of the background counts from the TRU energy channels. But, background compensation has definite limits in high background conditions. An alternative approach is to try to eliminate some of the background radionuclides from the sample. If the radon/thoron progeny are relatively free from attachment to other aerosol particles, some separation of the background radioactivity can be accomplished prior to collection of the aerosol. For example, in a fractionating CAM sampler head design based on inertial impaction alone, the mobile background aerosol particles are separated and carried away from the collection substrate along with the fine (usually submicrometer) fraction of the aerosol. For a filter collector design, the fractionation must be performed upstream of the filter, since an aerosol sampling filter will have a efficiency that approaches 100% for all particle sizes including those of freshly-formed radon/thoron progeny. In the development of our CAM sampler, we have incorporated fractionation stages upstream of the

filter to strip freshly formed, highly mobile radon/thoron progeny from the size distribution. Preliminary experiments have been conducted to demonstrate the feasibility of the concept.

A fourth problem of many contemporary CAM samplers is that an unbiased sample of aerosol does not reach the collection substrate. Losses on the internal walls of the sampler can substantially reduce the concentration of large particles detected by the CAM. In a previous study, we conducted wind tunnel tests with CAM samplers supplied by three vendors in which we examined the penetration of 5, 10, and 15 μm AED aerosol particles from the free stream to the sampling filters (McFarland et al., 1990). For one of the units, essentially no particles with sizes larger than 6 μm AED were able to penetrate through the flow system to the filter. One goal of the present development is that the CAM should permit penetration of at least 50% of aerosol particles of 10 μm AED. This size was selected by the U.S. EPA (1987) as representing the division between aerosol which could penetrate to the thoracic region of the human lung (≤ 10 μm AED) and that which would be deposited in the extra-thoracic regions.

A fifth factor, which will cause problems in determining the concentration of RDUs is that of non-uniformity of filter deposits. If aerosol particles are predominantly deposited near the edge of a filter, the counting efficiency will be reduced and the CAM will underestimate the concentration (Rodgers and McFarland, 1989). Should the deposit be primarily in the center of the filter, there would be an overestimation of concentration. Kleinmann and Valen (1983) tested a commercially available CAM sampler and observed substantial non-uniformities. In the study of three commercially available CAM samplers, McFarland et al. (1990) examined the areal deposition of 10 μm AED particles by analyzing subsamples cut from sampling filters. The coefficients of variation of areal deposition were 18% and 39% for the two units which did transmit significant concentrations of 10 μm AED aerosol particles.

In the present CAM sampler development, we have designed and fabricated a prototype which has been wind tunnel tested to determine the aerosol transport characteristics. Tests have been conducted to determine filter uniformity. Also, bench-type studies have been performed with freshly-formed radon daughters to ascertain the feasibility of using fractionators to separate the highly mobile background fraction from the distribution.

II. Prototype CAM

The prototype CAM sampler is shown schematically in Figure 1. Wind tunnel testing of the unit has been performed without the electronics assemblies, since the design and placement of those components does not interact with the aerosol flow path in the CAM. With reference to Figure 1, aerosol at a design flow rate of 57 L/min is drawn into the CAM though a diffusion screen system which is intended to serve two functions; namely, to collect highly mobile unattached background alpha-emitters and to uniformize the aerosol velocity profile. Further inside the unit, the air is directed through an electrical field in a condenser. The condenser is intended to provide essentially quantitative collection of charged

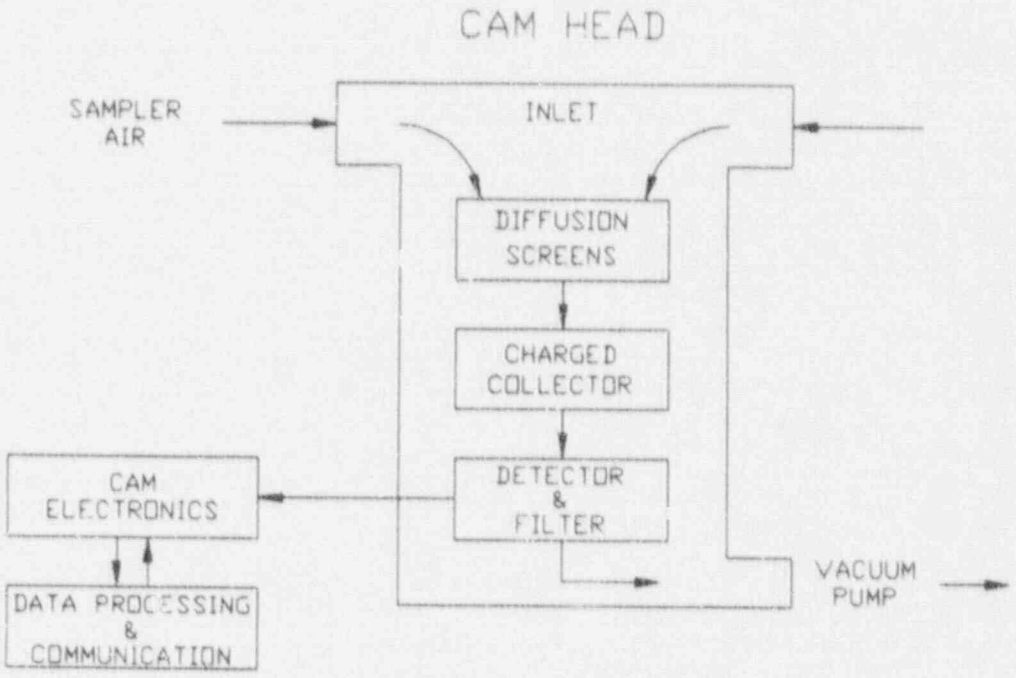

Figure 1. Schematic diagram of prototype CAM.

and unattached background radon/thoron progeny. After passing through the condenser, the aerosol flows into the gap between the filter and detector. In the current configuration, the detector can be as large as 49 mm diameter and the diameter of the open area of the filter can be as large as 42 mm. The filter is mounted in a special holder which, in turn, is inserted into the sampler in a drawer. During sampling, the filter is sealed in place with a mechanical cam arrangement. Airflow through the CAM is controlled with a critical flow venturi (Wright, 1954) and monitored with a mass flow meter (Sierra Instruments, Inc., Carmel Valley, CA).

III. Methodology and Test Apparatus

The wind tunnel used in the testing, Figure 2, has a basic cross section of 610 mm × 610 mm which is expanded to 1000 mm × 1000 mm at the test section. The expansion is designed to reduce blockage effects in the test section. Aerosol was generated with a vibrating jet atomizer (Berglund and Liu, 1973) from a mixture of nonvolatile oleic acid in ethanol. A fluorescent analytical tracer, sodium fluorescein, was added to the oleic acid in a ratio of 10% (m/V). During testing, samples of the oleic acid aerosol were collected on oilphobic glass slides and examined under a light microscope to determine the size. The resulting observed sizes were converted to AED by using the flattening factor of Olan-Figueroa et al. (1982) and the calculated density of the oleic acid/sodium fluorescein mixture.

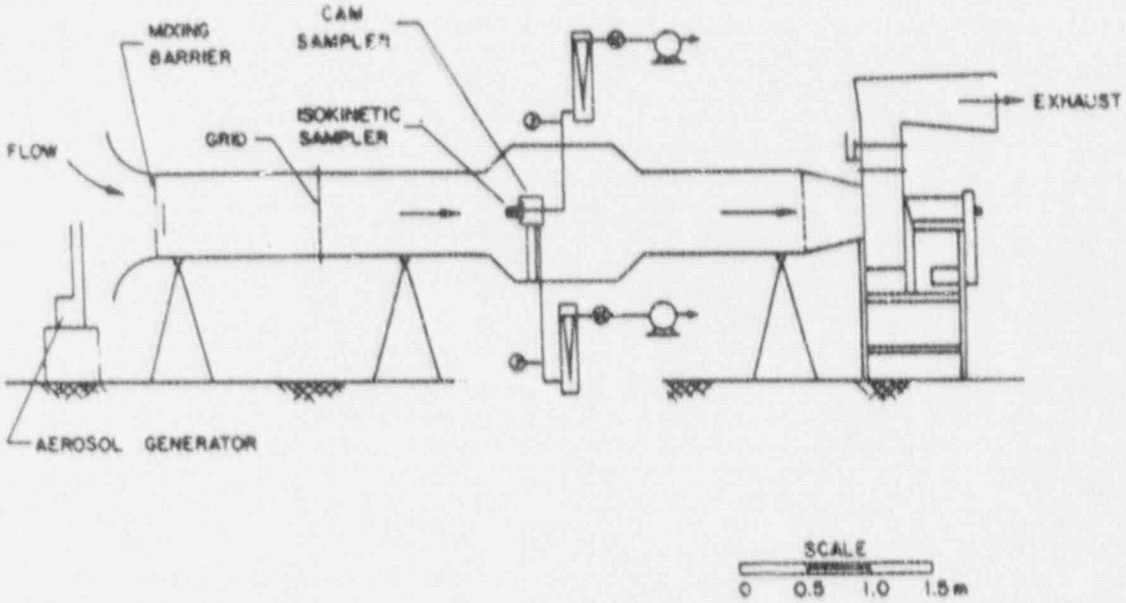

Figure 2. Wind tunnel used to characterize aerosol sampling attributes of the prototype CAM sampler.

Freshly formed aerosol was introduced into the wind tunnel through a mixing barrier and a grid plate. The purpose of these elements is to obtain a uniform aerosol concentration profile over the center 2/3 of the wind tunnel. the test section, the aerosol was simultaneously sampled with the C prototype and an isokinetic probe fitted with a filter collector. t the completion of a test, the filters were removed from the C and isokinetic probe and brought to an analysis laboratory where the sodium fluorescein was eluted and subsequently quantified. Aerosol penetration, P, through the CAM was calculated from:

$$P = \frac{m_{f,c}\, Q_{iso}}{m_{f,iso}\, Q_c} \qquad (1)$$

where: $m_{f,c}$ and $m_{f,iso}$ are the masses of fluorescein collected by the CAM and isokinetic filters, respectively; and, Q_c and Q_{iso} are the flow rates through the two samplers. At least triplicate tests were run at each condition in order to provide a measure of the reproducibility of the experiments.

The tests which involved determination of filter uniformity consisted of operating the CAM sampler in the wind tunnel for a period of time sufficient to collect an easily analyzable quantity of fluorescein, cutting the filter into 20 subsamples and then quantifying the fluorecein on each of the subsamples. Triplicate

experiments were conducted at each test condition.

The concept of using fractionators to remove high mobility background alpha-emitters from the aerosol size distribution was tested with the apparatus shown in Figure 3. High grade uranium ore was placed in a 200 L vessel as a means of generating radon daughters. Filtered room air was admitted into the vessel and then drawn into two commercially available CAM samplers. One of the CAM samplers had no fractionator and the other was fitted with an inlet which contained a screen and/or an electrostatic precipitator. The resulting energy spectra were analyzed for radon daughters in selected regions of interest. We also conducted experiments with partially aged radon daughters, where the radon daughters were given the opportunity to attach themselves to aerosol particles in room air. For these latter tests, the air exposed to the high grade uranium ore was discharged directly into a (200 m^3) laboratory environment. The two CAM samplers were positioned about 5 m from the radon daughter source. Again, comparisons were made between the counts accumulated with the fractionating CAM those detected with the unmodified CAM.

IV. Results

Since one of the key parameters in the design of a CAM sampler is the spacing between filter and detector, a set of tests was conducted to determine its effect of spacing upon aerosol penetration. Here, the sampler was operated at a flow rate of 57

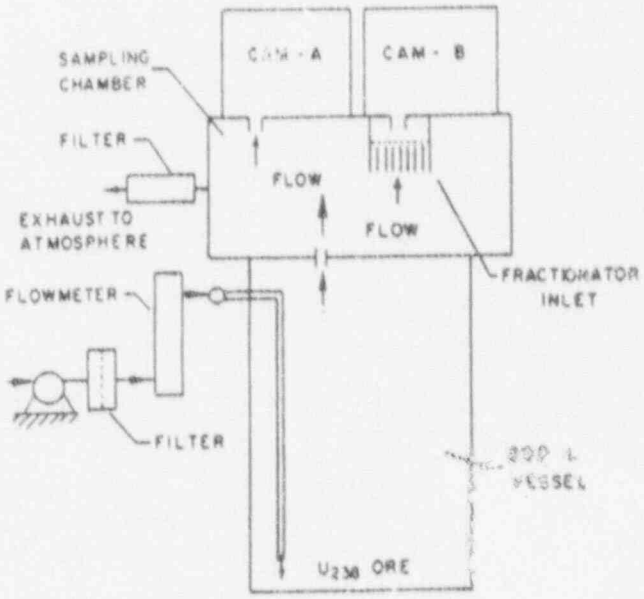

Figure 3. Test apparatus used to characterize the transmission of radon daughters through a fractionating inlet. CAM A had no special inlet and was used to provide a comparative reference with the fractionating inlet on CAM B.

L/min (2 cfm) in a wind speed of 1 m/s and challenged with 10 μm AED aerosol particles. The gap between filter and detector was set at various levels from 3.3 to 7.1 mm. It should be noted, however, that the actual minimum gap through which the aerosol flows is 2.03 mm smaller than the filter/detector gap due to the presence of the filter holder and the detector clamping ring. The results of these experiments, Table 1, show the penetration to be unaffected by filter/detector gap over the range of values tested. For all experiments we noted the penetration of 10 μm AED particles was between 85 and 87%. However, there was visual evidence of non-uniform deposits on filters for the 3.3 and 3.9 mm gaps, so a gap of 4.6 mm was selected for use in the CAM design.

The effect of wind speed on sampler performance is given in Table 2. The flow rate was 57 L/min, the particle size was 10 μm AED, and the wind speed was set at 0.3, 1, and 2 m/s. The values of penetration corresponding to these three wind speeds are 83, 87 and 88% with a standard deviation of about 3%, which indicates there is no substantial speed dependency over the range of speeds tested. No screen-type inlet fractionator was used during these tests.

Table 1. Penetration of aerosol through the prototype CAM sampler as a function of gap between filter and detector. Wind speed = 1.0 m/s, particle diameter = 10 μm AED, flow rate = 57 L/ min. No inlet screen. Minimum gap between filter holder and detector holder is 2.03 mm less than the filter/detector gap.

Filter/ Detector Gap (mm)	Penetration (percent)	Std. Dev. (percent)
3.3	87.1	0.9
3.9	85.9	1.7
4.6	87.1	2.7
5.8	86.3	1.7
7.1	86.7	1.7

Table 2. Penetration of aerosol as a function of wind speed. Flow rate = 57 L/ min, particle diameter = 10 μm AED. No inlet screen.

Wind Speed, m/s	Penetration (percent)	Std. Dev. (percent)
0.3	83.2	4.0
1.0	87.1	2.7
2.0	88.1	3.1

The variation of aerosol penetration with flow rate at a wind speed of 1 m/s is shown in Figure 4. Essentially 100% of 5.4 μm AED aerosol particles penetrate from the free stream to the sampling filter. At a size of 10 μm AED, the penetration values are 92%, 87% and 79% corresponding to flow rates of 28, 57, and 85 L/min, respectively. The cutpoint particle size (AED for which the penetration is 50%) is 17 μm for a flow rate of 57 L/min. No inlet screen was used during these tests.

The effect of including a fine mesh inlet screen with 0.11 mm diameter wires is shown in Figure 5. For those tests, the CAM was operated at a flow rate of 57 L/min in a wind speed of 1 m/s. It may be noted that the presence of the screen reduces the penetration of 10 μm AED particles from 87 to 71%. The cutpoint particle size is approximately 13 μm AED when the screen is used. Research is continuing on the design and placement of the screen elements.

Filter uniformity data for 10 μm AED aerosol particles are summarized in Table 3. The sampler was operated a flow rate of 57 L/min in a wind speed of 0.3 m/s for these tests. The locations on a filter from which each of the 20 subsamples were cut are identified in the drawing shown in Table 3. Test results have been normalized to a mean areal deposition of unity for each test. The coefficient of variation of areal deposition values is 7% for tests conducted either with or without a fine mesh screen over the inlet. Other tests which were conducted at flow rates of 28 and 85 L/min showed coefficients of variation of 4% and 8%, respectively.

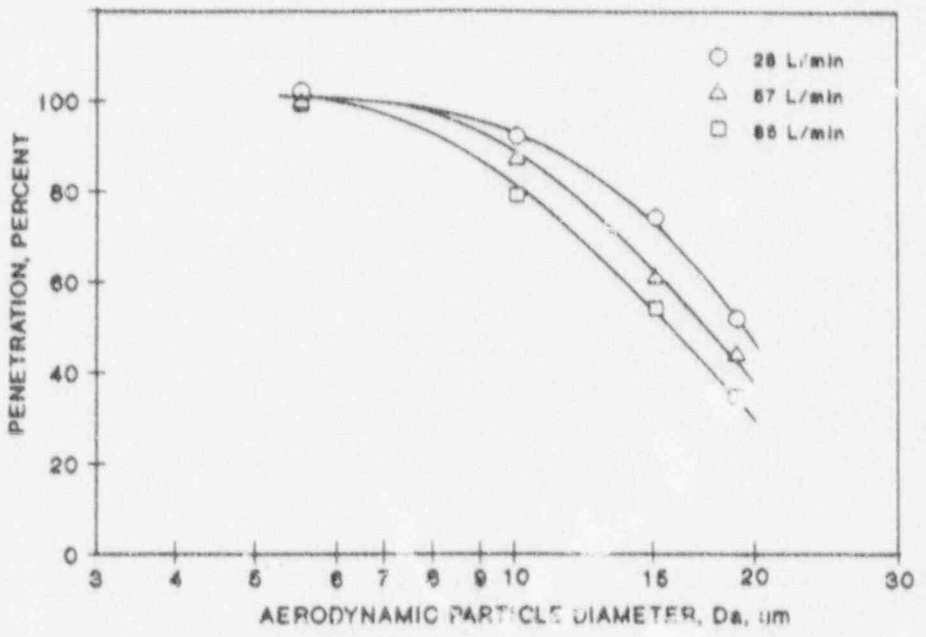

Figure 4. Effect of flow rate upon aerosol penetration. Wind speed = 1 m/s.

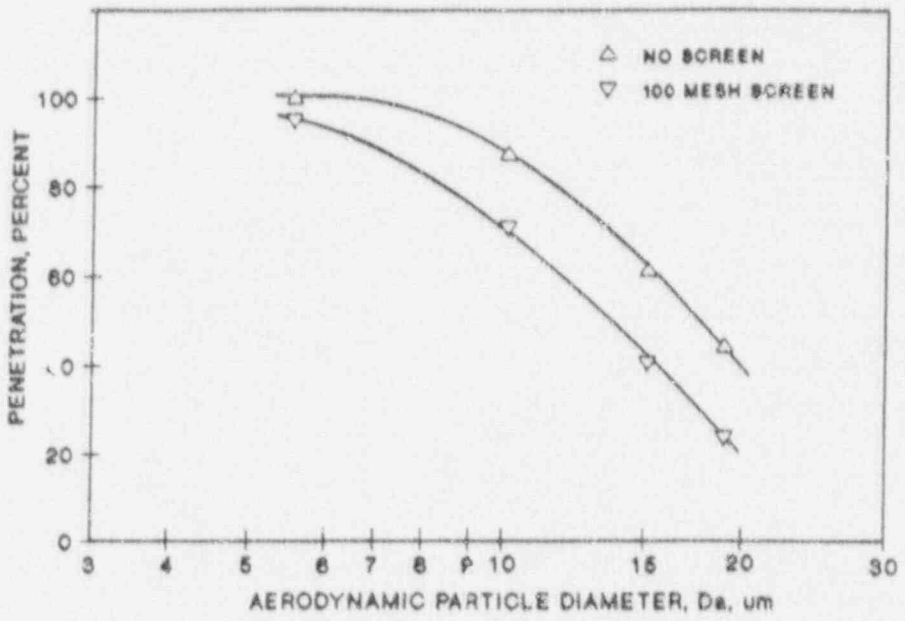

Figure 5. Effect of a 100 mesh inlet screen upon aerosol penetration. Flow rate = 57 L/min, Wind speed = 1 m/s.

Tests conducted to characterize the removal of freshly formed radon daughters showed the combination of a fine mesh screen and an electrostatic condenser eliminated 95% of the background radionuclides in the region of interest. Correspondingly, the removal of partially aged radon daughters was 33%.

V. Discussion

The CAM sampler prototype which is reported herein has a cutpoint which is greater than 10 µm AED when operated at a flow rate of 57 L/min with or without an inlet screen. We believe that a cutpoint of at least 10 µm should be used as a performance criteria for CAM samplers since this size can penetrate to the thoracic region of the human lung tree (ACGIH, 1985) and since particles of this size, or larger, can easily be generated under certain accident or release scenarios (Eldred et al., 1974; Perrin, 1987; Ballinger et al., 1988). From the standpoint of alarm considerations, it is also important that larger particles be effectively collected. The current standard for Pu-239 corresponds to the amount of alpha radiation which is emitted by a single particle of approximately 10 µm AED over an 8-hour period. Inadequate collection of larger particles could affect the ability of an instrument to correctly signal an alarm.

The performance of the prototype CAM in the collection of 10 µm AED particles at a flow rate of 57 L/min is relatively unaffected by

Table 3. Filter uniformity areal deposition. Values are normalized to a mean of unity. Wind speed = 0.3 m/s, particle diameter = 10 μm AED and flow rate = 57 L/min. Three replicates at each condition. The ± values are standard deviations.

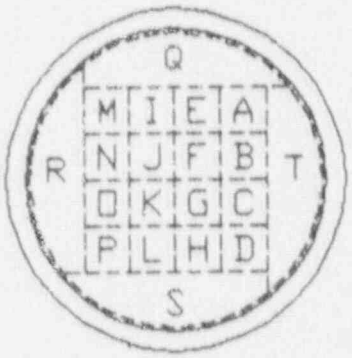

Sub-sample	Without an Inlet Screen		With a Fine Mesh Screen Inlet	
A	0.96	±0.05	0.94	±0.03
B	0.93	±0.01	0.88	±0.06
C	1.00	±0.03	0.89	±0.05
D	1.04	±0.08	1.00	±0.05
E	0.95	±0.05	0.96	±0.02
F	0.94	±0.03	1.02	±0.02
G	1.01	±0.01	1.04	±0.03
H	1.06	±0.07	1.05	±0.05
I	0.97	±0.01	1.00	±0.02
J	0.93	±0.02	1.10	±0.05
K	1.03	±0.02	1.08	±0.06
L	1.02	±0.04	1.08	±0.02
M	1.13	±0.03	0.97	±0.02
N	1.09	±0.08	1.08	±0.06
O	1.12	±0.02	1.04	±0.03
P	1.07	±0.05	1.04	±0.02
Q	0.90	±0.03	0.94	±0.04
R	0.94	±0.02	0.98	±0.03
S	1.01	±0.03	1.03	±0.03
T	0.91	±0.02	0.89	±0.03
Coefficient of Variation, %	0.07		0.07	

wind speed over the range of 0.3 to 2 m/s, showing penetration values of approximately 95% for these conditions. In clean room laboratory environments, the recommended mean air speed is approximately 0.5 m/s (ASHRAE, 1987), a value which is encompassed by the range of test conditions. It is anticipated that sampling biases would be primarily associated with high wind speeds (Durham and Lundgren, 1980) so it is expected the prototype CAM should perform well as an area sampler in a laboratory where the air velocity is within the tested range. Also, flow rate over the range of values of 28 to 85 L/min does not have a substantial effect on the sampling performance; thus, if a sampler is operated at a flow rate which deviates from the design condition of 57 L/min, the characteristics of the sample will not be greatly affected.

The uniformity of deposits of 10 μm AED aerosol particles on sampling filters is 7%, as represented by the coefficient of variation of 20 subsamples cut from each test filter. This is a lower values than noted in earlier tests with two commercially available CAM samplers which were able to transmit significant fractions of 10 μm AED aerosol particles (McFarland et al., 1990).

Preliminary experiments with a prototype inlet which fractionates high mobility background alpha-emitters show 95% of freshly formed radon daughters can be removed from the size distribution prior to collection of the aerosol by the sampling filter. When the radon daughters were allowed to become partially attached to ambient aerosol particles, the removal dropped to 33%. For certain sampling situations, the use of inlet fractionators could provide a relative enrichment of the TRU fraction of the aerosol and thereby improve the quality of alarm signals.

VI. References

ACGIH (1985). Particle size-selective sampling in the workplace. Report of the ACGIH Technical Committee on Air Sampling Procedures. American Conference of Governmental Industrial Hygienists, Cincinnati, OH.

Alexander, J.M. (1966). A continuous monitor for prompt detection of airborne plutonium. *Health Physics* 12:553-556.

ASHRAE (1987). *1987 ASHRAE Handbook - Heating Ventilating and Air Conditioning Systems and Applications.* Am. Soc. of Heating, Refrigerating and Air Conditioning Engineers, Inc., Atlanta, GA.

Ballinger, M.Y., J.W. Buck, P.C. Owczarski and J.E. Ayer (1988). Methods for describing airborne fractions of free fall spills of powders and liquids. NUREG/CR-4997 (PNL-6300). Battelle Pacific Northwest Laboratories, Richland, WA.

Berglund, R.N. and B.Y.H. Liu (1973). Generation of monodisperse aerosol standards. *Environ. Sci. & Technol.* 7:147-153.

Biermann, A. and L. Valen (1984). CAM particle deposition evaluation. In: Griffith, R.V., ed. Hazards Control Department Annual Technology Review. Livermore, CA. Lawrence Livermore National Laboratory. UCRL-5007-83.

Durham, M.D. and D.A. Lundgren (1980). Evaluation of aerosol aspiration efficiency. *J. Aerosol Sci.* 11:179-188.

Elder, J.C., M. Gonzales and H.J. Ettinger (1974). Plutonium size characteristics. *Health Physics* 27:45-53.

Kaifer, R.C., J.F. Kordas, D.L. Phelps, C.T. Prevo, A.H. Biermann, D.W. Reuppel, D.L. Sawyer, R.M. Delvasto, T.J. Merrill and R.F. Salbeck (1986). *IEEE Transactions on Nuclear Science* 34:601.

Kirchner, R.A. (1966). A plutonium particle size study in production areas at Rocky Flats. *American Industrial Hygiene Assoc. J.* 27:396-401.

McFarland, A.R., C.A. Ortiz and J.C. Rodgers (1990). Performance evaluation of continuous air monitor (CAM) sampling heads. *Health Physics* 58:275-281.

Olan-Figueroa, E.O., A.R. McFarland and C.A. Ortiz (1982). Flattening coefficients for DOP and oleic acid droplets deposited on treated glass slides. *Am. Ind. Hyg. Assoc. J.* 43:395-399.

Perrin, M-L (1987). Plutonium aerosol size distributions in a reprocessing plant during decommisioning operations. In: Kenoyar, J., Vallerio, E. and B. Murphy, Eds. Proc. 1985 DOE Workshop on Workplace Aerosol Monitoring. PNL Report No. PNL-SA- 14255.

Rodgers, J.C. and A.R. McFarland (1989). Factors affecting the performance of alpha continuous air monitors. Presented at the

34th Health Physics Society Annual Meeting, June 1989. LA-UR-89-7920.

Tait, G.W.C. (1956). Determining the concentration of airborne plutonium dust. *Nucleonics* 14 (No. 1): 53-55.

U.S. Environmental Protection Agency (1897). Ambient air quality standards for particulate matter. 40 CFR Parts 50-53 and 58. *Federal Register* 52:24634-24750.

Wright, B.M. (1954). A size selecting sampler for airborne dust. *Brit. J. of Industrial Medicine* 11:284-288.

VII. Acknowledgements

Funding for this study was provided by Los Alamos National Laboratory to the Texas A&M Research Foundation under Purchase Order No. 5-LJ8-1688V-1. We wish to express our appreciation for this support. Several individuals have made contributions to the development and testing of the sampler including Messrs. Murray E. Moore and Christopher T.R. Boyce. Their efforts are gratefully acknowledged.

DISCUSSION

MERCIER: Is this a prototype or have you made many installations of this kind? How do you see this in the future?

McFARLAND: The unit we showed is a prototype. The Los Alamos National Laboratory is currently encouraging evaluations by instrument manufacturers who have shown an interest in commercializing the device. I believe they call this a technology transfer program.

LAICHTER: Do you have any calculations regarding the minimum detectable activity of your instrument for alpha emitters?

McFARLAND: The part we have shown deals only with the physical arrangements. The electronic apparatus combined with the physical apparatus will be tested in Los Alamos facilities this fall. I can tell you what our criterion is. We wish to detect on the order of a couple of counts per minute in the plutonium channels, but that remains to be seen. We hope the field experiments will be completed by the time the next DOE/NRC Conference takes place.

MULCEY: You made some comments on eliminating non-attached radon daughters. Have you done anything on eliminating the attached fraction of radon daughters, they are important, too?

McFARLAND: The experiments we conducted were related to the unattached fraction. We did some rather preliminary experiments in looking at room air with the attached fraction and we also made some calculations. As a design goal, we are trying to strip particles with equivalent aerodynamic size of less than about 0.03 μm. The particles are, roughly, 10 times the size of the unattached radon daughters. With our screen approach, we are attempting to push it up into this higher size range.

SCHOLTEN: You said that plutonium particles of greater than 10 μm are not inhalable. That is true. But I don't think that it is permissible to inject into the environment particles bigger than 10 μm, despite that they are not inhalable. You have to measure them, also.

McFARLAND: Your point is well taken that the size range of the particles does exceed 10 μm. In some experiments that have been conducted to look at plutonium size distributions, there was as much as 20% of the material associated with sizes larger than 10 μm, depending upon the source. Our desire is not to fractionate at 10 μm but to draw in as large a sample of the larger particles as possible. We are not purposely segregating the 10 μm particles; we are saying we want to have a cut point of at least 10 μm.

SCHOLTEN: Would it be possible to measure the radon daughter polonium-210 separately? In our laboratory we are working with polonium-210. Is it possible to distinguish between radon daughters?

McFARLAND: What we have mostly looked at are the gross counts over the entire range of radon daughters. We have attempted to look individually at Radon A and Radon C, but we have not gone farther than that.

KURZ: First of all, I am glad to see you are trying some front end fractionators to eliminate interfering r on daughters. I think that is a great idea. Do you have on the spectrum of the remaining radon daughters that we could look at? What is the resolution of the detector system? Did you consider using a virtual impactor as they have at Argonne Labs? Why did you decide to use a diffusion battery rather than a virtual impactor?

McFARLAND: We have looked at several options. The experimental data that we showed here were based strictly on the use of the screened inlet. We have probably run a couple of hundred tests and the sort of spectrum that you see here is fairly typical of the spectra that we have determined. The spectra come off the instrument channel by channel; and, we have smoothed out the curve. I think you can get a general idea of what the characteristics of the spectra look like.

KURZ: How big is the detector?

McFARLAND: We used both 1 in. and 2 in. detectors. The data we showed were associated with a flow rate of 1 cfm and a 1 in. detector.

Measurement system for alpha and beta aerosols with vide dynamic range and krypton 85 masking

Hanns-Peter Wichmann, Wiederaufarbeitungsanlage Karlsruhe Betriebsgesellschaft mbH. Eggenstein-Leopoldshafen, Federal Republic of Germany

Heinrich Tiggemann, Deutsche Gesellschaft zur Wiederaufarbeitung von Kernbrennstoffen mbH, Hannover, Federal Republic of Germany

Hans-Jürgen Kreiner, FAG Kugelfischer KGaA, Erlangen, Federal Republic of Germany

Abstract

In manufacture and reprocessing of fuel elements, waste gases as well as the ambient vent air have to be monitored for alpha and beta emitting aerosols which are discharged via the stacks of the buildings. A monitor is described which can measure the low activity concentrations to be expected in normal operation as well as activity concentrations which exceed the limit values by several orders of magnitude. Simultaneously, the interference effects of high noble gas activity concentrations (krypton 85) are suppressed to maximum extent. With a measuring range of 50 to 10^{12} Bq/m^3 for beta emitting aerosols, the monitor is also suitable for emission monitoring during depressurization of the containment in nuclear power stations.

1 Problem definition

When reprocessing fuel elements, it is necessary to monitor the vessel and ambient vent air for beta emitting aerosols.

Emission of radioactive substances via the vent air is inherent in the process. Gaseous radionuclides, essentially the noble gas ^{85}Kr, are liberated during dissolution of the fuel in the dissolver and are discharged with the dissolver waste gas. Emission with the stack vent air thus involves radioactive gaseous substances and aerosols.

The aerosols occurring directly or as a result of noble gas decay pass into the waste gas or ambient vent air systems. Here, they are passed through numerous waste gas cleaning systems and filter sections.
Downstream of the aerosol filters, the air is discharged via the stack into the environment.

As low activity concentrations are to be expected in normal operation, measurements must be extremely sensitive. The waste gas rates must also be monitored in limit value operation. This is rendered more difficult by the fact that, during dissolution of a fuel element, an additional ^{85}Kr cloud of high activity concentration occurs for several hours.

2 Principle of operation of the monitor FHT 59 ST

A bypass flow of 1.4 m^3/h is taken from the sampling system (see Fig.1). This air flow is heated by a pipe heater to prevent the temperature falling below the dew point. The wide dynamic measuring range measurement system (Fig.2) consists of a monitor with 2 measuring points operating on the stepping filter principle.

With Measuring Point 1, directly above the dust collection point, in the event of the beta limit value being exceeded and for the eventuality of the beta limit value possibly being exceeded by several orders of magnitude, the high activity concentrations are determined by means of gamma measurements for the beta aerosols, employing the known beta/gamma ratio. With Measuring Point 2, in normal operation, the activity concentrations up to the point where the limit value is reached are recorded by means of alpha and beta measurement. At the same time, this measuring point is used to record the activity concentrations where the alpha limit value is exceeded for alpha aerosols up to the point where the alpha limit value is exceeded by several orders of magnitude, and for beta activity concentrations up to several times the bottom measuring range limit of Measuring Point 1.

At Measuring Point 2, there is a purging system which ensures that any ^{85}Kr present in aerosols and accumulated on the filter material is purged from the filter.

In normal operation, the filter is allowed to collect dust for one hour and is then advanced to Measuring Point 2. At this measuring point, the filter is first purged before measurement to ensure that the beta measurement is not disturbed by the effect of ^{85}Kr (maximum beta energy ca.),67 MeV).

At Measuring Point 2, a ZnS-coated plastic scintillation counter is used which combines simultaneous alpha/beta measurement with good alpha/beta selectivity and is distinguished by a high counting rate stability. The preamplifier takes the form of special electronic circuitry with a linearity range covering 6 decades.

During dissolution of fuel rods and, for example, for radioactivity emission of 10% of the alpha or beta limit value, the cycle time is changed to 6 minutes of dust collection and measurement time. This has the effect of improved time-related resolution on the one hand and extension of the measuring range up to approx. 50 MBq/m^3 at Measuring Point 2 on the other hand.

For Mesuring Point 1, a ZnS-coated plastic scintillation counter is used as well; this is however shielded from the dust collection area with a graphite plate and a lead plate. Here the aerosol radioactivity measurement is typically carried out by means of gamma measurement.

The graphite plate fitted directly above the dust collection point has been dimensioned so that high energy beta radiation, such as the radiation from ^{106}Rh with a maximum energy of 3.5 MeV, is also totally absorbed with minimum bremsstrahlung. The lead plate between graphite layer and detector reduces the intensity of the gamma radiation.

With a beta activity concentration in excess of 0.5 MBq/m^3, the detection limit of Measuring Point 1 is exceeded, so that the measuring ranges of Measuring Points 1 and 2 overlap by two decades.

The two measuring points together completely cover a range of beta activity concentrations of 50 to 10^{12} Bq/m^3.

The measuring range for the alpha aerosols between the bottom measuring range limit and an activity concentration of 3.7×10^6 Bq/m^3 is completely covered by Measuring Point 2.

3 Interference effect of high filter radioactivity on the measuring points

As high levels of activity can accumulate on the filter strip, the reel onto which the strip is wound can become the "source". Here, only the nuclides emitting gamma radiation are relevant, as alpha and beta radiation is absorbed by the coiled filter strip or the fitted shield.

If one assumes an emission of 10 times the beta limit value (6.7×10^{11} Bq) during dust collection on a filter strip, according to the flow rate ratio of sampling and vent air (1.4 to 600 m^3/h), a beta activity of 1.6×10^9 Bq will accumulate on the filter. Taking into account the fraction 0.5 if gamma emitting nuclides, this would result in a relevant activity of 8×10^8 Bq.

Measuring Point 1. Here, the radioactivity on the coiled filter strip is located at a distance of 25 to 38 cm from the detector. For ^{137}Cs this will result, in the case of a point source at a minimum distance of 25 cm, without taking account of shield materials, in a dose rate of approximately 1 mSv/h.

In addition, at least 8 cm of lead shield has to be taken into account, which leads to a dose rate of approx. 0.15 µSv/h ($\mu_{Pb} = 1.1\ cm^{-1}$) at the location of Detector 1. This corresponds to an increase in the background rate of 1 s^{-1} in the gamma channel. In contrast to this, due to the external assumed radiation field of 10 µSv/h with all-round shielding of 3 cm, a dose rate of approx. 10 µSv/h $\cdot\ e^{-3.3} \approx 0.37$ µSv/h is to be expected in the event of stray radiation. Altogether, this would result in an increase in the background rate of 3.5 s^{-1}.

Taking into account the considerable uncertainties in the estimate quoted, in spite of the conservative assumptions used as a basis, a background rate of 10 s^{-1} will be applied below. This will result in a bottom measuring range limit ofr the gamma channel of 5×10^5 Bq/m^3.

Measuring Point 2. A similar estimation of the dose rate increase due to the dust-coated filter strip (minimum distance 12 cm, minimum lead layer 6 cm) results in a dose rate of approx. 6 µSv/h. This corresponds to the background rate in the beta channel of 40 s^{-1}. The increase in the alpha channel is less than $1 \times 10^{-2} s^{-1}$. If, for reasons of conservativeness, a background rate in the beta channel of 100 s^{-1}, and of $1 \times 10^{-2} s^{-1}$ in the alpha channel are taken as a basis, the following bottom measuring range limits will be abtained for a measuring time of 6 min: 125 Bq m^3 in the beta channel, and 1.6 Bq/m^3 in the alpha channel in the case of stray radiation.

4 Interference effect of krypton 85 on Measuring Point 1

For a ^{85}Kr activity concentration of 1.7×10^9 Bq/m^3 and an effective gas volume of approx. 100 cm^3 at the dust collection point of Measuring Point 1, an effective ^{85}Kr activity of 170 kBq will result.

As the gamma emission probability for ^{85}Kr is only 4×10^{-3}, as opposed, e.g., to 0,85 for ^{137}Cs, with a response capability of approx. 3×10^{-5} s^{-1}/Bq, a counting rate of approx. 0.024 s^{-1} will be obtained for ^{137}Cs. This rate is negligible in comparison with the background rate of about 3 s^{-1} caused by an external homogeneous radiation field of 10 µSv/h.

During the official test it could be demonstrated that, with the present state of the art of science and technology, a dynamic measuring range extending over almost 12 decades can be successfully achieved. Fig. 3 gives a view of the monitor.

Acknowledgements

The autors wish to thank Frau Coroli, Frau Jonker, Dr. Frenzel, Herr Hüsgen, Dr. Iwatschenko-Borho, Dr. Lin, Herr Rothhaupt, Herr Rupp, Herr Schapat, Dr. Schmitt, Herr von Wallenberg, all of FAG Kugelfischer, Erlangen, as well as Frau Kastl and Herr Schloss, Wiederaufarbeitungsanlage Karlsruhe, for their active cooperation on this monitor.

(Received on Juni 1, 1989; in English version on June 26, 19)

SESSION 14

CONTAINMENT VENTING

Thursday: August 16, 1990
Co-Chairmen: J. L. Kovach
P. Mulcey

CONTAINMENT VENTING
SLIDING PRESSURE VENTING PROCESS FOR PWR AND BWR PLANTS

PROCESS DESIGN AND TEST RESULTS

B. Eckardt
Federal Republic of Germany
KWU Group of Siemens AG

Abstract

In order to reduce the residual risk associated with hypothetical severe nuclear accidents, nuclear power plants in Germany as well as in certain other European countries have been or will be backfitted with a system for filtered containment venting.

During venting system process design, particular importance is attached to the requirements regarding, for example, high aerosol loading capability, provision for decay heat removal from the scrubber unit, the aerosol spectrum to be retained and entirely passive functioning of the scrubber unit. The aerosol spectrum relevant for process design and testing varies depending on aerosol concentrations, the time at which venting is commenced and whether there is an upstream wetwell, etc. Because of this the Reactor Safety Commission in Germany has specified that SnO_2 with a mass mean diameter of approximately 0.5 µm should be used as an enveloping test aerosol.

To meet the above-mentioned requirements, a combined venturi scrubber system was developed which comprises a venturi section and a filter demister section and is operated in the sliding pressure mode. This scrubber system was tested using a full-scale model and has now been installed in 14 PWR and BWR plants in Germany and Finland.

Depending on the specific requirements of each project, units have been installed for mass flows of between 3 and 14 kg/s, decay heat removal of up to 480 kW from the scrubber unit and an aerosol loading capacity of several hundred kilograms. The scrubber unit is between 2 and 4 m in diameter, depending on the design mass flow, and around 8 m high.

In the course of the experimental program to test scrubber operation, it was

necessary to perform hydraulic functional tests and removal efficiency tests at pressures from 1 to 10 bar and temperatures between 50 and 190 °C using air, steam and mixtures of the two.

To perform these tests, the JAVA scrubber test facility was erected enabling a section of the system to be tested on a scale of 1 : 1.

Tests were conducted to determine the removal efficiencies for $BaSO_4$, uranine and SnO_2 aerosols as well as elemental iodine under various pressure and temperature conditions. To prevent coagulation effects of a significant magnitude, low aerosol concentrations of around 0.1 to 1 g/m^3 were employed.

To achieve high removal efficiencies in boiling scrubber fluid and during operation above atmospheric pressure, it was necessary to modify the venturi section and the filter demister section. Following completion of these optimization measures, medium-energy venturi operation was sufficient to achieve $BaSO_4$ removal efficiencies of around 99 % in the venturi section.

Retention of the micro-aerosol SnO_2 in the water pool was also demonstrated to be around 99 % during high-energy venturi operation.

The removal efficiencies of the entire combined scrubber unit were found to be greater than 99.95 % for all the aerosols employed in the tests. These removal efficiencies are also in good agreement with the decontamination factors determined for this scrubber unit during the ACE Phase A tests, namely:

for mixed aerosol (Mn, Cs and I;	MMD 1 - 1.5 µm)	$> 10^5$
for DOP	(MMD 0.7 µm)	$> 5 \cdot 10^3$

The iodine retention capability was demonstrated using iodine with a radioactive tracer. Discriminating iodine sampling filters designed for I_2 and CH_3I retention were employed to determine the removal efficiency.

The removal efficiencies established for iodine were > 99 % over the entire operating pressure and temperature range and at various venturi flow velocities.

Owing to the use of discriminating iodine sampling filters, it was also possible to determine that the removal efficiency for organic iodide is in the range of 85 - 95 %.

Iodine revolatization experiments were performed with scrubbing water conditioned with NaOH and $Na_2S_2O_3$. Using an air/steam mixture having an air content of around 10 % by volume, it was possible to demonstrate that iodine revolatization within the entire scrubber unit is < 0.2 % over a period of 24 hours.

In order to meet special requirements for high organic iodide retention

($\geq$ 99 %), a completely passive sliding pressure version using an integrated sorption bed which does not need active heating equipment was developed which achieves an organic iodide retention efficiency of more than 99 %.

1 Introduction

The general requirements to be met by venting system designs are that such as system must have as high a retention and loading capability as possible but should be of simple design, without active components.
After a number of basic studies using venturi scrubbers and filter demisters had been completed, a two-stage filter system was selected.

2 Requirements

Because of their significant influence on the process design and verification program, some of the most important requirements are described below:

- Particle size distribution
  Because of its considerable influence on the retention capability of the system, the aerosol distribution was calculated in the course of parametric studies based on experiments. Analysis of these parameters revealed that aerosol mass mean diameters of less than 1 µm down to 0.65 µm could be expected, primarily on account of the long-term effects of concrete-melt interaction.
  Aerosol spectra still having a relevant submicron content are also encountered when venting is performed via an upstream suppression pool since these pools primarily retain larger aerosols.
  Therefore, in view of the ongoing investigations, it has been specified that the design of aerosol filtration equipment be based on aerosol fractions having a large submicron content for the sake of conservatism. Because of this, the German Reactor Safety Commission specified that tin dioxide (SnO_2) having a mass mean diameter of approximately 0.5 µm generated by a plasma torch should be used as an enveloping test aerosol.
- Passive removal of decay heat from the filter

PWR	BWR
> 7 kW	$\geq$ 200 kW

- Filter loading capacity
  Demonstration with SnO_2 for the following venting system flows:

PWR	BWR
$\geq$ 60 kg	$\geq$ 30 kg

- Filter efficiency

Aerosols	$\geq$ 99.9 %
Iodine (elem.)	$\geq$ 90 %

- Flow rate
  Depending on the reactor type and the point in time at which venting is initiated the resulting flow rates were:
  3 kg/s - 14 kg/s

Other general requirements applied to the filter design included the following:

- The filter should be able to operate in a passive and fully autonomous manner.
- The system must have no adverse effect on the existing standard of safety.
- Any associated dynamic loads - arising, for example, during steam condensation - must also be determined.
- All verification tests have to be performed under representative test conditions and were to cover both steady-state and transient as well as full-load and part-load operating conditions.
- Special requirements from other European countries, e.g. the TVO venting systems in Finland for which 480 kW of decay heat needs to be removed from the filter or the Soviet reactors which have an aerosol size distribution with an MMD of 0.5 µm, also required consideration.

3 Retention Process

The filtered venting system consists of a wet scrubber with venturi nozzles followed by a combined droplet separator and stainless-steel-fiber filter demister housed in a pressure vessel.

To activate the system, the isolation valves are opened by remote control from the control room (see Fig. 1 for example of German PWRs)

A separate battery power supply as well as provisions for remote valve actuation guarantee reliable valve operation.

Another solution used for the BWRs in Finland, TVO 1 and TVO 2, is also shown in Figure 1. Activation of this system is effected using rupture discs which open passively.

The venturi scrubber (Fig. 2) is operated at pressures close to the prevailing containment pressure levels due to the provision of a throttling orifice in the filter discharge line. The venting flow entering the scrubber is injected into a pool of water via a small number of submerged, short venturi nozzles.The ratio of the diameter of the aerosols and the venturi throat precludes any clogging.

As the vent gas passes through the throat of the venturi nozzle, the incoming gas flow develops a suction which causes scrubbing water to be entrained with it and, on account of the large difference between the velocity of the scrubbing water particles and that of the incoming vent flow, a large proportion of the aerosols are removed.

At the same time, the particles of the entrained scrubbing water provide large mass transfer surfaces inside the throat of the nozzle, which permit effective sorption of iodine. Optimum retention of iodine in the pool of water inside the scrubber is attained by conditioning the water with caustic soda and other additives. In view of the mechanisms occurring inside the venturi, most of the iodine and aerosol particles are in fact separated inside the throats of these nozzles.

The pool of water surrounding the nozzles acts as the primary droplet separation section and also serves as a secondary stage for retention of aerosols and iodine.

The gas exiting from the pool of water still contains small amounts of hard-to-retain aerosols as well as scrubbing water droplets. In order to ensure high retention efficiencies even over prolonged periods of time - for example, 24 hours - a high-efficiency droplet separator and micro-aerosol filter demister is provided as a second retention stage.

A throttling orifice installed downstream of the scrubber unit provides for critical expansion of the cleaned gas, which is subsequently released to the environment through a separate stack.

A second scrubber version is based on operation close to atmospheric pressures for venting containments with lower design pressures, e.g. 2 bar absolute.

This version is likewise designed to retain most of the aerosols in the scrubber section. Even under extremely low flow conditions the reduced venturi retention efficiency is fully compensated for by the filter demister.

During the qualification tests of this version, the same level of retention efficiency was achieved as with the sliding pressure version.

Both venturi scrubber versions provide a retention efficiency for aerosols of 99.95 % and more. This retention capability also applies to micro-aerosols of less than 0.5 µm so that, for example, variations in the particle size distribution of the aerosols cannot diminish the removal efficiency. The retention efficiency for elemental iodine under all operating conditions including overpressure conditions is above 99 %. The retention efficiency of organic iodide was found to be better than 85 to 95 %.

Furthermore, the venturi scrubber pool is designed such that evaporation of the pool water caused by the decay heat generated by the aerosols in the water will likewise not lead to an unacceptable drop in the pool water level.

The decay heat removal requirements of > 7 kW for the German PWRs and up to 480 kW for the TVO BWR plants can be handled in the pool without water makeup for 24 hours.

Because of high organic iodide retention requirements in special cases of $\geq$ 99 %, an additional venturi scrubber version was developed.

This version has an integrated sorption bed with provisions for continuous passive heating based on the principles of throttling and self-heating, and also operates under sliding pressure conditions.

The retention rates are:

for organic iodide $\geq$ 99 %

for elemental iodine $\geq$ 99.9 %

This version was developed in 1989 in response to special requirements and is not presented in detail in this paper.

4 Verification Program

The pretests performed for the purpose of process selection were conducted under atmospheric pressure and room temperature conditions on individual sections of the process such as the venturi and the metal-fiber filter demister. After final selection of the process, it was then necessary to perform functional tests under representative conditions. These tests covered aerosol removal efficiency tests as well as tests for iodine retention at a full-scale test facility, especially at pressures above atmospheric.
A full-scale test facility was erected specifically for the purpose of conducting the tests of this verification program.

5 JAVA Test Facility at Karlstein

Figure 3 shows the flow diagram and the test parameters of the JAVA test facility. The scrubber test vessel houses full-scale retention elements. In the various test series performed, both short and long venturis were installed.
The facility can be operated as a closed loop or as an open circuit connected to a steam boiler (22 MW) and a suppression tank. A summary of the main test parameters is also given in Figure 3.
Equipment for aerosol and iodine injection as well as measurement was installed upstream and/or downstream of the scrubber and filter sections.
Each test was monitored from a central control desk. This desk was equipped for continuous recording of all physical data measured at the JAVA facility.

6 Aerosol Generation

Aerosol generation and injection had to be performed at different system operating pressures (up to a maximum of 10 bar), depending on the test being conducted. Therefore, the methods usually employed for aerosol injection had to be modified.

A separate upgrading program was conducted on the following equipment to qualify them for operation within system pressure ranges of 1 to 6 or 1 to 10 bar:

- plasma torches (for SnO_2 generation)
- rotating brush powder disperser and belt dosing unit (for $BaSO_4$ injection)
- spray equipment (for uranine aerosol generation)
- spray equipment (for iodine injection).

A detailed description of the methods selected for aerosol generation cannot be given in this summary.

The aerosol concentrations of less than 0.1 g/m³ expected under containment venting conditions were unable to be continuously simulated during the SnO_2 test series.

As far as the generation of test aerosols was concerned it was, however, known that high aerosol concentrations could - even in the case of short residence times - result through coagulation in a significant increase in the size of the originally small test aerosols.

In order to obtain sufficiently small-sized test aerosols, it was therefore decided to use short residence times (duration between aerosol generation and arrival at the scrubber) and in this way it was possible to adequately prevent coagulation effects which could also arise with test aerosol concentrations of around 0.5 g/m³.

Figure 4 shows an SEM photomicrograph of the enveloping test aerosol SnO_2.

Figure 5 contains a comparison of the aerosol spectra that were generated against an aerosol spectrum that was derived from NAUA distribution calculations. This comparison reveals that particularly SnO_2 can be regarded as a conservatively enveloping test aerosol on account of its high submicron content.

6.1 Measuring Techniques

As a departure from customary sampling techniques performed at atmospheric pressure, aerosol sampling was conducted under realistic operating conditions at a pressure above atmospheric and using thermal tracing to establish temperatures above the corresponding saturated steam temperatures in order primarily to avoid agglomeration affects and any significant deposits in the instrument lines.

Samples of the main process gas flows were taken isokinetically at specified measuring locations, high-efficiency filters being used to remove the aerosols from the sample flows.

The material retained on the sample filtering elements was then evaluated by the AES (atomic emission spectroscopy) and gravimetric techniques. The aerosol particle size distributions were measured by the light scattering method as well as using a scanning electron microscope.

7 Iodine Removal

From the literature it was known that chemically conditioned scrubbing water pools displayed good iodine retention properties. Likewise, removal equipment such as venturis as well as irrigated packed wire-mesh filters were known to have good sorption characteristics an account of their large mass transfer surfaces.
Since the combined venturi scrubber presented herein constituted separating elements of this kind connected in series, high removal efficiencies were expected from the start.
Theoretical investigations performed in advance of system design using a droplet model to study the iodine removal capability of the venturi showed furthermore the significant effect had by operating temperature and pressure on removal efficiency.
Therefore it was necessary for a full-scale system mockup to be built for the purpose of verifying the iodine removal efficiency during short-term as well as long-term operation.

7.1 Performance of Test for Iodine Removal

This test was performed at the JAVA test facility using an aqueous I_2 solution containing I-123 as a tracer. The use of a tracer enabled a sufficient accuracy of measurement to be attained even at low iodine concentrations of between 10^{-3} and 10^{-5} g/m^3, which made it possible for decontamination factors in excess of 100 to be verified.

Figure 6 shows the equipment used for iodine injection. The aqueous I_2 solution having a pH of 3 and containing the I-123 tracer was pumped out of a storage tank by a piston pump into a forced-circulation evaporator. Here the solution was evaporated and the resultant gas superheated to about 30 to 50 °C above the system operating temperature. The system temperature on the scrubber inlet side

was selected such as to ensure that the temperature of the liquid would be in a superheated condition of > 10 °C.

7.2 Iodine Sampling and Measurement

Two iodine sampling systems were provided, one in the DN 150 inlet pipe immediately upstream of the venturi scrubber (contaminated gas side) and one in the DN 150 discharge line immediately downstream of the metal-fiber filter demister (clean gas side). The two systems were of identical design and are depicted in Figure 6. The samples were taken via a hook-shaped probe attached to a short, thermally-traced, flexible stainless-steel hose. A manifold connected the hose to three thermostatically-controlled heating chambers arranged in parallel and containing iodine adsorbers operated successively. Prior to entry into the iodine adsorbers the pressure of the gas sample was reduced to atmospheric inside an adjustable pressure-reducing valve. The temperature of the gas in the metal hose up to the reducing station was set at 200 °C and was brought down to 140 °C inside the heating chambers in order to prevent condensation.

The discriminating iodine adsorbers were installed vertically inside the heating chambers and comprised the following equipment when viewed in the direction of flow:

- aerosol filter
- absorbent material impregnated with potassium iodide
- absorbent material impregnated with silver nitrate
- downstream condenser operating at a temperature of < 40 °C.

The filters were additionally qualified in laboratory tests with respect to their discriminating I_2/CHI_3 removal efficiency under the relevant operating parameters.

8 Test Results

In the following a few of the results obtained from the numerous tests performed will be presented. These results were obtained after a wide range of different design optimizations had been effected; for example:

- modification of the venturi design in order to be suitable for operation in boiling liquid and particularly at elevated operating pressures and velocities.
- selection of the optimum venturi throat velocity range and air-to-water ratio.
- optimization of the filter demister design as well as operating flow velocities.

The results have been subdivided according to medium- or high-energy venturi operation, and long or short venturis, as shown in Tables 1 and 2..
Some of the iodine test results are presented in Table 3. These data incorporate correction factors based on pipe factors determined for the contaminated and clean gas sides.
In addition to the measurements of removal efficiency at different temperatures and venturi throat velocities, particular mention should be made of the long-term iodine revolatization tests.

8.1. Aerosol Retention

Medium-energy venturi operation tests were performed using soluble uranine and nonsoluble $BaSo_4$ aerosols having mass mean diameters in the region of 1 µm.
Even under low flow conditions, almost all of the aerosols (between 97 and 99 %) were retained in the venturi section.
As a result of the combination of venturis with a metal-fiber filter demister, even at system pressures of 1 to 10 bar retention efficiences of > 99.99 % were verified under full-flow conditions and also at reduced gas flows - due to the greater efficiency of the second section (see Fig. 2).
In keeping with the requirements specified by the German Reactor Safety Commission, SnO_2 was generated by means of plasma torches for use as a test aerosol in the final series of tests. In the course of these tests, aerosol mass mean diameters of 0.5 µm were attained. For these tests the venturi section was operated in the high-energy mode, that is by using a reduced number of venturis operated with a higher pressure drop. Due to this mode of operation, again almost all of the aerosols (95 to 99 %) were removed in the venturi section.
The total removal capability of the entire scrubber unit tended to decrease at higher operating pressures as well as lower vent flow rates.
However, in general the retention efficiency of the entire unit was nevertheless > 99.95.

8.2 Iodine Retention

The total iodine removal efficiency of the entire unit was determined in short-term and long-term tests.
The elemental iodine removal efficiencies provided by this two-stage filtration equipment were consistently > 99.4 %. These results have even been obtained under operating conditions that have an unfavorable effect on gas sorption, such as the following:

- elevated system operating pressures, and
- reduced venturi velocities under atmospheric conditions.

Iodine revolatization tests yielded revolatization rates of < 0.2 % over an operating period of 24 hours and using an air content in the vent flow of 10 % by volume.
Furthermore, as a result of the capability of the measuring techniques to discriminate between elemental iodine and organic iodide, it was possible to verify an average organic iodide removal efficiency of 85 to 95 %.

9 Conclusions

The venting process tested in detail in the course of the JAVA test series revealed that under all operating modes, including sliding pressure, especially as a consequence of the selected two-stage design of the process, extremely high removal efficiencies can be attained for both large-diameter aerosols and micro-aerosols, namely $\eta > 99.95$ % for aerosols and $\eta > 99$ % for elemental iodine.
These results are also in good agreement with the removal efficiency determined in the ACE Series A tests for the micro-aerosol DOP of likewise $\eta \geq 99.95$ %.
The specific design of the system for sliding pressure operation has resulted in compact overall dimensions which means that, despite the high mass flows of up to 14 kg/s, the system is capable of being backfitted in existing buildings.
Siemens filtered containment venting systems have now been installed at the BWR units TVO 1 und TVO 2 in Finland as well as in all West German BWR plants (total of seven).
Furthermore, systems for filtered containment venting have up to now already been installed in five West German PWR plants.

SIEMENS

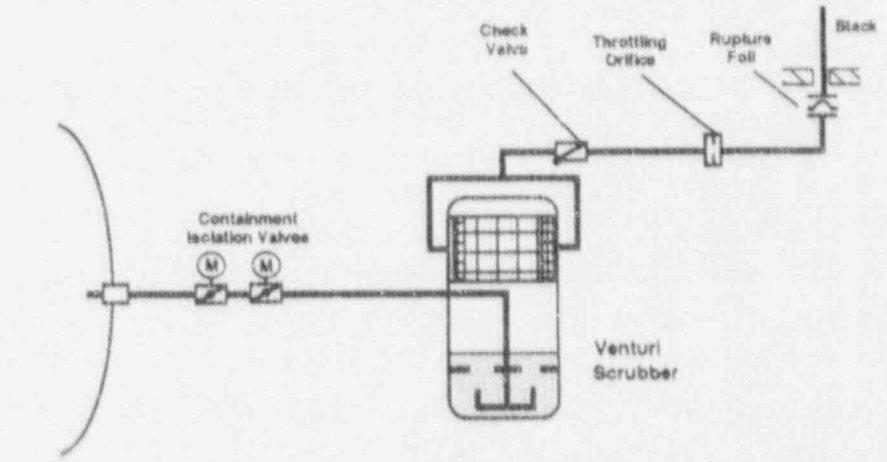

German PWRs

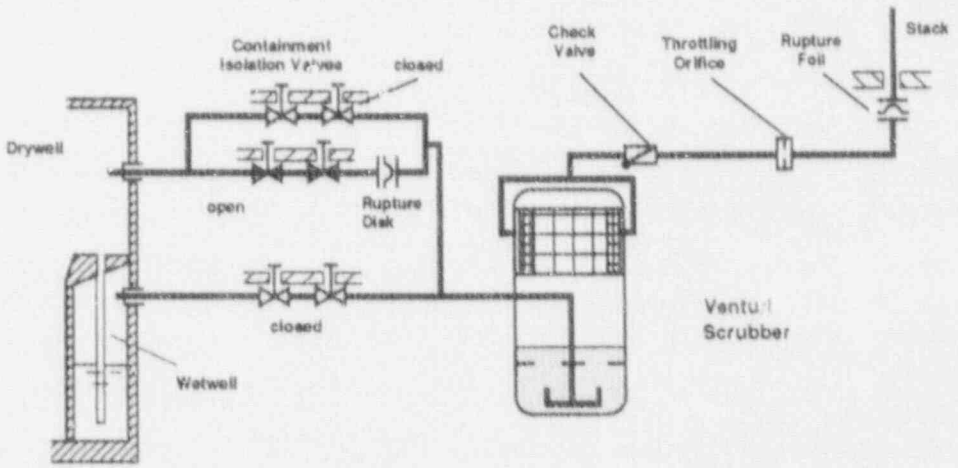

TVO BWRs in Finland

Removal efficiency:

Aerosols >99.95 %
Elemental iodine >99 %

Verified at the full-scale JAVA test facility at Karlstein.

Containment Venting
Sliding Pressure Venting Process
Flow Diagrams
Fig. 1

SIEMENS

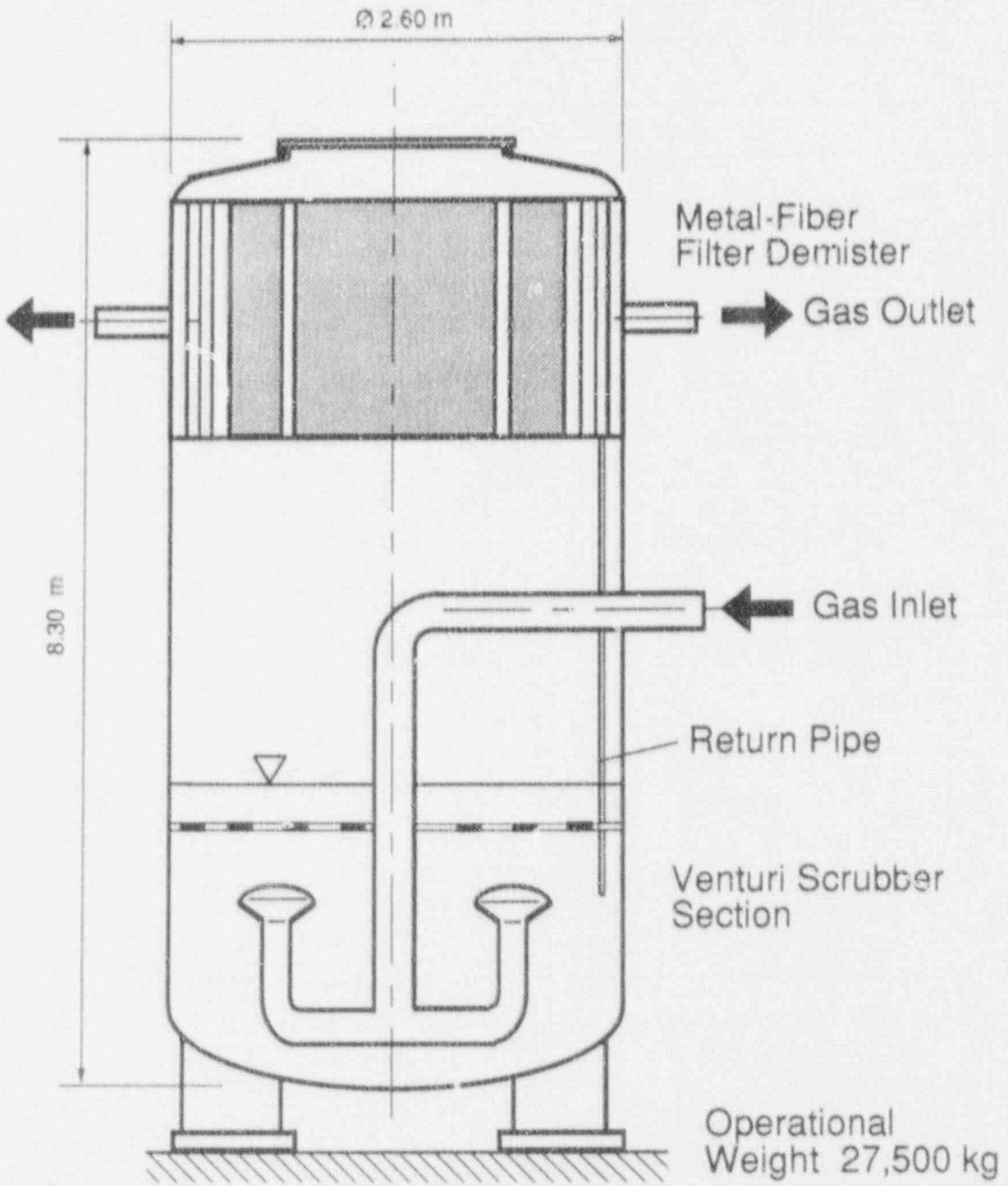

Containment Venting
Combined Venturi Scrubbing Unit
for 1300 MWe PWR Plants
Fig. 2

UB KWU
US 331
FI/01.90
13-67-A

SIEMENS

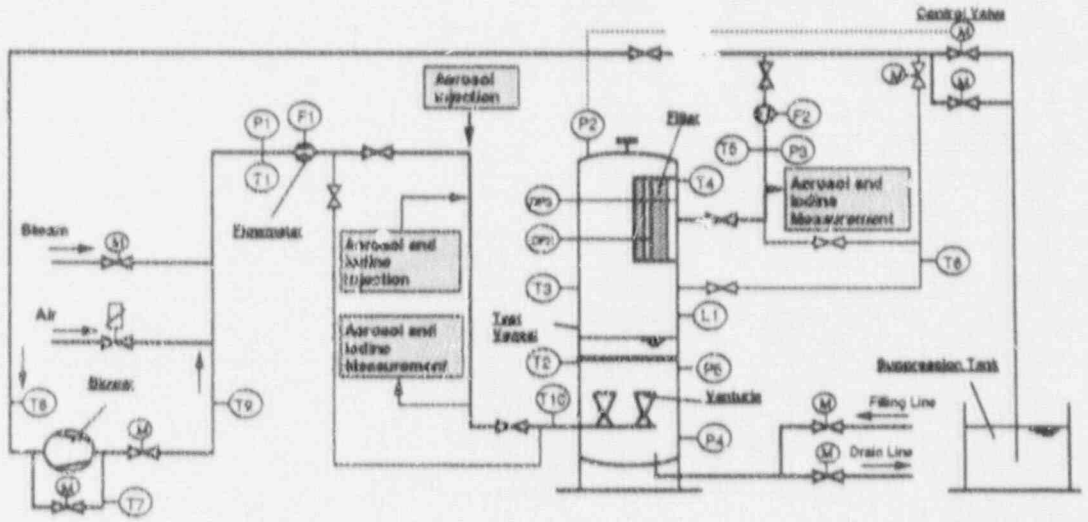

Flow Diagram

JAVA Test Facility in Karlstein

Test Parameters

Pressure	1 - 10 bar
Temperature	50 - 200 °C
Flowrate	300-3,000 m3/h
Mass flow	0.05 - 4.0 kg/s
Carrier gas	Air / steam
Aerosol concentration	SnO_2 / $BaSO_4$ 0.1 -0.6 g/m3 Uranine ≤ 0.001 g/m3

Operating Modes

Steady-state recirculation operation

Steady-state once-through operation

Transient once-through operation (startup simulation)

Containment Venting
Test Facility and Parameters
Fig. 3

UB KWU
S 331
13-02-8

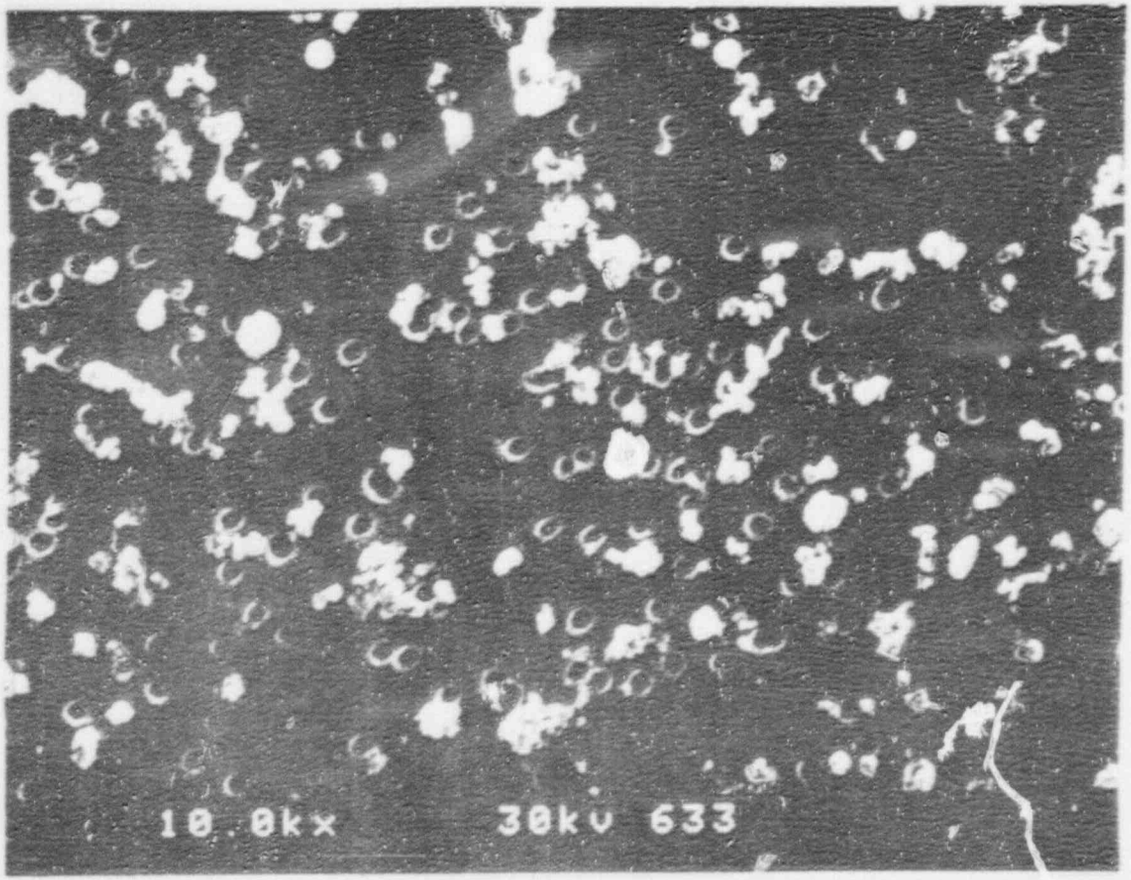

Containment Venting
SEM Photomicrograph of Test Aerosol SnO_2 Generated by Plasma Torch
Fig. 4

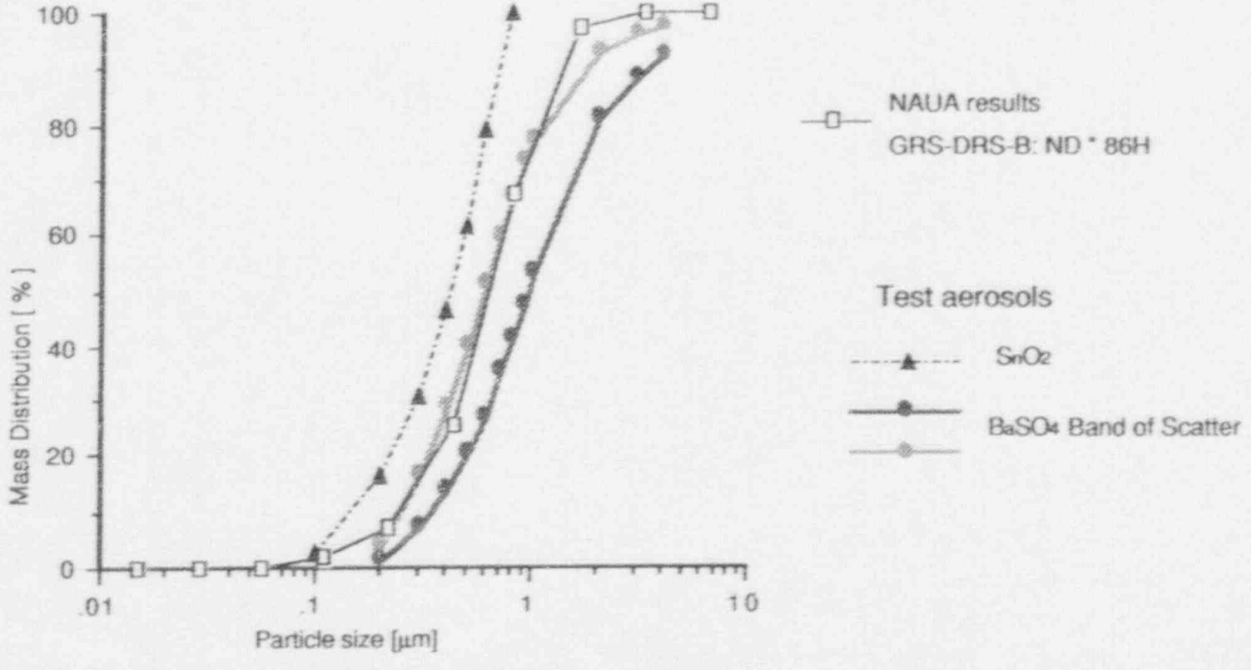

Containment Venting
Aerosol Spectra
Fig. 5

SIEMENS

Dose Rate Injection

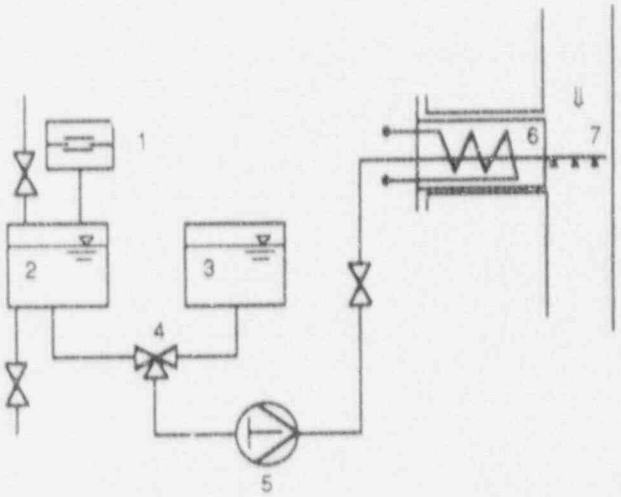

Iodine - Injection

1 Steam Barrier
2 Tank for conc. Iodine Solution
3 Deionate Storage Tank
4 Three Way Valve
5 Dosing Pump
6 Steam Generator
7 Distributer

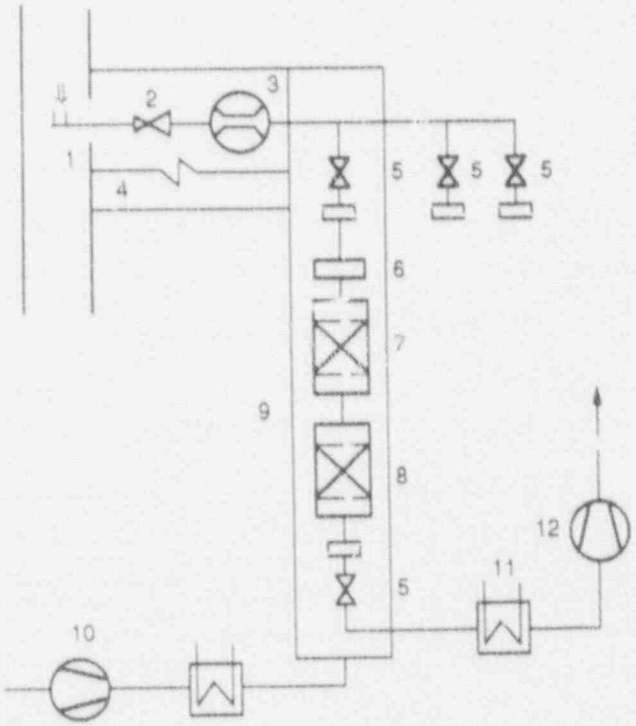

Iodine Sampling Device (schematic)

1 Hooke Injection
2 Pressure Reduction
3 Flow Meter
4 Heater
5 Valves
6 Aerosolfilter
7 Iodinefilter elem.
8 Iodinefilter org.
9 Thermo Chamber
10 Heating Blower
11 Condenser
12 Suction Pump

Containment Venting/ JAVA - Test Facility
Iodine - injection and Sampling
Fig 6

UB KWU
S 331
Et /06.90
09-05-E

SIEMENS

Test No.	Test Aerosol	Venturi Operation	Pressure [bar]	Temp. [° C]	Gas Flow [m^3/h]	Medium	Density [kg/m^3]	Contaminated Gas Concentration [mg/m^3]	Total Removal Efficiency [%]	Partial Removal Efficiency [%]
091 UL	Uranine	Medium - Energy	2. 4	102	1000	Air/ Steam		0.79	99. 999	
093 UL	Uranine	Medium - Energy	6	123	600	Air/ Steam		1.2 6	99. 999	
0105 UL	Uranine	Medium - Energy	3	113	1220	Air/ Steam		0.45	99. 998	
039 AD	$BaSO_4$	Medium - Energy	6	169	1000	Steam/ Air	3.07	227	99.999	
041 AL	$BaSO_4$	Medium - Energy	8	126	1000	Air/ Steam	6. 678	229	99.999	
040 AL	$BaSO_4$	Medium - Energy	10	129	1000	Air/ Steam	8. 394	114	99.997	
413 AL	$BaSO_4$	Medium - Energy	2	94	600	Air		356	99.996	
922 AD	SnO_2	High-Energy	4. 1	154	1250	Steam/ Air	2. 18	498	99.998	99.5
921 AD	SnO_2	High-Energy	4. 1	152	1050	Steam/ Air	2. 17	390	99.991	99. 3
927 AD	SnO_2	Medium - Energy	1.8	163	650	Steam/ Air	0.90	520	99.967	95.8

Aerosol Removal Efficiency Tests
Short Venturi with Metal-Fiber Filter Demister
Table 1

UB KWU
U 331
09-08-E

Test No.	Test Aerosol	Pressure [bar]	Temp. [° C]	Gas Flow [m ³/h]	Medium	Contaminated Gas Concentration [mg/ m ³]	Total Removal Efficiency [%]	Partial Removal Efficiency [%]
944 AD	$BaSO_4$	1.9	175	2000	Steam/ (Air)	107	> 99.999	99.2
818 AL	$BaSO_4$	2.0	106	1200	Air/ (Steam)	132	>99.999	98.9
820 AL	$BaSO_4$	2.0	112	1000	Air/ (Steam)	152	>99.999	98.9
819 AL	$BaSO_4$	2.0	114	600	Air/ (Steam)	128	99.996	97.7
826 AL	$BaSO_4$	3.3	119	1000	Air/ (Steam)	362	99.998	99.6
929 AD	SnO_2	2.2	188	2000	Steam/ (Air)	352	99.99	Water level
933 AD	SnO_2	2.4	172	2000	Steam/ (Air)	352	99.99	max.
930 AD	SnO_2	1.8	187	1500	Steam/ (Air)	400	99.97	min.
932 AD	SnO_2	1.5	161	600	Steam/ (Air)	440	99.97	min.
934 AD	SnO_2	1.9	145	1500	Steam/ (Air)	343	99.99	max.

Aerosol Removal Efficiency Tests
Long Venturi with Metal -Fiber Filter Demister
Table 2

UB KWU
U9 141
09-87-E

Test No.	Venturi Type	pH*	Pressure [bar]	Gas Flow [m³/h]	Gas Composition	Removal Efficiency [%]	Iodine Revolatization
903 ID - D	short	9. 6	4. 3	1200	Steam (air + CO_2)	99. 8%	----
905 ID - D	short	9. 5	1. 9	450	"	99. 9%	----
900/903 ID - D	short	12. 5 -9. 5	4. 3	1200	90% by vol. Steam/ 9% by vol. air < 1% by vol. CO_2	----	1.1×10^{-2} - 3.2×10^{-3} %/h
910 ID - D	long	9. 3	1. 8	2000	Steam (air + CO_2)	99. 9%	----
913 ID - D	long	8. 9	1. 8	450	"	> 99. 9%	----
907/ 903 ID - D	long	12. 7 - 9	1. 8	2000	82 - 90 % by vol. steam 18 - 10 % by vol. air < 1 % by vol. CO_2	----	1.1×10^{-3} %/h

* 0.2 % by wt. thiosulfate

Iodine Removal and Revolatization Results
Venturi with Metal-Fiber Filter Demister
Table 3

UB KWU
U 331
09-10-E

DISCUSSION

CEDERQVIST: You claim in your paper that you have about 85% to 95% efficiency for removal of methyl iodine. Can you substantiate it? Sometimes you can have you can have very high efficiency for removal of methyl iodine during transient operation, but not during long term operations. Do you think there is a risk that efficiency will go down?

ECKARDT: It was demonstrated that the measuring technique consisted of discriminating iodine samplers. It was found during the test that about 1% of the iodine was organic iodide. When we back calculated the organic iodide retention between inlet measurements and outlet measurements, we found consistent values between 85% and 95%. We tested over periods of many hours.

KOVACH: How would you compare the hygroscopic properties of SnO_2 and $BaSO_4$ to the mainly Cs salt aerosols generated in an accident?

ECKARDT: During the JAVA test series it was found that the SnO_2 and $BaSO_4$ retention efficiencies are conservatively low in comparison to soluble aerosols like Uranin (pool-specific). In addition during the ACE tests with the Siemens Venturi scrubber it was confirmed that retention efficiencies for Cs-aerosols of $>3 \cdot 10^5$ could be obtained (approximately 10 times higher than SNO_2 results during the JAVA tests).

INVESTIGATIONS INTO THE DESIGN OF A FILTER SYSTEM FOR PWR CONTAINMENT VENTING

H.-G. Dillmann, J.G. Wilhelm

Kernforschungszentrum Karlsruhe GmbH
Laboratorium für Aerosolphysik und Filtertechnik II
Postfach 3640, D-7500 Karlsruhe 1
Federal Republic of Germany

Abstract

The reactors of power stations in the Federal Republic of Germany are being or have already been equipped with systems for containment venting under severe accident conditions. Two different offgas cleaning systems are available. One system, realizing a complete passive filtering concept, which will be discussed below, consists of a multistage metal fiber filter for coarse particulates and aerosol removal and an additional molecular sieve filter for gaseous iodine retention connected in series.

The requirements made with respect to aerosol filtration includes among others the capability of retaining 60 kg of a recondensing aerosol with a 0.5 µm mean geometric mass diameter.

$BaSO_4$ and SnO_2 were used as tracer aerosols in the experiments. In various test filters comprising several metal fiber stages loadings up to 13 kg/m² SnO_2 and up to ~ 20 kg/m² $BaSO_4$ were measured. All the decontamination factors were > 1000.

Vaporous iodine is removed on molecular sieve filters (zeolite filters) subsequent to airborne particulate filtration. As Ag-zeolites act as catalysts in the H_2/O_2 reaction and thus might give rise to a violent exothermal reaction, the catalytic effect was suppressed by substituting mixed doping for doping solely with silver. The removal efficiencies achieved with Ag-zeolites and zeolites with mixed doping in air-steam mixtures are indicated, and investigations of the catalytic behavior in air-steam-H_2 mixtures are described.

I. Introduction

Continued evaluation of experimental and theoretical work on aerosol concentration and on the spectrum of particulate sizes in the containment atmosphere has led to the specification of additional stricter requirements with respect to the dust storage capability of the filter systems used for containment venting in German PWRs.

By modifications of the design the dust storage capability was greatly enhanced; additional evidence was provided on the filter performance. As regards the removal efficiency to be achieved (requirement ≥ 99.9%) no modifications had to be taken into account because also in the experiments with the least favorable spectra of particulate sizes of the tracer aerosols values ≥ 99.99% were attained in practically all cases. Despite the combustion of hydrogen in the containment which had to be ensured by use of igniters, it is assumed in a conservative approach that a hydrogen residue is still present in

the offgas. Molecular sieves have been developed whose catalytic activity on the H_2/O_2 reaction was suppressed by binary doping.

II. The Loadability of the HEPA Filters

According to the results of research work it must be expected that approximately 40 kg of mass have to be accommodated at the moment of pressure relief in the containments of German PWRs. A 50% safety allowance has been made in addition to this mass. The mean particulate diameter was fixed at the conservative value of 0.5 µm and a recondensing aerosol was specified. With that type of tracer aerosol and with other aerosols whose particulates differed in their properties loading experiments were performed.

III. Tracer Aerosols Used

$BaSO_4$, TiO_2 and SnO_2 have been used as tracer aerosols. $BaSO_4$ is a color pigment, which is supplied with different grain size distributions (Fig. 1). The flowability of all tracer aerosols has been ensured by adding small amounts of Aerosil ($\leq$ 2 vol.%, Aerosil is an extremely fine SiO_2 powder) so that plugging can be avoided in the dispersing equipment. The mean particulate diameter ranged from 0.8 to 1.2 µm.

A further tracer aerosol, TiO_2, was evaporated in an arc generated argon plasma in order to distribute the aerosols very finely. The recondensed primary particulates make up an agglomeration spectrum and were fed into the test equipment (~ 0.05-0.2 µm). It was possible to use TiO_2 both alone and mixed with other tracer aerosols, e.g. to shift the spectrum.

Rather large amounts of SnO_2 were used as tracer aerosol; they had likewise been produced by plasma evaporation, in this case as metallic tin powder, followed by oxidation. A mean particulate diameter of 0.4-0.5 µm is achieved in that evaporation. (Fig. 2)

IV. Description of the Test Rigs

The test rigs described in earlier publications were used for the loading tests /1, 2/.

In addition, a test bench of Battelle, Frankfurt, was used for some large filter loading tests because of the infrastructure equipment available at that company (large plasma torch and large steam generator). The test bench is represented in Fig. 3.

V. Description of the Filters Tested

In some experiments the filters corresponded to the usual design, namely

2.5 kg/m²	30 µm fibers in the prefilter
1.5 kg/m²	22 µm fibers in the prefilter
1.5 kg/m²	12 µm fibers in the prefilter
1.5 kg/m²	8 µm fibers in the prefilter
4.5 kg/m²	2 µm fibers in the main filter.

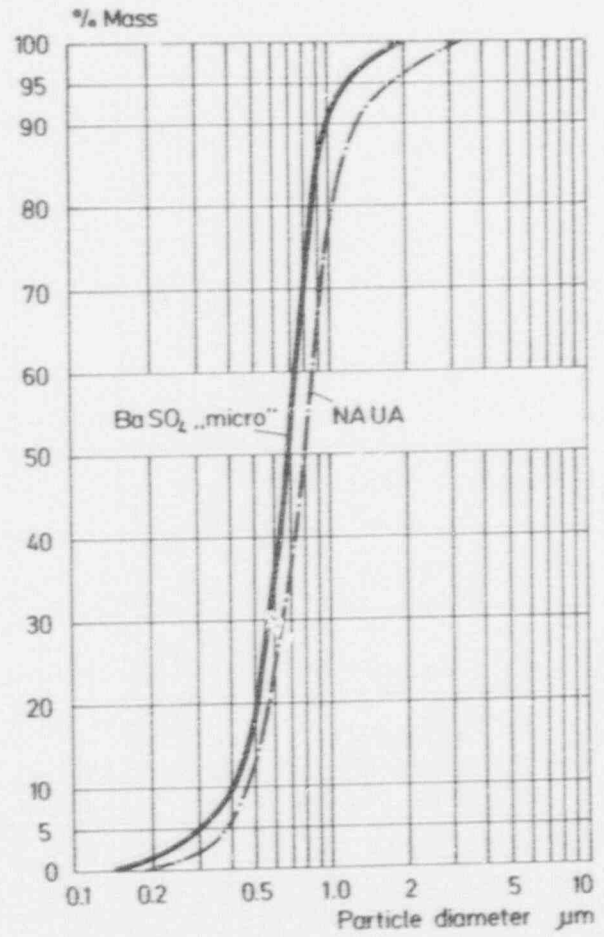

Fig. 1

Particle distribution of Ba SO_4 „micro"

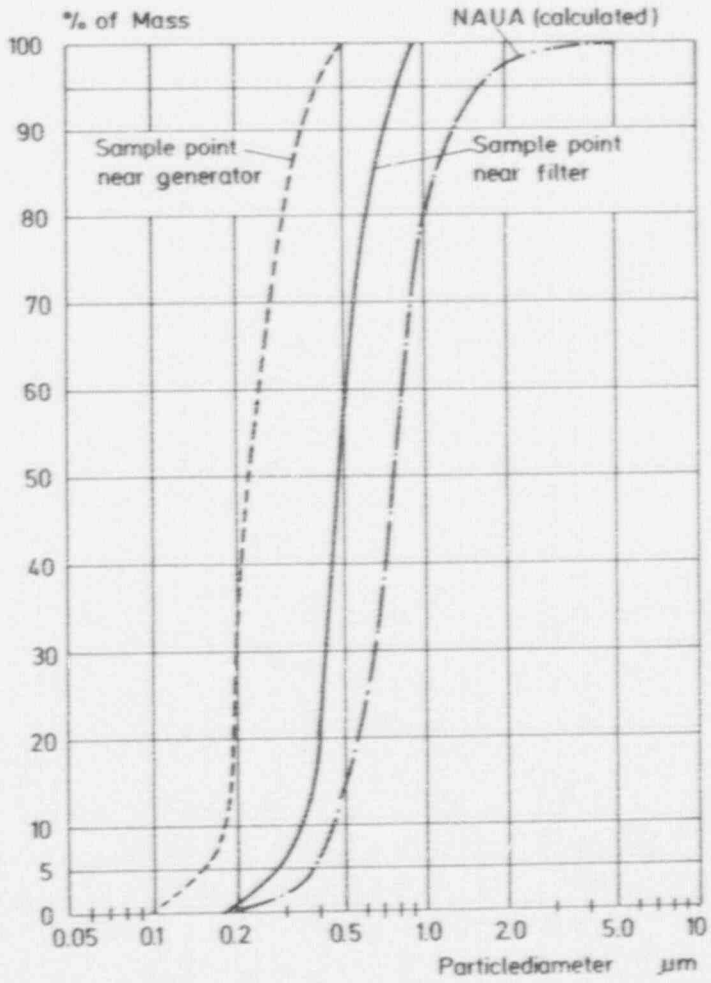

Fig. 2

Particle size distribution of SnO_2

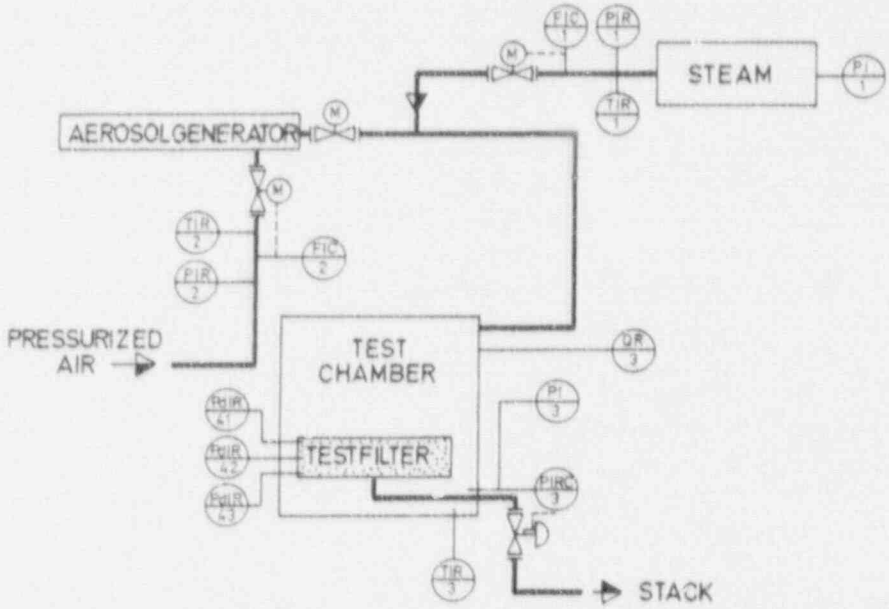

Fig. 3 FILTER TEST RIG

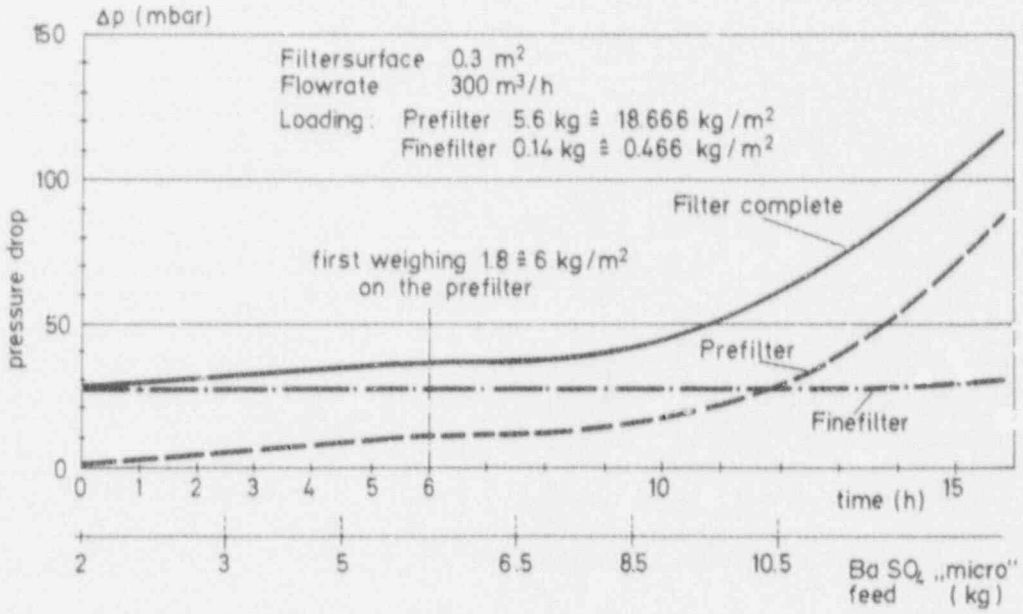

Fig. 4 Filter loading test with $BaSO_4$ „micro"

In some experiments the fine filter stage comprised half the number (only three) of layers with 2 µm fibers because the hindmost layers in direction of flow serve solely to achieve extremely high removal efficiencies and do not contribute to attaining maximum loadability.

For the finalizing tests on maximum loading the prefilter was augmented by fiber cores of 40-65 µm fibers with different layer thicknesses.

VI. Loading Experiments with $BaSO_4$

Test filters were examined for their dust storage capability using $BaSO_4$ aerosols. Fig. 4 shows the pressure loss curve in the course of loading. The tests had to be terminated at 105 mbar rise in pressure differential. A ' kg loading was measured at the filter with 0.3 m^2 filter surface ich corresponds to ~ 19 kg/m^2. The aerosol masses removed in the pipew rk between the feed point and the filter was not taken into account.

VII. Loading Tests with Mixed Aerosol

In order to determine the loadability of metal fiber filters using a tracer aerosol to which a much higher portion of fine substances than in the pure $BaSO_4$ aerosol had been added, the $BaSO_4$ aerosol (Blanche Fix) was mixed in the gas phase with the very fine aerosol TiO_2 (using the plasma evaporation method). Experience with this tracer aerosol had been accumulated both in the methods of preparation and detection. Mixing with $BaSO_4$ at the ratio 1:1 gives a bimodal mixed aerosol with 10% of the mass less than 0.2 µm in size and a median value of approx. 0.7 µm. For comparison a fine fraction of ≤ 1% at the time of venting can be determined with the NAUA code for < 0.2 µm particulate diameter. Titanium dioxide was fed approx. 3 m upstream of the test filter into the TAIFUN test section, $BaSO_4$ approx. 2 m upstream of the filter, using the technique described before, in order to keep low the aerosol losses and to get a good mixture. With this tracer aerosol the loading plot shown in Figure 5 was recorded.

The plot makes evident that the reserves for loading the metal fiber filters are sufficient also in cases where there is a very high fraction of very small particulates. After the filter had been dismantled at 105 mbar pressure differential it was weighed. The gain in weight was 1.95 kg for 0.3 m^2 face area which is equivalent to 6.5 kg/m^2 loading at 80 mbar rise in pressure differential.

In order to comply with the specification above the maximum mass to be removed on the filter installed downstream of a throttle is 2 kg/m^2 with the envisaged face area (approx. 75 mbar pressure loss). Pressurized filters of smaller dimensions which are installed upstream of a throttle are expected to remove 5 kg/m^2 at the maximum (pressure loss approx. 90 mbar).

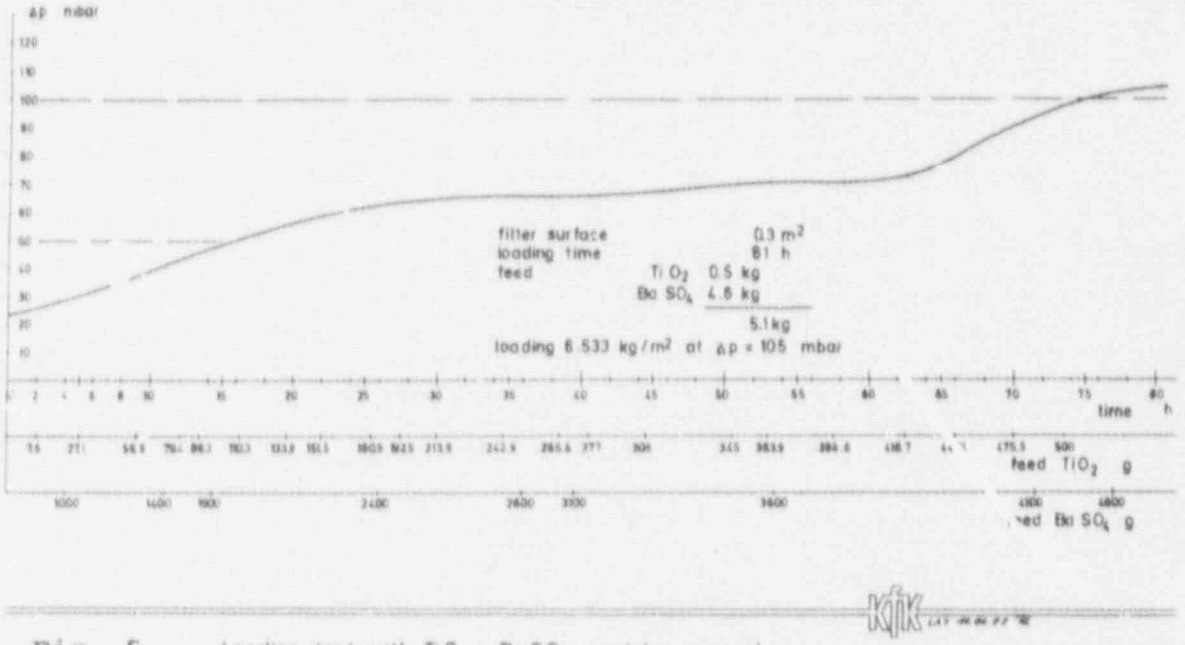

Fig. 5 Loading test with TiO_2 + $BaSO_4$ - mixing aerosol

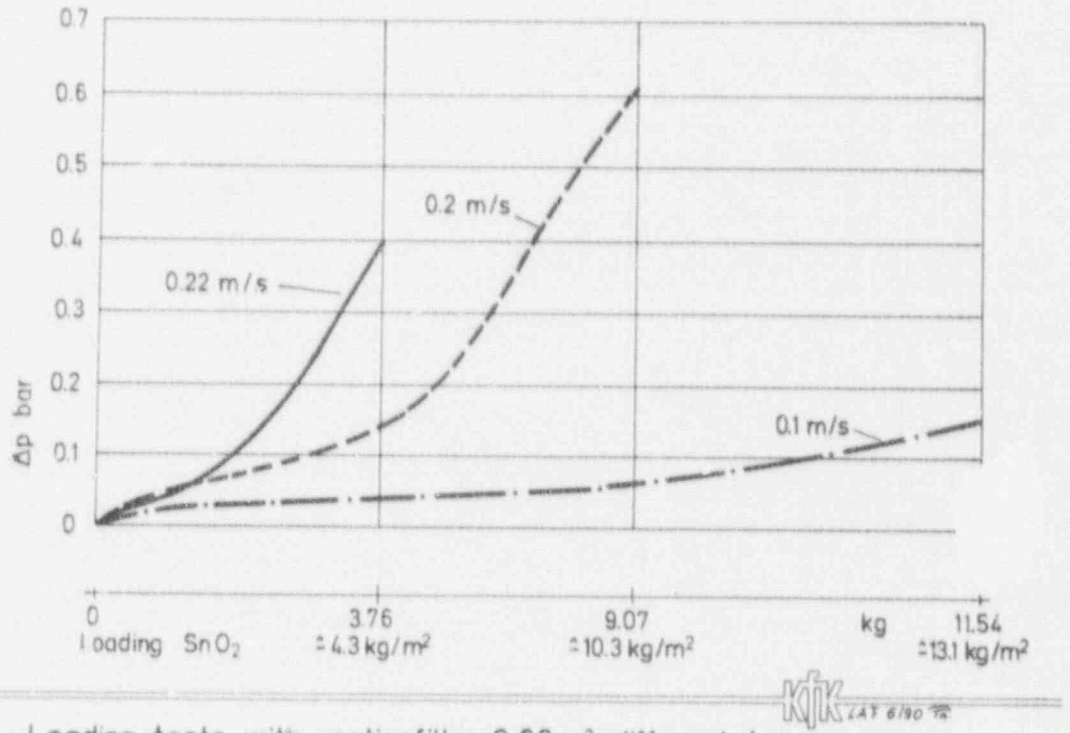

Fig. 6 Loading tests with ventingfilter 0.88 m², different types
Aerosol: SnO_2, $d_{50\%}$ ~ 0.5 µm particlediameter

Loading Tests with SnO_2

As verification tests required by a advisory committee loading tests with SnO_2 tracer aerosol were performed on filters with 0.9 m^2 filter area. Two different filter elements and two different face velocities were investigated.

The steam to air ratio was approx. 2:1. The system pressure was 4 bar in two experiments and approx. 1.5 bar in one experiment performed at approx. 145 °C. This corresponds to the conditions expected to prevail during venting provided that the filters are installed upstream and downstream, respectively, of the throttle.

The loading tests are represented in Figure 6. Figures 7 and 8 show typical SEM micrographs as well as the aerosol spectrum of the SnO_2 particulates. In the first test the total loading attained was approx. 13 kg/m^2 at 0.1 m/s face velocity and at 150 mbar pressure differential. The rated pressure differential in that experiment was 1 bar which means that the reserves are remarkable.

At twice the face velocity, i.e. 0.2 m/s, loading as determined by weighing was approx. 10 kg/m^2 at approx. 600 mbar pressure differential.

When a filter of much simpler design was used downstream of the throttle the loading was approx. > 4 kg/m^2 at about 0.22 m/s face velocity. The pressure differential attained was approx. 400 mbar.

It appeared in all tests that interruptions in operation caused a reduction in the pressure differential which means that upon resumption of operation the pressure differential was lower with the same system pressure and under identical atmospheric conditions. In order to stay on the conservative side, this effect was not taken into account when the filter was designed.

VIII. Behavior of a Loaded Cold Filter Simulation of Resumption of Operation

Startup Test

To clarify the behavior of a cold filter during startup while it is exposed to steam, one existing filter (loading 6.53 kg/m^2) was subjected to a "cold startup test" in order to simulate the phase of condensation.

Conditions of Testing

Filter temperature: 25 °C carrier gas at the beginning of exposure: humid air at 80 °C, air-steam ratio about 1:1, additional tracer feed, heating of the loaded test filter through condensation up to a value above the dew point.

Figure 9 shows the temperature and pressure plots. The pressure drop is caused by condensation at the structures of the particulates removed. The agglomerates undergo shrinkage and become more compact bodies with reduced flow resistance /3/.

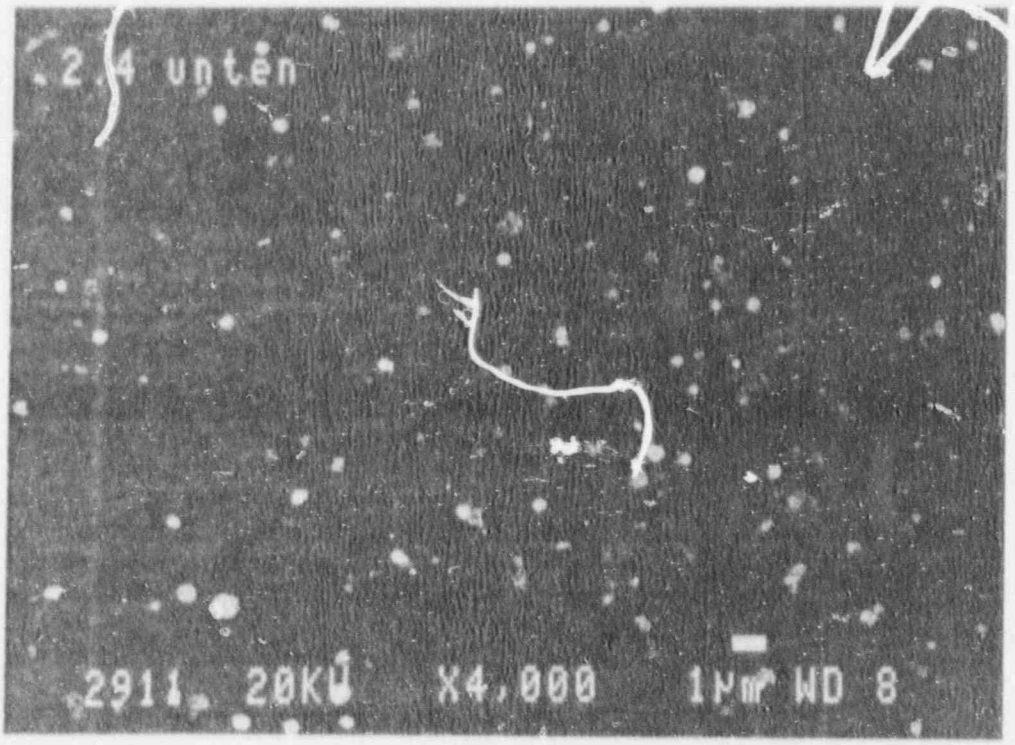
2.4 unten
2911 20KV X4,000 1µm WD 8

Fig. 7

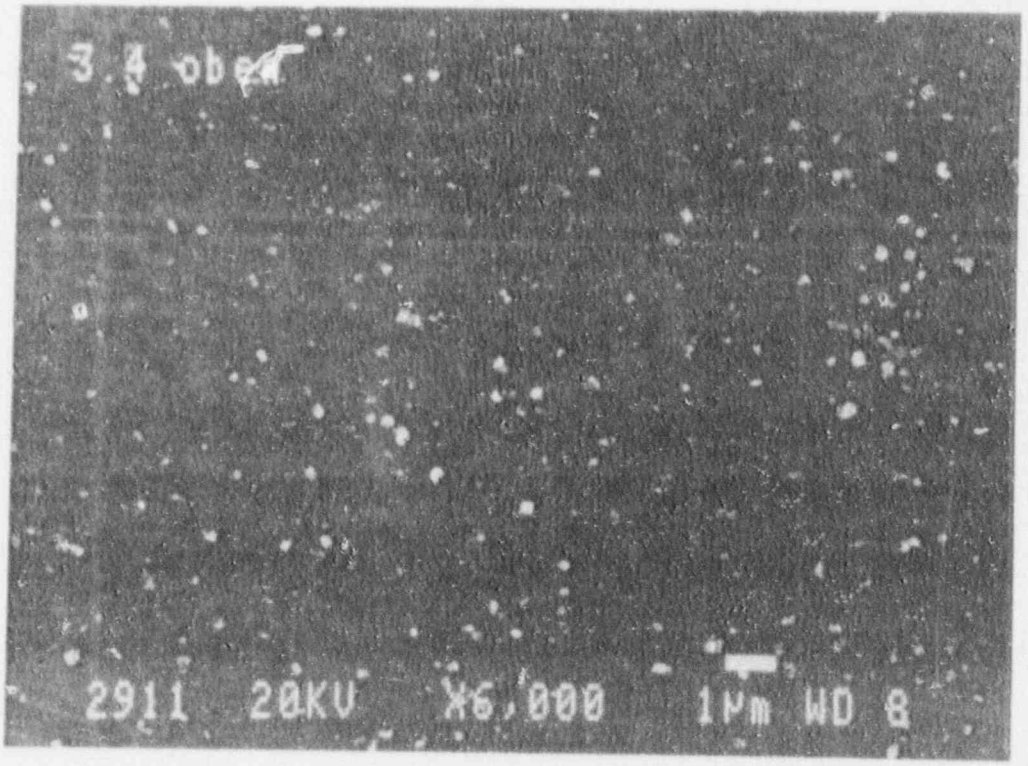
3.4 oben
2911 20KV X6,000 1µm WD 8

Fig. 8

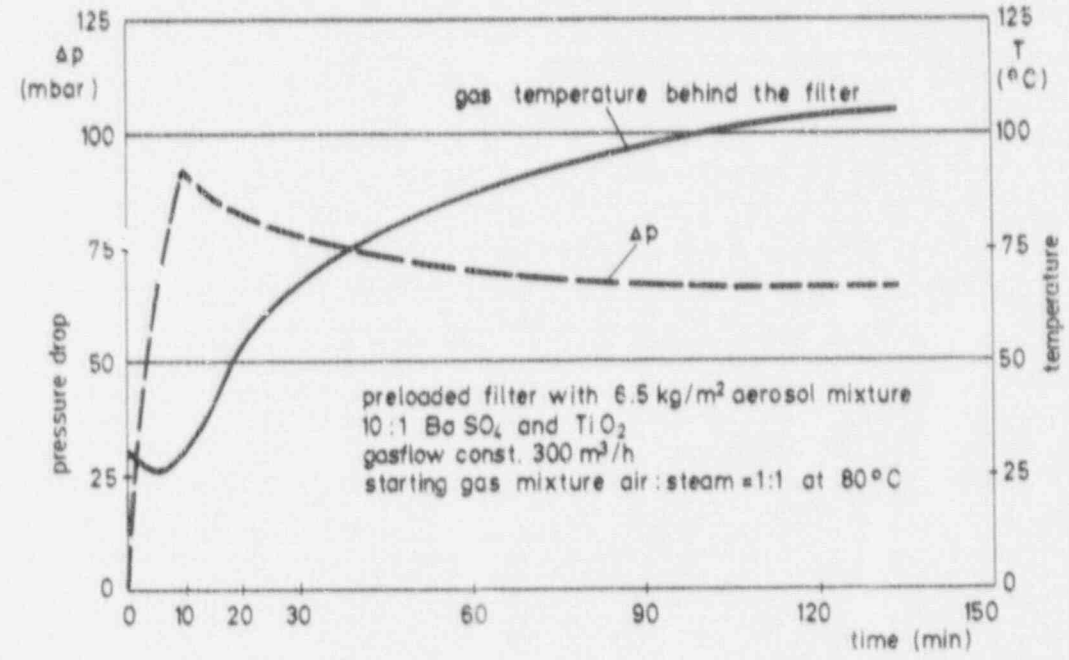

Fig. 9 Starting test with a preloaden filter with air - steam mixture 1:1

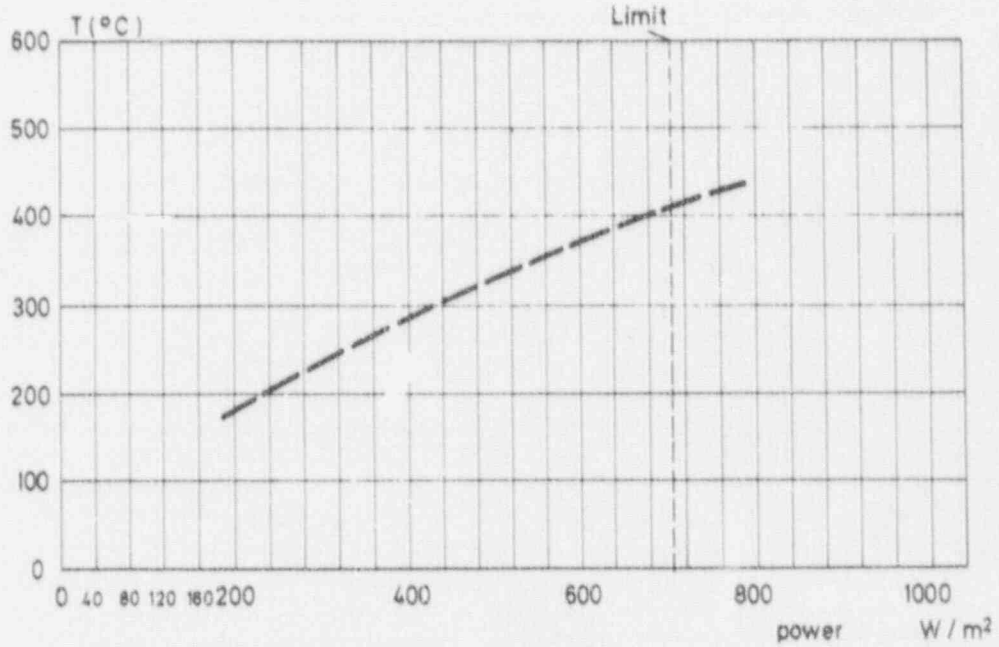

Aerosol filter stage (Flowrate = 0 m³/h)

Fig. 10 Temperature as a function of decay heat

IX. The Temperature Behavior

The materials used in venting filters resist temperatures of up to 400 to 500 °C. During filter operation the filters are cooled by the air-steam mixture; when disconnected, the filters should release the decay heat of the fission products without requiring active cooling measures, i.e. solely through convection and heat radiation. Since the relevant computations are very complex, true-scale filter modules with electric heaters integrated in the layers of the metal fiber filters and in the molecular sieve layers were heated. At constant temperatures of approx. 400 °C in the layers establishment of the temperature equilibrium was awaited and the electric power feed was measured (Fig. 10 and 11). It appears that the decay heat to be expected can be removed in a passive mode without cooling.

X. The Results of the Advanced Containment Experiments (ACE)

Under an international program some venting systems were intercompared in Richland, Washington, within the framework of the Advanced Containment Experiment.

Among others, several scrubbers and filter systems as well as combinations of both were investigated. On the KfK metal fiber filters decontamination factors of several 10^6 were obtained for cesium and manganese aerosols. The decontamination factor for iodine was 60,000 when the tracer aerosol was CsI. The relatively low DF suggests that some of the iodine had penetrated the particulate filter as a gas. The test filters had not been equipped with a sorption filter stage for iodine removal. In the preliminary test involving DOP as the tracer aerosol DFs of about 50,000 were measured. This means that the KfK metal fiber filters attained the highest decontamination factors achieved so far in these comparisons. The increase in pressure differential of the filters was 60-80 mbar (Fig. 12); in the test AA 20 the pressure increased faster in the prefilter at the end of testing; however, it dropped quickly again at constant volume flow rate. The pressure drop at the fine filter remained constant. The effect might be attributable to a typical feature of the ~ 60% CsOH aerosol fraction.

XI. Molecular Sieves for Iodine Filtration during Depressurization

The technique of filtering gaseous radioiodide from the offgas of the containment during depressurization should satisfy as far as possible the following requirements:

- passive simple removal method requiring no additional energy;
- high removal efficiency with respect to elemental and organic iodine;
- avoiding additional sources of risks, e.g. by radiolytic production of hydrogen, ignition of hydrogen-oxygen mixtures, and concentration of hydrogen bearing mixtures due to steam condensation;

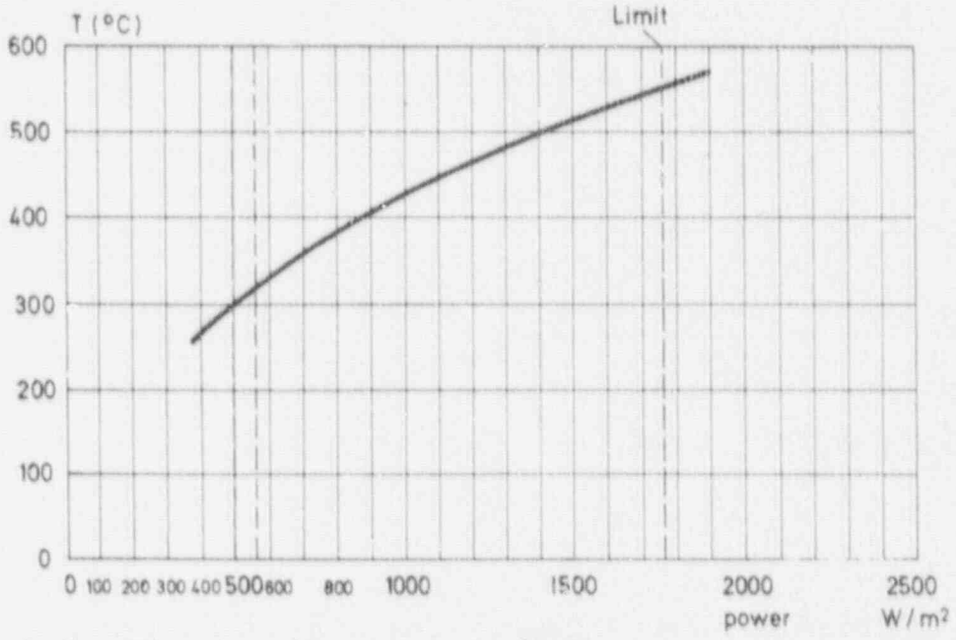

Fig. 11 Temperature as a function of decay heat

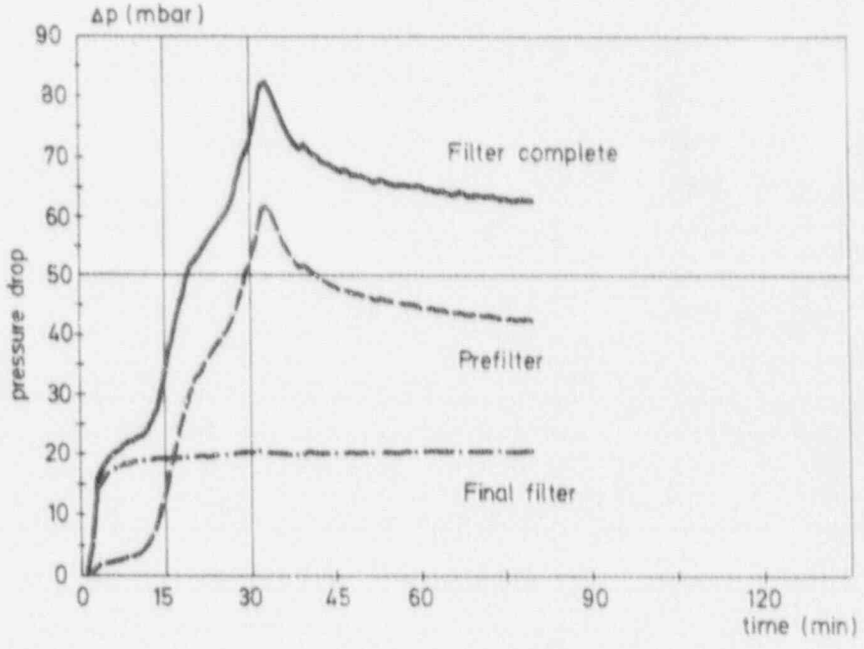

Fig. 12 ACE - Loading test with venting filter

- resistance of the removing medium to the constituents of the offgas including the reaction gases from the interaction of core melt with structural material (e.g. core melt/concrete) and elevated temperatures;

- resistance of the removal medium and of the iodine removed to high radiation doses;

- removal of the iodine such that no further measures are required during the period of decay. (The half-life of I-131 decides upon the decay time).

Radioiodide can be removed at elevated temperatures most conveniently and by passive means through filtration in a deep bed filter using silver containing molecular sieves as the sorbent material.

Already at the 20th Air Cleaning Conference it was reported about the removal efficiency of silver doped molecular sieves under the conditions of temperature and humidity to be expected during depressurization of the containment /4/. A multiplicity of further test results are meanwhile available on these materials /5/. Recent experimental activities have been focused on the development of the binary doped molecular sieves, on the measurement of their removal efficiency for elemental iodine, and on the study of the catalytic properties of these sorbent materials with respect to H_2/O_2 reactions in steam-air mixtures. Molecular sieve doping has been optimized inasmuch as catalytic properties have been suppressed and the highest possible removal efficiencies achieved. In the present report data are indicated which have been obtained during the measurement of binary doped molecular sieves envisaged for installation in the filters which are operative during depressurization.

XII. Behavior of Molecular Sieves in Steam-Air Mixtures

In the course of depressurization of the containment of a German pressurized water reactor offgas temperatures between about 160 °C (opening) and about 120 °C (closure) may be expected. The molecular sieve filter is installed in all cases downstream of the throttle and operates at a pressure which is determined by the flow resistance of the filter and of the subsequent pipework.

The relief of the pressurized steam-saturated containment offgas to a pressure close to atmospheric pressure involves drying of the offgas. The dew point in the filter can be underrated only during the startup phase while the filter still at ambient pressure is exposed to the offgas. It is assumed that preheating (an active energy consuming measure) of the flow path and the filter is renounced.

Molecular sieves absorb water while releasing much adsorption heat and are very much heated by that process. It has been shown in an experiment that while a test filter is exposed to initially saturated steam a temperature prevailed in the sorbent material which was well above the steam temperature and condensation in the sorbent material can be excluded for the entire startup phase. The temperature plot in a filter accommodating 22.2 kg molecular sieve and exposed to

an air-steam mixture is shown in Figure 13. The filter element was 610 x 610 mm in overall size with 75 mm layer thickness of the sorbent material. In the cold condition (36 °C) it was exposed to a steam-air mixture (dew point temperature 96 °C at the moment of entrance of the cold test bench). The temperature measuring points were arranged in the inflowing air 20 cm upstream of the filter with 1.5 cm and 3.7 cm, respectively, of the layer thickness of the sorbent material.

Figure 13 exhibits a very fast rise in temperature (> 100 °C) of the sorbent material within about 2 min as well as a temperature of the sorbent material which is permanently above the gas temperature. The maximum adsorption heat of the molecular sieve for H_2O is 3000 kJ/kg, 715 kcal/kg).

Table 1: **Removal Efficiency of a Binary Doped Molecular Sieve for I-131 in a Steam-Air Mixture**

Sorbent material: Molecular sieve, spherical shape, diam. 1 - 3.5 mm

Sweep gas: Steam-Air mixture 2.9:1; temperature 145 °C, pressure 1 bar, linear air velocity 31.2 cm/s

Test medium: I-127 + I-131 mixture as elemental iodine or organic iodine compound

Removal efficiency in %			
Bed depth (cm) Residence time (s)	2.5 0.08	5.0 0.16	7.5 0.24
Type A, I_2	99.74	99.973	99.981
Type A, I_2	99.46	99.946	99.966
Type A, CH_3I	84.7	96.8	99.21
Type A, CH_3I	79.6	94.4	98.1
Type B, I_2	99.930	99.973	99.983
Type B, CH_3I	95.0	99.74	99.974
Type C, I_2 *	98.7	99.19**	99.931
Type C, CH_3I	83.8	97.0	99.33

* Sorbens material conditioned for 15 h with steam air mixture + 6% H_2, before loading with I_2

** mechanical leak in 2nd test bed

The results of some investigations of the removal of elemental iodine and methyl iodide from an air-steam mixture are indicated in Tab. I. They show that high removal efficiencies (> 99.9%) can be attained. The molecular sieve specimens were conditioned with the air-steam mixture for 3-3.5 h prior to exposure and after loading with iodine (0.5-1 h) they were flushed with the air-steam mixture for 16-17 h in order to make up for any desorption processes (Test rig: Fig. 14). The experiment involving CH_3I was performed within a flushing period of only 1 h duration. A multitude of experiments carried out at an earlier date did not reveal an influence exerted by the duration of flushing. The sorbent material used in the experiment enumerated last in Tab. I was treated for 15 h at 145 °C with a steam-air mixture at the ratio 2.7:1, with 6% hydrogen added, before the removal efficiency was determined in order to detect any hydrogen induced changes of the material. In another two experiments 6% hydrogen was added to the steam-air mixture over the entire duration of the experiment (Tab. II). The equipment was not fully automated so that the duration of the experiment could only be extended to 6 h at the maximum.

Table 2: Removal Efficiency of a Binary Doped Molecular Sieve for Elemental Iodine in a Steam-Air Mixture with 6% H_2

Sorbent material: Molecular Sieve, type C, spherical shape, diam. 1 - 3.5 mm

Sweep gas: Experiment I: 47% steam, 47% air, 6% H_2, V_{1in} 31.2 cm/s
Temperature: 145 °C, pressure 1 bar

Experiment II: 65% steam, 29% air, 6% H_2, V_{1in} 50 cm/s
Temperature: 145 °C, pressure 1 bar

Exp. I	Bed depth (cm)	2.5	5.0	7.5
	Residence time (s)	0.08	0.16	0.24
	Removal efficiency (%)	97.9	99.42	99.86
Exp. II	Bed depth (cm)	2.5	5.0	8.0
	Residence time (s)	0.05	0.1	0.16
	Removal efficiency (%)	90.4	96.6	99.34

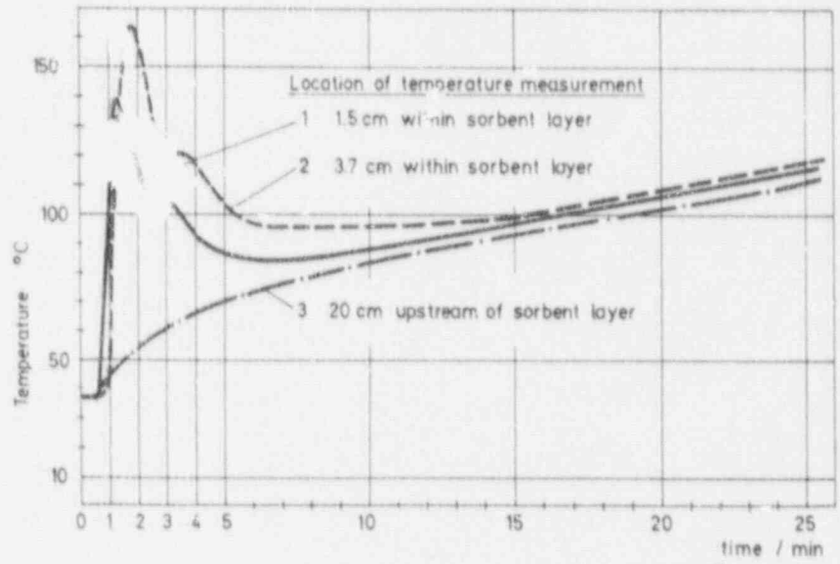

Fig. 13 Development of temperatures in gas and sorbent during start - up phase

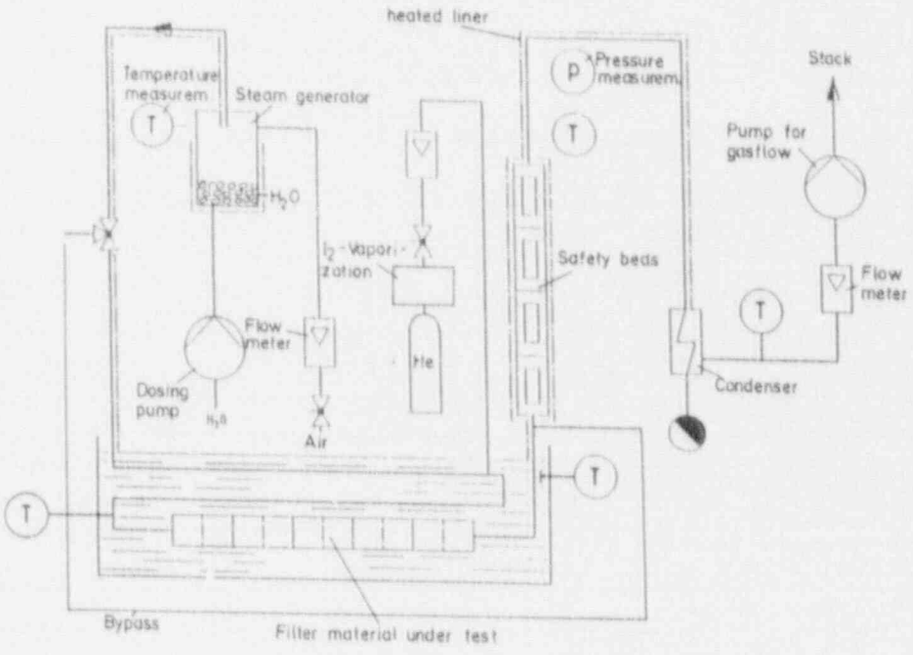

Fig. 14 Test rig for Iodine removal efficiency of sorbens

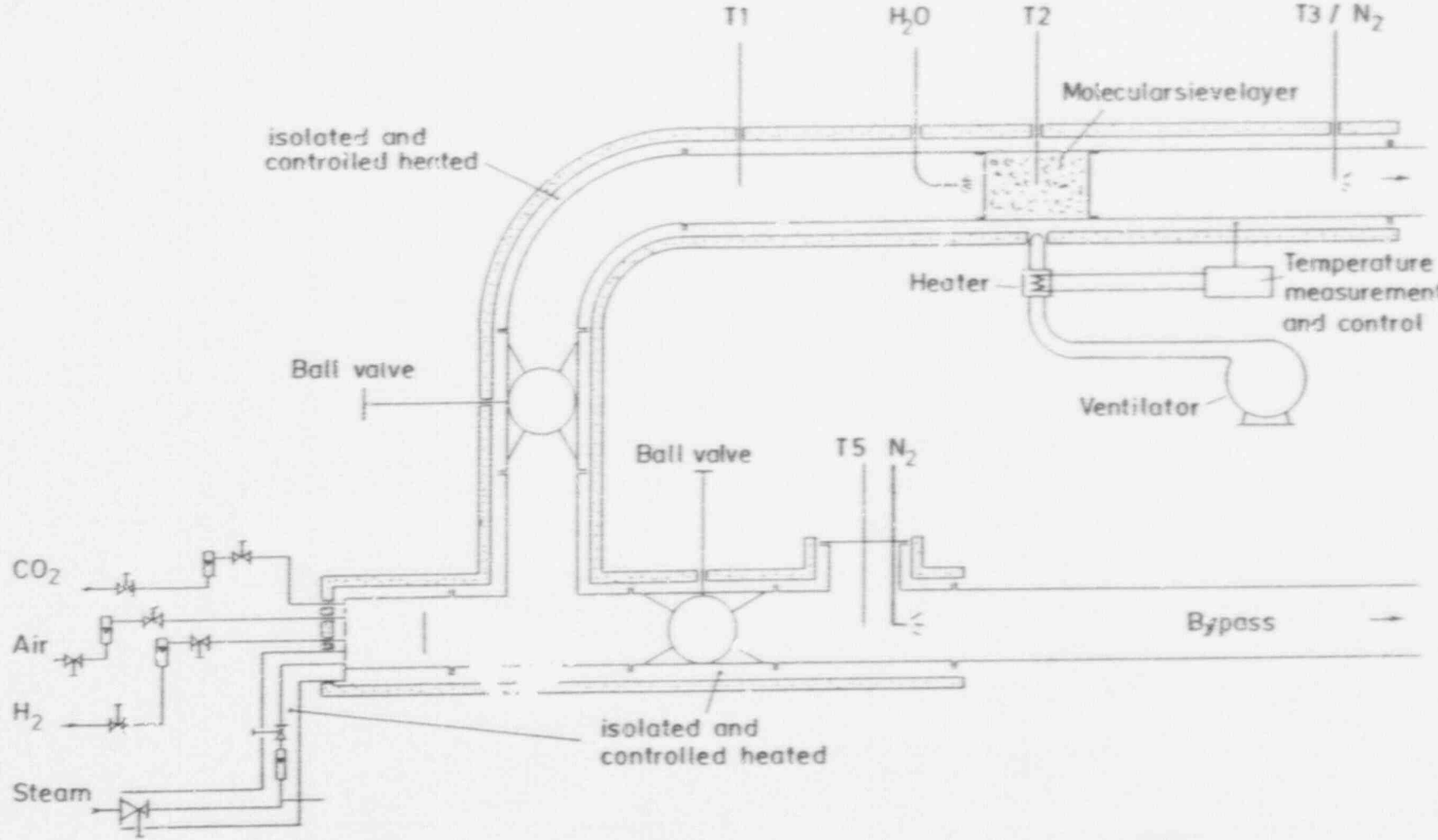

Fig. 15

KfK LAF 7/90

Testrig for H_2-Experiments with Molecularsieves

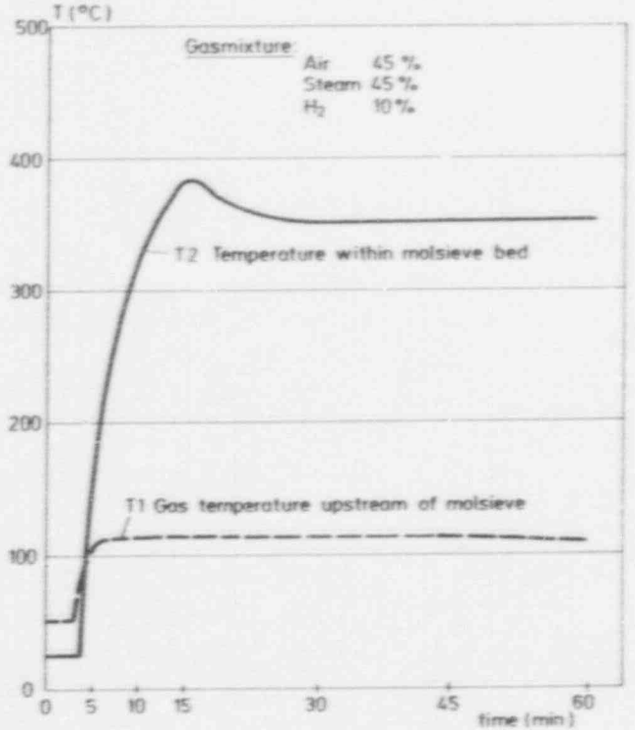

Fig. 16

Catalytic behaviour of a AgX-molecular sieve

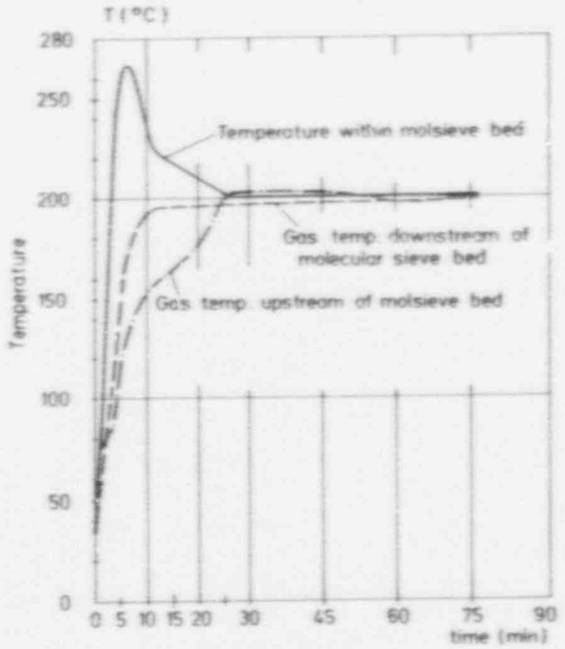

Fig. 17

Temperature behaviour
of a binary doped molecular sieve

XIII. Experiments on the Catalytic Activity of the Molecular Sieve

The investigations were made with the equipment shown in Fig. 15. The majority of the tests were performed with a conservative steam-air mixture as regards the air fraction, namely at the ratio 1:1. The hydrogen fraction in the total gas mixture was set at 5, 10 and 15%. The linear gas velocity around the sorbent material was fixed at 10, 20 and 30 cm/s. To record also the heat effect due to adsorption of the steam during the startup phase the dry molecular sieve was challenged abruptly by switching the gas flow from the by-pass section to the test section. The pipe section ending shortly in front of the molecular sieve bed was heated before switching; the pipe section with the sorbent material was heated to the temperature of the inflowing steam beginning with startup in order to compensate for the heat losses of the molecular sieve bed (2.5 cm in diameter).

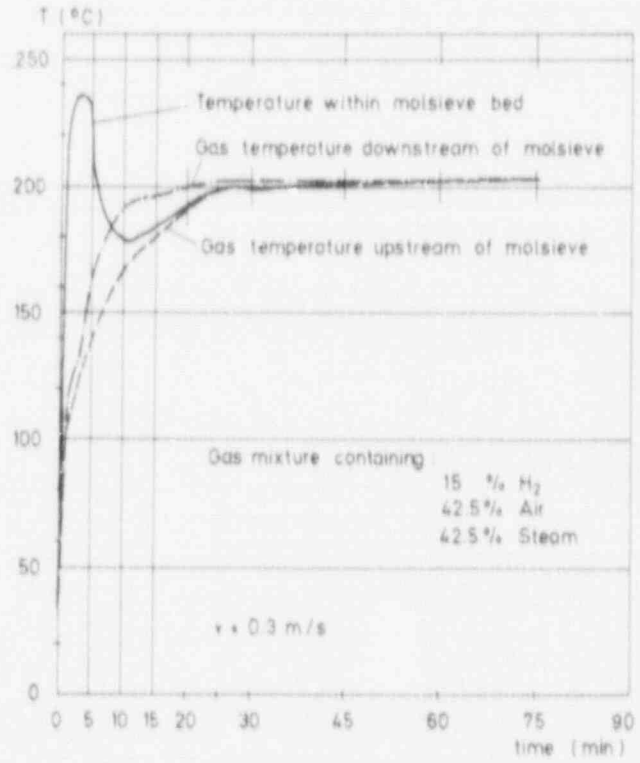

Fig. 18 Temperature behaviour of a binary doped molecular sieve

The catalytic reaction of the exclusively silver doted molecular sieve produced the maximum heat effect with 10% hydrogen fraction and 10 cm/s linear gas velocity. Figure 16 shows the typical temperature plot in the inflowing gas mixture and in the molecular sieve bed in one of these experiments. After a temperature maximum occurring at the beginning around the molecular sieve bed and caused by the amount of heat released by H_2O adsorption and H_2/O_2 reaction a constant overall temperature difference of about 230 °C established between the inflowing gas mixture and the sorbent material due to the catalytic reaction of hydrogen with the oxygen present in the air.

Figure 17 shows the temperature plot when a binary doped molecular sieve is used. During startup of the initially low temperature molecular sieve a temperature develops very quickly around the layer of the molecular sieve which lies above the temperature of the inflowing gas mixture. This higher temperature decreases within a time interval determined essentially by the gas velocity and hence by the amount of water supplied per unit of time and attains again a level near the gas temperature. This is also shown in Fig. 18 under different conditions.

In a great number of further experiments the suppression of the catalytic properties of the molecular sieve due to binary doping could be demonstrated for the individual molecular sieve batches.

IVX. References

/1/ Dillmann, H.-G., Pasler, H.: "Experimental Investigations of Aerosol Filtration with Deep Bed Fiber Filters", CONF-820833, Vol. 2, p. 1160 (1983).

/2/ Wilhelm, J.G., Dillmann, H.-G., Gerlach, K.: "Testing of Iodine Filter Systems under Normal and Post-Accident Conditions", CONF-720823, Vol. 1, p. 434 (1972).

/3/ Franklin, H., Knutson, E.O, Hinchliffe, L.E.: "A Humidity Effect in the Flow Resistance of Loaded Fibrous Filters", Atmospheric Environment, Vol. 10, p. 911 (1976).

/4/ Dillmann, H.-G., Pasler, H., Wilhelm J.G.: "Offgas Cleaning Devices for Containment Venting", CONF-880822, Vol. 9, p. 709 (1989).

/5/ Reichert, U., et al.: "Zeolithe als Sorbens für die Iodabscheidung bei der Druckentlastung", PSF-Jahresbericht 1989, KfK-Bericht 4700, S. 142-149, (to be published).

DISCUSSION

KOVACH: I would like to say that I am very glad you have decided to switch to some material other than silver adsorbents. As we discussed at the last Air Cleaning Conference, their use could create more of a hazard than assistance in some units. Maybe it is a help that we have had a lot of success in this country with silver-lead combination absorbents to prevent this type of application.

MULCEY: Did you perform specific investigations on the hygroscopic nature of the aerosol to be filtered with regard to the pressure drop increase?

DILLMANN: Not directly, but the ACE Experiments with approximately 60% of CsOH have been finished successfully. In a real accident the content of CsOH in the containment atmosphere will be in the range of a few percent.

EXPERIMENTAL STUDY ON AEROSOL REMOVAL EFFICIENCY FOR POOL SCRUBBING UNDER HIGH TEMPERATURE STEAM ATMOSPHERE

J. Hakii
Nuclear Power Plant Planning Div., Tokyo Electric Power Co.,Inc.
1-3, Uchisaiwai-cho, 1-chome, Chiyoda-ku, Tokyo, 100, JAPAN

I. Kaneko and M. Fukasawa
Nuclear Engineering Laboratory TOSHIBA Corporation
4-1 Ukishima-cho, Kawasaki-ku, Kawasaki, 210, JAPAN

M. Yamashita
Nuclear Reactor Design Division, TOSHIBA Corporation
8 Shinsugita-cho, Isogo-ku, Yokohama, 235, JAPAN

M. Matsumoto
Nuclear Power Engineering Department, HITACHI Ltd.
1-1, Saiwaicho 3-chome, Hitachi-shi, Ibaraki-ken, 317, JAPAN

ABSTRACT

Removal efficiencies of particulate materials in water pools were studied. The experiments were carried out for many different parameters such as geometric, thermal hydraulic and aerosol properties. The experiments were performed with the scrubbing pool which is a cylindrical pressure vessel of 1 meter in diameter and 5 meters high.

From the experimental results, it was confirmed that the efficiency strongly depended on scrubbing depth, particle diameter and steam fraction of carrier gas. The efficiency increased significantly when the steam fraction exceeded 50 vol.%.

Moreover, the authors confirmed the efficiency reduction phenomenon at boiling pools, which had been theoretically predicted. As the results, the efficiency for the boiling pool decreased to a half of that for a subcooled pool in the case of 2.7 meters scrubbing depth.

INTRODUCTION

There are many facilities which contain water in nuclear power plants. These facilities will serve as a particulate material catcher.

When particles (aerosol) included in a mixture of incondensable gases and condensable steam are released into water pools, the aerosol is expected to be retained in water.

In the present study, experiments were carried out in order to investigate the 'scrubbing effect', which means the removal phenomenon for the aerosol material in water pools.

Carrier gas injected into a water pool forms bubbles and aerosol

is suspended in the bubbles. The suspended aerosol moves to the surface of the bubble through several driving forces such as gravitational settling, inertial deposition, diffusional deposition and steam condensation. Aerosol is expected to be retained in the water, when it has just arrived at, and deposited on the surface of a bubble. Table 1 shows models for aerosol deposition velocity adopted for the prototype SPARC code (1).

Table 1 Calculation models for pool scrubbing (prototype SPARC code)

• Gravitational Settling Velocity	$V_g = \frac{\rho_p \cdot d_p^2 \cdot C_c \cdot g}{18\mu}$
• Inertial Deposition Velocity	$V_c = \frac{V_b^2 \cdot \rho_p \cdot d_p^2 \cdot C_c}{4\mu D_b} \sin^2\theta$
• Diffusional Deposition Velocity	$V_D = 2\left(\frac{D \cdot V_b}{\pi D_b}\right)$
• Deposition Velocity by steam condensation or evaporation	$V_v = \frac{W_v}{\left(\frac{M_w (P_g + P_w)}{R \cdot T_0}\right)}$

ρ_p : particle density	W_v : average vapor flux into a bubble
d_p : particle diameter	M_w : average molecular weight at the surface
C_c : Cunningham slip correction factor	P_g : total pressure at pool surface
g : acceleration due to gravity	P_w : water vapor pressure
μ : gas viscosity	T_0 : interface temperature
V_b : bubble rise velocity	R : gas constant
D_b : bubble diameter	D : particle diffusivity
θ : angle measured from vertical pole	

The SPARC code, which was released by U.S. NRC, is used for scrubbing effect analysis. The authors referred these models when test conditions were chosen.

The test conditions had been expanded to cover a wide range of conditions to investigate various situations.

TEST CONDITIONS

There are many factors which affect aerosol deposition velocities as shown in Table 1. The authors selected eight parameters considering geometric, thermal hydraulic and aerosol properties. The parameters and their ranges are shown in Table 2. Standard values were selected for each parameter and tests were carried out while varying only one parameter. This clarifies the influence by a specific parameter.

Polystyrene LATEX particle was used in this test, because its diameter is fixed and its density is unity. The authors didn't change particle density parametrically, because the aerodynamic diameter was used for evaluating results. Consequently, particle diameter was chosen for aerosol property and sometimes, CsI was also used for comparison with LATEX. For the thermal hydraulic property, some fundamental factors were chosen. They are pool water temperature, carrier gas temperature, carrier gas steam fraction, and carrier gas flow rate. Scrubbing depth and injection nozzle diameter were chosen for geometric property.

Table 2 Scrubbing test conditions

Parameter		Standard value	Range
Geometric property	injection nozzle diameter (cm)	15	1～15
	scrubbing depth (meters)	2.7	0～3.8
Hydraulic property	pool water temperature (℃)	80	20～110
	carrier gas temperature (℃)	150	20～300
	steam fraction (vol.%)	50	0～80
	carrier gas flow rate (L/min)	500	300～2000
Aerosol property	particle diameter (μm)	0.2～1.0	0.2～1.0
	material	LATEX	LATEX,CsI

It is expected that a bubble formed in a boiling pool would get larger as it goes up in the pool, because pool water evaporate to the inside of the bubble. Therefore, it will be difficult for aerosol to move toward the surface of a bubble against the water vapor flux. In order to investigate this efficiency reduction phenomenon, the authors carried out several tests under boiling pool conditions.

It should be noticed that bubble diameter and its rise velocity are also important parameters for both inertial deposition and diffusional deposition velocity, as shown in Table 1. As bubble rise velocity depends on its diameter, only bubble diameter should be considered. In these tests, injection nozzle diameter and flow rate were varied, instead of varying the bubble diameter itself. The authors consider that the bubble diameter distribution formed under these conditions, is more suitable for a real scrubbing phenomenon than uniformly controlled bubbles. It was reported as a result of BCL/EPRI experiments, that the bubble diameter distribution does not depend on hydraulic and geometric conditions. The mean value of bubble diameter and the geometric standard deviation were reported to become about 5.6 millimeter and about 1.5 respectively, under various conditions (2).

TEST APPARATUS

Figure 1 shows the test apparatus. This is composed of carrier gas generation system (air compressors and steam boiler), aerosol generator, scrubbing pool, pool water control system and exhaust gas treatment system.

Carrier gas generation system can serve air/steam mixture gas at a 2000 N·L/min maximum flow rate at 6 kg/cm^2-G maximum gas pressure and 300°C maximum gas temperature.

The aerosol generator is an atomizer type. The solution contained aerosol is injected into carrier gas using air pressurized by 2-3 kg/cm^2 versus carrier gas and the solution pressurized at the same pressure as carrier gas.

Figure 2 shows scrubbing pool details. It is a cylindrical pressure vessel, 1 meter in diameter and 5 meter high. It has 5 pairs of windows, 20 cm in diameter. Maximum scrubbing depth is 3.8 meters.

The pool water control system can heat or cool the pool water by circulating pool water through two external heat exchangers. This system can control the pool water temperature from room temperature to 120°C.

The exhaust gas treatment system is located down stream from the scrubbing pool. Two pressure control valves maintain carrier gas pressure in the scrubbing pool. This system also has a heat exchanger and an industrial wet scrubber. The former is used to cool exhaust gas and the latter is used to remove aerosol.

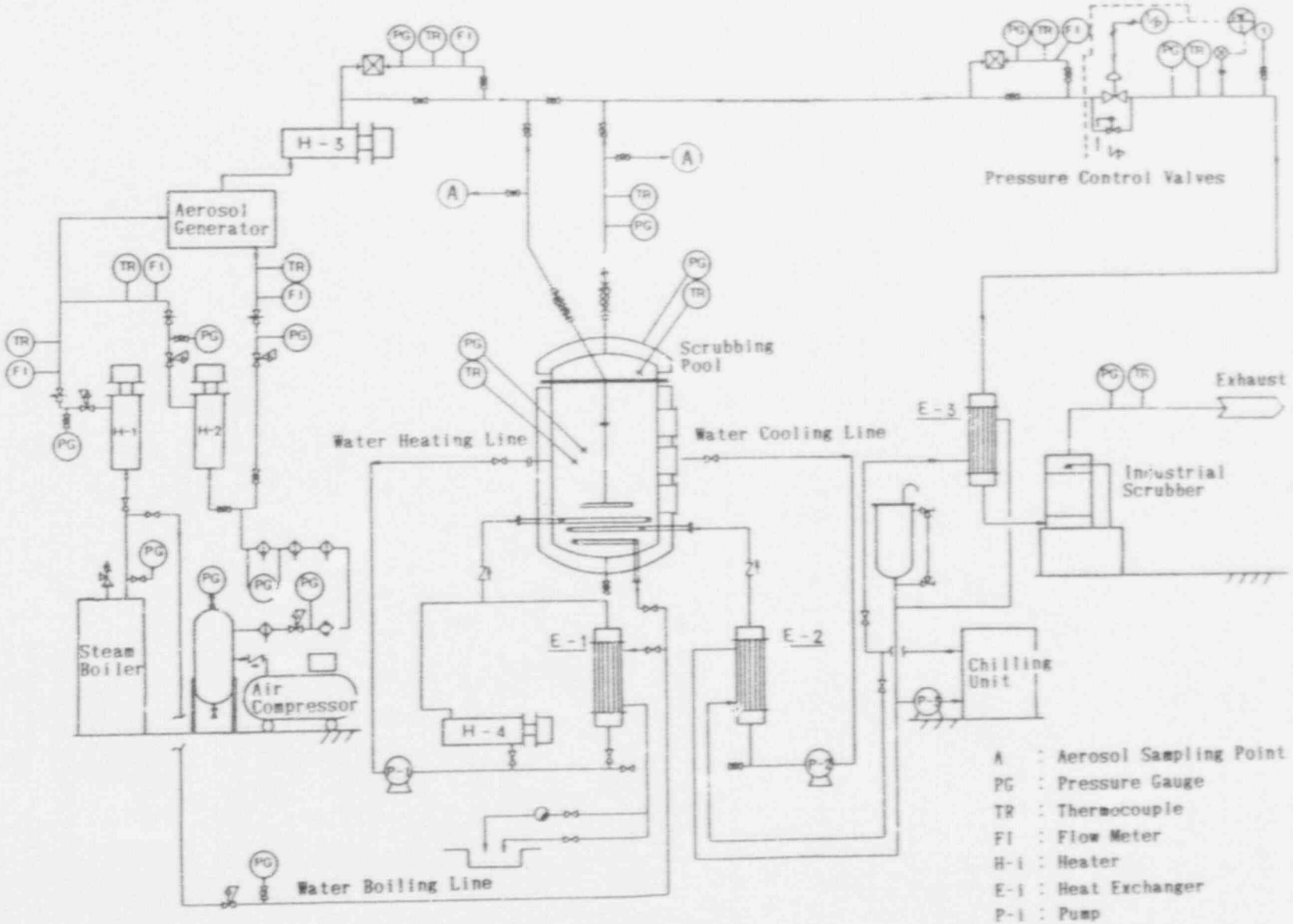

Figure 1 Test apparatus

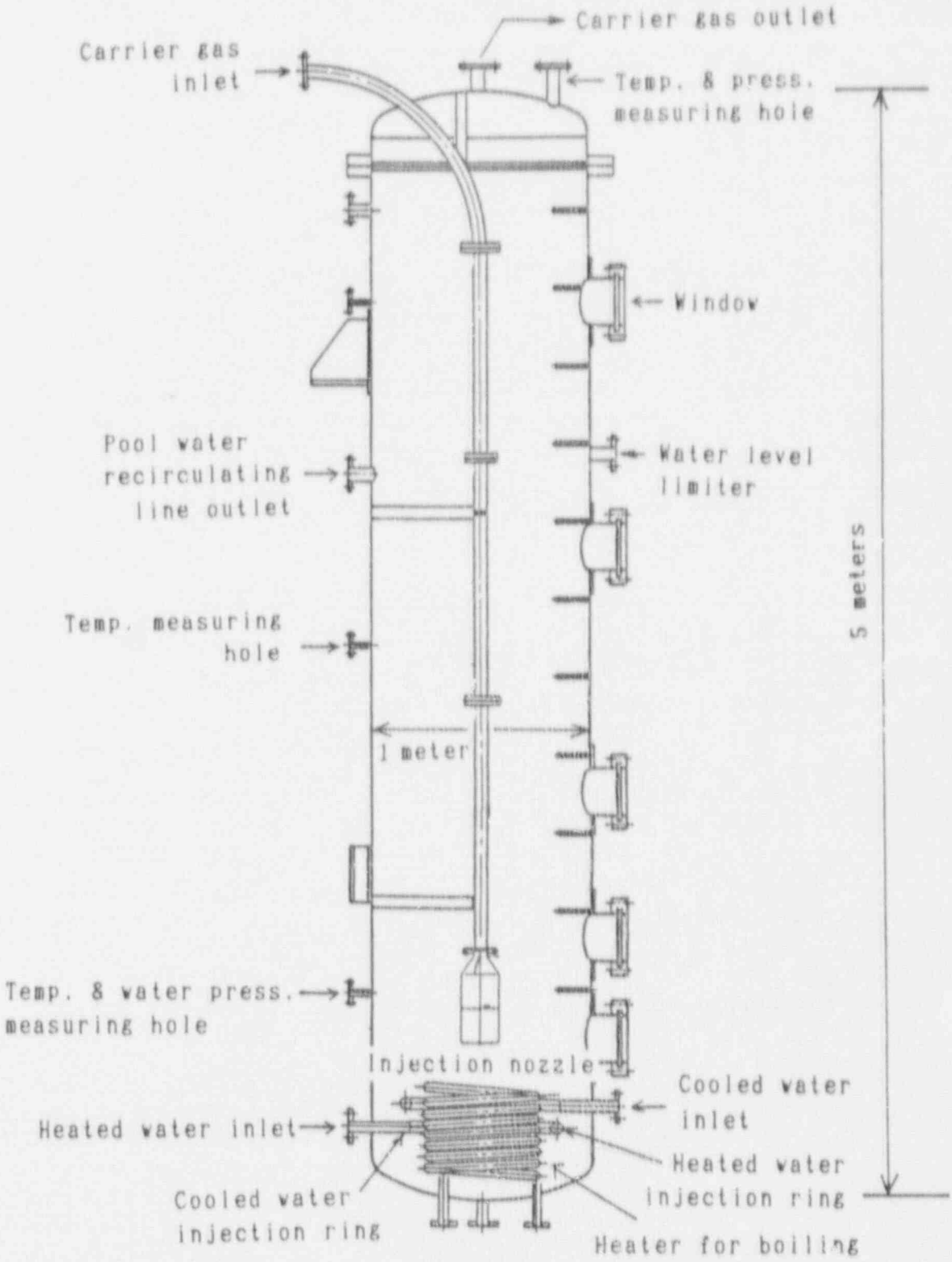

Figure 2 Scrubbing pool

AEROSOL MEASURING METHOD

In these tests, two kinds of aerosol material were used. One was LATEX and the other was cesium iodine. These aerosols were measured by different methods. Explanations of each measuring method follow (refer to Fig. 3).

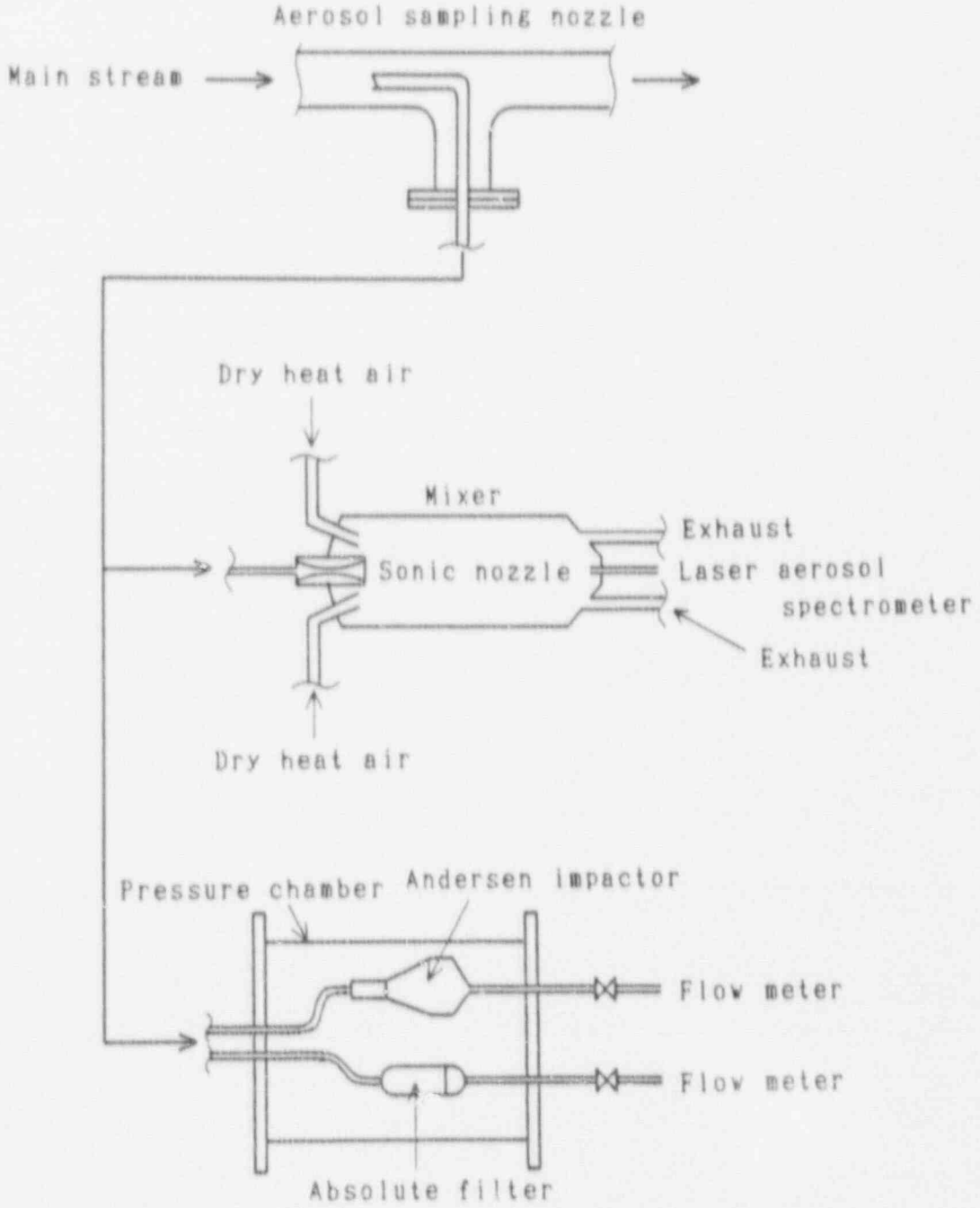

Figure 3 Aerosol measuring system

LATEX MEASUREMENT

Polystyrene LATEX particles were used in the test. The particle diameters were 0.21, 0.31, 0.56 and 1.0 micro meter.

The aerosol sampling nozzles look like a pitot tube. They are in main line located down stream and up stream from the scrubbing pool. Aerosol is extracted from main stream by the sampling nozzles.

In aerosol measurement, the most severe condition is when aerosol exists in a pressurized steam mixture gas. In this case, the authors used the sonic nozzle to reduce the sampled gas pressure. This sonic nozzle also provides a constant flow, which depends on its critical flow. Just after this depressurization, the sampled gas is diluted 150 times by highly dried air at the same temperature. Most of the diluted gas was exhausted and a few 10 cc/sec of the gas was cooled to room temperature. During this cooling, a mist contamination by steam condensation would not happen, because the gas dew point had been reduced below room temperature by that dilution. The cooled gas is introduced to a laser aerosol spectrometer and its particle diameter and number concentration are measured.

Generally, it is expected that particle diameters and number concentrations are disturbed by those complicated processes. In this test, this disturbance is kept small by following reasons, (1) using fixed diameter LATEX, (2) adopting a diameter range, which is unlikely to deposit and (3) designing the sampling lines to be unlikely to deposit. The authors performed the calibration tests using a vacant scrubbing pool under various conditions. As the results , the difference in particle number concentrations between sampling points down stream and up stream from the pool was 20 % at the maximum.

CsI MEASUREMENT

Cesium iodide is so hygroscopic that it tends to absorb water vapor in carrier gas. Due to this property, it is expected that differences in steam fraction would change the CsI particle diameter. The CsI particle diameter will be small, if the same dilution process as the LATEX measurement is used. The reason is that the process strongly decreases the sampled gas steam fraction.

For CsI measurement, a conventional Andersen impactor was used. However, it was not used under atmospheric conditions. The impactor was used at the same temperature and pressure as sampled gas to maintain the original diameter.

An Andersen impactor is usually used under depressurized conditions obtained by a suction pump. In this test, since the impactor is sometimes used under highly pressurized condition, calibration tests using LATEX were carried out. Results confirmed that the impactor can be used with only general theoretical compensation.

TEST RESULTS

In this test, many different parameters, which expanded to wide range, were introduced. Some important results are as follow. The removal effect is defined as the ratio of entrance aerosol concentration to the exit aerosol concentration, which is called the 'decontamination factor'.

The value for each parameter follows the standard values in Tabl 2, if no special remarks are included in the figures. In the stan ard condition, steam/air carrier gas is 150 °C temperature at 2.0kg/cm^2-G pressure, 500 L/min flow rate and 50 vol.% steam fraction, pool temperature is 80°C and its scrubbing depth is 2.7 meter, and the injection nozzle is 15 cm diameter. The carrier gas is injected into water trough the downward injection nozzle.

INJECTION NOZZLE DIAMETER EFFECT

Figure 4 shows the injection nozzle diameter effect, which is 6, 10 and 15cm, on the DF. This figure also shows the carrier gas flow rate effect on the DF. The results show that the DF does not depend on either injection nozzle diameter or flow rate, but the difference of the DF caused by particle diameter is ranged for one order. The DF was about 100 for 1 micro meter LATEX.

The fact that DF does not depend on either injection nozzle diameter or flow rate means the bubbles diameter distribution is almost the same under those conditions. This result is consistent with the experimental results obtained from BCL/EPRI (3).

For comparison between extremely different conditions, several tests using the 1 cm diameter injection nozzle were carried out. Results showed that the small nozzle DF increased to 10 times higher than that for a large one. This seems to be caused by inertial deposition velocity, increased with an increase in the injected gas velocity.

SCRUBBING DEPTH EFFECT

Figure 5 shows the effect of scrubbing depth, which varied from 0 to 3.8 meters, on the DF. The results show that the DF increases exponentially with an increase in the depth. The DF for 1 micro meter LATEX is about 10 for 1.1 meter depth and about 500 for 3.8 meter depth.

The DF is about 2 for 0 meter depth. This seems to be caused by inertial deposition at the injection nozzle exit.

STEAM FRACTION EFFECT

Figure 6 shows that the effect of steam fraction in carrier gas varied from 0 to 80 vol.% on the DF. The DF increases with an increase in steam fraction above 50 vol.%, while it slightly deviates around 100 below 30 vol.%.

FLOW RATE EFFECT

Figure 7 shows that the effect on the DF when carrier gas flow rate ranged for 300 to 1000 L/min. The results show that DF hardly depends on the flow rate. Notice that there was no steam fraction in this case.

This results means that the bubble diameter distribution does not depend on the flow rate, as mentioned before.

BOILING POOL EFFECT

The boiling pool test was carried out for two scrubbing depths, 1.6 meter and 2.7 meters. The pool water temperature was 110 °C and the pressure above the upper pool surface was equal to its saturation vapor pressure. Figure 5 shows the DF for a boiling pool, compared with a subcooled pool (80 °C). From these results, the predicted reduction in DF is not observed for the 1.6 meter scrubbing depth. However, The boiling pool DF for 2.7 meter depth is a half that of the subcooled pool. The heat energy per pool volume, supplied at the boiling test, was 9.6 KW/m^3.

DISCUSSION

COMPARING WITH OTHER TEST RESULTS

The scrubbing test results for a small injection nozzle, 1 cm diameter, were reported by BCL/EPRI (3). Some scrubbing tests were also carried out in the authors experiments. Figure 8 shows a comparison between BCL/EPRIs and the authors' test results under almost the same test conditions. The DF values for authors' test for particle diameter, ranged from 0.3 to 0.5 micro meter, are consistent with BCL/EPRI's. Moreover, the DF of the authors' test for 1 micro meter particle diameter were linearly interpolated between the BCL/EPRI's DF. It is concluded that these test results are consistent with each other.

The tests on nearly saturated pool water were also reported by BCL/EPRI. It is said that the differences in the DF, between boiling and subcooled pool water, were very small. On the other hand, tests on boiling pool water were carried out in the authors' experiment. Results confirmed that the DF in boiling pool water decreased to a half of that in subcooled pool water. These different results seems to mean that the DF depends on the evaporation rate from pool water into the bubble. Therefore, it should be noted that the heat energy, supplied in pool water, or the evaporation rate, would be one of the important parameters, when the DF evaluation in boiling pool water is required.

COMPARING WITH MODELS

Calculation by prototype SPARC were carried out and compared

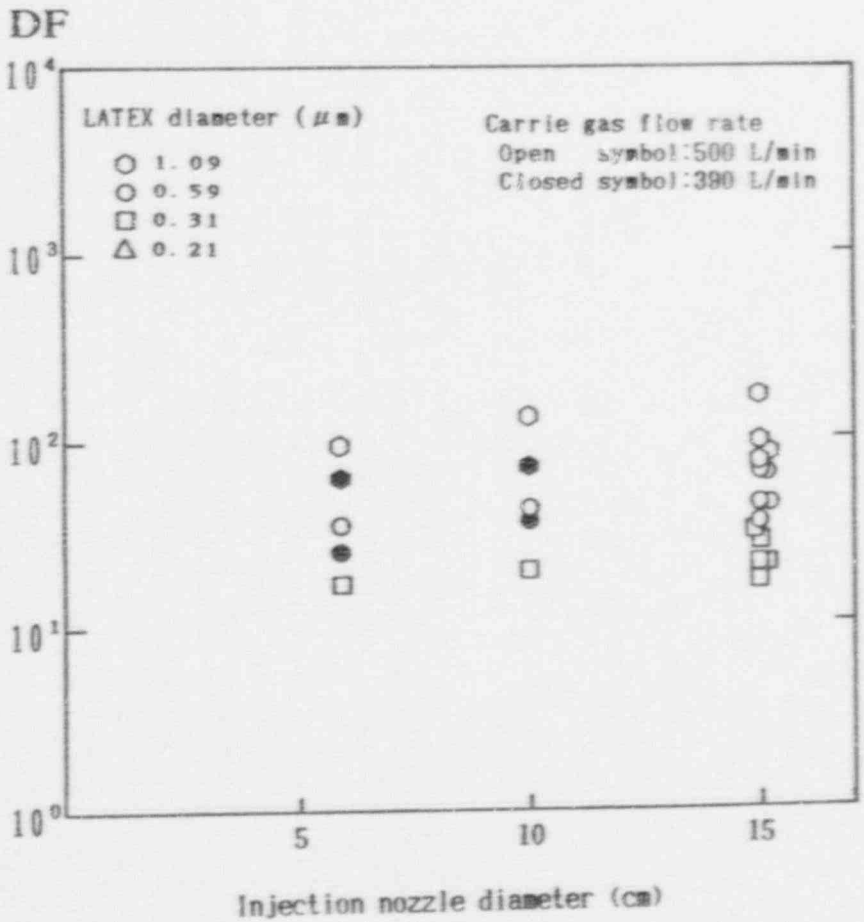

Figure 4 The effect of diameter of injection nozzle on the DF

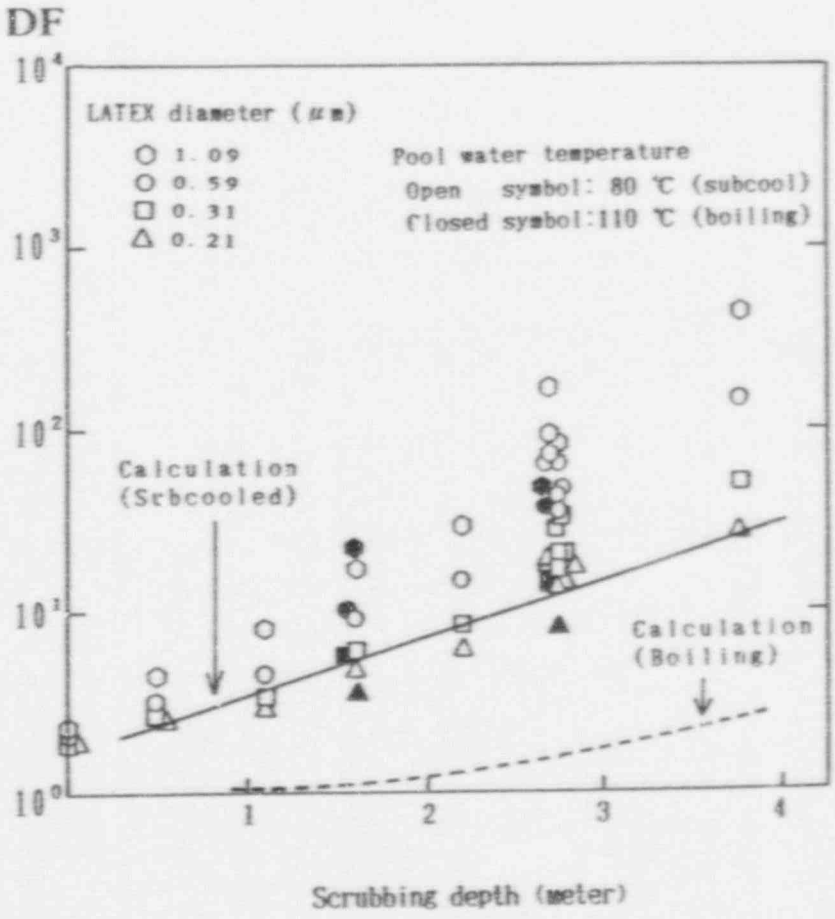

Figure 5 Scrubbing depth and pool water effect on DF compared with prototype SPARC calculation for 1 micro meter LATEX.

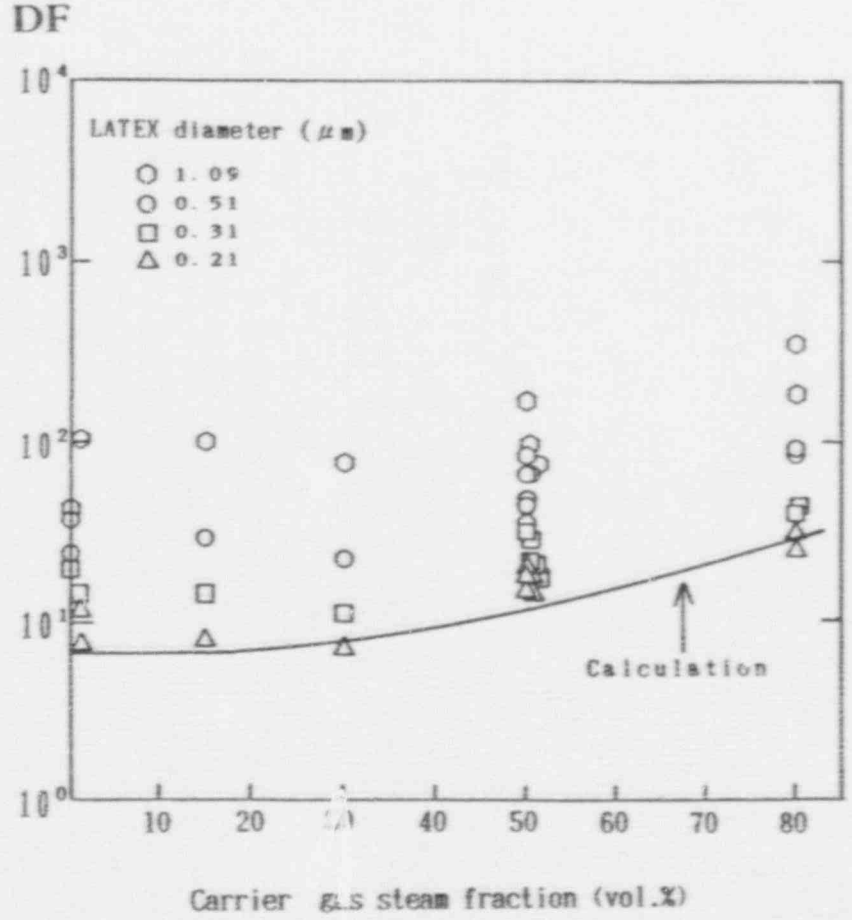

Figure 6 Carrier gas steam fraction effect on DF compared with prototype SPARC calculation for 1 micro meter LATEX.

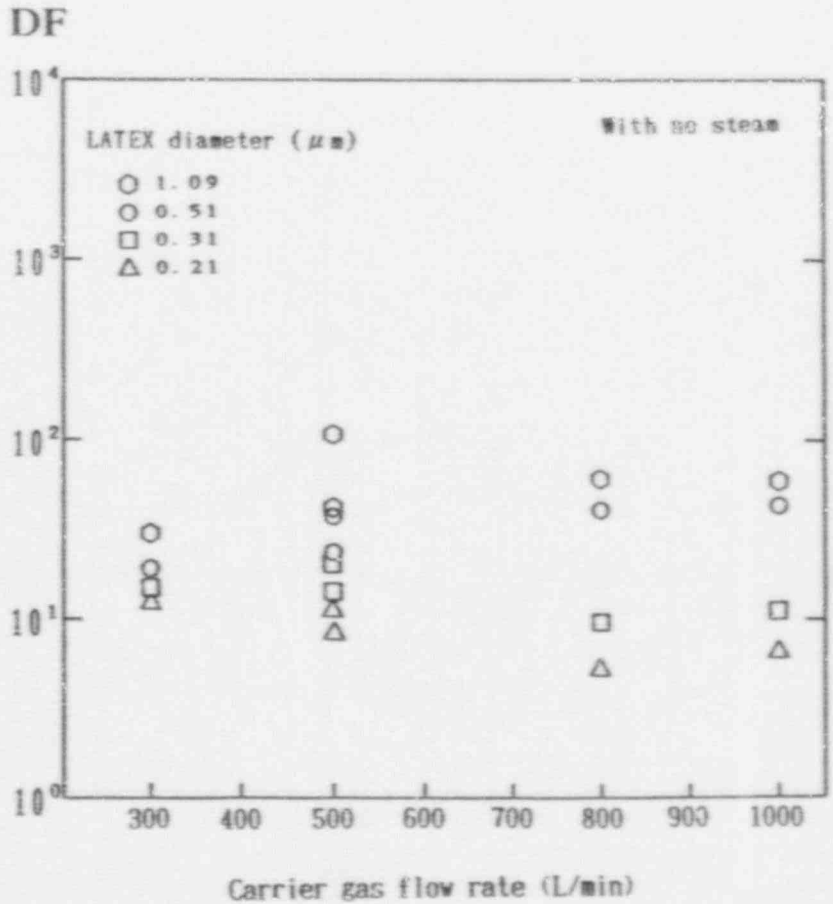

Figure 7 Carrier gas flow rate effect on DF

with the authors test results. However, it should be noticed that the absolute values for the SPARC DF were always lower than that for BCL/EPRI's experimental DF (4).

A comparison between the calculations and the test results was carried out for 1 micro meter LATEX.

Figure 5 shows a comparison between measured and calculated DF for the scrubbing depth effect on DF. As mentioned above, the calculated DF is always lower than the measured DF, but the trends are consistent with each other.

Figure 6 also shows a comparison for the carrier gas steam fraction effect on the DF. The calculated DF is also conservative, but the trend is well comparable.

It was predicted that the DF at boiling pool would reduce, because of pool water evaporation toward the inside of the bubble. Figure 5 also shows a comparison between measured and calculated DF values at a boiling pool. Calculated DF at a boiling pool is 8 times lower than that at a subcooled pool. The increasing evaporation rate, due to the energy supplied to pool water, was not modeled in prototype SPARC. If it was modeled, the calculated DF value would be smaller than the present. On the other hand, the measured DF value at the boiling pool is about a half of that measured at the subcooled pool, in spite of supplying 9.6 KW heat energy.

It is difficult to explain these differences from only these results. However, it is assumed to be one of the reasons that hydraulic turbulence, raised by boiling water, increases inertial deposition velocity in the bubble.

It has been reported that a new version SPARC has already been developed, using BCL/EPRI test results. The new version SPARC seems to be consistent with the authors test results, except for the boiling situation.

CONCLUSION

In these experiments, DF measurements were carried out for many different parameters such as scrubbing pool geometry, hydraulic conditions and aerosol conditions. Results confirmed that the DF hardly depended on thermal hydraulic conditions, but that scrubbing depth and particle diameter are important parameters. This means that the scrubbing DF can be roughly decided by the facility geometry and the scrubbed material property.

These test data are consistent with those obtained from the other experiment and calculation. However, since the present calculation for boiling pool seems to be so conservative, a new model should be developed.

These data offer basic and important information regarding the questions about how much aerosol material is removed by plant facilities under various situations.

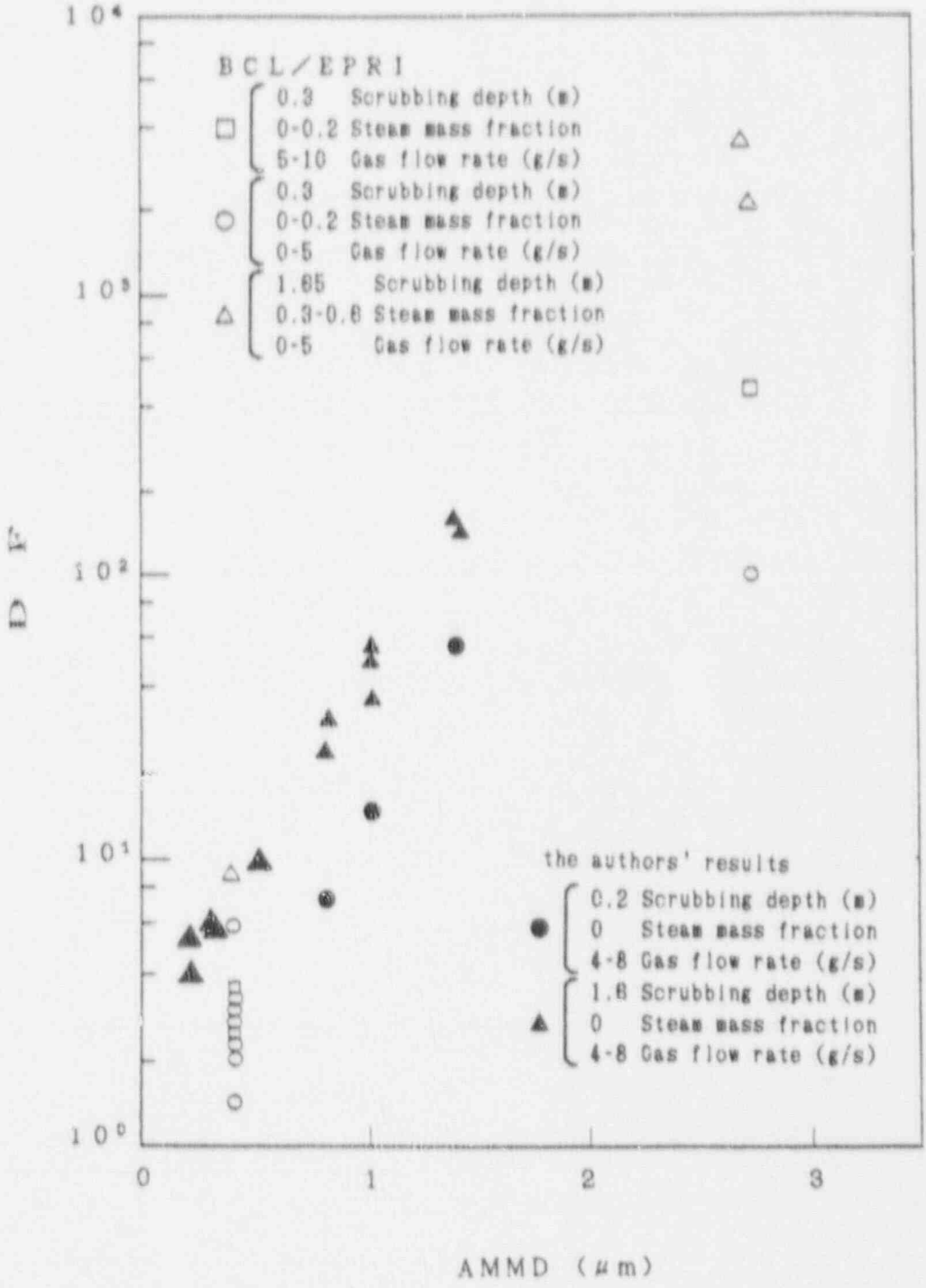

Figure 8 comparison DF for 1 cm diameter injection nozzle between the authors' results and BCL/EPRI's test.

ACKNOWLEDGEMENT

This study has been performed as a joint study by Tokyo Electric Power Co. Inc., Tohoku Electric Power Co. inc., Chubu Electric Power Co. Inc., Hokuriku Electric Power Co. Inc., Chugoku Electric Power Co. Inc., Japan Atomic Power Co. Inc., Toshiba Corporation, and Hitachi Ltd.

REFERENCES

(1) ' Technical bases and user's manual for the prototype of a Supression Pool Aerosol Removal Code (SPARC) ', NUREG/CR-3317, PNL-4742, May 1985.

(2) D.D. Paul, L.J. Flanigan and R.N. Oehlberg, ' Radionuclide scrubbing in water wools -- gas-liquid hydrodynamics ', Proceedings of ANS Topical Meeting: Fission Product Behavior & Source Term Research, Jul. 1984.

(3) M.R. Kuhlman, J.A. Gieseke, M. Merilo and R. Oehlberg, ' Scrubbing of fission product aerosols in LWR water pool under severe accident conditions', Proceedings of An International Symposium on Source Term Evaluation for Accident Conditions by IAEA, Oct. 18th - Nov. 1st 1985.

(4) P.C. Owczarski and W.K. Winegardner, ' Validation of SPARC, a suppression pool aerosol capture model ', Proceedings of An International Symposium on Source Term Evaluation for Accident Conditions by IAEA, Oct. 18th - Nov. 1st 1985.

Impact of the filtered venting system design upon the total radioactive release in case of a severe accident and a comparison of European requirements

Hans Cederqvist — ABB Atom, S-721 63 Västerås, Sweden
Kjell Elisson — ABB Atom, S-721 63 Västerås, Sweden

Gustaf Löwenhielm — Swedish State Power Board, S-162 87 Vällingby
Erika Appelgren — Swedish State Power Board, S-162 87 Vällingby

Abstract:

Filtered containment venting systems have been introduced in several nuclear power plants in Europe. The objective is to relieve the containment overpressure in a controlled way during a severe accident involving core-melt.

The release of fission products when operating the venting system has been compared to that resulting from diffuse leakage from the containment. The conclusion is that the diffuse leakage of gaseous and particulate species can not be neglected in comparison to that resulting from operating the filtered containment venting system.

Representative European requirements related to filtered containment venting have been analyzed and compared.

1. INTRODUCTION

Since 1988, all Swedish nuclear power plants, nine ABB Atom BWRs and three Westinghouse PWRs have been equipped with filtered containment venting systems (FCVS). The need to go beyond the original design basis accident for accident mitigation was recognized during the late 70's as a result of international studies and the TMI-accident in the U.S. The fundamental role of a proper functioning containment in order to prevent large releases also became apparent.

As the first nuclear power plant in the world, the Barsebäck 1&2 BWRs in 1985 were equipped with a FCVS comprising a shared gravel bed filter of high capacity. (1).

At that time, discussions were underway to introduce FCVS also on other Swedish nuclear power plants. The experience from Chernobyl confirmed the importance of containment integrity and accelerated the ongoing programme aiming at mitigating severe accidents (class 9-accidents) in Swedish nuclear power plants.

The major elements of this programme are:

- filtered containment venting, see figure 1.1,
- increased reliability of the containment spray system by connecting dieseldriven pumps,
- introduction of emergency operating procedures that cover the whole range of a severe accident from the initiating event to restoration of a stable situation,
- education and training of operators in order to increase their capability to handle an accident situation.

This programme is further described in (2).

The FCVS used in Sweden (except Barsebäck) is the FILTRA/MVSS where MVSS stands for Multi Venturi Scrubber System (3).

The basic function of the FCVS is to prevent containment overpressurization by relieving excess pressure through a filter. The system plays an important role in the accident mitigating strategy adopted in Sweden, which aims at preventing severe accidents involving core melt from causing unacceptable radioactive releases, especially of land-contaminating products such as Cs.

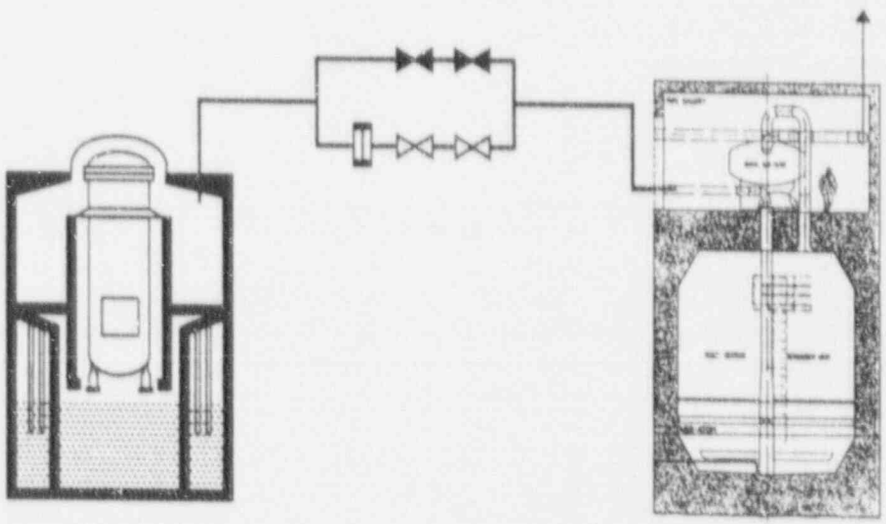

Figure 1.1: Conceptual lay-out of Filtered Containment Venting System (FILTRA/MVSS)

In a severe accident situation, the release to the environment will emanate from two sources, i.e. diffuse leakage from the pressurized containment and discharge from the FCVS, when operated.

The objective of this paper is to discuss and compare these two release paths in order to conclude what requirements should be applied regarding the separation efficiency of the FCVS.

This paper is based upon a large study performed by the Swedish State Power Board (SSPB) aiming at determining the diffuse leakage and its effect upon the accessability to vital systems during a severe accident (4). The results for the Forsmark 1&2 BWRs (2x1000 MWe) have been utilized.

It should be recognized, however, that the processes involved in a severe accident especially in the containment are complex and to a large extent plant specific.

1.2 Design basis accident sequence

The total blackout of all AC current has been chosen as the design basis severe accident sequence in all Swedish nuclear power plants. Numerous potential sequences involving small and large LOCAs, transients etc have been analyzed but the total blackout was found to be usable as envelope also for these. Plant specific versions of the MAAP 3.0 code have been applied.

To give an example of the analysis with MAAP 3.0 the results from a total blackout sequence for Forsmark 1&2 is presented in the following, as shown in figure 1.2. The analysis concerning fission product release is terminated at 24h when electrical power is assumed to be available again.

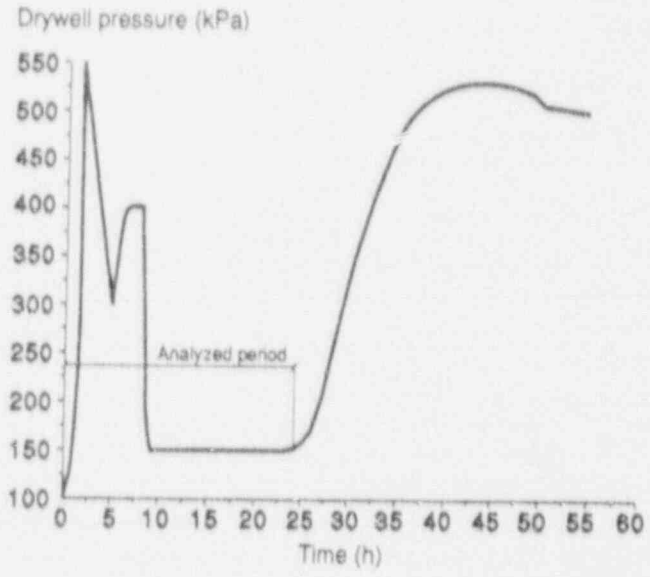

Figure 1.2: Design Basis Accident Sequence (Total Blackout)

The scenario starts with a total blackout and thus loss of core cooling and residual heat removal systems. Scram is initiated and the reactor water level starts to decrease while the pressure in the reactor is maintained at approximately 7 MPa. The batteries are assumed to be available for the specified duration (2 h) maintaining the safety relief valves and the containment isolation operable.

Depressurization of the reactor pressure vessel is initiated at low water level in the reactor and this leads to total core uncovery and increased fuel temperatures (12-13 minutes).

After 25-30 minutes, zircaloy oxidation starts and hydrogen is produced. As the metal-water reaction is exothermal, this oxidation leads to further increased fuel temperatures.

After 1 h, the core starts to melt and a total of 30 % of the zircaloy is assumed to be oxidized. This is more than originally predicted by the MAAP 3.0 code which is non-conservative in this case.

After 1.4 h, the core melt has progressed so far that the melt ("corium"=mixture of uranium dioxide, zircaloy, zirconium oxide and steel) starts to flow to the lower plenum of the reactor pressure vessel. The time to melt-through of the reactor vessel is assumed to be short, 1 minute, occurring through a control rod drive housing. The pressure in dry-well is increased due to the combined effect of H_2-generation and flashing of water after melt-through.

The resulting fast increase in the dry-well pressure will cause the FCVS to be initiated automatically after 1.7 h due to opening of the rupture disc at 550 kPa, equal to the containment design pressure. The simultaneous blow of steam to wetwell, venting and cooling of the core melt in the lower water-filled drywell will result in a pressure decrease which will be reversed once boiling starts in lower drywell and wetwell.

A reduction in drywell pressure is achieved when the containment spray system is assumed to be initiated, i.e. after 8h.

The pressure increase after 24h is caused by the water reaching boiling temperature and fill-up of the containment achieved by operating the spray system.

Manual control of the FCVS is possible during the whole sequence.

2. SOURCE TERM

The calculations of the accident sequence, core melt progression, thermal hydraulics and the transport and retention of fission products have been performed with the MAAP 3.0 code as described in section 1.2. These calculations also give the source term to the FCVS. The source term to the reactor building, caused by diffuse leakage, is based on the pressure and fission product content in the reactor vessel and drywell given by the MAAP calculations.

The following total amount of radioactivity is assumed to be released to the FCVS.

Table 2.1 Source Term to FCVS

Noble gases	100% (of core inventory)
I (CsI, I_2, CH_3I)	2.2%
Cs (CsOH, CsI)	2.3%
Te	3.5%
Mo-group	1.6E-3%
Sr-group	6.5E-3%

3. ASSUMPTIONS FOR THE DIFFUSE LEAKAGE CALCULATIONS

To calculate the diffuse leakage, the pressure and the fission product content in the reactor vessel and the drywell are needed. As the leakage calculations, as shown in Section 4, are quite complicated, it was necessary to simplify the results from the MAAP 3.0 code.

The time, therefore, has been subdivided into four periods:

A. 1600-6100 s, from start of fission product release from the fuel to vessel failure.

B. 6100-15000 s, from vessel failure until all non-condensible gases are collected in the wetwell gas phase.

C. 15000-28800 s, until the containment spray starts

D. 28800-86400 s, until water reaches nominal top core level

During each time period the pressure and fission product content in each node were assumed to be constant.

The fission products can be present in the reactor vessel, the drywell and the wetwell. The transport of fission products between these volumes is given by the MAAP 3.0 code calculations.

The diffuse leakage will occur from:

- isolation valves
- personnel locks
- equipment hatches
- penetrations

Of these, isolation valves give the completely dominating contribution. No dry leakage paths from the wetwell to the reactor building could be identified. Therefore only fission products in the reactor vessel and drywell will contribute to the diffuse leakage. In Figure 3.1 is shown how the noble gases are divided between the reactor vessel and drywell.

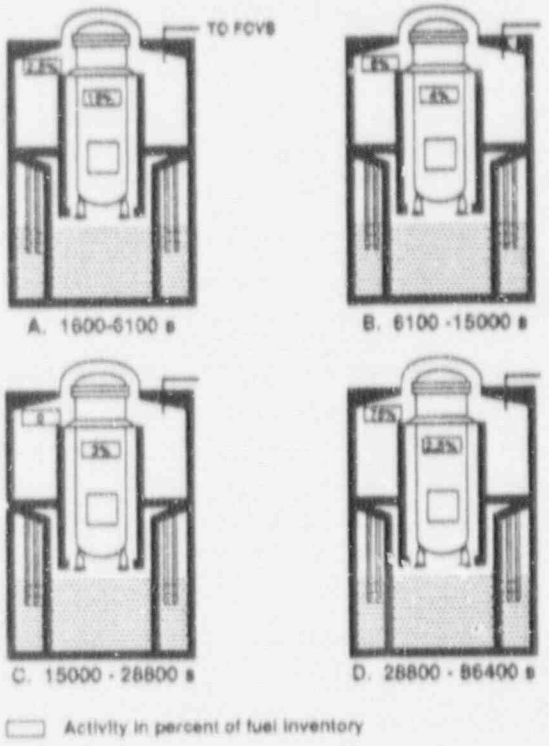

Figure 3.1: Distribution of source term inside containment

All values are chosen somewhat higher than the mean value for each time period.

During the first time period (A) up to vessel failure fission products are released from the fuel. After automatic depressurization of the reactor vessel to the wet-well the pressure in the vessel will be limited to 500kPa. The reason why fission products are found in the drywell is the pressure increase in the wetwell gas phase, caused by hydrogen, which does not condense in the condensation pool. When the wetwell pressure exceeds the drywell pressure with 50 kPa, the vacuum breakers will open and release activity to the drywell.

In the second time period (B), after vessel failure there is a continuous transport of non-condensibles to the wetwell gas phase. The exception is the non-condensibles in the vessel, where the gaseous airborne fission products are trapped due to the slighuly higher pressure. Thus in the third time period (C) negligible amounts of fission products are assumed to be present in the drywell until the containment spray is initiated.

Steam will then condense in the drywell and cause an underpressure compared to the wetwell, the vacuum breakers will open, and most of the gaseous fission products will be transported from the wetwell gas phase to the drywell during time period D.

4. RELEASE FROM THE CONTAINMENT BY DIFFUSE LEAKAGE

In connection with the work to implement the mitigating measures at the Ringhals and Forsmark plants, the radiological habitability in vital areas was investigated (5). The dose rates in such areas are affected by the radioactive materials in the containment and FCVS piping, contaminated systems, the noble gas plume and diffuse leakage.

As the design sequence was a total blackout (as described in Section 1.2) it was realized that the emergency ventilation would not be in operation. The main purpose of the investigation at that time was to determine the problems associated with the radioactive materials staying in buildings outside the containment.

In this paper, however, the emphasis is to judge the release to the environment caused by the diffuse leakage and compare it to the release through the FCVS.

4.1 Leakage from the containment

It proved not possible to use the leakage criteria (1 %/24 hours) given in USNRC Regulatory Guide 1.3, because a severe accident situation is very different from a DBA event such as a large LOCA accident.

At the Swedish Power Board reactors, isolation valves covered with water in a large LOCA accident have less stringent leakage requirements than those in gas media. In a total black-out situation many of the valves, covered with water in the DBA accident, will be in gas phase leading to a larger release. Another important difference is that the scram system with nitrogen tanks have valves with fail safe in open mode. This means that when the battery capacity is exhausted (after at least 2 hours) only the check valves in this system would stop activity release but with a considerably larger leakage.

Important for the containment leakage are the conditions, such as the activity distribution and pressure, in the containment. These conditions have been described in Section 3. The method used to calculate the activity transport has been the following:

1. Select volumes in which the activity is to be calculated.
2. Estimate the leakage factor between these volumes.
3. Solve the differential equations set up. These were simplified by assuming that the amount and distribution of radioactive matter and pressure in the containment were constant during the four time periods.

The volumes selected and the leakage paths between these are shown in Figure 4.1. Notice that the reactor building has been divided into primary and secondary parts. The primary part of the reactor building are those areas into which leakage from the containment can occur, such as rooms in direct contact with the containment or with systems connected to the reactor vessel or drywell volumes. The remaining area in the reactor building is labeled the secondary part and includes refuelling floor, corridors, lifting shafts, etc.

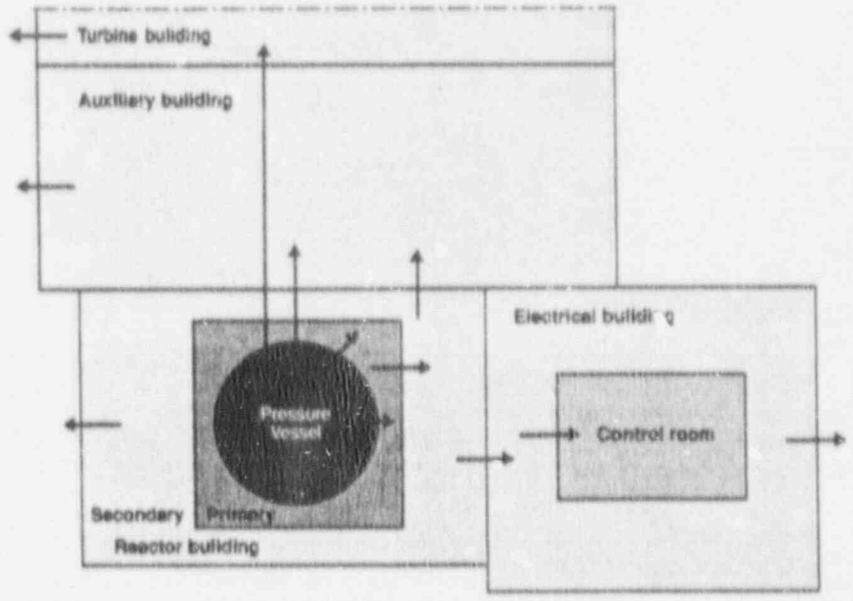

Figure 4.1 - Leakage paths

The leakage rates from individual volumes are expressed as the leakage factors, defined as

$$L = \frac{v}{V}$$

where: v = leakage in $Nm^3/24$ h
V = leaking volume in Nm^3

The leakage factors from the containment to the surrounding buildings are shown in Table 4.1.

Table 4.1 - Leakage factors

Time period	A	B	C	D
Leakage factor for				
Reactor Vessel	0.40	0.37	0.59	0.30
Drywell	0.006	0.003	0.006	0.002

The total leakage is obtained by multiplying the leakage factor with the activities in the reactor vessel and drywell given in Figure 3.1.

The release during the analyzed 24 hours is then 1.4 % (of which 1.3 % from the reactor vessel) of the gaseous activity.

It should be pointed out that the diffuse leakage characteristics depend upon the accident sequence.

4.2 Leakage paths to the environment

If the emergency ventilation is in operation most of the iodine will be ventilated to charcoal filters where more than 99 % will be retained. For the analyzed sequence, in which the emergency ventilation will not function, a part of the activity will leak to the environment unfiltered, but a large fraction is estimated to deposit within the building.

The transport of radioactive materials in surrounding buildings and to the environment according to the leakage paths in Figure 4.1 have been calculated (4) but these results are not presented in this context.

The most important leakage path involves leakage directly from the reactor building (secondary volume) to the environment. This will result in a ground release whereas discharge from the FCVS takes place from a separate stack.

4.3 Sensitivity analysis

A considerable effort was made to estimate the uncertainties. Most important for the activity release to the environment is the uncertainty of the containment leakage to the surrounding buildings. It was found difficult to estimate the uncertainty of this leakage due to fluctuating results from leakage measurements. The release to the environment, as well as the dose rates calculated are directly proportional to the leakage factors.

4.4 Summary of the diffuse leakage

The total leakage of noble gases during the analyzed 24h is 1.4 % of the core inventory. As 1.1 % of the iodine is assumed to be found in gaseous form, the corresponding leakage would be about 0.015 %. However, the elementary iodine has a tendency of being trapped on surfaces. It is assumed that these retention processes in the systems and buildings will lead to a DF corresponding to 2-10.

These processes are not assumed to affect the organic part of the iodine but the release of gaseous iodine will be less than 0.01 % of the iodine inventory.

For particulate species the retention in systems and buildings depends upon the following factors:

- particle size distribution
- concentration
- chemical form
- humidity in atmosphere
- residence time
- transport paths
- etc.

These processes have been studied in several international experiments, e.g. the LACE program (6).

It is a complex task to determine the diffuse leakage of particulates to the environment. A complete modeling of the processes and systems involved would be required to calculate the resulting release and this is beyond the scope of this investigation.

However, based on an analysis of the involved systems and volumes, DFs in the range 50-500 were judged to be appropriate for the retention process, and the resulting release of Cs due to diffuse leakage will be 10^{-3} - 10^{-4} % of the core inventory.

5. DISCHARGE VIA THE FILTERED VENTING SYSTEM

The FCVS installation is shown in figure 1.1.

The Swedish requirements focus upon the potential release of land-contaminating fission products such as Cs and state that in a core melt accident the total release of Cs to the environment shall be less than 0.1 % of the core inventory (for 1800 MWt).

In order to determine the available source term in case of a core melt numerous calculations e.g. with the MAAP 3.0 code have been performed. Based on these calculations, the Swedish utilities determined that the following decontamination factors were to be applied for the FCVS:

BWR	100
PWR	500

The DF is applied to all fissions products except noble gases and organic iodine.

The source term described in section 2.1 is assumed to be released to the FCVS during 24h.

For the BWRs, the resulting nominal release will be:

I (as Cs I)	0.02 %
Cs (CsOH and CsI)	0.02 %
Te	0.03 %
Mo, Sr	$<10^{-4}$ %

Consequently, the release of radioactive land-contaminating species will be smaller than the stipulated requirement.

The actual release of fission products, e.g. Cs will be several orders of magnitude smaller due to that the realistic DF in the FILTRA/MVSS for Cs is larger than 10^4. This has been shown in the Swedish verification programme and the ACE-tests (8).

The release of Cs due to diffuse leakage will be of the same magnitude as the discharge from the FCVS with a DF in the range 2000 - 20000.

The corresponding figure for I will be 300-1000. However, the release of iodine will be dominated by CH_3I.

6. EUROPEAN REQUIREMENTS

Requirements regarding the installation of filtered containment venting systems today exist in virtually all European countries utilizing nuclear power.

Sweden was the first country to introduce these requirements, but has been followed by e.g. Germany and Switzerland where installation of efficient FCVS has been done or is underway.

The release of noble gases in a severe accident is deemed as an acceptable sacrifice in order to prevent the possibility of land contamination resulting from releases of Cs and I.

No separation requirements therefore exist for noble gases and organic iodine.

The following DFs are applied:

		Aerosols	Iodine
Sweden	BWR	100	100
	PWR	500	500
Germany	BWR & PWR	1000	10
Switzerland	BWR & PWR	1000	100

The consent seems to be that a DF in the range 100-1000 is sufficient to prevent the available source term from causing unacceptable damage.

All installed or planned FCVS in these countries have DFs that exceed the stipulated requirements. It should be noted that in Sweden the requirement concerns the resulting release of Cs as described in Section 5.

When analyzing the existing differences between the countries, the following can be concluded:

Sweden

- Large emphasis upon sturdy design in order to withstand dynamic effects (e.g. hydrogen deflagration).
- Manual initiation of FCVS is not accepted requiring high filter performance over a large turn-down ratio (1-100% of full flow) and stabilization of rupture disc.
- Filter located outside in a separate building.
- Connection of FCVS to drywell (BWRs).

Germany

- More credit taken for operator action and containment performance during an accident.
- Filters located inside existing structures or in a separate building.
- Connection of FCVS to wetwell (BWRs).

Switzerland

- No automatic initiation of FCVS allowed. Filters located inside or outside.
- Connection of FCVS to drywell and wetwell (BWRs).

The most typical design severe accident scenario is the total black-out sequence .

The initiation time after an accident depends upon the scenario and varies from 3h to 30h.

The typical requirement is the possibility to relieve 1 % of the nominal thermal power. However, the flow rate does also depend upon containment design, scenario etc. Flow-rates from 2-14 kg/s have been specified.

7. CONCLUSION

The performed comparison between the release from the FCVS and that resulting from diffuse leakage has shown that the importance of the diffuse leakage can not be neglected. An important observation is that the diffuse leakage will be dominated by the direct leakage from the reactor pressure vessel through the primary system piping, thus by-passing the containment.

Since diffuse leakage causes release on ground level, it is of great importance not only for systems accessability but also for land-contamination in the vicinity of the plant.

References:

1. K. Elisson, "Filtered containment venting", International Symposium on Severe Accidents in Nuclear Power Plant, 21-25 March, 1988, Sorrento, Italy.

2. L. Högberg, "The Swedish Nuclear Safety Program", Nuclear Safety, vol. 29, No. 4, Oct-Dec 1988.

3. K. Elisson and L. Lindau "Filtered containment venting in Sweden", 20th DOE/NRC, Nuclear Air Cleaning Conference, Aug 1988, Boston, Mass.

4. E. Appelgren et al, "Radiological consequences of diffuse leakage - Forsmark 1&2", SSPB Report PK-126/87 (in Swedish).

5. G. Löwenhielm et al, "Mitigating measures at the Ringhals NPP: Accident management from a radiological point of view", International Symposium on Severe Accidents in Nuclear Power Plant, 21-25 March, 1988, Sorrento, Italy.

6. F. Rahn et al, "Summary of the LWR Aerosol Containment Experiments (LACE) program", International Symposium on Severe Accidents in Nuclear Power Plant, 21-25 March, 1988, Sorrento, Italy.

7. L. Öhlin et al, "FILTRA/MVSS - Result of Aerosol and Iodine Collection Tests", ACE-phase A (to be published).

DISCUSSION

WILHELM: With respect to the use of sprays in a serious accident, did you calculate what air/hydrogen concentrations you might reach by condensing steam inside the containment? Calculations in Germany show clearly that if you do this, you create an explosive mixture because when the steam is down, hydrogen will be increased in concentration. Steam is an inhibitor. If the inhibitor is taken out of the mixture of steam, air, and hydrogen, the atmosphere may become explosive.

CEDERQVIST: Yes, a lot of effort has been devoted to calculating the risk of hydrogen explosions and this has had a very important impact on our design of filter systems.

DESIGN AND FULL SCALE TEST OF A SAND BED FILTER

Maurice KAERCHER
Head of nuclear circuits and lay out Division
Design Department
Electricité de France
LYON, FRANCE

Abstract

All French PWR plants are equiped with a containment venting system. This system is designed and implemented by Electricité de France (Design Department) with the technical support of Safety Authorities (Institute of Protection and Nuclear Safety of Atomic Energy Commission).

This paper covers the following items ;

- main assumptions, sizing and design requirements,
- basic design of the filter resulting from PITEAS R & D program carried out between 1983 and 1989 at Cadarache nuclear center,
- full scale tests performed in 1990 on FUCHIA loop at Cadarache
  . description of the loop using plasma torches to generate CsOH aerosols in a steam - air flow,
  . preliminary results concerning thermohydraulic and thermic behaviour under residual power simulated filtration efficiency with CsOH aerosols and iodine,
- complementary design including :
  . hydrogen risk during condensation period,
  . radiological shieldings of the filter,
  . heat removal after the filter closure,
- conclusion on the validation of the filter.

1. Introduction

Since the publication of the WASH 1400 report, and after the TMI 2 accident, studies and experimental programs have been carried out to deepen knowledge about the evolution and consequences of serious accidents which can happen on reactors. These studies have enabled families of accidents to be brought to light originating from multiple failures and which could lead to meltdown and containment loss.

To avoid or limit the consequences of such accidents, Electricité de France (EDF) have set up ultimate procedures (U procedures). These procedures are especially aimed at assuring fuel cooling and avoiding or delaying loss of containment integrity.

Scenario studies showed that in many cases of containment integrity loss, its internal pressure was able to increase slowly over several days under the combined effects of steam and incondensable gas releases from core concrete interaction.

This pressure increase could cause a containment failure and an important uncontrolled release of radiation into the environment. Now it is a fact that an adequate management of such a release by controlling flow, activity and time of aperture would permit the risk zone to be sufficiently limited so that, in accordance with studies carried out by the Civil Safety Authorities, population evacuation would be possible.

It was therefore decided to place a decompression - filtration system of the simplest design on the containment to assure a reduction of released radiation, except rare gas and gaseous iodine, by a factor of 10.

The choice of technical filtration properties was defined resulting from the PITEAS Research and Development program lead by the Institute of Protection and Nuclear Safety (IPSN) in collaboration with Electricity de France (EDF).

The system was then tested at full scale under conditions representative of accident conditions.

All PWR reactors installed in France are equipped with it.

2. Design hypothesis of venting system

Results of accident scenario studies show that the containment pressure remains below the design pressure in the first 24 hours. Thus the filter design criteria from the thermodynamic and aerosol viewpoints was fixed at conditions existing in the containment 24 hours after the start of the accident.

The filter is put into operation when the pressure in the containment reaches the design pressure. The gas flow rate through the filter was specified in such a way that its evacuation capacity assures that the design pressure is not exceeded. This sized the filter to give a gas flow rate of 3.5 kg/s.

From the aerosol characterization viewpoint, various sensitivity studies carried out, show that 24 hours after the start of the accident, the aerosol properties (concentration and

granulometry), are relatively independent of the source (flow and granulometry) and that in the area of release values which can be expected and for dry containment designs of the EDF type, the concentration after 24 hours is most often less than 0.1 g/m^3 and the AMMD is about 5 µm.

As for granulometry, taking account of the fact that the efficiency in the considered area diminishes for the smaller granulometries, the AMMD was fixed at 1 µm in order to determine the filtering medium and to guarantee the factor of 10 searched for.

The main design hypothesis are grouped in appendix A.

3. Description of decompression filtration system

3.1 Général description (see figure 1).

The decompression-filtration system from upstream to downstream consistes primarily of :

- a containment penetration with double insulation made by two valves in series located outside the containment, and as close as possible to it.
- an orifice plate reducing pressure to atmospheric (with the exception of pressure losses)
- a sand filter
- a device for measuring radiation released
- an independent evacuation duct located inside the normal effluent stack of the plant.

With the exception of the containment penetration (with its isolating valves), the system is not safety classified nor designed for earthquakes, it concerns a complementary installation.

3.2 Special Points

3.2.1 Circuit conditioning under normal plant operation

The principle of a permanent circuit conditioning during normal plant operations was selected in order to guard against the humidification of the system (protection from corrosion) and particularly of sand.

This conditioning is achieved by assuring that the installation is continuously scavenged by dry filtered air.

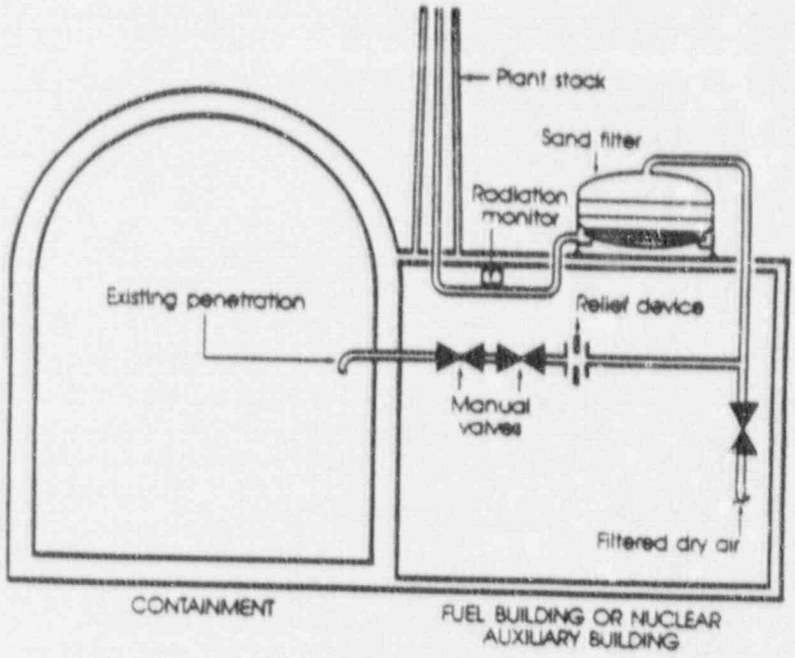

Fig.1: General Diagram

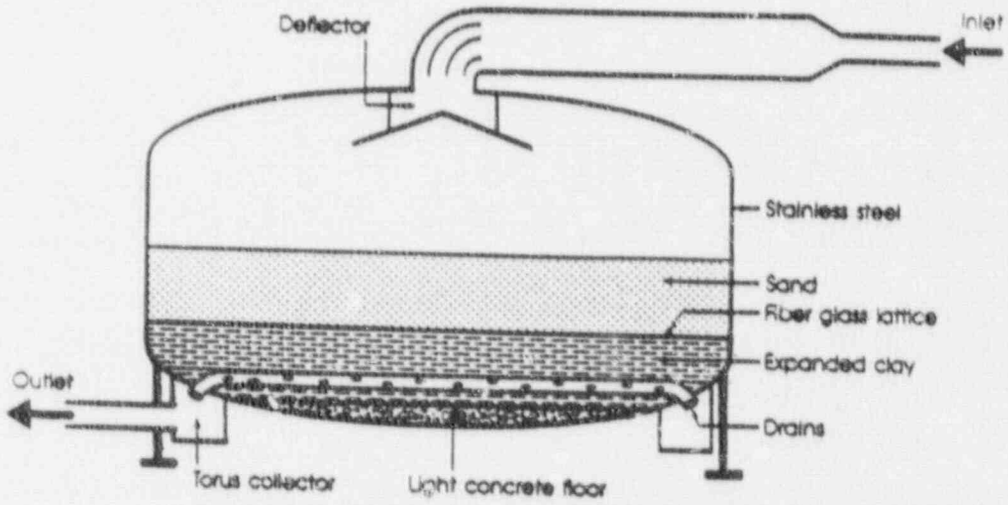

Fig.2: Sand Bed Filter Section

3.2.2 Condensation

The aim is to avoid under established operating conditions, any condensate accumulation during the implementation of the system, in the bottom of stack.

Maintaining this objective is guaranteed by the following arrangements :

- adequate thermal insulations of the device

- discharges via an independent small diameter duct (400 mm) located inside the normal effluent plant stack assuring a speed sufficiently high to ensure condensate entrainment.

3.2.3 Measuring device for released radiation

A device is provided downstream of the filter enabling the released radiation to be measured if the circuit is put into operation. The detector in the process of being qualified will permit iodines, cesiums, and rare gas to be separately measured.

3.2.4. Evacuation duct

This duct is inside the normal plant stack for the following reasons :

- no climatic loadings (particularly wind)

- better dilution of accidental phase release due to the air flow supply extracted from the nuclear island buildings.

3.2.5. Operating conditions

From the principle viewpoint, it seems worthwhile recalling that safety depends on the containment and that this fundamental principle should not be brought into question by the existence of a venting device permitting a controlled opening to be made in this containment and that in consequence it would be preferable to postpone as long as possible, and if possible to avoid putting of device into operation, by taking account of its mechanical resistance proporties.

This being specified, the decision to put the system in service then out of service is the responsibility of the Power Station Director in conjunction with the local and national level of the authority who is in charge of the crisis management.

The system is put into service by opening the containment isolating valves (after closing the incoming conditioning air). The internal containment pressure is then about 5 bars.

The specific start up criteria of the system are specified in the serious accident intervention guide prepared jointly by

Electricité de France and the Safety Authorities.

3.2.6. Design of sand filter

3.2.6.1. Efficiency and filtering medium

Tests on the PITEAS loop (see paragraph 4) permitted the definition of the following conditions :

- 10 cm/s gas mixture velocity in the filter corresponding to a filtering surface of about 40 m^2,
- filtering bed of 80 cm,
- filtering medium made of "Cattenom" sand of granulometry corresponding to a mass medium diameter of 0.6 mm and a standard deviation less than 2,
- gas mixture reduced to near atmospheric pressure,
- a maximum filtering medium pressure drop of 10^4 Pa.

3.2.6.2. Description (see figure 2)

The sand filter is a vertical axis cylinder with the torispherical upper and lower ends with the following characteristics :

- diameter : 7.32 m
- height : 4 m
- empty weight : 12 tons
- operational weight : 92 tons.

The sand bed support comprises an expanded clay layer with a basket system for gas recuperation and a cellular concrete floor in the filter bottom.

For all sites except Fessenheim, this filtration section is installed on the roof of a nuclear island building, the PWR 900 MWE series being fitted with a system common to two twinned plants.

4. Research and Development program for the sand filter

The program called PITEAS developed to define the sand filter, evolved in two stages : the first one, carried out in the laboratory, permitted the selection of sand to meet the specification : filtration coefficient more or egal to 10 ; the second, made on the pilot loop, studied the system's thermal behaviour and defined its field of use. Finally a full scale test

was made on the FUCHIA loop.

4.1. Laboratory tests

Laboratory tests were carried out on a sand column, 80 cm high and 20 cm diameter. For these trials, the uncondensable gases (CO and CO2) were replaced by air, giving the following test gas mixture properties :

- temperature : 140°C
- pressure : slightly above atmospheric pressure
- composition % w/w : air 68%, steam 32%.

The gas velocity through the filter varied around set point of 10 cm/s (tests at 7 cm/s and 14 cm/s).

The aerosols used were made from cesium carbonate. A parametric study of the AMMD influence was done.

The tests of relatively short durations (1 hour) were carried out in 2 ways :

- under thermal equilibrium conditions (steady state operating conditions) for the filter.
- under transient thermal conditions, that is with a filter at ambient temperature at start of test.

The filtering medium used was sand, from "Cattenom" produced in the High Mosell valley. Different granulometeries obtained by sieving were tried : 1.6 - 1.2 - 0.7 - 0.5 and 0.42 mm for the mass medium diameter, deviation being less than 2.

A complete parametric study of the purifying coefficient as a function of the aerosol diameter, sand granulometry and gas velocity through the filter was made under steady state operating conditions (see figure 3). In transient operating conditions punctual measurements, confirmed the results obtained under steady state conditions. Pressure drops under both operating conditions were very similar (see figure 3). No indication of clogging was detected during the tests. The aerosol sand load obtained during the tests reached 1300 g/m2 for 0.7 mm sand and 191 g/m2 for 0.5 mm sand. The re-entrainment of aerosols deposited under the action of the gas current, was the subject of 2 tests with a 0.5 mm sand with an initial load of 144 g/m2 and gas velocity of 7 cm/s ; the fraction released over one hour was less than 10^{-4}.

From these results a sand granulometry was selected corresponding to a mass medium diameter of 0.6 mm and a standard deviation below 2. Under these conditions, a filtration coefficient significantly above 10 is obtained, and a pressure drop for the set

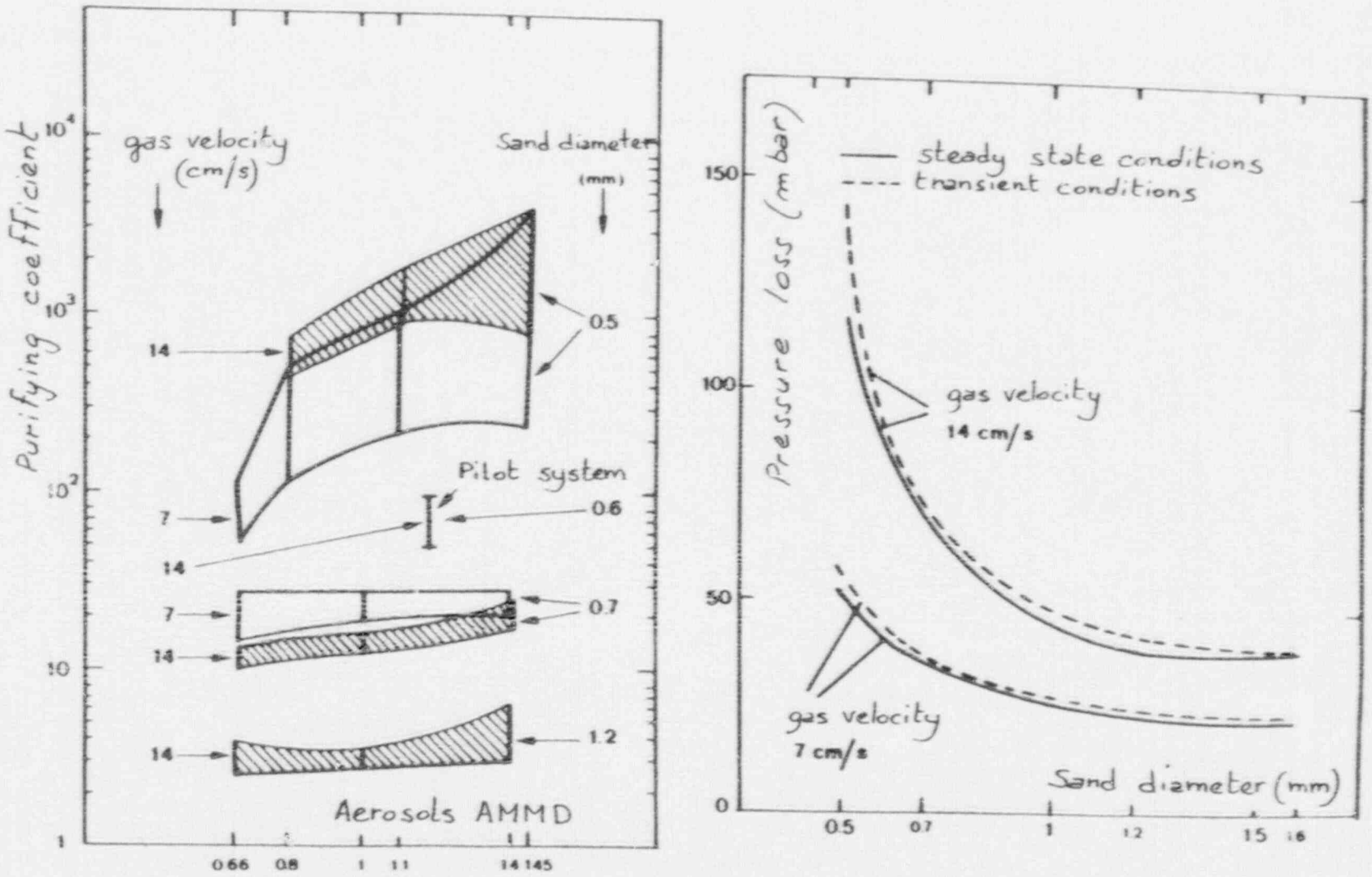

Figure 3 : LABORATORY TESTS RESULTS

velocity 10 cm/s, below the 10^4 Pa limit which was imposed.

4.2. Tests on pilot system (PITEAS loop)

The second part of the program was carried out on the pilot loop with the selected sand quality. To identify the filter's field of use, three test series were run.

- a first series to characterize the filter's thermal behaviour,
- a second series to check out the results obtained in the laboratory,
- a third series to study the filter's performance under various operating conditions.

4.2.1. Description of test system

The main composents of the test system are shown in figure 4.

The sand bed is a cylinder of 1 meter diameter and 0.8 m high.

Instrumentation essentially consists in measuring the sensitive points of the installation, pressures, temperatures, and air and vapour flow rates.

Aerosols are generated by the acoustic pulverization of an aqueous cesium carbonate solution. Tests were carried out with aerosols of AMMD of 1.17 - 2.15 - and 4.7 µm obtained from different solution concentrations, by sparger condensers. The cesium was analysed by atomic absorption spectrometry in solution samples taken from the system and from the effluent tanks.

4.2.2. Thermodynamic behaviour of the filter

The test objective was to evaluate filter blockage risks by flooding, in the condensation phase of the vapour, during the start up phase when the filter is cold. The filter's behaviour was followed during temperature measurements at different points of the sand bed and pressure drop measurements.

The tests were carried out at two gas velocities through the filter ; 5 and 10 cm/s. Various gas compositions were tested :

- air 68%, steam 32%
- air 35%, steam 65%
- steam 100%

The thermal balance on the three transient phases (condensation, evaporation and reheating) enables the duration of these phases to be calculated. The values obtained confirmed the measurements. The calculations also give an estimation of the condensed water mass. It is about 23 kg for the gas mixture. These low values in relation to free volume available between the sand

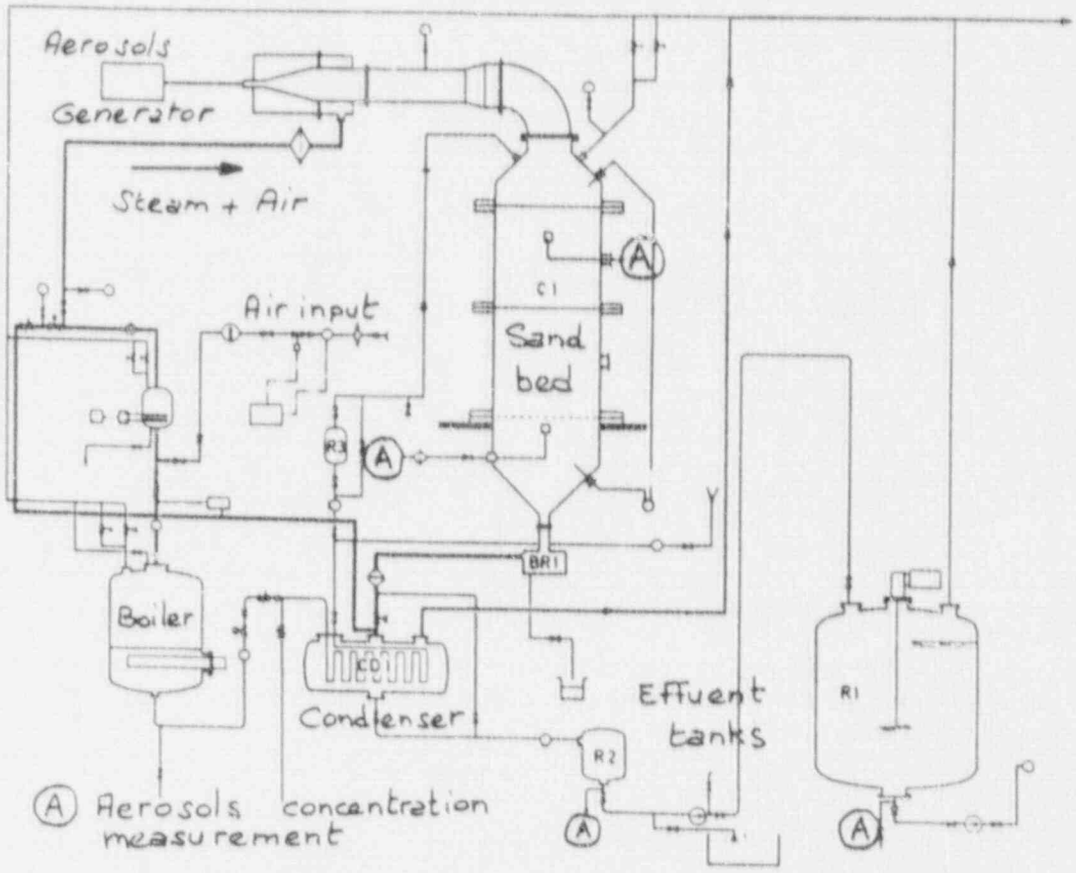

Figure 4 : SCHEMATIC DIAGRAM FOR PILOT SYSTEM (PITEAS LOOP)

particules, which is close to 240 L, explain the minor influence of condensation on pressure drop.

4.2.3. System efficiency under steady state operating conditions

A series of tests made after preheating the filter to the gas temperature, confirmed, the results obtained in the laboratory ; filtration coefficients cross check (see figure 3), and salting out is low.

4.2.4. System efficiency under transient operating conditions

The test revealed a significant drop of the purification coefficient during the condensation phase.

This phenomena seams to be linked to a Cesium hydroxyde entrainment by water produced by condensation, in contact with the cold sand.

This phenomena, which at the beginning concerns the whole sand mass of the filter, progressively reduces as the drying front propages itself. The dried upper part of the sand then progressively recovers its maximum efficiency, and the global efficiency of the system increases.

The curve of figure 5 concerns a test made with a lower mix temperature upstream of the filter favourising condensation and shows the increase of the filtration coefficient.

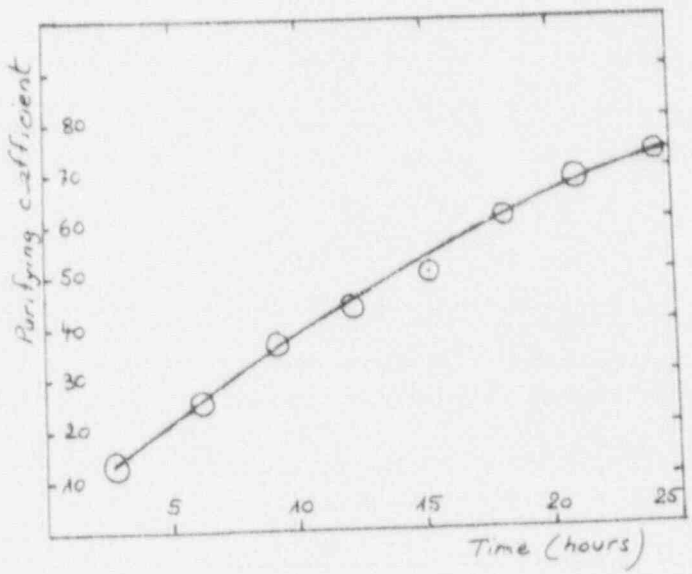

Figure 5 : System efficiency under transient conditions.

4.2.5. Molecular iodine retention

A test aimed at examining molecular iodine behaviour in contact with sand was carried out under steady state operating conditions with 32% steam in the gas. This test revealed a good momentary iodine retention and a notable salting out under the action of a gas blowing made 24 hours after the test. The filter seems to act as delay line for iodine.

5. FULL SCALE TESTS ON THE FUCHIA LOOP

A full scale decompression-filtration system called the FUCHIA loop was erected at Cadarache in 1989 (schématic diagram see figure 6). The FUCHIA loop is virtually identical to the venting system implemented on PWR in France.

Several different kinds of tests were performed : thermohydraulic, filtration, thermic and salting out tests.

These tests were performed on a fully insulated filter from January 10th 1990 to February 19th. A partially desinsulated filter was tested from March 6th to the end of April 1990. The following preliminary results only concern the fully insolated sand filter and have to be confirmed.

5.1. Thermohydraulic test

5.1.1. Description

The filter is fed during 30 hours with an air-steam mixture (35 % air, 65 % steam, temperature 140°C) maximizing the condensation effects. There is no aerosols generation.

About 30 temperature measurements, mostly taken at different levels in the sand, were recorded during the test. The quantities of condensed water at the low points of the circuit were measured.

5.1.2. Preliminary results

The thermohydraulic results are in accordance to the calculated elements and PITEAS results :

- the temperature field is homogeneous with a few degrees loss at the circumference and a almost symetrical distribution,
- the sand reaches its nominal temperature after a condensation transient of 15 hours,
- the pressure loss is close to the expected value,
- no important condensation is noticed in the system.

MD : Flow measurement
MT : Temperature measurement
P : Pressure loss measurement
A : Aérosols measurement (concentration and granulometry) and iodine concentration.

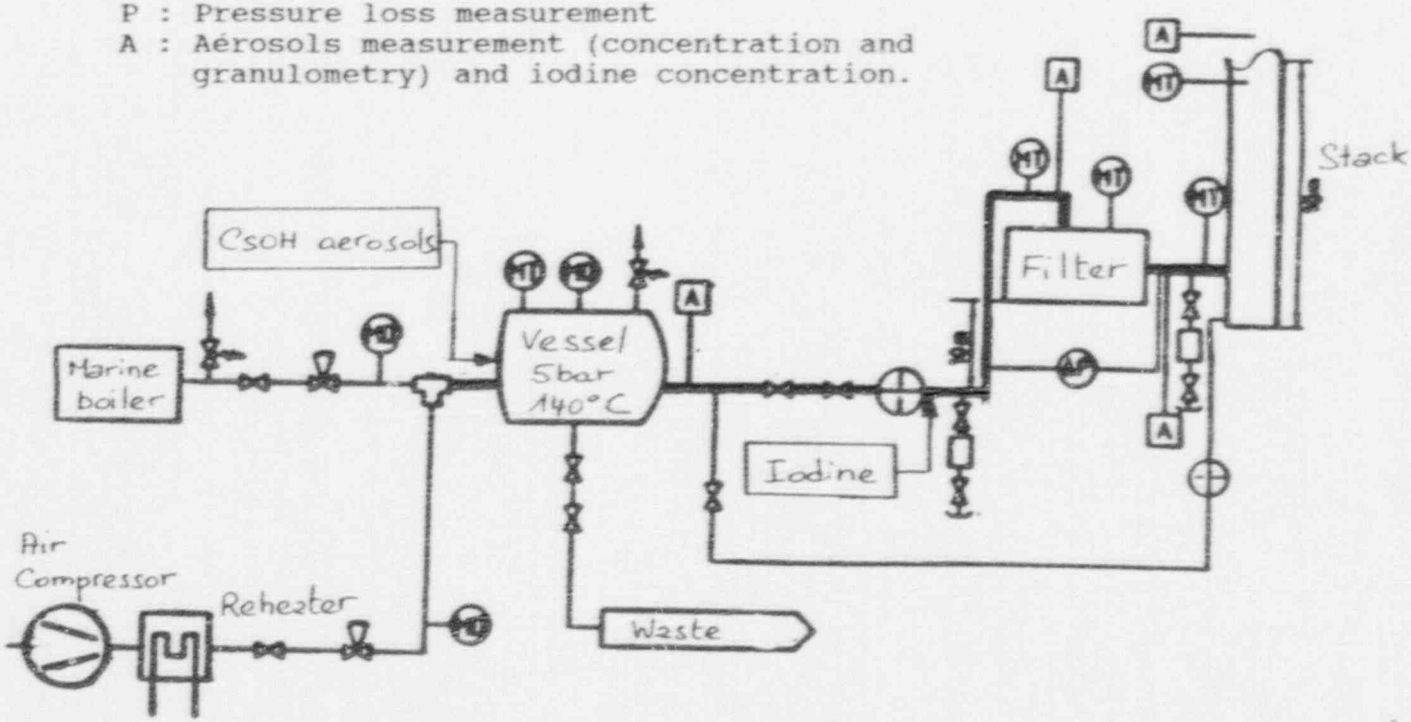

Figure 6 : **Schematic Diagram for Full Scale Test** (Fuchia Loop)

5.2. filtration test

5.2.1. Description of filtration test

The sand filter is blown through by an air-steam mixture (35 % air, 65 % steam et a temperature of 140°C) during 50 hours.

During the first 25 hours, cesium aerosols are generated by means of plasma torches with an AMMD of 1 µm at a flowrate of 513 g/hour.

- iodine is introduced in molecular form at a flowrate of 70 g/hour.

During the following 25 hours then neither aerosols nor iodine are generated.

5.2.2 Preliminary results

the filtration efficiencies on cesium and iodine are evaluated by :

- mesuring cesium and iodine concentration above and below the sand filter.
- mesuring cesium aerosols AMMD and concentration above and below the sand filter by impactor (ANDERSEN 2000).
- three dimensionnal cartography in the sand by means of core samples.

The main primary results are the following

- the AMMD of cesium aerosols measured above the sand filter is near 1 µm (standard deviation about 2.3)
- the average flow of cesium aerosols above the sand filter is near 150 g/h, that means that 350 g/h of the 500 g/h generated do not reach the sand filter. 30 % of the aerosols stick to the pipes before reaching the sand filter.
- the concentration of aerosols given by concentration and granulometry measurements are coherent.
- the diagram (see figure 7) gives the efficiency for cesium hydroxyde measured on the sand filter as a function of time.
- for iodine an average efficiency of 20 seams to be observed but this result has to be confirmed,
- a very low salting out is noticed during the period without aerosols generation.

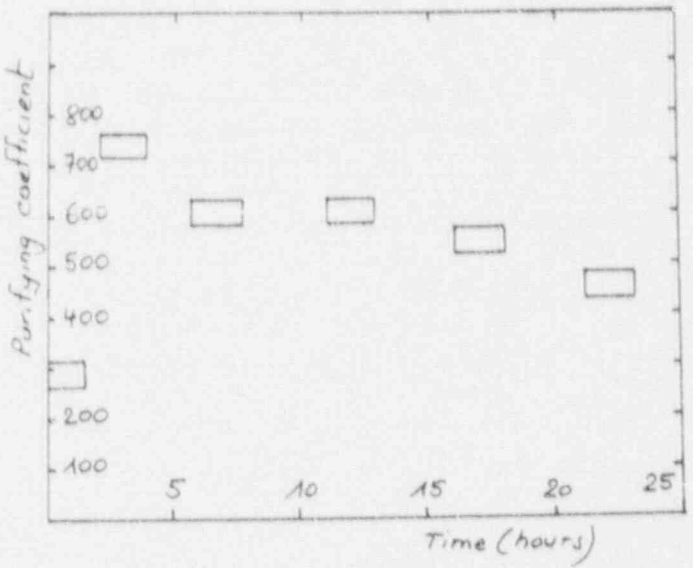

Figure 7 : Efficiency on cesium hydroxyde.

5.3. Thermic and Salting out test

After the filtration tests the thermal behaviour and the fission product salting out are checked over ten days. The residual power is simulated by electrical heating and a cooling is carried out by blowing fresh air (10 % of normal flow). After ten days the temperature the temperature measured are near 100°C. The salting out ratio noticed during this period of time is not significant.

6. COMPLEMENTARY DESIGN

The following points must be taken into account when putting the decompression-filtration system of the containment into operation.

6.1. Hydrogen risk in the filter

This risk is extremely short-lived and could occur when the filter is put in operation in a situation where the upstream gas mixture contains a significant quantity of hydrogen.

This would imply a scenario in which hydrogen, produced in large quantities, had not burned previously inside the containment and where there is a high steam concentration. Condensation would then lead to hydrogen enrichment of the gas mixture in the pipework

and filter during the temperature buildup transient in the metal parts upstream of the filter.

Although combustion of the mixture is unlikely (there is no specific source of energy) and although it is improbable that this combustion would destroy the filter, it cannot decively proved.

Provisions must therefore be taken to provide against this occurence. These measures consist in providing a preheating system.

This system uses an electric heater downstream of the conditioning fan. It's supplied by normal power supply or by an independent electric generator. The system is able to heat the pipe, the filter top and the upper sand bed part in a few hours. It was tested on a french unit (Cattenom 4).

6.2. Radiation protection : on-and off-site traffic

The surveys undertaken show that, as regards on-site and off-site protection, biological shielding is necessary for direct and indirect dose rate values (skyshine) induced by the limit values corresponding to the radioactivity trapped in the filter for the most pessimist hypothesis with an extreme source term.

With regard to direct radiation, the neutralizing effect procured by a sand bed ring (25 cm) significantly reduces the direct dose level, to such an extent that no further provisions are necessary.

Decision has been taken for the implementation of installations aimed at limited protection with respect to sky effect (indirect dose rates), leading to on-site and off-site dose rate values which are not significantly penalizing.

Contraints related to seismic resistance of supporting structures result in technically different solutions being adopted for different series of plants : concrete slab or structure to be filled with water.

6.3. Thermal behaviour after filter closure

When the system is shut off, the heat dissipated in the filter raises the temperatures in the sand. The target was not to exceed 300°C in the sand (CsOH meltdown is 315°C).

For normal dissipated heat values (below the extreme source term/10), the sand temperatures do not exceed the target values from the FUCHIA results, even with the insulated filter.

For high values and the insulated filter, it would be necessary to use an air sweeping cooling device using the conditioning fan, or to provide a water cooling device on the

filter dome.

7 CONCLUSIONS

The Laboratory tests and then the PITEAS program on a reduced scale model, enabled the main design parameters of the sand filter to be defined. This filter was subjected to a full scale test on the FUCHIA loop. The perfect control of representative test conditions resulted in a reasonable spread of the first test results and permitted the following conclusions to be drawn :

- On the thermohydraulic plan, the influence of the condensation phenomena on the flow conditions in the loop and on the filtration efficiency is small.

- The filtration efficiency measured is higher than that observed in the reduced scale tests. This efficiency measured for the decompression system is further increased by deposits inside the piping.

- The residual power can be evacuated by blowing fresh air at 10% of normal flow.

- Salting out levels observed on the test periods are low.

Although many measurements are still in the process of analysis, particularly those concerning aerosol distribution in the sand, these preliminary results fully validate the design options of the filters installed on PWR power stations in France and confirm their high efficiency.

APPENDIX A : DESIGN ASSUMPTIONS

SAND BED FILTER DESING

Minimum efficiency : 10

No interaction with other systems

Passive system

No seismic design

flowrate : 3,5 kg/s

Time allowed before operation : at least 24 hours

CONTAINMENT ATMOSPHERE

5 bar
140°C

Composition

Air : 33 %
Steam : 29 %
CO_2 : 33 %
CO : 5 %

Aerosols : average diameter : 1 to 5 µm
total mass : 5 kg
activity : about 10^6 Ci

DISCUSSION

HANDYSIDE: Are you confident that the physical and chemical forms of CS and I used in your test are the same those expected in a reactor accident?

KAERCHER: From the point of view of cesium, we have selected, for FUCHIA tests, an aerosol which maximized the negative effect of condensation, i.e., CsOH is a soluble aerosol. In addition, accident studies showed that the proportion of CsOH in Cs releases is important. From point of view of iodine, accident studies showed that most of the iodine releases are CsI or I_2. The behavior of CsI is described by CsOH (both are soluble) and I_2 is tested in full scale tests.

BERGMAN: What is the expected sand bed filtration efficiency for particle sizes such as 0.1 µm.

KAERCHER: No test was performed with 0.1 µm particles during our program. The reason is that this size is far from the expected size, which is between 1 and 5 µm. A theoretical analysis has shown that sand bed filtration efficiency increases when particle size decreases below 1 µm. Consequently, filtration efficiency for smaller particles, such as 0.1 µm, is not less than the value measured during FUCHIA tests with 1 µm particles.

CLOSING COMMENTS OF SESSION CO-CHAIRMAN KOVACH

I think it was an interesting session. We learned about a technology that is currently being refined. You can see that there are several different applications aimed at the same problem and its solution, using the different criteria, different performance requirements, and different technology. It is a very interesting field, but at the same time my belief is that we need additional test data, particularly to make sure that our evaluation challenges do, in fact, closely simulate accident conditions.

SESSION 16

PANEL SESSION: NUCLEAR AIR CLEANING PROGRAMS AROUND THE WORLD

Thursday: August 16, 1990
Co-Chairmen: G.R. Plumb
V. Friedrich

Panel Members:
Mr. Lambert Scholten, *The Netherlands*
Dr. M. Lee Hyder, *U.S.A.*
Mr. Christopher Cheh, *Canada*
Mr. David Holman, *United Kingdom*
Mr. Ian Handyside, *United Kingdom*
Mr. Philippe Mulcey, *France*
Mr. Hans Cederqvist, *Sweden*
Dr. Juergen Wilhelm, *Germany*
Dr. Yasuo Hirose, *Japan*
Mr. Vilmos Friedrich, *Hungary*

OPENING COMMENTS OF PANEL SESSION CO-CHAIRMAN PLUMB

THE DUTCH NUCLEAR PROGRAMS
L. C. Scholten

NUCLEAR AIR CLEANING PROGRAM IN USA
M. L. Hyder

NUCLEAR AIR CLEANING R&D PROGRAMS IN CANADA
C. H. Cheh

UNITED KINGDOM ATOMIC ENERGY AUTHORITY PROGRAMS
D. Holman

DEVELOPMENTS IN THE AREA OF REGULATORY MATTERS IN THE UK
I. Handyside

NUCLEAR AIR CLEANING PROGRAMS IN PROGRESS IN FRANCE
P. Mulcey

A SHORT OVERVIEW OF THE PROGRAMS IN SWEDEN
H. Cederqvist

NUCLEAR AIR CLEANING ACTIVITIES IN GERMANY
J. G. Wilhelm

AIR CLEANING PROGRAMS RELATING TO THE FIRST JAPANESE COMMERCIAL REPROCESSING PLANT
Y. Hirose

NUCLEAR AIR CLEANING PROGRAMS IN HUNGARY
V. Friedrich

OPENING COMMENTS OF PANEL SESSION CO-CHAIRMAN PLUMB

In this session we will try to cover such topics as the international development of systems, equipment, test methods, and regulations as they relate to reactors, fuel storage, reprocessing, management of high, intermediate, and low level wastes, other fuel cycle activities, and finally non-fuel cycle activities. We will try to deal with them, first, in a generic manner and then go to particular developments of special note.

THE DUTCH NUCLEAR PROGRAM

L. C. Scholten
N.V. KEMA
P.O. Box 9035
NL-6800 ET Arnhem, The Netherlands

The Dutch nuclear program is limited. In our country we have two power reactors, a BWR and a PWR and an ultra-centrifuge fuel enrichment plant. There were plans to build new plants, but directly after the Tsjernobyl accident our government postponed the decision and ordered a new study on the safety of nuclear energy. That study is now completed and at the moment under discussion. A facility for waste storage on land is to be built. The first stage for low-level waste is under design and construction will start soon. Later, the facility will be enlarged for storing spent fuel for the next 100 years.

The filter systems at the reactors and the enrichment plant are tested by our company on a regular base. For the testing we have adopted the ASME-N510 standard and the ASTM-D3803 standard for charcoal. We are not obliged to follow these codes exactly; our test methods have been approved by the nuclear inspectorate. More details of the testing methods are in papers at the nuclear air cleaning conferences organized by the European Commission.

At the Dutch power plant containment vent filters will be placed. In December 1988 the nuclear inspectorate has ordered to install containment vent filters by 1992. In practice that means that they will be installed during refueling outage in spring 1992. At this moment it is not yet decided which type of filter will be used. For the PWR a sliding pressure unit of modified Siemens-KWU design is foreseen. For the BWR a decision will be taken when the results of level-2 calculations with the STCP are available. We expect that a filter working at atmospheric pressures will be used.

Furthermore research is going on for the penetration of ultra-fine particles through HEPA-filters. Those small particles, smaller than ≈ 1 μm and down to 1 nm, are believed to creep through HEPA filters with the same mechanism as plutonium particles. We still have to verify our theory experimentally. Therefore we are working together with the CEA in France, where the depth penetrations are examined with the peeling technique explained at this conference.

In the international field, we share in the ACE-program and subsequent programs, i.e., large scale tests for studying the behavior of aerosols inside containments during severe accidents.

A special case is our BWR. It is a small one, only 60 MWe, built as a demonstration plant in 1968. It is built according to GE-specifications with a MARK-I like containment. It is the only BWR in the world with natural circulation, so without internal pumps. Therefore, it serves now a model for the SBWR design of GE. In fact some of our reactor engineers are accredited at GE for some years.

NUCLEAR AIR CLEANING PROGRAMS IN USA

M. Lee Hyder
Westinghouse Savannah River
P.O. Box 616
Aiken, SC 29802

In many respects, my review of U.S. air cleaning programs may be a fairly easy task since many of these have been reported at this Conference. However, I have been able to identify some other activities that were presented. In addition, you may know of some that I have missed. If so, I hope you will bring them forward, as Dr. Plumb has suggested. It is apparent to me that the U.S. programs, though containing some significant areas of new work, are not as extensive as they may have been in past years. In part, this is a natural consequence of a maturing industry. After all, there are more than 40 years of air cleaning studies that have been reported at these conferences. It is now possible for engineers to construct excellent air cleaning systems of considerable complexity for many purposes using standard commercial components. But this reduced level of effort also reflects the considerably diminished level of new construction in the U.S. nuclear industry, that inevitably is reflected in the level of research and development in this area and others.

I would like to describe the U.S. programs in the manner that Dr. Plumb has suggested by talking first about generic programs. Much of what I have to say deals with aerosols and particulate cleaning. We have heard at this Conference about the work done at Livermore National Laboratory on the development of metal filters. We have heard of work on the characterization of aerosols and of the performance of filter equipment being done by Argonne National Laboratory and at New Mexico State University. We have heard of at least two groups who are working on filter testing using various particulate generators to challenge the HEPA filters. Still, it is my impression that the U.S. work on aerosols is more extensive than has been reported here. I know from talking with people working in this area, that the field is a broad one. It is a significant area of research at several of our universities and there are national and international meetings held in this field which go well beyond the interests on the nuclear industry. I hope that we will continue to draw technology into our nuclear programs from this resource. An active generic area that has been referred to occasionally but not specifically mentioned in any one paper, is the development of models and codes for severe accidents dealing with movement of both aerosol and gaseous radioactivity. It is foreseeable that during the coming few years there will be a great deal of effort, directed into fitting some of these fairly newly developed codes to experimental data in order to validate them.

Turning to the area of air cleaning regulations and standards, we have been made aware here of numerous changes which are in progress in this country. The updating of the NRC Regulatory Guide 1.52, the recent issuance of new versions of ANSI Standards ASME N509 and N510, and the progress of work on the AG-1 Code will all have significant effects on future air cleaning development. Additionally, the recent modification of the absorber test methods, reflected in the test standards, will come in time to be reflected in practice, as well, although it appears that things are not moving very fast from what we have heard here.

With these thoughts in mind, I will look at some of the specific activities underway in developing air cleaning information for specific areas, beginning with the support of nuclear reactors. One of the largest such activities has only been lightly discussed at this conference because it is privately conducted research of a proprietary nature. I refer to the work coordinated by the Electric Power Research Institute, the so called LACE and ACE programs on reactor accident phenomena. This work is being done in collaboration with partners from many countries. We have heard about some, including the Dutch presentation. As I understand it, these studies have recently included various concepts for reactor containment venting, including some of those that we heard about this morning, as well as generic studies of iodine behavior in accident situations. Outside of these programs, there is only a limited amount of work in support of nuclear reactor operation. I have to mention that we maintain at the Savannah River Site a continuing program related to aerosol and adsorber research as well as research

on natural air circulation. Some of this is being done to develop the kind of code validation that I mentioned earlier. Additionally, this is an area that may see some new construction. The anticipated design and construction of one or even several new production reactors may be the basis for future work by the Department of Energy, (DOE) and its contractors. Also, as we have heard at this meeting, the firms involved in advanced power reactor design have no doubt been addressing various air cleaning problems, and their work may become more apparent in the future.

In the area of nuclear fuel reprocessing, I am sad to report our activities in this country have sunk to a rather low level. There is pioneering work centered at Oak Ridge National Laboratory, and that lab gave a paper in this field during this conference. In my discussions with Dr. Jubin and Mr. Birdwell, they told me that this is a very limited area of research right now. Of the remaining areas of nuclear industry research, the most active by far is waste management, and it has many aspects. We have heard about the design of waste and fuel repositories with ventilation as an essential part of the design. The cleanup and concentration of waste from several DOE sites, which has gotten considerable attention, and no doubt will have more, includes several areas of air treatment development. I can mention specifically, for example, work being done at the Idaho Chemical Processing Plant on catalytic reduction of nitrogen oxides and the recent development and construction of an off-gas system for the melter and solidification building at the Savannah River Waste Defense Processing Facility which is scheduled to be put into operation during the coming winter. This process includes several interesting problems involving air cleaning, as it must handle substantial quantities of benzene in one part of the process as well as mercury vapors. The performance of this equipment should, I think, be an interesting topic for the next air cleaning conference. Also, there will be work during the coming period on other waste management efforts at the various DOE sites, including the planned Hanford waste solidification facility, and a number of waste incineration programs. Other areas of the nuclear fuel cycle, including uranium refinement and fuel manufacturing, appear to be adequately covered by existing technology. I know of no new developments in these areas. In conclusion, I would like to emphasize that we still don't feel that we know everything, particularly in areas relating to sorbents, formation and migration of aerosols, and some of the other phenomena that might be encountered in potential reactor accident situations. I expect that there will be work continuing in these areas, and that we will be hearing more about them in future conferences.

NUCLEAR AIR CLEANING R&D PROGRAMS IN CANADA

Christopher H. Cheh
Ontario Hydro
Chemical Research Department
800 Kipling Avenue
Toronto, Ontario, M8Z 5S4 Canada

All CANDU generating stations are equipped with various gas treatment systems. The Off-Gas Management System, the Reactor Ventilation System (or Contaminated Exhaust System), and the D2O Vapour Recovery System reduce gaseous radioactive emissions during normal station operation whereas the Emergency Filtered Air Discharge System is designed for post-accident containment clean up. These systems installed at Ontario Hydro's CANDU stations are briefly described in a previous paper (1). In the following, R&D programs on gaseous radionuclides in Canada will be briefly discussed.

Carbon-14 R&D Program

In 1980, Ontario Hydro initiated a carbon-14 development program to reduce emissions from our nuclear generating stations. A removal process using calcium hydroxide at ambient temperature was developed from bench scale to full scale engineering system for both moderator cover gas system and nitrogen annulus gas system.

During replacement of the pressure tubes of Pickering NGS-A Units 1 and 2, carbon-14 contaminated dust was found in the annulus gas system. Elaborate work procedures had to be followed by retubing workers to avoid personal contamination. This affected the retubing schedule. A study was therefore carried out to find a way to decontaminate the annulus gas systems of Units 3 & 4 prior to retubing. It was learned that, in a nitrogen filled annulus gas system, carbon-14 forms hydrogen cyanide (HCN), which then polymerizes and crystallizes out on the annulus gas system surfaces. Even at a high temperature, the carbon-14 species decomposed very slowly. The decomposition products are H_2O, NH_3, and CO_2 at temperatures up to 300°C. The decomposition of the polymer material is normally incomplete. Pyrolysis, however, is enhanced when a source of oxygen is provided (2). Consequently, it was proposed that oxygen be added to the annulus gas to oxidize the carbon-14 which could then be purged from the system.

A carbon-14 removal unit was assembled to remove carbon-14 from the moderator cover gas at NPD NGS. This unit was later modified and used to remove carbon-14 from the purge of the annulus gas at Pickering NGS Units 3 & 4. Details of this carbon-14 removal program are summarized in a paper presented at this conference (3).

Tritium R&D Program

Both Atomic Energy of Canada Limited and Ontario Hydro have installed large scale tritium removal facilities to extract tritium from D_2O. The AECL Chalk River Tritium Extraction Plant uses their proprietary wet-proof catalyst and liquid phase catalytic exchange process followed by cryogenic distillation (4). Ontario Hydro's Tritium Removal Facility at Darlington NGS uses the vapour phase catalytic exchange process to extract tritium from D_2O and then separate the tritium by cryogenic distillation (5).

The Canadian Fusion Fuels Technology Project was formed in 1982 to undertake research and engineering in tritium technology and robotics for fusion applications. The total program is about $10 million per annum including contributions from subcontractors and cost sharing with external projects. The technology program is subdivided into three major elements; Systems and Engineering; Safety and Facilities Engineering; and Technology Applications. These major program elements include specific activities on: blanket and first wall systems; fusion fuel systems; safety and the environment; risk, reliability and maintenance; engineering services; remote handling; and technology transfer. An overview of the scope of the program is covered by two papers published in 1988 (6,7). Some of the projects Ontario Hydro Research Division has been involved in include hydrogen isotope separation (8), tritium dispersion and behaviour in the environment (9), and tritium immobilization (10).

Iodine R&D Program

The adsorption/chemisorption capacity of personal respirator canisters towards H_2S/SO_2 and CH_3I has been tested to determine whether these canisters met the specification of Ontario Hydro for use in our nuclear stations (11). Methods for in-station testing of charcoal filters and cold iodine analysis are also being developed.

The performance of charcoal filters under post-LOCA conditions had been tested and reported at the 20th DOE/NRC Nuclear Air Cleaning Conference (12,13).

A photochemical technique of removing both organic and inorganic forms of radioactive iodine from air developed by AECL is reviewed in a paper presented at this conference (14).

Aerosol Research Program

A multi-purpose aerosol research facility is being constructed in three stages to study ambient, high temperature and high humidity, and low temperature conditions, respectively. First stage of construction is now complete. The facility will support fundamental aerosol research, HEPA and charcoal filter testing, insulator studies and flow measurement calibration. Detailed design of the facility is given in an Ontario Hydro Research Division Report (15).

There is often a need to verify filter performance under normal operating conditions or to obtain information on filter performance under extreme conditions, eg. operation for long periods or at high temperature and high humidity. Work in this field was started in a modest way by assembling a system to characterize the performance of the small HEPA filters used in respiration systems (16).

An active and important area of research is the investigation of the behaviour of liquid aerosols formed in containment by a LOCA (17, 18). An understanding of aerosol behaviour in this situation is important because aerosols may act as carriers of non-gaseous radionuclides and therefore are responsible for transport of these species within containment and their release to the environment.

Noble Gases R&D Program

Technical and economic feasibility of applying the noble gas removal technology to remove Xe isotopes from the containment building air following an accident will be studied at WNRE.

Because of the short notice I had to be a panel member, I am sure I have omitted some of the R&D programs in Canada.

References

1. C. H. Cheh, "Review and Studies of Gas Treatment and Ventilation Systems in Ontario Hydro's Nuclear Generating Stations", Proceedings of a European Conference held in Luxembourg on 14-18 October, 1985, pp 218-230.

2. F. R. Greening, "The Characterization of Carbon-14 Rich Deposits Formed in the Nitrogen Gas Annulus Systems of 500 MWe CANDU Reactors", Radiochemica Acta 47, 209-217 (1989).

3. S. D. Chang, C. H. Cheh, P. J. Leinonen, "Demonstration of Carbon-14 Removal at CANDU Nuclear Generating Stations", 21st DOE/NRC Nuclear Air Cleaning Conference, Aug. 12-15, 1990.

4. W. J. Holtslander, T. E. Harrison, J. D. Gallagher, "The Chalk River Tritium Extraction Plant Construction and Early Commissioning", Fusion Technology 14, pp 484-488, Sept., 1988.

5. S. K. Sood, R. A. P. Sissingh, O. K. Kveton, "Removal and Immobilization of Tritium from Ontario Hydro's Nuclear Generating Stations", Fusion Technology 8, pp 2478-2485, Sept., 1985.

6. D. P. Dautovich, "Overview of Canadian Fusion Nuclear Technology Effort", Proceedings of the First International Symposium on Fusion Nuclear Technology, Tokyo, Japan, Apr. 10-19, 1988.

7. D. P. Dautovich, R. R. Stasko, "Overview of Canadian Fusion Fuels Technology Program on Safety", Fusion Technology 14, pp 401-406, Sept., 1988.

8. C. H. Cheh, "Large Scale Gas Chromatographic Demonstration System for Hydrogen Isotope Separation", Fusion Technology 14, pp 567-573, 1988.

9. R. M. Brown, G. L. Orgram, F. S. Spencer, "Field Studies of HT Behaviour in the Environment", Fusion Technology 14, pp 1165-1181, 1988.

10. W. T. Shmayda, N. P. Khernal, "Uranium for Hydrogen Isotope Removal from Inert Gas Streams", Proceedings of the First International Symposium on Fusion Nuclear Technology, Tokyo, Japan, April 10-19, 1988.

11. T. Jarv, "H2S/SO2 and CH3I Performance Testing of Respirator Canisters: MSA Window-Cator Gas Mask 'Type N', Ontario Hydro Research Division Report 87-303-H, Dec. 22, 1987.

12. J. C. Wren, C. J. Moore, A. C. Vikis, R. J. Fluke, "A Study of the Performance of Charcoal Filters Under Post-LOCA Conditions", Proceedings of the 20th DOE/NRC Nuclear Air Cleaning Conference, pp 786-801, 1988.

13. J. C. Wren, C. J. Moore, "Long-term Desorption of CH_3I from a TEDA-impregnated Charcoal Bed Under Post-LOCA Conditions", Proceedings of the 20th DOE/NRC Nuclear Air Cleaning Conference, pp 1117-1129, 1988.

14. A. C. Vikis, C. J. Evans, R. MacFarlane, "Photochemical Removal of Radioactive Iodine From Air", 21st DOE/NRC Nuclear Air Cleaning Conference, Aug. 12-15, 1990.

15. H. Leung, "Design of a Multipurpose Aerosol Research Facility", Ontario Hydro Research Division Report 88-69-K, July 22, 1988.

16. H. Leung, M. Mackay, "Evaluation of Filters Using Spectrofluorimetry and CNC Methods", Ontario Hydro Research Division Report 88-173-K, Aug. 8, 1988.

17. G. Orgram, A. Lemyk, "Water Aerosol Leakage Experiments Nov. 1988: Droplet Size Distributions Measured by FSSP", Ontario Hydro Research Division Report 90-36-P, Feb., 1990.

18. G. Orgram, A. Lemyk, "Water Aerosol Leakage Experiments Nov. 1989: Filter Measurement of Cs in Vent Line", Ontario Hydro Research Division Report 89-285-P, Jan., 1990.

UNITED KINGDOM ATOMIC ENERGY AUTHORITY PROGRAMS

David Holman
UKAEA
AEE - Winfrith
Dorchester, Dorset
United Kingdom DT2 8DH

A large number of waste management facilities are currently planned or are under construction in the United Kingdom. They include about 5 cement encapsulation plants, a couple of super- compactors, and equipment we are developing for reactor decommissioning, particularly on some of the old gas cooled reactors. In addition, there is some ongoing refurbishment of active handling facilities. Each of the systems has relatively simple off-gas treatment; predominantly double HEPA filtration for the removal of particulate. I suppose the major differences in the U.K. are now almost total utilization of the type of circular filters Dave Loughborough spoke about at this conference. The excellent sealing and remote handling techniques associated with the push-through capabilities developed by the staff at Harwell have made use of this type of filter almost universal in the U.K. Several very large systems have been installed including a couple of units that deal with up to 100,000 cu. ft/min. Examples are our reprocessing plant, our reactor installations, and some of the major radioactive materials handling facilities around the U.K. Because of the wide use of circular filters with their improved seal arrangements, we were able to overhaul our facility design codes and now we specify 99.99% removal instead of 99.95%, which had been the norm before. Indeed, we are getting penetrations of less than 0.005% and even down as low as 0.001%, approaching the efficiency of the material itself.

On the subject of fuel reprocessing, I believe most people at the conference are aware that British Nuclear Fuels in the U.K. are planning to commission their oxide processing plant in 1992. The off-gas treatment technologies for this plant were established quite some time ago and their designs were frozen. The systems involve only a primary condenser and demisters on the dissolver off-gas line with an acid scrubber for NO_x removal and an alkali scrubber for iodine and C-14 retention, all backed up by double HEPA filters. Krypton-85 removal using cryogenic or fluorocarbon techniques was not considered necessary or cost effective, although the possibility to retrofit such a system has been included in the building design. Currently, a major new program in the U.K. is aimed at the future reprocessing plants; a plant we call "Son of THORP" is aimed for the year 2010-2015.

Using environmental impact considerations and due to the cost of large off-gas scrubbers, it has been shown clearly that it is worthwhile to evaluate alternative and advanced technologies. The key features that have been looked at as part of waste minimization program are reduced off-gas flows with recycle of the off-gases within the dissolver off-gas and the vessel vent off-gas systems whenever possible. The use of improved stainless steel-lined cells reduces in-leakage, lowers cell ventilation requirements, and leads to smaller HEPA installations then are currently specified by THORP. Segregation and treatment of the vessel vent system will lead to reduced transfer of organic materials to the dissolver, leading to organic iodine problems. Steps to minimize radioiodine residues in the raffinate coming forward to the purex system will lead to reduced difficulties of iodine bleeding out into the off-gas systems all the way through the purex purification process, a source of difficulties for many reprocessing plants. We are currently examining volume intensified scrubbers and jet spray towers to reduce the size of the acid and the alkali scrubbers at the head end of the reprocessing vessel off-gas treatment systems. We will also require improved NO_x abatement both because of its chemical toxicity and to enable krypton-85 systems to be considered at the back end of the process.

Currently, there is work in the U.K. on selective and non-selective catalytic NO_x abatement and a new technique (which I am not aware of being studied anywhere else in the world) that uses corona discharge. This is a high voltage system that is very similar to electrostatic precipitators but is operated under higher voltage. With this system you can convert NO_x to NO_2. If the corona discharge is operated with continuous alkali irrigation, NO_x can be removed to very low levels in a single unit. An advantage of the corona discharge system is that it is also capable of removing both organic and

inorganic iodine simultaneously because it completely converts organic iodides to CO_2 and iodine oxides that can be removed by an alkali scrubber system.

Schemes to lower C-14 discharges, in particular C-14 that arises from carbon monoxide, are also being examined. Another novel application is selective removal of various key isotopes by membrane-type processes. At the moment, the program involves looking at membrane materials and trying to find selective membranes which will remove the key radionuclides. The successful implementation of off-gas flow minimization coupled with new improved NO_x abatement techniques should allow us to use krypton-85 removal in any future plant. In particular, I think, the chromatographic technique described earlier at this Conference by Dr. Ringel of Julich looks particularly attractive in that context. In the ways I have outlined, future reprocessing plants will be installed in the U.K. that will achieve a markedly lower environmental impact than any existing or planned plants in operation anywhere in the world at this time. I hope we shall be able to report some of the developments of this work at the next Nuclear Air Cleaning Conference.

DEVELOPMENTS IN THE AREA OF REGULATORY MATTERS IN THE UK

Ian Handyside
Her Majesty's Inspectorate of Pollution
Room A512
Romney House
43 Marsham Street
London, England SW1P 3PY

As you probably know, we opted at an early stage for gas cooled reactors in the U.K. Currently there is a hold on further development of nuclear power in my country. However, we have one PWR design which is currently well advanced in construction. It is going to be located at a place called Sizewell. It is based on the Snupps design. We also have in place a public inquiry for a PWR plant at another site and we are waiting for results of that inquiry.

So far as reprocessing is concerned, there is a significant development at Sellafield in that the plant for vitrification of high level wastes is now on stream and, perhaps by the time of the next conference, there will be some useful information on performance of gas clean-up systems.

On the subject of waste disposal in the UK, we are currently actively searching for a new disposal site and we anticipate that one will be available early in the next century.

On fusion, we have the JET facility constructed and it is at an early stage of operation, but quite soon it will be taking in large inventories of tritium and by the time of the next conference there will likely be some useful information on its management.

There is not a lot to report on the nuclear regulation front in the UK, although one change that will come forward by the end of the year is that research establishments such as AEA, including Harwell, will come under the formal regulations that apply to civil nuclear installations.

Much more fundamental on the regulatory scene is a major initiative that will become law soon. We are introducing an Environmental Protection Act that will apply to the most polluting non-radioactive substances. This is to be based on the concept of integrated pollution regulation and will require each operator to adopt the best practical environmental option for waste disposal. Operators will also be required to use best available technology not entailing excessive cost, to minimize discharges of waste from plant. I think there has been reference to a similar concept in amendments to the US Clean Air Act that are going through the regulatory system in the US.

NUCLEAR AIR CLEANING PROGRAMS IN PROGRESS IN FRANCE

Philippe Mulcey
Institut de Protection et de Sûreté Nucléaire
DPT/SPIN/SEIP, bâtiments 389, 393
CEN/SACLAY
91191 Gif-Sur-Yvette
Cedex, France

I shall try to give a short presentation of the nuclear air cleaning programs in progress in France. First, concerning reactors, a good presentation was given this morning of the sand-belt filter and, in particular, a full-scale test of a filter unit at Cadarache, so I shall not elaborate more on it. On this topic, we also have a big program in Cadarache called PHEBUS-PF that involves simulating very severe accidents in a PWR. Associated with this big program, laboratory studies about iodine and aerosol measurement techniques for use during such severe accidents are in progress.

Concerning reprocessing plants, the trapping of all species of gaseous and particulate iodine before release to the stack is one of the most important things to do from the point of view of volatile radioisotopes. The program we have in progress is to use an iodine scrubber to transform gases, such as molecular iodine and methyl iodide, into solid and stable particulate of iodine oxides. This technique was initially proposed by our Canadian colleagues at Whiteshell, the team of Andy Vikis. At present laboratory tests are being conducted on a pilot scale facility at flow rates ranging from of 100 to 300 m3/hr in order to study the influence of humidity, NO_x concentration, iodine concentration, on the efficiency of the process.

Concerning waste management, we have an important program in France for incineration of TRUS. From the point of view of air cleaning, the two major points are first, the improvement in our knowledge of the source term, that includes all gases and aerosols that are to be filtered and improve our understanding of all operating conditions of the incinerators. The second major point is our research and development program on appropriate filtration systems. That is to say, a search for systems that can reduce secondary wastes as much as possible, and, when possible, to collect aerosols as such to make storage easier. Two different techniques are under study in our laboratories: one, is gas microfiltration derived from liquid technology and leads to an interesting application to gaseous filtration. The second study is directed toward the use of granular beds.

Concerning the dismantling of nuclear facilities, we are looking at the emission of aerosols from dismantling tools and here too, there are two directions for our R & D programs. One is improvement in our knowledge of the source term, including the concentration and size distribution of emitted aerosols. The second is research on appropriate filtration systems. One of them is under study in our laboratories. It refers to a new design of a cleanable electrostatic filter.

For all nuclear facilities, we are looking at the effects of fires in rooms and ventilation ducts. We are elaborating for a source term data base applicable to many materials and components that emit aerosols, gases, and heat during fires in order to develop ventilation strategies for fires in nuclear facilities. This activity has mainly resulted in the development of a computer code that describes the behavior of ventilation networks under fire conditions, (SIMEVENT code). For this it is necessary to couple to the ventilation code the codes that are able to describe heat generation and heat transfer as well as aerosol production and transfer inside the facility.

Regarding filter testing, a paper was presented during this Conference on the realtime detection of a fluorescent aerosol. As you may know, the HEPA filter tests in France are performed according to Standard NF-X-44011 which suffers from a delayed response of the content of aerosol sampled upstream and downstream from the filter. An attempt is made to incorporate all the sequences of measurement into a realtime detection apparatus. Modeling pressure drop evolution of HEPA filters is in progress from existing models and experimental data obtained with a peeling technique of the filter

media. A paper was given yesterday on this topic. We also have a study in progress to model granular bed filters, and an experimental program on liquid aerosol filtration to study removal efficiency and resistance during loading. As you know, the behavior of liquid aerosols in filter media is different than the behavior of solid aerosols and this difference affects the development of pressure drop and efficiency during loading. This is being studied in the Center at Fontenay-aux-roses. The last point I want to point out concerns migration of aerosols through HEPA filter media. A study on thermo-migration of ultra fine particles through HEPA filters is being conducted in collaboration with Lambert Scholten from KEMA Laboratories (The Netherlands).

A SHORT OVERVIEW OF THE PROGRAMS IN SWEDEN

Hans Cederqvist
ABB Atom AB
Service Division
S-721 63 Vateras
Sweden

I will present a short overview of the situation in Sweden. Presently, we have 12 nuclear power plants in operation, 9 BWRs, 3 PWRs. A preliminary decision to phaseout nuclear power hangs over us like an ominous cloud, but we are doing everything we can to change this decision, you may be sure. We have in operation a central storage for spent fuel which is located underground; we have presently about 2,000 tons there. Because it is located 50 meters below ground level, it needs a lot of ventilation and a large portion of the facility consists of ventilation systems. The ventilation systems are mostly of a conventional type.

We also have a central storage facility for intermediate waste, close to the Forsmark plant. We have a fuel factory where we employ conventional filter technology. A new facility that has been placed into operation is a low-level incinerator in Straswick where filters for removal of dioxin has been installed and are presently in operation.

It is very easy to summarize what has been happening in nuclear air cleaning in Sweden in recent years. Air cleaning research has been completely dominated by filter containment systems and a big effort has been made to develop systems that can be demonstrated to work under accident conditions and to install them into the various nuclear power plants with all the procedures and accessories that are needed to make these systems function. The program began in 1985 and today we have reached the situation where we have containment filter systems in all the plants. It has been a major effort which now is concluded.

The ABB Atom

BWRs employ a unique design for treating off-gases. It is a combination of a sand-bed and small charcoal columns where we use adsorption-desorption. They have been in operation since 1980. The regulations applied include the US NRC Regulatory Guide 1.52 plus Swedish regulations that have been issued by the Radiation Protection Agency in 1985. We presented them here at the Nuclear Air Cleaning Conference in 1986.

To summarize the situation in Sweden, we have no large programs underway; we try to optimize the systems that are presently in operation, to improved efficiency, and to decrease the cost of operation.

NUCLEAR AIR CLEANING ACTIVITIES IN GERMANY

Juergen Wilhelm
Kernforschungszentrum Karlsruhe GmbH
Postfach 3640
D-7500 Karlsruhe 1
Federal Republic of Germany

I would like to restrict my discussion to nuclear air cleaning activities in Germany. Only limited activities are now going on in the Federal Republic of Germany. I tried to get some information about what is going on in the German Democratic Republic but it seems that hardly anything goes on there. Work is underway in the Federal Republic of Germany on containment venting with reard to filtration based on a combination of stainless steel roughing and fine filters with a DF similar to or better than that achieved with HEPA filters. The main point of interest at the moment is the development of relatively small filter units that can be located inside the containment. Some of these filters are under construction and will be installed in nuclear plants. Besides avoiding additional costs for filter construction, this special concept keeps the particulate material inside the reactor containment. Problems of handling extremely high radioactivity materials and the need for additional shielding are avoided in the case of a core meltdown. Similar considerations apply to the use of Venturi scrubbers combined with stainless steel filter, i.e., use of existing buildings for the filter system so that new buildings are not necessary. We had to optimize the stainless steel filter with respect to its loading capacity for aerosols by enabling it to accommodate 60 kg of aerosol with a mass medium diameter of 0.5 μm which is generated from tin dioxide with a plasma torch. Because the filter capacity for these particles is at least 60 kg, the capacity for larger particles will be much higher, namely by a factor of 5 or more. For use in the future in nuclear power stations with a proposed new containment design, the development of a large stainless steel filter is being considered at the Karlsruhe Nuclear Research Center. The new containment design is intended to withstand a steam explosion, a hydrogen explosion, and a core meltdown accompanied by melt penetration through the pressure vessel. This means complete confinement in the case of a very severe reactor accident acutally the most serious reactor accident one can assume. The idea is to cover the steel containment with a concrete containment and to have connections between the steel containment and the concrete containment to carry the pressure from the steel containment to the high-strength concrete containment. A containment built this way will withstand static pressures of around 40 - 50 bars and short pressure peaks of more than 100 bars.

I heard at this Conference the opinion that future reactors will not need air cleaning system. My feeling is that even though we will have a new design, air cleaning will be needed because I have never seen or heard of a containment with locks and penetrations that are absolutely tight. I can't imagine that 100% leak-tightness can be guaranted because operating a reactor one has to bring people and material into the containment, one has to take steam out of the containment, one has to bring water in, and so on.

The new double containment has annular rooms between the steel containment and the concrete containment. The idea is that concrete containment will have openings and the air inside the annular rooms will be exchanged by a stack draft effect as it is heated up (Fig. 1). The air will cool and steel containment, heated by the decay heat of the core. Therefore, the steel containment is cooled in a passive mode. The air from the annular rooms will have to be filtered because it may contain activity leaking from the inner containment. At the moment, German standards allow a leakage of 0.25% per day of the volume of the inner containment. The filter one has to use for the new containment concept will be rather large. The airflow needed for cooling the inner steel containment after a core meltdown is on the order of some 100 m^3/s. Therefore, only the air will be filtered from that part of the containment where penetrations and leakage may occur. These are penetrations which are closed under conditions of normal operation, but it still may have some leakage. At Karlsruhe around 30 people are working on the new containment concept, named containment 2000. That doesn't mean that the containment 2000 will be built in Germany with certainty, but it does mean that experienced people are working on a new design and hope for public acceptance. My personal feeling is, if one does not do new

CHIMNEYS

REMOVAL OF DECAY HEAT

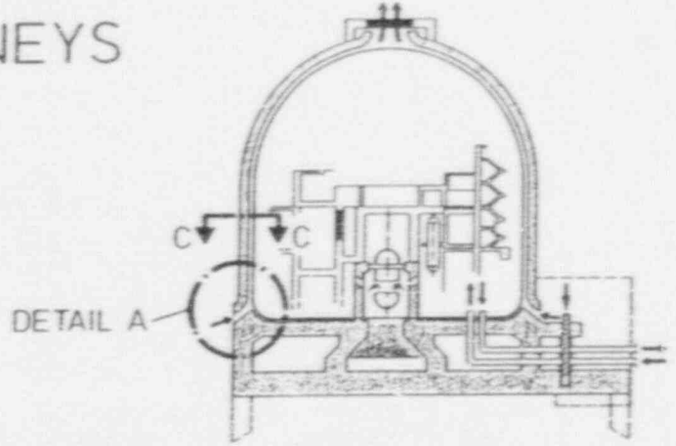

SECTION C-C

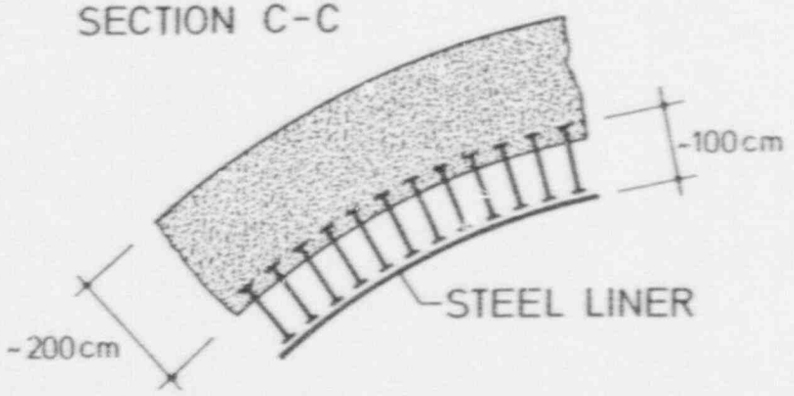

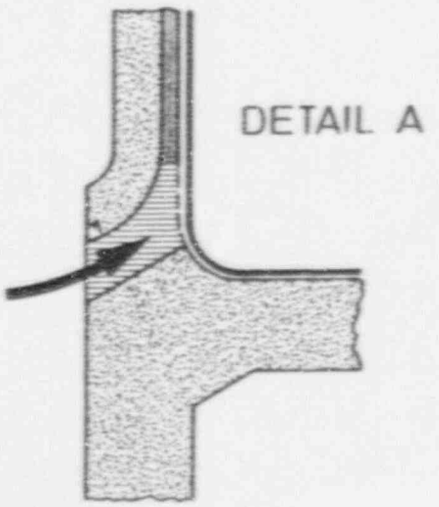

FIG. 1	INSTITUT FÜR MASSIVBAU UND BAUSTOFFTECHNOLOGIE UNIVERSITÄT KARLSRUHE (TH)	1990

t'ings in the power reactor safety area one may never be able to build more nuclear power stations in the future.

Another part of the work in Germany is concerned with the dismantling of decomissioned reactors. Here, aerosol generation due to cutting heavy components is being examined. We are looking for the best method that will produce the lowest possible amount of aerosols. Also under development in Germany is a code for calculating filter stresses that include high air velocity, gas compressibility, high humidity, the effect of condensation processes, and shock waves, as well as supersonic flow in the ventilation systems.

Going to reprocessing, it can be said that Germany will not build a reprocessing plant, strictly speaking, for political reasons; there are no technical reasons. Therefore, work on reprocessing is down. There are some residual activities because the system which was developed for the off-gas system of the reprocessing plant, including the vessel and dissolver off-gas systems, has been sold to Japan and some additional measurements will be done. Further, some work is done on off-gas cleaning of incineration plants. One important thing is the fact that dioxin has to be trapped in the off-gas of incineration plants. The startup of a new incineration plant showed the concentration of dioxin to be rather high, but with a better design of the process the concentrations may be lower. In total, the amount of research and development in the nuclear air cleaning field is at a low level at the moment. Most of the groups working previously in nuclear air cleaning are now using their knowledge and experience to solve problems of conventional air cleaning. For example, the KfK work on the high strength HEPA filters is the background for a recleanable HEPA filter for application in conventional industry. As I see it, the admissible concentrations for the release of substances like cadmium and heavy metals will be so low in Germany in the future that I think we can use our special knowledge to benefit the conventional field.

AIR CLEANING PROGRAMS RELATING TO THE FIRST JAPANESE COMMERCIAL REPROCESSING PLANT

Yasuo Hirose
Hitachi Ltd.
3-1-1 Saiwai-cho, Hitachi-shi
Japan

My presentation will put special emphasis on the air cleaning programs related to the first Japanese commercial reprocessing plant. This project is the biggest nuclear issue in Japan these days. The plant is going to be located at the northern-most part of the main island of Japan, facing the Pacific Ocean. Officially, construction will start next year and is scheduled to be completed by the end of 1997. A detailed design and regulatory procedure is underway at the moment. The plant is specified to be capable of storing 3,000 metric tons of uranium in the pool facility. Eight hundred metric tons of uranium will be processed per year from spent fuel 50% derived from BWRs and 50% from PWRs. It is specified that the spent fuel assemblies will have burned 45,000 megawatts per ton average and 55,000 megawatts per ton maximum. Several Japanese industrial groups, including nuclear power plant manufacturers, have been selected to take part in the construction of the plant. French technology has been introduced extensively into the main part of the Purex process. In addition we are using the reduced pressure evaporation technology and we are using the German iodine retention technology. We will have the safest and most reliable and efficient reprocessing plant. I should add that U.S. safeguard proven technology will be introduced, also. Our policy is to demonstrate technical reliability by many test programs. Here are some pertinent data about this special process. The air cleaning system can be divided into the shear-dissolver off-gas, the vessel off-gas and the vitrification off-gas sections. After careful evaluation of the environmental radiation risk, no other volatile fission product but iodine was designed to be removed from the gaseous effluent of the plant. So far as dissolver off-gas cleaning is concerned, radioactive particles and iodine are to be removed in the remotely maintainable filtering system using high efficiency demisters, and heaters, HEPA filters, and solid iodine-collecting adsorbents. The technology has been reported to this Air Cleaning Conference by our German colleagues. It is planned to eliminate iodine from all liquid streams and to transfer it to the gaseous stream as much as possible by providing iodine desorbers. There will be high retention capability for iodine within the plant in the form of a highly stabilized and compacted waste. These are safety feature of this new reprocessing plant.

The alternative absorbent has been discussed at this Air Cleaning Conference several times by our colleagues. Although German technology could have been demonstrated in an operating plant, we have ourselves made a careful selection of structure materials for iodine at higher temperature. Disposal of iodine-129 waste is a future obligation to be considered carefully. It is my belief that after impregnated solid waste has absorbed iodine chemically it is stable enough to be stored for something like 40 years while waiting to decide on a final conditioning method. It has been decided, moreover, that unused space should be provided in order to install additional cleaning capabilities for possible future demand for collecting volatile products other than iodine. Each component of the processing facility, such as fuel receiving and storage, head end, separation, purification, conversion, and the numerous steps of waste treatment, including the storage, evaporation, and incineration has its own best set of gas cleaning systems. They consist, typically, of scrubbers, condensers, mist separators, and HEPA filters. Taking into account possible iodine contamination, special off-gas cleaning systems are provided on storage tanks and separation processes. Air cleaning technology associated with the vitrification process will be demonstrated in the pilot plant at Tokai. It is a special safety feature in Japan that containments will be used to prevent spread of radioactivity to the environment even under very severe accident conditions.

DISCUSSION

HANDYSIDE: Vitrified high-level waste in storage needs cooling. Do you intend to include air cleaning systems for stored vitrified high-level wastes?

HIROSE: We are going to provide double walls.

HANDYSIDE: But no gas treatment?

HIROSE: No.

MERCIER: I have a small question on the vitrification comment in your presentation. You mentioned a ruthenium filter, can you give some information on the nature of this filter?

HIROSE: As a matter of fact I am not so much involved in this particular technology, but there will be a substantial amount of ruthenium. I think it will be collected with a scrubbing solution and sent back to the highly radioactive liquid waste concentrator. Just for safety, we are going to include a ruthenium filter.

NUCLEAR AIR CLEANING PROGRAMS IN HUNGARY

Vilmos Friedrich
Institute of Isotopes of the Hungarian
Academy of Sciences
P.O. Box 77
H-1525 Budapest, Hungary

In Hungary within the nuclear fuel cycle, we have one nuclear power plant with four reactors of 440 megawatts electrical each. This is a Soviet produced pressurized water reactor, type VVER-440. The spent fuel from these reactors is transported back to the USSR after five years storage at the nuclear power plant site according to the present contract.

Among non-fuel cycle facilities we have one research reactor plus one small reactor for educational and training purposes. We have one isotope production laboratory that prepares as its main product different kind of radioiodine isotopes. It can produce 40-100 curie per week of I-131 that are used for industrial and medical applications.

At the moment, Hungary has one disposal site for low-level radioactive wastes that originate from non-fuel-cycle facilities and designing a bigger disposal site for low- and medium-level wastes. Although the nuclear power plant is now completed, the construction of this disposal site has been delayed for more than two years due to strong public opposition at the site.

Concerning air cleaning activities, first, the nuclear power plant does not have conventional containment type construction. You may say that it is a special kind of confinement system. It has a control room ventilation system consisting of aerosol filters and carbon adsorbers. The aerosol filters contain plastic fibers and the carbon filters contain non-impregnated charcoal. The off-gas cleaning system consists of a catalytic hydrogen recombiner, dryer, and a carbon delay line for noble gases. The main safety features are a sprinkler system for confinement and a localization tower that is a new development in the Russian designs. The only reactors which have this localization tower are in Hungary, Finland, and Czechoslovakia. They contain bubble plates filled with boric acid solution for steam condensation and for scrubbing aerosols. There is also a post-accident recirculation system which consists of glass fiber aerosol filters and carbon adsorbers which, at the moment contain non-impregnated carbon. Unfortunately, there is no regulation or standard in Hungary for testing any kind of nuclear filters, a very poor situation. My laboratory has developed in-situ testing methods and equipment for HEPA filter testing in nuclear power plants. The test method is based on the British sodium chloride test. We couldn't use the DOP test due to the presence of plastic fibers in the aerosol filters. We are now working on developing in-situ carbon testing methods but, unfortunately, the present construction of the carbon adsorbers in our nuclear power plant is such that even if we got bad results from testing, the carbon cannot be changed. That is a problem at the moment and developing some in-situ testing methods for the nuclear power plant is a part of our research and development work. Part of the development work was done as part of a coordinated research program organized by the IAEA. In addition, some investigations are being conducted on performance of HEPA filters and charcoal units under severe conditions of high humidity and high temperature. Part of this work was also performed within the framework of the IAEA coordinated research program. Development of predictive computer codes is underway to evaluate and predict carbon performance because, at the moment, we are not able to perform in-situ testing of the carbon. At a presentation yesterday, I spoke about this program.

Finally, I would like to ask a question of the IAEA representative who is here. As far as I know, the IAEA is now going to initiate a revision of the safety features of the European-Russian type of nuclear power plant, the type VVER. Is it possible to inquire whether the air cleaning and filtration points of view within IAEA are such as to revise the requirements in these countries.

DISCUSSION

PLUMB: In response to the specific request, we will, of course, take note of the needs associated with VVER safety features in air cleaning and consider them within the Secretariat. We will observe due process when resolving the matter.

INDEX OF AUTHORS AND SPEAKERS

LIST OF ATTENDEES

AMEND, Juergen
Kernforschungszentrum Karlsruhe
Postfach 3640
D-7500 Karlsruhe 1
Germany

ANDERSON, Wendell L.
RR 4
Box 4172
LaPlata, MD
20646

ARNDT, Tim
Westinghouse Hanford S2-02
P.O. Box 1970
Richland, WA
99352

AVIDA, Ram
Nuclear Research Center Negev
P.O. Box 9001
Beer-Sheva
ISRAEL 84190

BAINARD, W. Dale
Washington Public Power Supply
3000 George Washington Way
Richland, WA
99352

BANTON, Steven
Pacific Gas & Electric Co.
Diablo Canyon Nuclear Power Plt.
P.O. Box 56
Avila Beach, CA 93424

BATEMAN, Jim
Flanders Filters, Inc.
P.O. Box 1708
Washington, NC
27889

BELLAMY, Ronald R.
Radiological Protection Branch
U.S. Nuclear Regulatory Com.
475 Allendale Rd.
Prussia, PA 19406

BENDER, Larry
AirGuard Industries
3807 Bishop Lane
Louisville, KY
40218

BERGMAN, Werner
Hazards Control Dept., L-386
Lawrence Livermore National Lab.
P.O. Box 5505
Livermore, C[illegible] '550

BERRY, Daniel
Rochester Gas & Electric
2048 Ridge Rd.
P.O. Box 148
Ontario Center, NY 14530

BIRDWELL, Joseph
Bldg. 7601
Oak Ridge National Lab.
P.O. Box 2008
Oak Ridge, TN 37831-6306

BISHARA, Amin T.
Suite 488
Plant Technical Services, Inc.
500 Grapevine Highway
Hurst, TX 76054

BOND, Leroy
Technical Papers Division
Lydall Inc.
P.O. Box 1960
Rochester, NH 03867

BRAUER, Fred P.
P7-35
Pacific Northwest Lab.
P.O. Box 999
Richland, WA 99352

BRAUN, H.
Ministry of Environment, Nature
Conservation & Reactor Safety
5300 Bonn
Germany

BRESSON, James F.
Dames & Moore
6100 Indian School Rd.
Albuquerque, NM
87110

BURWINKEL, Paul
Georgia Power Co.
Plant Vogtle
Waynesboro, GA
30830

CARLON, Hugh R.
U.S Army Chemical Research
Development & Engineering Center
Aberdeen Proving Grounds, MD
21010-5423

CARLSON, James
Univ. of California
6851 Heath Ct.
Pleasanton, CA
94588

CEDERQVIST, Hans
ABB Atom AB
Service Division
S-721 63 Vasteras
Sweden

CHEH, Christopher
Chemical Research-Process Chem.
Ontario Hydro-Research Div.
800 Kipling Ave. Toronto
M8Z 5S4 Canada

CHIPUL S., Miguel
Com. Federal de Electricidad
Officina de Ingenieria DOS BOCAS
APTO. Postal No. 178
Veracruz, Ver., Mexico

CHRISTIAN, J. D.
Idaho Chemical Processing Plant
Westinghouse Idaho Nuclear Co.
Idaho Falls, ID
83403

CICHELLO, John P.
Cleveland Electric Illum.
Perry Nuclear Power Plant
P.O. Box 5000
Cleveland, OH 44101

CROSBY, David W.
Air Techniques Div
Hamilton Associates, Inc.
1716 Whitehead Rd.
Baltimore, MD 21207

CROSS, Sherri
A5-10
U.S. Dept. of Energy
P.O. Box 550
Richland, WA 99352

CRUICKSHANK, Robin
Arizona Public Service
P.O. Box 52034
Phoenix, AZ
85072-2034

CURHAM, John J.
Public Service Electric & Gas
Salem Generating Station
P.O. Box 326
Hancocks Bridge, NJ 08038

DENARD, David W.
Duke Power Company
Oconee Nuclear Station
Seneca, SC
29665

DEVENA, Stan
Wolf Creek Nuclear Corp.
P.O. Box 411
Burlington, KS
66839

de WITT, H.
Brenk Systemplanung
Heinrichsallee 38
D-5100 Aachen
Germany

DHINGRA, Sada
MS 1796
Arizona Public Service Co.
P.O. Box 52034
Phoenix, AZ 85072-2034

DILLMANN, Hans-Georg
Kernforschungszentrum Karlsruhe
Postfach 3640
D-7500 Karlsruhe 1
Germany

DOERSAM, Michael A.
Barnebey & Sutcliffe Corp.
P.O. Box 2526
Columbus, OH
43216

DORAN, Jerry
Nebraska Public Power District
P.O. Box 499
Brownville, NE
68321

DORMAN, Richard
24 Balmoral Rd
Salisbury
Wiltshire
SPI 3PX United Kingdom

DORON, Eliahu
Nuclear Research Center Negev
P.O. Box 9001
Beer-Sheva
Israel 84109

DUNBAR, Al
Charcoal Service Corp.
P.O. Box 3
Bath, NC
27808

DYKES, D.M.
Westinghouse Savannah River
Savannah River Site
Aiken, SC
29808

EARLE, George W.
Westinghouse Savannah River Co.
Savannah River Site
Aiken, SC
29808

ECKARDT, Bernd
Abt. S 331
Siemens AG - UB KWU
Postfach 101063
D-6050 Offenbach, Germany

EDWARDS, James R.
Charcoal Service Corp
P.O. Box 3
Bath, NC
27808

ELLIOTT, William H.
EG&G
Rocky Flats Plant
P.O. Box 464
Golden, CO 80402-0464

ENNEKING, Joseph
Nuclear Consulting Services
P.O. 29151
Columbus, OH
43229

EPPERSON, Stephen A.
WSRC, Bldg. 735-11A
Savannah River Site
Aiken, SC
29802

EVANS, A. Gary
Savannah River Site
Westinghouse Savannah River
Aiken, SC
29808

EVANS, John S.
IPH
Harvard School of Public Health
665 Huntington Ave.
Boston, MA 02115

FAVIS, Fred
Bechtel National Inc.
50 Beale St.
San Francisco, CA
94105

FIRST, Melvin W.
Harvard Air Cleaning Laboratory
School of Public Health
665 Huntington Ave.
Boston, MA 02115

FLIS, Christine
Cook Nuclear Plant
Indiana Michigan Power
One Look Place
Bridgman, MI 49106

FLYNN, Kevin D.
Mail Code D2B
Southern California Edison
P.O. Box 128
San Clemente, CA 92674-0128

FOX-WILLIAMS, Kathy
MS LE-13, Airdustrial Bldg. S
Dept. of Energy
Olympia, WA
98504

FRANKENBERG, Ronald E.
CVI Incorporated
P.O. Box 2138
Columbus, OH
43216

FRANKLIN, Ben
American Air Filter
215 Central Avenue
Louisville, KY
40208

FREEMAN, Peter
Nuclear Consulting Services
P.O. Box 29151
Columbus, OH
43229

FRENCK, Roland L.
DT-12
Eng'g. & Operations Support
U.S. Dept. of Energy
Washington, DC 20545

FRETTHOLD, J.
EG&G Rocky Flats
P.O. Box 464
Golden, CO
80402-0464

FRIEDRICH, Vilmos
Institute of Isotopes of
the Hungarian Academy of Sci.
P.O. Box 77
H-1525 Budapest, Hungary

FULLER, David
TU Electric
304 Spanish Tr. Dr.
Granbury, TX
76048

FUNK, John
Hanford Environmental Health
1826 Birch
Richland, WA
99352

FURRER, Juergen
Kernforschungszentrum Karlsruhe
Postfach 3640
D-7500 Karlsruhe 1
Germany

GARCIA, Andrew G.
EG&G
Rocky Flats
P.O. Box 464
Golden, CO 80402-0464

GAZDEK, Jim
Argonne National Lab.
P.O. Box 2528
Idaho Falls, ID
83401

GEER, John A.
2395 Dartmouth Ave.
Boulder, CO
80303-5209

GHOSH, Deep
Southern Company Services
P.O. Box 2625
Birmingham, AL
35202

GILBERT, Alan
Vokes Limited
Henley Park
Guildford
England GU3 2AF

GILBERT, Humphrey
Consultant
P.O. Box 704
McLean, VA
22101

GILL, Charles
Region III
U.S. Nuclear Regulatory Comm.
799 Roosevelt Rd.
Glen Ellyn, IL 60137

GILMORE, Robert D.
Suite 104
Environmental Health Sci
Nine Lake Bellevue Bldg.
Bellevue, WA 98005

GLADDEN, David J.
STEDP-MT-TM-CB
U.S. Army
Dugway Proving Grounds
Dugway, UT 84022

GODAS, Thommy
National Institute of Radiation
Protection
Box 60204
S-10401 Stockholm
Sweden

GOLES, Ronald W.
Process Technology / MS G601
Battelle Pacific Northwest
P.O Box 999
Richland, WA 99352

GORDON, Mike
MS/PV-11
U.S. Dept. of Ecology
State of Washington
Olympia, WA 98504

GRAVES, Curt
Nuclear Consulting Services
P.O. 29151
Columbus, OH
43229

GREEN, Claude A.
Stearns Catalytic Div.
United Engineers
30 S. 17th St.
Philadelphia, PA 19102

GREEN, Melvin
Codes & Standards Div.
ASME
345 East 47th St.
New York, NY 10017

GREGORY, William S.
Group N-6, MS K557
Los Alamos National Lab.
P.O. Box 1663
Los Alamos, NM 87845

GRUBER, Mark
Prairie Island Plant
1717 Wakonade Dr. E.
Welch, MN
55089

GU Xiaochun
Shanghai Textile Res. Institute
545 Lan Zhou Rd.
Shanghai
People's Republic of China

GUEST, Alan
Ontario Hydro Research Div.
800 Kipling Ave.
Toronto, Ontario
M8Z 5S4 Canada

GURHAM, Jack
Salem Generating Station
Public Service Electric & Gas
P.O. Box 236
Hancocks Bridge, NJ 08038

GUSTAVSSON, Borje
ABB ATOM AB
ASEA Brown Boveri
S-721 63 Vasteras
Sweden

GUTTMANN, Jack
MS 16-H3
U.S. Nuclear Regulatory Comm.
Washington, DC
20555

HALL, G. Robert
Stearns-Roger Div.
UE&C
JACADS Johnston Atoll, Box 134
APO San Francisco, CA 96305

HANDYSIDE, Ian
Her Majesty's Inspect. of
Pollution
Room A512, Romney House
43 Marsham Street
London, England SWIP 3PY

HANSON, Wallace
Idaho National Engineering Lab.
EG&G Idaho
P.O. Box 1625
Idaho Falls, ID 83412

HAYES, John J.
MS OWFN 14B20
US Nuclear Regulatory Comm.
Washington, DC 20555

HAYES, Timothy W.
Southern Company Services
P.O. Box 2625
Birmingham, AL
35202

HERRMANN, Franz J.
Wiederaufarbeitungsanlage
Karlsruhe Betriebsgesellschaft
7514 Eggenstein-Leopoldshafen
Germany

HILLEY, James R.
Duke Power Company
P.O. Box 33189
Charlotte, NC
28242

HIROSE, Yasuo
Hitachi Ltd.
3-1-1 Saiwai-cho
Hitachi-shi
Japan

HOBART, Sue
Suite 200
Adams & Hobart
2025 Gateway Place
San Jose, CA 95110

HOFFMAN, J. R.
Florida Power & Light
P.O. Box 14000
Juno Beach, FL
33408

HOLMAN, David
UKAEA
AEE - Winfrith
Dorchester, Dorset
DT2 8DH United Kingdom

HOMICH, Laurence L.
U.S. Army/Descom
Letterkenny Army Depot
Chambersburg, PA
17201-4150

HUGHES, M. B.
M.C. Air Filtration
Motney Hill Rd.
Gillingham, Kent
ME8 7TZ England

HYDER, M. Leo
Westinghouse Savannah River
P.O. Box 616
Aiken, SC
29802

IHNEN, Merlin W.
Martin Marietta Energy Systems
P.O. Box 1410
Paducah, KY
42001

JACOX, Jack
Jacox Associates
P.O. Box 29720
Columbus, OH
43229

JANNAKOS, K.
Kernforschungszentrum Karlsruhe
Postfach 3640
D-7500 Karlsruhe 1
Germany

JAX, David
Detroit Edison, Fermi-2
6400 N. Dixie Highway
Newport, MI
48166

JOHNSTON, H. Stephen
President CH/BD
Delta Filter Corp.
14 Arch St.
Watervliet, NY 12189

JOSS, Gregg E.
Rochester Gas & Electric
Ginna Station
1503 Lake Rd.
Ontario, NY 14519

JUBIN, Robert T.
Bldg. 7601
Oak Ridge National Lab
P.O. Box 2008
Oak Ridge, TN 37831-6306

KAERCHER, Maurice
EDF. Septen
12-14, avenue Dutrievoz
Villeurbanne 69628
Cedex, France

KAGAWA, Alan
Evanite Fiber Corp.
P.O. Box E
Corvallis, OR
97339

KAID, Latif
Charcoal Service Corp.
P.O. Box 3
Bath, NC
27808

KANEKO, Itaru
Nuclear Enginee. ng Lab
Toshiba Corporation
4-1, Ukishima-cho, Kawasaki-ku
Kawasaki, 210 Japan

KARAKAOJA, Paavo
Imatran Voima Oy
P.O. Box 112
Vantaa, 01601
Finland

KIM, Yo Sun
Korea Atomic Energy Research
P.O. Box 7
Daedukdanji, Chungnam
Korea

KING, Robert
MS 11
Dept of Ecology
State of Washington
Olympia, WA 98505

, Carol A.
Corp., Ste. 205
Parry Highway
, PA
0

KI , Gary Q.
Bldg 2000 MS-6054
Martin Marietta Energy System
P.O. Box 2008
Oak Ridge, TN 37831-6054

KIRKLAND, John
Health Protection - 221-25F
Westinghouse Savannah River
P.O. Box 616
Aiken, SC 29802

KITTELSON, Richard
Niagara Mohawk Power Co.
8653 Braewood Dr.
Baldwinsville, NY
13027

KLAES, Leo J.
WT 10C143 H-K
Tennessee Valley Authority
400 W. Summit Hill Dr.
Knoxville, TN 37902

KLAUBER, Douglas W.
Hollingsworth & Vose
Townsend Rd.
West Groton, MA
01472

KOHLER, Gerhard M. A.
Kraftanlagen AG Heidelberg
6900 Heidelbberg,
Im Breitspiel 7
Germany

KONDO, Yoshikazu
Adv. Reactor & Ncl. Fuel Cycle
Hitachi Works
1-1 Saiwaicho 3 Chome Hitachi-
Ibaraki-ken, 317 JAPAN

KONO, Fumitaka
Toshiba Engineering Corp.
8-Somsigota Ospgp-ku
Yokoha City
235 Japan

KOVACH, J. Louis
Nuclear Consulting Services
P.O. Box 29151
Columbus, OH
43229-1035

KRANZ, Eugene
Northern States Power
1518 Chestnut Ave. N.
Minneapolis, MN
55403

KUMAR, Viswa S.
Center for Energy MS 3045
Toledo Edison Co.
300 Madison Ave.
Toledo, OH 43652

KURZ, Jerome L.
Kurz Instruments, Inc.
2411 Garden Rd.
Monterey, CA
93940

LAGUS, Peter
Suite M
Lagus Applied Technology Inc.
11760 Sorrento Valley Rd
San Diego, CA 92121

LAICHTER, Y.
Nuclear Research Center - Negev
P.O. Box 9001
Beer Sheva
Israel

LaRUE, Joseph
G 6-16
Westinghouse Hanford Co.
P.O. Box 1970
Richland, WA 99352

LEIBOLD, Hans
Kernforschungszentrum Karlsruhe
Postfach 3640
D-7500 Karlruhe 1
Germany

LEONARD, Len
ANPROG
Unit 15
10631 Bloomfield Ave.
Los Alamitos, CA 90720

LI Qi-dong
Dept. of Nuclear Sciences
Fudan University
Shanghai
People's Republic of China

LOCKWOOD, Ian Roberts
Hollingsworth & Vose (Europe)
Postlip Mills
Winchcombe, Crus
England

LOUGHBOROUGH, David
AEA Technology
Harwell Laboratory
Didcot, Oxon
OX11 ORA England

LYTTON, Russ
Duke Power Company
P.O. Box 1006
Charlotte, NC
28201-1006

MAKAM, Suri
MC N-50
Public Service Electric & Gas
P.O. Box 236
Hancocks Bridge, NJ 08038

McFARLAND, Andrew R.
Mechanical Engineering
Texas A & M Univ.
College Station, TX
77843-3121

McHUGH, Kevin
Lydall Inc.
1 Wakefield St.
Rochester, NH
03867

McINTYRE, Julie A.
MS K499
Industrial Hygiene Group
Los Alamos National Lab.
Los Alamos, NM 87545

McVEAN, Michael T.
TU Electric
P.O. Box 2300
Glen Rose, TX
76043

MERCIER, Jean-Pierre
CEA/CEN BP 6
60-68 Ave du General Leclerc
92265 Fontenay-aux-Roses
Cedex, France

MESSINA, Gary D.
HEFCO
3651 Hempland Road
Lancaster, PA
17601

MEYER, Steve
Union Electric Co.
P.O. Box 620
Fulton, MO
65251

MILLER, William H.
Sargent & Lundy Co.
55 E. Monroe St.
Chicago, IL
60603

MOELLER, Dade W.
Office of Continuing Education
Harvard School of Public Health
677 Huntington Ave.
Boston, MA 02115

MONROE, David L.
Martin Marietta Energy System
P.O. Box 2003
Oak Ridge, TN
37831-7324

MONSON, Paul
Westinghouse Savannah Site
Savannah River Laboratory
Aiken, SC
29808

MOORE, Glen
Flanders Filters, Inc.
P.O. Box 1708
Washington, NC
27889

MORRIS, K.
AEA Technology
Harwell Laboratory
Didcot, Oxon
OX 11 ORA England

MOTOI, Victoria
WAK GmbH
Postfach 1263
7514 Eggenstein-Leopoldshafen
Germany

MOY, Roger H.
Rm. 1468
Pacific Gas & Electric
77 Beale St.
San Francisco, CA 94105

MUKHI, Sudesh
Rm 1028
Con Edison Co.
4 Irving Place
New York, NY 10003

MULCEY, Philippe
IPSN/DPT/SPIN/SEIP
CEN/SACLAY, batiment 389
91191 Gif-Sur-Yvette
Cedex, France

MULLALLY, James
G6-06
Westinghouse Hanford Co.
P.O. Box 1970
Richland, WA 993532

MURROW, Jack
Murrow's Monitors
4 Carmel Ave
El Cerrito, CA
94530

NELSON, Jack R.
HEPA Corporation
3071 East Coronado St.
Anaheim, CA
92806

NERI, E.
ENEA-CASACCIA, Bldg. T-21
s.p. Anguillarese no. 301
S. Maria di Galeria
0060 Rome, Italy

NESBITT, Loyd B.
M/C 736
General Electric Nuclear Energy
175 Curtner Ave.
San Jose, CA 95125

NOVICK, Vincent
EP-207
Argonne National Lab.
9700 S. Cass Ave.
Argonne, IL 60439

OLSON, Peter
Flakt Inc.
P.O. Box 2300
Glen Rose, TX
76048

ORNBERG, Stephen C.
Sargent & Lundy
55 E. Monroe
Chicago, IL
60540

ORTIZ, John
Los Alamos National Lab.
P.O. Box 1663
Los Alamos, NM
87545

OTSUKA, Kazuhiko
Nitta Industries Corp
172 Ikezawa-cho Yamatokoriyama
Nara Prefecture
639-11 Japan

PAGE, James A.
Martin Marietta Energy Systems
P.O. Box 1410
Paducah, KY
42001

PARKIN, Philip H.
Ontario Hydro
700 University Ave.
Toronto, Ontario
M5G 1X6 Canada

PATEL, Manu C.
TU Electric Co., LB-81
400 N. Olive Street
24th fl, Skyway Tower
Dallas, TX 75201

PARTHASARATHY, Partha S.
MS 45/7/A31
Bechtel National Inc.
50 Beale St.
San Francisco, CA 94119

PAUL, Joseph D.
Westinghouse Savannah River Co.
802 East Martintown Rd.
North Augusta, SC
29841

PAULING, Ned B.
United Engineers & Const.
30 South 17th St.
Philadelphia, PA
19101

PEARSON, John R.
NCS Corporation
4555 Groves Rd. #41
Columbus, OH
43232

PEST, Mark E.
Arizona Public Service
Lichfield Park
502 Cascade Drive
Phoenix, AZ 85034

PHILIPPE, Marc
CEA-CEN
Fontenay-aux-Roses
bat. 18 60-68 Av du Gel Leclerc
BP no.6 92265 Cedex, France

PHILIPPI, Hardy M.
Atomic Energy of Canada
Chalk River
Ontario
KOJ 1JO Canada

PIERCE, James G.
CVI Inc.
P.O. Box 2138
Columbus, OH
43216

PIERCE, Mary E.
Hollingsworth & Vose
Townsend Road
West Groton, MA
01472

PLATINI, Massimo
Univ. di Roma
Ple A Moro No. 2
Rome
Italy

PLATZ, Mike
Evanite Fiber Corp.
P.O. Box E
Corvallis, OR
97339

PLUMB, G. R.
IAEA
Wagramerstrasse 5
P.O. Box 100
1150 Vienna, Austria

PORCO, Richard
Consultant
130 Glenwood Drive
Monroeville, PA
15146

PORTER, Greg
Pacific Gas & Electric Co.
P.O. Box 56
Avila Beach, CA
93424

POWELL, Dennis
Nuclear Consulting Services
P.O. Box 29151
Columbus, OH
43229

PYSH, W.A.
Techno Corporation
620 West 6th Street
Erie, PA
16507

RABEKOFF, Wendy
Fluor Daniel Inc.
333 Michelson Drive
Irvine, CA
92730

RABON, Rod L.
Bldg. 706-17C
Savannah River Site
Westinghouse Savannah River
Aiken, SC 29808

RAJA, Sri K.
Farr Co.
2221 Park Place
El Segundo, CA
90245

RAMM, Dave
Hollingsworth & Vose
1485-6 ENP Court
Concord CA
94520

RAMSDELL, James V.
Atmospheric Sciences Dept.
Battelle Pacific Northwest
P.O. Box 999
Richland, WA 99352

REINERT, Bruce B.
Industrial Hygiene Grp. MS K499
Los Alamos National Lab.
P.O. 1663
Los Alamos, NM 87545

REMICK, Forrest J.
MS 16-H3
U.S. Nuclear Regulatory Comm.
Washington, DC
20555

RHODES, William G.
General Electric Co.
P.O. Box 1072
Schenectady, NY
12301

RICKETTS, Craig I.
Kernforschungszentrum Karlsruhe
LAF II, Postfach 3640
D-7500 Karlsruhe 1
Germany

RINGEL, H. D.
KFA-Juelich
5170 Julich 1
Postfach 1913
Germany

ROBERSON, Philip W.
McGuire Nuclear Station
Duke Power Co.
Charlotte, NC
28242

RODGERS, John
MS K483
Los Alamos National Lab.
P.O. Box 1663
Los Alamos, NM 87545

ROESKE, Tom
Pall Corporation
2200 Northern Blvd.
East Hills, NY
11548

ROUSH, Dale
Ellis & Watts
4400 Glen Willow Lake Ln.
Batavia, OH
45103

ROWLAND, William D.
US Dept. of Energy
P.O. Box A
Aiken, SC
29801

SALISBURY, Scott
MS K-486
Los Alamos National Lab.
P.O. Box 1663
Los Alamos, NM 87545

SALO, Paivi
Finnish Centre for Radiation &
Nuclear Safety
P.O. Box 268
SF-00101 Helsinki, Finland

SAVORNIN, Jacques
CEA - IPSN
BP no. 6
92265 Fontenay aux-Roses
Cedex, France

SCHERR, Rodney W.
Savannah River Site
Westinghouse Savannah River
Aiken, SC
29808

SCHOLTEN, Lambert C.
N.V. KEMA
P.O. Box 9035
NL-6800ET, Arnhem
The Netherlands

SCHWARTZ, Barry
Sargent & Lundy
55 E. Monroe
Chicago, IL
60690

SEAM, Balbir C.
Bechtel Corp.
9801 Washington Blvd.
Gaithersburg, MD
20878

SEEL, Richard
General Dynamics
14 Holmes St.
Mystic, CT
06355

SEIBERT, Jeff
Pall Corporation
2200 Northern Blvd.
East Hills, NY
11548

SHEPARD, Robert L.
NL-007, Rm N-162
Off. of Nuclear Regulatory Res.
U.S. Nuclear Regulatory Comm.
Washington, DC 20555

SICKELS, Dave
ECO Air Products, Inc.
9455 Cabot Drive
San Diego, CA
92126

SMITH, Luther H.
Kaiser Engineers Hanford
P.O. Box 888
Richland, WA
99352

SMITH, Phillip R.
Dept. of Mechanical Eng.
New Mexico State Univ.
Box 30001
Las Cruces, NM 88003-001

SOFFER, Leonard
MS NLS-324
U.S. Nuclear Regulatory Comm.
Washington, DC
20555

SONODA, Takayuki
Nuclear Power Plant Eng'g Dept.
Hitachi Works, Hitachi, Ltd.
1-1 Saiwaicho 3 chome, Hitachi-
Ibaraki-ken, 317 Japan

STAHL, William C.
Set-Point Control Inc.
1100 Jadwin Ave., # 175
Richland, WA
99352

STEVENS, Don
Pall Corporation
2200 Northern Blvd.
East Hills, NY
11548

TINKLIN, B. T.
M.C. Air Filtration
Motney Hill Rd.
Gillingham, Kent
ME8 7TZ England

TORGERSON, David F.
AECL Research
Whiteshell Laboratores
Pinawa, Manitoba
ROE 1LO Canada

VanTRIEU, Vi
United Engineers & Constructors
30 S. 17th St.
Philadelphia, PA
19101

VENDEL, Jacques
IPSN/DPT/SPIN/SEIP
CEN/SACLAY, batiment 389
91191 Gif-sur-Yvette
Cedex, France

VERMILYA, Donald Scott
Bldg. 706-15C
Savannah River Site
Aiken, SC
29808

VIGNAU, B.
CEA/IRD/DERDCA/DGR
Service de Latelier Pilote
BP. 171
30205 Bagnols sur Cedex, France

VIKIS, A. C.
AECL Research
Whiteshell Laboratories
Pinawa, Manitoba
ROE 1LO Canada

VOGAN, Thomas
Sargent & Lundy
55 East Monroe St.
Chicago, IL
60603

VRESK, Josie
Argonne National Lab.
9700 S. Cass
Argonne, IL
60439

WALKER, Bob
Atomic Evergy Control Board
270 Albert St.
Ottawa, Ontario
K1P 559 Canada

WALKER, Jimmy N.
Bldg. 703-H
Savannah River Site
Westinghouse Savannah River
Aiken, SC 29801

WALTMON, Roy
Martin Marietta Energy Systems
P.O. Box 1410
Paducah, KY
42011

WATSON, Brian W.
A.E.A. Technology
Wigshaw Lane
Culcheth Warrington
WA3 4NE England

WATSON, J.H.P.
Institute of Cryogenics
Univ. of Southampton
Southampton
SO9 5NH England

WEADOCK, Anthony A.
Office of Safety Policy &
Standards, EH-352
U.S. Dept. of Energy
Washington, DC 20545

WEBER, Larry
Pall Corporation
2200 Northern Blvd.
East Hills, NY
11548

WEIDLER, Raymmd R.
Duke Power Co
P.O. Box 1006
Charlotte, NC
28201-1006

WEINERT, Arnd
Environmental & Prot. Dept.
TUEV SUEDWEST E.V.
Postfach 103262, D-6800
Mannheim 1, Germany

WHITE, E. R.
Rockwell-INEL
P.O. Box 1469
Idaho Falls, ID
83403

WICHMANN, Hanns-Peter
WAK GmbH
Postfach 1263
7514 Eggenstein-Leopoldshafen
Germany

WIEBE, Peter
Ontario Hydro
700 University Ave.
Toronto, Ontario H11 F22
M5G 1X6 Canada

WILHELM, Juergen
Kernforschungszentrum Karlsruhe
Postfach 3640
D-7500 Karlsruhe 1
Germany

WILLIS, Charles A.
MS EWW-360
Div. Radiation Prot & Emergency
Preparedness
U.S. Nuclear Regulatory Comm.
Washington, DC 20555

WOODS, Paul
MS 6006
Arizona Public Service Co.
P.O. Box 52034
Phoenix, AZ 85072-2034

YOSHINO, Hirokazu
Plant & System Planning Dept.
Toshiba Corporation
8, Shinsugita-cho, Isogo-ku
Yokohama 235, Japan

YOW, F. J. Roland
Corp. Consult & Development
P.O. Box 12728
Research Triangle Park, NC
27709

ZARBO, Robert
Arizona Nuclear Service
405 Redondo Dr. S.
Litchfield Park, AZ
85340

ZDON, Edward
#414
955 E. 3rd St.
Long Beach, CA
90802

ZHANG, YingZhong
Light Industrial Engineering
Design Institute
No. 611, Qi Pu Road
Shanghai, 200085
People's Republic of China

ZIEMER, Paul
Assistant Sec. for Environment,
Safety and Health
U.S. Dept. of Energy
Washington, DC 20555

NRC FORM 335 (2-89) NRCM 1102, 3201, 3202

U.S. NUCLEAR REGULATORY COMMISSION

BIBLIOGRAPHIC DATA SHEET

(See instructions on the reverse)

1. REPORT NUMBER (Assigned by NRC, Add Vol., Supp., Rev., and Addendum Numbers, if any.)
NUREG/CP-0116
CONF-900813
Vol. 2

2. TITLE AND SUBTITLE
Proceedings of the 21st DOE/NRC Nuclear Air Cleaning Conference
Sessions 9 - 16
Held in San Diego, California
August 13 - 16, 1990

3. DATE REPORT PUBLISHED
MONTH: February
YEAR: 1991

4. FIN OR GRANT NUMBER

5. AUTHOR(S)
M. W. First, Editor

6. TYPE OF REPORT

7. PERIOD COVERED (Inclusive Dates)

8. PERFORMING ORGANIZATION - NAME AND ADDRESS (If NRC, provide Division, Office or Region, U.S. Nuclear Regulatory Commission, and mailing address; if contractor, provide name and mailing address.)
Harvard School of Public Health
The Harvard Air Cleaning Laboratory
665 Huntington Avenue
Boston, MA 02115

9. SPONSORING ORGANIZATION - NAME AND ADDRESS (If NRC, type "Same as above"; if contractor, provide NRC Division, Office or Region, U.S. Nuclear Regulatory Commission, and mailing address.)
Office of Nuclear Safety
U.S. Department of Energy
Washington, DC 20585

Office of Nuclear Regulatory Research
U.S. Nuclear Regulatory Commission
Washington DC 20555

International Society of Nuclear Air Treatment Technologies, Inc.
P.O. Box 29246
Columbus, OH 43229

Harvard School of Public Health
The Harvard Air Cleaning Laboratory
665 Huntington Avenue
Boston, MA 02115

11. ABSTRACT (200 words or less)

This document contains the papers and the associated discussions of the 21st DOE/NRC Nuclear Air Cleaning Conference. Major topics are: (1) chemical processing systems, (2) reactor operations, (3) incineration and vitrification, (4) particulate filter developments, including filter testing and response to physical and temperature stress, (5) adsorption and testing of activated carbon and adsorber systems, (6) severe accident mitigation including modeling of emergency response systems, (7) nuclear waste management systems, (8) carbon removal, (9) monitoring and measurement systems, (10) the development of standards and regulations and concerns with existing standards and regulations, and (11) nuclear air cleaning activities around the world.

-14

12. KEY WORDS/DESCRIPTORS (List words or phrases that will assist researchers in locating the report.)
NUCLEAR AIR CLEANING CONFERENCE

13. AVAILABILITY STATEMENT
Unlimited

14. SECURITY CLASSIFICATION
(This Page)
Unclassified
(This Report)
Unclassified

15. NUMBER OF PAGES

16. PRICE

NRC FORM 335 (2-89)

THIS DOCUMENT WAS PRINTED USING RECYCLED PAPER.

UNITED STATES
NUCLEAR REGULATORY COMMISSION
WASHINGTON, D.C. 20555

120555139531 1 1AN19A19B
US NRC-OADM
DIV FOIA & PUBLICATIONS SVCS
TPS PDR-NUREG
P-223
WASHINGTON DC 20555